Università degli Studi di Udine

Dottorato di Ricerca
in Ingegneria Industriale e dell'Informazione

Ph.D. Thesis

Structural Analysis and Control of Dynamical Networks

Supervisor:
Franco Blanchini

Candidate:
Giulia Giordano

Doctorate Coordinator:
Paolo Gardonio

Udine, March 2, 2016

Author: **Giulia Giordano**

Author's Web Page: `https://users.dimi.uniud.it/~giulia.giordano`

Author's e-mail: giulia.giordano@uniud.it

Author's address:

Dipartimento di Matematica e Informatica
Università degli Studi di Udine
Via delle Scienze, 206
33100 Udine
Italia

Abstract

A dynamical network is comprised of a finite number of subsystems, each having its own dynamics, which interact according to a given interconnection topology. Dynamical networks are a powerful modelling tool to represent a large number of systems in different contexts, ranging from natural to man-made systems, and have a peculiar feature: the global behaviour is the outcome of an ensemble of local interactions. Hence, dynamical networks can be analysed so as to understand how local events can lead to global consequences and can be controlled by acting locally so as to achieve the desired global behaviour. The analysis and the control of dynamical networks are structural when they are grounded on the topology of the interconnection graph, along with qualitative, parameter-free specifications.

Structural analysis aims at assessing properties for a whole family of systems having the same structure and is particularly suited for natural systems, which can exhibit an extraordinary robustness in spite of large uncertainties and intrinsic variability. In this thesis, results and procedures are presented to structurally assess relevant properties, such as stability, boundedness and the sign of steady-state input-output influences, for a wide class of systems whose Jacobian admits the so-called BDC-decomposition, which embodies the sum of the effects of single local interactions. A structural classification is also proposed, to discriminate between systems that can possibly or exclusively admit instability related to oscillations or to multistationarity, for systems with a sign-definite Jacobian and for systems composed of the interconnection of stable monotone subsystems; a graph-based classification is given and applied to examples of artificial biomolecular networks.

In a dynamical network described by a graph, subsystems are associated with nodes and interactions with arcs. When the interactions are not given, they can be decided by a control system. In particular, network-decentralised control aims at governing the global behaviour of a dynamical network through controllers that are associated with the arcs of the interconnection graph, hence act locally and have access to local information only. Despite the restricted information constraint, a large class of systems can be always stabilised resorting to a network-decentralised controller. Both linear systems composed of independent subsystems, connected by the control action, and nonlinear compartmental systems are considered; the robustness and optimality properties of the devised network-decentralised control are investigated and several application examples are proposed, spanning from traffic control and data transmission to synchronisation and vehicle platooning. Network-decentralised estimation is also considered, for systems composed of identical agents; a robustness result is provided, exploiting the smallest eigenvalue of the generalised Laplacian matrix associated with the interaction graph.

Structural analysis and network-decentralised control synthesis are presented in this work as complementary facets of the same approach, which can streamline each other. Structural analysis can help explain the robustness of natural systems, so that the clever resources of nature can be mimicked to improve the control strategies designed for man-made systems; at the same time, local interactions can be engineered in biomolecular systems, as is done for artificial systems, to obtain the desired global behaviour. This virtuous circle will hopefully result in innovative approaches for biotechnologies and large-scale network engineering, aimed at improving the quality of our daily life.

Sommario

Una rete dinamica è composta da un insieme finito di sottosistemi, ciascuno con la propria dinamica, che interagiscono secondo una precisa topologia di interconnessioni. Le reti dinamiche consentono di rappresentare efficacemente un gran numero di sistemi nei contesti più svariati, che includono sia i sistemi naturali sia quelli ingegneristici, e hanno una caratteristica distintiva: il comportamento globale è il risultato di un insieme di interazioni locali. Perciò, le reti dinamiche possono essere analizzate al fine di comprendere come eventi locali possano portare a conseguenze globali e possono essere controllate per mezzo di azioni locali, per ottenere il comportamento globale desiderato. L'analisi e il controllo di reti dinamiche si possono dire strutturali quando si basano esclusivamente sulla topologia del grafo delle interconnessioni e su informazioni qualitative, che prescindono dai parametri.

L'analisi strutturale si propone di determinare proprietà che valgono per un'intera famiglia di sistemi aventi la stessa struttura ed è particolarmente utile nel caso di sistemi naturali, che spesso manifestano una straordinaria robustezza nonostante la presenza di grandi incertezze e di un'intrinseca variabilità nei parametri. In questa tesi, si presentano risultati e procedure che consentono di valutare da un punto di vista strutturale proprietà di interesse, quali la stabilità, la limitatezza e il segno dell'influenza ingresso-uscita a regime, per una vasta classe di sistemi la cui matrice Jacobiana ammette la cosiddetta decomposizione BDC, che esprime la somma degli effetti dovuti a singole interazioni locali. Si propone inoltre una classificazione strutturale che consente di distinguere tra sistemi che possono ammettere o che ammettono esclusivamente instabilità legata a fenomeni oscillatori o a multistazionarietà, per sistemi con una matrice Jacobiana a segno definito e per sistemi formati dall'interconnessione di sottosistemi monotoni stabili; una classificazione basata su grafi è proposta e applicata a esempi di reti biomolecolari artificiali.

In una rete dinamica descritta da un grafo, i sottosistemi sono associati ai nodi e le interazioni agli archi. Quando le interazioni non sono date, esse possono essere decise da un sistema di controllo. In particolare, il controllo decentralizzato nel senso delle reti mira a governare il comportamento globale di una rete dinamica per mezzo di controllori che sono associati agli archi del grafo di interconnessione, dunque agiscono localmente e hanno a disposizione soltanto informazioni locali. Nonostante il vincolo dovuto alla limitata informazione disponibile, una vasta classe di sistemi può essere sempre stabilizzata ricorrendo a un controllore decentralizzato nel senso delle reti. Si considerano sia sistemi lineari costituiti da sottosistemi indipendenti, connessi dall'azione di controllo, sia sistemi compartimentali nonlineari; si studiano le proprietà di robustezza e di ottimalità del controllo proposto, che è decentralizzato nel senso delle reti, e si propongono molteplici esempi di applicazione, che spaziano

da controllo del traffico e trasmissione di dati fino a sincronizzazione e controllo di colonne di veicoli. Si considera inoltre una procedura di stima decentralizzata nel senso delle reti, per sistemi formati da agenti identici; si fornisce un risultato di robustezza, che si avvale del minimo autovalore della matrice Laplaciana generalizzata associata al grafo di interazione.

L'analisi strutturale e la sintesi di controllori decentralizzati nel senso delle reti sono presentate in questa tesi come aspetti complementari dello stesso approccio, che possono aiutarsi l'un l'altro. L'analisi strutturale può aiutare a spiegare la robustezza dei sistemi naturali, di modo che le efficienti strategie della natura possano essere imitate per migliorare gli algoritmi di controllo progettati per i sistemi costruiti dall'uomo; allo stesso tempo, le interazioni locali nei sistemi biomolecolari possono essere ingegnerizzate, come accade nel caso dei sistemi artificiali, per ottenere il comportamento globale desiderato. Questo circolo virtuoso consentirà auspicabilmente approcci innovativi per le biotecnologie e per l'organizzazione di reti di grandi dimensioni, al fine di migliorare la qualità della nostra vita quotidiana.

Acknowledgements

In these beautiful years of doctoral studies, I have been lucky enough to meet several skilled and talented researchers, from whom I have learned a lot.

I am grateful to all the people of both the departments I have been connected with in Udine (*Dipartimento di Ingegneria Elettrica, Gestionale e Meccanica* and *Dipartimento di Matematica e Informatica*), for providing a stimulating working and learning environment – special thanks are due to **Dimitri Breda**, **Edda Dal Santo**, **Pietro Giannattasio**, **Roberto Petrella** and **Rossana Vermiglio** for interesting scientific discussions – and to all the people, from several institutions, with whom I have had the opportunity to interact and collaborate. In particular, I would like to thank:

• **Frank Allgöwer**, who hosted me at the Institut für Systemtheorie und Regelungstechnik, Universität Stuttgart, along with **Christian Ebenbauer** and **Nicole Radde**, and all the members of the IST group with whom I had stimulating discussions, especially **Viktor Avrutin**, **Debdas Paul**, **Caterina Thomaseth** and **Patrick Weber**;
• **Claudio Altafini** (Linköping University) and **Patrizio Colaneri** (Politecnico di Milano), the reviewers of my doctoral thesis, for their suggestions and comments that really helped me improve this work;
• **Daniele Casagrande** and **Umberto Viaro**, for our interesting scientific discussions and for the research problems we have handled together;
• **Carlo Drioli** and **Gian Luca Foresti**, who involved me in the study of a visual servoing application for tracking a moving target;
• **Gianfranco Fenu** and **Felice Andrea Pellegrino**, for introducing me to robotics and for hosting several deep research meetings at the University of Trieste;
• **Mirko Fiacchini**, **John-Jairo Martinez Molina** and **Olivier Sename**, who hosted me at the Institut National Polytechnique in Grenoble;
• **Elisa Franco**, for introducing me to the fascinating world of biology since 2012, when she was mentoring me during my stay at the California Institute of Technology, and for hosting me at the University of California at Riverside;
• **Paolo Gardonio**, the coordinator of this doctoral programme, for organising a wide range of training activities and events;
• **Renato Lo Cigno** and **Michele Segata**, for interesting discussions at the University of Trento concerning vehicle-to-vehicle communication and vehicle platooning;
• **Stefano Miani**, for interesting discussions and for involving me in the Franco-Italian collaborative research programme Galileo 2014;
• **Pier Luca Montessoro**, who provided me with fundamental support and involved

me in research projects about biometric recognition and distributed scheduling;
• **Richard M. Murray**, who hosted and mentored me within the SURF program at the California Institute of Technology;
• **Sorin Olaru** and **Vasso Reppa**, who hosted me at Supélec and introduced me to fault detection and isolation;
• **Fabio Zanolin**, for his suggestions and explanations, and for his precious guidance during my first teaching experience.

My deepest gratitude goes to my supervisor **Franco Blanchini**, for his invaluable advice, his care and his kindness. Working with him has been a challenging and enriching experience. He has set an example for me of how a good researcher should be, with his expertise, insight, creativity and with his genuine and contagious enthusiasm for research. I heartily thank him for all he has taught me, which I have treasured and I hope to have the possibility of teaching in turn, one day.

Udine, March 2, 2016 Giulia

Contents

List of Figures

List of Tables

1

Introduction

A large number of systems, in the most different contexts, can be modelled as *dynamical networks*: in fact, phenomena related both to the evolution of quantities over time (*dynamics*) and to interconnections among several units (*networks*) are ubiquitous in natural systems, as well as in complex artificial systems.

A dynamical network can be regarded as the interplay of a finite number of subsystems, each having its own dynamics, interconnected by suitable interactions, which enforce a relationship between the dynamics of the individual subsystems. The behaviour of the overall system, then, depends on the internal dynamics of the individual subsystems and on the topology of the interconnection network. Interestingly, the interactions are *local* (since each of them is related to a single interconnection link in the network topology), but their impact results in *global* consequences, affecting the behaviour of the overall system. This motivates us

- on the one hand, to study the mechanisms that produce the global system behaviour based on the ensemble of local interactions, keeping in mind that *local events have a global outcome* (analysis);
- on the other hand, to devise control strategies that obtain the desired global behaviour by deciding the local interactions based on local information, according to the motto: *think globally, act locally* (control).

In particular, both analysis and control can rely on the peculiar structure of the system under consideration, defined in terms of the graph representing the interconnection topology.

The goal of *structural analysis* for dynamical networks is to assess behaviours and phenomena based on the system structure only (essentially, on the graph topology, along with qualitative information about the subsystem dynamics and about the interaction functions). Hence, parameter-free criteria can be devised to check if a whole family of systems, all having the same structure, enjoys a relevant property.

This is especially important when dealing with natural systems, which are plagued by huge uncertainties and whose parameters are highly dependent on environmental and working conditions: by means of a structural investigation, it may be possible to explain how they can perform their specific, proper tasks in completely different conditions, thus revealing the structural source of the extraordinary robustness of nature and of living organisms.

The goal of *network-decentralised control synthesis*, instead, is to control or coordinate the behaviour of a large number of subsystems resorting to local controllers, which decide their strategy based on local information only. This means that each control agent, associated with a link of the network, decides local interactions based on information about the subsystems associated with the nodes connected by that specific link. Under proper structural assumptions, it is always possible to govern the overall behaviour of the system, achieving stability, by simply controlling local interactions, based on the knowledge of local dynamics only.

This is particularly relevant for complex systems, composed of several geographically sparse units, when it is impossible to build a centralised and omniscient controller that governs the system, due to hard constraints on the information available in each portion of the network.

The aim of this thesis is to propose a unified view of the analysis and the control of dynamical networks, carried out from a structural standpoint. It is worth underlining that (structural) analysis and control synthesis, albeit requiring in general different tools and approaches, are far from being disjoint. In fact, analysis is well suited for natural systems, while control of course refers to man-made systems; and a virtuous circle can be built since the analysis of natural systems can help engineers learn from nature and control man-made systems resorting to a biologically-inspired control design, while local interactions in natural systems (once their spontaneous functioning has been deeply understood) can be engineered with the same systematic, bottom-up approach that is used for building complex artificial systems (this is the goal of synthetic biology).

Thesis Overview and Contribution

The thesis presents a unified study of the structural analysis and control of dynamical networks,[1] and is articulated in three main parts.

Structural Properties, Dynamical Networks, Fundamental Concepts and Results

Part I deals with the common background and the fundamental concepts that will be recurrent throughout the thesis. First of all, structural properties are defined in Chapter 2 as properties enjoyed by all of the systems belonging to a family, specified without numerical bounds. Therefore, a structural property can be assessed according to parameter-free criteria, exclusively based on qualitative information

[1] Most of the results have been previously published in peer-reviewed conference or journal papers, or are currently under review or in preparation. The corresponding publications are always referenced; for the sake of completeness, almost all of the proofs (which can be found in the articles) have been either reported or sketched in the thesis as well.

about the considered family of systems. Possible qualitative information that can be available about functions (hence, about systems) are provided and discussed. Moreover, fundamental properties that are usually worth assessing are listed and described in detail, and their significance is motivated by examples. The concept of dynamical network is further investigated in Chapter 3, where the relationship with compartmental systems is examined (actually, dynamical networks can be regarded as a generalisation of compartmental systems). The structure of a dynamical network is formally associated with its graph representation and with the corresponding incidence matrix. Then, both structural analysis and control synthesis for the particular case of dynamical networks are presented, explaining how a structural approach can exploit the peculiarities of these systems. Fundamental concepts from several mathematical theories and essential results are reported in Chapter 4. Some basic concepts of graph theory (fundamental for defining and handling structures of dynamical networks) are summarised. The theory of chemical reaction networks is presented [HJ72, Fei72, Hor73a, Hor73b, FH74], along with fundamental established results such as the zero-deficiency theorem [Fei87], and the limits of mass action kinetics (representing the rate of a reaction depending on the concentration of the reactants) are discussed, proposing a generalised approach where reaction rates are generic functions of the concentrations of the involved species [BF11b]. As a key point on which the forthcoming investigation is based, a special structure named the BDC-decomposition is presented [BFG12, BG14, GCFB15]; such a decomposition exploits the fact that, for any system whose Jacobian matrix is the positive linear combination of rank-one matrices, this Jacobian can be written as the product of three matrices, one depending on a vector of positive parameters, the other two expressing the Jacobian *structure*. A useful integral formula [Kha02] is exploited to show that the BDC-decomposition is indeed a global property, and not only a local property. It is important to stress that the BDC-decomposition actually decomposes the system Jacobian (hence, the overall set of linearised interactions occurring in the system) into the sum of several basic local interactions that, summed up, result in the global dynamic effect. It can thus be seen as a picture of the "*local interactions, global behaviour*" effect that has been previously mentioned. It turns out that, for systems admitting a BDC-decomposition, some important quantities associated with the Jacobian matrix, for instance the determinant and the coefficients of the characteristic polynomial, are multi-affine functions of the positive parameters. Consequently, a vertex result is presented that exploits multi-affinity for testing the structural sign of a function in a hypercube in the parameter space [BFG12, BG14, GCFB15]. Multi-affinity also allows to invoke the fundamental mapping theorem [Bar94] and the zero exclusion theorem, to obtain a sufficient condition for robust stability. Some hints about fundamental concepts of the topological degree theory and its applications to the equilibria and the stability of dynamical systems [OC95, Hof90] are also briefly reported; a more thorough overview of the theory is in Appendix D.

The core contribution of the thesis is in Parts II and III, which deal respectively with structural analysis and control synthesis for dynamical networks.

Structural Analysis of Dynamical Networks

Part II, devoted to structural analysis, has a special focus on (bio)chemical and biological systems, although the proposed results are applicable for a much wider class of systems, not necessarily describing the dynamics and the interconnections that rule the behaviour of living organisms, biomolecules and chemical species. However, for these systems, whose features are investigated more in depth in Chapter 5, the need of a structural analysis is particularly felt, due to their inherent robustness in spite of severe uncertainties. A survey of the most investigated properties in the literature is proposed in Chapter 5 and some results are proposed for the structural detection of fundamental properties [BFG12], such as the capacity of exhibiting oscillations or perfect adaptation, simply exploiting multi-affinity (in fact, it can be shown that systems belonging to a wide class of biochemical and biological systems always admit a BDC-decomposition, and the proposed criteria are valid for any system admitting this decomposition); criteria to structurally assess stability and to rule out oscillatory instability are also discussed.

Chapter 6 structurally investigates stability and boundedness of biochemical systems, with generic monotonic reaction rates (not necessarily of the mass action form), by absorbing the non-linear system in a linear differential inclusion and looking for a polyhedral Lyapunov function, which can be found by a recursive procedure based on an associated discrete-difference inclusion [BG14]. Stability properties can be studied by decomposing the chemical reaction network into elementary reactions (local interactions) and propagating each of them independently to assess the stability properties of the global system. The results actually apply in general to any system admitting a BDC-decomposition. A discrete-event interpretation of the numerical procedure is proposed. Moreover, the results obtained by analysing the system in concentration coordinates are compared to those obtained by analysing the system in reaction coordinates [BG15a]. It is also shown that, for a set of fundamental motifs, structural stability cannot be assessed by means of quadratic Lyapunov functions, while it can be proved based on polyhedral Lyapunov functions [BG15b]. An example illustrates the fact that, in some cases, resorting to smooth structural Lyapunov functions is impossible: to prove structural stability, the only possibility is employing polyhedral Lyapunov functions. A catalogue of several nontrivial networks, whose stability and boundedness have been tested by means of the proposed procedure, is reported in Appendix A, while some details on the code implementing the procedure, which is available online, are in Appendix B.1.

The steady-state behaviour of a class of biological systems is investigated in Chapter 7 (and, again, the results can be immediately extended to consider generic systems admitting a BDC-decomposition). [GCFB15] The system exhibits a structural steady-state input-output influence if the variation of the steady-state output value, upon a perturbation due to a constant input, always has the same sign as the input, or the opposite sign, or is zero, independent of the parameter values; otherwise, the influence is indeterminate. When a persistent additive input is applied

to a single state variable and a single state variable is taken as the system output, the results for all the possible input-output pair combinations can be visualised in the structural influence matrix, whose entries express the sign of the steady-state influence on each variable of an external persistent input applied to each variable. Exploiting multi-affinity, structural influences can be assessed based on a simple vertex algorithm; as an alternative, a tree-like recursive algorithm is proposed for systems whose Jacobian entries are independent. Appendix B.2 presents and briefly discusses the code implementing the vertex procedure, which is available online.

Finally, Chapter 8 proposes a structural classification of biochemical systems (which can be easily applied to any system with a sign-definite Jacobian), based on their capacity of possibly/exclusively exhibiting transitions to instability of the oscillatory type (related to a pair of complex eigenvalues crossing the imaginary axis) or of the real type (related to a real eigenvalue crossing the imaginary axis at the origin and associated with multistationarity). [BFG14] The classification is extended to the case of systems that can be seen as the interconnection of unconditionally stable monotone subsystems [BFG15b]; this more general result can be applied to analyse (and to streamline the robust design and synthesis of) several synthetic biochemical networks [KWW06, KW11, BCFG14, CGK$^+$16].

Network-Decentralised Control of Dynamical Networks

In Part III, the focus is on the control of dynamical networks. In particular, in Chapter 9, network-decentralised state-feedback strategies are proposed to stabilise linear systems composed of several dynamically decoupled subsystems (which are then interconnected by the control action). The rule of the game, for network-decentralised control, is that control agents, each associated with a link of a given interconnection topology, can decide their strategy based on the sole knowledge of the state variables associated with the subsystems they connect. These restricted information constraints result in a block-structured feedback matrix, where structural zero-blocks enforce the lack of information available to the controllers; such a feedback matrix turns out to have the same block structure as the transpose of the overall input matrix of the system. When the subsystems do not share unstable eigenvalues (a generically satisfied property), any stabilisable system can be stabilised by means of a network-decentralised controller. Furthermore, for identical subsystems where each input affects a pair of subsystems, with input sub-matrices that differ for the sign only (which is typically the case for flow networks), network-decentralised stabilisability is shown to be equivalent to the presence of a connection with the external environment (namely, of an agent affecting a single subsystem). [BFG13, BFG15a]

Chapter 10 analyses the case of nonlinear systems with a compartmental structure, where two types of flows connecting pairs of compartments are possibly present, depending either on the difference of the state of the two compartments, or on the state of the starting compartment only. The saturated network-decentralised

strategy proposed in [BBGP13] is tailored and adapted to this case. Necessary and sufficient structural conditions for stabilisability are proposed and the robustness and asymptotic optimality properties of the devised network-decentralised control are discussed: the control is intrinsically robust since it does not require the knowledge of the involved functions (apart from qualitative monotonicity assumptions), it is still effective in the case of switching topologies and it can face a time-varying and unknown exogenous demand; optimality is ensured in terms of the minimal Euclidean norm of the asymptotic controlled flow. An alternative network-decentralised control is proposed to guarantee the satisfaction of positivity constraints during the whole system evolution. [BFG+16] Finally, the possibility of equipping the control arcs with integrators is explored, in order to ensure, along with decentralised asymptotic optimality, exact convergence to the desired set-point.

Several applications of the network-decentralised control approach are proposed in Chapter 11, ranging from traffic control problems (where at each node the traffic splits in several queues, each having a different destination, and a robust and asymptotically optimal network-decentralised control can be found that is independent of the traffic splitting rates and just needs information about the cumulative buffer content) [BGM14] and data transmission systems [BFG+16] to a network-decentralised channel sharing communication protocol [BCGM16], from clock synchronisation to the control of vehicle platoons.

Chapter 12 considers the dual framework of network-decentralised control: network-decentralised estimation. A local estimation problem is formulated: each node of the network is seen as an agent striving to reconstruct its own state having exclusively information exchanges with the neighbouring agents. Conditions for network-decentralised detectability are provided. Moreover, the choice of the observer gain and the proposed observer are robustified to tackle the case of unknown and switching topologies, exploiting a result on the smallest eigenvalue of the generalised Laplacian matrix and on the corresponding worst case (the smallest generalised Laplacian eigenvalue of all the connected graphs with a given number of nodes). [GBF+15]

1.1 Notation and Acronyms

It will be impossible to keep the notation completely coherent through all of the chapters. However, some notations will be recurrent throughout the thesis. Typically, Greek letters (α, β, γ, ...) will denote scalars, Roman letters (a, b, c, ...) vectors, capital Roman letters (A, B, C, ...) matrices, calligraphic letters ($\mathcal{A}$, $\mathcal{B}$, $\mathcal{C}$, ...) sets. Moreover, the following notation will be used.

- $\mathbb{N}$ is the set of natural numbers, including 0; $\mathbb{Z}$ is the set of integer numbers; $\mathbb{R}$ is the set of real numbers, while $\mathbb{R}_+$ is the set of non-negative real numbers;
- given a matrix M, $M^\top$ is its transpose, $\ker(M)$ is its kernel (null space, set of vectors x such that $Mx = 0$), while its left kernel (or left null space) is the set

of vectors x such that $x^\top M = 0$ (hence, it corresponds to $\ker(M^\top)$), $\text{span}(M)$ is its column space;

- given a square matrix A, $\text{tr}(A)$ is its trace (sum of diagonal elements), $\det(A)$ is its determinant, $\sigma(A)$ is its spectrum (set of the eigenvalues); an eigenvalue is called stable if its real part is strictly negative, unstable otherwise[2];
- e_h denotes a vector of the standard basis in $\mathbb{R}^n$ (a vector whose hth component is 1, while the others are 0);
- $\bar{1}_n$ denotes the vector of ones having dimension n (sometimes the dimension is not explicitly stated, but it is clear from the context);
- given a function $\Psi : \mathbb{R}^n \to \mathbb{R}$, its unit ball is the set

$$\mathcal{N}[\Psi, 1] = \{x : |\Psi(x)| \leq 1\};$$

- given a smooth function $\Psi : \mathbb{R}^n \to \mathbb{R}$, its gradient $\nabla\Psi(x)$ is the column vector

$$\nabla\Psi(x) = \left[\frac{\partial\Psi}{\partial x_1}(x)\ \frac{\partial\Psi}{\partial x_2}(x)\ \ldots\ \frac{\partial\Psi}{\partial x_n}(x)\right]^\top;$$

- a locally Lipschitz function $\Psi : \mathbb{R}^n \to \mathbb{R}$ is positive definite if $\Psi(0) = 0$ and $\Psi(x) > 0$ for all $x \neq 0$, positive semidefinite if the strict inequality is replaced by a weak inequality; the function $\Psi(x)$ is negative (semi)definite if $-\Psi(x)$ is positive (semi)definite;
- if A and B are matrices (or vectors) of the same dimension $m \times n$, then $A > B$, $A < B$, $A \geq B$, $A \leq B$ have to be intended componentwise ($A_{ij} > B_{ij}$, $A_{ij} < B_{ij}$, $A_{ij} \geq B_{ij}$, $A_{ij} \leq B_{ij}$ for all $1 \leq i \leq m$ and $1 \leq j \leq n$);
- in the space of symmetric matrices, $Q \prec P$, $Q \preceq P$, $Q \succ P$, $Q \succeq P$ denote that $P - Q$ is positive definite, positive semidefinite, negative definite, negative semidefinite (namely, the function $x^\top(P - Q)x$ is positive definite, positive semidefinite, negative definite, negative semidefinite);
- $\|x\|_p$, with integer $1 \leq p < \infty$, denotes the vector p-norm:

$$\|x\|_p = \sqrt[p]{\sum_{i=1}^{n} |x_i|^p}$$

for finite p and

$$\|x\|_\infty = \max_i |x_i|;$$

- if $P \succ 0$ is a symmetric (square) matrix, then $\|x\|_P = \sqrt{x^\top P x}$;
- given any vector norm $\|\cdot\|$, the corresponding induced matrix norm is

$$\|A\| \doteq \sup_{x \neq 0} \frac{\|Ax\|}{\|x\|};$$

[2] A more detailed overview concerning stability of equilibria and related results, including criteria based on eigenvalues, is reported in Appendix C.

- for $x \in \mathbb{R}^n$, the sign and saturation vector functions $\text{sign}(x)$ and $\text{sat}(x)$ (for given bounds $x_i^- \leq x_i \leq x_i^+$) are defined componentwise, respectively, as

$$[\text{sign}(x)]_i \doteq \begin{cases} 1 & \text{if} \quad x_i > 0 \\ 0 & \text{if} \quad x_i = 0 \\ -1 & \text{if} \quad x_i < 0 \end{cases}$$

and

$$[\text{sat}(x)]_i \doteq \begin{cases} x_i^+ & \text{if} \quad x_i > x_i^+ \\ x_i & \text{if} \quad x_i^- \leq x_i \leq x_i^+ \\ x_i^- & \text{if} \quad x_i < x_i^- \end{cases}$$

The following acronyms are also recurrent throughout the thesis.

- DNA: DeoxyriboNucleic Acid
- LMI: Linear Matrix Inequality
- LTI: Linear Time Invariant
- MAK: Mass Action Kinetics
- ODE: Ordinary Differential Equation
- OTI: Oscillatory Transition to Instability
- RNA: RiboNucleic Acid
- RTI: Real Transition to Instability
- TI: Transition to Instability

I

Background and Fundamental Concepts

2

Structural: More Than Robust

A property can be said *structural* for a class of systems (specified by given features that constitute its *structure*) when it is enjoyed by all of the systems in the class.

The structure of a system captures its inherent nature, its essence; hence, a structural property has a necessary connection to the essence of the system under investigation and holds for all of the systems characterised by the same structure (*i.e.*, for all of the systems belonging to the class specified by that structure). Then how is a structure determined, *i.e.*, how is the class of systems specified? This is an important point, especially because the term *structural* is often confused with *robust*, and used to express the same concept, while a crucial distinction should be made.

Usually, the concept of robustness refers to a class of systems expressing the possible deviations of a system from a given "nominal condition"; such deviations may be due to modelling uncertainties or to perturbations, and are assumed to be bounded. Consider, for instance, a parameterised family of systems: if any system of the family exhibits a certain property, for any choice of the parameter values *within given bounds*, then the property is *robust*; conversely, if any system of the family exhibits the property *regardless of the chosen parameter values* (without numerical bounds), then the property is *structural*.

It is therefore apparent that the concept of structural property (which is the key theme of the present chapter) is much more general and much more demanding. It is general, since it can refer not only to a family of *parametric* realisations, but also to a family of *functional* realisations (where the functions are simply required to satisfy some qualitative properties, such as, *e.g.*, monotonicity), or to any family of systems having a common *structure* that may be expressed, for instance, by the topology of an associated graph (as will be seen in Chapter 3). It is demanding, since the satisfaction of a structural property is a strong requirement, difficult to prove.

However, once a property has been proved to be structural for a given class of systems (structural analysis), or once a controller for a class of systems has been built satisfying special constraints based on the corresponding structure (network-decentralised control synthesis), the benefits are considerable. Engineers have been striving for decades to build robust systems, which work even under conditions that vary with respect to the nominal one, while natural systems often preserve some fundamental properties in the most diverse environmental conditions, practically

independent of parameter values: they are "more than robust". To mathematically explain their extraordinary robustness, a structural analysis is needed. Also, in the case of artificial systems, a control strategy often needs to be decided with limited information about the system and its parameters. When the aim is to design a controller that is able to accomplish the desired task with topology-dependent limitations, a network-decentralised approach to synthesis is beneficial.

Adopting a structural viewpoint is as powerful as challenging, and in this thesis the challenge is accepted, focusing in particular on dynamical networks.

2.1 Structural Properties

A property is structural if it is satisfied by all the systems of a family specified by a *structure* without numerical bounds. The following definition [BF11b, BF14] underlines the fundamental difference with respect to the less demanding concept of robust property.

Definition 2.1. *Given a family $\mathcal{F}$ of systems and a (relevant) property $\mathcal{P}$, $\mathcal{P}$ is a* robust property *with respect to $\mathcal{F}$ if any system $f \in \mathcal{F}$ has the property $\mathcal{P}$. $\mathcal{P}$ is a* structural property *if, moreover, the family $\mathcal{F}$ is specified without numerical bounds.*

Example 2.1. *Given the property of Hurwitz stability (a matrix is Hurwitz stable if all of its eigenvalues have negative real part), consider the matrices*

$$M_1 = \begin{bmatrix} -a & b \\ c & -d \end{bmatrix} \quad \textit{and} \quad M_2 = \begin{bmatrix} -a & -b \\ c & -d \end{bmatrix},$$

where a, b, c and d are positive coefficients. If $0 \leq b, c \leq 1$ and $2 \leq a, d \leq 3$, matrix M_1 is robustly Hurwitz stable. *Conversely, matrix M_2 is* structurally Hurwitz stable *(for any choice of positive values a, b, c, d).*

Example 2.2. *In the case of a nonlinear parameterised family, such as*

$$\dot{x}(t) = f(x(t), p), \quad x(t) \in \mathbb{R}^n, \quad x(0) = x_0 \in \mathbb{R}^n, \quad t \geq 0,$$

where $f(\cdot, \cdot)$ is a fixed function and $p = [p_1 \dots p_k]$ is a vector of (constant or time-varying) positive parameters, a property is structural if it holds for any choice of p. Yet, a family is not necessarily defined by resorting to parameters. For instance, the family of systems

$$\dot{x}(t) = f(x(t)), \quad x(t) \in \mathbb{R}^n, \quad x(0) = x_0 \in \mathbb{R}^n, \quad t \geq 0,$$

can be considered, where $f(\cdot)$ belongs to a family $\mathcal{F}_f$ of functions satisfying certain assumptions. Then, a property is structural if it holds for any $f(\cdot) \in \mathcal{F}_f$.

A given system *structure* can be specified into a dynamic *realisation* by choosing specific functions, along with specific parameter values.

2.2 Qualitative Information about Functions

A system structure may be specified by providing qualitative information about the functions involved. Some examples of qualitative specifications for scalar functions ($f : \mathbb{R} \to \mathbb{R}$) are the following. [BF11b]

- **Smoothness**: $f(\cdot)$ is continuous, or continuously differentiable, or of class C^k in general.
- **Positive constant**: $f(\cdot) = k > 0$.
- **Bounded**: $|f(\cdot)| < M$ for a certain constant $M > 0$.
- **Positive bounded**: $0 < f(\cdot) < M$ for a certain constant $M > 0$.
- **Linearity**: $f(\cdot)$ is linear.
- **Strict monotonicity**: $f(\cdot)$ is strictly increasing, or strictly decreasing.
- **Monotonicity**: $f(\cdot)$ is non-decreasing, or non-increasing.
- **Unbounded monotonicity**: $f(\cdot)$ is (strictly) monotonic and asymptotically unbounded.
- **Bounded monotonicity**: $f(\cdot)$ is (strictly) monotonic and asymptotically constant.
- **Exact nullity in an open interval**: $f(\cdot)$ is exactly null below or above a given threshold.
- **Sigmoid**: $f(\cdot) = s(\cdot)$ is sigmoidal, see the cases with $n \geq 2$ in Fig. 2.1 (a); $s(0) = s'(0) = 0$, it is non-decreasing and asymptotically constant ($0 < s(\infty) < \infty$), with a single inflection point (its first derivative has a unique maximum point, $s'(x) \leq s'(\bar{x})$ for some $0 < \bar{x} < \infty$).
- **Complementary sigmoid**: $f(\cdot) = c(\cdot)$ is complementary sigmoidal, see the cases with $n \geq 2$ in Fig. 2.1 (b); $c(x) = s(\infty) - s(x)$, where $s(\cdot)$ is sigmoidal (hence $c(\cdot)$ is non-increasing, $0 < c(0) < \infty$, $c'(0) = 0$, $c(\infty) = 0$ and it has a single inflection point).
- **Cropped sigmoid**: $f(\cdot)$ is a cropped sigmoid, or a cropped complementary sigmoid (examples are shown in Fig. 2.2).
- **Shifted sigmoid**: $f(\cdot)$ is a shifted (cropped) sigmoid or a shifted (cropped) complementary sigmoid (this is obtained by adding a constant to a sigmoidal, or complementary sigmoidal, function).

For more general functions ($f : \mathbb{R}^n \to \mathbb{R}^m$), the above properties can be assumed to hold for single components and with respect to specific arguments. For instance, given the system $\dot{x} = Sf(x) + Rg(x)$, denoting by $f_j(\cdot)$ and $g_j(\cdot)$ the components of the vector functions $f(\cdot)$ and $g(\cdot)$, respectively, in the (scalar) differential equation

$$\dot{x}_i = \sum_{j=1}^{m} \left[s_{ij} f_j(x_1, \ldots, x_n) + r_{ij} g_j(x_1, \ldots, x_n) \right],$$

with $s_{ij}, r_{ij} \geq 0$, the scalar function $f_j(\cdot)$ is assumed to be decreasing in x_i and increasing in the other variables, while $g_j(\cdot)$ is sigmoidal in all of its arguments.

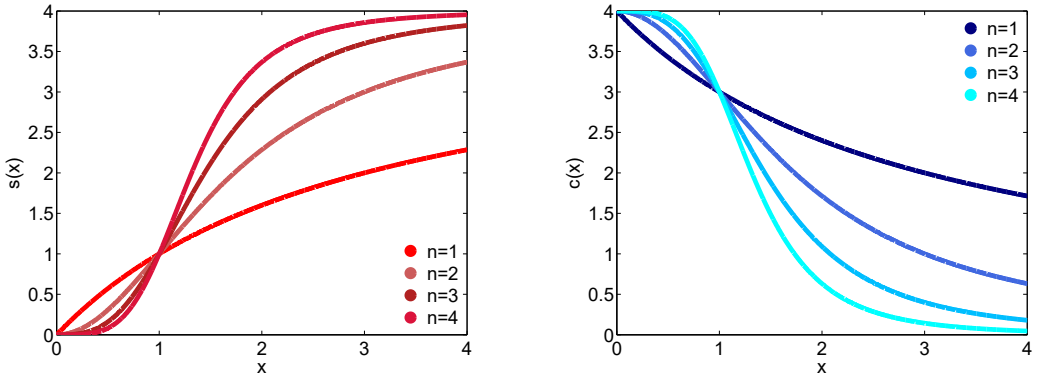

(a) $s(x) = \frac{\alpha x^n}{\beta + x^n}$ (b) $c(x) = \frac{\gamma}{\delta + x^n}$

Figure 2.1: Example of function $s(x) = \frac{\alpha x^n}{\beta + x^n}$, with $\alpha = 4$ and $\beta = 3$, and of function $c(x) = \frac{\gamma}{\delta + x^n}$, with $\gamma = \alpha\beta = 12$ and $\delta = \beta = 3$, for different values of n; note that $s(x) + c(x) = s(\infty) = c(0) = \alpha$. For $n \geq 2$, $s(x)$ is a sigmoidal function, while $c(x)$ is a complementary sigmoidal function.

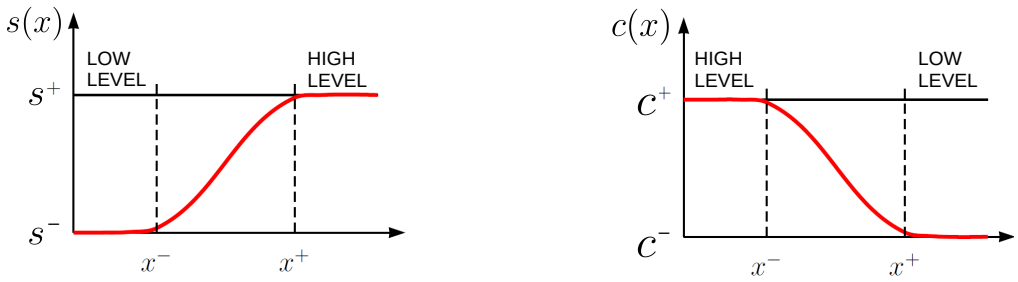

Figure 2.2: Example of a cropped sigmoidal function (left) and of a cropped complementary sigmoidal function (right).

2.3 Properties of Interest

The goal of a structural analysis is to assess the structural properties of a dynamic system. It is often interesting to determine if the system is structurally

- bounded (*i.e.*, the system solution $x(t) = \varphi(t, x(0))$ is bounded for any initial condition $x(0)$ in the assigned domain);
- sign-definite (*i.e.*, its Jacobian matrix has sign-definite entries);
- (mono)stable (*i.e.*, the system admits a unique stable equilibrium, see Fig. 2.3, left);
- bistable (*i.e.*, the system admits three equilibria, of which two are stable and one is unstable, see Fig. 2.3, right), or multistable in general;
- oscillatory (*i.e.*, the system state or output variables exhibit sustained oscillations, see Fig. 2.4);
- monotone (*i.e.*, the evolution operator preserves a given order in the state

space, see Fig. 2.5);
- positive (*i.e.*, the positive orthant is invariant for positive inputs);
- adaptive (*i.e.*, the system initially reacts to an external stimulus, but, after a transient, the original pre-stimulus condition is restored, see Fig. 2.6);
- persistent (*i.e.*, after having received an input and changed its state and output accordingly, the system remains in the new condition also after the stimulus has been suppressed, see Fig. 2.7);
- spiking (*i.e.*, a stimulus produces a strong reaction followed, after some time, by a relaxation, see Fig. 2.8);
- resilient (or robust, *i.e.*, the system can face damages and work properly even under failure of some components, by self-recovering or by successfully adapting to the change in conditions, see Fig. 2.9).

It may also be interesting to determine if the system can structurally exhibit bifurcations (often associated with oscillations or with multistability). Some of the listed properties will be examined more in depth in the following.

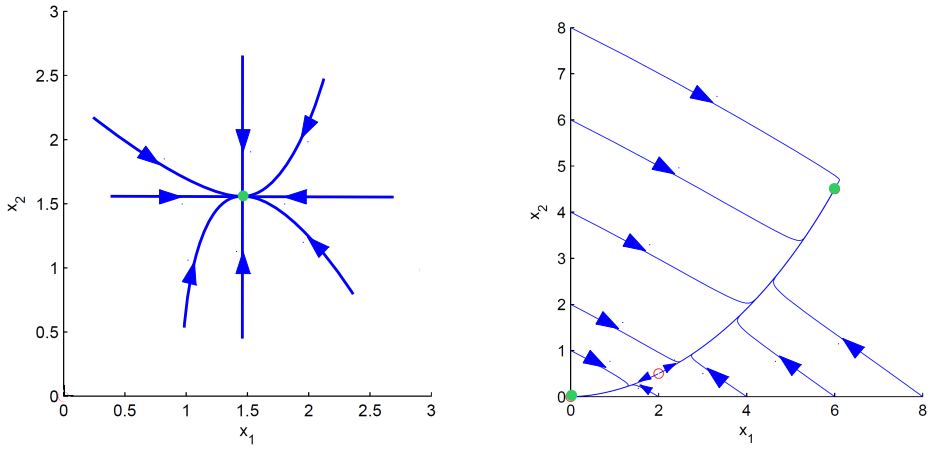

Figure 2.3: A monostable system (left) and a bistable system (right): phase-space portrait. Green dots denote stable equilibria, red circles unstable equilibria; blue curves are trajectories of the system.

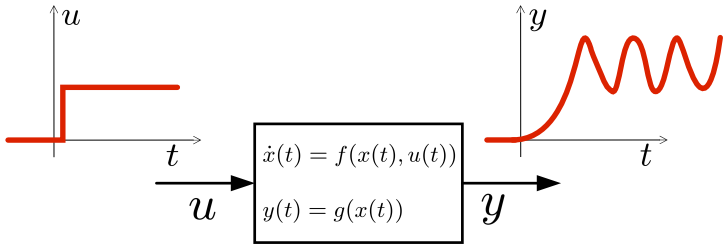

Figure 2.4: An oscillating system.

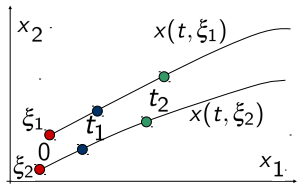

Figure 2.5: Monotone system trajectories: $\xi_1 \geq \xi_2$ implies that $x(t,\xi_1) \geq x(t,\xi_2)$ for all $t \geq 0$.

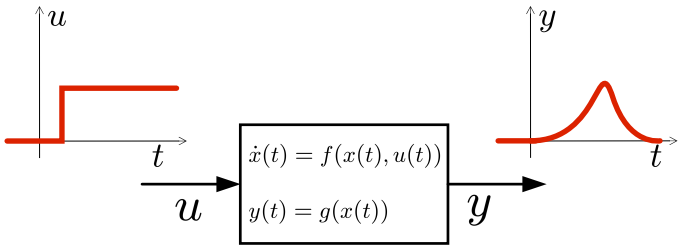

Figure 2.6: An adaptive system.

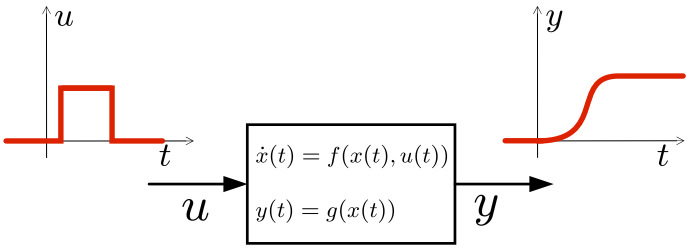

Figure 2.7: A persistent system.

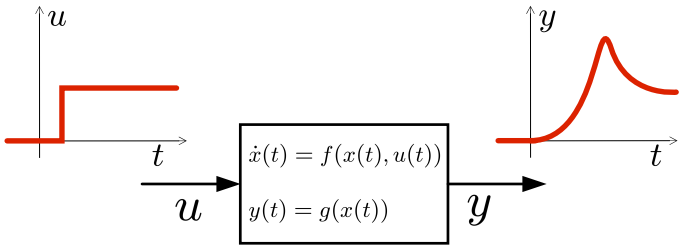

Figure 2.8: A spiking system.

2.3.1 Boundedness

The trajectories are typically bounded in systems where the variables cannot diverge due to physical/natural constraints (*e.g.*, the solutions of biochemical systems are globally bounded due to mass conservation constraints and degradation reactions).

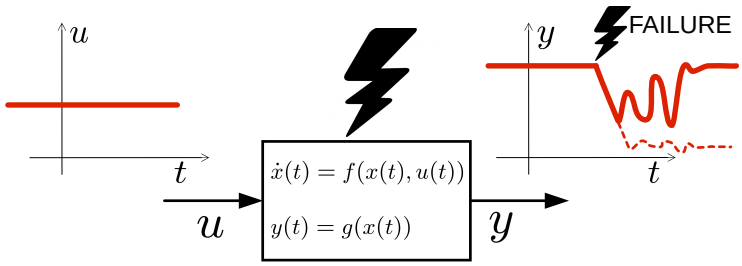

Figure 2.9: A resilient system (contrasted to a non-resilient system, dotted line).

Example 2.3. *A class of systems for which boundedness is assured is*

$$\dot{x}_i = -\alpha_i x_i + \sum_{j=1}^{m} g_{ij}(x), \quad i = 1, \ldots, n \tag{2.1}$$

where $\alpha_i > 0$ and each $g_{ij}(x)$ is a globally bounded function (for instance, a sigmoidal function, either cropped or not). The system has globally bounded solutions, regardless of both the exact expression of the functions $g_{ij}(x)$ and the value of the positive coefficients α_i.

2.3.2 Sign-Definiteness

Given a generic nonlinear system $\dot{x} = f(x)$, where $x \in \mathbb{R}^n$ and $f : \mathbb{R}^n \to \mathbb{R}^n$, the system Jacobian matrix J, $[J]_{ij} = \frac{\partial f_i}{\partial x_j}$, may be sign-definite. This means that its entries (which are functions of the parameters) cannot assume both positive and negative values.

This is an interesting structural property: independent of the chosen functions and parameters, the Jacobian exhibits a given sign pattern. This may happen, for instance, when the functions describing the dynamics of a system are monotonic and appear suitably in the system equations.

Remark 2.1. *A given Jacobian sign pattern may be the structure that identifies a family of systems (cf. Chapter 8).*

Surprisingly, most natural systems have a sign-definite structure.

Example 2.4. Activation/inhibition loops in biochemical systems. *[Son15] In (bio)chemical systems, most of the interactions are either negative (inhibitory) or positive (activating): activation and inhibition, being opposite phenomena, lead to opposite signs in the partial derivatives composing the system Jacobian matrix. Activation and inhibition feedback loops are common structures in large biochemical networks: the simplest examples, involving just two interacting species, are shown in Fig. 2.10.*

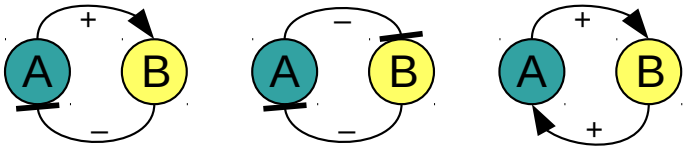

(a) (b) (c)

Figure 2.10: Activation/inhibition feedback loops: (a) activation-inhibition, (b) mutual inhibition, (c) mutual activation. Pointed arrowheads indicate activation, hammer arrowheads indicate inhibition.

Given two interacting chemical species A and B, suppose that the rate of change of A is affected by the concentration of B, and vice versa. *The corresponding dynamical system, modelling the time evolution of the concentrations $a(t)$ of A and $b(t)$ of B, in the presence of a constant mass addition of both, is*

$$\begin{aligned}\dot{a} &= a_0 + f(a,b)\\ \dot{b} &= b_0 + g(a,b).\end{aligned}$$

Then

- *either B is an* activator *of A (for instance, an enzyme that helps catalyse the production of A, or a protein whose presence enhances the expression of the gene that produces A) and then the partial derivative $\frac{\partial f(a,b)}{\partial b}$ is always positive, or at least non-negative;*
- *or B is an inhibitor of A (for instance, an enzyme that helps degrade A, or a protein that represses the gene that produces A), and then $\frac{\partial f(a,b)}{\partial b}$ is always negative, or at least non-positive.*

Similarly, A is either an activator of B, hence $\frac{\partial g(a,b)}{\partial a} \geq 0\,(>0)$, or an inhibitor of B, hence $\frac{\partial g(a,b)}{\partial a} \leq 0\,(<0)$. Also phenomena of auto-activation and auto-inhibition (positive or negative auto-regulation) may occur. However, auto-inhibition (or auto-degradation) is the most common, hence diagonal entries are typically negative.

The Jacobian matrix of the system is therefore always (structurally) sign-definite. Assuming that A is an activator, B is an inhibitor and both species are auto-degrading, the resulting Jacobian sign pattern is

$$sign(J) = sign\left(\begin{bmatrix}\frac{\partial f}{\partial a} & \frac{\partial f}{\partial b}\\ \frac{\partial g}{\partial a} & \frac{\partial g}{\partial b}\end{bmatrix}\right) = \begin{bmatrix}- & -\\ + & -\end{bmatrix}.$$

This is an example of activation-inhibition *loop, as in Fig. 2.10 (a). As usual in the field of control theory, this minimal negative feedback structure guarantees set-point regulation (or homeostasis, as a biologist would call it).*

In the case of mutual inhibition*, each species inhibits the other, as in Fig. 2.10 (b) and the resulting sign pattern of the Jacobian is*

$$sign(J) = \begin{bmatrix} - & - \\ - & - \end{bmatrix}.$$

Such a system can memorise which of the two species was last activated externally, hence enabling "biological memory". In fact, if an external input signal transiently increases the concentration of A over that of B, then A will repress B (which, being at a lower concentration, will not be able to repress A); assuming that A can maintain its high level due to the influence of external variables, the situation will persist until some other external factor allows B to increase over A.

In the case of mutual activation*, each species activates the other, as in Fig. 2.10 (c) and the resulting sign pattern of the Jacobian is*

$$sign(J) = \begin{bmatrix} - & + \\ + & - \end{bmatrix}.$$

If now some external input signal transiently increases the concentration of A over that of B, then B will be activated by A and will, in turn, enhance A even more. Therefore, a sufficiently large external signal applied to either A or B results in a large increase in both species. This minimal positive feedback structure is fundamental in biomolecular systems that amplify signals.

2.3.3 Stability

The stability property is the most studied by control engineers, who are often seeking stabilising controllers for potentially unstable plants. On the contrary, natural systems are often stable. For example, in biochemical systems, species concentrations tend to spontaneously reach a stable steady-state value. Even though biochemical systems are usually stable by their nature, their stability analysis is of interest, especially when it is carried out with a structural approach: in fact, it is important to mathematically prove the property of the model corresponding to the considered system (to check if the model is viable) and to structurally guarantee stability of highly uncertain models for any choice of the functions (provided they satisfy some qualitative requirements) along with their parameters.

Example 2.5. *Matrix*

$$M = \begin{bmatrix} -a & b \\ -c & -d \end{bmatrix},$$

with a, b, c, $d > 0$, *is* structurally Hurwitz stable*, since* $tr(M) = -(a+d) < 0$ *and* $\det(M) = ad + bc > 0$*. Therefore, its eigenvalues have negative real part regardless of the chosen parameter values.*

Example 2.6. *Matrix*

$$M = \begin{bmatrix} a & b \\ -c & d \end{bmatrix},$$

with a, b, c, $d > 0$, *is* structurally unstable, *since* $tr(M) = a + d > 0$ *and* $\det(M) = ad + bc > 0$*: hence, regardless of the chosen parameter values, its eigenvalues have positive real part.*

A brief survey of definitions and results on stability is provided in Appendix C.

2.3.4 Bifurcations

Dynamic phenomena may cause the appearance of sudden discontinuities: a small, smooth change in the value of a parameter may result in a sudden change in the system evolution and in a completely different steady-state behaviour. When chaotic dynamics are present, the dependence on initial conditions is so sensitive that small differences in initial states lead to trajectories that are abruptly diverging, even on finite time intervals. Varying a parameter may change not only the stability properties of a given equilibrium, but also the number of equilibria: when one of these situations occur, the system is said to undergo a *bifurcation*. Bifurcation theory, or bifurcation analysis, allows to study the changes in the qualitative behaviour of the solutions of a family of differential equations describing a dynamical system, due to parameter variations. [Str94, AP95, Kuz98, BV13]

Given the continuous-time dynamical system

$$\dot{x}(t) = f(x(t), p),$$

where $x \in \mathbb{R}^n$ is the system state and the function f is smooth in x and p (a real parameter), an *equilibrium point* or *fixed point* of the system is a constant steady-state solution (a vector $\bar{x}$ such that $f(\bar{x}, p) = 0$); a *periodic solution* of the system is a trajectory $x(t)$ such that $x(t + T) = x(t)$ for a minimum $T > 0$ and $\forall\, t$; an *invariant set* is a set such that any trajectory starting from an initial condition within the set remains in the set $\forall\, t$; an *isolated invariant set* is a bounded invariant set a neighbourhood of which contains no other invariant set. Both equilibrium points and periodic orbits (associated with periodic solutions) are invariant sets. A periodic orbit is called a *limit cycle* if it is isolated. The *positive limit set* of a system is the set of points to which trajectories converge as $t \to \infty$, while the *negative limit set* is the set of points to which trajectories converge as $t \to -\infty$: their union constitutes the *limit set* of the system. An attractor is a bounded invariant set to which trajectories starting from all sufficiently nearby initial conditions converge as $t \to \infty$. A *candidate operating condition* of a system can be defined as any possible steady-state solution of the system, regardless of its stability properties: an equilibrium point, periodic orbit or any other invariant subset of the limit set. [Lev10] A stable candidate operating condition is an actual *operating condition* for the system.

Thus, a *bifurcation* is a change in the number or in the stability properties of candidate operating conditions of a nonlinear system, which occurs when a parameter is varied; the bifurcation is said to occur at the *critical value* (bifurcation point, or bifurcation value) of the *bifurcation parameter*. Bifurcations from a nominal operating condition can only occur at parameter values for which the condition either loses stability or ceases to exist.

Local bifurcations occur in the proximity of an equilibrium point (a small-amplitude limit cycle or a pair of equilibrium points, for instance, can bifurcate from a nominal equilibrium point as the parameter is varied) and are revealed by changes in the local stability properties of equilibria as parameters pass through critical thresholds. A parameter change may cause the stability properties of an equilibrium to change (in continuous-time dynamical systems, this means that the real part of an eigenvalue corresponding to a certain equilibrium point is crossing zero), or may cause the appearance or disappearance of equilibrium points.

If the nominal operating condition of a system is not stable beyond the critical parameter value at which a bifurcation occurs, and a new candidate operating condition emerges from the nominal one at the critical parameter value, then: if the new operating condition is stable and occurs beyond the critical parameter value, the bifurcation is *supercritical* (there is an alternative operating condition near the nominal one), while if the new operating condition is unstable and occurs prior to the critical parameter value, the bifurcation is *subcritical* (the system must leave the vicinity of the nominal operating condition for parameter values beyond the critical one).

Some examples of bifurcations occurring due to a real eigenvalue transitioning through 0 are reported next.

Example 2.7. *A* **saddle-node bifurcation** *occurs when two equilibria (typically one stable, node, and the other unstable, saddle) exist before the bifurcation point, collapse into a single equilibrium at the bifurcation point and disappear afterwards (or the other way round, of course). For instance, as visualised in Fig. 2.11, for the scalar differential equation*

$$\dot{x}(t) = \mu - x(t)^2,$$

with $x(t)$, $\mu \in \mathbb{R}$*: if* $\mu > 0$*, there are two equilibria, one stable* ($\bar{x}_1 = \sqrt{\mu}$) *and the other unstable* ($\bar{x}_2 = -\sqrt{\mu}$)*, being the Jacobian given by the scalar* $-2\bar{x}$*; if* $\mu = 0$*, the two equilibria collide into the only equilibrium* $\bar{x}_0 = 0$ *(non-hyperbolic); if* $\mu < 0$ *there are no equilibria and all the orbits tend to* $-\infty$*.*

Example 2.8. *A* **transcritical bifurcation** *occurs when an equilibrium exists independently of the value of the parameter, another equilibrium exists and collides with the previous one at the bifurcation point. After the collision, they exchange their stability type. For instance, as visualised in Fig. 2.12, for the scalar differential equation*

$$\dot{x}(t) = \mu x(t) + x(t)^2,$$

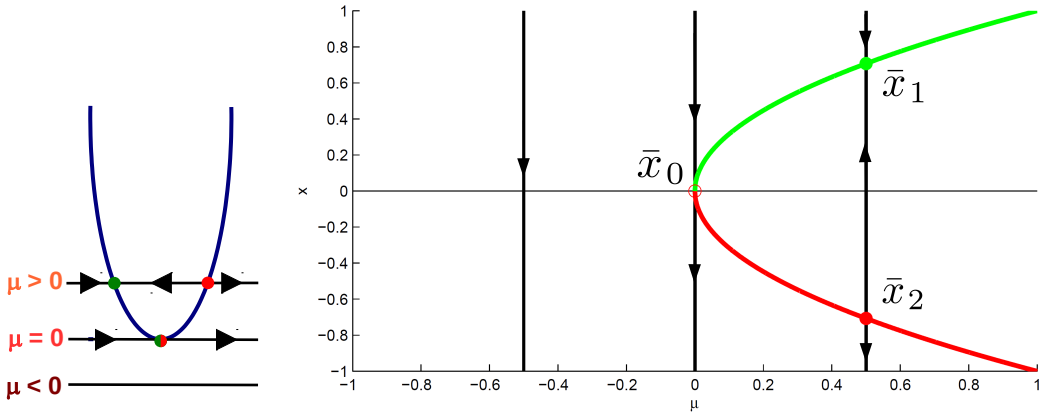

Figure 2.11: The saddle-node bifurcation in Example 2.7: visualisation (left) and corresponding bifurcation diagram (right; stable equilibria are in green, unstable equilibria in red).

with $x(t)$, $\mu \in \mathbb{R}$, the origin is always an equilibrium $\bar{x}_0$ (always existing independently of μ), another equilibrium $\bar{x}_1 = -\mu$ always exists and collides with $\bar{x}_0$ for $\mu = 0$. For $\mu > 0$, $\bar{x}_0$ is unstable and $\bar{x}_1$ is stable, while it is the opposite for $\mu < 0$ (since the Jacobian is $2\bar{x} + \mu$).

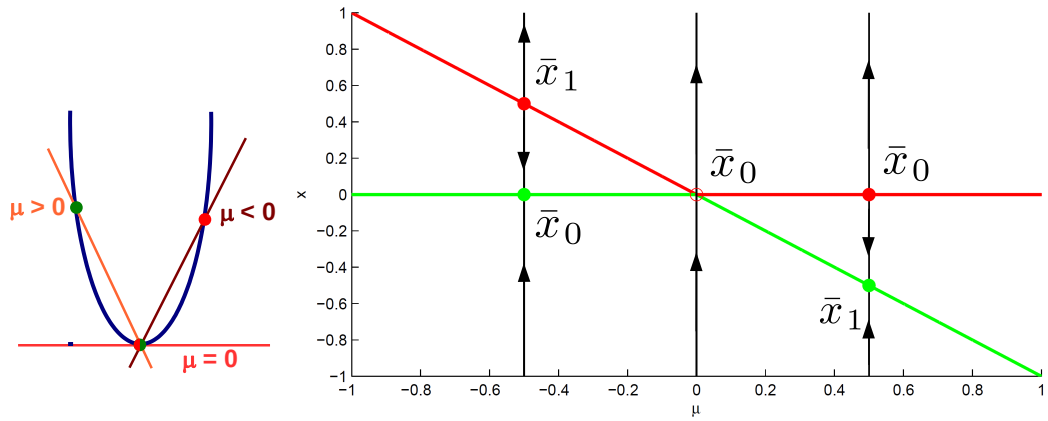

Figure 2.12: The transcritical bifurcation in Example 2.8: visualisation (left) and corresponding bifurcation diagram (right; stable equilibria are in green, unstable equilibria in red).

Example 2.9. *A* **pitchfork bifurcation** *occurs when an equilibrium exists independently of the value of the parameter, while two other equilibria exist on one side of the bifurcation point, both collide with the previous one at the bifurcation point and disappear afterwards. In the process, an exchange of stability type occurs. Systems whose right-hand side is an odd function typically undergo pitchfork bifurcations. For instance, for the scalar differential equation*

$$\dot{x}(t) = \mu x(t) - x(t)^3,$$

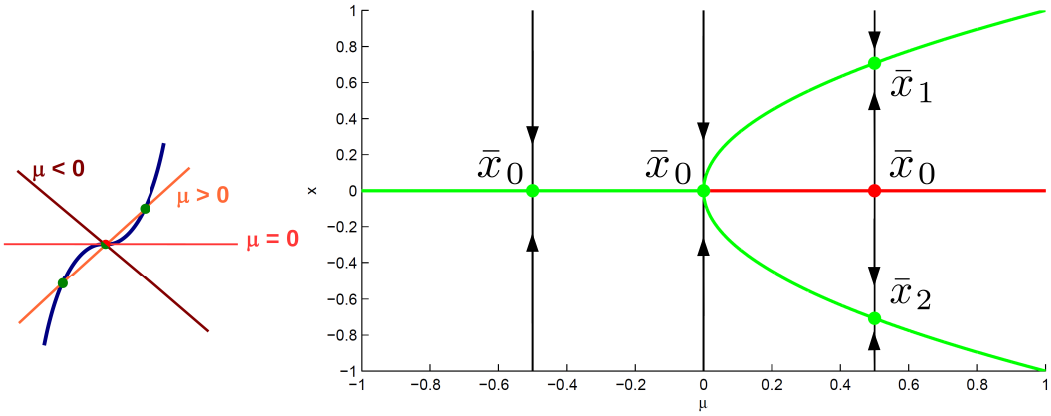

Figure 2.13: The pitchfork bifurcation in Example 2.9: visualisation (left) and corresponding bifurcation diagram (right; stable equilibria are in green, unstable equilibria in red).

with $x(t)$, $\mu \in \mathbb{R}$, $\bar{x}_0 = 0$ *is an equilibrium point* $\forall\ \mu$. *A bifurcation from the origin occurs at* $\mu = 0$, *since* $\bar{x}_0$ *is the only (stable) equilibrium point for* $\mu \leq 0$, *but as* $\mu > 0$ $\bar{x}_0$ *loses stability (because the Jacobian is* $\mu - 3\bar{x}^2$*) and two additional (stable) equilibria appear, at* $\bar{x}_{1,2} = \pm\sqrt{\mu}$, *which bifurcate from the origin at the critical parameter value* $\mu_c = 0$. *This is visualised in Fig. 2.13.*

A **Hopf bifurcation** occurs instead if, as a consequence of parameter variations, the equilibrium point of a dynamical system loses stability due to a pair of complex conjugate eigenvalues of the Jacobian matrix crossing the imaginary axis, while all of the other eigenvalues remain stable (they have a negative real part for all parameter values). A periodic solution locally appears from the equilibrium as the parameter crosses the critical value. In the neighbourhood of a Hopf bifurcation, under generic assumptions, the equilibrium point can generate a small-amplitude limit cycle. A system with a stable limit cycle can exhibit self-sustained oscillations, since trajectories for different initial states converge to the limit cycle and any small perturbation from the closed trajectory causes the system to return to the limit cycle. Hence, a Hopf bifurcation generates a periodic solution because, when the real parts of the eigenvalues are negative, the fixed point is a stable focus; as soon as they cross zero and become positive, the fixed point becomes an unstable focus, with orbits spiraling out. Since this change of stability is local, sufficiently far from the fixed point the phase portrait will be qualitatively unaffected: a periodic orbit will appear where the near and far trajectory flows find a balance. [vdH04]

Here the 2D version of the Hopf bifurcation theorem is reported, which was already known to Andronov around 1930 [AVK66] and suggested by Poincaré [Poi92]; in 1942 Hopf proved the result for arbitrary finite dimensions [Hop42].

Theorem 2.1. *In the two-dimensional case, consider the system*

$$\begin{cases} \dot{x} = f_k(x, y) \\ \dot{y} = g_k(x, y) \end{cases}$$

where k is a parameter. Let (x_0, y_0) be a fixed point of the system, possibly depending on k; the eigenvalues of the linearised system at the fixed point are given by $\lambda(k) = \alpha(k) \pm j\beta(k)$. Suppose that for a certain value of k, $k = k_0$, the following statements hold

- *$\alpha(k_0) = 0$, $\beta(k_0) = \omega \neq 0$ (conjugate pair of purely imaginary eigenvalues), with $sgn(\omega) = sgn\left(\frac{\partial g_k}{\partial x}\right)_{k=k_0}(x_0, y_0)$,*
- *$\left(\frac{d\alpha(k)}{dk}\right)_{k=k_0} = d \neq 0$ (the eigenvalues cross the imaginary axis with nonzero speed),*
- *$\gamma = \frac{1}{16}(f_{xxx} + f_{xyy} + g_{xxy} + g_{yyy}) + \frac{1}{16\omega}(f_{xy}(f_{xx} + f_{yy}) - g_{xy}(g_{xx} + g_{yy}) - f_{xx}g_{xx} + f_{yy}g_{yy}) \neq 0$, with $f_{xy} = \left(\frac{\partial^2 f_k}{\partial x \partial y}\right)_{k=k_0}(x_0, y_0)$ etc.*

Then a unique curve of periodic solutions bifurcates from the origin into the region $k > k_0$ if $\gamma d < 0$ or $k < k_0$ if $\gamma d > 0$. The origin is a stable fixed point for $k > k_0$ (respectively $k < k_0$) and an unstable fixed point for $k < k_0$ (respectively $k > k_0$) if $d < 0$ (respectively $d > 0$); the periodic solutions are stable (respectively unstable) if the origin is unstable (respectively stable) on the side of $k = k_0$ where the periodic solutions exist. The amplitude of the periodic orbits grows like $\sqrt{|k - k_0|}$, while their period tends to $2\pi/|\omega|$ as k tends to k_0. The bifurcation is called supercritical if the bifurcating periodic solutions are stable, subcritical if they are unstable.

Example 2.10. *Consider the equation $\ddot{x} - (k - x^2)\dot{x} + x = 0$, which, if $u = x$, $v = \dot{x}$, can be written as the first-order ODE system*

$$\begin{cases} \dot{u} = v \\ \dot{v} = -u + (k - u^2)v \end{cases}$$

The origin is a fixed point $\forall\, k$, with eigenvalues $\lambda(k) = \frac{k \pm j\sqrt{4-k^2}}{2}$. Therefore, the system has a Hopf bifurcation for $k = 0$: $\omega = -1$, $d = \frac{1}{2}$, $\gamma = \frac{1}{16}(0 + 0 - 2 + 0) = -\frac{1}{8}$; the bifurcation is supercritical and there is a stable limit cycle (isolated periodic orbit) if $k > 0$ for each sufficiently small k.

Example 2.11. *Hopf bifurcations can arise in biological systems: for instance, [WH95, WH96] are about the smallest chemical reaction system with Hopf bifurcation, which has been considered in [KTS08] as well. Hopf bifurcations also occur in the*

system called the Brusselator,[1] *modelling an autocatalytic chemical reaction, in which a chemical species acts to increase the rate of its own producing reaction. The differential equations are*

$$\begin{cases} \dot{x} = 1 - (b+1)x + ax^2y, \\ \dot{y} = bx - ax^2y, \end{cases}$$

where a and b are constant parameters, real and positive. The only equilibrium of the system is $(1, \frac{b}{a})$; the system Jacobian evaluated at the equilibrium is

$$J_{(1,\frac{b}{a})} = \begin{bmatrix} b-1 & a \\ -b & -a \end{bmatrix}.$$

The characteristic polynomial is $s^2 + (1 + a - b)s + a$; because of Descartes' rule of signs, since $a > 0$, if $b < a+1$ the equilibrium is stable (two eigenvalues with negative real part), while if $b > a + 1$ it is unstable (two eigenvalues with positive real part).

For a fixed value of a, as b varies, the equilibrium point undergoes a change in stability. To prove that a Hopf bifurcation is occurring at $b = a + 1$, it suffices to show that

- *the Jacobian eigenvalues are purely imaginary and nonzero when $b = a + 1$: in fact, the solutions of $s^2 + a = 0$ are $s = \pm j\sqrt{a}$*
- *the rate of change of the eigenvalues real part is nonzero when $b = a + 1$: $d = \frac{\partial}{\partial b}\frac{b-a-1}{2} = \frac{1}{2} \neq 0$*
- $\gamma = \frac{(a+1)(a+2)}{4\omega} \neq 0$

Since $\omega = -\sqrt{a}$, then $\gamma < 0$ and the bifurcation is supercritical: a stable limit cycle exists, with approximate period $2\pi/|\omega| = 2\pi/\sqrt{a}$.

2.3.5 Monostability and Bistability

Many simple systems have a unique steady state that is globally asymptotically stable (monostability), but systems with multiple attractors can arise (for instance, from complex interaction between processes that would be globally stable if isolated).

Bistability is a widespread phenomenon in nature, which explains a large number of phenomena, *e.g.*, in cellular functioning (decision-making processes in cell cycle progression, cellular differentiation, apoptosis) and can be generated by a positive feedback loop (as in the mutual activation case in Example 2.4, where A activates B and B activates A) with a very sensitive regulatory step. The principle of bistability underlies as well the operation of several man-made systems, such as mechanical

[1] The model was proposed by Ilya Romanovich Prigogine at the Free University of Brussels, hence the model name.

toggle-switches, flip-flops and memories in digital electronics (bistability is suitable for storing binary data: one stable state can represent a 0 bit and the other a 1 bit).

Consider the system

$$\dot{x} = g(x) - kx,$$

where $x \in \mathbb{R}_+$, $k > 0$ and $g(x) = \frac{\alpha x^n}{\beta + x^n}$ is a hyperbolic function if $n = 1$, a sigmoidal function if $n > 1$.

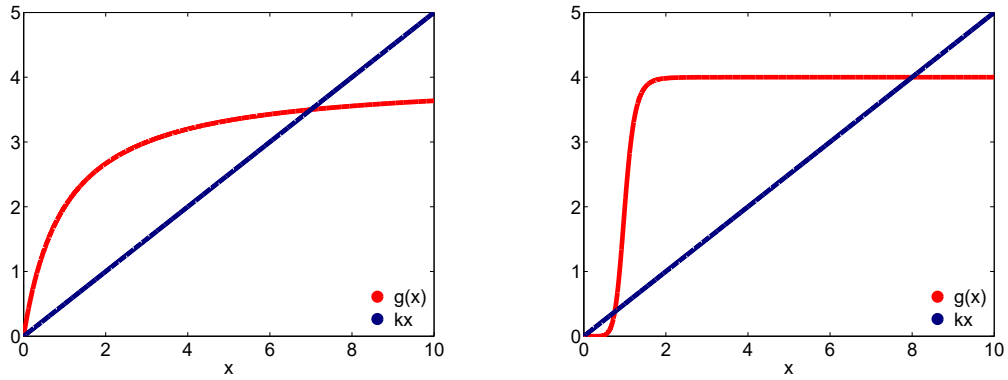

Figure 2.14: Monostability vs. bistability: (a) hyperbolic function ($n = 1$), leading to a single stable equilibrium; (b) sigmoidal function ($n = 8$), generating bistability.

Fig. 2.14 shows the plots of both the terms $g(x)$ and kx, with the choice $\alpha = 4$, $\beta = 1$ and $k = 1/2$, when (a) $n = 1$, and (b) $n = 8$. In the case $n = 1$, the two curves have an intersection at the origin and another with abscissa $\bar{x} = 7$. For $x < \bar{x}$, $g(x) > kx$ (hence $\dot{x} > 0$); for $x > \bar{x}$, $kx > g(x)$ (hence $\dot{x} < 0$). Therefore, $x(t)$ converges to $\bar{x}$, which is the unique stable steady state ($\bar{x}_0 = 0$ is unstable). When $n > 1$, instead, the curves have three intersections, having abscissae $\bar{x}_1 = 0$ and, in the case $n = 8$, $\bar{x}_2 = 0.75$ and $\bar{x}_3 = 8$. For $x < \bar{x}_2$, $kx > g(x)$, hence $x(t)$ converges to zero. For $\bar{x}_2 < x < \bar{x}_3$, $g(x) > kx$ and, for $x > \bar{x}_3$, $kx > g(x)$; hence, in both cases $x(t)$ converges to $\bar{x}_3$. Therefore, when $g(x)$ is sigmoidal, two stable steady states are created, one low and one high, along with an intermediate, unstable state.

Remark 2.2. *Functions of the form $\frac{\alpha x^n}{\beta + x^n}$, along with their complementary functions $\frac{\gamma}{\delta + x^n}$, appear frequently in biochemistry. In the hyperbolic form, $n = 1$, they are called Michaelis-Menten functions (used to model enzyme kinetics, as well as binding of transcriptional activators and repressors); in the sigmoidal form, $n > 1$, they are called Hill functions (where the so-called Hill coefficient n expresses the level of cooperativeness of the ligand binding). [Alo06] It is clear, then, that in biochemical systems a higher cooperativeness level can induce a bistable behaviour.*

The monostable or bistable behaviour depends on the qualitative shape of the curves, determined by the value of n. While a bistable system can be resting in

either of two stable steady states, separated by an unstable state, in a multistable system, more in general, two or more stable steady states are present.

Example 2.12. *The system [Wil09]*

$$\begin{cases} \dot{x}_1 = 2k_1x_2 - k_2x_1^2 - k_3x_1x_2 - k_4x_1 \\ \dot{x}_2 = k_2x_1^2 - k_1x_2 \end{cases}$$

can admit at most three steady states: the trivial $\bar{x}_1^{(1)} = \bar{x}_2^{(1)} = 0$ *and the pair* $\bar{x}_1^{(2,3)} = (k_1 \pm \sqrt{k_1 D})/(2k_3)$, $\bar{x}_2^{(2,3)} = (\bar{x}_1^{(2,3)})^2/k_1$, *where* $D = k_1 - 4k_3k_4$. *For* $D > 0$, *all of the three steady states are real, and the second and third are always positive; at* $D = 0$, *a saddle-node bifurcation occurs and the second and third steady states collapse into a single one, while for* $D < 0$ *just the trivial equilibrium exists. It can be shown that, for* $D > 0$, *the first and third steady states are always stable, while the second is a saddle point (hence, unstable). This system can therefore exhibit bistability. The system phase-space portrait for* $k_1 = 8$, $k_2 = k_3 = 1$, $k_4 = 1.5$, *with the equilibria and some trajectories, is shown in Fig. 2.3, right.*

2.3.6 Oscillations

Building oscillators is crucial to provide timing in man-made systems; for example, all synchronous electronic circuits rely on a "clock" signal (a periodic signal, usually a square wave) to govern their activity. But oscillations are fundamental in everyday life as well, for timing human activities (pendulum clocks work based on the harmonic oscillations of a swinging bar), and can even make life much happier by producing music (stringed musical instruments generate their sound thanks to vibrating strings, woodwinds thanks to the vibrations of an air column, induced by a sharp edge that splits the airstream or by a vibrating reed, or reeds). Oscillations can be produced by external inputs (as happens in the case of a string, or of a reed) or can be self-generated, typically by systems having an unstable equilibrium associated with a pair of complex eigenvalues with non-negative real part (this is the case of oscillators). Periodic biochemical and biophysical rhythms are ubiquitous characteristics of living organisms. Rhythmic phenomena occur at all levels of biological organisation, from unicellular to multicellular organisms, with periods ranging from fractions of seconds to years [Gol97]; a lot of physiological properties show periodic changes almost synchronous to the 24 hours cycle of light and darkness on earth (and are therefore called *circadian rhythms*) [Win80].

The simplest oscillations can arise from two-component networks, such as

$$\begin{cases} \dot{x} = f(x, y), \\ \dot{y} = g(x, y), \end{cases} \tag{2.2}$$

where $x, y \in \mathbb{R}$. Bendixson's negative criterion states that, if $\partial f/\partial x + \partial g/\partial y$ is of constant sign (not identically zero) in a region $\mathcal{D}$ of the (x, y) plane, then there can

be no periodic solution of system (2.2) entirely lying in $\mathcal{D}$. The system (2.2) can have in general one or more steady-state solutions satisfying

$$\begin{cases} 0 = f(\bar{x}, \bar{y}), \\ 0 = g(\bar{x}, \bar{y}). \end{cases}$$

The stability of such steady states is determined by the eigenvalues λ of the Jacobian matrix evaluated at the steady state

$$J_{(\bar{x},\bar{y})} = \begin{bmatrix} (\partial f/\partial x)_{(\bar{x},\bar{y})} & (\partial f/\partial y)_{(\bar{x},\bar{y})} \\ (\partial g/\partial x)_{(\bar{x},\bar{y})} & (\partial g/\partial y)_{(\bar{x},\bar{y})} \end{bmatrix} = \begin{bmatrix} j_{11} & j_{12} \\ j_{21} & j_{22} \end{bmatrix}.$$

The steady state is stable if $\Re(\lambda)$ is negative for both of the eigenvalues of J, namely, the roots of the characteristic equation $\lambda^2 - \mathrm{tr}(J)\lambda + \det(J) = 0$. In view of Descartes' rule of signs:

- if $\det(J) < 0$, then J has one positive and one negative eigenvalue, resulting in a saddle point;
- if $\det(J) > 0$ and $\mathrm{tr}(J) < 0$, the steady state is stable;
- if $\det(J) > 0$ and $\mathrm{tr}(J) > 0$, then there is an unstable node or focus.

Since the trace and determinant of J depend continuously on the parameters, if by varying a parameter k the trace $\mathrm{tr}(J)$ can go from negative to positive values, with $\det(J) > 0$, then the steady state loses stability at $\mathrm{tr}(J) = 0$ (for $k = k_{crit}$). At the *bifurcation point*, $\mathrm{tr}(J) = 0$, the eigenvalues are purely imaginary numbers, $\lambda = \pm j\omega$, $\omega = \sqrt{j_{11}j_{22} - j_{12}j_{21}}$. Close to the bifurcation point, for $k \approx k_{crit}$, small amplitude limit-cycle solutions surround the steady state and the period of oscillation is close to $2\pi/|\omega|$: periodic solutions arise due to a *Hopf bifurcation* at $k = k_{crit}$.

Oscillations often arise due to a Hopf bifurcation, which can occur in a two-component network under some requirements. If both j_{11} and j_{22} are always negative, then $\mathrm{tr}(J)$ never changes sign and a Hopf bifurcation cannot occur (cf. Bendixson's negative criterion): thus, one of them must be positive for some parameter values. If j_{11} and j_{22} are of opposite sign, then j_{12} and j_{21} must also be of opposite sign in order for $\det(J)$ to be positive (otherwise there cannot be a pair of complex eigenvalues). Four characteristic sign patterns of the Jacobian matrix can typically produce Hopf bifurcations in two-dimensional systems:

$$J = \begin{bmatrix} + & + \\ - & - \end{bmatrix}, \qquad \begin{bmatrix} + & - \\ + & - \end{bmatrix}, \qquad \begin{bmatrix} - & + \\ - & + \end{bmatrix}, \qquad \begin{bmatrix} - & - \\ + & + \end{bmatrix}.$$

Example 2.13. Lotka-Volterra model. *[Lot20, Vol26] The system*

$$\begin{cases} \dot{x}_1 = k_1 x_1 - k_2 x_1 x_2 \\ \dot{x}_2 = k_2 x_1 x_2 - k_3 x_2 \end{cases}$$

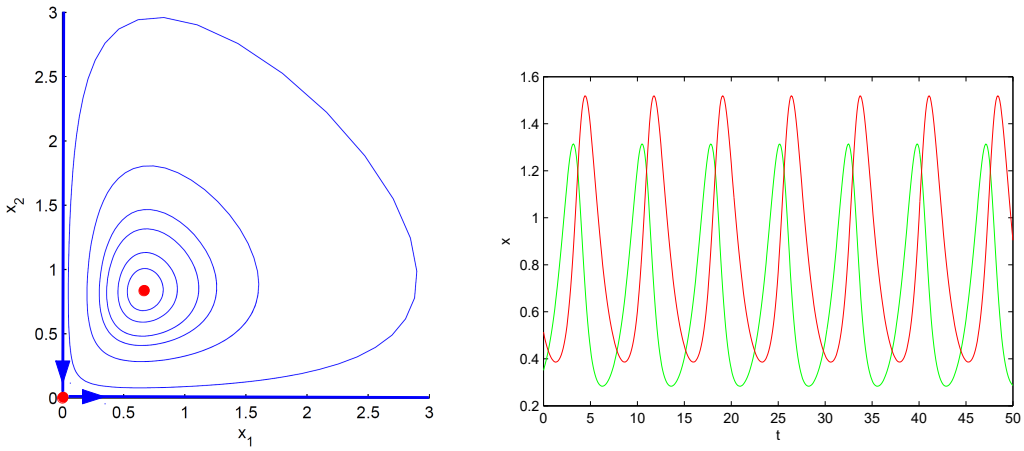

Figure 2.15: Lotka-Volterra oscillator: phase-space portrait (left) and time evolution starting from initial conditions $[0.35\ 0.51]^\top$ (right).

where k_1, k_2, k_3 are positive parameters, admits two equilibria, the trivial $\bar{x}_1 = \bar{x}_2 = 0$ and the positive $\bar{x}_1 = k_3/k_2$, $\bar{x}_2 = k_1/k_2$. The system Jacobian matrix is

$$J = \begin{bmatrix} k_1 - k_2\bar{x}_2 & -k_2\bar{x}_1 \\ k_2\bar{x}_1 & k_2\bar{x}_1 - k_3 \end{bmatrix}.$$

The Jacobian computed at the two equilibrium points is

$$J_{(0,0)} = \begin{bmatrix} k_1 & 0 \\ 0 & -k_3 \end{bmatrix},$$

hence the origin is a saddle-point (unstable), and

$$J_{(k_3/k_2, k_1/k_2)} = \begin{bmatrix} 0 & -k_3 \\ k_1 & 0 \end{bmatrix},$$

which has a pair of purely imaginary complex eigenvalues $s = \pm j\sqrt{k_1 k_3}$, responsible for the onset of oscillations. A phase-space portrait showing the equilibria and some orbits, along with the system time evolution starting from initial conditions $[0.35\ 0.51]^\top$, is reported in Fig. 2.15 for $k_1 = 10$, $k_2 = 12$ and $k_3 = 8$. However, it must be stressed that the oscillatory nature of the positive equilibrium of the system does not depend on the specific choice of parameter values.

Example 2.14. Van der Pol model. *The system*

$$\begin{cases} \dot{x}_1 = x_2 \\ \dot{x}_2 = (1 - x_1^2)x_2 - x_1 \end{cases}$$

only admits the equilibrium $\bar{x}_0$ at the origin, which is unstable (the corresponding Jacobian has two complex conjugate eigenvalues with positive real part). As shown

in Fig. 2.16 (left), the orbits tend to a limit cycle either from infinity or escaping from $\bar{x}_0$. Fig. 2.16 (right) shows instead the time evolution starting from an initial condition lying on the limit cycle: $[-1.45\ 0.819]^\top$.

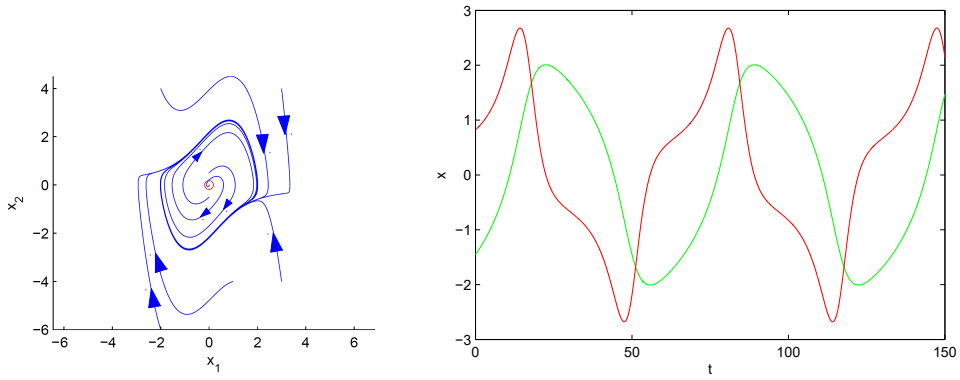

Figure 2.16: Van der Pol oscillator: phase-space portrait (left) and time evolution starting from initial conditions $[-1.45\ 0.819]^\top$ (right).

2.3.7 Monotonicity

Monotone systems [Hir88, Enc05, Son07, Smi08] enjoy remarkable properties that can be exploited to facilitate both the analysis [AS04b, GS07, ADLS06, DLAS07, Son07, AS08, WS08, ADLS10, BT11, BFG15b] and the control [AS03, CF06a] of dynamical systems.

Denote by $x(t) = \varphi(t, \xi)$ the solution at time t of the initial value problem

$$\dot{x}(t) = f(x(t)), \qquad x(0) = \xi,$$

where $f : \mathcal{X} \to \mathbb{R}^n$ is a locally Lipschitz vector field and x takes values in a closed set $\mathcal{X} \subset \mathbb{R}^n$; the solutions are unique and defined for all $t \geq 0$. Assume that a partial order denoted by $\succeq$ is defined on $\mathcal{X}$; a partial order is a binary relation satisfying the following axioms:

- reflexivity: $x \succeq x$, $\forall\, x \in \mathcal{X}$;
- transitivity: $x \succeq y$ and $y \succeq z$ implies $x \succeq z$, $\forall\, x, y, z \in \mathcal{X}$;
- antisymmetry: $x \succeq y$ and $y \succeq x$ implies $x = y$, $\forall\, x, y \in \mathcal{X}$.

Assume also that the defined partial order is closed: if $x(n) \to x$ and $y(n) \to y$ for $n \to \infty$ and $x(n) \succeq y(n)$ for all n, then also $x \succeq y$. Then, the system is monotone if $x(0) \succeq y(0)$ implies $\varphi(t, x(0)) \succeq \varphi(t, y(0))$, $\forall\, t \geq 0$.

In $\mathbb{R}^n$, a possible partial order is that in which $x \succeq y$ if $x_i \geq y_i$ for all $i = 1, \ldots, n$; in general, partial orders associated with any possible orthant in $\mathbb{R}^n$ can be defined.

In fact, a closed partial order relation can be defined by introducing a closed pointed positive convex cone $\mathcal{K} \subset \mathbb{R}^n$ and claiming that $x \succeq y$ if and only if $x - y \in \mathcal{K}$.

Example 2.15. *In $\mathbb{R}^2$, the "northeast" order can be defined as $(\bar{x}, \bar{y}) \geq (x, y)$ iff $\bar{x} \geq x$ and $\bar{y} \geq y$: $(\bar{x}, \bar{y}) - (x, y) = (\bar{x} - x, \bar{y} - y) \in \mathcal{K}_{ne}$, where $\mathcal{K}_{ne} = \{(a, b) : a \geq 0, b \geq 0\}$. Conversely, the "northwest" order is defined as $(\bar{x}, \bar{y}) \geq (x, y)$ iff $\bar{x} \leq x$ and $\bar{y} \geq y$: $(\bar{x}, \bar{y}) - (x, y) = (\bar{x} - x, \bar{y} - y) \in \mathcal{K}_{nw}$, where $\mathcal{K}_{nw} = \{(a, b) : a \leq 0, b \geq 0\}$.*

Formally, a cone $\mathcal{K} \subseteq \mathbb{R}^n$ is a nonempty, convex[2] set that is closed under multiplication by a positive scalar and pointed (*i.e.*, $\mathcal{K} \cap -\mathcal{K} = \{0\}$). Assume also that $\mathcal{K}$ is closed ($\partial\mathcal{K} \subseteq \mathcal{K}$) and has nonempty interior ($\text{int}\mathcal{K} \neq \emptyset$). Then, the cone $\mathcal{K}$ can induce the following order relations in $\mathbb{R}^n$:

- $x \succeq y$ iff $x - y \in \mathcal{K}$,
- $x \succ y$ iff $x \succeq y$ and $x \neq y$,
- $x \succ\succ y$ iff $x - y \in \text{int}\mathcal{K}$.

A signature tuple $(s_1, \ldots, s_n)$, where $s_i = 1$ or -1 $\forall$ i, defines the order $x \geq_s y$ if and only if $s_i x_i \geq s_i y_i$ $\forall$ i. The cones $\mathcal{K}_s = \{x \in \mathbb{R}^n : x \geq_s 0\}$ are denoted as orthant cones; the positive orthant cone, defined by $s = (1, \ldots, 1)$, is also called the cooperative cone. [Enc05]

Example 2.16. *Given the "northeast" order in $\mathbb{R}^n$, associated with the first orthant $\mathcal{K}_{ne} = \mathbb{R}^n_+$: $x \geq y$ means that $x_i \geq y_i$ for all i; $x \gg y$ means that $x_i > y_i$ for all i; $x > y$ means that $x_i \geq y_i$ for all i and, moreover, for at least one component j, $x_j > y_j$.*

A system is therefore monotone if, for all $x \succeq y$ and all $t \geq 0$, $\varphi(t, x) \succeq \varphi(t, y)$; if the partial order $\succeq$ is induced by the positive orthant $\mathcal{K}_{ne} = \mathbb{R}^n_+$, the system is cooperative. A system is strongly monotone if $x \succ y$ implies $\varphi(t, x) \succ\succ \varphi(t, y)$ for all $t > 0$.

When dealing with monotone systems, Metzler matrices are fundamental.

Definition 2.2. *Matrix A is a* Metzler matrix *if it has nonnegative off-diagonal entries: $a_{ij} \geq 0$ for all $i \neq j$.*

A linear system $\dot{x} = Ax$ is:

- monotone if $x_0 \geq y_0$ implies $\varphi(t, x_0) \geq \varphi(t, y_0)$ for all $t \geq 0$, and this is true iff A is a Metzler matrix;
- strongly monotone if $x_0 > y_0$ implies $\varphi(t, x_0) \gg \varphi(t, y_0)$ for all $t > 0$, and this is possible if A is Metzler and irreducible.[3]

[2] A set $\mathcal{C}$ is convex if the line segment between any two points in $\mathcal{C}$ lies in $\mathcal{C}$: for any $x, y \in \mathcal{C}$ and any real ϑ with $0 \leq \vartheta \leq 1$, $\vartheta x + (1 - \vartheta)y \in \mathcal{C}$.

[3] Given matrix $A \in \mathbb{R}^{n \times n}$ and the associated directed graph $\mathcal{G}(A)$ with n nodes, where (i, j) is an arc iff $a_{ji} \neq 0$, A is irreducible if $\mathcal{G}(A)$ is strongly connected (each node can be reached, starting from any other node, by following arcs in the direction in which they point).

Of course, the above concept can be generalised by considering any orthant cone $\mathcal{K}_s$ and the corresponding directions of the componentwise inequalities.

More in general, a nonlinear system is monotone with respect to the partial order induced by a generic orthant cone $\mathcal{K}_s$, in the case of class C^1 vector fields $f(x)$, $x \in \mathcal{X}$, if and only if the Jacobian matrix of the system, possibly after changing sign to some of its row-and-column pairs (according to the signature that defines $\mathcal{K}_s$), is Metzler for all $x \in \mathcal{X}$.

With the additional hypothesis of irreducibility, strongly monotone systems are obtained: for systems strongly monotone with respect to orthants, $x(0) > y(0)$ implies that $x_i(t) > y_i(t)$ for all i. Strongly monotone systems have peculiar dynamical properties: no chaotic dynamics can occur and not even limit cycles can arise.

Input-to-state monotonicity can be defined by considering the system

$$\dot{x} = f(x, u)$$

and assuming that the solution $x(t) = \varphi(t, \xi, u)$ at time t with initial conditions $x(0) = \xi$ is defined for all inputs $u(\cdot)$ and all times $t \geq 0$. Then, the system is *input-to-state monotone* if there are orders in the state and input spaces (corresponding to an assigned signature) such that

$$\xi \geq \tilde{\xi}, \quad u(t) \geq \tilde{u}(t) \, \forall \, t \geq 0 \quad \text{imply} \quad \varphi(t, \xi, u) \geq \varphi(t, \tilde{\xi}, \tilde{u}) \quad \forall \, t \geq 0.$$

It is *input-to-state anti-monotone* if the input has a negative effect on the state:

$$\xi \geq \tilde{\xi}, \quad u(t) \leq \tilde{u}(t) \, \forall \, t \geq 0 \quad \text{imply} \quad \varphi(t, \xi, u) \geq \varphi(t, \tilde{\xi}, \tilde{u}) \quad \forall \, t \geq 0.$$

If an output $y = g(x)$ is present, the system is *input-output monotone* (respectively, *input-output anti-monotone*) if it is *input-to-state monotone* (respectively, *input-to-state anti-monotone*) and, moreover, the output map $g(\cdot)$ preserves the order as well (this means that the components $g_i(\cdot)$ are either monotone non-increasing or monotone non-decreasing functions, depending on the assigned signature that defines an order in the output space).

Monotone systems have well-defined characteristics and constitute a well-behaved set of building blocks for arbitrary systems; moreover, cascades of such systems inherit the same properties. Therefore, interestingly, a system can be analysed by decomposing it as an interconnection of monotone subsystems. [AS04a, DESZ07]

2.3.8 Positivity

Often, for real systems, intuitive physical considerations guarantee the non-negativity of the solutions. In the corresponding mathematical model, non-negative initial conditions (possibly, in the presence of positive input sequences) must generate trajectories that are confined in the non-negative orthant. The fact that a system

naturally has non-negative state variables must be taken into account when designing a controller, not to alter the natural positivity of the system.

Interestingly, in the linear case, positivity is equivalent to monotonicity: both properties hold iff the state matrix is Metzler (in the continuous-time case; non-negative in the discrete-time case).

In the nonlinear case, conversely, there are positive systems that are not monotone, and monotone systems that are not positive (examples are provided in [BCV15]). For instance, in dimension 1 each system $\dot{x} = f(x)$, with regular f, is monotone, but it is not necessarily positive; any chemical reaction network is positive, but it is not monotone in general. However, the fact that a monotone nonlinear system, under mild smoothness assumptions, has a Jacobian matrix that is Metzler, when evaluated at any equilibrium point, corresponds to local positivity of the linearised system.

2.3.9 Perfect Adaptation

The insensitivity of system properties to parameter variations and uncertainties in the components, as well as in the environment, is essential for both biological and man-made systems. Adaptation and compensation mechanisms are needed to preserve the system functionality in spite of changing conditions and persistent external perturbations. A system is adaptive if its output initially responds to a stimulus, but then, after a transient response, returns to the pre-stimulus value even though the stimulus persists. If the output converges exactly to the pre-stimulus level, adaptation is called perfect, while it is called partial if the output only returns close to, but not exactly to, the pre-stimulus level.

It is worth pointing out that the word *adaptive* is used with a completely different meaning in control theory, where a control system is called adaptive if it automatically changes its parameters, depending on those of the controlled system, in order to assure a certain property.

Interesting examples of perfect adaptation in nature are offered by bacterial chemotaxis [BL97, SPO97, ASBL99], eukaryotic gradient sensing [LI02] and yeast osmoregulation [MGUMvO09]. Efforts have been made to determine motifs that can achieve perfect adaptation [MTES$^+$09] and to design biomolecular network modifications that enable perfect adaptation [WSA12]. Perfect adaptation obeys the internal model principle [Son03] and is equivalent to the presence of integral feedback [YHSD00] and of zeros at the origin in the system transfer function [DUR08].

In fact, perfect adaptation (seen as a robust property, due to the interconnection structure and independent of parameter values) can be formulated in terms of integral feedback control. The standard solution to develop a system that robustly tracks a desired steady-state output value, or function, is a control scheme that feeds back to the system the time integral of the system error (the difference between the actual and the desired output), as shown in Fig. 2.17: if the closed loop system is stable, the steady-state error is driven to zero regardless of perturbations in the input or in

the parameters. Any equally robust solution leading to zero steady-state error (and, thus, perfect adaptation) must be equivalent to integral control. [YHSD00]

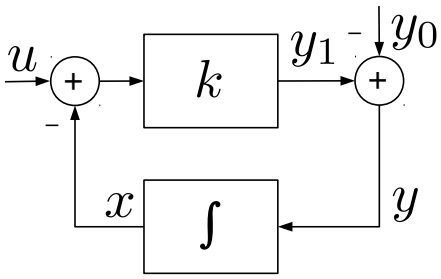

Figure 2.17: Integral feedback control. A process with gain k has input u; the difference between the actual output y_1 and the desired steady-state output y_0 (a constant) gives the error y, whose time integral x is fed back into the system: $\dot{x} = y$, $y = y_1 - y_0 = k(u - x) - y_0$. Provided that $k > 0$, $y \to 0$ as $t \to \infty$ because at steady-state $\dot{x} = y = 0$.

Consider an asymptotically stable linear time invariant (LTI) system

$$\begin{cases} \dot{x} = Ax + Bu, \\ y = Cx + Du, \end{cases}$$

where $x \in \mathbb{R}^n$ is the state vector, $u \in \mathbb{R}$ is the input, $y \in \mathbb{R}$ the output and $A \in \mathbb{R}^{n \times n}$, $B \in \mathbb{R}^{n \times 1}$, $C \in \mathbb{R}^{1 \times n}$, $D \in \mathbb{R}$, with all the eigenvalues λ_i of matrix A having $\Re(\lambda_i) < 0$, $i = 1, \ldots, n$. At steady state ($\dot{x} = 0$), $y = (D - CA^{-1}B)u$. For all constant input values u (neglecting the trivial case in which $[C \quad D] = 0$), $y = 0$ if and only if

$$\det \begin{bmatrix} A & B \\ C & D \end{bmatrix} = 0.$$

Therefore, a LTI dynamical system has perfect adaptation if and only if its transfer function has a zero at the origin. This condition is satisfied if and only if there exists a constant row vector $k \in \mathbb{R}^n$, $k \neq 0$ such that $k[A \quad B] = [C \quad D]$ (the matrix rows are not linearly independent). Hence, if $z = kx$, then $\dot{z} = k\dot{x} = k(Ax + Bu) = Cx + Du = y$. The condition $\dot{z} = y$ means that integral feedback control is an inherent property of the system; this is proved to be equivalent to robust perfect adaptation.

In the case of a nonlinear system, if the system has robust perfect adaptation, then its linearisation around the equilibrium point must have perfect adaptation. Hence, robust perfect adaptation reveals that an integral control is embedded in the system.

Consider a nonlinear system of the form

$$\begin{cases} \dot{x} = Ag(x) + Bu, \\ y = Cx + Du, \end{cases}$$

admitting an asymptotically stable equilibrium point $(\bar{x}, \bar{u})$. To check if the system has perfect adaptation, a constant perturbation on the input, with respect to the equilibrium input value, must be introduced. To determine if, after a transient, the system responds by returning to the equilibrium value prior to the perturbation, consider the linearised system around the equilibrium point,

$$\begin{cases} \dot{z} = Jz + Bv, \\ w = Cz + Dv, \end{cases}$$

where $z = x - \bar{x}$, $v = u - \bar{u}$ and J is the system Jacobian matrix. The perfect adaptation condition is equivalent to requiring that

$$\det \begin{bmatrix} J & B \\ C & D \end{bmatrix} = 0,$$

with the additional condition $\det J \neq 0$, which is assured by the asymptotic stability of the equilibrium point.

Example 2.17. *The system*

$$\dot{x} = \begin{bmatrix} a & b \\ c & d \end{bmatrix} x + \begin{bmatrix} g \\ 0 \end{bmatrix} u = Ax + Bu,$$

$$y = \begin{bmatrix} nc & nd \end{bmatrix} x = Cx,$$

with A stable (and $D = 0$), is structurally perfectly adaptive*, since*

$$\det \begin{bmatrix} a & b & g \\ c & d & 0 \\ nc & nd & 0 \end{bmatrix} = \det \begin{bmatrix} A & B \\ C & D \end{bmatrix} = 0,$$

regardless of the chosen parameter values.

3

Dynamical Networks

Dynamical networks are composed of a finite number of subsystems, each possibly having its own dynamics, interconnected by suitable interactions (which can be seen as generalised "flows"). Complex networks of interacting components, ranging from technological to natural networks, are ubiquitous in every aspect of daily life. Hence, a wide variety of real systems can be modelled in a dynamical-network framework [BBV08, ME10, RC10, Bar12], for instance:

- chemical and biochemical processes (gene regulatory networks, signalling pathways, metabolic networks) [Lot20, Fei87, Fei95a, Fei95b, CF05, Alo06, CF06b, Cha06, MC08, CWLA05, DK09, IA10, CB11, DVM14];
- biological and ecological systems [Vol26, Lev68, May74, Lev75, PL85, DLR03, DLLR03, EK05, DLR05, DRJ07, DGR$^+$09, MDJ$^+$11];
- economical networks, social networks and opinion dynamics [FJ99, EK10, FIA11, Alt12, CF12, DCB12, Alt13, ACFO13, FRTI13, MJB14, VFFO14, AL15, JMFB15, FIRT15, Fri15, RFTI15, BCGV15, BCGV16];
- consensus and synchronisation systems [OSM04, BGP06, OSFM07, RBA07, CFSZ08]; [SWX08, SAS10, CCSZ11, CZ14];
- flow networks [AZ07, OnZ07, BBP10, WvdS13a, WvdS13b, DBO$^+$13, BP15];
- water distribution networks [LK69, BBGP13];
- inventory management and production-distribution systems [SP85, BYZ95, BRU97, BMU00, BT06, SPTK08, BBP10, BPA15];
- power networks and smart grids [IA09, Far10, SHPB12];
- transportation networks [AI98, MOnL08];
- traffic and congestion management systems [Ift96, Ift99];
- vehicle platooning and formation flight of aircrafts [RI96, WCS96, AR98, D'A98, RBA07, SH07, PTB03];
- telecommunication and data communication networks [MS82, MP95, EV89, ID90, ID02]; ...

This chapter presents the distinctive features of dynamical networks, along with the graph representation that constitutes an effective visual representation of the *structure* of a dynamical network. The structural approach discussed in Chapter 2 is specialised to the case of dynamical networks, exploiting their special characteristics for both structural analysis and network-decentralised control synthesis.

3.1 Local Interactions, Global Behaviour

Dynamical networks can be seen as a generalisation of the concept of *compartmental system*. Compartmental systems [God83, JS93], first arisen in a biological and physical context (with applications to physiology, pharmacokinetics, metabolism, epidemiology, ecology, *etc.*), are fundamental both

- for the dynamic modelling of processes that are subject to conservation laws (such as mass balance) in various fields [Jac72, And83, KKA84];
- for the formulation of flow and congestion control problems [BG06, HHB06].

A compartmental system is the ensemble of a finite number of compartments (individual units, corresponding to amounts of homogeneous material) interconnected by flows of material. The compartments may either occupy different physical spaces (so that the flow between compartments corresponds to moving material between different physical locations) or the same physical space (so that the exchange of material between compartments corresponds to the transformation of one substance into another). Compartmental systems have some fundamental properties.

- Transfer flows connect at most two compartments.
- Proper "mass" conservation constraints hold for material transfers between compartments and from/to the external environment. Denoting by x the state vector associated with the ensamble of compartments (where each state variable is the amount of material in the corresponding compartment), the total "mass" $\bar{1}^\top x$ is preserved in the absence of connections with the external environment, *i.e.*, for a closed system; conversely, in the presence of exchanges with the external environment, the total mass variation $\bar{1}^\top \dot{x}$ corresponds to the difference between the sum of inflows and the sum of outflows.
- The state variables must be non-negative, since they represent the quantity of material in each compartment. Hence, compartmental systems are positive systems: the non-negative orthant is forward invariant, and forward controlled-invariant for any non-negative input sequence [FR00, BF02].
- Compartmental systems are monotone [AS03, CF06a, Smi08].

Dynamical networks are not necessarily positive systems and do not need to include mass conservation constraints. Moreover, while flows in compartmental systems require interactions between at most two compartments, for dynamical networks each "flow" can result from interactions among more than two subsystems.

The distinctive feature of dynamical networks is that the interactions occur locally, since flows involve a subset of the subsystems only; however, *local events have global consequences*, since they determine the behaviour of the overall system. It is therefore interesting to study:

[**A**] [**Analysis**] how the global behaviour is affected by the local interactions (analysis) and, in particular, by their "structure" (structural analysis);

[C] [**Control Synthesis**] how a desired global behaviour can be obtained by deciding the local interactions, given their "structure" (control synthesis), possibly under constraints depending on the "structure" itself (structural control synthesis).

To understand more precisely what a structure is, in the special case of dynamical networks, their graph representation needs to be introduced.

3.1.1 Graph Representation and Structure

A *graph* $\mathcal{G}$ is constituted by a set of *nodes* and a set of *arcs* connecting pairwise the nodes, as in Fig. 3.1, left. More formally, a graph is defined as the ordered pair $\mathcal{G} = (\mathcal{N}, \mathcal{A})$, where:

- the nodes are the elements of the set $\mathcal{N} = \{1, 2, \ldots, n\}$, whose cardinality $|\mathcal{N}| = n$ is the *order* of the graph;
- the arcs are the elements of the set $\mathcal{A}$, which is a 2-element subset of $\mathcal{N}$, $\mathcal{A} \subseteq \{\{n_1, n_2\} : n_1, n_2 \in \mathcal{N}\}$, and whose cardinality $|\mathcal{A}|$ is the *size* of the graph. Note that, for *directed* graphs (with *directed* arcs), the set $\mathcal{A}$ is composed of *ordered* pairs of nodes (n_i, n_j), such that $(n_i, n_j) \neq (n_j, n_i)$.

If, conversely, the elements of $\mathcal{A}$ are subsets of $\mathcal{N}$ each including a number of elements between 2 and $|\mathcal{N}|$ (not necessarily the same for all of the elements of $\mathcal{A}$), then $\mathcal{A}$ is said to be the set of the hyperarcs and the resulting pair $\mathcal{G} = (\mathcal{N}, \mathcal{A})$ is called a hypergraph (see Fig. 3.1, right). Some fundamental concepts of graph theory will be summarised in Section 4.1.

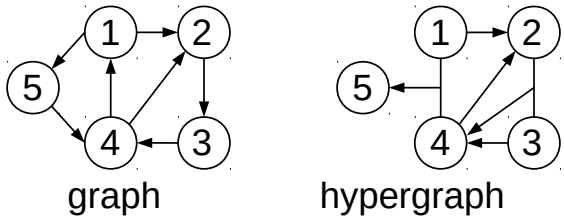

Figure 3.1: A graph of size 7 (left) and of a hypergraph of size 5 (right), both having order 5.

All dynamical networks admit a graph (or, more in general, a hypergraph) representation, in which nodes represent subsystems and arcs represent flows, or interactions. A graph *strictu senso* can be associated with compartmental system, where flows always require the interaction of at most two compartments. In the more general case of dynamical networks, it may be necessary to resort to a hypergraph, since interactions can involve more than two subsystems and are then associated with hyperarcs. For the sake of simplicity in the exposition, however, hypergraphs and hyperarcs will be often referred as graphs and arcs.

In general, in the considered dynamical networks, interactions with entities that are external to the system may occur as well. In this case, also arcs involving just one node can be considered, as in Fig. 3.2, to represent a connection with the "external environment". External connections may be seen as connections between a node of the graph and a fictitious node (node 0) representing the external environment.

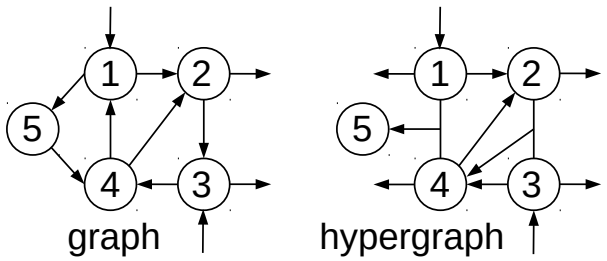

Figure 3.2: An example of a graph (left) and of a hypergraph (right) with external connections.

Which is, then, the structure of a dynamical network?
A thorough description of a dynamical network is provided by three basic elements:

- the *interaction topology*, corresponding to the associated graph;
- the *internal dynamics* of the subsystems (describing the inner, spontaneous behaviour that each subsystem-node would exhibit if isolated from the rest of the system-graph);
- the *interaction functions* (functional expressions associated with the connections-arcs in the graph).

The precise knowledge of internal node dynamics and of interaction functions is not fundamental for describing the essence of a dynamical network. The most essential component is clearly the first: to obtain a *structural representation* of a dynamical network, the nodes and the arcs can be seen just as "black-boxes" (which can be possibly required to satisfy some qualitative properties), while the topology of the interconnections among the nodes in the graph needs to be known exactly. Therefore, the structure of a dynamical network is the corresponding graph, along with possible qualitative requirements on the subsystem dynamics and on the interaction functions.

It is worth stressing that the graph can be associated with a matrix that fully describes its interconnection topology: the incidence matrix B, whose rows are associated with nodes and whose columns are associated with arcs (of course, its rows and its columns can be arbitrarily permuted, by assigning a different order to nodes and arcs). Each entry b_{ij} of matrix B is 1 if the jth arc enters node i, -1 if it leaves node i and 0 otherwise. This means that, for proper graphs (not externally connected), matrix B has zero-sum columns; this is not true in general for hypergraphs and for externally connected graphs.

For instance, the incidence matrices associated with the graph and hypergraph shown in Fig. 3.1 are, respectively,

$$B_{\mathcal{G}} = \begin{bmatrix} -1 & 0 & 0 & 1 & 0 & -1 & 0 \\ 1 & -1 & 0 & 0 & 1 & 0 & 0 \\ 0 & 1 & -1 & 0 & 0 & 0 & 0 \\ 0 & 0 & 1 & -1 & -1 & 0 & 1 \\ 0 & 0 & 0 & 0 & 0 & 1 & -1 \end{bmatrix}, \qquad B_{\mathcal{H}} = \begin{bmatrix} -1 & 0 & 0 & -1 & 0 \\ 1 & -1 & 0 & 0 & 1 \\ 0 & -1 & -1 & 0 & 0 \\ 0 & 1 & 1 & -1 & -1 \\ 0 & 0 & 0 & 1 & 0 \end{bmatrix}.$$

Hence, in the following, a graph (hypergraph) will be formally associated with its incidence matrix, which is an equivalent description of the graph structure.

3.2 A Twofold Goal

Analysis and control synthesis for dynamical networks are needed in different situations.

- **[A]** The interaction topology is *fixed*, the internal dynamics of the subsystems are *fixed* and the interaction functions are *fixed* as well; then, the aim is to investigate how the local interactions produce the global behaviour.
- **[C]** The interaction topology is *fixed*, the internal dynamics of the subsystems are *fixed*, but the interaction functions *can be decided*; the aim is then to choose the local interactions so as to produce the desired global behaviour. Even though the control strategy is decided locally, the goal is to govern the dynamics of the whole system.

Also, the two approaches of analysis and synthesis are especially meant for

- **[A]** natural systems (this is the domain of *system theory* applied to the natural world, recently capturing a strong interest under the name of *systems biology*, which aims at understanding the design principles underlying the functioning of biological systems, based on system-theoretical tools and techniques);
- **[C]** man-made systems (this is the broad realm of engineering, and *control theory*).

Analysis and synthesis are far from being disjoint: they have a tight bond, since

- engineers can learn from nature when designing control strategies (and most often natural systems are organised as dynamical networks in which the global behaviour is determined by the sum of a huge number of local interactions);
- local interactions can be engineered in natural systems that spontaneously exhibit a dynamical network structure (such as chemical and biochemical reaction networks and biomolecular systems, where interactions among species or molecules occur locally and then produce a global behaviour: complex metabolic networks and pathways) so as to obtain the desired global behaviour.

Nature has developed effective strategies to deal with highly complex dynamical networks, ensuring an extremely robust and reliable behaviour, in spite of severe uncertainties, intrinsic noise and environmental fluctuations. Conversely, engineers often experience difficulties in controlling much simpler artificial networks. Both natural and artificial networks face the same needs and challenges: for instance, in the most diverse external conditions, living organisms preserve a sturdy and resilient functioning, thanks to the adjusted regulation provided by enzymes; and power networks and smart grids, with dynamically changing loads and connections, should exhibit the same efficiency and promptness. To reach this goal, can engineers unravel and then adopt nature's strategy? There are many examples of biologically-inspired design of dynamical networks: for instance, agents can be coordinated by mimicking collective animal behaviour such as flocking, swarming, shoaling, as shown in Fig. 3.3 (this is the approach of the so-called *swarm robotics* [BFBD13]); the optimal disposition of wind turbines in a wind farm can be decided inspired by fish schooling [WLD10]; formation flight of aircraft can mimic bird flocking [AR98, PTB03]. Engineering local biochemical interactions to design from the bottom-up new large scale biological circuits with specific functionalities is the main goal of *synthetic biology*, which aims at building complex functional biomolecular systems made of simple components, as complex computational systems are built made of nanometric silicon devices (the analogy is illustrated in Fig. 3.4) [End05, DWS07, Alo06, Alo07a, EL00, KWW06, KW11, FFK$^+$11, FGFM14]. Suitable microscopic shapes and machines can also be built by engineering interactions at the molecular level, as shown in Fig. 3.5 [ABY$^+$10, DBC12].

On the one hand, studying, analysing and modelling the interactions among the bricks that compose and sustain life and among living creatures in nature is interesting *per se*. On the other hand, once an insight has been gained into the basic functioning of nature, it is much easier to imitate it in order to both (i) build artificial systems having the same astounding efficiency and resilience, and (ii) forge new biomolecular circuits with the desired behaviour (and it must not be forgotten that designing artificial biological systems and synthetic biochemical circuits can help a deeper understanding of natural biological design [MvO09]).

Therefore, analysis and synthesis are not only complementary facets of the same approach, but can also aid and streamline each other in a virtuous circle.

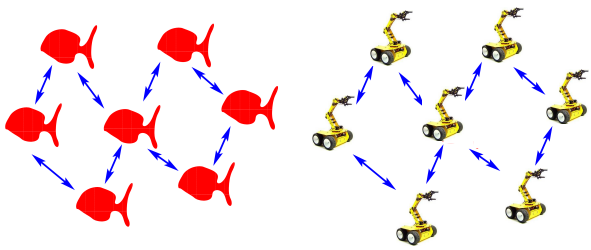

Figure 3.3: Robotic agents can be coordinated, for example, by mimicking a shoal of fish.

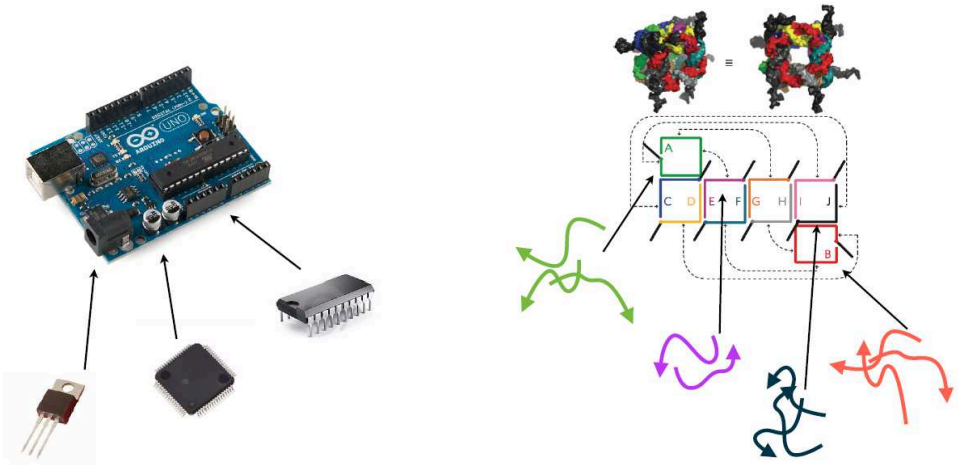

(a) Industrial assembly. (b) Molecular assembly.

Figure 3.4: Analogy between industrial and molecular assembly: (a) electronic components as sub-blocks of a computational system, ©Arduino microcontroller; (b) biochemical components as sub-blocks of cubic RNA-based scaffolds, [ABY+10].

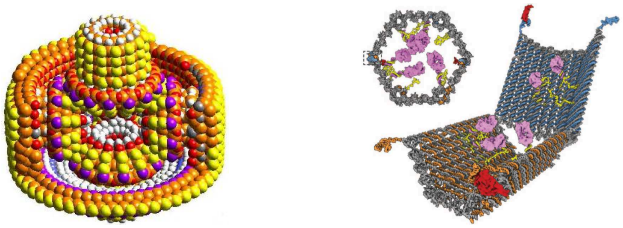

(a) Molecular gear. (b) DNA box.

Figure 3.5: Molecular machines: (a) molecular differential gear, ©1997 Institute for Molecular Manufacturing; (b) DNA box for targeted transport of molecular payloads [DBC12].

Recall now the distinction made above between *fixed* (in the case of analysis) and *decidable* (in the case of control synthesis) features. Of course a quantity, or function, that is *fixed* is not necessarily *known*; it simply cannot be changed or decided. Often, what is fixed is completely *unknown*, or only partially known. In the case of dynamical networks, the internal node dynamics and the interaction functions are unknown or *uncertain* in most cases. Hence, a *structural approach* to the analysis of dynamical networks is beneficial: the properties and behaviours of a dynamical network are assessed based on its structure only, independent of precise parameter values and functional expressions. Conversely, what can be decided is (obviously) always known. Yet, the choice can be subject to restrictions, due to constraints that need to be satisfied. Whenever these *constraints depend on the interconnection topology* of the dynamical network, hence on its structure, a structural approach to the control of dynamical networks is beneficial to govern the dynamics of the whole

systems by means of local agents with structurally restricted information.

Structural analysis aims at studying phenomena and behaviours based exclusively on the intrinsic nature (*i.e.*, the structure) of the system under consideration. A structural approach to the analysis of dynamical networks:

- [**local interactions structure**] takes into account exclusively the structure (essentially, the graph topology along with qualitative properties) of the local interactions among subsystems;
- [**parameter-free**] is *independent of parameter* values;
- [**global behaviour**] aims at explaining robustness and characteristic behaviours of the global system.

Structural analysis of dynamical networks will be dealt with in Part II.

When the system is controlled or coordinated by agents making their decisions based on restricted information, the restriction is likely to depend on the topology of the interactions (the system structure). Then, the control strategy must be such that:

- [**local interactions**] a control agent is associated with each arc of the graph, allowing local interactions to be decided;
- [**local structure-based information**] local interactions are decided based on local information only (the meaning of *local* depends on the graph topology);
- [**global behaviour**] the aim is to control or coordinate the global system behaviour.

In Part III, the concept of *network-decentralised control* will be introduced: a control is network-decentralised if each control agent, associated with an arc of the graph, decides its strategy exclusively based on information about the subsystems associated with the nodes it interconnects.

4

Essential Mathematical Concepts and Results

This chapter presents some indispensable mathematical concepts, outlines some fundamental theories and provides essential results that will be useful throughout the thesis.

4.1 Graph Theory

As seen in Chapter 3, a *graph* is described by the ordered pair $\mathcal{G} = (\mathcal{N}, \mathcal{A})$, where $\mathcal{N} = \{1, 2, \ldots, n\}$ is a set of *nodes* (whose cardinality $|\mathcal{N}| = n$ is the *order* of the graph) and $\mathcal{A} \subseteq \{\{n_1, n_2\} : n_1, n_2 \in \mathcal{N}\}$ is a set of *arcs* connecting pairwise the nodes (whose cardinality $|\mathcal{A}| = m$ is the *size* of the graph); an example is shown in Fig. 4.1. Hypergraphs are graphs in which each arc (denoted as hyperarc) can connect more than two nodes. Two nodes of a graph are *adjacent* if they are connected by an arc.

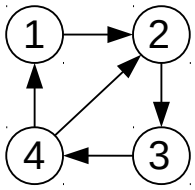

Figure 4.1: An example of a graph of size 5 and order 4.

A graph $\mathcal{G}_s = (\mathcal{N}_s, \mathcal{A}_s)$ is a *subgraph* of $\mathcal{G} = (\mathcal{N}, \mathcal{A})$ if $\mathcal{N}_s \subseteq \mathcal{N}$ and $\mathcal{A}_s \subseteq \mathcal{A}$ (all of the nodes and all of the arcs in the subgraph belong to graph $\mathcal{G}$ as well).

A graph may be *directed*, if a direction is assigned to each of its arcs, or *undirected* otherwise. In the present thesis, a direction for all arcs will be almost always indicated in the graphs; however, for some purposes, the arc orientation may be neglected.

Some special graph topologies are discussed in the following.

- A *bipartite graph* is a graph whose node set can be partitioned into two sets, $\mathcal{N}_1$ and $\mathcal{N}_2$, so that each arc connects a pair of nodes belonging one to $\mathcal{N}_1$ and

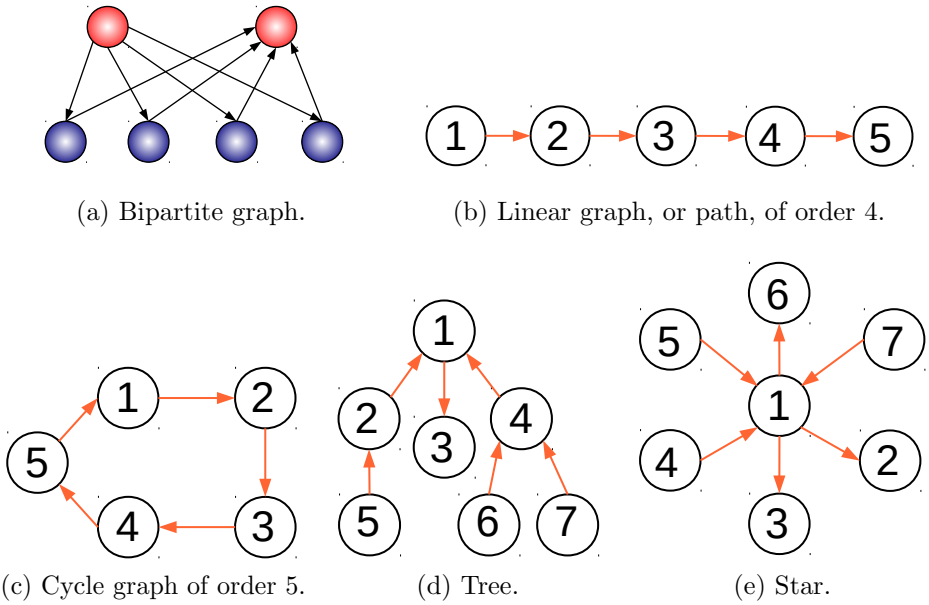

(a) Bipartite graph. (b) Linear graph, or path, of order 4.

(c) Cycle graph of order 5. (d) Tree. (e) Star.

Figure 4.2: Special graph topologies.

one to $\mathcal{N}_2$; namely, no arc exists that connects either two nodes in $\mathcal{N}_1$, or two nodes in $\mathcal{N}_2$ (see Fig. 4.2 (a)).

- A *linear graph* or *path graph* of order k is a graph whose nodes can be listed in order, $n_1, \ldots, n_{k+1}$, so that the (undirected) arcs are (n_i, n_{i+1}) for $i = 1, \ldots, k$; nodes n_1 and n_{k+1} are denoted as the *extrema* of the path (see Fig. 4.2 (b)). In an *oriented* path (or directed path), all the arcs must have a path-consistent orientation (for instance, the path in Fig. 4.2 (b) is oriented). If a linear graph occurs as a subgraph of another graph, it is a path in that graph.

Connectivity. In an undirected graph, a pair of nodes (i, j) (which is unordered) is *connected* if a path leads from i to j (and disconnected otherwise). An undirected graph is then *connected* if every unordered pair of nodes in the graph is connected. In a directed graph, an *ordered* pair of nodes (i, j) is *strongly connected* if a directed path leads from i to j; the ordered pair is *weakly connected* (or connected) if an undirected path leads from i to j (regardless of the direction of the involved arcs). A directed graph is then *strongly connected* if every ordered pair of nodes in the graph is strongly connected and *weakly connected* if every (ordered) pair of nodes in the graph is weakly connected.

- A *cycle graph* of order $k \geq 2$ is a graph whose nodes can be listed in order, $n_1, \ldots, n_k$, so that the (undirected) arcs are (n_{i-1}, n_i) for $i = 2, \ldots, k$ in addition to (n_k, n_1) (see Fig. 4.2 (c)). In an *oriented* cycle (or directed cycle), all the arcs must have cycle-consistent orientation (for instance, the cycle in Fig. 4.2 (c) is oriented). If a cycle graph occurs as a subgraph of another graph, it is a cycle in that graph.

- A *tree* is a (weakly) connected graph with no cycles (see Fig. 4.2 (d)). In a tree, a root (or internal node) is a node with at least two connections, while a leaf is a node with a single connection. A tree that consists of a single root (and where all of the other nodes are leaves) is denoted as a *star* (see Fig. 4.2 (e)). A tree is a *spanning tree* of a graph $\mathcal{G}$ if it is a subgraph of $\mathcal{G}$ including every vertex of $\mathcal{G}$ (a spanning tree of a *connected* graph $\mathcal{G}$ can be defined as the maximal set of arcs of $\mathcal{G}$ that contains no cycle, or as the minimal set of arcs that connects all nodes; there can be several spanning trees of a connected graph, while a graph that is not connected does not admit a spanning tree).
- A *forest* is a disjoint union of trees, *i.e.*, a graph with no cycles that is not connected; the spanning forest of a disconnected graph is the union of more spanning trees, one for each connected component of the graph.

Some matrices can be introduced to mathematically describe a graph topology.

D: If the number of connections for a node of the graph (namely, the number of arcs, either incoming or outgoing, attached to the node) is denoted as *degree* of the node, then the diagonal *degree matrix* $D \in \mathbb{N}^{n\times n}$ can be defined, whose diagonal entry d_{ii} is the degree of the ith node.

A: A fundamental matrix is the symmetric *adjacency matrix* $A \in \{0,1\}^{n\times n}$. Its entry a_{ij} is 1 if nodes i and j are connected by an arc (in either direction) and 0 otherwise.

B: The relationship between nodes and arcs is captured by the *incidence matrix* $B \in \{-1,0,1\}^{n\times m}$, whose entry b_{ij} is 1 if the jth arc enters node i, -1 if it leaves node i and 0 otherwise; matrix B has zero-sum columns.

L: The *Laplacian matrix* of the graph is defined as the difference between the degree matrix and the adjacency matrix: $L = D - A$. Hence, in the Laplacian matrix, the diagonal entries l_{ii} are equal to the number of arcs involving node i, while the off-diagonal entries l_{ij} are equal to -1 if nodes i and j are connected, 0 otherwise.

The Laplacian matrix has several interesting properties:

- $L = BB^\top$;
- $-L$ is a Metzler matrix with negative diagonal entries;
- L is weakly diagonally dominant and symmetric positive semidefinite: $L \succeq 0$;
- L is singular, with the algebraic multiplicity of its zero eigenvalue equal to the number of connected components in the graph (*i.e.*, if the whole graph is connected, zero has multiplicity equal to one);
- L has the eigenvector $\bar{1} = [1 \dots 1]^\top$ associated with the eigenvalue zero: $L\bar{1} = 0$, and also $\bar{1}^\top L = 0$;
- the second smallest eigenvalue of L is the algebraic connectivity (or Fiedler value) of the graph and is zero if the graph is not connected;
- L can be interpreted as a particular matrix discretisation of the Laplace operator (hence its name; an alternative name is Kirchhoff matrix).

The relationship $L = BB^\top$ between the incidence matrix and the Laplacian matrix justifies the choice of providing an equivalent description of a graph by means of its incidence matrix only, which actually contains all the necessary information.

The matrices characterising the graph in Fig. 4.1 are:

$$D = \begin{bmatrix} 2 & 0 & 0 & 0 \\ 0 & 3 & 0 & 0 \\ 0 & 0 & 2 & 0 \\ 0 & 0 & 0 & 3 \end{bmatrix}, \qquad A = \begin{bmatrix} 0 & 1 & 0 & 1 \\ 1 & 0 & 1 & 1 \\ 0 & 1 & 0 & 1 \\ 1 & 1 & 1 & 0 \end{bmatrix},$$

$$B = \begin{bmatrix} -1 & 0 & 0 & 1 & 0 \\ 1 & -1 & 0 & 0 & 1 \\ 0 & 1 & -1 & 0 & 0 \\ 0 & 0 & 1 & -1 & -1 \end{bmatrix}, \qquad L = \begin{bmatrix} 2 & -1 & 0 & -1 \\ -1 & 3 & -1 & -1 \\ 0 & -1 & 2 & -1 \\ -1 & -1 & -1 & 3 \end{bmatrix}.$$

In the presence of a connection with the external environment, namely, of at least one arc that is attached to a single node of the graph (as discussed in Chapter 3, the external environment can be seen as a fictitious node 0, not included in the graph, that accounts for the external world surrounding the graph), the *generalised incidence matrix* has no longer zero-sum columns and the *generalised Laplacian* is no longer singular. The matrices corresponding to the externally connected graph in Fig. 4.3 are:

$$D = \begin{bmatrix} 3 & 0 & 0 & 0 \\ 0 & 4 & 0 & 0 \\ 0 & 0 & 3 & 0 \\ 0 & 0 & 0 & 4 \end{bmatrix}, \qquad A = \begin{bmatrix} 0 & 1 & 0 & 1 \\ 1 & 0 & 1 & 1 \\ 0 & 1 & 0 & 1 \\ 1 & 1 & 1 & 0 \end{bmatrix},$$

$$B = \begin{bmatrix} -1 & 0 & 0 & 1 & 0 & -1 & 0 & 0 & 0 \\ 1 & -1 & 0 & 0 & 1 & 0 & 1 & 0 & 0 \\ 0 & 1 & -1 & 0 & 0 & 0 & 0 & -1 & 0 \\ 0 & 0 & 1 & -1 & -1 & 0 & 0 & 0 & 1 \end{bmatrix}, \qquad L = \begin{bmatrix} 3 & -1 & 0 & -1 \\ -1 & 4 & -1 & -1 \\ 0 & -1 & 3 & -1 \\ -1 & -1 & -1 & 4 \end{bmatrix}.$$

In the sequel, we will mainly refer to generalised Laplacian and incidence matrices.

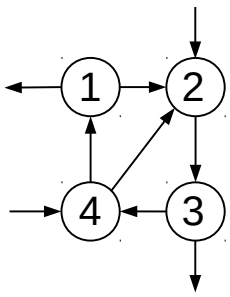

Figure 4.3: An example of an externally connected graph of size 9 and order 4.

4.2 Chemical Reaction Networks and Mass Action Kinetics

Chemical reaction networks can be modelled by means of systems of ordinary differential equations (ODEs), describing the dynamics of the concentrations of the species involved in the reaction environment. In the sequel, chemical species will be denoted with uppercase letters, their concentrations with the corresponding lowercase letter: for example, the chemical species X has concentration x.

The most common approach for converting a chemical reaction network into an ODE system is given by mass action kinetics (MAK). [CBHB09, Ang09]

A general chemical reaction can be written in the form

$$\sum_{j=1}^{n} a_j X_j \xrightarrow{k} \sum_{j=1}^{n} b_j X_j, \tag{4.1}$$

where X_j are the chemical species (reactants, or reagents, when they appear on the left-hand side, products when they appear on the right-hand side), a_j and b_j are the stoichiometric coefficients (non-negative integers) and $k > 0$ is the reaction rate constant. Equivalently, by exploiting a vector representation,

$$AX \xrightarrow{k} BX, \tag{4.2}$$

where $A = [a_1 \dots a_n]$, $B = [b_1 \dots b_n]$ and $X = [X_1 \dots X_n]^\top$.

A reversible reaction can be written as

$$\sum_{j=1}^{n} a_j X_j \underset{k^-}{\overset{k^+}{\rightleftharpoons}} \sum_{j=1}^{n} b_j X_j,$$

which is a compact notation grouping the forward and backward reactions, with reaction rate constants k^+ and k^- respectively:

$$\begin{cases} \sum_{j=1}^{n} a_j X_j \xrightarrow{k^+} \sum_{j=1}^{n} b_j X_j, \\ \sum_{j=1}^{n} b_j X_j \xrightarrow{k^-} \sum_{j=1}^{n} a_j X_j. \end{cases}$$

The compact notation (4.2) is still available, although now A and B are two-row matrices instead of row vectors.

A system of r chemical reactions can thus be written in the form

$$\sum_{j=1}^{n} a_{ij} X_j \xrightarrow{k_i} \sum_{j=1}^{n} b_{ij} X_j, \qquad i = 1, \dots, r \tag{4.3}$$

where $k_i > 0$ is the reaction rate constant of the ith reaction. Reversible reactions are assumed to be split into the forward and the backward reactions. In the matrix-vector form (4.2), $A = [a_{ij}] \in \mathbb{N}^{r \times n}$, $B = [b_{ij}] \in \mathbb{N}^{r \times n}$ and $k = [k_1 \dots k_r] \in \mathbb{R}^r_+$, $k_i \neq 0 \ \forall i$.

It is assumed that each species appears in the reaction network (4.3) with at least one nonzero stoichiometric coefficient and that $\forall\ i$, $\mathrm{row}_i(A) \neq \mathrm{row}_i(B)$, to avoid trivial reactions such as $X \xrightarrow{k} X$ or $X + Y \xrightarrow{k} X + Y$.

A typical method for deriving the dynamics of a reaction network is based on the law of mass action, which states that the rate of an elementary reaction (a reaction that proceeds through only one transition state) is proportional to the product of the concentrations of all the involved reactants, each with an exponent equal to the corresponding stoichiometric coefficient. In the case of stoichiometrically (but not kinetically) equivalent reactions, such as $X \xrightarrow{k} Y$ and $2X \xrightarrow{k} 2Y$, the law of mass action can be assumed to apply to the reaction involving the minimum number of molecules necessary for the reaction to occur.

By applying the law of mass action to the general chemical reaction network (4.3), the dynamics of the species concentrations are given by the system

$$\dot{x}(t) = (B - A)^\top K x^A(t), \quad t \geq 0, \tag{4.4}$$

where $K = \mathrm{diag}\{k_1, \ldots, k_r\}$ and, for $x = [x_1 \ldots x_n]^\top \in \mathbb{R}^n$ and $A = [a_{ij}] \in \mathbb{N}^{r\times n}$, $x^A \in \mathbb{R}^r$ is the column vector whose ith component is the product $x_1^{a_{i1}} \cdot \cdots \cdot x_n^{a_{in}}$. For example, given a matrix A and a vector x, vector x^A can be computed as follows:

$$A = \begin{bmatrix} 2 & 4 \\ 6 & 8 \end{bmatrix}, \quad x = \begin{bmatrix} x_1 \\ x_2 \end{bmatrix} \quad \Longrightarrow \quad x^A = \begin{bmatrix} x_1^2 x_2^4 \\ x_1^6 x_2^8 \end{bmatrix}.$$

The kinetic equations are linear if and only if each row of A contains just a 1 entry, while all the remaining entries are equal to zero (*i.e.*, each reaction is unimolecular). In this case, $x^A = Ax$ and, defining $M \in \mathbb{R}^{n\times n}$ as $M = (B - A)^\top KA$, (4.4) becomes

$$\dot{x}(t) = Mx(t), \quad t \geq 0. \tag{4.5}$$

Reaction networks of the form (4.3) can describe not only closed systems, for which conservation of mass holds, but also open systems, in which mass can be added or removed: the reactions $X \xrightarrow{k} \emptyset$ and $\emptyset \xrightarrow{k} X$ represent, respectively, mass removal and mass addition, and correspond to the differential equations $\dot{x} = -kx$ and $\dot{x} = +k$.

System (4.4) can be rewritten using a different notation that involves the stoichiometric matrix [DP12]

$$S \doteq (B - A)^\top \in \mathbb{Z}^{n\times r} \tag{4.6}$$

and the vector of reaction rate functions

$$f(x(t)) \doteq Kx^A(t) \in \mathbb{R}^r, \tag{4.7}$$

resulting in a system of the form

$$\dot{x}(t) = Sf(x(t)). \tag{4.8}$$

In the presence of influxes or outfluxes, represented by vector $u \in \mathbb{R}^v$, the system can be rewritten in the more general form

$$\dot{x}(t) = Sf(x(t)) + Vu(t), \tag{4.9}$$

where matrix $V \in \mathbb{R}^{n\times v}$.

Here a general matrix-vector framework based on mass action law has been presented, but of course the equations corresponding to simple chemical reaction systems can be derived immediately, based on mass action kinetics, without resorting to the computation of matrices A, B and of vector x^A.

Example 4.1. *For the reaction*

$$aX + bY \xrightarrow{k} mP,$$

with $n = 3$ *and* $r = 1$, $A = \begin{bmatrix} a & b & 0 \end{bmatrix}$, $B = \begin{bmatrix} 0 & 0 & m \end{bmatrix}$, $K = k$, $x^A(t) = x^a y^b$. *Hence, the species concentration dynamics are described by the system*

$$\begin{cases} \dot{x} = -akx^a y^b, \\ \dot{y} = -bkx^a y^b, \\ \dot{p} = mkx^a y^b. \end{cases}$$

Example 4.2. *The reversible reaction, split into the forward and backward reactions,*

$$X \underset{k_2}{\overset{k_1}{\rightleftharpoons}} Y \qquad \Longleftrightarrow \qquad X \xrightarrow{k_1} Y, \quad Y \xrightarrow{k_2} X$$

has $n = 2$ *and* $r = 2$, $A = \begin{bmatrix} 1 & 0 \\ 0 & 1 \end{bmatrix}$, $B = \begin{bmatrix} 0 & 1 \\ 1 & 0 \end{bmatrix}$, $K = diag\{k_1, k_2\}$. *The corresponding system is*

$$\begin{cases} \dot{x} = -k_1 x + k_2 y, \\ \dot{y} = k_1 x - k_2 y, \end{cases}$$

which is linear:

$$M = (B - A)^\top K A = \begin{bmatrix} -1 & 1 \\ 1 & -1 \end{bmatrix} \begin{bmatrix} k_1 & 0 \\ 0 & k_2 \end{bmatrix} \begin{bmatrix} 1 & 0 \\ 0 & 1 \end{bmatrix} = \begin{bmatrix} -k_1 & k_2 \\ k_1 & -k_2 \end{bmatrix}.$$

Example 4.3. *The reversible reaction involving species* X_1 *and* X_2 *corresponds to the dynamics*

$$X_1 + X_2 \underset{k_2}{\overset{k_1}{\rightleftharpoons}} 2X_1 \qquad \begin{cases} \dot{x}_1 = k_1 x_1 x_2 - k_2 x_1^2, \\ \dot{x}_2 = -k_1 x_1 x_2 + k_2 x_1^2. \end{cases}$$

Example 4.4. *The reversible reaction involving species* X_1, X_2 *and* X_3 *corresponds to the dynamics*

$$X_1 + X_2 \underset{k_2}{\overset{k_1}{\rightleftharpoons}} 2X_3 \qquad \begin{cases} \dot{x}_1 = -k_1 x_1 x_2 + k_2 x_3^2, \\ \dot{x}_2 = -k_1 x_1 x_2 + k_2 x_3^2, \\ \dot{x}_3 = 2k_1 x_1 x_2 - 2k_2 x_3^2. \end{cases}$$

Example 4.5. *The chemical reaction network is associated with the system*

$$\begin{cases} X_1 \xrightarrow{k_1} X_1 + X_2 \\ X_3 \xrightarrow{k_2} X_3 + X_4 \\ X_2 + X_4 \xrightarrow{k_3} X_5 \end{cases} \qquad \dot{x} = \begin{bmatrix} 0 & 0 & 0 \\ 1 & 0 & -1 \\ 0 & 0 & 0 \\ 0 & 1 & -1 \\ 0 & 0 & 1 \end{bmatrix} \begin{bmatrix} k_1 x_1 \\ k_2 x_3 \\ k_3 x_2 x_4 \end{bmatrix}.$$

Example 4.6. *A typical reaction network involves a substrate X_1 that interacts with an enzyme X_3 to generate a product X_4 by means of an intermediate species X_2. The corresponding reactions*

$$X_1 + X_3 \underset{k_2}{\overset{k_1}{\rightleftharpoons}} X_2 \xrightarrow{k_3} X_3 + X_4$$

can be expanded and associated with the system

$$\begin{cases} X_1 + X_3 \xrightarrow{k_1} X_2 \\ X_2 \xrightarrow{k_2} X_1 + X_3 \\ X_2 \xrightarrow{k_3} X_3 + X_4 \end{cases} \qquad \dot{x} = \begin{bmatrix} -1 & 1 & 0 \\ 1 & -1 & -1 \\ -1 & 1 & 1 \\ 0 & 0 & 1 \end{bmatrix} \begin{bmatrix} k_1 x_1 x_3 \\ k_2 x_2 \\ k_3 x_2 \end{bmatrix}.$$

4.2.1 Conservation Laws and Stoichiometric Compatibility Class

In some chemical reaction networks, it may happen that the corresponding differential equations are redundant: the sum of some of the partial derivatives is zero; hence, the sum of the corresponding state variables is a constant (which depends on the initial conditions). This expresses the conservation of the total amount of some substance that may be present in different forms (for instance, $x + x^* = x^{tot}$, where x is the species in the active form, while x^* is the species in the inactive form). In the presence of k conservation laws, k differential equations of the system can be replaced with k algebraic equations (the conservation laws, indeed).

The conservation laws are synthetically represented by the left kernel of the stoichiometric matrix S: $\ker(S^\top) = \{x \in \mathbb{R}^n : S^\top x = 0\}$. If $\operatorname{rank}(S) = h \leq \min\{n, r\}$, then the system has $n - h$ conservation laws (since $n - h$ is the dimension of $\ker(S^\top)$).

In the presence of conservation laws, the whole space $\mathbb{R}^n$ can be seen as partitioned in stoichiometric compatibility classes, each uniquely identified by the initial condition x_0, where the system evolution $x(t) = \varphi(t, x_0)$ is confined for all $t > 0$. A stoichiometric compatibility class can be expressed as

$$\mathcal{C}(x_0) = \{x_0 + \operatorname{span}(S)\} \cap \mathbb{R}^n_+, \tag{4.10}$$

where $\operatorname{span}(S)$ denotes the range (column space) of matrix S. Note that each stoichiometric compatibility class is a positively invariant set for the system (namely, for any initial condition in this set, the solution remains in it).

4.2.2 Positivity

The variables in biochemical systems must have non-negative values, since they represent the concentrations of chemical species. Hence, the non-negativity of the solutions must be guaranteed: non-negative initial conditions must generate trajectories confined in the non-negative orthant.

A rigorous proof is provided in [CBHB09], to show that the class of *essentially non-negative* systems is non-negative and that systems derived through mass action kinetics actually belong to that class.

Definition 4.1. *Function* $f = [f_1 \dots f_n]^\top : \mathbb{R}^n_+ \to \mathbb{R}^n$ *is* essentially non-negative *if, for all* $i = 1, \dots, n$, $f_i(x) \geq 0$ *for all* $x \in \mathbb{R}^n_+$ *such that* $x_i = 0$, *where* x_i *denotes the* i*th component of* x.

The linear function $f(x) = Mx$, where $M \in \mathbb{R}^{n \times n}$, is essentially non-negative if and only if M is Metzler (namely, it has non-negative off-diagonal entries).

Consider the system

$$\dot{x}(t) = f(x(t)), \quad x(0) = x_0, \tag{4.11}$$

where $f : \mathcal{D} \to \mathbb{R}^n$ is a locally Lipschitz function and $\mathcal{D}$ is an open subset of $\mathbb{R}^n$.

Recall that the set $\mathcal{U} \subseteq \mathcal{D}$ is *invariant* with respect to (4.11) if $x_0 \in \mathcal{U}$ implies that $x(t) \in \mathcal{U}\ \forall\, t \geq 0$ and the following fundamental result holds as a consequence of Nagumo's theorem. [Nag42]

Lemma 4.1. *Given the dynamical system* (4.11) *and the set* $\mathcal{U} \subset \mathcal{D}$, *closed with respect to* $\mathcal{D}$, *then* $\mathcal{U}$ *is an invariant set with respect to* (4.11) *if and only if,* $\forall\, x \in \mathcal{U}$, $\lim\limits_{h \to 0^+} \inf\limits_{y \in \mathcal{U}} \frac{\|x + hf(x) - y\|}{h} = 0$, *where* $\|\cdot\|$ *denotes the Euclidean vector norm on* $\mathbb{R}^n$.

This allows to prove that [CBHB09]

- $\mathbb{R}^n_+ \subset \mathcal{D}$ is an invariant set with respect to (4.11) if and only if $f : \mathcal{D} \to \mathbb{R}^n$ is essentially non-negative;
- if $f : \mathbb{R}^n_+ \to \mathbb{R}^n$ is defined as $f(x) = (B - A)^\top K x^A$, then it is locally Lipschitz and essentially non-negative.

It follows that $\mathbb{R}^n_+$ is invariant for the dynamical system (4.4).

Alternatively, the same positivity result for mass action kinetics can be obtained from the observation that all negative terms in the differential equation corresponding to $\dot{x}_i$ vanish when $x_i = 0$; hence, if $x(0) \in \mathbb{R}^n_+$ (namely, $x(0) \geq 0$ componentwise), then the solution $x(t) \in \mathbb{R}^n_+$ for all $t \geq 0$.

4.2.3 Zero-Deficiency Theorem

Among the celebrated results provided by the structural analysis of chemical reaction networks [HJ72, Fei72, Hor73a, Hor73b, FH74], the zero-deficiency theorem and the one-deficiency theorem [Fei87, Fei88, Fei95a, Fei95b] are well-renowned and have fostered a lot of subsequent work [CF05, CF06b, Cha06, And08, Han10, vRJ13].

The *zero-deficiency theorem* is fundamental to assess the existence and the stability properties of (positive) equilibria in chemical reaction networks, independent of the value of the reaction rate constant k, under mass action kinetics assumptions.

Consider a graph $\mathcal{G}_{cr}$, called *complex-reaction graph*, whose nodes are the complexes and whose arcs are the reactions, with their generic reaction rate constant (see Fig. 4.4): $\mathcal{G}_{cr} = (\mathcal{C}, \mathcal{R})$, where $\mathcal{C}$ is the set of complexes and $\mathcal{R}$ is the set of reactions (ordered pairs of complexes). In the case of Fig. 4.4, $\mathcal{C} = \{A;\ 2B;\ A+C;\ D;\ B+E\}$ and $\mathcal{R} = \{(A, 2B);\ (2B, A);\ (A+C, D);\ (D, A+C);\ (B+E, A+C);\ (D, B+E)\}$. A complex-reaction graph is in *normal form* if each complex appears only once; here graphs in normal form will be considered.

A complex $\mathcal{C}_i$ is said to *react to* a complex $\mathcal{C}_j$ if $(\mathcal{C}_i, \mathcal{C}_j) \in \mathcal{R}$ and to *react from* a complex $\mathcal{C}_k$ if $(\mathcal{C}_k, \mathcal{C}_i) \in \mathcal{R}$. A complex $\mathcal{C}_i$ is said to be *connected to* a complex $\mathcal{C}_j$ if there exists a sequence of complexes $\mathcal{C}_{\sigma(k)}$, $k = 1, \ldots, s$ that starts from $\mathcal{C}_i$ ($\sigma(1) = i$) and ends up to $\mathcal{C}_j$ ($\sigma(s) = j$), such that $\mathcal{C}_{\sigma(k)}$ reacts either to or from $\mathcal{C}_{\sigma(k+1)}$ for all $k = 1, \ldots, s-1$; this by no means implies directionality of the intermediate reactions. Conversely, a *path* exists from $\mathcal{C}_i$ to $\mathcal{C}_j$ if there exists a sequence of complexes $\mathcal{C}_{\sigma(k)}$, $k = 1, \ldots, s$ that starts from $\mathcal{C}_i$ ($\sigma(1) = i$) and ends up to $\mathcal{C}_j$ ($\sigma(s) = j$), such that $\mathcal{C}_{\sigma(k)}$ reacts to $\mathcal{C}_{\sigma(k+1)}$ for all $k = 1, \ldots, s-1$.

A *linkage class* $\mathcal{L} \subseteq \mathcal{C}$ is a maximal connected component of the graph, namely, a maximal set of connected complexes: all complexes belonging to $\mathcal{L}$ are connected to each other, but none of them is connected with complexes not in $\mathcal{L}$. Linkage classes form a partition of the complex set $\mathcal{C}$: the network in Fig. 4.4 is partitioned into two linkage classes.

Given the corresponding complex-reaction graph, a chemical reaction network is said to be *reversible* if $(\mathcal{C}_i, \mathcal{C}_j) \in \mathcal{R}$ implies $(\mathcal{C}_j, \mathcal{C}_i) \in \mathcal{R}$; *weakly reversible* if the existence of a path from $\mathcal{C}_i$ to $\mathcal{C}_j$ implies the existence of a path from $\mathcal{C}_j$ to $\mathcal{C}_i$ as well. Reversibility and weak reversibility are local properties, which do not imply a connection between all of the complexes in the network; also, a network can be weakly reversible even though not every complex is connected to every other (cf. the network in Fig. 4.4).

Denote by:

- C the number of complexes, $C = |\mathcal{C}|$;
- L the number of linkage classes;
- R the reaction rank, *i.e.*, the dimension of the stoichiometric (sub)space: $R = \text{rank}(S) = \dim[\text{span}(S)]$.

The reaction rank reveals that the positive system (4.8) evolves in a R-dimensional

affine manifold: the stoichiometric compatibility class (4.10).

The *deficiency* Δ of a chemical reaction network is then defined as

$$\Delta = C - L - R$$

and is a non-negative, integer number.

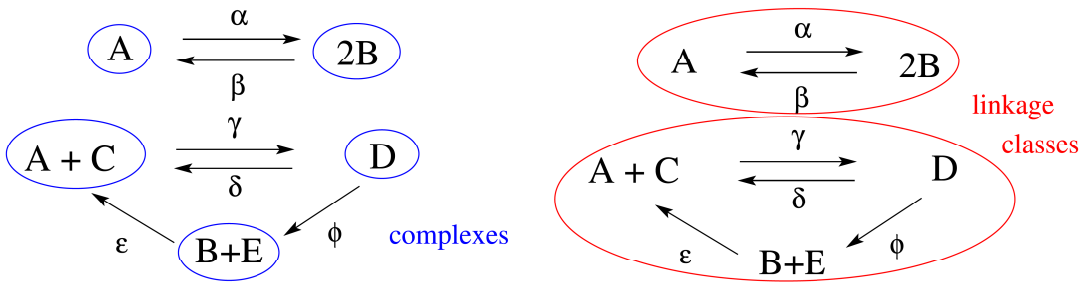

Figure 4.4: Examples of a complex-reaction graph, along with the indication of complexes and linkage classes. The above linkage class is reversible, while the bottom linkage class is weakly reversible (hence, the whole graph is weakly reversible).

In the case of Fig. 4.4, $C = 5$, $L = 2$ and $R = 3$, since

$$S = \begin{bmatrix} -1 & 1 & -1 & 1 & 1 & 0 \\ 2 & -2 & 0 & 0 & -1 & 1 \\ 0 & 0 & -1 & 1 & 1 & 0 \\ 0 & 0 & 1 & -1 & 0 & -1 \\ 0 & 0 & 0 & 0 & -1 & 1 \end{bmatrix}.$$

Hence, $\Delta = 0$.

In a mass action kinetics framework, weakly reversible networks having deficiency $\Delta = 0$ enjoy particular properties, as shown in [Fei87, Fei95a].

Theorem 4.1. (Zero-Deficiency Theorem.) *Given a weakly reversible network where the reactions are of the mass-action-kinetics type, assume that its deficiency is zero. Then, for all choices of reaction rate constants, there is a unique (positive) equilibrium $\bar{x}$ in each stoichiometric compatibility class $\mathcal{C}(x(0))$ and such an equilibrium is asymptotically stable (globally in int$(\mathbb{R}^n_+)$) in each stoichiometric compatibility class.*

The proof employs the fact that entropy $\sum_{i=1}^{n} x_i \ln(\frac{x_i}{\bar{x}_i}) - x_i + \bar{x}_i$ is a Lyapunov function [Lya66]. Although the theorem is based on assuming mass action, hence polynomial, kinetics, a generalisation can be proposed that holds when reaction rates of the form $ka^p b^q$ are replaced by $k\theta_a(a)^p\theta_b(b)^q$, where $\theta_i(\cdot)$ are suitable functions. [Son01]

When restricting to the stoichiometric compatibility class $\mathcal{C}(x(0))$ associated with the given initial condition $x(0)$, global stability of the unique equilibrium follows.

However, since there is a continuum of stoichiometric compatibility classes depending on $x(0)$, there is also a continuum of equilibria: when conservation laws are present, any neighbourhood of $\bar{x}$ contains infinitely many other equilibrium points. Hence, if not restricting to the stoichiometric compatibility class, the equilibrium point is only marginally stable.

For networks of higher deficiency ($\Delta \geq 1$), other results have been proved, such as the one-deficiency theorem; in this case, necessary conditions for multistationarity (namely, the network capacity of exhibiting multiple equilibria in $\mathbb{R}^n_+$ within a single stoichiometric compatibility class, for some choice of the reaction rate constants) are provided concerning networks with deficiency $\Delta = 1$, along with an algorithm to test them. [Fei88, Fei95b]

4.2.4 Generalised Mass Action Kinetics

The dynamics of a reaction network can be derived based on the law of mass action; yet, it is important to underline that this semi-empirical law (phenomenologically explained based on collision-theory-like reasonings) has limited validity and implies an approximation. The law of mass action, in fact, requires that the reaction occurs in a well-mixed compartment, with constant temperature and involving a high number of molecules (*i.e.*, of the order of magnitude of the Avogadro number $N_A = 6.022 \cdot 10^{23}$). Moreover, it is valid for reactions proceeding through only one transition state (*i.e.*, elementary reactions). Although elementary reactions may occur, they are not the rule. Generally, a reaction occurs by means of following steps and thus proceeds through more transitions. Hence, approximations different from mass-action can be adopted under suitable assumptions (such as time-scale separation).

Example 4.7. *The generation rate of the product of the reaction*

$$2A + B \xrightarrow{k'} C \tag{4.12}$$

is expressed by $k'a^2b$ according to mass action kinetics. Yet, the reactions that are really likely to occur are

$$A + B \underset{h}{\overset{k}{\rightleftharpoons}} X, \qquad X + A \xrightarrow{r} C. \tag{4.13}$$

Then the overall reaction occurs in two following steps and the production rate is limited by the slowest of the two. Expressing the reaction rate by means of a mass action kinetics approach would lead to a misleading simplification.

Based on the law of mass action, the equations corresponding to the chemical reaction in (4.12) *are*

$$\begin{cases} \dot{a} = -2k'a^2b \\ \dot{b} = -k'a^2b \\ \dot{c} = k'a^2b \end{cases} \tag{4.14}$$

while the equations corresponding to (4.13) *are*

$$\begin{cases} \dot{a} = -kab + hx - rax \\ \dot{b} = -kab + hx \\ \dot{x} = kab - hx - rax \\ \dot{c} = rax \end{cases} \tag{4.15}$$

Concentration dynamics are significantly different in the two cases. However, if it is assumed that the dynamics of x are much faster (hence x has already reached steady state, $\dot{x} = 0$), then $x = \frac{kab}{h+ra}$ and the system becomes

$$\begin{cases} \dot{a} = -2\frac{kr}{h+ra}a^2b \\ \dot{b} = -\frac{kr}{h+ra}a^2b \\ \dot{c} = \frac{kr}{h+ra}a^2b \end{cases} \tag{4.16}$$

Interestingly, (4.16) *has the same structure as* (4.14) *for "large enough" values of h ($h \gg ra$, so that $\frac{kr}{h+ra} \approx \frac{kr}{h} \doteq \hat{k}$).*

Analogously, the reaction

$$A + B + C \xrightarrow{k'} D, \tag{4.17}$$

associated with the mass action kinetics system

$$\begin{cases} \dot{a} = \dot{b} = \dot{c} = -k'abc \\ \dot{d} = k'abc \end{cases} \tag{4.18}$$

is more likely to actually occur as the reaction network

$$A + B \underset{h}{\overset{k}{\rightleftharpoons}} X, \qquad X + C \xrightarrow{r} D, \tag{4.19}$$

associated with system

$$\begin{cases} \dot{a} = \dot{b} = -kab + hx \\ \dot{x} = kab - hx - rcx \\ \dot{c} = -rcx \\ \dot{d} = rcx \end{cases} \tag{4.20}$$

Again, if $\dot{x} = 0$, then $x = \frac{kab}{h+rc}$ and the system becomes

$$\begin{cases} \dot{a} = \dot{b} = \dot{c} = -\frac{kr}{h+rc}abc \\ \dot{d} = \frac{kr}{h+rc}abc \end{cases} \tag{4.21}$$

which has the same structure as (4.18) *for $h \gg rc$, so that $\frac{kr}{h+rc} \approx \frac{kr}{h} \doteq \hat{k}$.*

Therefore, mass action kinetics can be regarded as an approximation of actual reaction functions, which is valid under some assumptions. An alternative analysis involves generalised mass action kinetics: reaction rates are expressed by general *functions* of the concentrations of all the participating molecules. It can be assumed that these functions, despite unknown, have certain suitable properties: usually, they are nonnegative, continuously differentiable and monotonic (either decreasing or increasing) in each argument; moreover, they are zero when at least one of the arguments is zero.

In Example 4.7, the rate of generation of the product becomes $g(a, b)$ with a generalised approach, where $g(\cdot, \cdot)$ is a function satisfying general assumptions.

Example 4.8. *With the generalised approach, the dynamical system corresponding to the reversible reaction in Example 4.2 becomes*

$$\begin{cases} \dot{x} = -g_x(x) + g_y(y) \\ \dot{y} = g_x(x) - g_y(y) \end{cases}$$

and that corresponding to the reversible reaction in Example 4.3 becomes

$$\begin{cases} \dot{x}_1 = g_{12}(x_1, x_2) - g_1(x_1) \\ \dot{x}_2 = -g_{12}(x_1, x_2) + g_1(x_1). \end{cases}$$

Example 4.9. *Consider the chemical reactions:*

$$\emptyset \xrightarrow{u_1} X_1 \xrightarrow{g_1(x_1)} X_2 \xrightarrow{g_2(x_2)} X_3 \xrightarrow{g_3(x_3)} X_4$$
$$pX_1 + X_4 \xrightarrow{g_{14}(x_1, x_4)} \emptyset$$

X_1 is supplied to the system with a constant influx u_1, and a chain of reactions generates X_4; a negative feedback loop is introduced by the reaction between X_1 and X_4. The system dynamics can be written as

$$\begin{cases} \dot{x}_1 = u_1 - g_1(x_1) - p\, g_{14}(x_1, x_4) \\ \dot{x}_2 = g_1(x_1) - g_2(x_2) \\ \dot{x}_3 = g_2(x_2) - g_3(x_3) \\ \dot{x}_4 = g_3(x_3) - g_{14}(x_1, x_4) \end{cases}$$

where $g_1(x_1)$, $g_2(x_2)$, $g_3(x_3)$ are smooth, strictly increasing functions that are zero at the origin, while $g_{14}(x_1, x_4)$ is smooth, strictly increasing in both arguments and zero when either x_1 or x_4 are zero. The dynamics can be equivalently written in the compact form (4.9)*:*

$$\begin{bmatrix} \dot{x}_1 \\ \dot{x}_2 \\ \dot{x}_3 \\ \dot{x}_4 \end{bmatrix} = \begin{bmatrix} -1 & 0 & 0 & -p \\ 1 & -1 & 0 & 0 \\ 0 & 1 & -1 & 0 \\ 0 & 0 & 1 & -1 \end{bmatrix} \begin{bmatrix} g_1(x_1) \\ g_2(x_2) \\ g_3(x_3) \\ g_{14}(x_1, x_4) \end{bmatrix} + \begin{bmatrix} 1 \\ 0 \\ 0 \\ 0 \end{bmatrix} u_1. \tag{4.22}$$

Thus, biochemical network models can be generically expressed by systems of first order differential equations [BF11b]

$$\dot{x}_i = \sum_{j\in\mathcal{J}_i} f_{ij}(x_i, x_j) + \sum_{h\in\mathcal{H}_i} g_{ih}(x_i, x_h) + \sum_{k\in\mathcal{K}_i} s_{ik}(x_k) + \sum_{d\in\mathcal{D}_i} c_{id}(x_d), \qquad i = 1, \ldots, n,$$

where functions f_{ij} are strictly increasing (associated with production), g_{ih} are strictly decreasing (associated with degradation), s_{ik} and c_{id} are associated with monotonic nonlinear terms (sigmoidal and complementary sigmoidal respectively); $\mathcal{J}_i, \mathcal{H}_i, \mathcal{K}_i, \mathcal{D}_i$ denote the subset of variables affecting x_i through each type of function. Such models are particularly apt for studying *structural properties*, assessed independent of the specific realisation of the functions: qualitative knowledge about the functions is often sufficient to achieve structural conclusions on the system behaviour.

4.3 BDC-decomposition

Consider the generic nonlinear system

$$\dot{x}(t) = g(x(t)), \tag{4.23}$$

where $x \in \mathcal{D} \subseteq \mathbb{R}^n$, $g : \mathcal{D} \subseteq \mathbb{R}^n \to \mathbb{R}^n$ is a continuously differentiable function, and $\mathcal{D}$ is an open, convex domain.

Definition 4.2. *System* (4.23) *admits a BDC-*decomposition *iff, for any $x \in \mathcal{D}$, $J(x) = \partial g/\partial x$ can be written as the non-negative linear combination of rank-one matrices, namely*

$$J(x) = \sum_{h=1}^{q} R_h D_h(x) = \sum_{h=1}^{q} B_h D_h(x) C_h^\top, \tag{4.24}$$

where B_h and $C_h^\top$ are column and row vectors, respectively, so that $R_h = [B_h C_h^\top]$ are rank-one matrices, and are independent of x, while $D_h(x)$, $h = 1, \ldots, q$, are non-negative scalar functions depending on x.

Note that a rank-one matrix R_h can always be written as the product of a column vector B_h and a row vector $C_h^\top$. In a compact form,

$$J(x) = BD(x)C,$$

where $D(x)$ is a diagonal matrix with non-negative diagonal entries $D_h(x)$, B is the matrix formed by the columns B_h and C is the matrix formed by the rows $C_h^\top$.

It is worth stressing that the above definition holds for any x in the domain $\mathcal{D}$, hence, in particular, for any equilibrium point $\bar{x} \in \mathcal{D}$ (such that $g(\bar{x}) = 0$).

Remark 4.1. *Although Definition 4.2 allows some of the diagonal elements $D_h(x)$ to be possibly zero, often the analysis will be restricted to points x at which, for all h, $D_h(x)$ are strictly positive.*

This decomposition has been proposed and exploited in [BFG12, BG14, GCFB15]. Not *any* system admits a BDC-decomposition. Of course, any Jacobian matrix can be written as $J(x) = \sum_{h=1}^{q} R_h D_h(x)$, where $D_h(x)$, $h = 1, \ldots, q$, are scalar functions associated with the partial derivatives and R_h are constant matrices. Yet, it may happen that $D_h(x)$ are not sign-definite, and/or that R_h do not have rank 1. For instance, the simple Jacobian matrix $J = \begin{bmatrix} -\mu & \omega \\ \omega & -\mu \end{bmatrix} = \mu R_1 + \omega R_2$ does not admit a BDC-decomposition, even though $\mu, \omega > 0$, because R_1 and R_2 have rank 2. Nonetheless, for a wide class of models, including (bio)chemical reaction networks, a BDC-decomposition (having a graph interpretation that will be described later) always exists, and can be easily and systematically computed. Consider the system

$$\dot{x}(t) = Sf(x(t)) + f_0, \tag{4.25}$$

where the state $x(t) \in \mathbb{R}^n_+$ represents species concentrations evolving over time, $f(x(t)) \in \mathbb{R}^m$ is a vector of reaction rate functions and $f_0 \in \mathbb{R}^n$ is a vector of constant influxes ($f_0 \geq 0$ componentwise); $S \in \mathbb{Z}^{n \times m}$ is the stoichiometric (flow) matrix of the system, whose entries $[S]_{ij}$ represent the net amount of the ith species produced or consumed by the jth reaction, excluding the contribution of constant influxes. Denote by $\bar{x}$ the equilibrium point, such that $Sf(\bar{x}) + f_0 = 0$. This class of models includes any chemical reaction network, or any phenomenological biomolecular model (*e.g.*, gene regulatory models, signalling networks, *etc.*) that can be written as an equivalent chemical reaction network. Also models typically used in ecology and population dynamics (such as Lotka-Volterra systems) can be rewritten as in (4.25), where $x(t)$ and $f(x(t))$ represent population density and growth rate functions.

Assumption 4.1. *Each function $f_j(\cdot)$, for $j = 1, \ldots, m$, is nonnegative and continuously differentiable, with sign-definite (*i.e.*, always positive, always negative or always zero) partial derivatives in the interior of the positive orthant.*

Assumption 4.2. *Each function $f_j(\cdot)$, for $j = 1, \ldots, m$, is zero if and only if at least one of its arguments is zero. Furthermore, if $[S]_{ij} < 0$, then $f_j(\cdot)$ must have $x_i(t)$ as an argument.*

Remark 4.2. *Assumption 4.2 ensures that* (4.25) *is a positive system (in fact, $\dot{x}_i \geq 0$ for $x_i = 0$), since the considered class of systems is intended to model biochemical and biological systems. For the existence of a BDC-decomposition, system positivity is not necessary in general: the fundamental requirement is the sign-definiteness of the partial derivatives. For instance, the system*

$$\begin{cases} \dot{a} = -k_1 a - k_2 b + a_0, \\ \dot{b} = h_1 a - h_2 b, \end{cases}$$

with $k_1, k_2, h_1, h_2 > 0$, is not necessarily positive (when $a = 0$, $\dot{a}$ may be negative if b is large enough), but its Jacobian indeed admits a BDC-decomposition. Note that, depending on the considered domain $\mathcal{D}$, the same system may admit or not a BDC-decomposition; and it may happen that the system admits a BDC-decomposition if $\mathcal{D} = \mathbb{R}^n_+$, but not if $\mathcal{D} = \mathbb{R}^n$. For example, the system

$$\begin{cases} \dot{a} = -ab - a + a_0, \\ \dot{b} = -ab - b + b_0, \end{cases}$$

whose Jacobian is

$$J(a, b) = \begin{bmatrix} -(b+1) & -a \\ -b & -(a+1) \end{bmatrix},$$

admits a BDC-decomposition if the domain is the positive orthant, but not if it is the whole plane (because, in this latter case, the variables are no longer sign-definite).

The following result guarantees that systems of the form (4.25) always admit a BDC-decomposition.

Proposition 4.1. *Any system falling in the class* (4.25) *admits a BDC-decomposition: $J(x) = BD(x)C$. Matrices B and C can be built systematically, based on the stoichiometric matrix S and on qualitative information about $f(\cdot)$.*

Proof. The statement can be proved constructively, by rewriting equation (4.25) as

$$\dot{x} = \sum_{j=1}^{s} S_j \; f_j(x) + f_0,$$

where S_j is the jth column of matrix S. The corresponding Jacobian is

$$J(x) = \sum_{j=1}^{s} S_j \begin{bmatrix} \dfrac{\partial f_j}{\partial x_1} & \dfrac{\partial f_j}{\partial x_2} & \cdots & \dfrac{\partial f_j}{\partial x_n} \end{bmatrix}.$$

Denoting by $D_1(x), D_2(x), \ldots, D_q(x)$ the absolute values of all the non-zero partial derivatives, it can be written

$$J(x) = \sum_{h=1}^{q} B_h D_h(x) C_h^\top,$$

where

- $D_h(x) = \left| \frac{\partial f_j}{\partial x_i} \right|$ for some i and j;
- $B_h = S_j$, the column of S associated with f_j;
- $C_h^\top$ has a single non-zero entry in the ith position, equal to the sign of $\frac{\partial f_j}{\partial x_i}$.

□

It is now described more in detail how to construct the decomposition matrices. First of all, identify all the distinct, non-zero partial derivatives $\frac{\partial f_j}{\partial x_i}$ and take their absolute values, denoted as D_h; second, assign an order to elements D_h and build the diagonal matrix $D = \text{diag}\{D_1, \ldots, D_q\} \in \mathbb{R}^{q \times q}$. Then, in correspondence to each element $D_h = \left|\frac{\partial f_j}{\partial x_i}\right|$, matrix $B \in \mathbb{Z}^{n \times q}$ includes the column S_j of S associated with f_j. Since each function f_j may depend on p_j different variables, the corresponding column S_j will be repeated p_j times in matrix B. Finally, in correspondence to each element $D_h = \left|\frac{\partial f_j}{\partial x_i}\right|$, matrix $C \in \mathbb{Z}^{q \times n}$ includes a row that has a $+1$ or -1 entry in the ith position (corresponding to the variable x_i with respect to which the derivative in D_h is taken), while the other entries are zero; the sign of the non-zero entry depends on the sign of the corresponding derivative.

The BDC-decomposition is built step by step in the following example.

Example 4.10. *Consider the metabolic network proposed by [CWLA05], p. 106, defined by reactions* $\emptyset \xrightarrow{a_0} A$, $A + B \xrightarrow{f_{ab}} C + D$, $D \xrightarrow{f_d} B$, $C \xrightarrow{f_c} \emptyset$. *Species* B *and* D*, involved in the second and third reactions, are linked by a mass conservation constraint:* $b + d = K$ *is constant. Hence,* $\dot{d} = -\dot{b}$ *and variable* d *can be neglected, so as to obtain the* reduced-order *system*

$$\begin{cases} \dot{a} = a_0 - f_{ab}(a, b) \\ \dot{b} = -f_{ab}(a, b) + f_d(K - b) \\ \dot{c} = f_{ab}(a, b) - f_c(c). \end{cases}$$

This system can be rewritten as in model (4.25) *defining* $x = \begin{bmatrix} a & b & c \end{bmatrix}^\top$,

$$S = \begin{bmatrix} -1 & 0 & 0 \\ -1 & 1 & 0 \\ 1 & 0 & -1 \end{bmatrix}, \quad f(x) = \begin{bmatrix} f_{ab}(a, b) \\ f_d(K - b) \\ f_c(c) \end{bmatrix}, \quad f_0 = \begin{bmatrix} a_0 \\ 0 \\ 0 \end{bmatrix}.$$

The Jacobian matrix and its BDC*-decomposition are*

$$J = \begin{bmatrix} -\alpha & -\beta & 0 \\ -\alpha & -(\beta + \delta) & 0 \\ \alpha & \beta & -\gamma \end{bmatrix}$$

$$= \underbrace{\begin{bmatrix} -1 & -1 & 0 & 0 \\ -1 & -1 & 0 & 1 \\ 1 & 1 & -1 & 0 \end{bmatrix}}_{=\text{B}} \underbrace{diag\{\alpha, \beta, \gamma, \delta\}}_{=\text{D}} \underbrace{\begin{bmatrix} 1 & 0 & 0 \\ 0 & 1 & 0 \\ 0 & 0 & 1 \\ 0 & -1 & 0 \end{bmatrix}}_{=\text{C}},$$

where the Greek letters denote partial derivatives, in absolute value: $\alpha = \partial f_{ab}/\partial a > 0$, $\beta = \partial f_{ab}/\partial b > 0$, $\gamma = \partial f_c/\partial c > 0$, $\delta = |\partial f_d/\partial b|$. *To compute the* BDC*-decomposition, choose an order for the non-zero partial derivatives: 1)* α*, 2)* β*, 3)* γ *and 4)* δ*. Then:*

1) the first column of B corresponds to S_1, associated with the reaction rate function $f_{ab}(\cdot,\cdot)$, and the first row of C has a 1 entry in the first position, corresponding to variable a;
2) the second column of B corresponds to S_1, associated with $f_{ab}(\cdot,\cdot)$, and the second row of C has a 1 entry in the second position, corresponding to b;
3) the third column of B corresponds to S_3, associated with $f_c(\cdot)$, and the third row of C has a 1 entry in the third position, corresponding to c;
4) the fourth column of B corresponds to S_2, associated with $f_d(\cdot)$, and the fourth row of C has a -1 entry in the second position, corresponding to b (since δ is the opposite of $\partial f_d/\partial b < 0$).

Column S_1 is repeated twice in B because $f_{ab}(\cdot,\cdot)$ has two arguments.

Remark 4.3. *The BDC-decomposition is not unique. Even when an order for the diagonal entries of D is assigned, the sign of both B_k and $C_k^\top$ can be changed, resulting in matrices $\hat{B}$ and $\hat{C}$, and still $J = \hat{B}D\hat{C}$. More in general, B_k can be divided and $C_k^\top$ can be multiplied by the same quantity. The only requirement is that matrix D, containing the free non-negative parameters, is diagonal.*

The proposed approach for computing the BDC-decomposition can be extended to non-positive systems (cf. Remark 4.2) and also to the case of dependencies between partial derivatives. For instance, the system

$$\begin{cases} \dot{a} = a_0 - f_{ab}(a-b) \\ \dot{b} = f_{ab}(a-b) - f_b(b) \end{cases}$$

with

$$S = \begin{bmatrix} -1 & 0 \\ 1 & -1 \end{bmatrix}, \quad f = \begin{bmatrix} f_{ab}(a-b) \\ f_b(b) \end{bmatrix}, \quad f_0 = \begin{bmatrix} a_0 \\ 0 \end{bmatrix},$$

would have the BDC-decomposition

$$J = \begin{bmatrix} -\alpha & \beta \\ \alpha & -(\beta+\gamma) \end{bmatrix} = \underbrace{\begin{bmatrix} -1 & -1 & 0 \\ 1 & 1 & -1 \end{bmatrix}}_{=B} \underbrace{\operatorname{diag}\{\alpha,\beta,\gamma\}}_{=D} \underbrace{\begin{bmatrix} 1 & 0 \\ 0 & -1 \\ 0 & 1 \end{bmatrix}}_{=C}$$

if considering the three parameters $\alpha = \partial f_{ab}/\partial a > 0$, $\beta = |\partial f_{ab}/\partial b|$ and $\gamma = \partial f_b/\partial b > 0$. However, since $\beta = \alpha$, two parameters only, α and γ, are needed. Hence:

$$J = \begin{bmatrix} -\alpha & \alpha \\ \alpha & -(\alpha+\gamma) \end{bmatrix} = \underbrace{\begin{bmatrix} -1 & 0 \\ 1 & -1 \end{bmatrix}}_{=B} \underbrace{\operatorname{diag}\{\alpha,\gamma\}}_{=D} \underbrace{\begin{bmatrix} 1 & -1 \\ 0 & 1 \end{bmatrix}}_{=C}.$$

Also when the Jacobian of system (4.25) has independent (hence sign-definite, due to Assumption 4.1) entries, the system always admits a BDC-decomposition.

Remark 4.4. *A system can admit a BDC-decomposition when an external input u is present, affecting the system, or when one of the system parameters is considered as an external input u,*

$$\dot{x}(t) = g(x(t), u(t)),$$

as long as $g(\cdot, \cdot)$ is continuously differentiable and the system Jacobian $J(x, u)$ can be written as the positive (or non-negative) linear combination of rank-one matrices, as in (4.24).

The BDC-decomposition can be an interesting tool and play a key role when assessing *structural* properties. For a *family* of systems admitting a BDC-decomposition, the concept of *structure* can be defined as follows.

Definition 4.3. *The* structure *of a family of systems admitting a BDC-decomposition is given by the matrices B and C. A* realisation *of the structure is given by a choice of the positive (or non-negative) diagonal entries of D, $D_k > 0$ ($D_k \geq 0$), $k = 1, \ldots, q$.*

The BDC-decomposition is a structural representation associated with the Jacobian matrix of the system, which can be equivalently represented by a graph whose nodes and arcs denote, respectively, species and interactions among them. Examples are provided by the graphs in Fig. 4.5. Each arc is associated with positive parameters that are in the diagonal of D; if the arc has k tails, it is associated with k parameters. The arc corresponds to k identical columns of matrix B (having a negative entry in the positions associated with the nodes from which the arc tails start, a positive entry in the positions associated with the nodes reached by the arc arrows, zero entries elsewhere) and to k rows of matrix C, each having a single non-zero entry in one of the positions associated with the nodes from which the arc tails start.

Note that, according to the considerations in Section 3.1.1, this graph – actually, a hypergraph – is fully represented by the stoichiometric matrix S, which is its incidence matrix.

Example 4.11. *Consider the system*

$$\begin{cases} \dot{a} = -f_{ab}(a, b) + f_c(c) \\ \dot{b} = -f_{ab}(a, b) - f_b(b) + f_c(c) + f_c^*(c) \\ \dot{c} = f_{ab}(a, b) + f_b(b) - f_c(c) - f_c^*(c) \end{cases} \tag{4.26}$$

with

$$S = \begin{bmatrix} -1 & 1 & 0 & 0 \\ -1 & 1 & -1 & 1 \\ 1 & -1 & 1 & -1 \end{bmatrix}, \quad f = \begin{bmatrix} f_{ab}(a, b) \\ f_c(c) \\ f_b(b) \\ f_c^*(c) \end{bmatrix}.$$

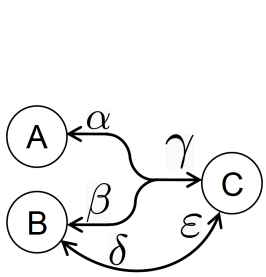

(a) System in Example 4.11.

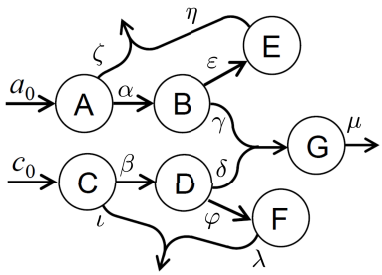

(b) System in Example 7.5.

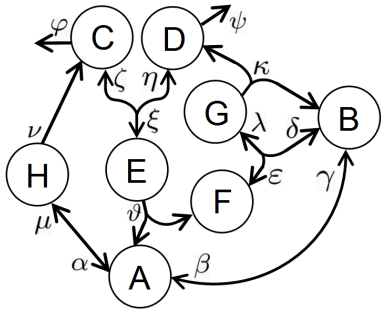

(c) System in Section 7.6.1.

Figure 4.5: Three examples of graphs corresponding to the Jacobian structure. [GCFB15]

Denoting by $\alpha = \partial f_{ab}/\partial a$, $\beta = \partial f_{ab}/\partial b$, $\gamma = \partial f_c/\partial c$, $\delta = \partial f_b/\partial b$ *and* $\varepsilon = \partial f_c^*/\partial c$ *the positive partial derivatives, the system Jacobian matrix, along with its BDC-decomposition,*

$$J = \begin{bmatrix} -\alpha & -\beta & \gamma \\ -\alpha & -(\beta+\delta) & \gamma+\varepsilon \\ \alpha & \beta+\delta & -(\gamma+\varepsilon) \end{bmatrix} \tag{4.27}$$

$$= \underbrace{\begin{bmatrix} -1 & -1 & 1 & 0 & 0 \\ -1 & -1 & 1 & -1 & 1 \\ 1 & 1 & -1 & 1 & -1 \end{bmatrix}}_{=\mathrm{B}} \underbrace{diag\{\alpha,\beta,\gamma,\delta,\varepsilon\}}_{=\mathrm{D}} \underbrace{\begin{bmatrix} 1 & 0 & 0 \\ 0 & 1 & 0 \\ 0 & 0 & 1 \\ 0 & 1 & 0 \\ 0 & 0 & 1 \end{bmatrix}}_{=\mathrm{C}} \tag{4.28}$$

corresponds to the graph in Fig. 4.5 (a).

Remark 4.5. *The BDC-decomposition has an obvious connection with the system Jacobian, as shown by both its definition and its construction in the proof of Theorem 4.1. However, it is not just a local property, or a linearisation. Consider, for instance, the two scalar systems*

$$\dot{x} = \pm x^3,$$

both admitting the equilibrium $\bar{x} = 0$. By computing the Jacobian at the equilibrium, in both cases, it is impossible to draw conclusions on its stability: $J_{\bar{x}} = \pm 3x^2|_{x=\bar{x}} = 0$. However, both of the systems can be written as $\dot{x} = \pm x^2 x = \pm D_1(x)x$, where $D_1(x) = x^2 \geq 0$. Hence, the structure $B = \pm 1$ and $C = 1$ not only yields a BDC-decomposition of the Jacobian ($J(x) = BD(x)C$, for $D(x) = 3x^2$), but also a global representation *for the system (by choosing $D_1(x) = x^2$). This aspect will be better explained in the next section. By means of such a global representation, the original nonlinear system can be absorbed in a linear differential inclusion, which can help assessing the stability properties of its equilibrium at zero (as will be shown in Chapter 6).*

4.3.1 BDC-decomposition as a Global Property: a Useful Integral Formula

Based on a simple but powerful integral formula, it can be shown that the BDC-decomposition associated with a system is not only a local, but also a *global property*.

Given a continuously differentiable function $g(x)$, $g : \mathcal{D} \subset \mathbb{R}^n \to \mathbb{R}^n$, where $\mathcal{D}$ is an open convex domain containing the origin and $g(0) = 0$, then

$$g(x) = \left(\int_0^1 \frac{\partial g}{\partial x}(\sigma x) d\sigma \right) x, \quad \forall\, x \in \mathcal{D}$$

(see [Kha02], p. 108, Exercise 3.23).

More in general, it can be shown that, for arbitrary $g(0)$,

$$g(x) - g(0) = \left(\int_0^1 \frac{\partial g}{\partial x}(\sigma x) d\sigma \right) x, \quad \forall\, x \in \mathcal{D}. \tag{4.29}$$

In fact, denoting by $\varphi(\sigma) \doteq g(\sigma x)$ for $0 \leq \sigma \leq 1$,

$$g(x) - g(0) = \varphi(1) - \varphi(0) = \int_0^1 \varphi'(\sigma) d\sigma = \int_0^1 \frac{\partial g}{\partial x}(\sigma x) d\sigma \quad x,$$

since

$$\frac{d\varphi}{d\sigma}(\sigma) = \frac{\partial g}{\partial x}(\sigma x) \frac{d(\sigma x)}{d\sigma} = \frac{\partial g}{\partial x}(\sigma x) x.$$

Then, reconsider system (4.25), with $x \in \mathcal{D}$ open and convex,

$$\dot{x}(t) = Sf(x(t)) + f_0,$$

along with the equilibrium condition

$$0 = Sf(\bar{x}) + f_0.$$

Denoting $z \doteq x - \bar{x}$ and subtracting the two equations, the shifted system

$$\dot{z} = S[f(z + \bar{x}) - f(\bar{x})] \tag{4.30}$$

is obtained; since the system admits a BDC-decomposition, as previously shown, for any fixed equilibrium $\bar{x}$ its Jacobian can be written as $J(z) = BD(z)C$, hence the system can be equivalently rewritten (not linearised) as

$$\dot{z} = [BD(z)C]z. \tag{4.31}$$

In fact, an immediate application of the integral formula (4.29) to the right-hand side of system (4.30) provides

$$\dot{z} = \left[\int_0^1 J(\sigma z + \bar{x})d\sigma\right] z,$$

where J is the Jacobian of the function $\psi(z) \doteq Sf(z + \bar{x}) = Sf(x)$. In view of the BDC-decomposition, equivalently

$$\dot{z} = \left[B\left(\int_0^1 \operatorname{diag}\left\{\frac{\partial f_i(\sigma z + \bar{x})}{\partial x_j}\right\} d\sigma\right) C\right] z.$$

Therefore, denoting by

$$\Gamma_{ij}(z) = \int_0^1 \frac{\partial f_i(\sigma z + \bar{x})}{\partial x_j} d\sigma, \tag{4.32}$$

it follows that

$$D(z) = \int_0^1 \operatorname{diag}\left\{\frac{\partial f_i(\sigma z + \bar{x})}{\partial x_j}\right\} d\sigma = \operatorname{diag}\left\{\int_0^1 \frac{\partial f_i(\sigma z + \bar{x})}{\partial x_j} d\sigma\right\} = \operatorname{diag}\left\{\Gamma_{ij}(z)\right\}. \tag{4.33}$$

It is worth underlining that, due to monotonicity of the functions $f_i(\cdot)$, whose integral is computed on a non-zero interval, $\Gamma_{ij}(z)$ is strictly positive and admits a maximum and a minimum in any closed and bounded domain:

$$\nu < \nu_{ij} \leq \Gamma_{ij}(z) \leq \mu_{ij} < \mu.$$

Hence the integral formula (4.29), which will be useful in Chapters 6 and 10, allows the computation of the BDC-decomposition with a uniquely determined matrix $D(z)$.

It is worth stressing that a system admits a "global" BDC-representation of the form (4.31) *if and only if* it admits a "local" BDC-decomposition $J = BDC$.

Proposition 4.2. *A nonlinear system* (4.25)*, admitting equilibrium* $\bar{x}$*, can be equivalently written in the form*

$$\dot{z} = BD(z)Cz,$$

where $z = x - \bar{x}$*, if and only if it admits a* BDC*-decomposition, according to Definition 4.2.*

Proof. If $J(x) = BD(x)C$ for any x in the domain, then, denoting $z = x - \bar{x}$, $J(z) = BD(z)C$ holds for any z. Then, integration exploiting the integral formula (4.29) entails the result, as shown in the derivation above. Conversely, if system (4.25) is equivalent to $\dot{z} = BD(z)Cz$, then linearisation immediately provides $J(z) = BD(z)C$, hence $J(x) = BD(x)C$. □

Note that, if $\bar{x}$ is not an equilibrium point, the nonlinear system (4.25) can be equivalently written as

$$\dot{z} = BD(z)Cz + \hat{f}_0,$$

where $z = x - \bar{x}$ and $\hat{f}_0 = Sf(\bar{x}) + f_0$.

By exploiting the BDC-decomposition, some interesting structural results can be derived, which hold regardless of the value of the positive diagonal entries of matrix D. A first result concerns the number of equilibrium points of the nonlinear system.

Theorem 4.2. *Consider a nonlinear system* (4.25)*, defined on an open and convex domain $\mathcal{D}$, admitting a BDC-decomposition with D having a positive diagonal. If in $\mathcal{D}$ there are more than one distinct equilibrium points, then the system Jacobian $J = BDC$ cannot be structurally nonsingular.*

Proof. Given the system $\dot{x} = Sf(x) + f_0$, consider two distinct equilibrium points $\bar{x}$ and $\tilde{x}$. Then, both equilibrium conditions $0 = Sf(\bar{x}) + f_0$ and $0 = Sf(\tilde{x}) + f_0$ must hold. Since the equality $S[f(x) - f(\bar{x})] = BD(z)Cz$, with $z = x - \bar{x}$, can be written for any x, it is possible to choose $x = \tilde{x}$. This choice provides $S[f(\tilde{x}) - f(\bar{x})] = BD(z)Cz = 0$, in view of the equilibrium conditions. Since $z = \tilde{x} - \bar{x} \neq 0$, being $\tilde{x} \neq \bar{x}$ (the equilibria are distinct by assumption), then $BD(z)C$ must be singular. □

Hence, if $J = BDC$ is structurally nonsingular, there cannot be more than one equilibrium point: the equilibrium (if any) must be unique.

Another results concerns monotonicity. As mentioned earlier, a monotone nonlinear system has a Jacobian matrix that is Metzler, when evaluated at any equilibrium point.

Proposition 4.3. *The system* (4.25)*, admitting a BDC-decomposition*

$$J(x) = \sum_{k=1}^{q} B_k C_k^\top D_k(x),$$

is structurally monotone if and only of $B_k C_k^\top$ are Metzler matrices for all k.

Proof. Sufficiency is immediate, since the non-negative linear combination of Metzler matrices is of course a Metzler matrix. Necessity can be proved by contradiction: should $B_k C_k^\top$ have a negative off-diagonal entry, for some k, then, for large enough values of $D_k(\bar{x})$, the resulting matrix $J(\bar{x})$ would have a negative off-diagonal entry as well, hence it would not be Metzler for some $\bar{x}$, and the system would not be structurally monotone. □

4.4 Exploiting Multi-Affinity

As will be shown later, for a system admitting a BDC-decomposition, some important functions, such as the determinant and the coefficients of the characteristic polynomial of the Jacobian, are multi-affine functions of the diagonal entries of matrix D.

A fundamental result states that a multi-affine function defined on a hypercube reaches its minimum (and maximum) value on a vertex of the hypercube ([Bar94], Lemma 14.5.5). The following theorem will be useful for structural analysis [BFG12, BG14, GCFB15].

Theorem 4.3. *Given the hypercube*

$$\mathcal{C}_x = \{x \in \mathbb{R}^n : 0 \leq x_k \leq C,\, k = 1, \ldots, n\},$$

and the multi-affine function $h : \mathcal{C}_x \to \mathbb{R}$, denote by $x^{(v)}$ the vertices of the hypercube $\mathcal{C}_x$, $v = 1, \ldots, 2^n$, where $x^{(1)} = [C\ C\ \ldots\ C]$. Then:

a) $h(x) > 0$ for all x in the interior of $\mathcal{C}_x$ if and only if $h(x^{(v)}) \geq 0$ for all v and $h(x^{(1)}) > 0$;
b) $h(x) < 0$ for all x in the interior of $\mathcal{C}_x$ if and only if $h(x^{(v)}) \leq 0$ for all v and $h(x^{(1)}) < 0$;
c) $h(x) = 0$ for all x in $\mathcal{C}_x$ if and only if $h(x^{(v)}) = 0$ for all v.

Proof. Just the first claim is proved, since the derivation is similar for the others. Necessity is immediately based on continuity arguments. Sufficiency can be proved by contradiction. Since a multi-affine function defined on a hypercube reaches its minimum (and maximum) value on a vertex of the hypercube, it must be $h(x) \geq 0$ in the whole cube. Assume there is an internal point $x^* > 0$ of the hypercube such that $h(x_1^*, x_2^*, \ldots, x_n^*) = 0$. Consider variations along the direction of $0 \leq x_1 \leq C$. The restricted function is linear and nonnegative; hence, since it is zero in one point, it must be zero in the extrema: $h(0, x_2^*, \ldots, x_n^*) = h(C, x_2^*, \ldots, x_n^*) = 0$. Fix $x_1 = C$, corresponding to the second condition: the new point $(C, x_2^*, \ldots, x_n^*)$ is in the relative interior of the $(n-1)$-dimensional cube where $x_1 = C$. Then the same argument can be repeated along the direction of x_2, to conclude that $h(C, C, x_3^*, \ldots, x_n^*) = 0$. Proceeding in the same way for all the directions gives $h(C, C, C, \ldots, C) = 0$, in contradiction with $h(x^{(1)}) > 0$. □

Remark 4.6. *If x has n components, it is necessary to check 2^n vertices; hence, an algorithm exploring the sign of $h(x)$ on all vertices has exponential complexity. However, remarkably, checking the sign on a* finite *number of vertices can provide information on the sign in the whole hypercube.*

The BDC-decomposition of a matrix, defined in (4.24), is a multi-affine function of the coefficients D_h, because $[B_h C_h^\top]$ are rank-one matrices. [Bar94] This property can be exploited for structurally assessing properties of the associated system (see Chapters 5, 6 and 7).

4.4.1 The Mapping Theorem

The mapping theorem ([Bar94], Sections 14.6-14.10) is a fundamental tool in the robust stability analysis of polynomials with multi-affine uncertainty structures; it provides a sufficient condition for stability based on an overbounding family of polynomials: the convex hull of the original family.

Definition 4.4. *The convex hull conv$\mathcal{I}$ of the set $\mathcal{I}$ is the smallest convex set including $\mathcal{I}$, or equivalently the intersection of all the convex sets that include $\mathcal{I}$. When $\mathcal{I} \subseteq \mathbb{R}^n$, the convex hull is the set of all the convex combinations of points in $\mathcal{I}$,* i.e.*, the set of all the points of the form*

$$\sum_{i=1}^{n} \lambda_i x_i \quad \textit{with} \quad x_i \in \mathcal{I}, \quad \lambda_i \geq 0 \, \forall \, i, \quad \sum_{i=1}^{n} \lambda_i = 1.$$

Theorem 4.4. (Mapping theorem). *Let $Q \subset \mathbb{R}^l$ be a hyper-rectangle with vertices $\{q^{(i)}\}$ and $f : Q \to \mathbb{R}^n$ a multi-affine function. If the range of f is denoted by $f(Q) = \{f(q) : q \in Q\}$, then conv $f(Q) =$ conv $\{f(q^{(i)})\}$.*

Proof. See [Bar94]. □

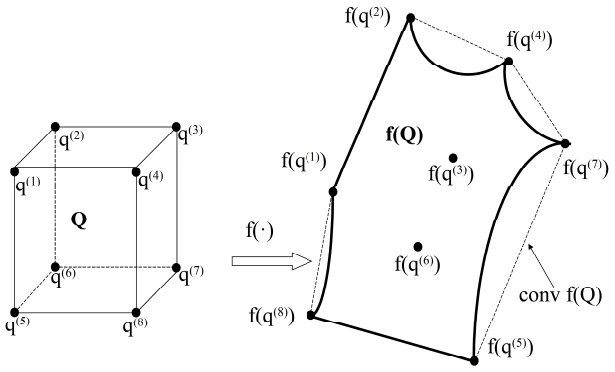

Figure 4.6: Geometric visualisation associated with the mapping theorem.

A geometric visualisation is shown in Fig. 4.6. To have an example of a possible application, consider an uncertain polynomial $p(s, q)$ of degree n in the complex variable s, whose real coefficients $a_i(q)$ are continuous, multi-affine functions of a vector of real uncertain parameters $q \in \mathbb{R}^l$, with $q_i \in [q_i^-, q_i^+]$:

$$p(s, q) = a_0(q) + a_1(q)s + \cdots + a_n(q)s^n, \quad \text{with} \quad a_n(q) \neq 0 \, \forall \, q \in Q,$$

$$q = [q_1 \, q_2 \, \ldots \, q_l],$$

$$Q = \{q : q_i^- \leq q_i \leq q_i^+, \, i = 1, \ldots, l\}.$$

Of course, $p(s,q)$ can be thought of as a two-dimensional vector in the complex plane; both real and imaginary parts are multi-affine (real) functions of the parameters. Then, if the coefficient vector $a(q)$ is considered, the mapping theorem provides a simple description of the convex hull of the coefficient set: $\operatorname{conv} a(Q) = \operatorname{conv}\{a(q^{(i)})\}$.

For a fixed frequency $s = \jmath\omega$, the *value set* of the polynomial can be defined as

$$p(\jmath\omega, Q) = \{p(\jmath\omega, q) : q \in Q\}$$

and is the set of the possible values of the polynomial for a given s, when q is varying. The mapping theorem allows to state that $\operatorname{conv} p(s,Q) = \operatorname{conv}\{p(s,q^{(i)})\}$.

If the roots of $p(s,q)$ for all $q \in Q$ need to be studied, in order to check robust stability (which is guaranteed if $p(s,q)$ has roots in the open left half complex plane for all $q \in Q$), an extension of the Nyquist stability criterion provides a robustness criterion: the Nyquist criterion must hold for all the possible polynomials obtained with different choices of q. The following theorem can be demonstrated based on continuity arguments.

Theorem 4.5. (Zero exclusion theorem). *The polynomial $p(s,q)$, whose coefficients are multi-affine functions of the parameter vector q, is robustly stable for all $q \in Q$ if and only if $p(s,\bar{q})$ is stable for some $\bar{q} \in Q$ and $0 \notin p(\jmath\omega, Q)\,\forall\,\omega \geq 0$.*

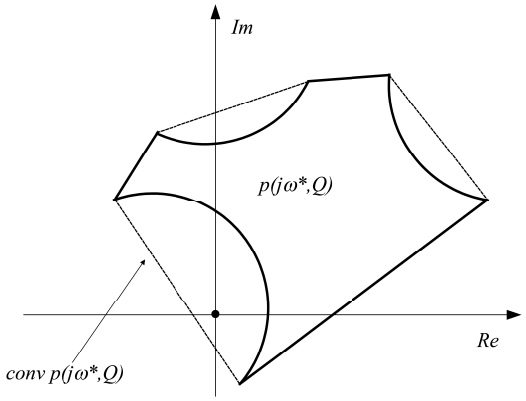

Figure 4.7: Inconclusive robust stability test based on the mapping theorem, showing that the criterion is sufficient only: zero belongs to the convex hull, but not to the actual value set.

Thanks to the mapping theorem, it is possible to have a sufficient condition for stability if the convex hull of the original family is used as a tight overbound. Being grounded on an overbound, a stability analysis based on the mapping theorem provides sufficient but not necessary conditions; in fact, zero may be a point of the convex hull, but not of the original family. As shown in Fig. 4.7, it might happen that, at some frequency ω^*, $0 \in \operatorname{conv} p(\jmath\omega^*, Q)$ but $0 \notin p(\jmath\omega^*, Q)$: the true value set remains unknown. Yet the mapping theorem provides a sufficient condition, since if $0 \notin \operatorname{conv} p(\jmath\omega^*, Q)$, of course $0 \notin p(\jmath\omega^*, Q)$.

Note that the mapping theorem and the zero exclusion theorem apply to any parametric polynomial whose coefficients are multi-affine functions of the parameters. Interestingly, this is the case of systems admitting a BDC-decomposition.

Theorem 4.6. *Theorems 4.4 and 4.5 apply to the characteristic polynomial of any system admitting a BDC-decomposition.*

Proof. By definition, the Jacobian of any system that admits a BDC-decomposition can be written as the positive linear combination of rank-one matrices. Therefore, the coefficients of the characteristic polynomial are multi-affine functions of the Jacobian entries and the assumptions required by the mapping theorem and by the zero exclusion theorem are satisfied. □

4.5 Results from Topological Degree Theory

The *topological degree* $d(f, \mathcal{S}, p) \in \mathbb{Z}$ is a useful notion to investigate the solutions of the equation $f(x) = p$ in a given open set $\mathcal{S} \subseteq X$,[1] where $f : \bar{\mathcal{S}} \to X$ is a continuous function, $p \in X$ and $p \notin f(\partial\mathcal{S})$ (namely, $f(z) \neq p$ for all $z \in \partial\mathcal{S}$) and X is a topological space (often a metric space). The topological degree theory can be fruitfully applied to the study of both fixed points and zeros of functions, and also to the study of dynamical systems and stability theory. [Hof90, Zan96, OC95]

A more detailed overview of the topological degree theory is provided in Appendix D; the reader is referred to [Sch69, Llo78, Dei85, FG95, OJCC06, Feč08, Ams14] for a thorough handling of the theory and its applications. Here, just a few applications of the theory that will be used in Chapter 8 are reported, along with some useful observations that are immediately based on the presented results.

Consider the dynamical system

$$\dot{x}(t) = f(x(t)), \tag{4.34}$$

where $f : \mathbb{R}^n \to \mathbb{R}^n$ is a sufficiently smooth function. Assume that the system solution $x(t) = \varphi(t, x(0))$ (for any given initial condition $x(0)$) is unique and depends continuously on the initial condition. Note that, of course, $x(t) = \varphi(t, x(0))$ must be continuous, and even differentiable, in the variable t. Assume, moreover, that all the system solutions are globally uniformly asymptotically bounded in an *open* ball $\mathcal{S}$: namely, for any compact set $\mathcal{S}_0 \subseteq \mathbb{R}^n$ including $\mathcal{S}$, there exists $T > 0$ (depending on $\mathcal{S}_0$) such that $\varphi(t, x(0)) \in \mathcal{S}$ for any $x(0) \in \mathcal{S}_0$ and any $t \geq T$. Then, the existence of (at least) an equilibrium point is automatically assured based on the results in [Srz85], see also [RW02, RW04].

Once the existence of equilibria is guaranteed, it is interesting to inquire into their number and their stability properties. To this aim, the topological degree theory turns out to be very powerful. The degree is here defined for functions f that are continuous in $\bar{\mathcal{S}}$ and also continuously differentiable in $\mathcal{S}$, with p a regular value of f.

[1] Given a set $\mathcal{S}$, $\bar{\mathcal{S}}$ denotes its closure, int$\mathcal{S}$ its interior, $\partial\mathcal{S}$ its boundary.

Definition 4.5. *Given* $f \in C(\bar{\mathcal{S}}) \bigcap C^1(\mathcal{S})$, $\bar{x} \in \mathcal{S}$ *is a* critical point *of* f *if the determinant of the Jacobian matrix evaluated at* $\bar{x}$ *is zero:* $\det(J_f(\bar{x})) = 0$. *Moreover, let* $Z_f = \{x \in \mathcal{S} : \det(J_f(x)) = 0\}$; *if* $p \notin f(Z_f)$, *then* p *is a* regular value *of* f.

Using Sard's lemma, the following definition can be provided.

Definition 4.6. *Consider* $f \in C(\bar{\mathcal{S}}) \bigcap C^1(\mathcal{S})$ *and* $p \notin (f(Z_f) \bigcup f(\partial\mathcal{S}))$. *Then, the* degree of f at p with respect to $\mathcal{S}$ *is defined as*

$$d(f, \mathcal{S}, p) = \sum_{x \in f^{-1}(p)} \text{sign}[\det(J_f(x))], \tag{4.35}$$

where $\text{sign}(t) = 1$ *for* $t > 0$ *and* $\text{sign}(t) = -1$ *for* $t < 0$.

Since $p \notin f(Z_f)$, $f^{-1}(p)$ is finite, hence (4.35) is well defined. Then the following result holds (descending from Lemma 2 in [Hof90]).

Theorem 4.7. *Assume that the system* (4.34) *has solutions that are globally uniformly asymptotically bounded in an open ball* $\mathcal{S} \subset \mathbb{R}^n$ *and admits* $N < \infty$ *equilibria* $\bar{x}_i$, $i = 1, \ldots, N$, *each contained in* $\mathcal{S}$, *none of which is a critical point. Then*

$$\sum_{i=1}^{N} \text{sign}\left[\det(J(\bar{x}_i))\right] = (-1)^n. \tag{4.36}$$

From this fundamental theorem, several useful consequences can be drawn, once the analytical expression of the Jacobian matrix has been determined as a function of the generic equilibrium point. First of all, notice that (4.36) is equivalent to

$$\sum_{i=1}^{N} \text{sign}\left[\det(-J(\bar{x}_i))\right] = 1, \tag{4.37}$$

which is convenient since it is independent of the system dimension.

For instance, under boundedness assumptions, if $\det(-J) > 0$, regardless of the specific values of the parameters and of the equilibrium point, and there are no degenerate equilibria, then the equilibrium must be unique. In fact, if there were two or more equilibria, the sum in (4.37) (in which all of the addends must be 1, being $\det(-J)$ always positive) would be more than 1.

If $\det(-J) < 0$ for a given equilibrium point $\bar{x}_j$, then $\bar{x}_j$ must be unstable (in fact, if $\det(-J) = p_0$, the constant term of the characteristic polynomial, is negative, then there is at least an eigenvalue with positive real part); hence, at least other two equilibria must exist of degree 1, so that $-1 + \mathbf{1} + \mathbf{1} = 1$ and (4.37) is satisfied. Of course other n equilibria might exist, with n even, so that (4.37) is satisfied.

If there are two stable equilibria, then at least another equilibrium must exist of degree -1, so that $1 + 1 - \mathbf{1} = 1$ (of course, again, there might be other n equilibria, with n odd), so that (4.37) is satisfied.

Note that assuming that all of the equilibria are contained in a proper open set $\mathcal{S}$ (or, equivalently, that there are no equilibria on the boundary of $\mathcal{D}$, whenever a closed set $\mathcal{D}$ is considered) is crucial, as shown by the following example.

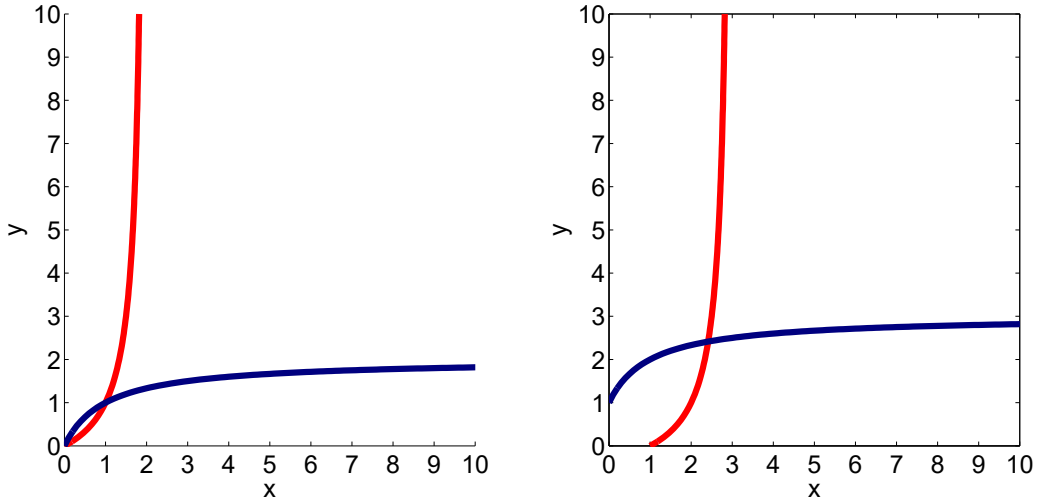

(a) An equilibrium is on the boundary of $\mathbb{R}^n_+$. (b) No equilibria on the boundary of $\mathbb{R}^n_+$.

Figure 4.8: Nullclines of the systems in Example 4.12.

Example 4.12. *Consider the system*

$$\begin{cases} \dot{x} = -x + 2\frac{y}{1+y} \\ \dot{y} = -y + 2\frac{x}{1+x} \end{cases}$$

defined on the domain $\mathcal{D} = \mathbb{R}^n_+$ *(in fact, it can be seen that the positive orthant is a positively invariant set for the system), which admits two equilibrium points:* $\bar{x}_1 = (0,0)$ *and* $\bar{x}_2 = (1,1)$*, such that* $\bar{x}_1 \in \partial\mathcal{D}$*, while* $\bar{x}_2 \in int\mathcal{D}$ *(the nullclines are shown in Fig. 4.8, (a)). The Jacobian matrix is*

$$J = \begin{bmatrix} -1 & \frac{2}{(y+1)^2} \\ \frac{2}{(x+1)^2} & -1 \end{bmatrix}$$

and $\det(-J_{\bar{x}_1}) = -3 < 0$*, while* $\det(-J_{\bar{x}_2}) = \frac{3}{4} > 0$*. Hence,* (4.37) *is not satisfied, being* $\operatorname{sign}[\det(-J_{\bar{x}_1})] + \operatorname{sign}[\det(-J_{\bar{x}_2})] = -1+1 = 0$*. However, this happens because the assumptions of Theorem 4.7 are not satisfied: indeed,* $\bar{x}_1$ *belongs to the boundary of* $\mathcal{D}$*. If the system*

$$\begin{cases} \dot{x} = 1 - x + 2\frac{y}{1+y} \\ \dot{y} = 1 - y + 2\frac{x}{1+x} \end{cases}$$

is considered, then the equilibrium $\bar{x}_1 = (k,k)$ *in* $\mathcal{D} = \mathbb{R}^n_+$ *is unique and lies in the interior of* $\mathcal{D}$*, as shown by the nullclines represented in Fig. 4.8, (b). As expected based on Theorem 4.7,* $\operatorname{sign}[\det(-J_{\bar{x}_1})] = 1$*. In fact,* $\det(-J_{\bar{x}_1}) = 1 - \frac{4}{(k+1)^4}$*, which is positive, being* $k > \sqrt{2} - 1$*.*

II

Structural Analysis of Dynamical Networks

5

A Foreword on Biochemical Systems

This part of the thesis is devoted to the structural analysis of dynamical networks. The focus is especially on biochemical and biological systems, due to their strong robustness properties in spite of a high level of uncertainty. These particular features, which will be discussed in this chapter, make natural systems particularly suitable and interesting to be structurally analysed. [Gio12b]

It is worth stressing that, although the results are often formulated in terms of biochemical or biological systems, the proposed analysis tools can be applied to much more general classes of systems. In fact, essentially, the results in Chapters 6 and 7 simply require that the system admits a BDC-decomposition, while the results in Chapter 8 require that the system either has a sign-definite Jacobian or is the sign-definite interconnection of stable monotone subsystems.

5.1 Biology: a System-Theoretic Approach

The high complexity and astounding efficiency of living organisms has gained the attention of many researchers: cellular networks are mapped and analysed with the goal of understanding how biological behaviours arise and of extracting general design principles and rules that can explain how certain networks can perform particular biological functions [MTES$^+$09]. To survive, all living organisms need to sense external stimuli and face variations in the environment [Fra11]. Cells process information, for survival and reproduction, by means of biochemical circuits made of many species of interacting molecules [HHLM99, KWW06]. Complex structures assemble, perform elaborate biochemical tasks and vanish when their work is done: these phenomena seem to be simple, since they are so spontaneous and efficient, but it is very difficult to understand the general design principles beneath their mechanisms [Alo06]. The dynamic processes, feedback control loops and signal processing systems underlying life [Son05] need to be explored and unraveled. Mathematical models can help describe biological systems with quantitative methods and from a whole-istic perspective [CR02]. A systemic attitude will streamline the identification of targets for novel pharmaceuticals and the understanding of their effects on the cell and the body as a whole; a global understanding of dynamic interactions among genes

and cellular environment will be the first step towards future gene therapies; also, more quantitative experimental methods will allow making falsifiable predictions [Pop34, Pop63], thus bringing modern biology closer to other established experimental sciences [Son05]. This inter-disciplinary approach to biology, requiring the joint effort of scientists with different backgrounds, such as biologists, chemists, physicists, mathematicians and engineers [Kit02], has led to the emerging field of systems biology.

Systems biology aims at understanding biology at a system level, through an inquiry of the structure and the dynamics of cellular and organismal functions: many properties of life arise from interaction among different parts of a cell or organism, so that the behaviour of a biological system as a whole cannot be explained by considering its isolated constituents. Molecular systems biology, in particular, is focused on life mechanisms at the cellular level, such as metabolic networks and pathways and cell signalling networks.

Among the pioneers of a system-level understanding of biology were Norbert Wiener [Wie48] and Ludwig von Bertalanffy [vB69], but the rising interest that makes systems biology an emerging area of research is due to the recent progresses in molecular biology: new and big data are provided, enabling experimental and applied work, allowing for mathematical and computational models of molecules, cells, organisms. As is discussed in [Son05], holistic studies have been already pursued in biological and biomedical engineering, biomathematics and biophysics and many quantitative theories have been developed, *e.g.*, of physiological regulation, metabolic pathways, insulin control, heart electrical patterns, neural and circadian oscillations; bioinformatics has helped in handling and analysing the huge and rapidly growing amount of data stored in biology databases, and has allowed the sequencing of genomes and the prediction of protein and DNA structure; mathematical ideas and algorithms have provided software tools that support the daily work of biologists and pharmaceutical researchers; new sophisticated approaches to data collection and measurement enable a quantitative study of microscopic dynamic interactions among cellular components and a system-level view of cells; at the same time, new theoretical approaches are required to interpret and organise these huge amounts of data. To better understand the network of dynamic interactions among molecules, systems biology adopts an integrated, systematic approach.

Tied to systems biology, a new and challenging field of research is emerging: synthetic biology, which aims at systematically designing from the bottom-up new large scale biochemical circuits. Synthetic circuits with specific functionalities, composed of nucleic acids and proteins, have already been built and promise to be programmable components in larger, integrated systems for nanomanufacturing, pattern formation and artificial biomaterials. [Fra11, Gio12a, BFG14] The creation of synthetic circuits [DWS07] can offer a powerful insight into the design principles present in nature [MvO09] and selected by evolution, which, although it works by random tinkering, seems to converge onto a defined set of basic circuit elements [Alo06, Alo03, Alo07b]. Yet, it is also useful in practical applications: new biotechnologies,

gene and cell therapy can improve human health and quality of life, and the ability of engineering genes and cells and of creating new biomolecular circuits is useful for devising innovative biotechnologies and drugs (for instance, some genes have been used as blocks to insert in a host genome, which is reprogrammed to induce the desired behaviour; yeasts and bacteria have been engineered to produce pharmaceuticals and remedies, such as insulin). [Fra11, Gio12a]

Developing reliable models is the main goal that systems and synthetic biology have in common, since it allows to gain a deeper understanding of the properties of natural complex systems, and to predict their dynamics, as well as to devise general design principles for engineering biomolecular networks that are synthesised *de novo*, so as to optimally and/or robustly tune their features.

5.2 Structural Analysis

Predictive mathematical models are crucial for highlighting the fundamental features of biological systems and the basic laws that rule the behaviour of living matter, in order to perform both the study of natural systems and the design of artificial gene circuits. [Kit02, WGC04, Alo06] Yet, developing suitable models for biological systems requires a remarkable endeavor: a significant challenge arises from the lack of exact quantitative knowledge and from the variability of parameters present in nature, which must be taken into account. Most data so far are qualitative rather than quantitative [Kit02] and a lot of system parameters are not exactly measured: at most, they may be known to lie within certain bounds, but the intrinsic variability inherently prevents from attaining precise knowledge about their values [ATS09]. Therefore, models are plagued by uncertainty (due for instance, in molecular systems, to the variability of reaction parameters and to the presence of unknown interactions).

Interestingly, although parametric uncertainty is a considerable and often intrinsic issue, biochemical networks are incredibly robust to component tolerance [Alo03] and the molecular circuitry of living organisms is able to perform robust regulatory tasks, despite the large variability of its components [Kit04, Alo07a, SWSK11, BF11b]; hence the need to understand the inherent roots of such an extraordinary robustness [GR07, Kit07].

So, given limited, qualitative information, what can be demonstrated about the behaviour of a biochemical system? [RBB10] Is it possible to state if a certain system is, for instance, always stable, or monotone, if it can exhibit oscillations, or perfect adaptation, regardless of parameter values (within a feasible domain)?

Yes, it is, provided that theoretic and computational tools are devised to analyse biological and biochemical systems independent of parameter values. *Structural properties* [NYWP07, SF10, BF11b] must be sought, which ground on the inherent nature of the system only. In this context, a control-theoretic approach is very powerful to structurally assess the key properties of biochemical dynamical systems and to help biotechnologists tune their performance and robustness.

In this part of the thesis, indeed, biochemical systems are the primary object of the investigation and are analysed, looking for *parameter-independent*, structural properties. Focusing on sign-definiteness, monotonicity and boundedness of interactions, given a family of biological systems (associated with a structure), it is possible to rule out behaviours that the structure cannot exhibit and to determine which are instead the potential dynamic outcomes that the structure can yield. The proposed structural analysis is based on the systematic methodologies proposed in [BF11b, BF11a, BFG12, BG14, BG15b, BG15a, GCFB15, BFG14, BFG15b] and founded on classical control-theoretic and system-theoretic methods, in particular on the analysis of the system Jacobian matrix, Lyapunov functions and invariant sets theory [BM15]. In most cases, the achieved structural criteria can be easily verified via numerical analysis (see Appendix B).

5.3 Assessing Properties: a Brief Overview

Dynamic behaviours of biological, biochemical and biomolecular systems have been investigated through various methods, ranging from statistical techniques [BSSS11] and numerical simulations [MI02] to graph-based approaches [DLAS07, RBB10], Petri-net approaches [AdLS07, Sol12] and qualitative modelling techniques [BF11b, BF11a, FB12, GFM13, FGFM14, BCFG14, CGK$^+$16].

Extensive numerical simulations [DJ02] exploring the parameter space are often employed to investigate structural (or robust) properties of biological systems [MI02, KC08]. However, even though numerical simulations can be useful to falsify a conjecture, by providing a counterexample, and can be the only viable method for analysing very complex systems, which cannot be tackled analytically, no campaign of numerical trials will ever provide an actual *warranty* of robustness. Fortunately, many analytical tools are available, based for instance on the renowned deficiency theory [Fei87, Fei95a, Fei95b, SMRMA07], the theory of monotone systems [Smi08, Son07, DLAS07], algebraic geometry and graph theory [CF05, CF06b, MC08, AS09, ADLS10, Min11, DP12, BFG14]. Control theoretic methods have also been employed [ESPP$^+$06], providing criteria based on the analysis of the Jacobian matrix [BFG12] and on Lyapunov theory and set-invariance [BM15, ATS09, CH08, BF11b, BG14]. Rigorous mathematical tools allow to demonstrate that certain biochemical networks structurally enjoy a given property, independent of specific parameter values. Among the properties of interest, particularly relevant for biochemical systems are robustness, monotonicity, perfect adaptation, the capacity of oscillating or of having multiple stable equilibria.

Robustness

Stability against external perturbations and internal variability is a common feature of living systems: evolution selects the fittest organisms, able to resist to diseases,

imperfections or damages of regulatory mechanisms and to survive in various conditions [Kit04, GR07]. Thus, complex biological systems must be robust against environmental and genetic perturbations to be evolvable [CWWL07]. Several reports have been published on how robustness is involved in various biological processes, showing examples of natural phenomena exhibiting robustness and studying the mechanisms that allow living systems to be robust [Kit07]. Robustness in biochemical networks has been analysed, in order to discover natural classes of robust networks [Kit04, Kit10, SWSK11, WAJS12], among which the famous case of bacterial chemotaxis [BL97, ASBL99, YHSD00], and to devise control strategies for achieving robustness [ESKD$^+$05, DIR$^+$12]. The link of robustness with complexity and redundancy has been investigated [TSE99, CD02a, CD02b].

Numerical simulations have been the most pervasive tool for a quantitative analysis of robustness in biological networks and for investigating how topological properties affect robustness [MI02, AC03, Tia04, GGMF05, GR07, KE09, KC08]. In [PIL05], for instance, the Jacobian eigenvalues for two, three and four node networks have been numerically computed to check whether some properties are robust to parameter variability: many interconnections recognised to be robustly stable have turned out to be the most frequent topologies in biological databases. But analytic approaches have been adopted too [SMRMA07]. Advanced mathematical tools have been employed to achieve parameter-independent conclusions on the dynamic behaviour of specific classes of biological systems. A geometric approach has been attempted to devise a graph-based robustness definition for biochemical networks [AK07]; the deficiency theory has provided general results to establish robust stability of a chemical reaction network [SF10, Fei87], as well as the theory of monotone systems [Son07]. Methods based on set-invariance and Lyapunov theory [ESPP$^+$06, ATS09, CH08, BF11b] have been employed too; in [BWW$^+$11] a robustness measure for gene regulation networks has been proposed, leading to convex optimisation problems. Robustness analysis of existing and well-known biochemical networks and pathways [BL97, ASBL99, YHSD00, BF11a] has provided consolidated knowledge useful for designing robust synthetic networks [BYWB07, Fra11].

Monotonicity

Monotonicity is an important structural property in several biological models. The theory of monotone systems [Hir88, MPS90, Smi08, BT11] has been widely applied to biochemical systems [AS03, AS04b, Enc05, GS07, Son07, WS08, ADLS06, AS08, ADLS10, BFG15b], following a graph-based approach to prove monotonicity of chemical reaction network models [DLAS07] and tackling large-scale biological networks by means of a decomposition into monotone subsystems [AS04a, DESZ07].

Adaptation

Adaptation is recurring in biological systems and is a fundamental feature for gradient sensing [LI02]. Among the biochemical systems having the property of adaptation, there are cellular sensory systems displaying fold change detection [SGH$^+$10], osmoregulation [MMGUvO08, MGUMvO09] and the robust molecular circuitry involved in bacterial chemotaxis [BL97, SPO97, ASBL99]. The flagellar motor of *Escherichia coli* cells is controlled by a cascade of signalling proteins, whose active or inactive state is determined by the presence of nutrient or toxin in the environment. The flagellar motion of *E. coli* presents a robustly stable and perfectly adaptive steady state: cells are sensitive to gradients, but steps in the nutrient or toxin concentration only temporarily alter the motion equilibrium (in order to move towards the nutrient or far from the toxin), which after a transient always returns to its stable mode, depending exclusively on the concentrations of signalling cascade proteins and binding rates, and not on external inputs: this has been shown by both analysis of an ordinary differential equation model [BL97] and experimental data [ASBL99] and has thus drawn the attention for further analysis. In [YHSD00] an integral feedback control structure has been shown to be present in the chemotaxis network and to guarantee its robust perfect adaptability: more in general a link has been established between perfect adaptation and integral feedback; by means of frequency response analysis, perfect adaptation has been associated with the presence of zeros in the system transfer function [DUR08]. Adaptation has also been explored analytically to highlight its link with the existence of an internal model [Son03]. Efforts have been made to determine motifs that can achieve perfect adaptation (showing through numerical simulations that the adaptability of three-node networks can be investigated solely based on their structure, regardless of the chosen reaction parameters [MTES$^+$09]) and to design biomolecular network modifications that enable perfect adaptation [CWWL07, KM11, WSA12].

Oscillations

Oscillations are fundamental in cells and organisms to provide the timing of life: the so-called circadian rhythms [Win80, CLD95, Dun99, BL00, HHS$^+$00, NII$^+$05, Wag05, KNN$^+$06, BTM$^+$08, QBM$^+$10, YFJ13]. The qualitative and experimental analysis of oscillations from a chemical and biological point of view [SS61, PC66, BR79, KEK81, LSA11] has been soon supported by mathematical analysis [Lot20, Vol26, Hig67, Rap76a, Rap76b, WLCA10] aimed at developing simple but realistic models of complex oscillatory biological processes [FPK$^+$09].

Oscillatory phenomena in biochemical systems have been understood in their pathway dynamics and their properties [BTM$^+$08], providing suitable models [Gol97, Con99, Gol07, QNKS07, QBM$^+$10] and underlining trade-offs between robustness and efficiency [CBD11]. The oscillatory behaviour of chemical and biochemical reaction networks has been analysed based on the theory of monotone systems

[GS07, AS08], on bifurcation theory [DK09], as well as on qualitative techniques founded on Lyapunov theory and Jacobian matrix analysis [FB12, BFG14, BFG15b]. Structural analysis of biochemical networks exhibiting an oscillatory behaviour has been recently considered also in [MC08, Min11], which, using the formalism of mass action kinetics, provide necessary conditions based on the network graph structure.

Mathematical analysis has helped look for general design principles, strategies and motifs [LE90, ROE90, VKBL02, Lew03, GP06, WCA06, NT08, TCM+08, TKSS09, LW10, BJ11, HH11, Ngu12], which are very useful for supporting the experiments and the actual realisation of synthetic chemical and biochemical oscillators, often *in vitro* [AWM98, EL00, ASMN03, PSF03, FWS+05, KCEO05, LS05, NII+05, WTL07, BSO+08, SCB+08, TMLSF09, TDG+10, SFM10, FFK+11, MPS+11, KW11]; a comparative analysis is provided in [PSGdB10].

Multistability

Efforts have been made to mathematically analyse, explain and forecast bistable behaviours in biochemical networks and biological systems [XF03, YM03, YSHM04, MHK04, MB04, VRMG04, TB05, WB05, CF06b, SP07, QNKS07, CEA08, DK09, FPK+09, RGBB09, Wil09, MY10, SGMGSG11, CGK+16] and more in general biochemical systems exhibiting multistability have been considered [AS04b, AFS04, CTF06, KST07, MC08, SGGS09, LW10, SGMGSG11, BF11a, BFG14, BFG15b]. Bifurcation analysis has helped detect bistability, multistability and hysteresis in biological models [AFS04], but bistability has also been inquired by means of Bayesian techniques for parameter space analysis [SKW12]. The theoretical investigation has been advancing in parallel to the construction of *in vitro* bistable circuits [GCC00, HPDC00, KWW06, SKW11, CA12, MTF14].

5.4 Structural Property Detection in Biochemical Systems

This section presents the systematic methodology proposed in [BFG12] to investigate the structural nature of oscillatory behaviours (related to Hopf-type bifurcations) and perfect adaptation, based on the analysis of the system Jacobian matrix, for systems admitting a BDC-decomposition.

Again, although the focus in [BFG12] is on biological and biochemical systems, it is worth stressing that the proposed results are applicable to any system admitting a BDC-decomposition. Based on the multi-affinity of the BDC-decomposition, simple criteria, easy to verify numerically, can be provided to check if a given model structurally has the potential to exhibit an oscillatory or an adaptive behaviour.

Systems of the form (4.9), namely

$$\dot{x}(t) = Sf(x(t)) + Vu(t), \tag{5.1}$$

with $x \in \mathbb{R}^n$, $S \in \mathbb{Z}^{n\times m}$, $f : \mathbb{R}^n \to \mathbb{R}^m$, $V \in \mathbb{R}^{n\times v}$ and $u \in \mathbb{R}^v$, of course admitting a BDC-decomposition, are considered here under boundedness assumptions.

Assumption 5.1. *The solutions of* (5.1) *are globally bounded.*

Conditions that exclude a certain type of instability relying on structural properties of the Jacobian (and the corresponding characteristic polynomial) are illustrated in the following two examples.

Example 5.1. *Consider the Jacobian matrix*

$$J = \begin{bmatrix} -(\alpha+\epsilon) & 0 & -\delta \\ \alpha & -\beta & 0 \\ -\epsilon & \beta & -(\gamma+\delta) \end{bmatrix},$$

where Greek letters denote positive partial derivatives. Clearly, J admits a BDC-decomposition. It can be verified that the characteristic polynomial has positive coefficients for any choice of the parameters and corresponding equilibria. Hence, the Jacobian cannot have positive real eigenvalues.

Example 5.2. *The Jacobian matrix*

$$J = \begin{bmatrix} -(\alpha+\epsilon) & 0 & -\delta \\ \alpha & -\beta & 0 \\ 0 & \beta & -\gamma \end{bmatrix},$$

where again Greek letters denote positive partial derivatives, has a characteristic polynomial with positive coefficients for any choice of the parameters and corresponding equilibria. Hence, the Jacobian cannot have positive real eigenvalues.

In both Examples 5.1 and 5.2, instability of equilibria can only arise in association with pairs of complex eigenvalues having positive real part. Can instability occur at all for the equilibria? It turns out that the system of Example 5.1 is unconditionally stable. Conversely, the system of Example 5.2 may become unstable for very large δ.

A similar analysis setup can be adopted for structurally detecting oscillatory behaviours and perfect adaptation.

5.4.1 Revealing Potential Oscillators

Consider the general model (5.1), under Assumption 5.1, and suppose that its Jacobian

$$J = \sum_{k=1}^{q} B_k C_k^\top D_k,$$

where $[B_k C_k^\top] = R_k$ are rank-one matrices and D_k are scalars, can be an unstable matrix for some choice of the parameters. Instability can be *exponential* (due

to nonnegative real eigenvalues) or *oscillatory* (due to complex eigenvalues with nonnegative real part). If structural conditions *exclude* exponential instability for J, any choice of parameters destabilising J yields oscillatory dynamics.

A condition to exclude exponential instability is:

$$\det(\lambda I - \sum_{k=1}^{q} R_k D_k) \neq 0, \quad \text{for} \quad \lambda \in \mathbb{R}^+.$$

Since D_k are arbitrary, positive scalars, they can be normalised as $0 < \underline{D}_k \leq 1$. In addition, to exclude zero eigenvalues, the condition becomes

$$\det(\lambda I - \sum_{k=1}^{q} R_k \underline{D}_k) \neq 0 \tag{5.2}$$

$$\text{s.t.} \quad \epsilon \leq \lambda \in \mathbb{R}^+, \epsilon > 0, \quad 0 < \underline{D}_k \leq 1. \tag{5.3}$$

Dividing by λ

$$\det\left(I - \sum_{k=1}^{q} R_k \frac{\underline{D}_k}{\lambda}\right), \quad \lambda \geq \epsilon$$

and taking $\bar{D}_k = \frac{\underline{D}_k}{\lambda}$, $0 < \bar{D}_k \leq \frac{1}{\epsilon}$, the problem is equivalent to analysing function:

$$f(\bar{D}) = \det\left(I - \sum_{k=1}^{q} R_k \bar{D}_k\right). \tag{5.4}$$

Proposition 5.1. *Consider the cube:*

$$\mathcal{C}_{\bar{D}} = \{\bar{D}_k : \quad 0 < \bar{D}_k \leq \Theta\}, \qquad \Theta = \frac{1}{\epsilon}. \tag{5.5}$$

Function $f(\bar{D})$ in (5.4) *is nonzero in the cube $\mathcal{C}_{\bar{D}}$ if and only if $f(\bar{D})$ is positive on each vertex of $\mathcal{C}_{\bar{D}}$.*

Proof. It is immediately based on Theorem 4.3, since $f(0) = 1$ is positive (where 0 is the zero vector). □

Proposition 5.1 provides a criterion to detect a potential oscillatory system.

Lemma 5.1. *If the determinant function* (5.2) *is positive on all the vertices of the parameter cube* (5.5)*, then system* (5.1) *under Assumption 5.1 can exhibit only oscillatory unstable linearised dynamics.*

Example 5.3. *Recall the system in Example 4.9, for which*

$$J = \begin{bmatrix} -1 & 0 & 0 & -p & -p \\ 1 & -1 & 0 & 0 & 0 \\ 0 & 1 & -1 & 0 & 0 \\ 0 & 0 & 1 & -1 & -1 \end{bmatrix} D \begin{bmatrix} 1 & 0 & 0 & 0 \\ 0 & 1 & 0 & 0 \\ 0 & 0 & 1 & 0 \\ 1 & 0 & 0 & 0 \\ 0 & 0 & 0 & 1 \end{bmatrix},$$

$D = diag\{d_1,\ d_2,\ d_3,\ d_4,\ d_5\} = \{\alpha, \beta, \gamma, \delta, \varepsilon\}$. *The determinant function is*

$$f = \det \begin{bmatrix} 1 + (\alpha + p\delta) & 0 & 0 & p\varepsilon \\ -\alpha & 1 + \beta & 0 & 0 \\ 0 & -\beta & 1 + \gamma & 0 \\ \delta & 0 & -\gamma & 1 + \varepsilon \end{bmatrix}$$

and is positive on all the 32 vertices, as can be numerically verified. Therefore, the system is a potential oscillator, since instability is necessarily associated with complex, unstable eigenvalues.

5.4.2 Revealing Perfect Adaptation

Consider a system of the form (5.1), with output $y = Nx(t)$. Suppose a constant perturbation is introduced on the input, with respect to its equilibrium value. If the system is perfectly adaptive, after a transient it responds by returning to the pre-perturbation equilibrium. As seen in Section 2.3.9, the linearised system

$$\begin{cases} \dot{z} = Jz + Vv \\ w = Nz, \end{cases} \tag{5.6}$$

being a linear time invariant dynamical system, has perfect adaptation if and only if its transfer function has a zero at the origin, which is equivalent to requiring that

$$\det \begin{bmatrix} J & V \\ N & 0 \end{bmatrix} = \det(H) = 0.$$

Assume that D_k, $k = 1, ..., q$, can be normalised as: $0 \leq \bar{D}_k \leq 1$. Since $\det(H)$ is a multi-affine function of the variables D_k, the next result immediately follows from Theorem 4.3.

Proposition 5.2. *Function $f(\bar{D}) = \det(H)$ is identically zero if and only if it is zero at each vertex of the cube $\mathcal{C}_{\bar{D}}$, defined consistently with expression* (5.5).

A zero at the origin assures zero response to a step input, provided that there is no cancellation, *i.e.*, no pole at the origin; hence,

$$\det(J) \neq 0.$$

This second condition can be verified by exploiting the same principle. Normalising D_k as $\epsilon \leq \bar{D}_k \leq 1$, with $\epsilon > 0$, it requires checking if $f(\bar{D}) = \det[J(\bar{D})]$ is sign definite on the cube defined by the possible values of $\bar{D}_k$.

Proposition 5.3. *Function $f(\bar{D})$ is nonzero inside the cube $\epsilon \leq \bar{D}_k \leq 1$ if and only if it has the same sign (either positive or negative) at all of the vertices.*

Example 5.4. *The system*

$$\begin{cases} \dot{x}_1 = u_1 - g_{12}(x_1, x_2) + g_3(x_3) - g_1(x_1) \\ \dot{x}_2 = u_2 - g_{12}(x_1, x_2) \\ \dot{x}_3 = g_{12}(x_1, x_2) - g_3(x_3), \end{cases}$$

where u_1 and u_2 are constant positive functions, while $g_1(x_1)$, $g_3(x_3)$ and $g_{12}(x_1, x_2)$ are smooth, strictly increasing in each argument and zero when either argument is zero, has Jacobian matrix:

$$J = \begin{bmatrix} -(\alpha+\eta) & -\beta & \gamma \\ -\alpha & -\beta & 0 \\ \alpha & \beta & -\gamma \end{bmatrix},$$

where Greek letters denote (positive) partial derivatives. It can be numerically verified that $\det(-J) > 0$. *If perturbations on input u_1 are considered and x_3 is taken as the system output, the condition*

$$\det \begin{bmatrix} -(\alpha+\eta) & -\beta & \gamma & 1 \\ -\alpha & -\beta & 0 & 0 \\ \alpha & \beta & -\gamma & 0 \\ 0 & 0 & 1 & 0 \end{bmatrix} = 0$$

is always satisfied, hence the system admits perfect adaptation to perturbations in u_1.

5.4.3 Stability and Bistability

Stability and D-Stability

When structurally investigating potential oscillations or perfect adaptation, stability (or instability) has an important role because (i) oscillations cannot be achieved if the system does not transition to instability due to a pair of complex eigenvalues crossing the imaginary axis; (ii) to have perfect adaptation, the system must be asymptotically stable. As discussed in Section 4.4.1, since the Jacobian of any system that admits a BDC-decomposition can be written, by definition, as the non-negative sum of rank-one matrices, then the coefficients of the characteristic polynomial are multi-affine functions of the Jacobian entries and the mapping theorem [Bar94] applies, providing a sufficient condition for robust stability (given by the zero exclusion theorem). Other conditions for stability, suitably tailored to the case of systems admitting a BDC-decomposition, will be provided in Chapter 6.

Interestingly, stability of the BDC-decomposition of the system Jacobian matrix is related to D-stability problems. A matrix A is said to be D-stable if the product DA is stable for all real positive definite diagonal matrices D. Hence, the problem of analysing robust stability of a matrix of the form $A^* = DA$, where D is a positive

definite diagonal matrix, is a D-stability problem. [Cro78] In the BDC-decomposition ($J = B\,D\,C$ as in (4.24)), assume that $q \geq n$ (which is a necessary condition for J to be invertible, otherwise asymptotic stability would be structurally lost due to an eigenvalue at the origin; in fact, the rank of a product of matrices is lesser or equal to the minimum rank of the factors). Consider now the matrix obtained from J by permuting its factors

$$J^* = D\,C\,B = D\,N \in \mathbb{R}^{q\times q}.$$

The dimension of J^* is q. Hence, for $q \geq n$, the spectral set of J is included in the spectral set of J^*: the eigenvalues of J^* are those of J plus the eigenvalue $\lambda = 0$ with multiplicity $q - n$. The presence of zero eigenvalues is a problem that can be dealt with numerically by means of an ε perturbation: $\varepsilon I + J^*$. The D-stability property has been proved to be equivalent to a μ-type condition [CFY95] and an approach based on Linear Matrix Inequalities (LMIs) has been proposed to test D-stability [GdOH98]; for large scale problems, this type of investigation may become highly complex and a probabilistic approach [CDT11] may be more effective.

Bistability

It has been shown how to exclude the presence of real positive eigenvalues, ruling out exponential transitions to instability (through the origin), hence revealing potential oscillations. Is it possible to rule out oscillatory transitions to instability, hence revealing potential bistability? If a system is monotone, instability can be only due to real unstable eigenvalues. More in general, to exclude oscillatory bifurcations, it is necessary to assure that

$$\det[j\omega I - J(D)] \neq 0,$$

with $\omega > 0$, for all diagonal matrices $D \succ 0$. Equivalently, normalising the expression to $\omega = 1$, it can be written that $\det[jI - J(D)] \neq 0$. Multiplying the expression by its conjugate provides the condition

$$h(D) = \det[jI - J(D)]\det[-jI - J(D)] \neq 0.$$

Function $h(D)$ is a real polynomial in the variables D_k, $k = 1, ..., q$. Then the problem reduces to determining if the polynomial $h(D)$ is copositive (*i.e.*, positive for $D_k > 0$). Unfortunately, $h(D)$ is not a multi-affine function of D_k: no vertex results based on Theorem 4.3 can be obtained and more sophisticated algorithms are required. For instance, stability analysis by means of positive polynomials has been considered in the literature (see [QD92], and [Las11] for more recent results and references).

6

Structural Stability and Boundedness of Biochemical Systems

The extraordinary robustness of biochemical systems can be explained based on the fact that they enjoy *structural* properties, independent of specific parameter values.

In this chapter, the main goal is assessing structural stability of biochemical reaction networks with monotonic reaction rates, *i.e.*, establishing if all the networks with a certain structure are stable, regardless of specific parameter values. Following [BG14], stability is investigated by absorbing the system equations in a linear differential inclusion and seeking a polyhedral Lyapunov function proper to the considered network *structure*. A numerical recursive procedure is devised to generate such a function. For a wide class of mono- and bimolecular reaction networks, named *unitary*, the procedure is shown to be very efficient since, due to the particular structure of the problem, it requires iterations in the space of integer-valued matrices. Even when a Lyapunov function certifying stability cannot be found, with a similar (but less conservative) procedure it is possible to test whether the system evolution is structurally bounded; in this case, the system equations are absorbed in a positive linear differential inclusion.

It is also briefly shown that the proposed numerical procedure can be interpreted in a discrete-event system framework.

To certify the effectiveness of the approach, many non-trivial biochemical reaction networks have been tested (which are thoroughly described in Appendix A, along with the outcomes of both a stability and a boundedness test) and well established models in the literature are analysed.

[BG14] considers systems in *concentration coordinates*, where the state variables are species concentrations. It is also shown, along the lines in [BG15a], that the proposed theoretical results can be applied to systems in *reaction coordinates*, as well. Stability of these systems, where the state variables are reaction rates, was first investigated by Al-Radhawi and Angeli. For these systems, the same numerical test as in [BG14] can be employed to find a polyhedral Lyapunov function and thus certify stability. Under suitable assumptions on the rank of structural matrices, it is proved that the test can be equivalently performed for the system in concentration coordinates or for the system in reaction coordinates, since it has the same outcome

in both cases.

Moreover, for basic motifs in biochemical networks (which admit piecewise-linear Lyapunov functions, based on the results in [BG14]), it is shown that stability cannot be structurally proved resorting to quadratic Lyapunov functions [BG15b] and even to smooth Lyapunov functions.

Most of the results apply not only for the considered class of biochemical reaction networks, but also for any system admitting a BDC-decomposition (see Section 4.3).

6.1 Background

Often, in chemical and biochemical networks, parameter values are widely uncertain, time-varying and depending on unpredictable factors due to specific environmental and working conditions. In spite of this, particular behaviours are extremely robust, since they depend on particular structures (often called *motifs*, [Alo07b]), regardless of specific parameter values. [Alo06] Structural analysis is a powerful tool to gain insight into this phenomenon.

Recall that a structural property (see Chapter 2) is satisfied by all the systems belonging to a class, characterised by a structure, regardless of parameter values [NYWP07, BF11b]; this concept is related with robustness [CH08, ESPP$^+$06], which is however a less demanding requirement: to be robust, a property just needs to be preserved by the system under large parameter variations.

Structural analysis of chemical reaction networks, begun in the early seventies [HJ72, Hor73a, Hor73b], has provided fundamental results, such as the zero-deficiency theorem and the one-deficiency theorem [Fei87, Fei95a, Fei95b], on which a lot of subsequent work is grounded [CF05, CF06b, Cha06, And08, Han10]. The zero-deficiency theorem (thoroughly presented in Section 4.2.3) provides a structural general sufficient condition (0-deficiency, which is immediately verifiable from an easy test on the network structure) to assure that a chemical network described by mass action kinetics admits a single positive stable equilibrium; the result is nicely proved by adopting the system entropy as a Lyapunov function. A fundamental assumption in the zero-deficiency theorem requires the reaction kinetics to be of the mass action type (hence polynomial, although a possible generalisation is proposed in [Son01]). However this assumption, although being widely accepted, is not necessarily satisfied, as discussed in Section 4.2.4.

It is therefore interesting to study the behaviour of networks for which the mass action kinetics assumption does not necessarily hold. In this chapter, structural stability is investigated for a wide class of (bio)chemical reaction networks, under the sole requirement of monotonicity of the reaction rates. To prove stability, polyhedral Lyapunov functions are employed, which have a successful history in the robustness analysis of uncertain systems (see [BM15] for a literature survey) and have been used to prove the stability of compartmental systems [MKO78]. Indeed, compartmental systems can be seen as monomolecular chemical reactions in which each species can

be transformed into another (*e.g.*, $A \xrightarrow{g(a)} B$). Under the assumption of increasing reaction rate functions, stability can be proved by adopting as a Lyapunov function the 1-norm, which is a particular *polyhedral* (*i.e.*, *piecewise-linear*) norm.

Polyhedral norms have been used as candidate Lyapunov functions for biochemical networks in [BF11b], [FB13], although applied to specific problems. Also piecewise-linear in rate Lyapunov functions have been recently considered in [ARA13, ARA14, ARA15] for the stability analysis of chemical reaction networks.

The main idea in this chapter is that of adopting polyhedral norms (including the 1-norm as a special case) as candidate Lyapunov functions to investigate structural stability of chemical reaction networks with general, monotonic reaction rates.[1]

A theoretical framework is proposed and leads to a numerical procedure to generate piecewise-linear Lyapunov functions, which may certify the stability of all chemical reaction networks with a certain structure. If a piecewise-linear Lyapunov function is derived, network stability is structural: under monotonicity assumptions, it is assured for all reaction rate functions.

General chemical networks are considered, both isolated and with external inputs, under general monotonicity assumptions on the involved reaction rate functions (hence, without restricting to mass action kinetics reactions). Based on the network structure only, a polyhedral Lyapunov function (actually a norm) is sought for the system; to this aim, the nonlinear system equations are absorbed in a linear differential inclusion. The existence of a polyhedral Lyapunov function is shown to be equivalent to the stability of a suitable discrete difference inclusion, based on which a numerical recursive procedure is proposed to generate the unit ball of the associated polyhedral norm. Whenever a polyhedral Lyapunov function is found, the proposed procedure structurally certifies the stability of the system *for any choice* of monotonic reaction rate functions. In the case of *unitary* reaction networks, in which the stoichiometric matrix has coefficients in $\{-1, 0, 1\}$, the procedure enormously benefits from the fact that iterations occur in the set of integer-valued matrices. As expected, the seminal results in [MKO78] follow as a special case, since the procedure generates the 1-norm for compartmental systems. It is also shown that, once a polyhedral Lyapunov function is found, local stability of the equilibrium can be investigated, in isolated systems, within the stoichiometric compatibility class. An interpretation of the recursive numerical procedure in terms of the evolution of a discrete-event system is briefly outlined. A similar procedure is reported as well, which can be adopted, even when structural stability is not satisfied, to prove at least boundedness of the state variables.

[1] The monotonicity assumption is satisfied by almost all biochemical systems. Since experimental data are often noisy and uncertain, the estimated parameters in the dynamical model are expected to be highly uncertain too, and even finding an analytical expression for the involved functions may be extremely challenging (this is why it is crucial to be able to *structurally* assess properties, regardless of precise parameter values and exact functional expressions). However, typically the qualitative trends of the interactions are reliably evaluated according to the dynamic or steady state correlation of biochemical quantities. [BF14]

Structural stability and boundedness of several networks are investigated in Appendix A based on the proposed methods. Surprisingly, non-trivial systems can be managed without difficulties, providing either a positive stability certificate (by finding a piecewise-linear function with quite a small number of vertices) or a negative certificate (non-existence of such a function).

The methods in [BG14] can also be recast to the framework proposed in [ARA13, ARA14, ARA15], where the system variables are reaction rates, instead of species concentrations. All the results provided in [BG14], including the computational procedure, apply in the reaction-coordinates setup as well, because the system in reaction coordinates has the same *structure* as the differential inclusion considered in concentration coordinates. Under suitable assumptions on the rank of structural matrices, it can be shown that the stability of the system in reaction coordinates is equivalent to the stability of the corresponding differential inclusion in concentration coordinates. For *unitary* networks, this means that the proposed computational procedure converges in the former case if and only if it converges in the latter.

Can the same structural (parameter-free) stability results be achieved resorting to different candidate Lyapunov functions? For instance, quadratic Lyapunov functions have been successfully employed for the robustness analysis of uncertain systems [ZDG96, SPS98, BEGFB94]. However, it is well known that, for proving *robust* stability of linear differential inclusions, quadratic Lyapunov functions are conservative, while polyhedral Lyapunov functions are not [BT80, MP86a, MP86b, MP86c, MP89]. Consistently with previous work, it is shown that *structural* stability of some fundamental chemical reaction network motifs cannot be proved by means of quadratic Lyapunov functions, although these motifs are structurally stable, as can be demonstrated based on polyhedral Lyapunov functions. A simple example shows that furthermore, in some cases, it is not possible to resort to smooth Lyapunov functions at all. This substantiates the effectiveness of a polyhedral-Lyapunov-function approach to the *structural* stability analysis of biochemical networks.

6.2 Absorbing the System in a Differential Inclusion

Consider the class of models

$$\dot{x} = Sg(x) + g_0, \tag{6.1}$$

where the state $x \in \mathbb{R}^n_+$ represents the concentration of biochemical species, $g(x) \in \mathbb{R}^m$ is a vector of functions representing the reaction rates and $g_0 \geq 0$ is a vector of constant influxes; $S \in \mathbb{Z}^{n \times m}$ is the stoichiometric matrix of the system, whose entries s_{ij} represent the net amount of the ith species produced or consumed by the jth reaction, excluding the contribution of constant influxes.

Assumption 6.1. *All the component functions of vector $g(x)$ are nonnegative and continuously differentiable. All their partial derivatives are positive in the interior of the positive orthant.*

Decreasing trends can be considered as well: in some cases, this just requires changing sign to g. An important case is that of a species which is present in a total amount $x_i^{tot} > 0$ and can be either active, x_i, or inactive, x_i^*, with $x_i + x_i^* = x_i^{tot}$. Since $0 \leq x_i \leq x_i^{tot}$, the activation term must be the only positive term in the right side of the equation. For instance, the equation

$$\dot{a} = -g_{in}(a, b) + g_{act}(a^{tot} - a, c) \tag{6.2}$$

includes the inhibition term g_{in} and the activation term g_{act}.

Assumption 6.2. *Each component function of vector $g(x)$ is zero if and only if at least one of its arguments is zero. Moreover, if $s_{ij} < 0$, then g_j must depend on x_i.*

Assumption 6.2, ensuring that $\dot{x}_i \geq 0$ for $x_i = 0$, is required to guarantee that (6.1) is a positive system. For instance, $g_{in}(a, b)$ in (6.2) can be of the form $\kappa\frac{ba}{1+a}$, but not of the form $\kappa\frac{b}{1+a}$.

Example 6.1. *A biochemical network is proposed in [FB12] representing an oscillator model inspired by the experimental system in [KW11], where a synthetic oscillator is built* in vitro. *The synthetic system is composed of two short synthetic genes, termed* genelets, *which are interconnected through their RNA outputs and, in the absence of enzymes, are activated (inactivated) thanks to the binding of a DNA activator (inhibitor) strand. A subset of the overall set of reactions, corresponding to the* activated *subsystem, is considered here as a standalone system. The corresponding chemical reactions*

$$A + B \xrightarrow{g_{ab}(a,b)} A^*, \qquad B^* \xrightarrow{g_b(b^*)} B,$$
$$C + A^* \xrightarrow{g_{ac}(a^*,c)} A + B^*, \qquad \emptyset \xrightarrow{c_0} C$$

involve the genelet species A (and its inactive form A^*), the inhibitor strand B (and its inactive form B^*) and the RNA output C. Along with the mass conservation constraints $a^{tot} = a + a^*$ and $b^{tot} = b + b^* + a^*$, these reactions correspond to the following ODEs for $x = [a\ b\ c]^\top$:

$$\begin{cases} \dot{a} = g_{ac}(a^{tot} - a, c) - g_{ab}(a, b) \\ \dot{b} = g_b(b^{tot} - a^{tot} + a - b) - g_{ab}(a, b) \\ \dot{c} = c_0 - g_{ac}(a^{tot} - a, c) \end{cases}$$

Then,

$$S = \begin{bmatrix} 1 & -1 & 0 \\ 0 & -1 & 1 \\ -1 & 0 & 0 \end{bmatrix}, \quad g(x) = \begin{bmatrix} g_{ac}(a^{tot} - a, c) \\ g_{ab}(a, b) \\ g_b(b^{tot} - a^{tot} + a - b) \end{bmatrix}, \quad g_0 = \begin{bmatrix} 0 \\ 0 \\ c_0 \end{bmatrix}.$$

Possible reactions, along with the corresponding reaction terms appearing in the proper equations, are in the following (non-exhaustive) list.

(a) $\emptyset \xrightarrow{a_0} A$: $\dot{a} = a_0$, a_0 constant
(b) $A \xrightarrow{g(a)} \emptyset$: $\dot{a} = -g(a)$
(c) $A \xrightarrow{g(a)} B$: $\dot{a} = -g(a),\ \dot{b} = g(a)$
(d) $A + B \xrightarrow{g(a,b)} \emptyset$: $\dot{a} = -g(a,b),\ \dot{b} = -g(a,b)$
(e) $A + B \xrightarrow{g(a,b)} C$: $\dot{a} = -g(a,b),\ \dot{b} = -g(a,b),\ \dot{c} = g(a,b)$
(f) $A \xrightarrow{g(a)} B + C$: $\dot{a} = -g(a),\ \dot{b} = g(a),\ \dot{c} = g(a)$
(g) $A + B \xrightarrow{g(a,b)} C + D$: $\dot{a} = -g(a,b),\ \dot{b} = -g(a,b),\ \dot{c} = g(a,b),\ \dot{d} = g(a,b)$
(h) *Activation* $A^* + B \xrightarrow{g(a^*,b)} A$: $\dot{a} = g(a^{tot} - a, b),\ \dot{b} = -g(a^{tot} - a, b)$, with $a + a^* = a^{tot}$, where a^{tot} is the total concentration
(i) *Difference dependence* (see Example 6.1): $\dot{a} = g(a^{tot} - b^{tot} - a + b)$

Any network can be represented by a graph, whose nodes are associated with biochemical species and whose arcs represent interactions (reactions). Fig. 6.1 defines the arcs corresponding to the reactions in the above list. The graph of Example 6.1 corresponds to that in Fig. 6.2.

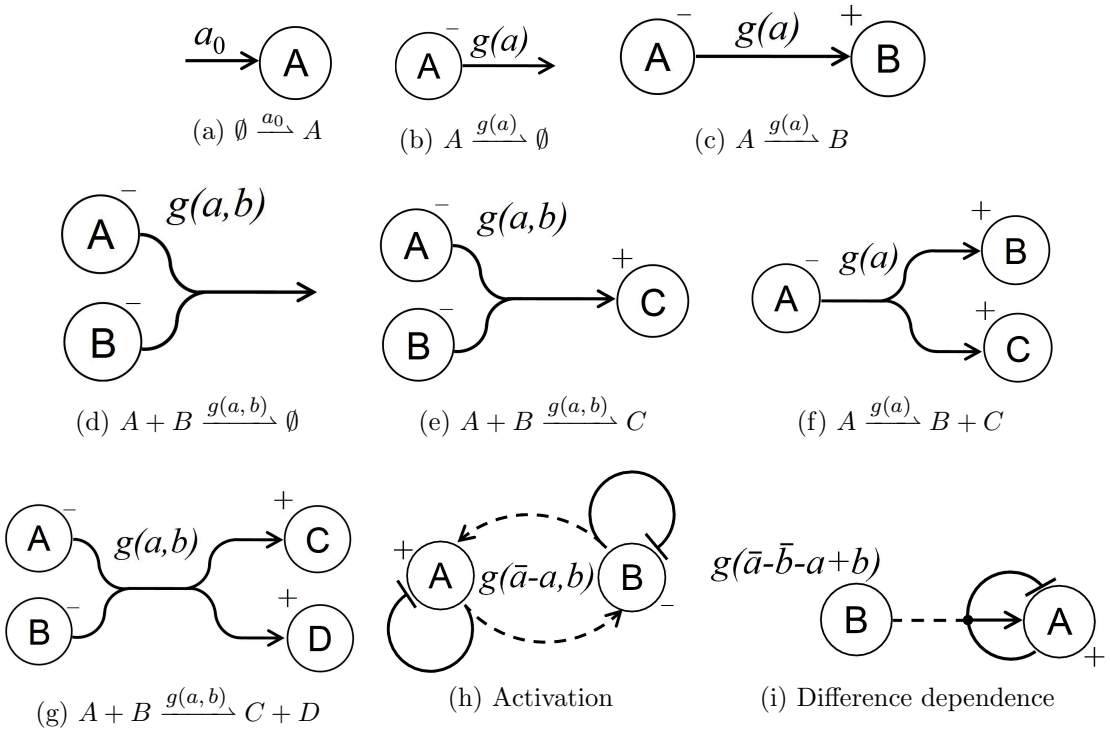

(a) $\emptyset \xrightarrow{a_0} A$ (b) $A \xrightarrow{g(a)} \emptyset$ (c) $A \xrightarrow{g(a)} B$
(d) $A + B \xrightarrow{g(a,b)} \emptyset$ (e) $A + B \xrightarrow{g(a,b)} C$ (f) $A \xrightarrow{g(a)} B + C$
(g) $A + B \xrightarrow{g(a,b)} C + D$ (h) Activation (i) Difference dependence

Figure 6.1: Graph representations of biochemical reactions. [BG14]

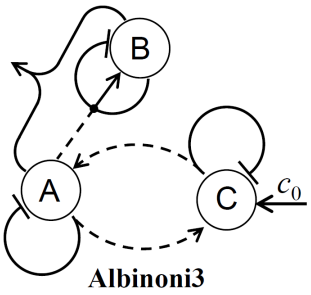

Figure 6.2: Graph of the network in Example 6.1. [BG14]

Assumption 6.3. *Functions $g_j(\cdot)$ in which each argument depends on a single variable x_i are admitted if $s_{ij}\frac{\partial g_j}{\partial x_i} < 0$ for each argument. Functions having as an argument the sum or difference of more variables, such as $g_j(x_i - x_k)$, or $g_j(x_i + x_k)$, are admitted if they appear in a single equation, $\dot{x}_k = \ldots$, where x_k is one of the variables of the linear combination, and $s_{kj}\frac{\partial g_j}{\partial x_k} < 0$.*

Hence, the diagonal entries of the Jacobian of $Sg(x)$ are negative and no autocatalytic reactions are considered. Also reactions of the form $A \rightharpoonup A + B$, often used to model gene expression, are not allowed. Nevertheless, a more complete gene expression model will be successfully analysed in Section 6.8.

Remark 6.1. *Ruling out autocatalytic reactions is not necessary at all for the proposed theoretical framework, or for the numerical procedure in Section 6.3.1, to be applicable. Simply, for networks with autocatalytic reactions, the polyhedral-function procedure would not converge and, of course, no structural stability certificate would be issued.*

Networks composed of reactions in the list (cf. Fig. 6.1) form a subset of those satisfying Assumption 6.3. These networks are also *unitary*, according to the next definition.

Definition 6.1. *The network is* unitary *if $s_{ij} \in \{-1, 0, 1\}$.*

Remark 6.2. *Requiring a network to be unitary is a restriction: for instance, multimolecular reactions of the type $nA + B \rightharpoonup P$, with $n > 1$, would be ruled out. However, two basic points are worth noticing.*

- *In the considered setup, the restriction is not theoretical, but essentially computational. In fact, the theory works in general, although the numerical procedure might not converge in finite time for non-unitary networks. This issue will be reconsidered in Section 6.3.2.*
- *Multimolecular reactions can be always expressed as a cascade of bimolecular reactions, which are unitary. For instance, $2A + B \rightharpoonup P$ can be decomposed as the pair of unitary reactions $A + B \rightharpoonup C$ and $C + A \rightharpoonup P$. Such a decomposition is justified, since trimolecular reactions are considered unlikely to happen and*

no reactions concurrently involving more than three molecules have yet been observed; therefore an overall reaction is more plausibly modelled by a chain of bimolecular steps (see, for instance, [EK05] Section 7.4 or [Lev99] Sections 2.1, 2.3).

Both isolated systems ($g_0 = 0$) and non-isolated systems ($g_0 \neq 0$) can be considered in the proposed framework. For $g_0 = 0$, as discussed in Section 4.2.1, the solution of the system is forced to stay in the *stoichiometric compatibility class* $\mathcal{C}(x(0))$:

$$x(t) \in \mathcal{C}(x(0)) = \{x(0) + \text{span}(S)\} \cap \mathbb{R}^n_+.$$

Example 6.2. *Consider the reactions*

$$X_1 \underset{g_2(x_2)}{\overset{g_1(x_1)}{\rightleftharpoons}} X_2, \qquad \emptyset \xrightarrow{g_{01}} X_1, \qquad \emptyset \xrightarrow{g_{02}} X_2$$

corresponding to the second order nonlinear system

$$\begin{bmatrix} \dot{x}_1 \\ \dot{x}_2 \end{bmatrix} = \begin{bmatrix} -1 & 1 \\ 1 & -1 \end{bmatrix} \begin{bmatrix} g_1(x_1) \\ g_2(x_2) \end{bmatrix} + \begin{bmatrix} g_{01} \\ g_{02} \end{bmatrix}.$$

Then, for $g_0 = 0$, the stoichiometric compatibility class is

$$\mathcal{C}(x(0)) = \{x_1 + x_2 = x_1(0) + x_2(0), \quad x_1,\ x_2 \geq 0\}.$$

To perform a structural analysis, the ε-modified system

$$\dot{x}(t) = -\varepsilon x(t) + Sg(x(t)) + g_0, \tag{6.3}$$

with $\varepsilon > 0$ arbitrarily small, is considered and the following definitions of stability are introduced.

Definition 6.2. *System* (6.1) *is*

i) ***structurally stable*** *if any equilibrium point $\bar{x}$ of the system with $\varepsilon = 0$ and $g_0 \geq 0$ (if such a point exists) is Lyapunov stable: there exists a continuous, strictly increasing and unbounded function $\omega : \mathbb{R}_+ \to \mathbb{R}_+$, with $\omega(0) = 0$, such that $\|x(t) - \bar{x}\| \leq \omega(\|x(0) - \bar{x}\|)$;*

ii) ***structurally convergent*** *if it is structurally stable and, for any $\varepsilon > 0$ and $g_0 \geq 0$, the perturbed system* (6.3) *has globally bounded solutions and admits an equilibrium which is globally asymptotically stable in $\mathbb{R}^n_+$.*

The previous definitions are structural, in that they do not require the knowledge of function $g(\cdot)$: hence, they hold for any choice of $g(\cdot)$ and its parameters, provided that it satisfies the stated assumptions. Note that the existence of an equilibrium is not always guaranteed.

Example 6.3. *The reaction network*

$$\begin{cases} \dot{a} = -g_{ab}(a,b) + a_0 \\ \dot{b} = -g_{ab}(a,b) + b_0 \end{cases}$$

has no equilibrium if $a_0 \neq b_0$. *Conversely, the reaction network*

$$\begin{cases} \dot{a} = -g_{ab}(a,b) + a_0 \\ \dot{b} = -g_{ab}(a,b) - g_b(b) + b_0 \end{cases}$$

admits an equilibrium iff $b_0 > a_0$.

The existence of equilibria typically requires boundedness of the system solutions, a problem that will be considered later (in Section 6.7), assuming ε-dissipation.

The infinitesimal parameter $\varepsilon > 0$ in (6.3) is required for technical reasons. The considered parameters are sign definite but, having unknown values, they can be arbitrarily close to zero. Therefore, after absorbing the system in a differential inclusion, to assess *asymptotic* stability, a natural degradation of the species (represented by $\varepsilon > 0$) needs to be considered in general. Considering a spontaneous degradation is reasonable in biochemical systems and, in practice, the introduction of ε in Definition 6.2 ii) does not lead to the classification as stable of systems which are unstable (namely, a wrong stability certificate for unstable systems cannot be produced). The presence of the degradation term is necessary for the system to tolerate persistent positive inputs. For instance, according to the definition, the system of Example 6.2 is structurally stable and convergent. Without any ε-degradation, it would produce unbounded solutions, unless $g_0 = 0$. For $g_0 = 0$, any of its equilibrium points is only marginally stable. However, it has the property of *asymptotic stability within the stoichiometric compatibility class*, a problem that will be faced later without considering any $\varepsilon > 0$.

Assume that an equilibrium $\bar{x} = \bar{x}(\varepsilon)$ exists $\forall\, \varepsilon \geq 0$.[2] To find a criterion for global asymptotic stability, the system is absorbed in a differential inclusion.

Denote $z \doteq x - \bar{x}$, hence $x = z + \bar{x}$. Since $0 = S\, g(\bar{x}) - \varepsilon\bar{x} + g_0$, it is possible to write

$$\dot{z}(t) = S\, [g(z(t) + \bar{x}) - g(\bar{x})] - \varepsilon z(t). \tag{6.4}$$

Note that this is not a linearisation: it is a *nonlinear shifted system*, which is globally (and not only locally) equivalent to the original system. For this system, the following proposition holds.

Proposition 6.1. *System* (6.4) *can be equivalently written as*

$$\dot{z}(t) = BD(z(t))C\; z(t) - \varepsilon z(t), \tag{6.5}$$

[2] As will be shown later, such an equilibrium indeed exists if the system passes the proposed computational test.

where matrix $B \in \mathbb{Z}^{n\times q}$ is formed by a selection of columns of S, $C \in \mathbb{Z}^{q\times n}$ and $D(z)$ is a diagonal matrix with nonnegative diagonal entries. q is the number of possible partial derivatives with respect to all arguments ($q \geq n$, $q \geq m$).

Proof. Consider the generic function $g_k(x_i, x_j)$ (the argument applies to functions of more than two variables as well) and write it as

$$\begin{aligned}
&g_k(z_i + \bar{x}_i, z_j + \bar{x}_j) - g_k(\bar{x}_i, \bar{x}_j) = \\
&\frac{g_k(z_i + \bar{x}_i, z_j + \bar{x}_j) - g_k(\bar{x}_i, z_j + \bar{x}_j)}{z_i} z_i + \frac{g_k(\bar{x}_i, z_j + \bar{x}_j) - g_k(\bar{x}_i, \bar{x}_j)}{z_j} z_j = \\
&\frac{\partial g_k(\tilde{x}_i, \bar{x}_j)}{\partial x_i} z_i + \frac{\partial g_k(\bar{x}_i, \tilde{x}_j)}{\partial x_j} z_j = (\pm D_{ki}) z_i + (\pm D_{kj}) z_j,
\end{aligned}$$

in view of the differential mean value theorem, where $\tilde{x}_i$ and $\tilde{x}_j$ are proper values in the intervals $[\bar{x}_i, z_i + \bar{x}_i]$ and $[\bar{x}_j, z_j + \bar{x}_j]$ respectively, while D_{ki} and D_{kj} are nonnegative scalar functions of $\bar{x}$ and z. The values $\tilde{x}_i$ and $\tilde{x}_j$ are not necessarily unique and depend on the function g_k.

Alternatively, the same expression can be derived by adopting the integral expressions (4.32) and (4.33) in Section 4.3.1. Ordering the partial derivatives D_{ki} and D_{kj} as D_1, D_2, etc., $D = \text{diag}\{D_1, D_2, \ldots, D_q\}$. Matrix B is achieved by replicating (up to the sign) each column of S, say the kth, a number of times equal to the arguments of g_k. In matrix C, c_{ki} is ± 1 if D_k is with respect to x_i, 0 if it is not. □

Example 6.4. *Consider the system of Example 6.1 and let $D_1 = -\frac{\partial g_{ac}}{\partial a}$, $D_2 = \frac{\partial g_{ab}}{\partial a}$, $D_3 = \frac{\partial g_{ab}}{\partial b}$, $D_4 = \frac{\partial g_{ac}}{\partial c}$, $D_5 = \frac{\partial g_b}{\partial a}$ be positive parameters. Then*

$$B = \begin{bmatrix} -1 & -1 & -1 & 1 & 0 \\ 0 & -1 & -1 & 0 & 1 \\ 1 & 0 & 0 & -1 & 0 \end{bmatrix},\ D = diag(D_1, \ldots, D_5),\ C = \begin{bmatrix} 1 & 1 & 0 & 0 & 1 \\ 0 & 0 & 1 & 0 & -1 \\ 0 & 0 & 0 & 1 & 0 \end{bmatrix}^\top.$$

Remark 6.3. *The system Jacobian J_ε evaluated at any point has exactly the same structure $J_\varepsilon = BDC - \varepsilon I$ as the matrix of* (6.5)*. Hence, it can be said that the system admits a BDC-decomposition (see Section 4.3).*

Remark 6.4. *Denoting by B_i the ith column of matrix B and by $C_i^\top$ the ith row of matrix C, Assumption 6.3 implies that*

$$C_i^\top B_i < 0 \quad \forall\, i. \tag{6.6}$$

For unitary networks, $C_i^\top B_i = -1\ \forall\, i$, with noteworthy numerical benefits.

System (6.5) is equivalent to the original nonlinear *shifted* system; if in (6.5) $D(z(t))$ is replaced by $D(t)$, a linear differential inclusion is obtained, such that all the trajectories of (6.5) are also trajectories of the differential inclusion. With an abuse,

the notation $\dot{z} = ...$ will be used instead of $\dot{z} \in ...$, since the differential inclusion will be actually studied as a standalone system. The goal will be to exploit the tight relationship between the original system and the associated linear differential inclusion, in order to show that stability of the original system can be structurally proved by means of a polyhedral Lyapunov function if and only if *that* function is a polyhedral Lyapunov function for the differential inclusion.

The following theorem can be stated.

Theorem 6.1. *Consider the linear differential inclusion*

$$\dot{z}(t) = \left[-\varepsilon I + \sum_{i=1}^{q} B_i D_i(t) C_i^\top\right] z(t), \quad z(0) = z_0 \tag{6.7}$$

where $D_i(t)$ are arbitrary nonnegative scalar piecewise-continuous functions.[3] *Then:*

1. *marginal stability of* (6.7) *for $\varepsilon = 0$ implies structural stability of any equilibrium of* (6.1)*;*
2. *asymptotic stability of* (6.7) *for $\varepsilon > 0$ implies structural convergence of* (6.1)*.*

Proof. If $\bar{x}$ is any equilibrium point, then, denoting by $z = x - \bar{x}$, the nonlinear system can be absorbed in the linear differential inclusion. All the solutions $z(t)$ are then solutions of (6.7) for $\varepsilon = 0$, hence stability of (6.7) implies structural stability.

In the case $\varepsilon > 0$, being the set of solutions of (6.5) a subset of the set of solutions of the differential inclusion (6.7), it is just necessary to prove that, if (6.7) is asymptotically stable, then (6.3) admits a steady state $\bar{x}$ for any $\varepsilon > 0$; its global stability is then immediate.

After some computations (see [BG14] for details), (6.3) can be written in the form of (6.7) with an additive constant term; indeed, replacing $D(z(t))$ with $D(t)$ leads to the differential inclusion

$$\dot{z}(t) = [-\varepsilon I + BD(t)C]z(t) + \tilde{g}_0.$$

If (6.7) is asymptotically stable, then the solutions of the differential inclusion are bounded; since they are a superset of the solutions of (6.3), then (6.3) has bounded solutions as well and it necessarily admits a steady-state value $\bar{x}$ (depending on ε). □

Remark 6.5. *Absorbing the trajectories of the nonlinear system in those of a linear differential inclusion is completely different from considering the system linearisation around an equilibrium point. The stability of the differential inclusion is a sufficient condition for the stability of the original system. As will be seen later, a polyhedral function exists for the former iff it exists for the latter.*

[3] Piecewise-continuous means that the number of discontinuity points is finite in each finite interval and, in each of these intervals, right and left limits are finite.

From the proof of Theorem 6.1 the next Corollary follows.

Corollary 6.1. *If the differential inclusion* (6.7) *is asymptotically stable, then* (6.3) *admits an equilibrium.*

The following equivalence is worth pointing out.

Proposition 6.2. *Marginal stability of* (6.7) *for* $\varepsilon = 0$ *is equivalent to its asymptotic stability for* $\varepsilon > 0$.

Proof. The statement is immediately proved since, given $D_i(t) \geq 0$ and denoting by $z_0(t)$ the solution corresponding to $\varepsilon = 0$, the solution corresponding to $\varepsilon > 0$ is

$$z_\varepsilon(t) = e^{-\varepsilon t} z_0(t).$$

□

In view of Proposition 6.2, the two claims of Theorem 6.1 can only be verified together.

6.3 Analysis of the Differential Inclusion

The stability of the differential inclusion (6.7) can be analysed by considering an associated discrete-time difference inclusion. Then, the main idea (depicted in Fig. 6.3) is the following: if all the possible discrete transitions starting from the vertices of the diamond (the unit ball of $\|x\|_1$) remain bounded, then the continuous-time solution remains trapped inside the convex hull of the reached points (stable case); conversely, if the difference inclusion diverges, so does the differential inclusion, since there exist continuous-time solutions arbitrarily close to the discrete-time solutions.

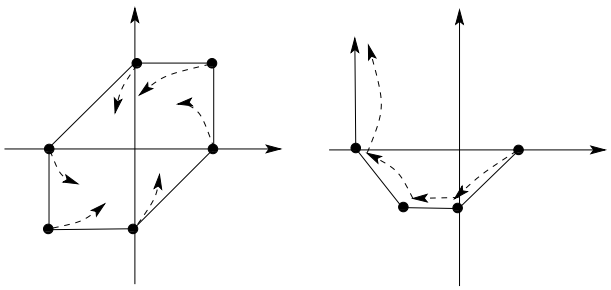

Figure 6.3: The idea: convergent case (left); divergent case (right). [BG14]

First consider the case $\varepsilon = 0$ in (6.7). Since $D_i(t)$ are arbitrary nonnegative, at best marginal stability can be proved.[4] For any state value $z \in \mathbb{R}^n$, the set of all

[4]For instance, $\dot{x}(t) = -D(t)x(t)$, $D(t) > 0$ is not necessarily asymptotically stable: the solution does not converge to 0 if $D(t)$ goes to 0 too quickly.

derivatives is included in a cone of directions $\pm B_i$:

$$\dot{z} \in \{v : \ v = \sum_{i=1}^{q} v_i D_i, \quad D_i \geq 0\}, \quad \text{where} \quad v_i = B_i C_i^\top z.$$

Therefore, if a common convex Lyapunov function exists for all the special systems

$$\dot{z} = B_i C_i^\top z, \tag{6.8}$$

with $i = 1, \ldots, q$, then the same function is a Lyapunov function for the differential inclusion (and the nonlinear system).

The solutions of (6.8) with initial state z_0 can be written as

$$z(t) = z_0 + \int_0^t B_i C_i^\top z(\sigma) d\sigma = z_0 + B_i \vartheta(t)$$

where $\vartheta(t) = \int_0^t C_i^\top z(\sigma) d\sigma$. To find ϑ, the variable $(C_i^\top z)$ can be considered, which satisfies the differential equation

$$\frac{d}{dt}(C_i^\top z) = (C_i^\top B_i)(C_i^\top z).$$

Its solution is $C_i^\top z(t) = C_i^\top z_0 e^{C_i^\top B_i t}$ and asymptotically converges to zero, since $C_i^\top B_i < 0$ (see Remark 6.4). Then $z(t)$ converges to a finite value z_∞. Without computing the integral, the limit can be achieved as the value such that

$$C_i^\top z_\infty = C_i^\top (z_0 + B_i \vartheta_\infty) = 0,$$

which yields $\vartheta_\infty = -C_i^\top z_0 / (C_i^\top B_i)$.

The dynamics (6.8) asymptotically drives the state from z_0 to

$$z_\infty = z_0 + B_i \vartheta_\infty = z_0 - \frac{B_i C_i^\top z_0}{C_i^\top B_i} = \left[I - \frac{B_i C_i^\top}{C_i^\top B_i} \right] z_0.$$

Then, the family of matrices

$$\mathcal{F} = \left\{ \Phi_i \doteq \left[I - \frac{B_i C_i^\top}{C_i^\top B_i} \right], \quad i = 1, \ldots q \right\} \tag{6.9}$$

can be considered, along with the discrete linear difference inclusion (actually a discrete-time switching system) $y(k+1) = \Phi(k) y(k)$, where $\Phi(k)$ is an arbitrary sequence in $\mathcal{F}$ and $y(k) \in \mathbb{R}^n$.

Consider then the two systems

$$\dot{z}(t) = BD(t)Cz(t), \quad D_i(t) \geq 0 \tag{6.10}$$

and

$$y(k+1) = \Phi(k) y(k), \quad \Phi(k) \in \mathcal{F}. \tag{6.11}$$

A technical lemma, thoroughly proved in [BG14], shows that any solution of the discrete-time system is approached by a continuous-time solution for large enough time.

Lemma 6.1. *Given systems* (6.10) *and* (6.11)*, both starting from the initial condition* $y(0) = z(0)$*, then* $\forall\, k > 0$ *and* $\forall\, \delta > 0$*, no matter how small, there exists* $t > 0$ *such that* $\|z(t) - y(k)\| < \delta$*.*

The result in Lemma 6.1 is interesting *per se*, because it proves that, in view of the peculiar properties of the considered systems, the stability of the continuous-time system implies that of the discrete-time system (while, in general, only the opposite is true). Moreover, based on Lemma 6.1, the following result in [BG14] can be proved, stating that discrete and continuous-time stability are equivalent.

Theorem 6.2. *Robust stability of the continuous-time system* (6.10) *is equivalent to robust stability of the discrete-time system* (6.11)*.*

Proof. If the continuous-time system (6.10) is stable, Theorem 5.2 in [Bla91] guarantees that there exists a convex and compact set including 0 in its interior (namely, a C-set), $\mathcal{S}$, which is robustly positively invariant for (6.10). Then, $\mathcal{S}$ must be robustly positively invariant also for (6.11). In fact, assume by contradiction that, for $y(0) \in \partial\mathcal{S}$ (the boundary of $\mathcal{S}$), it can be written

$$y(1) = \Phi_i y(0) \notin \mathcal{S} \quad \text{for some} \quad \Phi_i \in \mathcal{F}.$$

A neighbourhood $\mathcal{B}$ of $y(1)$ exists such that $\mathcal{B} \bigcap \mathcal{S} = \emptyset$. In view of Lemma 6.1 a continuous-time solution $z(t)$ exists that is arbitrarily close to $y(1)$ and, hence, enters the set $\mathcal{B}$. Yet, this violates the assumption that $\mathcal{S}$ is positively invariant for (6.10).

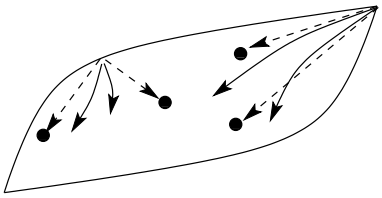

Figure 6.4: Continuous-time solutions (solid) point inside the cone defined by discrete-time solutions (dashed). [BG14]

If, conversely, the discrete-time system (6.11) is stable, then Theorem 5.1 in [Bla91] guarantees that there exists a C-set $\mathcal{S}$ which is positively invariant for (6.11). Hence, if $y(0) \in \partial\mathcal{S}$, by the definition of Φ_i,

$$y(1) = \Phi_i y(0) = \left[I - \frac{B_i C_i^\top}{C_i^\top B_i} \right] y(0) \in \mathcal{S}.$$

The Bouligand tangent cone to $\mathcal{S}$ in $y(0)$ (see Fig. 6.4) is defined as [BM15]

$$\mathcal{T}(y(0)) = \left\{ z : \lim_{h \to 0} \frac{\operatorname{dist}(y(0) + hz, \mathcal{S})}{h} = 0 \right\},$$

where $\mathrm{dist}(u, \mathcal{S}) = \inf_{v \in \mathcal{S}} \|u - v\|$ is the distance of u from the set $\mathcal{S}$. Since $y(0)$ and $y(1)$ are both in the convex set $\mathcal{S}$, their difference is in the tangent cone: for all i,

$$y(1) - y(0) = -\frac{B_i C_i^\top}{C_i^\top B_i} y(0) \in \mathcal{T}(y(0)).$$

The tangent cone to a convex set is convex. Therefore, by combining the vectors achieved for all i with arbitrary nonnegative coefficients $\tilde{D}_i \geq 0$, the derivative can be expressed as

$$\dot{z} = \sum_{i=1}^{q} (-\tilde{D}_i) \frac{B_i C_i^\top}{C_i^\top B_i} y(0) = \sum_{i=1}^{q} B_i D_i C_i^\top y(0) \in \mathcal{T}(y(0)),$$

where $D_i \doteq -\tilde{D}_i / (C_i^\top B_i) \geq 0$. Then Nagumo's theorem [Nag42, Bla91] can be invoked, which states that any convex and compact set $\mathcal{S}$ is positively invariant for (6.10) if and only if $\dot{z} \in \mathcal{T}(z)$ for all $z \in \partial\mathcal{S}$. Hence, it can be concluded that $\mathcal{S}$ is positively invariant for (6.10). Details are provided in [BG14]. □

Remark 6.6. *In general, the theorem holds in one direction only (namely, the differential inclusion is stable if the difference inclusion is stable) and the opposite is not true: for instance, taking $q = 1$ and the stable $A_1 = \left[\begin{smallmatrix} 0 & 1 \\ -1 & 0 \end{smallmatrix}\right]$, $I + D_1 A_1$ is unstable.*

Polyhedral Lyapunov function. Given a full row rank matrix $X \in \mathbb{R}^{n \times s}$,

$$V_X(x) = \inf\{\|w\|_1 : \ Xw = x, \ w \in \mathbb{R}^s\}$$

is a polyhedral norm; the vertices of its unit ball are the columns of matrix X and their opposites (see Fig. 6.5). Given a full column rank matrix $M \in \mathbb{R}^{s \times n}$, the dual function is

$$V^M(x) = \|Mx\|_\infty;$$

the facets of its unit ball are on the planes $M^k x = 1$ or $M^k x = -1$, where M^k is the kth row of M. Then, the positive definite function $V_X(x)$ ($V^M(x)$) is a weak Lyapunov function if it is non-increasing along all possible system trajectories.

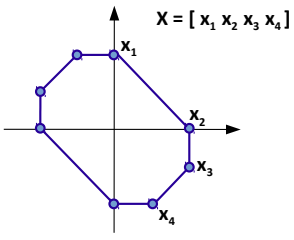

Figure 6.5: Polyhedral unit ball of a piecewise-linear Lyapunov function.

Theorem 6.2 admits the following corollary.

Corollary 6.2. (6.11) *is marginally stable and admits a weak polyhedral Lyapunov function if and only if* (6.10) *is marginally stable and admits the same weak Lyapunov function.*

Proof. By homogeneity, a norm is a weak Lyapunov function iff its unit ball $\mathcal{B}$ (which is a C-set) is positively invariant. In view of the proof of Theorem 6.2, such $\mathcal{B}$ is positively invariant for (6.11) if and only if it is positively invariant for (6.10). □

The main asymptotic stability result in [BG14] is the following.

Theorem 6.3. *If* (6.11) *admits a weak Lyapunov function, then*

1. (6.7) *is marginally stable for* $\varepsilon = 0$*;*
2. (6.7) *is asymptotically stable for* $\varepsilon > 0$*;*
3. (6.1) *is structurally convergent.*

6.3.1 Computational Procedure

The unit ball of a polyhedral Lyapunov function for (6.11) can be computed as follows. Given matrix X, let $Y = \mathrm{mr}(X)$ be its minimal polytopic representation (*i.e.*, the minimal subset of columns of X for which $V_X(x) = V_Y(x)$), achieved from X by removing all the redundant vertices. In the set of polyhedra, define the iterate:

$$X^{k+1} = \Psi(X^k), \tag{6.12}$$

where

$$\Psi(X) = \mathrm{mr}\,[X \quad \Phi_1 X \quad \cdots \quad \Phi_q X]\,.$$

The linear differential inclusion (6.11) admits a polyhedral Lyapunov function if and only if Ψ has a fixed point $\Psi(X) = X$. [AR08]

The computation of X^k can start from any arbitrary full row rank integer matrix X^0; for simplicity, set $X^0 = [-I \;\; I]$. Then the procedure works as follows.[5]

Procedure 6.1. ***Polyhedral function algorithm.***

1. *Fix* $\nu > 1$*, integer. Let* $X^0 := [-I \;\; I]$
2. *Compute the sequence* (6.12)*, until either*

   Successful stop: $X^k \equiv X^{k-1}$,

   Unsuccessful stop: $\max_{ij} |X^k|_{ij} > \nu$.

[5] A MATLAB implementation of the procedure is available at `http://users.dimi.uniud.it/~franco.blanchini/polychem.zip` (see also Appendix B.1).

Remark 6.7. *The quantity ν represents the maximum "tolerated escape"; for instance, the unsuccessful stop due to violation for $\nu = 10$ means that a trajectory has gone far away 10 times with respect to the initial ball size. In fact, if the procedure does not converge with a certain ν, there will be a continuous-time trajectory originating from $\|x(0)\|_1 \leq 1$ such that $\|x(t)\|_\infty$ approaches the value ν for large t, since continuous-time trajectories can get arbitrarily close to discrete-time trajectories. Since $\|x\|_1 \geq \|x\|_\infty$, ν corresponds to the accepted tolerance for the ratio of the maximum 1-norm during the transient evolution of the system to the initial 1-norm, and can be fixed accordingly. Moreover, if the convex hull of X includes the convex hull of X^0 in its interior, then the difference inclusion is unstable, hence no Lyapunov function exists: this will be proved soon, by resorting to the dual procedure.*

A dual procedure can be considered, having the same properties, in which the iterations are applied to the dual system

$$y(k+1) = \Phi(k)^\top y(k),$$

whose stability is equivalent to stability of the primal [BM15]; hence, the dual procedure converges iff the primal does. In case of convergence to a matrix $\bar{X}$, the primal system admits the polyhedral Lyapunov function $V^M(x) = \|\bar{X}^\top x\|_\infty$.

The dual procedure adopts the dual representation F for each set

$$\{x : -\bar{1} \leq Fx \leq \bar{1}\}$$

and proceeds backward in time. Starting from the dual set of the unit diamond, namely, from the unit box $\{x : -\bar{1} \leq F_0 x \leq \bar{1}\}$, where $F_0 = I$, the set sequence is computed backward in time, as follows. Let the pre-image be defined as

$$F_{k+1} = \Psi^{-1}(F_k) = \mathrm{mr}\left\{x : -\bar{1} \leq F_0 x \leq \bar{1}, \quad -\bar{1} \leq F_k \Phi_h x \leq \bar{1}, \quad h = 1, \ldots, q\right\}.$$

This is the set of all the states x in the original set, such that $\Phi_h x$ (and all their convex combinations) are in the set $\{y : -\bar{1} \leq Fy \leq \bar{1}\}$. The dual iteration is then

$$F_{k+1} = \Psi^{-1}(F_k). \tag{6.13}$$

Procedure 6.2. ***Polyhedral function dual algorithm.***

1. *Fix $\nu > 1$, integer. Let $F_0 := I$*
2. *Compute the sequence* (6.13)*, until either*

   Successful stop: $F_k \equiv F_{k-1}$,

   Unsuccessful stop: $\max_{ij} |F_k|_{ij} > \nu$.

The unsuccessful condition implies that the backward procedure has produced a set that has "collapsed inside" (the larger F, the smaller the set). The following result can then be invoked.

Proposition 6.3. *If the set represented by* $\{x : -\bar{1} \leq F_k x \leq \bar{1}\}$ *is included in the interior of the convex hull of the original one, then the procedure will not converge.*

The proof is reported in [BM96]. Since the dual procedure corresponds to the primal procedure applied to the dual system, the stopping criterion applies to the primal procedure as well, if the set obtained at a certain iteration includes the original one in its interior.

For unitary networks, the computation of the iterates turns out to be particularly efficient: if $C_i^\top B_i = -1$ for all i, indeed, then the sequence X^k is integer for any X^0 integer (because, for unitary networks, Φ_k as in (6.9) are integer matrices). Therefore, when assessing structural stability of unitary networks, polyhedral functions with integer vertices can be determined and it can be guaranteed that the procedure stops in a finite number of steps (since the number of integer matrices satisfying the condition $\max_{ij} |X|_{ij} \leq \nu$ is finite, then the iterate X^k can either leave the set or hit a fixed point).

Moreover, for unitary networks, the next corollary holds.

Corollary 6.3. *If* $C_i^\top B_i = -1$*, then stability of* (6.7) *is equivalent to the existence of a polyhedral Lyapunov function.*

An equivalence result can then be stated: a polyhedral function is a Lyapunov function for the nonlinear system if and only if it is a Lyapunov function for the linear differential inclusion.

Theorem 6.4. *System* (6.1)*, admitting a steady state* $\bar{x}$*, is stable with a polyhedral Lyapunov function* $V(x - \bar{x})$ *for any possible choice of functions* g *satisfying the stated assumptions if and only if* $V(z)$ *is a Lyapunov function for* (6.7) $\forall\, \varepsilon \geq 0$*.*

Proof. The proof is based on the fact that a Lyapunov function for the nonlinear system must be a local Lyapunov function for the linearised system $\dot{z} = Jz$ as well, where $J = BDC$ is the Jacobian, having exactly the same structure as the state matrix of the differential inclusion (cf. Remark 6.3). If g is arbitrary, then the diagonal matrix D (whose diagonal entries are the partial derivatives computed at $\bar{x}$) has arbitrary nonnegative diagonal entries. Details are in [BG14]. □

6.3.2 Non-Unitary Networks and Special Cases

The procedure can be applied to non-unitary systems without conceptual restrictions. However, since integer terms of magnitude greater than 1 can appear, the procedure might not converge in finite time. In this case, it may be useful to normalise the columns of B or the rows of C (this is always possible, because it is equivalent to

the substitution $D_i := \kappa D_i$), to get 1 as the maximum magnitude. For example, the reactions $2A + B \xrightarrow{g_{2ab}} C$, $B \xrightarrow{g_b} \emptyset$ and $C \xrightarrow{g_c} \emptyset$ correspond to

$$B = \begin{bmatrix} -1 & -1 & 0 & 0 \\ -\frac{1}{2} & -\frac{1}{2} & -1 & 0 \\ \frac{1}{2} & \frac{1}{2} & 0 & -1 \end{bmatrix}, \quad C = \begin{bmatrix} 1 & 0 & 0 & 0 \\ 0 & 1 & 1 & 0 \\ 0 & 0 & 0 & 1 \end{bmatrix}^\top.$$

In this case the procedure converges, although it generates a unit ball with non-integer vertices. Due to non-integer values, finite time convergence is not assured in general. Interestingly, decomposing the g_{2ab} reaction as $A + B \xrightarrow{g_{ab}} D$, $A + D \xrightarrow{g_{ad}} C$ or as $A + A \xrightarrow{g_{aa}} D$, $B + D \xrightarrow{g_{bd}} C$ still leads to convergence in both cases.

For some special structures there is no need to apply the procedure, since they always admit a polyhedral Lyapunov function. This is the case, for instance, of compartmental systems [MKO78], formed by arcs as in Fig. 6.1 (a), (b) and (c). Actually, also arcs as in Fig. 6.1 (d) are admitted.

Proposition 6.4. *Networks containing only reactions of the types in Fig. 6.1 (a), (b), (c) and (d) admit a polyhedral Lyapunov function $\|x\|_1$ (the proposed procedure, initialised with $[-I\ I]$, stops at the first step, yielding $[-I\ I]$).*

In fact, for each of these arcs, the iterate Ψ maps each versor $\pm e_h$ in another versor, thus Ψ has a fixed point $X = [-I\ I]$ and V_X is a polyhedral Lyapunov function; linearity assures that any combination of arcs of these types admits the same polyhedral Lyapunov function.

Applying the procedure can turn out to be unnecessary also in the case of networks which are subsets/supersets of others already tested. A network $\mathcal{N}_1$ is a subset of $\mathcal{N}_2$ if it is achieved from $\mathcal{N}_2$ by removing arcs; $\mathcal{N}_2$ is then a superset of $\mathcal{N}_1$.

Lemma 6.2. *If a biochemical network admits a polyhedral Lyapunov function, then any of its subsets admits a polyhedral Lyapunov function too. Conversely, if a biochemical network does not admit polyhedral Lyapunov functions, then none of its supersets can admit a polyhedral Lyapunov function.*

6.4 Mismatches in Local Dissipativity

In the proposed framework, asymptotic stability is assured by introducing an ε dissipativity. Yet, the same level of local dissipativity is added to each node. Does the system tolerate a mismatch in the dissipation terms? Instead of (6.3) and (6.7), a system may be considered where the dissipation terms are in general different:

$$\dot{z}(t) = \left[-\Delta + \sum_{i=1}^{q} B_i D_i(t) C_i^\top \right] z(t), \quad z(0) = z_0 \tag{6.14}$$

where Δ is a diagonal matrix with nonnegative elements (including $\Delta = \varepsilon I$ as a special case). Then, the following result is proved in [BG14].

Proposition 6.5. *Assume that the system passes the computational test with a Lyapunov function V_X. Hence, V_X is a Lyapunov function for* (6.14) *with $\Delta = 0$. Then V_X is a Lyapunov function for* (6.14) *if and only if it is a Lyapunov function for the Δ-system*

$$\dot{z}(t) = -\Delta z(t).$$

If each diagonal entry of Δ is bounded in an interval, checking if the provided Lyapunov function works for the Δ-system simply requires linear programming [Bla91]. The details are discussed in [BG14].

6.5 Local Asymptotic Stability within the Stoichiometric Compatibility Class

Introducing the ε perturbation may seem unnatural; on the other hand, if $\varepsilon = 0$, a polyhedral Lyapunov function can assure only marginal stability of the system. Still, for systems naturally evolving in a stoichiometric compatibility class, a test can be performed to guarantee at least local asymptotic stability of the equilibrium (if any).

Recall the following theorem from [BM15].

Theorem 6.5. *A linear time-invariant continuous-time system admits polyhedral Lyapunov functions if and only if it is stable (at least marginally) and there are no purely imaginary eigenvalues (*i.e.*, only $\lambda = 0$ is admitted).*

This result can be used to show that, if the system admits a polyhedral Lyapunov function, then asymptotic stability is equivalent to non-singularity *inside the stoichiometric compatibility class*. Let $z = x - \bar{x}$ and consider the orthogonal transformation

$$\begin{bmatrix} H^\top \\ K^\top \end{bmatrix} z = \begin{bmatrix} z_H \\ z_K \end{bmatrix}, \quad z = \begin{bmatrix} H & K \end{bmatrix} \begin{bmatrix} z_H \\ z_K \end{bmatrix},$$

where H is an orthonormal basis of $\ker[S^\top]$ (hence $H^\top S = 0$) and K is an orthonormal basis of $\mathrm{span}(S)$. If in (6.1) $g_0 = 0$, then $H^\top \dot{x} = 0$. By means of a state transformation, system (6.5) with $\varepsilon = 0$ can be rewritten as

$$\begin{bmatrix} \dot{z}_H \\ \dot{z}_K \end{bmatrix} = \begin{bmatrix} H^\top \\ K^\top \end{bmatrix} BDC \begin{bmatrix} H & K \end{bmatrix} \begin{bmatrix} z_H \\ z_K \end{bmatrix}.$$

Since B is formed by columns of S, $H^\top B = 0$ and

$$\begin{bmatrix} \dot{z}_H \\ \dot{z}_K \end{bmatrix} = \begin{bmatrix} 0 & 0 \\ B_K DC_H & B_K DC_K \end{bmatrix} \begin{bmatrix} z_H \\ z_K \end{bmatrix},$$

where $B_K = K^\top B$, $C_K = CK$ and $C_H = CH$. Therefore $z_H(t) = z_H(0)$ is constant. If $\bar{x}$ is an equilibrium in the same stoichiometric class of $x(0)$, then $z_H(0) = 0$ and

$$\dot{z}_K = B_K D C_K z_K.$$

Hence, it is enough to assess the asymptotic stability of this latter system. If a polyhedral Lyapunov function has been found for the original system, then also the z_K subsystem admits a polyhedral Lyapunov function, because it has been obtained by a linear state transformation. Therefore, in view of Theorem 6.5, the next proposition follows.

Proposition 6.6. *Assume that the system admits a polyhedral Lyapunov function. Let $\bar{x}$ be an equilibrium point in the stoichiometric compatibility class of $x(0) = x_0$. Assume that all the partial derivatives of the functions g_k are non-zero at the equilibrium. Then such an equilibrium is asymptotically stable iff $K^\top BDCK$ is structurally non-singular, where K is any basis of span(S).*

Since a non-singularity problem is considered, any basis K, not necessarily orthonormal, is suitable.

The only issue left is how to check the non-singularity of $K^\top BDCK = B_K D C_K$. To this aim, notice that

$$\psi(D_1, D_2, \ldots, D_q) = \det[-B_K D C_K]$$

is a multi-affine function of the nonnegative diagonal elements D_k of D. To verify whether $\psi(D_1, D_2, \ldots, D_q) \neq 0$, since D_k are *arbitrary* nonnegative scalars, they can be normalised as $0 \leq D_k \leq 1$. Then the unit hypercube

$$\mathcal{C}_D = \{D_k : 0 \leq D_k \leq 1,\, k = 1, \ldots, q\}$$

can be considered. Since matrices BDC and $B_K D C_K$ have the same structure, the function $\varphi(D_1, D_2, \ldots, D_q) = \det[-BDC]$ (which must be nonnegative if the system admits a polyhedral Lyapunov function) can be equivalently analysed. Denoting by $D^{(v)}$ the matrices corresponding to the vertices of the hypercube $\mathcal{C}_D$, the following result holds immediately, based on Theorem 4.3 (see [BG14] for a complete proof).

Proposition 6.7. $\det[-BDC] > 0 \;\forall\, D \succ 0$ *if and only if* $\det[-BC] > 0$ *and* $\det[-BD^{(v)}C] \geq 0 \;\forall\, v$.

In view of this result, non-singularity of the matrix inside the hypercube $\mathcal{C}_D$ can be assessed by simply checking the value of $\psi(D_1, D_2, \ldots, D_q) = \det[-K^\top BDCK]$ on the vertices of $\mathcal{C}_D$, thus on a finite number of points.

6.6 Discrete-Event System Interpretation

Chemical reaction networks have been often analysed resorting to discrete-event frameworks, employing for instance Petri nets [AdLS07, Sol12]. Also the proposed procedure admits a nice interpretation in terms of the evolution of a discrete-event system, which is briefly presented here by means of an example. Note that the considered discrete-event system, albeit similar to a Petri net, does not work as a Petri net; indeed, the number of tokens at the nodes here can be negative, which is not the case for Petri nets.

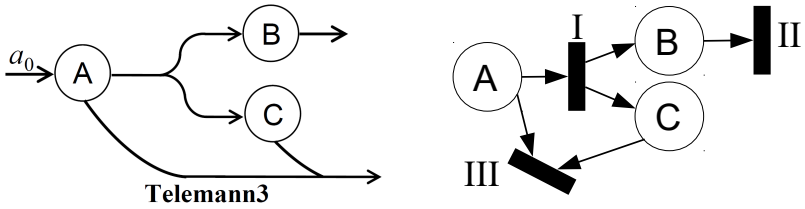

Figure 6.6: Graph and discrete-event representation of the system considered in Section 6.6.

Consider the system whose graph is in Fig. 6.6, along with its "Petri-net-like" discrete-event representation. The corresponding matrices B and C are

$$B = \begin{bmatrix} -1 & 0 & -1 & -1 \\ 1 & -1 & 0 & 0 \\ 1 & 0 & -1 & -1 \end{bmatrix} \quad \text{and} \quad C = \begin{bmatrix} 1 & 0 & 0 \\ 0 & 1 & 0 \\ 0 & 0 & 1 \\ 1 & 0 & 0 \end{bmatrix}$$

and the evolution of the discrete-time system $y(k+1) = \Phi(k)y(k)$ is determined by the matrices in the family $\mathcal{F}$, having the form $\Phi_i = I - \frac{B_i C_i^\top}{C_i^\top B_i}$, $i = 1, \ldots, 4$. Hence,

$$\Phi_1 = \begin{bmatrix} 0 & 0 & 0 \\ 1 & 1 & 0 \\ 1 & 0 & 1 \end{bmatrix}, \; \Phi_2 = \begin{bmatrix} 1 & 0 & 0 \\ 0 & 0 & 0 \\ 0 & 0 & 1 \end{bmatrix}, \; \Phi_3 = \begin{bmatrix} 1 & 0 & -1 \\ 0 & 1 & 0 \\ 0 & 0 & 0 \end{bmatrix}, \; \Phi_4 = \begin{bmatrix} 0 & 0 & 0 \\ 0 & 1 & 0 \\ -1 & 0 & 1 \end{bmatrix}.$$

The numerical procedure then monitors convergence of the sequence given by the evolution of the system according to each of these matrices, starting from the unit ball of the 1-norm: $X^0 = [-I \;\; I] = [-v_1 \; -v_2 \; -v_3 \;\; v_1 \;\; v_2 \;\; v_3]$. Consider just the positive vertices of X^0 (the evolution of the others can be immediately obtained, being the opposite). Vertex $v_1 = [1\ 0\ 0]^\top$ is transformed into $\Phi_1 v_1 = [0\ 1\ 1]^\top = v_4$, $\Phi_2 v_1 = \Phi_3 v_1 = [1\ 0\ 0]^\top = v_1$, $\Phi_4 v_1 = [0\ 0\ -1]^\top = -v_3$; vertex $v_2 = [0\ 1\ 0]^\top$ is transformed into $\Phi_1 v_2 = \Phi_3 v_2 = \Phi_4 v_2 = [0\ 1\ 0]^\top = v_2$, $\Phi_2 v_2 = [0\ 0\ 0]^\top$; vertex $v_3 = [0\ 0\ 1]^\top$ is transformed into $\Phi_1 v_3 = \Phi_2 v_3 = \Phi_4 v_3 = [0\ 0\ 1]^\top = v_3$, $\Phi_3 v_3 = [-1\ 0\ 0]^\top = -v_1$. The sole newly generated vertex is $v_4 = [0\ 1\ 1]^\top$ (always along with its opposite, of course). The procedure applied to v_4 gives $\Phi_1 v_4 = \Phi_4 v_4 = [0\ 1\ 1]^\top = v_4$,

$\Phi_2 v_4 = [0\ 0\ 1]^\top = v_3$, $\Phi_3 v_1 = [-1\ 1\ 0]^\top = v_5$. Applying the procedure to the only new vertex, $v_5 = [-1\ 1\ 0]^\top$, gives $\Phi_1 v_5 = [0\ 0\ -1]^\top = -v_3$, $\Phi_2 v_5 = [-1\ 0\ 0]^\top = -v_1$, $\Phi_3 v_5 = [-1\ 1\ 0]^\top = v_5$, $\Phi_4 v_5 = [0\ 1\ 1]^\top = v_4$. No new vertices are generated at this step, hence the procedure stops successfully: the system admits a polyhedral Lyapunov functions with 10 vertices, whose matrix $X = [v_1\ \ v_2\ \ v_3\ \ v_4\ \ v_5]$ is

$$X = \begin{bmatrix} 1 & 0 & 0 & 0 & -1 \\ 0 & 1 & 0 & 1 & 1 \\ 0 & 0 & 1 & 1 & 0 \end{bmatrix} \tag{6.15}$$

and whose unit ball is shown in Fig. 6.17 (a).

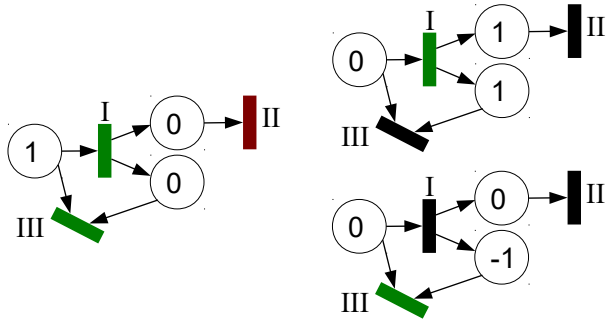

(a) Initial marking v_1.

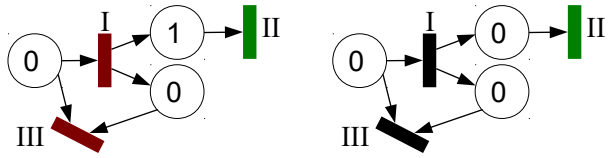

(b) Initial marking v_2.

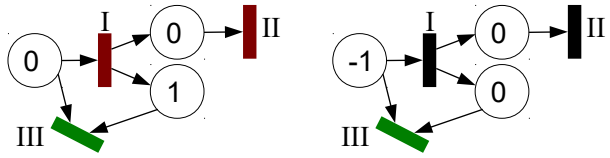

(c) Initial marking v_3.

Figure 6.7: Discrete-event interpretation of the procedure evolution: first step.

The evolution of the discrete-time system in the numerical procedure can be related to the evolution of a particular discrete-event system, in which the initial condition represents an "initial marking", assigning a number of tokens to each node, and a transition (associated with each of the black rectangles in Fig. 6.6, left, *i.e.*, with each of the reactions occurring in the network) is "enabled" whenever at least one of the starting nodes of the transition contains a non-zero number of tokens. When either the number of tokens in the starting node is positive, or

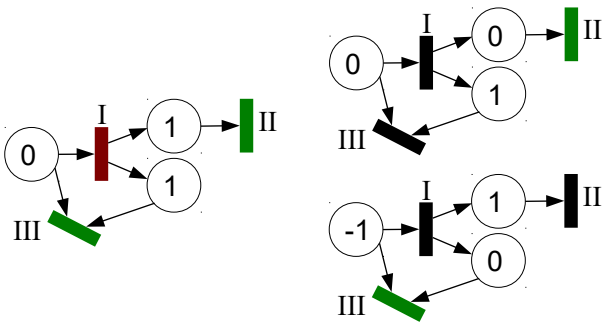

Figure 6.8: Discrete-event interpretation: second step. Initial marking v_4.

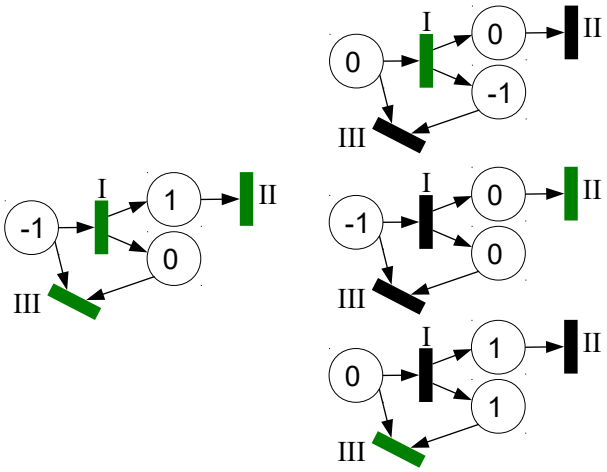

Figure 6.9: Discrete-event interpretation: third step. Initial marking v_5.

the starting nodes are two and the number of tokens is non-negative in both (and positive in at least one of them), then the transition takes tokens from the starting node(s) and moves them to the arrival node(s), if explicitly present (otherwise, they simply disappear). When either the starting node is one only and the number of tokens therein is negative, or the starting nodes are two and the number of tokens is non-positive in both (and negative in at least one of them), then the transition takes "holes" from the starting node(s) and moves them to the arrival node(s), again, if explicitly present. The evolution in the case of the considered system is shown in Figs. 6.7, 6.8 and 6.9: on the left side, the initial marking is illustrated, and enabled transitions are in green, non-enabled transitions in red; on the right side, the new marking generated by the action of each of the enabled transitions is illustrated. Reaction I corresponds to evolution matrix Φ_1 (and generates the same outcome for the same initial conditions), reaction II corresponds to evolution matrix Φ_2 (and again generates the same outcome for the same initial conditions), while reaction III corresponds to evolution matrices Φ_3 and Φ_4. In this latter case, the outcome of (at least) one of the two evolution matrices is the same as that of the transition related to reaction III in the discrete-event evolution, while the outcome of the other

(if different) is always the unchanged input vertex. Interestingly, the evolution is the very same as that of the numerical procedure, and the same new vertices are generated at each iteration.

Let $\Phi(k) \in \mathbb{Z}^{n\times n}$ represent the integer operator acting on the discrete-event system with state $\tau(k)$. Then we have the following.

Proposition 6.8. *Let $\tau(0) = [\tau_1(0) \dots \tau_n(0)]$ be any integer vector, whose components represent tokens and holes. The evolution of the discrete-event system with all possible operator sequences $\Phi(k) \in \mathcal{F}$ and initial marking τ generates a finite number of configurations if and only if Procedure 6.1 converges in finite time.*

This analogy has a conceptual interest, although the discrete-event approach does not present any computational advantage with respect to the numerical approach illustrated in Section 6.3.1, which is fairly efficient (especially for unitary networks).

6.7 Boundedness

If the associated differential inclusion admits a polyhedral function, then, in view of Theorem 6.3 and Corollary 6.1, the original system has a bounded solution. However, the system might be bounded as well, even though it does not pass the proposed stability test. Since boundedness is a fundamental property on its own [Ang11], it is worth being investigated; to this aim, a different test is provided, inspired by the proposed stability procedure, but less conservative. The idea is to absorb the system in a *positive* differential inclusion, by dividing and multiplying each negative term appearing in an equation by the variable associated with that equation, for instance

$$\dot{a} = \cdots - g(a,b) \cdots = \cdots - \frac{g(a,b)}{a}\, a \cdots = \cdots - k\, a \dots,$$

and then writing in the same way the same positive term in the other equations. An absorbing differential inclusion associated with a Metzler matrix is thus achieved.

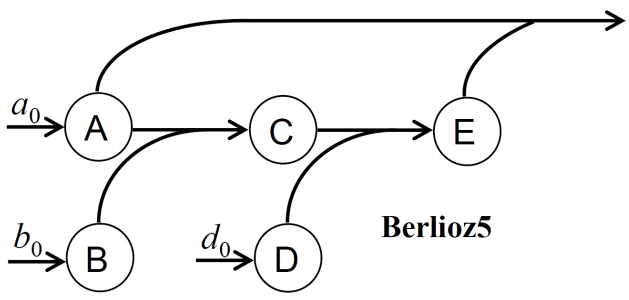

Figure 6.10: Graph of the network in Example 6.5. [BG14]

Example 6.5. *Consider the chemical system*

$$\begin{aligned} A + B &\xrightarrow{g_{ab}(a,b)} C, & \emptyset &\xrightarrow{a_0} A,\\ C + D &\xrightarrow{g_{cd}(c,d)} E, & \emptyset &\xrightarrow{b_0} B,\\ A + E &\xrightarrow{g_{ae}(a,e)} \emptyset, & \emptyset &\xrightarrow{d_0} D, \end{aligned}$$

corresponding to the graph named Berlioz5 in Fig. 6.10, and the associated ODE model

$$\begin{cases} \dot{a} = -g_{ab}(a,b) - g_{ae}(a,e) + a_0 \\ \dot{b} = -g_{ab}(a,b) + b_0 \\ \dot{c} = \ g_{ab}(a,b) - g_{cd}(c,d) \\ \dot{d} = -g_{cd}(c,d) + d_0 \\ \dot{e} = \ g_{cd}(c,d) - g_{ae}(a,e) \end{cases}$$

Denoting $\alpha = g_{ab}(a,b)/a$, $\beta = g_{ae}(a,e)/a$, $\gamma = g_{ab}(a,b)/b$, $\delta = g_{cd}(c,d)/c$, $\eta = g_{cd}(c,d)/d$, $\zeta = g_{ae}(a,e)/e$, *the system can be rewritten as*

$$\begin{bmatrix} \dot{a} \\ \dot{b} \\ \dot{c} \\ \dot{d} \\ \dot{e} \end{bmatrix} = \begin{bmatrix} -(\alpha+\beta) & 0 & 0 & 0 & 0 \\ 0 & -\gamma & 0 & 0 & 0 \\ \alpha/2 & \gamma/2 & -\delta & 0 & 0 \\ 0 & 0 & 0 & -\eta & 0 \\ 0 & 0 & \delta/2 & \eta/2 & -\zeta \end{bmatrix} \begin{bmatrix} a \\ b \\ c \\ d \\ e \end{bmatrix} + \begin{bmatrix} a_0 \\ b_0 \\ 0 \\ d_0 \\ 0 \end{bmatrix}.$$

Defining the matrices Φ_k as before, it can be seen that, for unitary systems, they are nonnegative but, unfortunately, not necessarily integer. Then, an iterative procedure can be used that is initialised with matrix I. The sequence X^k includes only nonnegative matrices, non-integer in general, and the condition $X^k = X^{k-1}$ means that the polyhedron defined as the convex hull of the columns of X^k and 0,

$$\mathcal{P} = \{x = X^k w : \ \sum_i w_i \leq 1, \ \ w_i \geq 0\},$$

is positively invariant for the discrete-time system and also for the differential inclusion. Yet, it can no longer be ensured that the procedure stops in a finite number of steps. Convergence of the procedure implies boundedness for $g_0 = 0$ and, assuming $\varepsilon > 0$, boundedness for any, arbitrary, constant $g_0 > 0$. Actually, it is sufficient that the additive term $g_0 > 0$ is bounded; this is relevant to systems including functions of the form $g(x_i^{tot} - x_i)$, with $0 \leq x_i \leq x_i^{tot}$, which can be handled just as bounded terms.

When, as in Example 6.5, the positive system is diagonally dominant, boundedness can be immediately inferred without resorting to the numerical procedure.

Proposition 6.9. *A system formed only by arcs (a), (b), (c), (d), (e), (g), (h) as in Fig. 6.1 is structurally bounded.*

Proof. The matrix is at least weakly diagonally dominant in presence of arcs (a), (b), (c), (d), (e), (g), (h); in the case of diagonal dominance, the unit simplex

$$\mathcal{P} = \{x : \sum_i x_i \leq 1, \quad x_i \geq 0\}$$

is positively invariant for both the discrete and the continuous-time systems. □

Diagonal dominance is not assured in the presence of arcs (f), (i).

6.8 Structural Stability Analysis of Well-Established Biochemical Models

Polyhedral functions can prove structural stability of some well-known models in the literature.

6.8.1 Enzymatic Reactions

Consider the reaction of an enzyme E binding to a substrate S to form a complex C; the product P results from the modification of the substrate S due to the binding with the enzyme E [Alo07b, DVM14, EK05].

$$\emptyset \xrightarrow{g_{s0}} S, \quad S + E \underset{g_c}{\overset{g_{es}}{\rightleftharpoons}} C \xrightarrow{g_c^*} P + E$$

Since $c + e = \kappa$ is constant, the equations for $x = [s \ e]^\top$ are

$$\begin{cases} \dot{s} = -g_{es}(e, s) + g_c(\kappa - e) + g_{s0} \\ \dot{e} = -g_{es}(e, s) + g_c(\kappa - e) + g_c^*(\kappa - e) \end{cases}$$

This system is bounded and, in view of Proposition 6.4, structurally stable with a Lyapunov function $\|x - \bar{x}\|_1$. Of course neither stability nor boundedness can be inferred for the final product P, which in general diverges.

6.8.2 A Metabolic Network

Reconsider the metabolic network proposed in Example 4.10, having reactions [CWLA05]

$$\emptyset \xrightarrow{g_{a0}} A, \quad A + C \xrightarrow{g_{ac}} B + D, \quad D \xrightarrow{g_d} C, \quad B \xrightarrow{g_b} \emptyset.$$

Since $c + d = \text{const}$, a system can be obtained in the variables a, b and c, as shown in Example 4.10. This system turns out to be structurally stable: the procedure generates a Lyapunov function whose unit ball has 10 vertices, while the dual unit ball has 12 facets.

6.8.3 Gene Expression

Both transcription and translation can be modelled by the reduced reactions [DVM14]

$$A + E \underset{g_c}{\overset{g_{ae}}{\rightleftharpoons}} C \xrightarrow{g_c^*} A + E + B.$$

In the case of transcription, E is RNA polymerase, A is DNA and B is produced mRNA. In the case of translation, E stands for ribosomes, A is mRNA and B is the produced protein. In both cases, C is an intermediate complex. This mechanism, in the variables a, c and e, is both bounded and structurally stable: the procedure generates a Lyapunov function with 12 vertices (the dual unit ball has 12 facets). Yet, if the final product B is considered, *e.g.*, by including a degradation reaction $B \xrightarrow{g_b} \emptyset$, the procedure does not converge. However, it can be proved that the system is stable (hence bounded): a, c and e, whose evolution is independent of b, converge to a steady state $\bar{a}$, $\bar{c}$ and $\bar{e}$; the equation for b is $\dot{b} = g_c^*(c) - g_b(b)$, therefore b also converges to a steady state.

6.8.4 MAPK Pathway

Consider the open-loop MAPK pathway equations

$$\begin{cases} \dot{y}_1 = g_{y13}(y^{tot} - y_1 - y_3) - g_{y1}(x, y_1), \\ \dot{y}_3 = g_{xy}(x, y^{tot} - y_1 - y_3) - g_{y3}(y_3), \\ \dot{z}_1 = g_{z13}(z^{tot} - z_1 - z_3) - g_{z1}(y_3, z_1), \\ \dot{z}_3 = g_{yz}(y_3, z^{tot} - z_1 - z_3) - g_{z3}(z_3), \end{cases}$$

where x is a constant input. The model results from the substitutions of $y_1+y_2+y_3 = y^{tot}$ and $z_1 + z_2 + z_3 = z^{tot}$ in the two phosphorylation processes, where y^{tot} and z^{tot} are constant total concentrations (see [CWLA05] p. 207 and also [FB13]). Numerical tests show that the system is bounded, but does not admit an overall Lyapunov function. In these cases, it is possible to adapt the framework and check only a subset of reactions. In fact, by separately analysing the two modules of the cascade, it can be seen that the considered system is robustly stable. For constant x, the y-subsystem admits a polyhedral Lyapunov function (the unit ball has 6 vertices, the dual 4 facets). Hence the y variables converge to a steady state, which is asymptotically stable in view of Proposition 6.6. Convergence of y_3 to a steady state allows to apply the same analysis to the z-subsystem.

6.9 Piecewise-Linear Lyapunov Functions in Reaction Coordinates

The stability results proposed so far concern systems in concentration coordinates, whose state variables are species concentrations. However, systems in reaction coordinates, whose state variables are reaction rates, can be considered too; their stability has been previously studied based on piecewise-linear in rate Lyapunov functions [ARA13, ARA14, ARA15].

In this section, it is shown that the same stability results hold for systems in reaction coordinates as well, at least for a special class of chemical reaction networks, which are called *regular*.

Definition 6.3. *System* (6.1) *is* regular *if (i) it admits an equilibrium point $\bar{x}$, and (ii) $g(\cdot)$ is left invertible (injective), so that, given $\bar{g} = g(\bar{x})$, $\bar{x}$ is unique.*

In the case of regular systems, an equilibrium exists for the system in reaction coordinates if and only if it exists for the system in concentration coordinates.

Define the new variable $r \doteq g(x) - g(\bar{x})$, which can be thought of as a "relative" reaction rate, such that $r \to 0$ iff $x \to \bar{x}$ (due to the regularity assumption). The corresponding dynamics are

$$\dot{r} = \left[\frac{\partial g}{\partial x}\right][Sg(x) + g_0] = \left[\frac{\partial g}{\partial x}\right] Sr. \tag{6.16}$$

Remark 6.8. *Reaction and concentration representations are both valid, in general, but may lead to different conclusions. For instance, given the* non-regular *system*

$$\begin{cases} \dot{a} = -g(a,b) + a_0 \\ \dot{b} = -g(a,b) + b_0 \end{cases}$$

consider the reaction variable $r = g(a,b)$ and the set

$$\mathcal{S}_{\nu,\mu} = \{(a,b) \geq 0 : 0 < \nu \leq g(a,b) \leq \mu\},$$

which is invariant for the system, provided that μ is large enough and ν is small enough. Indeed,

$$\dot{r} = \frac{\partial g(a,b)}{\partial a}\dot{a} + \frac{\partial g(a,b)}{\partial b}\dot{b} = -D_1(r - a_0) - D_2(r - b_0) \leq 0$$

for r large enough (take, for instance, $r \geq \max\{a_0, b_0\}$). Note also that $\dot{r} \geq 0$ for r small enough ($r \leq \min\{a_0, b_0\}$). This means that r is ultimately bounded in the interval $[\nu \;\; \mu]$. However, for $a_0 \neq b_0$, the concentration variables diverge (unless an ε-dissipation is assumed to be present), as it can be seen by noting that $\dot{a} - \dot{b} = a_0 - b_0$. Later, it will be shown that the analysis in reaction and in concentration coordinates lead in general to different results.

Proposition 6.10. *System* (6.16) *can be equivalently written as*

$$\dot{r}(t) = ED(z(t))F\, r(t), \tag{6.17}$$

where $E \in \mathbb{Z}^{m\times q}$, $F \in \mathbb{Z}^{q\times m}$ *is formed by rows of* S, *while* q *and* D *are as in* (6.5).

Proof. Matrix $[\partial g/\partial x]S$ can be equivalently expressed as the product EDF, where the diagonal entries D_j of D are the partial derivatives $\partial g_k/\partial x_h$, the entries of E are $|e_{ij}| = 1$ if g_k in D_j appears in the ith equation, 0 otherwise, and the jth row of F is the hth row of S if the derivative in D_j is with respect to x_h (or also a sum or difference of more rows of S, if the function has as an argument a sum or difference of more variables, see Assumption 6.3). □

Remark 6.9. *$D(z(t))$ is a matrix of partial derivatives, as in* (6.5), *but it is not the same matrix. Consider $\dot{x} = g(x) + g_0$, with steady state $0 = g(\bar{x}) + g_0$, and let $z = x - \bar{x}$ ($\bar{x}$ is fixed). Then $\dot{z} = g(z + \bar{x}) - g(\bar{x}) = g'(\tilde{z})z$,* for some *$\tilde{z}$. Conversely, if $r = g(x) - g(\bar{x})$, then $\dot{r} = g'(x)\dot{x} = g'(x)r$, where $x = z + \bar{x}$. In principle, a formal expression should be $D_{BC}(z(t))$ and $D_{EF}(z(t))$; however, this is not necessary because only the structural property that D has non-negative diagonal entries will be used.*

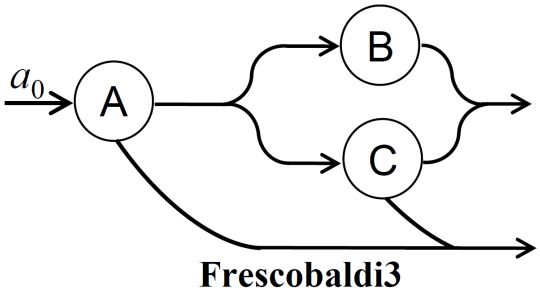

Figure 6.11: Graph of the network in Example 6.6. [BG14]

Example 6.6. *Consider the reaction network associated with the graph in Fig. 6.11. The system in concentration coordinates has equations*

$$\begin{cases} \dot{a} = a_0 - g_a(a) - g_{ac}(a,c) \\ \dot{b} = g_a(a) - g_{bc}(b,c) \\ \dot{c} = g_a(a) - g_{ac}(a,c) - g_{bc}(b,c) \end{cases}$$

corresponding to the general model (6.1) *with* $x = [a\ b\ c]^\top$,

$$S = \begin{bmatrix} -1 & -1 & 0 \\ 1 & 0 & -1 \\ 1 & -1 & -1 \end{bmatrix}, \quad g(x) = \begin{bmatrix} g_a(a) \\ g_{ac}(a,c) \\ g_{bc}(b,c) \end{bmatrix}, \quad g_0 = \begin{bmatrix} a_0 \\ 0 \\ 0 \end{bmatrix}.$$

Let $\alpha = \partial g_a(a)/\partial a$, $\beta = \partial g_{ac}(a,c)/\partial a$, $\gamma = \partial g_{ac}(a,c)/\partial c$, $\delta = \partial g_{bc}(b,c)/\partial b$ *and* $\epsilon = \partial g_{bc}(b,c)/\partial c$ *be positive parameters. Then* $D = diag\{\alpha, \beta, \gamma, \delta, \epsilon\}$,

$$B = \begin{bmatrix} -1 & -1 & -1 & 0 & 0 \\ 1 & 0 & 0 & -1 & -1 \\ 1 & -1 & -1 & -1 & -1 \end{bmatrix}, \; C = \begin{bmatrix} 1 & 1 & 0 & 0 & 0 \\ 0 & 0 & 0 & 1 & 0 \\ 0 & 0 & 1 & 0 & 1 \end{bmatrix}^\top.$$

Given $r = [g_a(a) - g_a(\bar{a}) \quad g_{ac}(a,c) - g_{ac}(\bar{a},\bar{c}) \quad g_{bc}(b,c) - g_{bc}(\bar{b},\bar{c})]^\top$, *the corresponding system in reaction coordinates is*

$$\dot{r} = \begin{bmatrix} \alpha & 0 & 0 \\ \beta & 0 & \gamma \\ 0 & \delta & \epsilon \end{bmatrix} Sr = \begin{bmatrix} -\alpha & -\alpha & 0 \\ -\beta+\gamma & -(\beta+\gamma) & -\gamma \\ \delta+\epsilon & -\epsilon & -(\delta+\epsilon) \end{bmatrix} r = EDFr,$$

where

$$E = \begin{bmatrix} 1 & 0 & 0 & 0 & 0 \\ 0 & 1 & 1 & 0 & 0 \\ 0 & 0 & 0 & 1 & 1 \end{bmatrix}, \quad F = \begin{bmatrix} -1 & -1 & 1 & 1 & 1 \\ -1 & -1 & -1 & 0 & -1 \\ 0 & 0 & -1 & -1 & -1 \end{bmatrix}^\top.$$

System

$$\dot{r}(t) = ED(t)Fr(t), \quad D_i(t) \geq 0, \tag{6.18}$$

has the same *structure* as system (6.10) and in the following, when relating BDC and EDF, it will be assumed that the diagonal entries of D are ordered in the same way in both expressions. Again, a spontaneous ε-degradation must be added to assess asymptotic stability; the system can be rewritten as

$$\dot{r}(t) = [-\varepsilon I + ED(t)F]\, r(t), \quad r(0) = r_0, \tag{6.19}$$

which has the same *structure* as system (6.7). Hence, all the reasoning and the results in [BG14] still hold in the new reaction coordinates framework. Then, the numerical procedure based on iterates (6.12) in the set of polyhedra can be employed to find a polyhedral Lyapunov function, thus ensuring stability of the system in reaction coordinates.

A strong analogy between the two formulations is shown by the following result.

Proposition 6.11. *Given a reaction network, consider the corresponding matrices* B *and* C *as in* (6.5)*, and the corresponding matrices* E *and* F *as in* (6.17)*. Then, the equality* $CB = FE$ *holds.*

Proof. Denote by S_i the ith column and by S^i the ith row of the stoichiometric matrix S, and by $\vec{e}_i$ the column versor having the ith element equal to 1, and all other elements equal to 0. Matrix B is composed by columns of S, $B = \begin{bmatrix} S_{j_1} & S_{j_2} \dots S_{j_q} \end{bmatrix}$, while F by rows of S, $F = \begin{bmatrix} (S^{i_1})^\top & (S^{i_2})^\top \dots (S^{i_q})^\top \end{bmatrix}^\top$ (more in general, a row of F could be a sum or difference of more rows of S); the rows of C are versors,

$C = \left[\vec{e}_{i_1} \;\; \vec{e}_{i_2} \ldots \vec{e}_{i_q}\right]^\top$ (more in general, a row of C could be a sum or difference of versors), while the columns of E are versors, $E = \left[\vec{e}_{j_1} \;\; \vec{e}_{j_2} \ldots \vec{e}_{j_q}\right]$. Whenever a row of F is the sum or difference of more rows of S, the corresponding row of C is the same sum or difference of the corresponding versors, and *vice versa* (*e.g.*, if $F_k^\top = S^1 - S^2$, then $C_k^\top = \vec{e}_1^\top - \vec{e}_2^\top$). The columns of B and of E (and the rows of C and F accordingly) can be always swapped so that the order of the indices $\{j_k\}$ (respectively, $\{i_k\}$) is the same. Then, consider the two matrix products and observe that, if the entry $[CB]_{uv} = \vec{e}_{i_h}^\top S_{j_l}$, the corresponding entry $[FE]_{uv} = S^{i_h}\vec{e}_{j_l}$ (and analogously for the case of linear combinations). The former expression selects the i_hth element of the j_lth column of S; the latter selects the j_lth element of the i_hth row of S, which is clearly the same. Hence, $CB = FE$. □

The following corollary ensures that the same computational benefits are guaranteed when applying the numerical procedure to the system in reaction coordinates.

Corollary 6.4. *A network is unitary in reaction coordinates iff it is unitary in concentration coordinates.*

Proof. In view of the equality $CB = FE$, $C_i^\top B_i = -1 \;\forall i$ iff $F_i^\top E_i = -1 \;\forall i$. □

It is interesting to investigate the connection between robust stability of the differential inclusion in concentration coordinates

$$\dot{z}(t) = [-\varepsilon I + BD(t)C]z(t), \quad D_i(t) \geq 0, \tag{6.20}$$

and robust stability of the system in reaction coordinates,

$$\dot{r}(t) = [-\varepsilon I + ED(t)F]r(t), \quad D_i(t) \geq 0. \tag{6.21}$$

In both cases, the existence of a polyhedral Lyapunov function ensures asymptotic stability of the system. For unitary networks, for which $C_i^\top B_i = -1$ (resp. $F_i^\top E_i = -1$), stability of (6.7) (resp. of (6.19)) is *equivalent* to the existence of a polyhedral Lyapunov function, according to Corollary 6.3. Once stability of the system has been shown in one of the two frameworks (because the numerical procedure converges and generates the unit ball of the corresponding polyhedral Lyapunov function), what can be inferred about stability of the system in the other framework?

Let $\eta(t) \doteq Cz(t)$ and $\xi(t) \doteq Fr(t)$. Consider the systems

$$\dot{\eta}(t) = [-\varepsilon I + CBD(t)]\eta(t), \quad D_i(t) \geq 0, \tag{6.22}$$

$$\dot{\xi}(t) = [-\varepsilon I + FED(t)]\xi(t), \quad D_i(t) \geq 0, \tag{6.23}$$

and the following definition.

Definition 6.4. *System* (6.23) *(resp.* (6.22)*) is* F-stable *(*C-stable*) if the subspace span(F) (span(C))*[6] *is invariant and all the trajectories starting from that subspace converge to zero for any* $D(t)$*.*

[6] span(A) denotes the column space of matrix A.

For a fixed $D(t)$, $FED = CBD$ in view of Proposition 6.11. Then, the following results hold.

Lemma 6.3. *If system* (6.21) *(resp.* (6.20)*) is asymptotically stable for any* $D(t)$*, then system* (6.23) *is* F*-stable (resp.* (6.22) *is* C*-stable).*

Proof. Fix a matrix $D(t)$. Given the solution $r(t)$ of (6.21) for initial conditions $r(0)$, $\xi(t) = Fr(t)$ is the solution of (6.23) for initial conditions $\xi(0) = Fr(0)$. If $r(t) \to 0$, then also $\xi(t) = Fr(t) \to 0$. □

Lemma 6.4. *Assume* $span(F) = span(C)$.[7] *If* (6.21) *(resp.* (6.20)*) is asymptotically stable for any* $D(t)$*, then* (6.22) *is* C*-stable (resp.* (6.23) *is* F*-stable).*

Proof. Since $FE = CB$, under the stated assumptions C-stability of (6.22) is equivalent to F-stability of (6.23), which is guaranteed by Lemma 6.3. Hence, starting from initial conditions of the form $\xi(0) = Cz(0)$, the solution $\xi(t) = Cz(t) \to 0$, where $z(t)$ is the solution of system (6.20). □

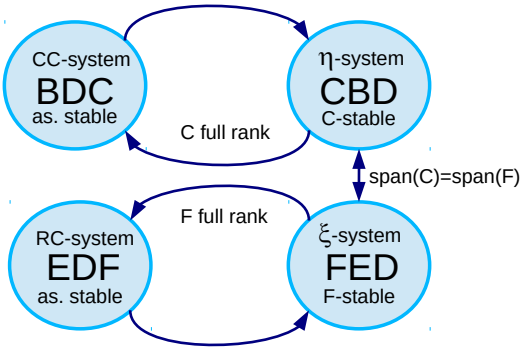

Figure 6.12: The connection between stability properties.

Lemma 6.5. *If* C *(resp.* F*) has full column rank and system* (6.22) *is* C*-stable (resp. system* (6.23) *is* F*-stable), then system* (6.20) *(resp.* (6.21)*) is asymptotically stable.*

Proof. Obviously, $\eta(t) = Cz(t) \to 0$ implies $z(t) \to 0$ if C has full column rank. The full rank assumption is fundamental; otherwise $Cz(t)$ may converge to zero, but $z(t)$ might diverge in the kernel of C. □

The connection between stability properties of the four systems (RC-system, in reaction coordinates; ξ-system; η-system; CC-system, in concentration coordinates) is summarised in Fig. 6.12 and leads to the main result of this section.

Theorem 6.6. *Assume that:*

[7] This means that $\text{rank}([F\ C]) = \text{rank}(F) = \text{rank}(C)$.

(i) both F and C have full column rank;
(ii) $span(F) = span(C)$.

Then the stability of system (6.20)*, in concentration coordinates, is equivalent to the stability of system* (6.21)*, in reaction coordinates.*

Since, for unitary networks, stability is equivalent to the existence of a polyhedral Lyapunov function, under the assumptions of Theorem 6.6 the outcome of the computational procedure must be the same.

Remark 6.10. *The injectivity assumption typically requires $m \geq n$ (the number of reactions is greater or equal to the number of species), while matrix F having full column rank typically requires $n \geq m$. Hence, the result in Theorem 6.6 particularly applies to the case $n = m$.*

6.10 Non-Polyhedral Lyapunov Functions

It is natural to wonder, at this point, whether structural stability of biochemical networks can be alternatively proved resorting to different (simpler, or smoother) Lyapunov functions.

The simplest possibility is resorting to quadratic Lyapunov functions; recall that the positive definite function

$$V_P(x) = x^\top P x, \qquad P \succ 0,$$

is a weak quadratic Lyapunov function for the system with state matrix A if $A^\top P + PA = -Q$ for a proper $Q \succeq 0$, or equivalently if $A^\top P + PA \preceq 0$. Quadratic Lyapunov functions have an ellipsoidal unit ball, as shown in Fig. 6.13.

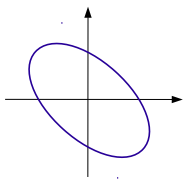

Figure 6.13: Ellipsoidal unit ball of a quadratic Lyapunov function.

To compare the effectiveness of polyhedral and quadratic Lyapunov functions for proving structural stability of chemical reaction networks, under the assumption of monotonicity of reaction rates, consider the basic chemical reaction motifs in Fig. 6.14, corresponding respectively to a chain of monomolecular reactions, a reversible monomolecular reaction, a bimolecular reaction, a bimolecular reversible reaction and a bimolecular-monomolecular reaction chain. In [BG15b], their stability has been structurally inquired by means of both quadratic and polyhedral Lyapunov functions, achieving the following result.

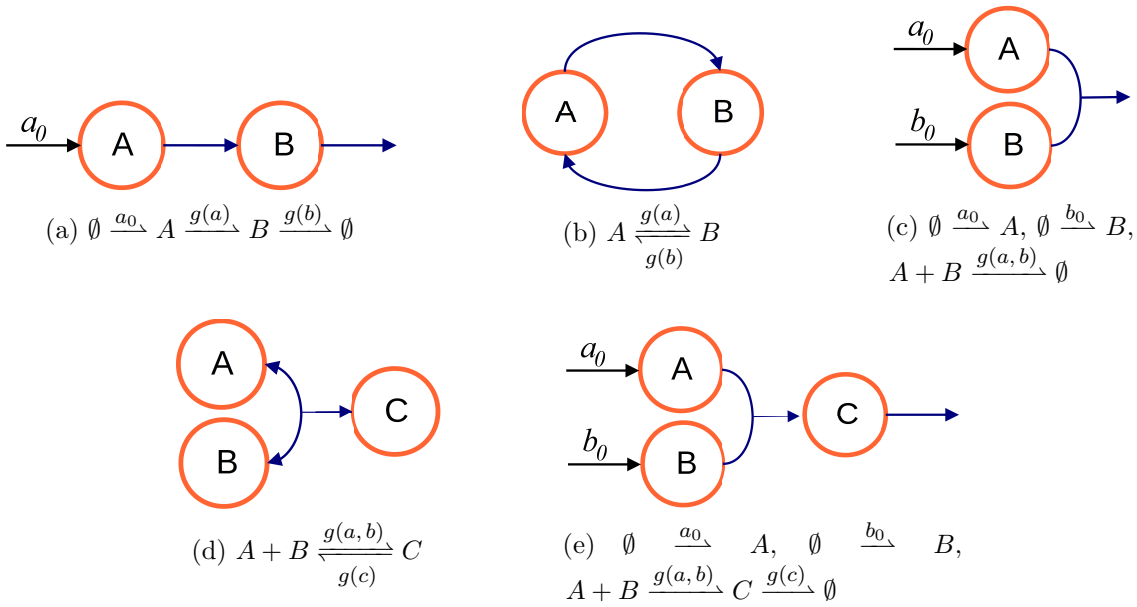

Figure 6.14: Graph representation of the considered basic motifs. [BG15b]

Proposition 6.12. *All of the chemical reaction networks in Fig. 6.14 are structurally stable and convergent, but none of them is structurally* quadratically *stable. Their structural stability can be proved resorting to polyhedral Lyapunov functions.*

For each case, the proof in [BG15b] shows in detail that, denoting by J the Jacobian matrix of the system, depending on the partial derivatives seen as positive parameters D_k, it is impossible to find a symmetric positive definite matrix P such that $J^\top P + PJ \preceq 0$ *for any choice of the parameters* $D_k > 0$; however, for all of the examined motifs, the numerical procedure proposed in [BG14] converges, ensuring the existence of a polyhedral Lyapunov function and, therefore, structural stability of the motif. The unit ball of the polyhedral Lyapunov functions corresponding to some of the motifs is shown in Fig. 6.15.

One could argue that the counterexamples are valid for the differential inclusion, but not for the original system. Yet, it must be reminded that *structural* (parameter-free) results are sought and that, as underlined in Remark 6.3, the Jacobian of the linearised original system (6.4) at the equilibrium $\bar{z} = 0$ has the same structure as the state matrix of system (6.5) ($J = BDC - \varepsilon I$). Therefore, if there is no quadratic Lyapunov function for the differential inclusion, there cannot be a local quadratic Lyapunov function that is *independent of parameter values*.

The networks analysed in Proposition 6.12 are simple but fundamental, being actual building blocks for huge and complex chemical reaction networks. Hence, for a network that contains one of these building blocks (practically, any reaction network), stability cannot be *structurally* investigated by means of quadratic Lyapunov functions.

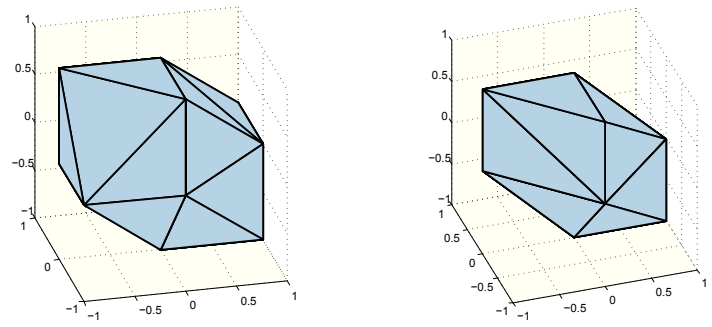

Figure 6.15: Unit ball of the polyhedral Lyapunov functions associated with the motif in Fig. 6.14 (d), left, and with the motif in Fig. 6.14 (e), right. [BG15b]

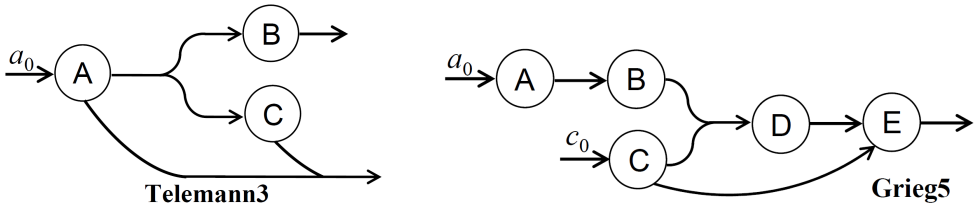

(a) $\emptyset \xrightarrow{a_0} A \xrightarrow{g(a)} B + C$, $B \xrightarrow{g(b)} \emptyset$, $A + C \xrightarrow{g(a,c)} \emptyset$

(b) $\emptyset \xrightarrow{a_0} A \xrightarrow{g(a)} B$, $\emptyset \xrightarrow{c_0} C \xrightarrow{g(c)} E \xrightarrow{g(e)} \emptyset$, $B + C \xrightarrow{g(b,c)} D \xrightarrow{g(d)} E$

Figure 6.16: Graph representation of the networks named Telemann3 and Grieg5. [BG14]

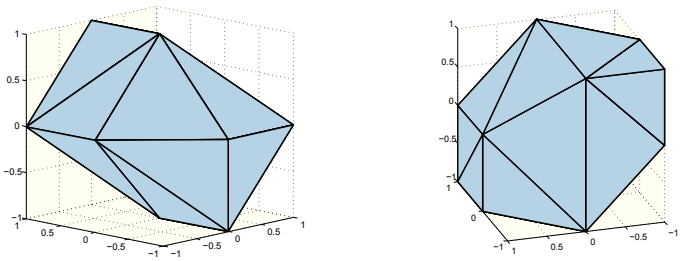

(a) Primal (b) Dual

Figure 6.17: Unit ball of the polyhedral Lyapunov functions (in concentration coordinates) associated with the network named Telemann3 in Fig. 6.16. [BG15a]

Example 6.7. *The chemical reaction networks in Fig. 6.16 include some of the basic motifs in Fig. 6.14. For these networks, according to Proposition 6.12, there is no hope to prove structural stability based on quadratic Lyapunov functions. However, the existence of a polyhedral Lyapunov function assures their structural stability, independent of parameters.*

Indeed, the network named Telemann3 in Fig. 6.16, which includes the motif in Fig. 6.14 (c), and therefore cannot be structurally quadratically stable, admits the polyhedral Lyapunov function with X as in (6.15)*, having the unit ball shown in*

Fig. 6.17 (a), and the dual with

$$F = \begin{bmatrix} 0 & 1 & 1 & -1 & 1 & 0 \\ 1 & 1 & 0 & 0 & 1 & 1 \\ 0 & 0 & 1 & 1 & -1 & -1 \end{bmatrix}^\top, \tag{6.24}$$

having the unit ball shown in Fig. 6.17 (b).

The reaction network named Grieg5 in Fig. 6.16, including the motifs in Fig. 6.14 (a), (c), (e), admits polyhedral Lyapunov functions whose unit ball has 22 *vertices in the primal case,* 68 *facets in the dual case.*

It can also be conjectured that the same negative result holds for logarithmic Lyapunov functions, such as entropy [Fei87, Han10], when considering more general reaction rates than mass action kinetics, since a logarithmic candidate Lyapunov function can be approximated as a quadratic function in a neighbourhood of the equilibrium.

In some interesting cases, it can be shown that a biochemical network whose structural stability can be proved resorting to polyhedral Lyapunov functions, by means of the procedure in [BG14], does not admit any smooth *structural* Lyapunov function.

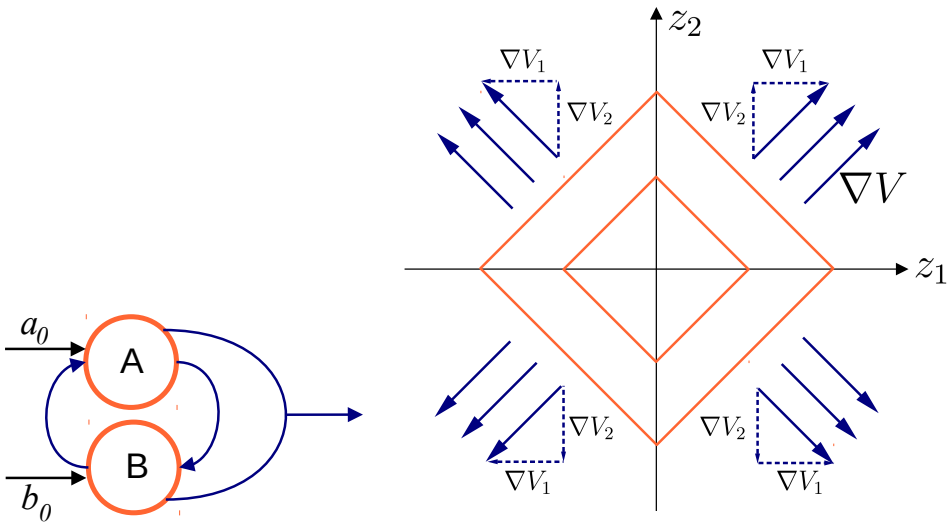

Figure 6.18: Example 6.8: graph (left) and unit ball of the Lyapunov function (right).

Example 6.8. *The simple system corresponding to the graph in Fig. 6.18 (left)*

$$\begin{cases} \dot{a} = -g_a(a) + g_b(b) - g_{ab}(a,b) + a_0 \\ \dot{b} = g_a(a) - g_b(b) - g_{ab}(a,b) + b_0 \end{cases}$$

(for which it is not difficult to see that an equilibrium always exists if all functions grow unbounded as a and b get large) has Jacobian matrix

$$J = \begin{bmatrix} -(\alpha+\beta) & \delta-\gamma \\ \beta-\alpha & -(\gamma+\delta) \end{bmatrix}.$$

Assume that the linearised system $\dot{z} = Jz$ admits the structural Lyapunov function $V(z)$, having gradient $\nabla V = [\nabla V_1 \quad \nabla V_2]$. This means that $\dot{V}(z) = \nabla V Jz < 0$ for any choice of $\alpha, \beta, \gamma, \delta > 0$. Detailed computations provide

$$\dot{V}(z) = [\beta(\nabla V_2 - \nabla V_1) - \alpha(\nabla V_2 + \nabla V_1)]z_1 + [\delta(\nabla V_1 - \nabla V_2) - \gamma(\nabla V_1 + \nabla V_2)]z_2 < 0.$$

For z_1, $z_2 > 0$, the inequality structurally *holds iff $\nabla V_2 = \nabla V_1 > 0$. For z_1, $z_2 < 0$, the inequality* structurally *holds iff $\nabla V_2 = \nabla V_1 < 0$. For $z_1 > 0$ and $z_2 < 0$, the inequality* structurally *holds iff $\nabla V_2 = -\nabla V_1 < 0$. For $z_1 < 0$ and $z_2 > 0$, the inequality* structurally *holds iff $\nabla V_1 = -\nabla V_2 < 0$. Based on the previous considerations, the function $V(z)$ is also decreasing when $z_1 = 0$, $z_2 \neq 0$ and when $z_1 \neq 0$, $z_2 = 0$. As shown in Fig. 6.18 (right), the only possible unit ball corresponding to such a function is the diamond. Hence, the unique structural Lyapunov function is polyhedral and no smooth Lyapunov functions can be found.*

6.11 Examples from the Catalogue

To evidence the potentiality of the proposed procedure, a stability test and a boundedness test have been performed for a large number of nontrivial biochemical networks, reported in Appendix A. [BG14] Each network is identified by the name of a musician and a number representing the order of the system.

Test results are summarised in Table A.1 (Appendix A, page 317), where in column CV (convergence) the outcome (Yes/No) of the procedure described in Section 6.3.1 is reported; in the Yes case, the number of vertices and the number of facets of the unit ball of the polyhedral function are indicated in the columns labelled as n_V and n_F, respectively. It can be noticed that the numbers n_V and n_F are surprisingly small, while in general polyhedral Lyapunov functions can be extremely complex [BM15]. Clearly the verdict on the existence of the function is always consistent, but the primal and the dual procedure may produce quite different numbers. The rank of S, reported in column r(S), evidences the dimension of the stoichiometric compatibility class; also the outcome (NCC=Yes/No) of the non-singularity test in the stoichiometric class is reported. To analyse the conservativeness of the test, random points (10^5) have been generated in the hypercube $\mathcal{C}_D$: column MR reports the sign of the maximum real part of the eigenvalues of all samples. All the networks whose eigenvalues have a positive random maximum real part are recognised as unstable, as expected. However, some networks that are locally marginally stable, according to the random eigenvalues outcome, do not pass the polyhedral function

Table 6.1: Results of the comparative numerical tests.

Network	CV_z	n_v	n_f	CV_r	n_v	n_f
Buxtehude3	No	-	-	No	-	-
Corelli3	Yes	6	6	Yes	6	6
Frescobaldi3	No	-	-	No	-	-
Telemann3	Yes	10	12	Yes	8	6
Boccherini4	No	-	-	No	-	-
Čajkovskij4	No	-	-	No	-	-
Gounod4	No	-	-	No	-	-
Offenbach4	No	-	-	No	-	-
Paganini4	Yes	14	18	Yes	12	8
Grieg5	Yes	22	68	Yes	52	22
Liszt5	Yes	28	66	Yes	52	22
Martucci5	No	-	-	No	-	-
Mahler6	Yes	12	62	No	-	-

CV = Convergence (Yes/No);
n_v = number of vertices (primal procedure);
n_f = number of facets (dual procedure).

test. The boundedness test is instead much less conservative, as evidenced by the results reported in the last column (BO=Yes/No).

The proposed numerical procedures appear effective and useful for detecting stability also in complex, quite large reaction networks: Table A.1 shows that systems up to 8-10 variables can be efficiently analysed, which is still surprising in the context of polyhedral functions, which are known to be computationally challenging.

A subset of the systems in Appendix A has been analysed both in concentration (z) and in reaction (r) coordinates: comparative test results are reported in Table 6.1. Column $\text{CV}_{z/r}$ shows whether the procedure converges (Yes/No) in concentration/reaction coordinates. In both cases, whenever the polyhedral function is found, the number of vertices and the number of facets of its unit ball are shown in the columns labelled as n_v and n_f respectively. All the networks in Table 6.1 correspond to regular systems. For all of them, apart from Mahler6, the assumptions of Theorem 6.6 hold and, as expected, the convergence outcome of the computational procedure is the same in the two frameworks. For the network named Mahler6, the procedure converges in concentration coordinates, but not in reaction coordinates; for this system, as can be verified, matrix F does not have full (column) rank.

For instance, the network named Telemann3 (see Fig. 6.16) admits in concentration coordinates the primal and dual polyhedral Lyapunov functions reported in (6.15) and (6.24) (the unit ball is shown for both cases in Fig. 6.17); in reaction coordinates, it admits the polyhedral Lyapunov function with

$$X = \begin{bmatrix} -1 & 1 & -1 & -1 \\ -1 & 1 & 1 & 1 \\ 1 & 1 & 1 & -1 \end{bmatrix},$$

whose unit ball is the cube of side 2, centered in the origin, and the dual function with $F = I$, the identity matrix, corresponding to the unit ball of the 1-norm (diamond).

6.12 Remarks

The proposed method to structurally assess stability and boundedness of biochemical reaction networks with monotonic reaction rates can admit several extensions. Further work in this framework aims at proving the existence of a positive equilibrium point for the system. An intriguing direction for further research concerns the global stability property; so far, global stability can be established under the assumption that an ε-degradation is present. Without any ε-degradation assumption, it has been shown that the existence of a polyhedral Lyapunov function (in concentration coordinates) assures just *local* stability of the equilibrium (if any), provided that matrix BDC is robustly non-singular. It would be interesting to understand whether, under appropriate conditions, it is possible to remove the assumption of ε-degradation and still ensure *global* stability.

7

Structural Steady-State Analysis of Biological Systems

The problem of identifying structural influences of external inputs on steady-state outputs is considered here, with a special focus on biological network models, following [GCFB15]. A *structural influence* is identified when, upon a perturbation due to a constant input, the ensuing variation of the steady-state output value has the same sign as the input (positive influence), the opposite sign (negative influence), or is zero (perfect adaptation), for any feasible choice of the model parameters. When persistent additive inputs are applied to a single state variable and outputs are taken as single state variables, all the resulting signs and zeros can constitute a structural *influence matrix*, whose (i, j) entry indicates the sign of the steady-state influence of the jth system variable on the ith variable (namely, the variation in the steady state of the ith variable, caused by an external persistent input applied to the jth variable). Each entry is structurally determinate if the sign of the variation does not depend on the choice of the parameters, but is indeterminate otherwise. In principle, determining the influence matrix requires exhaustive testing of the system steady-state behaviour in the widest range of parameter values. However, for any system admitting a BDC-decomposition, the influence matrix can be evaluated with an algorithm that tests the system steady-state behaviour only at a finite number of points (*i.e.*, the vertices of a hypercube defined in the parameter space). By means of the same algorithm, the structural effect of any perturbation, such as variations of relevant parameters, can be assessed as well.

In this chapter, a broad class of biological networks is considered; the method is applied to nontrivial models of biochemical reaction networks and population dynamics drawn from the literature, providing a parameter-free insight into the system dynamics.

7.1 Background and Motivating Examples

The general concept of *steady-state influence* concerns the effect of a persistent input applied to the system on the steady-state variation of a suitable output. This includes

perfect adaptation as a special case: as seen in Section 2.3.9, a variable embedded in a system is adaptive if, in the presence of a persistent input, after a transient it reverts to its pre-perturbation value, and adaptation is perfect if the pre-perturbation value is exactly recovered at steady state.

Suppose that a persistent input is applied to the system. Then, the steady-state variation of a system variable (regarded as an output) may have the same or the opposite sign of the applied input, or may be zero (perfect adaptation). A *structural influence* is present if the sign of the variation does not depend on the value of the system parameters. In particular, the effect of an external input *applied to each of the system variables* on the steady-state variation of each of the variables can be considered: in this case, the steady-state interactions can be represented by the structural *influence matrix*.

The problem of determining structural influences is well known in the field of ecology, and is related to the notion of community matrix [Lev68], which is the Jacobian matrix of the system of growth equations and thus describes interactions among and within species in a community near equilibrium. The community matrix, expressing direct effects only, was first qualitatively analysed in [Lev74, Lev75] in terms of signed entries, graphs and loops. The net steady-state effect, combining all direct and indirect effects, is expressed by the adjoint matrix of the negative of the community matrix. [Lev74, Lev75, DLR02, DLR03, DLLR03, DLR05] When the sign of some entries of the adjoint matrix is indeterminate, the net response predicted by the model is uncertain: to quantify this uncertainty, a weighted-predictions matrix was introduced [DLR02, DRJ07] that assigns a probability to the predicted sign of the response. Recently, a theoretical approach and an algorithm to determine the sign of changes in steady states upon parameter perturbations in biochemical reaction networks have been proposed in [Son14b, Son14a]. In [MF15], the structural variation in species concentrations/fluxes when a reaction in the network is altered has been studied, under qualitative assumptions (positivity, smoothness, monotonicity of rate functions). This type of investigation is focused on the *steady-state* response to external stimuli, in contrast with other approaches that consider the *dynamic* interactions between variables.

This chapter presents the computational approach proposed in [GCFB15] to *structurally* assess the steady-state input-output influences. The structural influence is *determinate* if, for any feasible choice of the system parameters, the steady-state variation in the output value is zero ('0', perfect adaptation), or its sign is concordant ('+') or discordant ('−') with the sign of the external stimulus. In contrast, if the sign of the variation depends on the magnitude of the parameters, the influence is *indeterminate* ('?'). A particular type of structural steady-state influences can be represented by means of the *influence matrix*: the (i, j) entry of this matrix represents the influence on variable i (output) of an additive input persistently applied to variable j. In ecological models (at least, in their Lotka-Volterra approximations), the structural influence matrix corresponds to the sign pattern of the adjoint of the negative of the community matrix. An efficient algorithm is proposed that allows to

compute structural steady-state variations due to external stimuli, and in particular the structural influence matrix, for any system admitting the BDC-decomposition described in Section 4.3. The structural sign of the input-output influence, for *any* feasible choice of the parameters, can be determined by checking just a *finite* number of points in the parameter space, corresponding to the vertices of the unit hypercube. This is possible because, for systems admitting a BDC-decomposition, the expression of the input-output influence turns out to be a multi-affine function defined on a hypercube, hence it reaches its extreme values on the vertices of the hypercube (as discussed in Section 4.4).

Recall that a wide class of biological systems, which can be written in terms of a "stoichiometry" matrix and a vector of "reaction rates", have a Jacobian matrix that always admits a BDC-decomposition where matrices B and C depend on the stoichiometry matrix and matrix D depends on the partial derivatives of the reaction rate functions (cf. Section 4.3).

A noteworthy feature of the algorithm proposed in [GCFB15] is that it can handle parametric dependencies between the entries of the Jacobian matrix; thus, the algorithm can assess structural sign determinacy of the influence even when the Jacobian matrix is not sign-definite. This is an advantage relative to the existing literature that considers solely matrices with independent entries. For systems with independent Jacobian entries, a tree-like recursive algorithm can be used to compute the influence matrix, which enhances computational efficiency. Also the case of marginally stable systems, whose trajectories evolve in the stoichiometric compatibility class associated with the initial conditions, is considered. For these systems, any persistent input might cause divergence of the trajectories in time; however, a structural input-output influence analysis can be carried out by considering impulsive, rather than persistent, inputs.

To show the effectiveness of the algorithm in explaining the intrinsic behaviour of the system in terms of steady-state response to external stimuli, several models of biochemical and ecological systems proposed in the literature are analysed.

First, some background is provided and the concept of influence matrix is introduced by means of two illustrative examples, which show what structural information can be obtained.

Example 7.1. *Consider the following Lotka-Volterra prey-predator model [May74]*

$$\begin{cases} \dot{H}(t) = H(t)[r(1 - H(t)/K) - aP(t)] + u_1, \\ \dot{P}(t) = P(t)(-b + cH(t)) + u_2, \end{cases} \tag{7.1}$$

where $H(t)$ are the prey and $P(t)$ the predators; a, b, c, r and K are positive parameters; u_1 and u_2 are persistent external inputs. The birth rate of the prey population is modelled with the Verhulst-Pearl logistic term $r(1 - H(t)/K)$. When $u_1 = u_2 = 0$, the stable equilibrium is E_0: $\bar{H}_0 = \frac{b}{c}$, $\bar{P}_0 = \frac{r}{a}\left(1 - \frac{b}{cK}\right)$ (other equilibria are E_1: $\bar{H}_1 = K$, $\bar{P}_1 = 0$ and E_2: $\bar{H}_2 = 0$, $\bar{P}_2 = 0$). Consider the equilibrium E_0

and suppose now that there is a constant injection or removal of prey or predators, i.e., *inputs u_1 or u_2 become non-zero and constant. How does this perturbation affect the equilibria? The perturbation is assumed to be sufficiently small, so that the equilibrium remains stable and non-zero, and does not disappear (for instance, for large negative values of u_i the equilibrium may not exist).*

Assume there is an injection or removal of prey, i.e., *input $u_1 \neq 0$, and denote as $\bar{H}$ and $\bar{P}$ the new coordinates of the equilibrium E_0. From the second equation,*

$$\bar{P}(-b + c\bar{H}) = 0,$$

so the steady-state value of the prey will be unchanged: $\bar{H} = b/c$. From the first equation

$$\bar{H}[r(1 - \bar{H}/K) - a\bar{P}] + u_1 = 0,$$

being $\bar{H}$ unchanged, it can be seen that $\bar{P}$ is an increasing function of u_1.

The conclusion is that, no matter how the parameters are taken within the domain where E_0 exists, after a transient the predator population variation $\bar{P} - \bar{P}_0$ has the same sign of u_1: $\bar{P} > \bar{P}_0$ if $u_1 > 0$, $\bar{P} < \bar{P}_0$ if $u_1 < 0$. Hence, the influence of u_1 on P is structurally positive. *Conversely, since $\bar{H} = \bar{H}_0$ is unchanged, the influence of u_1 on H is structurally zero. This phenomenon corresponds to* perfect adaptation*: a positive (negative) u_1 causes an initial increase (decrease) of the prey, but at steady-state the prey population converges to the unperturbed value $\bar{H}_0$, due to a compensating effect associated with the variation in the predator population.*

With similar computations it can be argued that, if a predator injection is considered (input $u_2 \neq 0$), the structural influence on H is negative and on P is positive: if $u_2 > 0$ ($u_2 < 0$ respectively), $\bar{H} < \bar{H}_0$ and $\bar{P} > \bar{P}_0$ ($\bar{H} > \bar{H}_0$ and $\bar{P} < \bar{P}_0$).

Since the steady-state values $\bar{H}$ and $\bar{P}$ are functions of u_1 and u_2, $\bar{H}(u_1, u_2)$ and $\bar{P}(u_1, u_2)$, implicitly defined by the equilibrium conditions, it is possible to equivalently compute and inspect the signs of the corresponding partial derivatives. Then, structurally, *$\partial\bar{H}/\partial u_1 = 0$, $\partial\bar{P}/\partial u_1 > 0$, $\partial\bar{H}/\partial u_2 < 0$, $\partial\bar{P}/\partial u_2 > 0$.*

To visualise at once the steady-state interactions between inputs applied to each system variable and outputs taken as a single system variable, a structural steady-state influence matrix *can be built, which in the following will be denoted as matrix M. The (i, j) entry of matrix M is '+', '−', or '0' if, for any feasible choice of the model parameters, an input u_j (representing a persistent external injection applied to the jth population) causes a change of the same sign, opposite sign, or no change in the steady state of the ith population (seen as an output). Based on the performed calculations, the influence matrix M for the prey-predator system* (7.1) *is:*

$$M = \begin{bmatrix} 0 & - \\ + & + \end{bmatrix}. \tag{7.2}$$

The prey-predator model is a sufficiently simple case where the influence matrix can be computed analytically. However, building matrix M in large and complex networks requires a more sophisticated and computationally efficient approach. Two issues are worth pointing out.

(a) An equilibrium (steady-state) may not exist, or it may be unstable. However, in many cases of practical interest in biology and ecology, the existence of a stable equilibrium is possible or even guaranteed. In the following, it is assumed that an equilibrium exists and is stable. In the concluding remarks, parameter-independent criteria for the existence of an equilibrium and its stability will be discussed.

(b) Especially in complex systems, some entries of M may not be structurally determinate, namely, the sign may depend on the choice of the system parameters. The structural influence matrix M has a '?' entry in the position (i, j) whenever the sign of the variation in the steady state of the ith variable, due to an additive input persistently applied to the jth variable, is not structurally determinate.

As shown in [DLR02, DLR03], the influence matrix M corresponds to the sign pattern of $\mathrm{adj}(-J)$, where J is the system Jacobian matrix computed at the equilibrium. This highlights the relationship between the system Jacobian and the structural influence matrix M.

For instance, for the prey-predator model (7.1), at the equilibrium E_0, the Jacobian matrix, along with its BDC-decomposition, is

$$J = \begin{bmatrix} -r\bar{H}/K & -a\bar{H} \\ c\bar{P} & 0 \end{bmatrix} = \begin{bmatrix} -\alpha & -\beta \\ \gamma & 0 \end{bmatrix} = \underbrace{\begin{bmatrix} 1 & 1 & 0 \\ 0 & 0 & 1 \end{bmatrix}}_{=B} \underbrace{\mathrm{diag}\{\alpha, \beta, \gamma\}}_{=D} \underbrace{\begin{bmatrix} -1 & 0 \\ 0 & -1 \\ 1 & 0 \end{bmatrix}}_{=C}. \tag{7.3}$$

Then it can be immediately seen that

$$\mathrm{adj}(-J) = \begin{bmatrix} 0 & -a\bar{H} \\ c\bar{P} & r\bar{H}/K \end{bmatrix} = \begin{bmatrix} 0 & -\beta \\ \gamma & \alpha \end{bmatrix}$$

has the same sign pattern shown in (7.2).

However, sign-definiteness of the Jacobian entries does not directly relate to the existence or absence of structural steady-state influences.

Example 7.2. *Consider a synthetic gene network designed to regulate the transcription rate of RNA species, which bind to form output products [FFM08, FM08, GFM13, FGFM14]. Two RNA species, transcribed by two separate genes, bind to form a product; the presence of self-repression loops causes their transcription rates to be equated at steady state. The system is described by the following equations [FFM08, FGFM14]:*

$$\begin{cases} \dot{g}_i = \alpha_i(g_i^{tot} - g_i) - \delta_i g_i r_i \\ \dot{r}_i = \beta_i g_i - \delta_i g_i r_i - k r_i r_j \end{cases}, \qquad i, j \in \{1, 2\}, \quad i \neq j,$$

where g_i are active gene template concentrations (active and inactive gene templates are present in a total amount $g_i^{tot} = g_i + g_i^*$), transcribed to produce RNA species

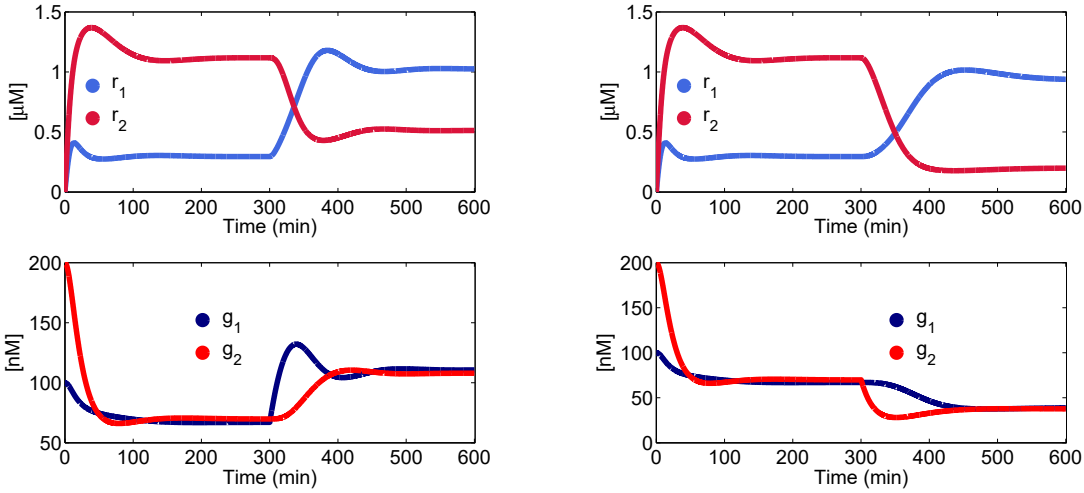

(a) g_1^{tot} is increased to 300 nM at $t^* = 300$ min (b) g_2^{tot} is decreased to 50 nM at $t^* = 300$ min

Figure 7.1: Simulation results for the self-repression two-gene rate regulatory network: time evolution of species concentrations. Top: free RNA concentrations. Bottom: active gene concentrations. Parameter values are consistent with the literature about synthetic gene networks: $\alpha_1 = \alpha_2 = 3{\cdot}10^{-4}$ s^{-1}, $\beta_1 = \beta_2 = 1 \cdot 10^{-2}$ s^{-1}, $\delta_1 = \delta_2 = 500$ M^{-1} s^{-1}, $k = 2 \cdot 10^{-3}$ M^{-1} s^{-1}; initially, $g_1^{tot} = 100$ nM and $g_2^{tot} = 200$ nM.

(with concentrations r_i), which in turn bind to form a product; α_i are gene activation rates, β_i are transcription rates, δ_i is the self-repression coefficient for subsystem g_i-r_i, while k is the product generation rate. Besides its rate regulatory task, it can be expected that this network exhibits tracking properties *when the total concentration of a gene template varies. In fact, if g_i^{tot} increases (this is equivalent to an input u_i acting on g_i), then, at steady state, g_i increases and so does r_i. Due to the increase in r_i, more binding sites are created, hence r_j decreases (the RNA species is more required). Stoichiometric self-inhibition is reduced and g_j increases. Of course, the concentration increases* provided that it can*: since the reagents bind according to a given stoichiometry, the expected increase can only occur if the reagent with the lowest concentration is augmented until it is no more a bottleneck for the output production. Still, the behaviour of r_j is not clearly predictable: the increase in r_i should increase its consumption, while the increase in g_j should increase its production. Does one of the two opposite effects structurally dominate?*

The system tracking properties may be inquired via simulation: results are shown in Fig. 7.1. It can be seen that, when g_1^{tot} increases, g_1 increases too and this leads to an increase in r_1 and in g_2, while r_2 decreases. Analogously, when g_2^{tot} decreases, g_2 decreases as well and this leads to a reduction in r_2 and in g_1, while r_1 increases. Yet, a simulation performed for a particular choice *of the parameters cannot provide a structural answer. Even a huge number of simulations with different parameter values cannot assure that the property holds in the whole parameter space, no matter*

how densely sampled.[1]

It is then fundamental to resort to a structural analysis. The Jacobian matrix for this network is

$$J = \begin{bmatrix} -(\alpha_1 + \delta_1 \bar{r}_1) & -\delta_1 \bar{g}_1 & 0 & 0 \\ \beta_1 - \delta_1 \bar{r}_1 & -(\delta_1 \bar{g}_1 + k\bar{r}_2) & 0 & -k\bar{r}_1 \\ 0 & 0 & -(\alpha_2 + \delta_2 \bar{r}_2) & -\delta_2 \bar{g}_2 \\ 0 & -k\bar{r}_2 & \beta_2 - \delta_2 \bar{r}_2 & -(\delta_2 \bar{g}_2 + k\bar{r}_1) \end{bmatrix}.$$

Note that J_{21} and J_{43} are structurally positive, in view of the equilibrium conditions $(\beta_i - \delta_i \bar{r}_i)\bar{g}_i = k\bar{r}_i\bar{r}_j$.

Computation of the steady-state influence shows that, for any feasible choice of the parameters, when g_1^{tot} increases, g_1 increases too and this leads to an increase in r_1 and in g_2, while r_2 decreases. Analogously, when g_2^{tot} decreases, g_2 decreases as well and this leads to a reduction in r_2 and in g_1, while r_1 increases. Hence, the rate regulatory system exhibits tracking properties at steady state for any feasible choices of the parameters. The influence matrix M, which can be computed as the sign pattern of $adj(-J)$, is

$$\begin{array}{c} \\ \\ \textit{effect on variable} \end{array} \begin{array}{c} \\ g_1 \{ \\ r_1 \{ \\ g_2 \{ \\ r_2 \{ \end{array} \begin{array}{c} \textit{input applied to variable} \\ \overbrace{}^{g_1}\ \overbrace{}^{r_1}\ \overbrace{}^{g_2}\ \overbrace{}^{r_2} \\ \begin{bmatrix} + & - & + & + \\ + & + & - & - \\ + & + & + & - \\ - & - & + & + \end{bmatrix} \end{array}.$$

Independent of the system parameters, an external input affecting r_i decreases both g_i and r_j, while increases g_j and r_i itself. The effect of an external input affecting g_i is the same that is obtained when incrementing g_i^{tot}. A powerful parameter-free insight has thus been gained into the system behaviour, in terms of sign of the change in the steady states of the variables due to an external stimulus.

The size and complexity of this second example are still tractable: the analytical computation of the influence matrix is tedious but possible. However, for large and complex systems, algebraic calculations are not scalable and a computational approach is needed. In this chapter, a systematic and efficient numerical method will be described for computing steady-state influences.

Remark 7.1. *As will be shown, with respect to [DLR02, DLR03, DLLR03, DLR05], the algorithm proposed in [GCFB15] can deal with the existence of constraints due to parameters repeated in more than one entry (*e.g.*, in Example 7.2, $\delta_1\bar{r}_1$ appearing in both J_{11} and J_{21}).*

[1] A property may hold everywhere except for a zero-measure set of points, which would be practically undetectable by means of a random analysis.

7.2 A Vertex Algorithm to Assess Structural Influences

An efficient algorithm to compute structural steady-state input-output influences is described in this section. The algorithm applies to any system admitting a BDC-decomposition (see Section 4.3); in this case, in fact, *parameter-independent steady-state influences* between the input and the output can be structurally assessed based on matrices B and C. The algorithm is based on the evaluation of the sign of the determinant of a matrix at a finite number of points.

Consider a general nonlinear system

$$\dot{x}(t) = f(x(t), u(t)), \tag{7.4}$$

$$y(t) = g(x(t)), \tag{7.5}$$

where $f(\cdot,\cdot)$ and $g(\cdot)$ are continuously differentiable, $x \in \mathbb{R}^n$, $u \in \mathbb{R}$ is an input and $y \in \mathbb{R}$ is an output. Assume that there exists an equilibrium point $\bar{x} > 0$ (componentwise), corresponding to $\bar{u}$, such that $f(\bar{x}, \bar{u}) = 0$, and consider the corresponding output steady-state value $\bar{y} = g(\bar{x})$. So both the steady-state values $\bar{x}(u)$ and $\bar{y}(u)$ are functions of u. The following standing assumptions are made.

- B1 The considered equilibrium $\bar{x}$ is asymptotically stable.
- B2 The input perturbation u is small enough to ensure that the stability of $\bar{x}(u)$ is preserved.[2]

The influence is determined by the derivative of the steady-state map that relates a given input u to a specific output y. For system (7.4)-(7.5), the implicit function theorem provides an analytical expression for the derivative of the steady-state input-output map:

$$\frac{\partial \bar{y}}{\partial \bar{u}} = \left.\frac{\partial g}{\partial x}\right|_{\bar{x}} \left(-\left.\frac{\partial f}{\partial x}\right|_{(\bar{x},\bar{u})} \right)^{-1} \left.\frac{\partial f}{\partial u}\right|_{(\bar{x},\bar{u})}. \tag{7.6}$$

Consider the linear approximation of the nonlinear system in a neighbourhood of the equilibrium $\bar{x}$. Then, denoting by $z(t) = x(t) - \bar{x}$, $v(t) = u(t) - \bar{u}$, $w(t) = y(t) - \bar{y}$, the linearised system is

$$\begin{cases} \dot{z}(t) = Jz(t) + Ev(t), \\ w(t) = Hz(t), \end{cases}$$

where $[J]_{ij} = \left.\frac{\partial f_i}{\partial x_j}\right|_{(\bar{x},\bar{u})}$, $[E]_i = \left.\frac{\partial f_i}{\partial u}\right|_{(\bar{x},\bar{u})}$ and $[H]_j = \left.\frac{dg}{dx_j}\right|_{\bar{x}}$. J is the Jacobian matrix, while E and H are a column and a row vector representing, respectively, how the input acts on the system state and how the output depends on the system state in the linearised system.

[2] The eigenvalues of the Jacobian matrix are continuous functions of its entries, which, in turn, are continuous functions of u.

Proposition 7.1. *For system* (7.4)-(7.5),

$$\frac{\partial \bar{y}}{\partial \bar{u}} = H(-J)^{-1}E = \frac{1}{\det(-J)} \det \begin{bmatrix} -J & -E \\ H & 0 \end{bmatrix}. \tag{7.7}$$

Proof. The first equality is immediate in view of (7.6). As for the second equality, since

$$\begin{bmatrix} -J & -E \\ H & 0 \end{bmatrix} = \begin{bmatrix} I_n & 0 \\ -HJ^{-1} & 1 \end{bmatrix} \begin{bmatrix} -J & -E \\ 0 & H(-J)^{-1}E \end{bmatrix},$$

where the matrices in the product are block-triangular and $H(-J)^{-1}E$ is a scalar, it follows that

$$\det \begin{bmatrix} -J & -E \\ H & 0 \end{bmatrix} = 1 \cdot \det(-J) \left[H(-J)^{-1}E \right].$$

□

Since the equilibrium is assumed to be stable, $\det(-J)$ is always positive. For any system whose Jacobian J admits a BDC-decomposition, to evaluate the sign of $\frac{\partial \bar{y}}{\partial \bar{u}}$, it suffices to consider the sign of

$$r(D) \doteq \det \begin{bmatrix} -J & -E \\ H & 0 \end{bmatrix} = \det \begin{bmatrix} -BDC & -E \\ H & 0 \end{bmatrix}. \tag{7.8}$$

To assess the *structural* influence on the output y due to the input u, it must be verified whether function $r(D)$ is sign-definite, namely, it has the same sign *for all* the possible choices of D. The following result states that the *structural* sign of $r(D)$ in (7.8) can be determined by checking a *finite* number of points, namely, the vertices of the unit hypercube

$$\mathcal{C}_D = \{D_k : 0 \leq D_k \leq 1,\, k = 1, \ldots, q\}.$$

Theorem 7.1. *[GCFB15] Denote by $D^{(v)}$ the matrices corresponding to the vertices of the hypercube $\mathcal{C}_D$, $v = 1, \ldots, 2^q$. Then:*

a) $r(D) > 0$ structurally if and only if $r(D^{(v)}) \geq 0$ for all v and $r(D) > 0$ for $D = I$;
b) $r(D) < 0$ structurally if and only if $r(D^{(v)}) \leq 0$ for all v and $r(D) < 0$ for $D = I$;
c) $r(D) = 0$ structurally if and only if $r(D^{(v)}) = 0$ for all v.

Proof. First, notice that $r(D)$ is multi-affine and positively homogeneous; hence, the sign of $r(D)$, with $D_i > 0$, does not change if D is scaled with a positive factor: $\text{sign}[r(D)] = \text{sign}[r(\varphi D)]$ for any positive φ. Indeed, consider $\varphi J = B(\varphi D)C$. Then

$$\begin{aligned} \det \begin{bmatrix} -\varphi J & -E \\ H & 0 \end{bmatrix} &= \det \begin{bmatrix} \varphi I_n & 0 \\ 0 & 1 \end{bmatrix} \det \begin{bmatrix} -J & -E \\ H & 0 \end{bmatrix} \det \begin{bmatrix} I_n & 0 \\ 0 & 1/\varphi \end{bmatrix} \\ &= \varphi^{n-1} \det \begin{bmatrix} -J & -E \\ H & 0 \end{bmatrix}. \end{aligned}$$

Therefore, $r(D)$ is positive (negative, zero) for all $D_i > 0$ if and only if it is positive (negative, zero) in all points $D_i > 0$ in the unit cube. The claims can then be proved based on Theorem 4.3 presented in Section 4.4. □

Based on Theorem 7.1, for any system (7.4) *admitting a BDC-decomposition*, the structural steady-state influence of *any* input provided to the system on *any* output of the form (7.5) can be tested as follows.[3]

Procedure 7.1. ***Vertex algorithm.***
Input: *Matrices B and C of the BDC-decomposition and matrices E and H appearing in* (7.8).
Output: *The steady-state structural influence sign $\sigma \in \{+, -, 0, ?\}$.*

1. *Let $\omega_{max} = \omega_{min} := 0$.*
2. *For $k = 0, 1, \ldots, 2^q - 1$, consider its binary representation $k_{bin} := [D_1, D_2, \ldots, D_q] \in \{0, 1\}^q$.*
   (a) *Let $D = diag\{D_1, D_2, \ldots, D_q\}$.*
   (b) *Let $\omega_{min} := \min\{\omega_{min}, sign[r(D)]\}$ and $\omega_{max} := \min\{\omega_{max}, sign[r(D)]\}$;*
3. *IF $\omega_{min} = 0$ and $\omega_{max} = 1$, then $\sigma := +$;*
4. *IF $\omega_{min} = -1$ and $\omega_{max} = 0$, then $\sigma := -$;*
5. *IF $\omega_{min} = 0$ and $\omega_{max} = 0$, then $\sigma := 0$;*
6. *IF $\omega_{min} = -1$ and $\omega_{max} = 1$, then $\sigma :=?$.*

The outcome of the procedure is one of the four cases represented in Fig. 7.2. Figures 7.2 (a)-(c) illustrate the cases where the sign of the output variation, when the input varies as a step function, is structurally determinate; Fig. 7.2 (d) depicts the case where no structural influence can be identified, because the output could either increase, decrease or not vary, depending on the specific choice of the parameters.

Remark 7.2. *The algorithm has exponential complexity: if the diagonal matrix D has dimension q, the sign of $r(D)$ must be explored on the 2^q vertices of the hypercube.*

The result exploits the fact that J is the positive linear combination of rank-one matrices, hence $r(D)$ is a multi-affine function defined on a hypercube (or a hyper-box) and reaches its extrema on the vertices (which is crucial in the proof of Theorem 7.1, since it is based on Theorem 4.3). In the general case of a convex combination of matrices that do not have rank one (hence, the system does not admit a BDC-decomposition), such a vertex result is not assured. For instance,

$$\det \begin{bmatrix} a & 0 \\ 0 & a-b \end{bmatrix} = a(a-b)$$

[3] A MATLAB implementation of the algorithm is available at `https://users.dimi.uniud.it/~franco.blanchini/influence.zip` (see also Appendix B.2).

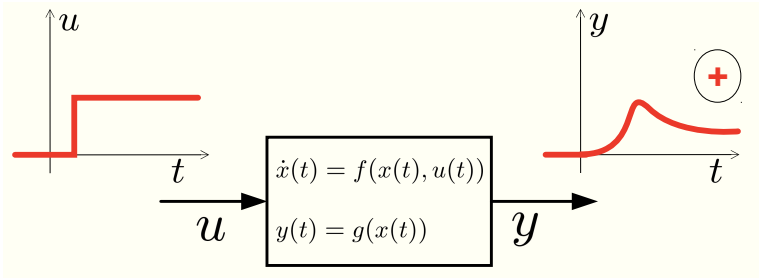

(a) Increase: the structural influence is '+'.

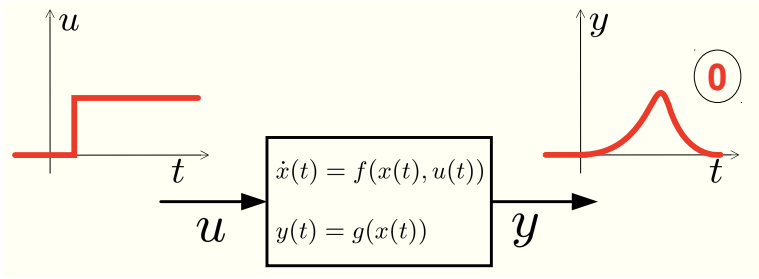

(b) Perfect adaptation: the structural influence is '0'.

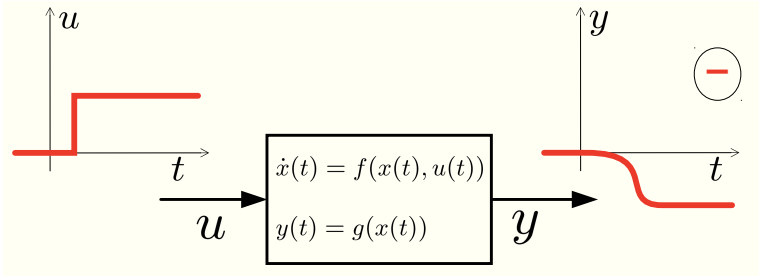

(c) Decrease: the structural influence is '−'.

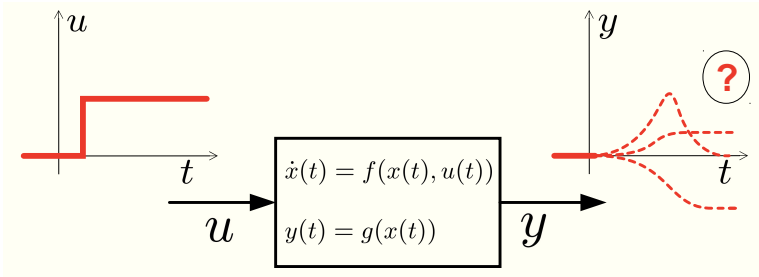

(d) Indeterminate: the structural influence is '?'.

Figure 7.2: Illustration of the structural input-output influence. The structural influence is determinate if a step in the input causes a positive (a), zero (b), or negative (c) change in the output steady state, for any feasible choice of the system parameters. The structural influence is indeterminate when the output variation can be positive, zero, or negative, depending on the system parameters (d). [GCFB15]

is not multi-affine in the parameters: given for instance the square $0 \leq a, b \leq 1$, this determinant is never negative on the four vertices; however, for $b = 1$ and $a = 1/2$, the determinant is $-1/4 < 0$. This happens because the matrix associated with a (which is the identity $I_2 \in \mathbb{R}^{2\times 2}$) has rank two.

Remark 7.3. *The vectors E and H are in general functions of the parameters, namely, of the partial derivatives (with respect to x and to u): $[E]_i = \frac{\partial f_i}{\partial u}\big|_{(\bar{x},\bar{u})}$ and $[H]_j = \frac{dg}{dx_j}\Big|_{\bar{x}}$. This not an issue, because $r(D)$ is still a multi-affine function of the parameters.*

The proposed approach can be used to establish the existence of a structural influence of *any input* on a given output. Since uncertain parameters (for example, in biochemical systems, binding rates, dissociation constants, or Hill coefficients) can be considered as inputs subject to variations, the method can be applied to identify the structural influence of a system parameter on the system outputs. This interesting case is illustrated with an example.

Example 7.3. *Consider the system*

$$\begin{cases} \dot{x}_1 = -pf_1(x_1, x_2) + f_3(x_3) + x_{1,0} \\ \dot{x}_2 = -pf_1(x_1, x_2) - f_2(x_2) + x_{2,0} \\ \dot{x}_3 = pf_1(x_1, x_2) - f_3(x_3) - f_4(x_3) \end{cases}$$

where p is a positive parameter considered as input, $u = p$. In its Jacobian

$$J = \begin{bmatrix} -\tilde{\alpha} & -\tilde{\beta} & \gamma \\ -\tilde{\alpha} & -(\tilde{\beta}+\delta) & 0 \\ \tilde{\alpha} & \tilde{\beta} & -(\gamma+\varepsilon) \end{bmatrix}, \qquad \tilde{\alpha} = p\alpha, \quad \tilde{\beta} = p\beta,$$

Greek letters denote the absolute value of the partial derivatives $|\partial f_j/\partial x_i|$. The characteristic polynomial has only positive coefficients; it can be shown by means of the Routh-Hurwitz criterion (the Routh-Hurwitz table is not reported here for brevity) that it is stable for any choice of the positive parameters. The BDC-decomposition and vector E are

$$J = \underbrace{\begin{bmatrix} -1 & -1 & 1 & 0 & 0 \\ -1 & -1 & 0 & -1 & 0 \\ 1 & 1 & -1 & 0 & -1 \end{bmatrix}}_{=\mathrm{B}} \underbrace{diag\{\tilde{\alpha}, \tilde{\beta}, \gamma, \delta, \varepsilon\}}_{=\mathrm{D}} \underbrace{\begin{bmatrix} 1 & 0 & 0 \\ 0 & 1 & 0 \\ 0 & 0 & 1 \\ 0 & 1 & 0 \\ 0 & 0 & 1 \end{bmatrix}}_{=\mathrm{C}},$$

$$E = \begin{bmatrix} -\zeta \\ -\zeta \\ \zeta \end{bmatrix},$$

where $\zeta = |\partial \dot{x}_i/\partial p| = f_1$ *(see Remark 7.3). If the variable* x_i *is considered as an output, then* $H = H_i$ *will have a* 1 *in the* i*th position and zero elsewhere. By means of the proposed vertex algorithm, the following steady-state influence of* p *on the variables* x_1*,* x_2 *and* x_3 *can be derived:*

$$\begin{matrix} & \overbrace{\phantom{\begin{bmatrix} - \end{bmatrix}}}^{p} \\ x_1\{ & \\ x_2\{ & \\ x_3\{ & \end{matrix} \begin{bmatrix} - \\ 0 \\ 0 \end{bmatrix}.$$

In this simple case, the results can be checked by direct computation of

$$\det \begin{bmatrix} -J & -E \\ H_i & 0 \end{bmatrix},$$

by considering H_i *associated with the considered variable (*e.g.*, for* x_1*,* $H_1 = [\ 1\ 0\ 0\ ]$*). It can be seen that both* x_2 *and* x_3 *are subject to a perfect adaptation with respect to variations of* p*. This fact, although surprising, can be explained by considering the system steady state:* $\bar{x}_3$ *and* $\bar{x}_2$ *depend on the constant influx only (since adding the first and third equation at steady state gives* $f_4(\bar{x}_3) = x_{1,0}$*, and subtracting the second to the first gives* $f_3(\bar{x}_3) + f_2(\bar{x}_2) = x_{2,0} - x_{1,0}$*), while* $\bar{x}_1$ *depends on* p *and can thus compensate any variation in* p*, preventing it from affecting* $\bar{x}_2$ *and* $\bar{x}_3$*.*

The observation in Example 7.3 can be generalised in the following proposition.

Proposition 7.2. *Consider a system of the form* (4.25)*, namely*

$$\dot{x}(t) = Sf(x(t)) + f_0,$$

and assume that the j*th reaction has rate* $f_j(\cdot) = p\tilde{f}_j(\cdot)$*, with* p *a positive parameter, and that (at least) one of the species, having concentration* x_i*, is involved as a reagent in the* j*th reaction only and in no other reactions (hence the corresponding column* J_i *of the Jacobian matrix contains one coefficient only). Then all the variables of the system are insensitive to variations in* p*, except for* x_i *itself.*

Proof. Since E and J_i are linearly dependent columns, the determinant in (7.8) is zero as long as h_i is zero. □

Note that, even though none of the conditions in Theorem 7.1 is satisfied, some useful (although non-structural) information can be derived as well, based on the computation of the function $r(D)$ for all the vertices of the hypercube. Consider for instance the case depicted in Fig. 7.3. The function has different signs at different vertices of the hypercube (actually, a cube in $\mathbb{R}^3$): it is neither always non-positive, nor always non-negative; yet, it is always zero at the vertices in which the parameter ϑ is zero. It cannot be said that the system output is perfectly adaptive (this would be the case if the function were zero for all vertices). However, it is perfectly adaptive if $\vartheta = 0$. Moreover, this suggests that the considered output is adaptive (see Fig. 7.4) for small enough values of ϑ.

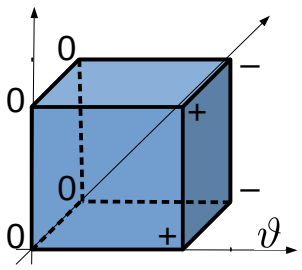

Figure 7.3: A function having different signs on different vertices of the cube.

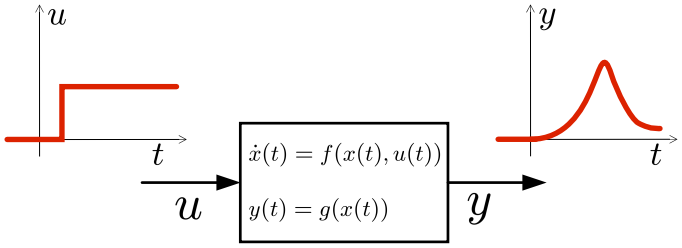

Figure 7.4: A non-perfectly adaptive system: when a persistent input is applied, after a transient the output returns very close to its pre-perturbation value.

7.3 Structural Influence Matrix

To assess the structural influence on the ith variable of a persistent, additive input applied to the jth variable [GCFB15], consider a system (7.4)-(7.5) having the form

$$\dot{x}(t) = f(x(t)) + Eu(t), \tag{7.9}$$
$$y(t) = Hx(t), \tag{7.10}$$

and take vectors $E = E_j$ and $H = H_i$ with a single non-zero entry equal to one

$$E_j = [0 \ \dots \ 0 \ \underbrace{1}_{\text{position } j} \ 0 \ \dots \ 0]^\top, \qquad H_i = [0 \ \dots \ 0 \ \underbrace{1}_{\text{position } i} \ 0 \ \dots \ 0].$$

If the system admits a BDC-decomposition, then each entry $[M]_{ij}$ of the influence matrix $M \in \mathbb{R}^{n\times n}$ can be generated by means of the numerical vertex algorithm described in Procedure 7.1, choosing the corresponding E_j and H_i. $[M]_{ij}$ is:

- '+' if the influence is positive for any realisation of the structure;
- '0' if there is perfect adaptation for any realisation of the structure;
- '−' if the influence is negative for any realisation of the structure;
- '?' if the influence is not structurally sign-definite.

As illustrated in Fig. 7.2, each entry of the influence matrix (or, more in general, any structural steady-state derivative) can be interpreted as the response of the system output to a step input.

Remark 7.4. *Consistently with the results in [DLR02, DLR03, DLLR03, DLR05, DRJ07], computing the influence matrix is equivalent to determining the sign pattern of the adjoint matrix adj*$(-J)$ *of* $-J$*, namely, the matrix such that* $(-J)^{-1} = adj(-J)/\det(-J)$.

Example 7.4. (Metabolic network: influence matrix). *Reconsider the system proposed in Example 4.10:* $\det(-J)$ *is structurally positive and the vertex algorithm provides the influence matrix*

$$M = \begin{bmatrix} + & - & 0 \\ - & + & 0 \\ + & 0 & + \end{bmatrix}.$$

Example 7.5. *The system in Fig. 4.5 (b) corresponds to the Jacobian matrix*

$$J = \begin{bmatrix} -(\alpha+\zeta) & 0 & 0 & 0 & -\eta & 0 & 0 \\ \alpha & -(\gamma+\varepsilon) & 0 & -\delta & 0 & 0 & 0 \\ 0 & 0 & -(\beta+\iota) & 0 & 0 & -\lambda & 0 \\ 0 & -\gamma & \beta & -(\delta+\varphi) & 0 & 0 & 0 \\ -\zeta & \varepsilon & 0 & 0 & -\eta & 0 & 0 \\ 0 & 0 & -\iota & \varphi & 0 & -\lambda & 0 \\ 0 & \gamma & 0 & \delta & 0 & 0 & -\mu \end{bmatrix}.$$

By means of the proposed algorithm, it can be verified that $\det(-J) > 0$ *structurally and*

$$M = \begin{bmatrix} + & - & + & + & - & - & 0 \\ + & + & - & - & - & + & 0 \\ + & + & + & - & - & - & 0 \\ - & - & + & + & + & - & 0 \\ ? & + & - & - & + & + & 0 \\ - & - & ? & + & + & + & 0 \\ + & + & + & + & - & - & + \end{bmatrix}.$$

Finally, some peculiarities of the influence matrix in two particular classes of systems are worth underlining.

First of all, consider the case of monotone systems (described in Section 2.3.7). Recall that a system of the form $\dot{x}(t) = f(x(t))$, with f differentiable, is *monotone* [Smi08, Son07] iff its Jacobian $J(x)$ is a *Metzler matrix* for any x (*i.e.*, its off-diagonal entries are nonnegative). The following result holds.

Proposition 7.3. *Given a monotone system, denote by* J *its Jacobian evaluated at a stable equilibrium. Then its influence matrix is such that* $[M]_{ij} \in \{+, 0\}$ *for all* (i, j)*. If furthermore* J *is irreducible,* $[M]_{ij} = +$ *for all* (i, j).

Proof. If J is a stable Metzler matrix (hence its diagonal entries are negative, see [FR00]), then $(-J)^{-1} \geq 0$, where the inequality has to be intended componentwise; if, moreover, the matrix is irreducible, the inequality is strict: $(-J)^{-1} > 0$. [HLMQ14] Since the equilibrium is stable, $\det(-J) > 0$. Then $\mathrm{adj}(-J) = (-J)^{-1}\det(-J) \geq 0$ (> 0 in the irreducible case), which proves the thesis. □

However, monotonicity is not necessary to have a positive influence matrix. In fact, there are stable matrices which are not Metzler, but for which all of the entries of $\mathrm{adj}(-J)$ are positive. For instance, the following matrix J is not Metzler:

$$J = \begin{bmatrix} -15 & 2 & 12 \\ -5 & -10 & 14 \\ 8 & -1 & -18 \end{bmatrix}. \quad \text{However,} \quad \mathrm{adj}(-J) = \begin{bmatrix} 194 & 24 & 148 \\ 22 & 174 & 150 \\ 85 & 1 & 160 \end{bmatrix}$$

is elementwise positive. Yet, interestingly, in this case matrix J is eventually positive (namely, it satisfies the Perron-Frobenius property with positive left and right eigenvectors, see [Nou06, AL15]). This suggests a connection between eventual positivity and elementwise positivity of the influence matrix, which will be worth investigating.

Another remarkable case is that in which some diagonal entries of the influence matrix are zero, as in the prey-predator case in Example 7.1, or even negative. Consider the system

$$J = \begin{bmatrix} -\alpha & \beta \\ -\gamma & \delta \end{bmatrix}, \quad \text{for which} \quad M = \begin{bmatrix} - & + \\ - & + \end{bmatrix}.$$

Assuming stability, if a constant additive input is applied to the first state variable, its own steady-state value decreases. This situation may arise because this is a non minimum-phase system; such systems have been recently studied in a biological context. [MCB+10, YKM13]

7.4 The Case of Marginally Stable Systems

As discussed in Section 4.2.1, some chemical reaction networks correspond to a marginally stable system, whose state is forced to stay inside the *stoichiometric compatibility class* associated with the initial conditions:

$$x(t) \in \mathcal{C}(x(0)) = \{x(0) + \mathrm{span}(S)\} \cap \mathbb{R}^n_+.$$

This happens, for instance, in the presence of mass conservation constraints. The rank of the stoichiometric matrix S (hence of B) corresponds to the dimension of the stoichiometric compatibility class. If matrix B is not full row rank, the system trajectories evolve inside a subspace having dimension smaller than n and, of course, BDC is structurally singular. It is assumed, however, that 0 is the only eigenvalue of the system having nonnegative real part.

In this case, to restrict the analysis to the stoichiometric compatibility class, a transformation can be considered that provides a full row rank $\tilde{B}$. Let $z(t) = x(t) - \bar{x}$, $v(t) = u(t) - \bar{u}$, $w(t) = y(t) - \bar{y}$ and consider the linearised system

$$\dot{z}(t) = BDCz(t) + Ev(t), \tag{7.11}$$

$$w(t) = Hz(t). \tag{7.12}$$

Given the state transformation

$$\begin{bmatrix} M \\ N \end{bmatrix} z = \begin{bmatrix} z_M \\ z_N \end{bmatrix}, \qquad z = \begin{bmatrix} P & Q \end{bmatrix} \begin{bmatrix} z_M \\ z_N \end{bmatrix},$$

where $M^\top$ is a basis of $\ker(B^\top)$ (ker denotes the kernel of a matrix; *i.e.*, $M^\top$ is such that $MB = 0$) and N is a basis of $\mathrm{span}(B)$, the transformed system is

$$\begin{aligned} \begin{bmatrix} \dot{z}_M \\ \dot{z}_N \end{bmatrix} &= \begin{bmatrix} 0 & 0 \\ NBDCP & NBDCQ \end{bmatrix} \begin{bmatrix} z_M \\ z_N \end{bmatrix} + \begin{bmatrix} ME \\ NE \end{bmatrix} v \\ &\doteq \begin{bmatrix} 0 & 0 \\ B_N DC_P & B_N DC_Q \end{bmatrix} \begin{bmatrix} z_M \\ z_N \end{bmatrix} + \begin{bmatrix} E_M \\ E_N \end{bmatrix} v, \end{aligned}$$

$$y = \begin{bmatrix} HP & HQ \end{bmatrix} \begin{bmatrix} z_M \\ z_N \end{bmatrix} \doteq \begin{bmatrix} H_P & H_Q \end{bmatrix} \begin{bmatrix} z_M \\ z_N \end{bmatrix}.$$

If $E_M = 0$, the *step response* of the system can be computed: $z_M(t) \equiv z_M(0) = 0$ $\forall t$ and the z_N-subsystem is asymptotically stable by assumption. Then $\det(-B_N DC_N)$ can be considered, along with the sign of

$$\det \begin{bmatrix} -B_N DC_Q & -E_N \\ H_Q & 0 \end{bmatrix},$$

and the analysis can be carried out without changes.

If instead $E_M \neq 0$, the equation for z_M would be $\dot{z}_M = E_M u$, so that $z_M(t) = z_M(0) + E_M ut$ would diverge. The analysis can be carried out by considering the *impulse response* of the system, namely, by assuming u to be the Dirac delta function. In this case, $z_M(t) \equiv z_M(0^+) = E_M$ is constant and can be considered as the input for the z_N-subsystem, which is asymptotically stable (therefore its impulse response converges to zero) so that the sign of the steady-state derivative is given by the sign of

$$\det \begin{bmatrix} -B_N DC_Q & -B_N DC_P E_M \\ H_Q & H_P E_M \end{bmatrix}.$$

In the previous cases, $B_N DC_Q$ has been assumed to be non-singular. If $B_N DC_Q$ is singular because C does not have full column rank, an additional state transformation can be considered that provides a full column rank $\tilde{C}$, as previously done for B. However, even when both B and C have full rank, matrix BDC can be structurally singular. In this case, as long as zero is a simple eigenvalue, the (i, j) entry of the structural influence matrix can represent the sign of the steady-state variation of the ith variable due to an impulsive additive input applied to the jth variable. Otherwise, unfortunately, it is useless to resort to further transformations.

Example 7.6. *Consider the system introduced in Example 4.11 and depicted in Fig. 4.5 (a). Its Jacobian matrix, provided in* (4.27) *along with its BDC-decomposition, is structurally singular. A mass conservation constraint is present, because $\dot{b} + \dot{c} = 0$*

in system (4.26)*, hence* $b+c$ *is constant. Since zero is a simple root of the characteristic polynomial* $p(s) = s^3 + (\alpha+\beta+\gamma+\delta+\varepsilon)s^2 + \alpha(\delta+\varepsilon)s$*, the influence matrix can be used to describe structural steady-state variations induced by impulsive inputs:*

$$M = \begin{bmatrix} 0 & ? & ? \\ 0 & + & + \\ 0 & + & + \end{bmatrix}. \tag{7.13}$$

While C *has full column rank,* $rank(B) = 2$*. Therefore, the analysis can be restricted to the stoichiometric compatibility class. A basis of* $ker(B^\top)$ *is given by the vector* $[0 \;\; 1 \;\; 1]^\top$*. Completing with a basis of* $span(B)$*, the following state transformation is achieved:*

$$T^{-1} = \begin{bmatrix} 0 & 1 & 1 \\ 0 & 1 & 0 \\ 1 & 0 & 0 \end{bmatrix}, \qquad T = \begin{bmatrix} 0 & 0 & 1 \\ 0 & 1 & 0 \\ 1 & -1 & 0 \end{bmatrix}.$$

To account for all the possible variable selections, take $E = I_3$ *and* $H = I_3$ *as the identity matrices, so that the influence* (i, j) *is achieved by selecting the* j*th column of* E *and the* i*th row of* H*. The transformed system becomes*

$$T^{-1}JT = \left[\begin{array}{c|cc} 0 & 0 & 0 \\ \hline \gamma+\varepsilon & -(\beta+\gamma+\delta+\varepsilon) & -\alpha \\ \gamma & -(\beta+\gamma) & -\alpha \end{array}\right] = \begin{bmatrix} 0 & 0 \\ B_N D C_P & B_N D C_Q \end{bmatrix},$$

$$T^{-1}E = \left[\begin{array}{ccc} 0 & 1 & 1 \\ \hline 0 & 1 & 0 \\ 1 & 0 & 0 \end{array}\right] = \begin{bmatrix} E_M \\ E_N \end{bmatrix},$$

$$HT = \left[\begin{array}{c|cc} 0 & 0 & 1 \\ 0 & 1 & 0 \\ 1 & -1 & 0 \end{array}\right] = \begin{bmatrix} H_P & H_Q \end{bmatrix}.$$

Denote by $E_M^{(j)}$ *the* j*th column of* E_M *and by* $H_Q^{(i)}$ *the* i*th row of* H_Q*. Now* $\det(-B_N D C_Q)$ *is structurally positive and, by considering the sign of*

$$\det \begin{bmatrix} -B_N D C_Q & -B_N D C_P E_M^{(j)} \\ H_Q^{(i)} & H_P^{(i)} E_M^{(j)} \end{bmatrix},$$

the (i, j) *entry of the influence matrix associated with the impulse response can be computed:*

$$M_{(scc)} = \begin{bmatrix} 0 & ? & ? \\ 0 & + & + \\ 0 & + & + \end{bmatrix}. \tag{7.14}$$

As expected, matrix (7.14) *is equal to* (7.13)*, which has been previously computed without any state transformation just because* $dim[ker(B^\top)] = 1$*. When the kernel has a higher dimension, a state transformation is necessary to compute the influence matrix in the stoichiometric compatibility class.*

Example 4.10, with mass conservation constraints, has been previously analysed in a reduced-order form, neglecting the variable $d = K - b$ (see Example 7.4). Yet, it is also possible to consider *all of the four variables*: in this case, the influence matrix in the stoichiometric compatibility class can be computed as illustrated in this section.

7.4.1 Laplace Domain: Step Response and Impulse Response

An interpretation of the proposed analysis can be provided in terms of transfer functions. Given a stable system with input $u(t)$ and output $y(t)$, the steady-state derivative $\frac{\partial \bar{y}}{\partial \bar{u}}$ is related to the transfer function $F(s) = Y(s)/U(s)$. Precisely, $\frac{\partial \bar{y}}{\partial \bar{u}} = F(0) = \frac{n(0)}{d(0)} = \frac{n_0}{d_0}$, where $n(s) = \sum_{h=0}^{k} n_h s^h$, $n_k = 1$, and $d(s) = \sum_{h=0}^{n} d_h s^h$, $d_n = 1$, $d_0 \neq 0$, are computed as

$$n(s) = \det \begin{bmatrix} sI - J & -E \\ H & 0 \end{bmatrix} \qquad \text{and} \qquad d(s) = \det (sI - J) .$$

This can be regarded as the asymptotic value of the system unit step response, as illustrated in Fig. 7.2. Indeed, if $u(t)$ is the Heaviside step function, whose Laplace transform is $U(s) = \frac{1}{s}$, the steady-state value of the step response, $\bar{y} = y(\infty)$, can be evaluated by applying the final value theorem:

$$\lim_{t \to \infty} y(t) = \lim_{s \to 0} sY(s), \tag{7.15}$$

provided that both the limits exist and are finite. Clearly, if the system is asymptotically stable, $y(t)$ converges to a finite value. Moreover, $\lim_{s\to 0} sY(s) = \lim_{s\to 0} sF(s)\frac{1}{s} = F(0)$ is finite, since there are no poles at the origin of the complex plane. Therefore, the hypotheses of the final value theorem are satisfied.

In the case of an asymptotically stable system, it is pointless to consider the impulse response: if $u(t) = \delta(t)$, Dirac's delta distribution, then $U(s) = 1$ and, since there are no poles at the origin, $\bar{y} = \lim_{s\to 0} sF(s) = 0$. However, if the system is marginally stable and zero is a simple eigenvalue, then $d_0 = 0$, $F(s) = \frac{n(s)}{sd'(s)}$ and the steady-state derivative can be seen as expressing the asymptotic value of the system impulse response: $\lim_{s\to 0} sF(s) = \lim_{s\to 0} \frac{n(s)}{d'(s)} = \frac{n_0}{d_1}$. In the proposed setup, performing the vertex test in Procedure 7.1 remains possible, since *all* of the polynomial coefficients are multi-affine functions of the parameters D_k.

7.5 A Tree-Like Algorithm

Most of the analysis in Section 7.3 focuses on flow-governed systems, in which simultaneous production and consumption occur: with a given reaction rate, one

or more species are converted into other species, leading to Jacobian matrices with coefficients appearing repeatedly on the same column (possibly with different sign). Yet, in several cases all the Jacobian entries are independent: hence, for systems admitting a BDC-decomposition (due to Assumption 4.1), J is a sign-definite matrix, as in the prey-predator system (7.1), having Jacobian (7.3).

When the entries are independent, the problem can still be solved by adopting the proposed vertex algorithm. However, this can involve a very large number of parameters. For instance, in Example 4.10 there are 4 parameters, thus 16 vertices; if all the non-zero entries were independent, there would be 128 vertices. If all the non-zero entries of Example 7.5 were independent, the number of vertices would be $2^{19} = 524288$.

Example 7.7. (Snowshoe hare population dynamics). *To describe the interactions among vegetation, snowshoe hare and predators in boreal forests, a simple model is proposed in [DRJ07], corresponding to the sign-definite community matrix*

$$J = \begin{bmatrix} -\alpha & -\beta & 0 \\ \gamma & -\delta & -\varepsilon \\ \varphi & \eta & -\psi \end{bmatrix} \tag{7.16}$$

having sign pattern

$$\Sigma_J = \begin{bmatrix} - & - & 0 \\ + & - & - \\ + & + & - \end{bmatrix}.$$

The influence matrix

$$M = \begin{bmatrix} + & - & + \\ ? & + & - \\ + & ? & + \end{bmatrix} \tag{7.17}$$

can be found by simply computing the adjoint, as well as by means of the proposed vertex algorithm, which involves 8 *parameters, hence* 256 *vertices.*

For systems with very high dimension, complexity could render the vertex algorithm unfeasible. Yet, complexity can be reduced by adopting a tree-like algorithm [GCFB15] that takes advantage of the sparsity of the Jacobian (namely, of the presence of several zero entries). To determine the influence matrix, the sign of the determinant (7.8) must be structurally assessed for all input-output pairs; equivalently, the sign of the entries of $\mathrm{adj}(-J)$, which are just determinants of sub-matrices, must be established.

Procedure 7.2. ***Tree Recursive Algorithm for Determinant Sign: TRADS(Σ_n).***
Input: $\Sigma_n \in \mathbb{R}^{n\times n}$, *the sign matrix which forms the root of the tree.*
Output: *The structural sign of the determinant of* Σ_n, $\sigma \in \{+, -, 0, ?\}$.

1. *Consider the first row of matrix* Σ_n.
2. *For each non zero entry* $[\Sigma_n]_{1i}$*, create a link to a new node, marked by '−' or by '+' depending on the sign of* $[\Sigma_n]_{1i}\,(-1)^{i+1}$*, and associate with this node the sign matrix* Σ_{n-1} *(of dimension* $n-1$*), which is the complementary matrix of the considered entry.*
3. *For each new node connected to the original node with a '−' arc, change sign to the first row of the corresponding matrix* Σ_{n-1}.
4. *Apply the procedure TRADS(*Σ_{n-1}*) to all the new nodes.*

The procedure stops when all of the sign matrices have dimension 1*. Then* $\sigma = +$ *if all the matrices are* $[+]$*, or* $[0]$ *with at least a* $[+]$ *matrix;* $\sigma = -$ *if all the matrices are* $[-]$*, or* $[0]$ *with at least a* $[-]$ *matrix;* $\sigma = 0$ *if all the matrices are* $[0]$*;* $\sigma = ?$ *otherwise.*

Obviously, the outcome of the procedure is the same if the matrix is altered by transposing it or by permuting rows and/or columns, with appropriate sign changes. This can be done at each iteration, preferably choosing the row or column having most zero entries.

Example 7.8. (Snowshoe hare population dynamics). *Consider the signed Jacobian matrix* (7.16)*, in Example 7.7. To find the sign of the structural influence on the third variable of an additive input persistently applied to the first variable, the algorithm (applied without transposing or permuting) produces*

$$\Sigma_4 = \begin{bmatrix} + & + & 0 & - \\ - & + & + & 0 \\ - & - & + & 0 \\ 0 & 0 & + & 0 \end{bmatrix}$$

$$\Sigma_3 = \begin{bmatrix} + & + & 0 \\ - & + & 0 \\ 0 & + & 0 \end{bmatrix}^{(+)} \quad \begin{bmatrix} + & - & 0 \\ - & + & 0 \\ 0 & + & 0 \end{bmatrix}^{(-)} \quad \begin{bmatrix} - & + & + \\ - & - & + \\ 0 & 0 & + \end{bmatrix}^{(+)}$$

$$\Sigma_2 = \left[\begin{bmatrix} + & 0 \\ + & 0 \end{bmatrix}^{(+)} \;\middle|\; \begin{bmatrix} + & 0 \\ 0 & 0 \end{bmatrix}^{(-)} \right] \left[\begin{bmatrix} + & 0 \\ + & 0 \end{bmatrix}^{(+)} \;\middle|\; \begin{bmatrix} - & 0 \\ 0 & 0 \end{bmatrix}^{(+)} \right] \left[\begin{bmatrix} + & - \\ 0 & + \end{bmatrix}^{(-)} \;\middle|\; \begin{bmatrix} + & - \\ 0 & + \end{bmatrix}^{(-)} \;\middle|\; \begin{bmatrix} - & - \\ 0 & 0 \end{bmatrix}^{(+)} \right]$$

$$\Sigma_1 = \left[\begin{bmatrix} 0 \end{bmatrix}^{(+)} \;\middle|\; \begin{bmatrix} 0 \end{bmatrix}^{(+)} \;\middle|\; \begin{bmatrix} 0 \end{bmatrix}^{(+)} \;\middle|\; \begin{bmatrix} 0 \end{bmatrix}^{(-)} \;\middle|\; \begin{bmatrix} + \end{bmatrix}^{(+)} \begin{bmatrix} 0 \end{bmatrix}^{(+)} \;\middle|\; \begin{bmatrix} + \end{bmatrix}^{(+)} \begin{bmatrix} 0 \end{bmatrix}^{(+)} \;\middle|\; \begin{bmatrix} 0 \end{bmatrix}^{(-)} \begin{bmatrix} 0 \end{bmatrix}^{(+)} \right]$$

Indices $[]^{(-)}/[]^{(+)}$ *mean that the sign of the first row is changed/unchanged. Since the final matrices are all* $[0]$ *with at least a* $[+]$*, the determinant is structurally positive, consistently with* $[M]_{31} = +$ *in* (7.17)*. Of course, the number of computations dramatically reduces if it is noticed that the most convenient choice at the beginning is the last row, or the last column, having a single non-zero entry.*

Remark 7.5. *In the worst case in which all the entries are non-zero, the tree algorithm would have a complexity of* $n!$*, where* n *is the matrix dimension. This complexity is negligible if compared to that of the vertex algorithm directly applied, which would be* 2^{n^2}*. For instance, for a* 5×5 *matrix, the complexity is* $5! = 120$ *instead of* 2^{25} *(roughly* $32 \cdot 10^6$*). In general, meaningful matrices are sparse; therefore, the operation count would be at most* $\nu_1 \cdot \nu_2 \cdot \ldots \cdot \nu_n$*, where* ν_i *is the number of non-zero entries of the* i*th row.*

Sparsity is typical in several cases of practical interest.

Example 7.9. (Population dynamics in Danish shallow lakes). *Two models are analysed in [DRJ07] to describe the interactions among* 10 *different species in Danish shallow lakes: model "I" considers modified or non-linear interactions in a model of eutrophic shallow lakes, while model "J" considers only linear trophic interactions in a model of mesotrophic lakes. In both cases, starting from a sign-definite community matrix A, a qualitative adjoint matrix $adj(-A)$ is computed. The qualitative adjoint matrices of the two models are then compared with experimental responses measured in field studies: model J is considered less reliable, because the resulting signs are largely inconsistent with the observed response. By means of the proposed algorithm, the structural influence matrices can be computed. The entries are all indeterminate for model "I". Also for model "J" most entries are indeterminate, however there are notable exceptions:* $[M]_{34} = +$, $[M]_{43} = -$, $[M]_{44} = +$, $[M]_{99} = +$ *have sign consistent with that reported in [DRJ07] and, interestingly, are not among the entries reported to be inconsistent with field observations.*

7.6 Examples

7.6.1 E. coli EnvZ-OmpR Osmoregulation

The proposed vertex algorithm can be applied to the biochemical network in Fig. 4.5 (c), representing the complex EnvZ-OmpR osmoregulation model in *Escherichia coli*, studied in [SF10], with additional auto-degradation reactions for species C and D. For this system, steady-state effects are not easy to foresee based on qualitative considerations. The system has Jacobian matrix

$$J = \begin{bmatrix} -(\alpha+\beta) & \gamma & 0 & 0 & \vartheta & 0 & 0 & \mu \\ \beta & -(\gamma+\delta) & 0 & 0 & 0 & -\varepsilon & \kappa+\lambda & 0 \\ 0 & 0 & -(\zeta+\varphi) & -\eta & \xi & 0 & 0 & \nu \\ 0 & 0 & -\zeta & -(\eta+\psi) & \xi & 0 & \kappa & 0 \\ 0 & 0 & \zeta & \eta & -(\xi+\vartheta) & 0 & 0 & 0 \\ 0 & -\delta & 0 & 0 & \vartheta & -\varepsilon & \lambda & 0 \\ 0 & \delta & 0 & 0 & 0 & \varepsilon & -(\kappa+\lambda) & 0 \\ \alpha & 0 & 0 & 0 & 0 & 0 & 0 & -(\mu+\nu) \end{bmatrix}.$$

By means of the vertex algorithm, it can be seen that $\det(-J)$ is structurally positive and the influence matrix is

$$M = \begin{bmatrix} + & + & + & + & + & + & + & + \\ + & + & + & + & + & + & + & + \\ + & + & + & 0 & + & 0 & + & + \\ 0 & 0 & 0 & + & + & + & + & 0 \\ + & + & + & + & + & + & + & + \\ ? & ? & ? & ? & ? & ? & ? & ? \\ + & + & + & + & + & + & + & + \\ + & + & + & + & + & + & + & + \end{bmatrix}.$$

7.6.2 Biofuel Production

In this section, two biofuel production models are *structurally* compared and it is shown that their peculiar properties can be inferred independent of parameter values. An important issue of microbial biofuel production methods, based on engineered bacteria, is that production cannot be unrestrictedly increased because biofuel is toxic to the cell that is producing it. Efflux pumps have been shown to be effective at increasing tolerance to biofuel, but an over-expression of efflux pumps hinders the growth of the cell population, hence decreases biofuel production: the toxicity of biofuel and of pump over-expression must then be properly balanced to maximise the biofuel output. Consider the two models for cell growth and biofuel production provided in [HD12]: in the former, efflux pumps are expressed at a constant level; in the latter, a synthetic feedback loop is implemented, using a biosensor to control efflux pump expression.

The feedback system is described by the equations

$$\begin{cases} \dot{n} = n\left[\alpha_n\left(1-\frac{n}{n_{max}}\right) - \delta_n b_i - \frac{\alpha_n p}{p+\gamma_p}\right] \\ \dot{R} = \alpha_R + k_R\left(\frac{I}{I+\gamma_I}\right) - \beta_R R \\ \dot{p} = \alpha_p + k_p \frac{1}{\frac{R}{1+k_b b_i}+\gamma_R} - \beta_p p \\ \dot{b}_i = \alpha_b n - \delta_b p b_i \end{cases},$$

where n is the cell density, R is the concentration of repressor proteins, p is the concentration of pumps, b_i is the concentration of intracellular biofuel; n_{max} is the maximum population size. Both biofuel toxicity and pump toxicity can prevent population growth. Repressor activation by the inducer is modelled as $I/(I+\gamma_I)$, where γ_I indicates the inducer value that corresponds to half maximal activation of the repressor and I can be considered as a constant input. Since R reaches its steady state independently of all other state variables, it can be considered just as an external inflow.

There are two possible equilibrium values for n: the trivial $\bar{n}=0$ (all the cells are dead) and the nontrivial $\bar{n}$, such that

$$\left[\alpha_n\left(1-\frac{\bar{n}}{n_{max}}\right) - \delta_n \bar{b}_i - \frac{\alpha_n \bar{p}}{\bar{p}+\gamma_p}\right] = 0.$$

Thus $[J]_{11}$, *i.e.*, the partial derivative computed at the equilibrium point, is simply $-\frac{\alpha_n \bar{n}}{n_{max}}$. Denote by φ_p the positive partial derivative of $\frac{p}{p+\gamma_p}$ with respect to p and by ψ_{b_i} the positive partial derivative of $k_p \frac{1}{\frac{R}{1+k_b b_i}+\gamma_R}$ with respect to b_i. The Jacobian matrix of the reduced system, including only the variables n, p, b_i, is then:

$$J_{FL} = \begin{bmatrix} -\frac{\alpha_n \bar{n}}{n_{max}} & -\alpha_n \bar{n}\varphi_p & -\delta_n \bar{n} \\ 0 & -\beta_p & \psi_{b_i} \\ \alpha_b & -\delta_b \bar{b}_i & -\delta_b \bar{p} \end{bmatrix}.$$

It can be seen that $\det(-J_{FL})$ is structurally positive and the influence matrix is

$$M_{FL} = \begin{bmatrix} + & ? & - \\ + & + & + \\ + & - & + \end{bmatrix}.$$

As expected, b_i is reduced by a positive input applied to p and augmented by a positive input applied to n; a positive input applied to b_i reduces n, due to the biofuel toxicity for the cells. The effect on n of an input applied to p is not structurally determinate, which is consistent with the considerations about the trade-off regarding efflux pumps expression: a significant level of p helps increasing cell tolerance to biofuel (enhancing population growth), but, when over-expressed, pumps burden cells (hindering population growth). The effect of the feedback, which allows modulating the expression of efflux pumps, is worth pointing out. In fact, an input applied to n increases p, to adjust it to the needs of a grown population, and an input applied to b_i also increases p, because more efflux pumps are needed to protect the cells from an increased level of toxicity.

Consider now the system in which efflux pumps are expressed at a constant level. The repressor equation is no longer present in the system, since an inducer is now directly used to control pump expression, while the other equations remain unchanged:

$$\begin{cases} \dot{n} = n\left[\alpha_n\left(1 - \frac{n}{n_{max}}\right) - \delta_n b_i - \frac{\alpha_n p}{p+\gamma_p}\right] \\ \dot{p} = \alpha_p + k_p\left(\frac{I}{I+\gamma_I}\right) - \beta_p p \\ \dot{b}_i = \alpha_b n - \delta_b p b_i \end{cases}$$

$$J_C = \begin{bmatrix} -\frac{\alpha_n \bar{n}}{n_{max}} & -\alpha_n \bar{n}\varphi_p & -\delta_n \bar{n} \\ 0 & -\beta_p & 0 \\ \alpha_b & -\delta_b \bar{b}_i & -\delta_b \bar{p} \end{bmatrix}.$$

It can be seen that $\det(-J_C)$ is structurally positive. The influence matrix is:

$$M_C = \begin{bmatrix} + & ? & - \\ 0 & + & 0 \\ + & - & + \end{bmatrix}.$$

The comparison between M_C and M_{FL} immediately highlights the effect of the feedback loop: all the structural influences are the same but those on p due to a persistent input applied to n and to b_i. In the absence of feedback, p is completely insensitive to both inputs applied to n and to b_i; feedback allows to tune the expression of efflux pumps, increasing it when a positive input is applied to n or to b_i. Thanks to the feedback regulation, pumps can be produced at the exact amount needed for increasing cell tolerance to toxic biofuel, without excessively burdening cells.

According to the sensitivity analysis performed in [HD12], the feedback model is almost insensitive to many system parameters, while a few key parameters (α_n, δ_n,

γ_p, n_{max}, α_b, δ_b) strongly influence growth and production. To assess if the sign of such an influence is independent of the other parameter values, a *structural* analysis can be performed by computing the determinant in (7.8) for each parameter κ, where $E_\kappa = [\partial\dot{n}/\partial\kappa \;\; \partial\dot{p}/\partial\kappa \;\; \partial\dot{b}_i/\partial\kappa]^\top$ and H selects the desired output among n, p and b_i. The influence of *parameter variations* on the steady-state of the state variables can be summarised as follows:

$$
\begin{array}{c}
\\ n\,\{ \\ p\,\{ \\ b_i\,\{
\end{array}
\begin{array}{c}
\overbrace{}^{\alpha_n}\overbrace{}^{\delta_n}\overbrace{}^{\gamma_p}\overbrace{}^{n_{max}}\overbrace{}^{\alpha_b}\overbrace{}^{\delta_b}\overbrace{}^{\alpha_p}\overbrace{}^{k_p}\overbrace{}^{\beta_p}\overbrace{}^{k_b}\overbrace{}^{\gamma_R} \\
\left[\begin{array}{ccccccccccc}
+ & - & + & + & - & + & ? & ? & ? & ? & ? \\
+ & - & + & + & + & - & + & + & - & + & - \\
+ & - & + & + & + & - & - & - & + & - & +
\end{array}\right]
\end{array}.
$$

The obtained structural influences are fully consistent with numerical results, but structural analysis gives a noteworthy advantage: the same trends are guaranteed to be achieved independently of the other system parameters.

7.6.3 Interactions at the Trans-Golgi Network

The interactions at the cellular Golgi apparatus are well studied (see for instance [TWH+13, WHO+15] and the references therein), but not yet completely understood in terms of exact modelling. Two different models describing PKD-CERT interactions at the trans-Golgi network in mammalian cells are proposed in [WHO+15], where sampling-based Bayesian analysis and perturbation experiments are performed for model calibration and validation. It is natural to wonder whether the two models present structural differences and, in case, which of the two is more suitable for describing actual interactions occurring in the network. To this aim, a comparative structural influence analysis is briefly provided here.

It can be shown that model A ("short distance shuttle") corresponds to a Jacobian matrix of the form

$$
J_A = \begin{bmatrix}
-(\alpha+\vartheta+\xi) & \pi & 0 & -\nu & -\mu & 0 & 0 \\
\vartheta+\xi & -(\beta+\pi) & 0 & \nu & \mu & 0 & 0 \\
0 & -\rho & -(\gamma+\sigma) & \kappa & 0 & 0 & 0 \\
0 & \rho & \sigma & -(\delta+\kappa) & 0 & 0 & 0 \\
0 & 0 & 0 & -\psi & -(\varepsilon+\varphi) & \lambda & 0 \\
0 & \tau & 0 & 0 & 0 & -(\zeta+\lambda) & \omega \\
0 & -\tau & 0 & \psi & \varphi & 0 & -(\eta+\omega)
\end{bmatrix},
$$

while model B ("neck swinging") has Jacobian

$$
J_B = \begin{bmatrix}
-(\alpha+\vartheta+\xi) & \pi & 0 & 0 & 0 & 0 & -\mu \\
\vartheta+\xi & -(\beta+\pi) & 0 & 0 & 0 & 0 & \mu \\
0 & -\rho & -(\gamma+\sigma) & \kappa & 0 & 0 & 0 \\
0 & \rho & \sigma & -(\delta+\kappa) & 0 & 0 & 0 \\
0 & 0 & 0 & 0 & -(\varepsilon+\nu) & \lambda & 0 \\
0 & \tau & 0 & -\psi & \nu & -(\zeta+\lambda+\varphi) & \omega \\
0 & -\tau & 0 & \psi & 0 & \varphi & -(\eta+\omega)
\end{bmatrix};
$$

in both cases, Greek letters denote positive parameters associated with partial derivatives.

Both $\det(-J_A)$ and $\det(-J_B)$ are not sign determined. The corresponding influence matrices are

$$M_A = \begin{bmatrix} ? & ? & ? & ? & - & - & - \\ + & + & ? & ? & + & + & + \\ - & - & ? & ? & - & - & - \\ + & + & ? & ? & + & + & + \\ ? & ? & ? & ? & ? & ? & ? \\ + & + & ? & ? & ? & ? & ? \\ ? & ? & ? & ? & ? & ? & ? \end{bmatrix}$$

and

$$M_B = \begin{bmatrix} ? & ? & - & - & - & - & - \\ + & + & + & + & + & + & + \\ - & - & ? & ? & - & - & - \\ + & + & + & + & + & + & + \\ ? & ? & - & - & ? & ? & ? \\ ? & ? & - & - & ? & ? & ? \\ ? & ? & + & + & + & + & + \end{bmatrix}.$$

This example shows how the structural influence matrix may be used to falsify a model. Influence matrices are useful, indeed, both for diagnostics and model validation: in fact, for instance, a structural sign of a matrix entry that is conflicting with experimental observations indicates that the model is not suitable for describing the observed phenomenon.

In this case, it is interesting to notice that the two influence matrices are fully consistent: there is no pair of corresponding entries having inconsistent signs. The influence matrix for model B is much more sign determined than that for model A, hence the sensitivity of the steady-state to parameter variations is higher for the "short distance shuttle" model.

7.6.4 An Enzymatic Cascade

While [GCFB15] was still under review, simultaneous work by Sontag [Son14a] was presented at a conference. Using completely different methods, [Son14b, Son14a] deal with a very similar (although more specific) problem: determining the sign of global changes in steady states upon perturbation of parameter values in individual modules, for biomolecular networks formed by the interconnection of several subsystems, in the presence of conservation laws that lead to stoichiometric constraints. The example of an enzymatic cascade is proposed and discussed in [Son14b, Son14a], where the structural signs of steady-state variations upon perturbation of *total amounts of species* are assessed based on the procedure by Sontag. The same results can be

obtained based on the methods proposed in [GCFB15] and presented in this chapter, which also allow to immediately compute the structural influence matrix for the system; the example and its structural analysis are reported here for the sake of completeness.

The chemical reactions proposed in [Son14b, Son14a]

$$E + M_0 \underset{g_a}{\overset{g_{em_0}}{\rightleftharpoons}} A \xrightarrow{g_a^*} M_1 + E, \qquad M_1 + G \underset{g_b}{\overset{g_{m_1g}}{\rightleftharpoons}} B \xrightarrow{g_b^*} M_0 + G,$$
$$M_1 + N_0 \underset{g_c}{\overset{g_{m_1n_0}}{\rightleftharpoons}} C \xrightarrow{g_c^*} N_1 + M_1, \qquad F + N_1 \underset{g_d}{\overset{g_{fn_1}}{\rightleftharpoons}} D \xrightarrow{g_d^*} N_0 + F,$$

along with the conservation laws

$$e + a = E_T, \quad g + b = G_T, \quad f + d = F_T,$$
$$m_0 + a + m_1 + b + c = M_T, \quad n_0 + c + n_1 + d = N_T,$$

where the letters with the subscript T indicate the total amount of enzymes and phosphatases, are equivalent to the reduced order ODE system

$$\begin{cases} \dot{a} = g_{em_0}(E_T - a, m_0) - g_a(a) - g_a^*(a) \\ \dot{b} = g_{m_1g}(M_T - a - b - c - m_0, G_T - b) - g_b(b) - g_b^*(b) \\ \dot{c} = g_{m_1n_0}(M_T - a - b - c - m_0, n_0) - g_c(c) - g_c^*(c) \\ \dot{d} = g_{fn_1}(F_T - d, N_T - c - d - n_0) - g_d(d) - g_d^*(d) \\ \dot{m}_0 = -g_{em_0}(E_T - a, m_0) + g_b^*(b) + g_a(a) \\ \dot{n}_0 = -g_{m_1n_0}(M_T - a - b - c - m_0, n_0) + g_c(c) + g_d^*(d) \end{cases}$$

together with the algebraic relationships

$$\begin{cases} e = E_T - a \\ f = F_T - d \\ g = G_T - b \\ m_1 = M_T - a - b - c - m_0 \\ n_1 = N_T - c - d - n_0 \end{cases}$$

The corresponding Jacobian matrix has the structure

$$J = \begin{bmatrix} -(\alpha+\gamma+\delta) & 0 & 0 & 0 & \beta & 0 \\ -\varepsilon & -(\varepsilon+\eta+\vartheta+\zeta) & -\varepsilon & 0 & -\varepsilon & 0 \\ -\kappa & -\kappa & -(\kappa+\mu+\nu) & 0 & -\kappa & \lambda \\ 0 & 0 & -\rho & -(\xi+\rho+\sigma+\tau) & 0 & -\rho \\ \alpha+\gamma & \vartheta & 0 & 0 & -\beta & 0 \\ \kappa & \kappa & \kappa+\mu & \tau & \kappa & -\lambda \end{bmatrix},$$

with $\det(-J) > 0$.

The structural effect of perturbations affecting the total amount of species can be computed as follows. The linearisation is of the form $\dot{x} = Jx + Eu$, $y = Hx + \hat{D}u$, hence, based on the decomposition $J = BDC$, the structural sign can be determined as

$$\operatorname{sign}\left(\det\begin{bmatrix} -BDC & -E \\ H & \hat{D} \end{bmatrix}\right).$$

The computation is straightforward, based on the techniques proposed so far, whenever the output is chosen as one of the variables of the reduced order system and matrix (actually, vector) E depends on a single parameter. In fact, in this case $\hat{D} = 0$, hence the parameter in vector E can be replaced by 1 (this is equivalent to dividing the whole column by the parameter). When, conversely, either E depends on more parameters (for instance, the choice $u = M_T$ leads to $E = \begin{bmatrix} 0 & \varepsilon & \kappa & 0 & 0 & -\kappa \end{bmatrix}^\top$) or $\hat{D} = 1$ (as happens for the choice $y = e$ when $u = E_T$, $y = f$ when $u = F_T$, $y = g$ when $u = G_T$, $y = m_1$ when $u = M_T$ and $y = n_1$ when $u = N_T$), then it is necessary to provide a sort of BDC-decomposition for vector E as well, $E = E_b D E_a$, and to compute

$$\operatorname{sign}\left(\det\begin{bmatrix} -BDC & -E_b D E_a \\ H & \hat{D} \end{bmatrix}\right).$$

Note that the above determinant is still a multi-affine function of the positive parameters associated with the partial derivatives.

The structural influences obtained with the approach in [GCFB15] are fully consistent with those in [Son14b, Son14a] and can be summarised as follows:

$$\begin{array}{c} \\ a\{ \\ b\{ \\ c\{ \\ d\{ \\ e\{ \\ f\{ \\ g\{ \\ m_0\{ \\ m_1\{ \\ n_0\{ \\ n_1\{ \end{array} \begin{array}{c} \overbrace{}^{E_T} \overbrace{}^{F_T} \overbrace{}^{G_T} \overbrace{}^{M_T} \overbrace{}^{N_T} \\ \left[\begin{array}{ccccc} + & - & + & + & - \\ + & - & + & + & - \\ + & + & - & + & + \\ + & + & - & + & + \\ + & + & - & - & + \\ - & + & + & - & - \\ - & + & + & - & + \\ - & - & + & + & - \\ + & - & - & + & - \\ - & + & + & - & + \\ + & - & - & + & + \end{array}\right] \end{array}.$$

Important quantities that can be experimentally measured are the concentrations of total active enzymes: $m_1 + b + c$ and $n_1 + d$. Taking as an output $y_m = m_1 + b + c = M_T - a - m_0$ and $y_n = n_1 + d = N_T - c - n_0$ and exploiting the technique discussed above to handle the case of a direct dependency of the output on the input ($\hat{D} \neq 0$), again the structural influences are consistent with those in [Son14b, Son14a]:

$$\begin{array}{c} \\ y_m\,\{ \\ y_n\,\{ \end{array} \overbrace{\begin{array}{cccccc} + & + & - & + & + \\ + & - & - & + & + \end{array}}^{\begin{array}{ccccc} E_T & F_T & G_T & M_T & N_T \end{array}}$$

Moreover, with the method in [GCFB15] the influence matrix for the reduced order system can be immediately computed:

$$M = \begin{bmatrix} + & + & - & - & + & - \\ - & + & - & - & - & - \\ - & - & + & + & - & + \\ - & - & - & + & - & - \\ ? & + & - & - & + & - \\ + & + & ? & + & + & + \end{bmatrix}.$$

7.6.5 Perfect Adaptation and Stoichiometric Adaptation

An interesting side result of the proposed approach is its ability to structurally identify *perfect adaptation*, a property widely observed and studied in the literature [YHSD00, DUR08, MTES+09, WSA12]. In this framework, in fact, a 0 influence represents a structural perfect adaptation. This phenomenon may occur in two different cases: the first is the trivial case in which there is no path leading from the input to the output variable in the system graph (this corresponds to a reducible Jacobian); the second is the case in which a path between the input and the output variables exists and has a zero complement, resulting in zero complementary feedback. [PL85, DLR02] An example of non-trivial structure that produces perfect adaptation is given by *stoichiometric adaptation*.

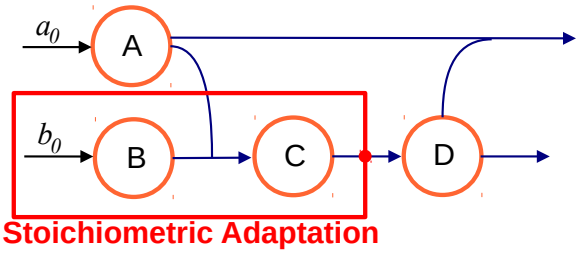

Figure 7.5: Example 7.10: a graph with stoichiometric adaptation.

Example 7.10. *(Stoichiometric adaptation.) Consider the graph in Fig. 7.5, corresponding to the reaction network*

$$\emptyset \xrightarrow{a_0} A, \quad A + D \xrightarrow{g_{ad}} \emptyset, \quad D \xrightarrow{g_d} \emptyset$$
$$\emptyset \xrightarrow{b_0} \mathbf{B}, \quad \mathbf{A} + \mathbf{B} \xrightarrow{g_{ab}} \mathbf{C}, \quad \mathbf{C} \xrightarrow{g_c} \mathbf{D}$$

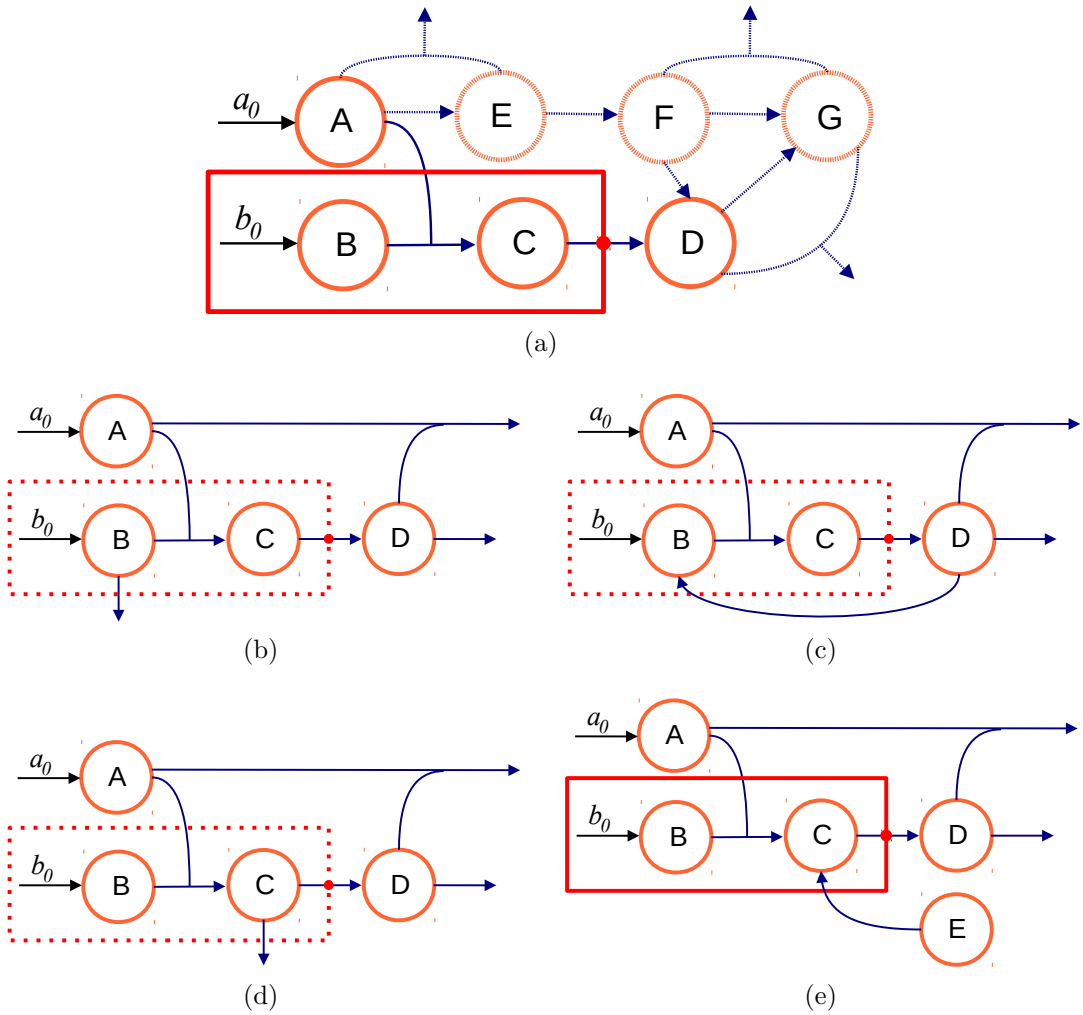

Figure 7.6: The stoichiometric adaptation module can be immersed in a generic network, as shown in (a), provided that no other reactions involve B or have C as a reagent. The networks in (b), (c) and (d) are no longer perfectly adaptive, while the network in (e) still exhibits perfect adaptation.

and to the system

$$\begin{cases} \dot{a} = -g_{ab}(a,b) - g_{ad}(a,d) + a_0 \\ \dot{b} = -g_{ab}(a,b) + b_0 \\ \dot{c} = g_{ab}(a,b) - g_c(c) \\ \dot{d} = g_c(c) - g_{ad}(a,d) - g_d(d) \end{cases}$$

with $b_0 > a_0$. *The corresponding Jacobian matrix has the structure*

$$J = \begin{bmatrix} -(\alpha+\mu) & -\beta & 0 & -\nu \\ -\alpha & -\beta & 0 & 0 \\ \alpha & \beta & -\gamma & 0 \\ -\mu & 0 & \gamma & -(\nu+\delta) \end{bmatrix},$$

with $\det(-J) > 0$*, and the proposed algorithm allows to verify that, if variable* c *is considered as an output, there is perfect adaptation in response to a persistent input applied to any of the variables, except for* b *and* c *itself. In fact, the influence matrix is*

$$M = \begin{bmatrix} + & - & - & - \\ - & + & + & + \\ \boxed{0} & + & + & \boxed{0} \\ - & + & + & + \end{bmatrix}.$$

Actually, it can be seen that such a structure corresponds to the presence of an integrator. Indeed, at the equilibrium, $g_c(\bar{c}) = b_0$*. Hence, if the variable* $w = b + c$ *is considered, its derivative* $\dot{w} = b_0 - g_c(c)$ *is zero at the equilibrium. Likewise, by considering* $w = c + d$*, it can be noticed that* $\dot{w} = g_{ab}(a, b) - g_{ad}(a, d) - g_d(d)$ *is zero at the equilibrium. The presence of the stoichiometric-adaptation motif (squared in Fig. 7.5 and corresponding to the reactions emphasised in boldface) in the system graph always ensures perfect adaptation, provided that no other reactions involve species* B *or have species* C *as a reagent (additional reactions where* C *is a product do not alter the perfect adaptation property). The reaction network in Fig. 7.6 (a) is an example. For instance, it can be seen that if either the reaction* $B \rightharpoonup \emptyset$*, or* $D \rightharpoonup B$*, or* $C \rightharpoonup \emptyset$ *is added, then the system no longer reveals perfect adaptation; while, if* $E \rightharpoonup C$ *is added, variable* c *is still perfectly adaptive with respect to persistent inputs applied to* a *or to* d *(see Fig. 7.6 (b)-(e)).*

Note that the presence of the stoichiometric-adaptation motif is sufficient, but not necessary for perfect adaptation. Two examples of systems exhibiting perfect adaptation without including the stoichiometric adaptation module are discussed in the next example.

Example 7.11. Verdi4. *The chemical reaction network in Fig. 7.7, left,*

$$\emptyset \xrightarrow{b_0} B \xrightarrow{g_b} A, \quad B + C \xrightarrow{g_{bc}} A, \quad A \xrightarrow{g_a} D, \quad C + D \xrightarrow{g_{cd}} \emptyset, \quad \emptyset \xrightarrow{c_0} C,$$

where the stoichiometric adaptation condition is violated by the presence of the reaction $B \xrightarrow{g_b} A$*, correspond to the system*

$$\begin{cases} \dot{a} = g_b(b) + g_{bc}(b, c) - g_a(a) \\ \dot{b} = -g_b(b) - g_{bc}(b, c) + b_0 \\ \dot{c} = -g_{bc}(b, c) - g_{cd}(c, d) + c_0 \\ \dot{d} = g_a(a) - g_{cd}(c, d) \end{cases}$$

with $2b_0 > c_0 > b_0$*, whose Jacobian matrix is*

$$J = \begin{bmatrix} -\alpha & \beta + \eta & \gamma & 0 \\ 0 & -(\beta + \eta) & -\gamma & 0 \\ 0 & -\eta & -(\gamma + \varepsilon) & -\delta \\ \alpha & 0 & -\varepsilon & -\delta \end{bmatrix}.$$

It can be checked that $\det(-J) > 0$ *and the influence matrix is*

$$M = \begin{bmatrix} + & + & \boxed{0} & \boxed{0} \\ + & + & - & + \\ - & - & + & - \\ + & + & - & + \end{bmatrix},$$

which shows that the variable a *is still perfectly adaptive with respect to persistent inputs applied to variable* c *or* d*.*

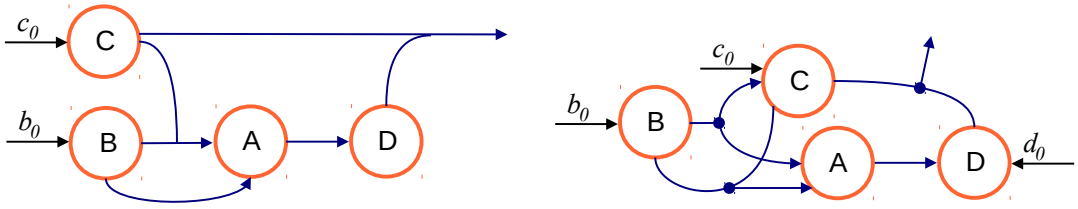

Figure 7.7: The graphs of the systems in Example 7.11: Verdi4 (left) and Wagner4 (right).

Wagner4. *The system*

$$\begin{cases} \dot{a} = g_b(b) + g_{bc}(b,c) - g_a(a) \\ \dot{b} = -g_{bc}(b,c) - g_b(b) + b_0 \\ \dot{c} = -g_{bc}(b,c) - g_{cd}(c,d) + g_b(b) + c_0 \\ \dot{d} = g_a(a) - g_{cd}(c,d) + d_0 \end{cases}$$

with $2b_0 + d_0 > c_0 > d_0$*, associated with the reactions*

$$\emptyset \xrightarrow{b_0} B \xrightarrow{g_b} A + C, \quad B + C \xrightarrow{g_{bc}} A, \quad A \xrightarrow{g_a} D, \quad C + D \xrightarrow{g_{cd}} \emptyset, \quad \emptyset \xrightarrow{c_0} C, \quad \emptyset \xrightarrow{d_0} D$$

(see the graph in Fig. 7.7, right), has a Jacobian matrix with the structure

$$J = \begin{bmatrix} -\alpha & \beta + \delta & \gamma & 0 \\ 0 & -(\beta + \delta) & -\gamma & 0 \\ 0 & \beta - \delta & -(\gamma + \zeta) & -\varepsilon \\ \alpha & 0 & -\zeta & -\varepsilon \end{bmatrix}.$$

It can be checked that $\det(-J) > 0$*; interestingly, the influence matrix is exactly the same as in the previous case (hence, again, variable* a *exhibits perfect adaptation whenever a persistent input is applied to variable* c *or* d*).*

7.7 Remarks

An efficient numerical algorithm has been proposed to *structurally* assess the steady-state input-output influence of a stimulus, regarded as a persistent input provided to

a system, on a system variable, regarded as an output: this simply requires checking the determinant of a matrix at a finite number of points (the vertices of the hypercube defined by the space of parameters). Under asymptotic stability assumptions, the steady-state influence can be used to describe the system response to a step input. In the case of marginally stable systems, it can be used instead to describe the system response to an impulsive input in the *stoichiometric compatibility class*, after a suitable state transformation. The influence matrix summarises the steady-state net influence on each variable due to an additive input persistently applied to a single variable. In some cases, entries with indeterminate sign are found in the influence matrix. Remarkably, several complex systems proposed in the literature have a surprisingly small fraction of indeterminate entries, so revealing an intrinsic robustness aspect in the system steady-state interactions.

Robust stability analysis may be a preliminary step for the application of the proposed algorithm. It has been assumed that the equilibrium exists and is locally stable. However, it may be necessary to check if this assumption holds. The existence of an equilibrium is assured if the system solutions are bounded. Some structural boundedness criteria have been suggested in Chapter 6, based on [BG14], along with stability criteria based on Lyapunov theory. Stability investigation can be also carried out with the methodologies described in the book by [Bar94] (and reported in Section 4.4.1). In fact, for a system admitting a BDC-decomposition, the characteristic polynomial

$$\det(sI - BDC) = p_0(D) + p_1(D)s + p_2(D)s^2 + \cdots + s^n$$

has coefficients $p_i(D)$ which are *multi-affine functions* of the coefficients D_k. Therefore, if reasonable bounds $0 < D_k^- \leq D_k \leq D_k^+$ can be assumed for each coefficient D_k (which is true based on the results in Section 4.3.1), then the graphical test based on the Mapping Theorem provides a nice sufficient condition for robust stability.

An important extension of the proposed approach (and algorithm) would be the inclusion of *a priori* information to determine structural influences. Consider for instance the community matrix associated with a stable three-dimensional system involving two species in competition, x_1 and x_2, preyed upon by a common predator x_3 ([Lev75], Figure 6b):

$$J = \begin{bmatrix} -a_{11} & -a_{12} & -a_{13} \\ -a_{21} & -a_{22} & -a_{23} \\ a_{31} & a_{32} & 0 \end{bmatrix}.$$

Its influence matrix is

$$M = \begin{bmatrix} + & - & ? \\ - & + & ? \\ ? & ? & ? \end{bmatrix}.$$

Without any additional information, the entry M_{33} of the influence matrix is '?'. However, if it is assumed that the system involving only the prey x_1 and x_2 is unstable,

so that $a_{11}a_{22} < a_{12}a_{21}$ (thus the overall system is stabilised by the presence of the predator), then $\hat{M}_{33} =$'$-$' and the influence matrix becomes

$$\hat{M} = \begin{bmatrix} + & - & ? \\ - & + & ? \\ ? & ? & - \end{bmatrix}.$$

Hence, a positive input to the predator population results in a steady-state decline in the abundance of the predator itself, due to the instability of the competing-prey subsystem.

8

Structural Classification of Oscillatory and Multistationary Biochemical Systems

Periodic and multistationary dynamics are relevant in several contexts, ranging from engineering and physics to biology. When models and parameters are uncertain, determining whether a system has the capacity to exhibit oscillations or multistationarity can be difficult. As discussed in Chapter 5, this issue is particularly pronounced for biological network models; hence, structural analysis is particularly important, since it is crucial to predict or rule out potential dynamic behaviours of a system *independent of parameter values*. In spite of considerable uncertainties, strong conclusions on the admissible dynamic behaviours of a system can often be achieved without detailed knowledge of its specific parameters, when a proper class of models is considered. A rich literature, related to Thomas' conjectures [Tho81], has focused on systems with a *sign-definite Jacobian*, providing cycle-based parameter-free criteria to identify potential oscillatory and multistationary dynamic outcomes.

This chapter reports the results in [BFG14], which considers dynamical systems with sign-definite Jacobian, associated with non-autocatalytic biochemical networks, and proposes a general, cycle-based classification of *multistationary and oscillatory behaviours*, which summarises and integrates several existing results in the literature. Distinguishing between transitions to instability due to a complex pair of eigenvalues or to a real eigenvalue crossing the imaginary axis, a complete characterisation is provided for candidate oscillatory and multistationary systems, based on the exclusive or simultaneous presence of positive and negative cycles in the Jacobian sign graph (where nodes are associated with species concentrations and arcs with signed Jacobian entries). Necessary and sufficient conditions are achieved, relying on the ability of locally scaling the *independent entries* of the Jacobian. This characterisation is robust with respect to model uncertainties, because it depends exclusively on the sign-definite Jacobian of the model, regardless of the chosen functions or parameters.

Although sign-definiteness of the system Jacobian is a strong requirement, it is actually satisfied by some relevant models in biochemistry and biology, which can thus be classified in the proposed framework. Significant molecular networks exhibiting

oscillations or bistability fall in the categories of *strong candidate oscillators or multistationary systems*; yet, in detailed models capturing the complexity of the cellular environment, often either the Jacobian is not sign-definite, or both positive and negative cycles are present (hence, both oscillatory and bistable behaviours are in principle possible).

To address a wider class of systems, the proposed structural classification is extended, following [BFG15b], to provide necessary and sufficient structural conditions for multistationarity and oscillations in *aggregate monotone systems*, defined as the interconnection of stable monotone components. The characterisation is then based on the presence of exclusively positive or exclusively negative cycles in the system *aggregate graph*, whose nodes are associated with the monotone subsystems.

The classifications proposed in [BFG14, BFG15b] apply to *in vitro* biomolecular networks such as those in [FFK$^+$11, KWW06, KW11, MPS$^+$11] and can thus aid the design of tunable and robust artificial biomolecular networks that are structurally well suited to achieve the desired dynamics.

8.1 Background

Understanding what interaction networks can generate multistationary and periodic behaviours in dynamical systems is fundamental in many different contexts; in particular, in the area of systems and synthetic biology, it is relevant both when analysing biochemical networks naturally present in an organism [GGG$^+$12, QNKS07] and when building artificial networks to achieve target dynamics. Due to the intrinsic variability and uncertainty of molecular systems, structural sources of multistationarity and periodicity need to be identified, based on parameter-free criteria. Many different tools have been employed to achieve structural conclusions on the behaviour of biochemical systems. For chemical reaction networks governed by mass-action kinetics, the zero deficiency theorem [Fei87] rules out the presence of oscillations and multistationarity regardless of specific kinetic rates, while cycle conditions associated with the presence of Hopf or saddle-node/pitchfork instability have been proposed using species-reaction graphs [CF05, CF06b, LW10, Min11] and algebraic geometry [DK09, DP12]. Chemical reaction networks are a very important class of models, but phenomenological models are often preferred in biology when pathways are not known in detail; and most criteria that apply for mass-action kinetics cannot account for Michaelis-Menten or Hill type kinetics, or for qualitative relationships. Graphical or algebraic conditions based on the Jacobian matrix enable a qualitative analysis also when the precise stoichiometry of the interactions is unknown. [MC08]

For generic systems with a sign-definite Jacobian, indeed, structural results can be achieved by studying *Jacobian graphs*, where species concentrations (states of the dynamical system) are associated with nodes and signed Jacobian entries linking different states are associated with arcs. Criteria based on the presence of

positive or negative cycles in the Jacobian graph have been proposed to explain multistationarity and oscillations in molecular and chemical systems [TCM+08]. Well known mathematical conjectures in this area have been formulated by Thomas [Tho81] (given a Jacobian graph, a negative cycle is a necessary condition for stable periodic behaviour, while a positive cycle is a necessary condition for multistationarity; see [DP12] for a very thorough survey) and proved in [Hir88, Gou98, Sno98], with several further extensions and refinements [Sou04, KST07, BC09, RC11].

Proper design of feedback loops enables the successful creation of many artificial biochemical networks exhibiting bistability [GCC00, ASMN03, KWW06, PFR12] or oscillations [EL00, SCB+08, TMLSF09, KW11, MPS+11, FFK+11]. However, this is extremely challenging in experimental systems; even *in vitro* artificial networks [KW11, MPS+11, FFK+11] with a small number of components are affected by unknown interactions that can create additional parasitic feedback loops of uncertain strength. Structural criteria are needed to predict dynamic outcomes of networks where several cycles (with potentially unknown magnitude) coexist.

Building on the vast literature flourished thanks to Thomas' conjectures, a structural classification of oscillatory and multistationary networks is proposed in [BFG14], based on the exclusive or concurrent presence of positive and negative cycles in the Jacobian graph. Non-autocatalytic systems having a sign-definite Jacobian are considered, whose *structure* is identified with the sign pattern of the Jacobian matrix and the corresponding directed graph. A structure can be specified into a dynamic *realisation* by choosing a specific set of functions, along with specific parameter values. Candidate dynamic behaviours are defined based on the admissible types of *transition to instability*, occurring when the Jacobian eigenvalues cross the imaginary axis due to a change in parameters. Multistationarity is associated with a real eigenvalue transitioning to instability (*i.e.*, changing sign from negative to positive), while oscillatory behaviours are associated with a complex pair of eigenvalues transitioning to instability (*i.e.*, whose real part changes sign from negative to positive) as parameter values change.

Weak (strong) candidate oscillators can possibly (exclusively) transition to instability due to a complex pair of eigenvalues, while weak (strong) candidate multistationary systems can possibly (exclusively) transition to instability due to a real eigenvalue. Following [BFG14], it is shown that a system can be classified as a strong candidate oscillator when all cycles in its structure are negative, as a weak candidate oscillator if there exists at least one negative cycle in its structure. Similarly, a system can be classified as a strong (weak) candidate multistationary system if its structure presents exclusively positive cycles (at least one positive cycle). Proofs rely on the topological degree theory (see [Hof90], along with the overview and references suggested in Section 4.5 and in Appendix D) and on the properties of sign-definite systems [MQ69]. The approach can be also used to characterise systems affected by delays, which are often present in models of gene networks [Lew03]: cycle-based sufficient conditions can be proposed to identify candidate oscillators and multistationary systems in the presence of delays.

Following [BFG15b], the classification is extended to the case of *aggregate monotone systems*, defined as the interconnection of stable monotone subsystems. The theory of monotone systems [Smi08, Son07] provides powerful robust analysis methods and simplifies the analysis of large, complex networks, which can be decomposed into interconnections of input-output monotone subsystems [AS03]: monotonicity (along with the existence of steady-state characteristics) facilitates the detection of multistationarity in systems of arbitrary size [AFS04] and, accompanied by small-gain conditions, provides necessary conditions for oscillations [AS08]. Many biochemical systems are monotone [Son07], or can be regarded as the interconnection of monotone subsystems: notable examples are the Cds-Wee1 network [AS03], the MAPK pathway [Son07], the Goldbeter oscillator [AS08] in *Drosophila*. Monotonicity is a property that can be verified without the exact knowledge of functional expressions and system parameters: therefore, criteria relying on monotonicity are robust with respect to modelling choices and parametric uncertainty.

Exploiting the fact that a monotone subsystem within a large network can be regarded as a single element having a sign-definite input-output mapping, the classification for sign-definite biochemical systems proposed in [BFG14] can be successfully scaled to consider interconnections of monotone subsystems, rather than interconnections of a multitude of individual molecular species, providing structural necessary and sufficient conditions for potential oscillatory and multistationary behaviours in aggregate monotone systems. [BFG15b] Focusing on networks comprised of stable monotone subsystems, strong candidate oscillators and multistationary systems can be characterised based on the exclusive presence of negative or positive cycles in the system aggregate graph; no strong conclusions can be drawn for aggregate graphs where positive and negative cycles are concurrently present. The approach is valid only for systems in which interactions between unconditionally stable monotone components are independent, so that they can be independently scaled (although this requirement is generally satisfied, interactions between bimolecular systems may be coupled by retroactivity or competition for common cellular resources).

A simple example clarifies the relevance of the proposed classification.

Example 8.1. *A nondimensional biomolecular model is considered in [BFG14], accounting for transcription and translation of two genes, where proteins reciprocally modulate their expression forming a feedback loop [EL00, KW11]:*

$$\begin{cases} \dot{r}_1 = \gamma_1 + H_1(p_2) - r_1, & \dot{p}_1 = \beta_1 r_1 - p_1, \\ \dot{r}_2 = \gamma_2 + H_2(p_1) - r_2, & \dot{p}_2 = \beta_2 r_2 - p_2, \end{cases} \tag{8.1}$$

where, for $i = 1, 2$, r_i are RNA species concentrations, p_i are protein concentrations, $H_i(\cdot)$ are Hill functions, and all Greek letters denote reaction rates that are constant

positive scalars. The system can be rewritten as

$$\begin{bmatrix} \dot{r}_1 \\ \dot{p}_1 \\ \dot{r}_2 \\ \dot{p}_2 \end{bmatrix} = \begin{bmatrix} -1 & 0 & 0 & 0 \\ \beta_1 & -1 & 0 & 0 \\ 0 & 0 & -1 & 0 \\ 0 & 0 & \beta_2 & -1 \end{bmatrix} \begin{bmatrix} r_1 \\ p_1 \\ r_2 \\ p_2 \end{bmatrix} + \begin{bmatrix} \gamma_1 + H_1(p_2) \\ 0 \\ \gamma_2 + H_2(p_1) \\ 0 \end{bmatrix} = \tilde{M} \begin{bmatrix} r_1 \\ p_1 \\ r_2 \\ p_2 \end{bmatrix} + \tilde{H}(p_1, p_2),$$

to evidence global boundedness of the two-gene system trajectories. In fact, $\tilde{M}$ is an asymptotically stable matrix and $\tilde{H}(p_1, p_2)$ is a bounded quantity, $\|\tilde{H}(p_1, p_2)\| \leq \eta$. The right-hand side of the equation is given by the sum of a linear term and a globally bounded nonlinear term. If the nonlinear part is neglected, an asymptotically stable linear system is achieved, which admits a global quadratic Lyapunov function $V(x) = x^\top P x$, where $\tilde{M}^\top P + P\tilde{M} = -Q$, with Q positive definite. Hence, all of the system solutions are globally ultimately bounded in an ellipsoidal set of the form $x^\top P x \leq k$, for some $k > 0$ which depends on P, Q and η (see [Kha02, BM15]).

Depending on the regulatory action of the proteins, hence on the type of Hill functions, the network presents a different number of equilibria and different possible dynamic behaviours.

Case (a):

$$H_1(p_2) = \alpha_1 \frac{p_2^n}{1 + p_2^n} \quad \textit{and} \quad H_2(p_1) = \alpha_2 \frac{p_1^n}{1 + p_1^n}.$$

A two-gene positive feedback loop is obtained, often encountered in developmental networks [Alo06, DRO+02], whose Jacobian is

$$J = \begin{bmatrix} -1 & 0 & 0 & \frac{\partial H_1}{\partial p_2} \\ \beta_1 & -1 & 0 & 0 \\ 0 & \frac{\partial H_2}{\partial p_1} & -1 & 0 \\ 0 & 0 & \beta_2 & -1 \end{bmatrix}, \qquad \textit{where} \quad \frac{\partial H_i}{\partial p_j} = \alpha_i \frac{n p_j^{n-1}}{(1 + p_j^n)^2}. \tag{8.2}$$

The system is non-autocatalytic: there is spontaneous degradation of each species, hence the diagonal terms of the Jacobian are negative. Moreover, all of the Jacobian entries, evaluated at a positive equilibrium, are sign definite: they do not change sign for arbitrary choices of the (positive) parameters α_i, β_i and n. Therefore, the Jacobian sign pattern is a structural property of this system and can be associated with a graph, where nodes correspond to the concentrations of biochemical species and are interconnected by positive ($+1$) or negative (-1) arcs according to the corresponding Jacobian entries,[1] as shown in Fig. 8.1 (a).

The characteristic polynomial is

$$p(s) = (s + 1)^4 - K, \qquad \textit{with} \quad K = \beta_1 \beta_2 \frac{\partial H_1}{\partial p_2} \frac{\partial H_2}{\partial p_1} > 0.$$

[1] Only the sign of each Jacobian entry is considered as the weight of the corresponding arc in the graph.

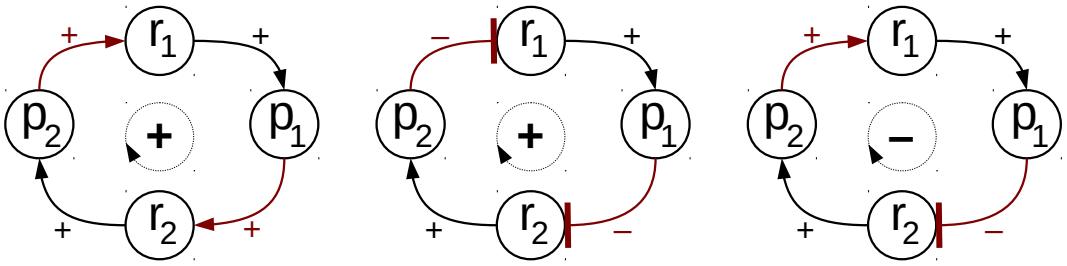

(a) Double positive feedback loop (overall positive cycle).

(b) Double negative feedback loop (overall positive cycle).

(c) Positive and negative regulation (overall negative cycle).

Figure 8.1: Graphs corresponding to different regulatory actions in the two-gene system (8.1).

As shown in [BFG14], for $n = 1$ there is a single positive equilibrium, while for $n > 1$ the system admits multiple (typically three) positive equilibria. The stability properties of an equilibrium can be examined based on the eigenvalues of the Jacobian matrix, which are the roots of its characteristic polynomial; when the parameters change, these roots change accordingly. If instability occurs, then it is due to a single real root which becomes positive: in fact, if $K > 1$, there is a single root having positive real part, and it is on the real axis, while, if $K < 1$, all of the roots have negative real part. Therefore, the system can only admit real (exponential) instability, arising due to a real eigenvalue changing sign from negative to positive. The transition to instability of the equilibrium is associated with the appearance of new equilibria.

Case (b):

$$H_1 = \alpha_1 \frac{1}{1+p_2^n} \quad \textit{and} \quad H_2 = \alpha_2 \frac{1}{1+p_1^n}.$$

System (8.1) *represents a two-gene double negative feedback loop, depicted in Fig. 8.1 (b), also known as toggle switch (a synthetic biological example is in [GCC00]; a natural example is the Cdc2-Wee1 network [AS03]). The same analysis performed for the two-gene double positive feedback loop can be repeated, getting similar results in terms of admissible transitions to instability, which can be only real (exponential), regardless of the considered equilibrium.*

Case (c):

$$H_1 = \alpha_1 \frac{p_2^n}{1+p_2^n} \quad \textit{and} \quad H_2 = \alpha_2 \frac{1}{1+p_1^n}.$$

When Hill functions have opposite regulatory roles, the network can behave as a two-gene oscillator [KW11]. The Jacobian is still a sign-definite matrix; however, $\frac{\partial H_1}{\partial p_2}$ and $\frac{\partial H_2}{\partial p_1}$ have opposite signs, due to the different slopes of the Hill functions, hence generate an overall negative *feedback loop, as shown in Fig. 8.1 (c). The characteristic polynomial is*

$$p(s) = (s+1)^4 + K, \qquad \textit{with} \quad K > 0.$$

The equilibrium conditions now admit a single intersection regardless of the value of α_i, β_i, and n, as is graphically shown in [BFG14]; since in this case $K < 0$, all of the Jacobian eigenvalues are complex, hence only oscillatory unstable dynamics can arise (and do arise when $K < -4$). In fact, for any given value of n there is only one equilibrium, whose stability properties can change depending on the values of α_i and β_i.

For details, the reader is referred to [BFG14], where equilibrium conditions and example trajectories in the $p_1 - p_2$ plane of the phase space are shown for different values of n in each of these three cases.[2]

The structural analysis of the simple two-gene system in Example 8.1 shows that, even without a precise knowledge of the involved functions, very strong conclusions on the possible dynamic behaviours of the system can be reached, independent of specific functions or parameter choices. In particular, a strong relationship has been highlighted between the presence of positive or negative cycles in the graph associated with the system and admissible transitions to instability.

8.2 Structural Classification

Consider the dynamical system

$$\dot{x} = f(x), \quad x \in \mathbb{R}^n, \tag{8.3}$$

where $f(\cdot)$ is continuously differentiable in all its components $f_i(\cdot)$, $i = 1, ..., n$, and may be any function satisfying the following assumptions.

Assumption 8.1. *All the solutions of system* (8.3) *are globally uniformly asymptotically bounded in a ball $\mathcal{S}$.*

As a consequence, the system admits an equilibrium point $\bar{x}$ in $\mathcal{S}$ (as discussed in Section 4.5; [Srz85], see also [RW02, RW04]).

Assumption 8.2. *For each component $f_i(\cdot)$, $\partial f_i/\partial x_j$ is either always positive, always negative, or always null in all the considered domain.*

Assumption 8.3. *The system is non-autocatalytic,* i.e., *for all i, $\partial f_i/\partial x_i < 0$.*

In the sequel, it will be always assumed that the above hypotheses are satisfied.

Since $f_i(\cdot)$ is monotonic (either non-increasing or non-decreasing) with respect to each argument, the Jacobian of system (8.3) is sign definite.

[2] A qualitatively similar study was carried out and validated by building synthetic bacterial circuits in [ASMN03], where analysis relied on the S-systems formalism [SV87].

Definition 8.1. *Given a system with a sign-definite Jacobian, its* structure *is the sign pattern matrix* $\Sigma = sign(J)$*. Matrix* Σ *can be associated with a directed* n*-node graph, whose arcs are positive* $(+1)$*, negative* (-1)*, or zero depending on the sign of the corresponding matrix entries.*

Graph examples are provided in Fig. 8.1.

Definition 8.2. *A* realisation *of the system structure* Σ *is given by any choice of functions* $f_i(\cdot)$*, along with specific parameter values,*[3] *which is compatible with* Σ*.*

For example, the structure corresponding to the two-node double positive feedback loop is

$$\Sigma = \begin{bmatrix} - & 0 & 0 & + \\ + & - & 0 & 0 \\ 0 & + & - & 0 \\ 0 & 0 & + & - \end{bmatrix}, \tag{8.4}$$

associated with the graph shown in Fig. 8.1 (a), while the specific model considered in Example 8.1 and its Jacobian matrix (8.2) are a possible realisation of this structure.

According to the definition proposed in Chapter 2, a property is *structural* if it is satisfied by any system with a given structure, independently of the specific realisation [BF11b]. Hence, a property is not structural if there exists at least one realisation which does not satisfy the property.

Definition 8.3. *Given a graph, a* cycle *is an oriented, closed sequence of distinct nodes connected by distinct directed arcs. A cycle is* negative *(respectively,* positive*) if the number of negative arcs is odd (respectively, even). The* order *of the cycle is the number of arcs involved in the cycle.*

For example, all of the two-gene networks in Example 8.1 have a single cycle; the double positive feedback system and the toggle switch exhibit an overall positive cycle, while the two-nodes oscillator presents an overall negative cycle.

Definition 8.4. *System* (8.3) *with structure* Σ *is* critical *iff all the negative cycles of its structure (if any) are of order two.*

Non-critical systems are considered here; the validity of the proposed results for possibly critical structures is briefly discussed in Section 8.2.1.

To define the concept of *transition to instability*, consider the parameter-dependent dynamical system (satisfying Assumptions 8.1–8.3)

$$\dot{x}(t) = g(x(t), \mu), \qquad x \in \mathbb{R}^n, \tag{8.5}$$

where μ is a real-valued parameter and $g(\cdot, \cdot)$ is a sufficiently smooth function, continuous in μ, satisfying all of the previously stated assumptions for every value

[3] Clearly, the choice of $f_i(\cdot)$ and its parameters uniquely determines the entries of the Jacobian matrix $J_{ij} = [\partial f_i / \partial x_j]$.

of μ. The structure Σ of system (8.5) is assumed to be invariant with respect to μ. Assumption 8.1 ensures that an equilibrium exists; all the following definitions refer to this equilibrium, which is, in general, a function of μ: $g(\bar{x}_\mu, \mu) = 0$. It is assumed that $\bar{x}_\mu$ depends continuously on μ. A suitable change of coordinates always allows to shift the equilibrium to the origin, without affecting the analysis. Indeed, if $z = x - \bar{x}_\mu$, then $\dot{z}(t) = g(z(t) + \bar{x}_\mu, \mu)$ and $g(\bar{z} + \bar{x}_\mu, \mu) = 0$ for $\bar{z} = 0$. The Jacobian matrix is unchanged, since $\frac{\partial g}{\partial z}\big|_{z=0} = \frac{\partial g}{\partial x}\big|_{x=\bar{x}_\mu}$. This equilibrium translation will be used in the following to simplify the notation.

Recall that a matrix is asymptotically stable if all its eigenvalues have a negative real part, while it is (asymptotically) unstable if at least one of its eigenvalues has a positive real part.

Definition 8.5. *System* (8.5) *undergoes a* Transition to Instability *at* $\mu = \mu^*$ *iff its Jacobian matrix* $J(\bar{x}_\mu)$ *is asymptotically stable in a left neighbourhood of* μ^**, and unstable in a right neighbourhood.*[4] *A TI is* simple *if at most a single real eigenvalue or a single pair of complex conjugate eigenvalues crosses the imaginary axis.*

In principle, many eigenvalues could leave the stability region simultaneously. However, since most systems have a *dominant* eigenvalue,[5] non-simple TIs are unlikely to occur.

Two types of simple TIs are considered, related to oscillatory and multistationary dynamic behaviours.

Definition 8.6. *System* (8.5) *undergoes an* Oscillatory Transition to Instability (OTI) *at* $\mu = \mu^*$ *iff its Jacobian matrix* $J(\bar{x}_{\mu^*})$ *has a single pair of pure imaginary eigenvalues, while all the other eigenvalues have negative real part:*

$$\sigma\left(J(\bar{x}_{\mu^*})\right) = \{\lambda_1, \lambda_2, \ldots, \lambda_n\}, \quad \textit{where} \quad \lambda_{1,2} = \pm j\omega,$$

with $Re(\lambda_k) < 0$ *for* $k > 2$ *and* $Re(\lambda_k) > 0$ *for* $k = 1, 2$ *in a right neighbourhood of* μ^**.*

Definition 8.7. *System* (8.5) *undergoes a* Real Transition to Instability (RTI) *at* $\mu = \mu^*$ *iff its Jacobian matrix* $J(\bar{x}_{\mu^*})$ *has a single zero eigenvalue, while all the other eigenvalues have negative real part:*

$$\sigma\left(J(\bar{x}_{\mu^*})\right) = \{\lambda_1, \ldots, \lambda_n\}, \quad \textit{where} \quad \lambda_1 = 0,$$

with $Re(\lambda_k) < 0$ *for* $k > 1$ *and* $Re(\lambda_1) > 0$ *in a right neighbourhood of* μ^**.*

[4] This definition holds for systems transitioning to instability from the right to the left neighbourhood of μ^* as well: it suffices to take $\hat{\mu} = \mu^* - \mu$ as the bifurcation parameter.

[5] A dominant eigenvalue (or complex pair of eigenvalues) has real part larger than any other eigenvalue of the system and substantially characterises the dynamic behaviour.

When an RTI occurs, the determinant of the Jacobian changes sign as the parameter crosses the stability limit. Indeed, the characteristic polynomial can be factored out as $p_\mu(\lambda) = [\lambda - z(\mu)]\tilde{p}_\mu(\lambda)$, with $\tilde{p}_\mu(\lambda)$ having roots with negative real part in a neighbourhood of $\mu = \mu^*$. Then $z(\mu) < 0$ for $\mu < \mu^*$, in view of the stability assumption, and $z(\mu) > 0$ for $\mu > \mu^*$. Since the constant term is $p_\mu(0) = -z(\mu)\tilde{p}_\mu(0) = -\det[J(\bar{x}_\mu)]$, the determinant changes sign at μ^*. As shown later in Corollary 8.2, under overall boundedness assumptions, this implies that an RTI causes the appearance of new equilibrium points. This is not the case for OTIs. These concepts are related to bifurcation theory (see Section 2.3.4 and [Str94, AP95, Kuz98, Mei07]): typically, RTIs are associated with zero-eigenvalue bifurcations [Str94], while OTIs are related to Andronov-Hopf bifurcations. Formally, however, additional assumptions are required for these bifurcations to occur, which complicates their mathematical analysis (a sample of this is provided in Section 2.3.4).

Consider now a system of the form (8.3), under Assumptions 8.1, 8.2 and 8.3, with a given *structure* Σ defined as the sign pattern matrix associated with the system Jacobian.

Remark 8.1. *An* alteration of (8.3) *is a system of the form* (8.5)*, such that for* $\mu = \mu_0, \quad g(x, \mu_0) = f(x)$ *and for* $\mu \neq \mu_0$ *the structure* Σ *is preserved, yielding the equilibrium* $\bar{x}_\mu$*.*

To structurally assess the system capacity to exhibit multistability or oscillations, the sign of the cycles in the corresponding directed graph can be examined. First of all, general definitions need to be stated for candidate oscillatory and multistationary systems. Based on these definitions, the necessary and sufficient conditions proposed in [BFG14] link the presence of negative and positive cycles in a structure to the oscillatory or multistationary nature of the system.

Definition 8.8. *A system of the form* (8.3)*, with structure* Σ*, is structurally*

i) a candidate oscillator in the weak sense *iff there exists an alteration* (8.5) *which admits an OTI;*
ii) a candidate oscillator in the strong sense *iff, for any alteration* (8.5)*, every simple TI (if any) is an OTI;*
iii) a candidate multistationary system in the weak sense *iff there exists an alteration* (8.5) *which admits an RTI;*
iv) a candidate multistationary system in the strong sense *iff, for any alteration* (8.5)*, every simple TI (if any) is an RTI.*

A weak candidate oscillator admits an unstable equilibrium point where trajectories spiral out of the equilibrium with oscillatory dynamics. A strong candidate oscillator admits transitions to instability exclusively of oscillatory nature. The two-gene oscillatory system described in Example 8.1 is a strong candidate oscillator, since unstable dynamics can arise only in association with complex conjugate eigenvalues, hence must be oscillatory. Conversely, a weak candidate multistationary

	Candidate oscillator	Candidate multistationary
Weak	A negative cycle exists	A positive cycle exists
Strong	All cycles are negative	All cycles are positive

Table 8.1: Table summarising the structural cycle-based classification of candidate oscillators and multistationary systems. [BFG14, BFG15b]

system admits unstable behaviours due to a real unstable eigenvalue. A strong candidate multistationary system can admit solely unstable dynamics due to a real unstable eigenvalue. In Example 8.1, both the two-gene double positive feedback loop and the toggle switch are strong candidate multistationary systems, since unstable dynamics can arise only due to a real unstable eigenvalue.

Necessary and sufficient conditions can be provided that characterise candidate oscillators and multistationary systems based on the sign of the cycles in their structure Σ: indeed, a system is a candidate oscillator in the strong sense iff all the cycles are negative, in the weak sense iff there is at least one negative cycle; conversely, a system is a candidate multistationary system in the strong sense iff all the cycles are positive, in the weak sense iff there is at least one positive cycle. The classification based on cycles in the system structure is summarised in Table 8.1.

Some of the proofs in [BFG14, BFG15b] are built with the following argument: given a condition $\mathcal{C}$ on a structure associated with a system $\dot{x}(t) = f(x(t))$, to prove that $\mathcal{C}$ is necessary for a certain structural property $\mathcal{P}$ to hold, it can be supposed by contradiction that $\mathcal{C}$ is not satisfied by the structure. Then, it can be shown that there always exists a realisation of the structure for which $\mathcal{P}$ does not hold.

To this aim, an alteration (8.5) of systems of the form (8.3) that leaves Σ unchanged can be useful to find, given a structure, a realisation which satisfies a property of interest. The proposed vector field alteration is achieved by means of $\nu_{\kappa,\epsilon}$ differential scaling maps. To simplify the notation, it is henceforth assumed that the equilibrium is at zero.

Definition 8.9. *A* differential scaling map $\nu_{\kappa,\epsilon}$ *(see for example Fig. 8.2), where* $\kappa,\ \epsilon > 0$ *are real parameters, is a strictly increasing, continuously differentiable, odd*[6] *scalar function, such that:*

$$\begin{cases} \nu_{\kappa,\epsilon}(x) = x \quad \textit{for} \quad |x| \geq \epsilon, \\ \frac{d\nu_{\kappa,\epsilon}(0)}{dx} = \kappa. \end{cases}$$

Therefore, a differential scaling map $\nu_{\kappa,\epsilon}$ has a scalable derivative at the origin and is the identity function outside the infinity-norm ϵ-ball.

[6] A function is odd iff $\nu_{\kappa,\epsilon}(-x) = -\nu_{\kappa,\epsilon}(x)$.

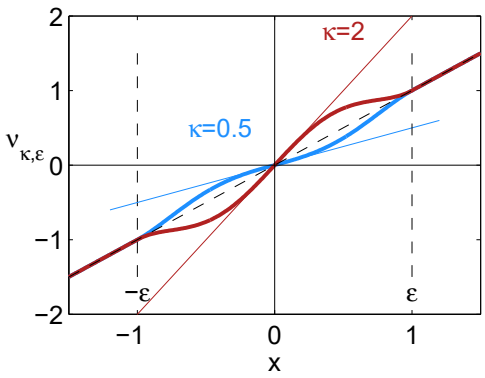

Figure 8.2: Plot of the $\nu_{\kappa,\epsilon}(x)$ differential scaling map in equation (8.6), with $\epsilon = 1$, $\kappa = 2$ (red) and $\kappa = 0.5$ (blue). [BFG14]

Example 8.2. *[BFG14] For illustrative purposes, consider:*

$$\nu_{\kappa,\epsilon}(x) = \begin{cases} x + \arctan[(\kappa-1)x]\left[1-\left(\frac{x}{\epsilon}\right)^2\right]^2 & \text{for} \quad |x| < \epsilon \\ x & \text{for} \quad |x| \geq \epsilon \end{cases} \tag{8.6}$$

The derivative of function (8.6) *inside the interval* $(-\epsilon, \epsilon)$ *is*

$$\nu'_{\kappa,\epsilon}(x) = 1 + \frac{(\kappa-1)\left[1-\left(\frac{x}{\epsilon}\right)^2\right]^2}{1+(\kappa-1)^2x^2} - \frac{4}{\epsilon^2}x\arctan[(\kappa-1)x]\left[1-\left(\frac{x}{\epsilon}\right)^2\right], \quad \text{for} \quad |x| < \epsilon,$$

while $\nu'_{\kappa,\epsilon}(x) = 1$ *for* $|x| \geq \epsilon$; $\nu'_{\kappa,\epsilon}(x) > 0$ *is continuous and positive for all* $\kappa > 0$, *and in* $x = 0$ *it is equal to* κ *as desired. This example function is plotted in Fig. 8.2.*

Alteration by differential scaling maps $\nu_{\kappa,\epsilon}$. The alteration obtained by composing the vector field $f(x)$ and a differential scaling map $\nu_{\kappa,\epsilon}$ results in the transformation

$$\dot{x} = f(\dots, x_i, \dots) \quad \to \quad \dot{x} = f(\dots, \nu_{\kappa,\epsilon}(x_i), \dots).$$

This operation:

a) does not alter the equilibrium $\bar{x}_i = 0$;
b) does not alter the sign of the Jacobian entries, *i.e.*, the structure Σ of the system;
c) changes the partial derivatives in $x_i = 0$ as:

$$\left.\frac{\partial f(\dots,\nu_{\kappa,\epsilon}(x_i),\dots)}{\partial x_i}\right|_{x_i=0} = \left.\frac{\partial f(\dots,\nu_{\kappa,\epsilon}(x_i),\dots)}{\partial \nu_{\kappa,\epsilon}}\frac{\partial \nu_{\kappa,\epsilon}(x_i)}{\partial x_i}\right|_{x_i=0} = \kappa\left.\frac{\partial f(\dots,x_i,\dots)}{\partial x_i}\right|_{x_i=0};$$

d) does not alter $\dot{x} = f(x)$ outside the ϵ-ball, hence preserves boundedness of the system solution.

If this alteration is applied to a vector field $f(x)$ in a neighbourhood of the origin as an equilibrium point, the elements of the Jacobian of f at $x = 0$ can be arbitrarily scaled without changing the value of the equilibrium. Hence, $\nu_{\kappa,\epsilon}$ alterations can be used to independently scale the magnitude of desired cycles and find, given a structure, a realisation that satisfies a property of interest. Even if different parameters κ_i are used to scale different arcs, it may be always assumed that $\kappa_i(\mu)$ are functions of a single parameter μ, consistently with (8.5).

The main results in [BFG14] can then be presented. The following proposition provides a characterisation of weak candidate oscillators, exemplified in the literature by the amplified negative feedback oscillators and incoherent oscillators described in [NT08] and by the toggle-switch/oscillator circuit in [ASMN03].

Proposition 8.1. *A non-critical system is a candidate oscillator in the weak sense if and only if its structure has at least one negative cycle (necessarily of order greater than two).*

Proof. Necessity can be proved by showing that, if there are no negative cycles, OTIs cannot occur.

First, consider structures corresponding to strongly connected graphs (namely, graphs where each node is connected to any other by an oriented path). In this case, as pointed out in [Son07], p. 68, the absence of directed negative cycles is equivalent to the absence of undirected negative cycles, which in turn guarantees monotonicity with respect to some orthant cone. Recall that a system is monotone with respect to some orthant cone if and only if its Jacobian is a Metzler matrix (namely, has non-negative off-diagonal entries), or becomes a Metzler matrix after a proper change in the sign of some variables. [Smi08, Son07] Since any Metzler matrix has a real dominant eigenvalue, any simple transition to instability is an RTI (therefore, the system does not admit undamped oscillations).

If instead the graph is not strongly connected, it can be partitioned into *strongly-connected components*: a node belongs to one (and only one) strongly-connected component iff it is connected to all the nodes in that component by an oriented path, and vice versa. If each strongly-connected component is collapsed into a single hyper-node, then the arcs connecting hyper-nodes (*i.e.*, connecting two nodes belonging to two different strongly-connected components) cannot form cycles (see, for instance, Fig. 8.3). Therefore, the graph composed by the M hyper-nodes corresponds to a block-triangular matrix

$$G = \begin{bmatrix} N_{11} & \mathbf{0} & \dots & \mathbf{0} \\ L_{21} & N_{22} & \dots & \mathbf{0} \\ \vdots & \vdots & \ddots & \vdots \\ L_{M1} & L_{M2} & \dots & N_{MM} \end{bmatrix},$$

where N_{ii} is the Jacobian matrix associated with the ith strongly-connected component (and is therefore equivalent to a Metzler matrix), while L_{ij} denotes the interconnection between the ith and the jth strongly-connected components.

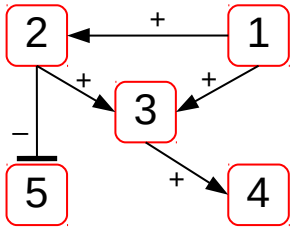

Figure 8.3: Graph formed by the hyper-nodes associated with strongly-connected components, corresponding to matrix (8.7).

For instance, the matrix corresponding to the graph in Fig. 8.3 is

$$G = \begin{bmatrix} N_{11} & \mathbf{0} & \mathbf{0} & \mathbf{0} & \mathbf{0} \\ L_{21} & N_{22} & \mathbf{0} & \mathbf{0} & \mathbf{0} \\ L_{31} & L_{32} & N_{33} & \mathbf{0} & \mathbf{0} \\ \mathbf{0} & \mathbf{0} & L_{43} & N_{44} & \mathbf{0} \\ \mathbf{0} & L_{52} & \mathbf{0} & \mathbf{0} & N_{55} \end{bmatrix} \tag{8.7}$$

Since matrix G is block-triangular, its spectrum is $\sigma(G) = \bigcup_i \sigma(N_{ii})$, where $\sigma(N_{ii})$ is the spectrum of N_{ii}. Therefore the overall not-strongly-connected graph corresponds to a matrix having a real dominant eigenvalue. This implies that any simple transition to instability is an RTI.

Sufficiency can be proved exploiting $\nu_{\kappa,\epsilon}$ differential scaling maps. If there exists a single negative cycle of order greater than two, then a $\nu_{\kappa,\epsilon}$ transformation can be applied to all remaining cycles, scaling down the κ parameter until all the other cycles are virtually eliminated: the interconnections are altered so that $\kappa_{ij} > 1$ for the arcs involved in the negative cycle, while small values $\kappa_{ij} \ll 1$ are assigned to the arcs not involved in the cycle. By reordering the nodes, a realisation can be always found having a Jacobian whose characteristic polynomial is[7]

$$p(s) = \prod_i (s + \beta_i) - \prod_i \gamma_i,$$

having all positive coefficients because by assumption $\beta_i > 0$, $\gamma_i \neq 0$ and $\prod_i \gamma_i < 0$ since the cycle is negative (details are in [BFG14]). Therefore the Jacobian has no real non-negative eigenvalues, in view of Descartes' rule of signs.

Then, the proof follows from the fact that any polynomial of order $n > 2$ of the form $\prod_i (s + \beta_i) + k$ has roots with positive real part for $k > 0$ large.[8] (Conversely, for $n = 2$ the two roots have negative real part and for $n = 1$ the root is real negative, hence the system is always asymptotically stable.) Therefore, for large γ_i, some of the

[7]Since the eigenvalues of a matrix are continuous functions of the matrix entries (see for instance [Wat07]), arbitrarily small entries can be neglected when computing the characteristic polynomial.

[8]This can be seen by building a Routh-Hurwitz table or by means of standard root locus techniques (see for instance [GK09]).

(necessarily complex) eigenvalues have positive real part (while all of the eigenvalues have negative real part for suitably small γ_i), hence there is always a realisation yielding an OTI. □

A characterisation of strong candidate oscillators, exemplified by the repressilator circuit [EL00] and the negative feedback oscillator models in [NT08], is provided in the following proposition.

Proposition 8.2. *A non-critical system is a candidate oscillator in the strong sense if and only if its structure has only negative cycles.*

Proof. Necessity can be proved by assuming that there is a positive cycle in the structure and applying the $\nu_{\kappa,\epsilon}$ differential scaling map, thus enhancing the positive cycle and scaling down arbitrarily close to zero all the other cycles. Proceeding as in the sufficiency part of the proof for Proposition 8.1, the characteristic polynomial of the realisation can be found as

$$p(s) = \prod_i (s + \beta_i) - \prod_i \gamma_i,$$

where $\prod_i \gamma_i > 0$, since the cycle is positive. Therefore, a realisation can be destabilised by driving one real root to cross the imaginary axis through the origin, generating an RTI.

The sufficiency proof employs algebraic tools from [MQ69] to prove that a structure with only negative cycles can solely present complex unstable eigenvalues. If the structure (sign pattern matrix associated with the Jacobian) has only negative cycles, the characteristic polynomial is

$$p(s) = \det(sI - J) = \sum_{i=0}^{n} p_k s^k, \tag{8.8}$$

where $p_n = 1$, because the characteristic polynomial is always monic, and

$$p_k = \sum_i \Delta_i^{(k)} (-1)^k,$$

where $\Delta_i^{(k)}$ are all the leading minors of order k of the Jacobian. Consider the following property, from Theorem 3.1 in [MQ69].

Property 8.1. *Given a matrix M with negative diagonal entries, such that all the cycles in it are non-positive, each leading minor of M having order k has sign $(-1)^k$.*

This implies that all the coefficients of the characteristic polynomial $p(s)$ are positive, hence no real positive roots are admitted. Therefore, if the system is destabilised, then a complex pair of eigenvalues with non-negative real part must exist, leading to an OTI. □

The following corollary can be proved as a consequence of the topological degree theory (outlined in Section 4.5 and Appendix D). This is a classical result due to Thomas [Tho94], proved in [BFG14] for completeness.

Corollary 8.1. *A strong candidate oscillator admits a single equilibrium.*

Proof. If the system of interest is a strong candidate oscillator, then its structure has only negative cycles. In view of the result proposed in [MQ69], the determinant of a realisation matrix $J(x)$ with only negative cycles, at *any* equilibrium point $\bar{x}$, satisfies:

$$\text{sign}[\det(J(\bar{x}))] = (-1)^n,$$

where n is the system dimension. Moreover, $\text{sign}[\det(J(\bar{x}))]$ does not change as a function of $\bar{x}$. Now, denoting the equilibria as $\bar{x}_i$, the topological degree theory provides the equality (4.36), reported below for convenience, which holds for globally bounded flows (see Theorem 4.7, corresponding to Lemma 2 in [Hof90]):

$$\sum_i \text{sign}[\det(J(\bar{x}_i))] = (-1)^n. \tag{8.9}$$

Since all the terms of the sum have the same sign, in the considered case, there must be a single equilibrium. □

The following proposition provides a characterisation of candidate weak multistationary systems, examples of which include amplified negative feedback oscillators and incoherent oscillators in [NT08], and again the toggle-switch/oscillator circuit in [ASMN03].

Proposition 8.3. *A non-critical system is a candidate multistationary system in the weak sense if and only if its structure has at least one positive cycle.*

Proof. Necessity (see also [Gou98] and [Sno98]) is immediate because, if there are no positive cycles, then the system is a candidate oscillator in the strong sense: the determinant of its Jacobian is never 0, therefore no 0 eigenvalues are admitted and no simple RTI can occur.

Sufficiency can be proved by exploiting a $\nu_{\kappa,\epsilon}$ differential scaling map. If a positive cycle exists, it can be magnified by independent scaling of the Jacobian entries in a realisation, so as to prove the existence of a realisation that admits a simple RTI. Details are in [BFG14]. □

Strong candidate multistationary systems can be finally characterised. Examples of these systems include the previously presented two-gene double positive feedback and the toggle-switch architectures in [AS03, GCC00].

Proposition 8.4. *A non-critical system is a candidate multistationary system in the strong sense if and only if its structure has positive cycles only.*

Proof. Necessity can be proved by contradiction: if not all the cycles are positive, then there exists a negative cycle. Hence, the system is a candidate oscillator in the weak sense and a realisation can be found that exhibits an OTI.

Sufficiency can be demonstrated along the lines of the necessity part of the proof of Proposition 8.1 (see [BFG14]): when all the cycles are positive, if the system admits a simple transition to instability, it must be an RTI. □

The two-gene positive feedback system and the toggle switch are also clear examples of the next result.

Corollary 8.2. *A strong candidate multistationary system, in which a simple RTI occurs at μ^*, admits additional equilibria in a right (unstable) neighbourhood of μ^*.*

*If these additional equilibria are non-singular (*i.e.*, if the determinant of the Jacobian is non-zero), then there are at least two additional equilibria.*

*If exactly two additional non-singular equilibria appear, and the Jacobian evaluated at those points, $J(\bar{x})$, has a single dominant eigenvalue (*e.g.*, if the system is irreducible), then these equilibria are asymptotically stable.*

Proof. If the system is a candidate multistationary system in the strong sense, its structure has only positive cycles and any simple transition to instability must be an RTI. This means that, for any realisation, the determinant of the Jacobian changes sign when the parameter μ crosses the critical value μ^*. For values $\mu < \mu^*$, the characteristic polynomial must have a positive constant term, hence $\text{sign}[\det(J(\bar{x}))] = (-1)^n$. For values $\mu > \mu^*$, conversely, $\text{sign}[\det(J(\bar{x}))] = -(-1)^n$. This means that the equality in (8.9) cannot be true in a right neighbourhood of μ^*, unless additional equilibrium points appear. If the additional equilibria are non-singular, *i.e.*, they have a non-singular Jacobian, they must be at least two for equality (8.9) to hold.

Assume now that exactly two additional equilibria appear, x_U, x_L, introduced by the transition to instability, and the original equilibrium is $\bar{x} = 0$, unstable by assumption. Then, it can be shown that $x_U \in \mathcal{U}$ and $x_L \in \mathcal{L}$, where $\mathcal{U}$ and $\mathcal{L}$ are positively invariant sets, such that the solutions originated in each of them are bounded (details are in [BFG14]). The proof is concluded by invoking a known result in the context of monotone systems (see, for instance [Jia91], page 458, Theorem D): since the two equilibria are unique in the bounded sets $\mathcal{U}$ and $\mathcal{L}$, they must be stable. □

8.2.1 Critical Systems

Non-critical systems have been considered so far in order to provide unified results. Here the validity of the characterisation is examined for possibly critical systems. Propositions 8.3 and 8.4, concerning candidate multistationary systems, hold for critical systems as well. The assumption comes into play when the characterisation of candidate oscillatory systems is considered.

For critical networks, the sufficiency part of Proposition 8.1 does not hold: the existence of negative cycles of order two does not assure that the system can oscillate. Consider, for instance, the system

$$\begin{cases} \dot{x}_1 = -b_1 x_1 + H_{12}(x_2), \\ \dot{x}_2 = -b_2 x_2 + H_{21}(x_1), \end{cases} \tag{8.10}$$

where b_1 and b_2 are positive constants, while H_{ij} are positive, bounded, monotonic functions: H_{12} is non-increasing and H_{21} is non-decreasing, which ensures the existence of a negative cycle. Then the system always admits a single, asymptotically stable equilibrium point. Oscillations would be possible if $b_1 = b_2 = 0$, in contrast with the assumption that negative self-loops must exist at each node. The necessity part of Proposition 8.1 still holds: if there are no negative cycles, the system cannot have equilibria with oscillatory instability.

In the presence of negative cycles only, instability must be oscillatory, hence Proposition 8.2 still holds. However, some critical systems cannot be destabilised at all, as is the case of (8.10).

If a critical system with only negative cycles (all of order two) were necessarily stable, Proposition 8.1 could be extended as follows.

Conjecture: A system is a candidate oscillator in the weak sense if and only if it has at least a negative cycle of order greater than two.

However, although the sufficiency part of this conjecture is true, the necessity part is unfortunately false, as shown by a counterexample in [BFG14] (a system with a positive cycle and a negative cycle of order two, which admits OTIs).

Finally, concerning critical systems, the following well-known result (see for instance [EK05], Chapter 6.5) is worth recalling.

Proposition 8.5. *If all the self-loops are negative, and all the other cycles are negative and of order two, then any equilibrium of the system is stable.*

8.2.2 Systems with Delays

Delay differential equations are often adopted to model molecular systems (*e.g.*, transcription, processing and transport of mRNA in genetic networks and transport of proteins across cellular membranes have been successfully captured by models with explicit delays [HH11, Lew03]). Local, cycle-based sufficient conditions for OTIs and RTIs can be stated in a wide class of systems affected by delays. Consider the delay differential equation model

$$\dot{x}(t) = f(x(t), x(t-\tau_1), x(t-\tau_2), \ldots, x(t-\tau_M)). \tag{8.11}$$

Under standard differentiability assumptions, the corresponding linearised system around an equilibrium point is

$$\dot{\xi}(t) = A_0\xi(t) + \sum_{k=1}^{M} A_k\xi(t-\tau_k). \tag{8.12}$$

Assume for simplicity that there are no delayed self-loops (*i.e.*, matrices A_k have zero diagonal entries for $k \geq 1$). Then, stability is ensured if the roots of

$$\det\left[A_0 + \sum_{k=1}^{M} A_k e^{-\tau_k s} - sI\right] = 0 \tag{8.13}$$

have negative real part. Consider the auxiliary system with all delays set to 0:

$$\dot{\zeta}(t) = \left[A_0 + \sum_{k=1}^{M} A_k\right]\zeta(t) = \bar{A}\zeta(t). \tag{8.14}$$

Matrix $\bar{A}$ is equal to the Jacobian that would be obtained by setting the delays $\tau_i = 0$ in system (8.11): $\dot{x}(t) = f(x(t), x(t), x(t), \ldots, x(t))$. Since equilibria are delay-independent, the delay-free system has the same equilibria as the delayed system.

Graphs can be associated with systems (8.12) and (8.14), where nodes correspond to species concentrations and signed, directed arcs correspond to the dynamic interactions among species (delayed or not), defined by matrices A_k, $k = 0, ..., M$. Any positive/negative cycle of (8.12) corresponds to a positive/negative cycle of (8.14), because delays do not change the sign of the cycles.

Proposition 8.6. *If the graph associated with system* (8.12) *has negative cycles only, the system exclusively admits OTIs.*

Proof. Assume by contradiction that the system admits a real transition to instability. Hence, one root of equation (8.13) crosses the imaginary axis with value $s = 0$. Yet, this turns out to be impossible if the system has only negative cycles (see [BFG14] for details). □

Proposition 8.7. *If the graph associated with system* (8.12) *has positive cycles only, the system exclusively admits RTIs.*

Proof. In the absence of negative cycles (possibly with the exception of self-loops), system (8.12) is a linear positive system with delay, hence matrix $\bar{A}$ in system (8.14) is a Metzler matrix. A *positive* linear system with delays (with no delayed self-loops) is stable if and only if its delay-free, auxiliary counterpart (8.14) is stable [HC04, LYW10] (see also [WLCA10], Theorem 6.5). Then, if all its cycles are positive, the auxiliary system (8.14) can transition to instability due to a pole in $s = 0$ only. Details are in [BFG14]. □

Since equilibria are delay-independent, if the auxiliary system presents multiple equilibria, so does the delayed system. It is worth pointing out that Proposition 8.5 is not valid in the presence of delays: indeed, the presence of a delay in a second order negative cycle may compromise stability.

8.3 Remarks

The presented theory can be easily extended to the case of systems restricted to specific regions of the state space (such as the positive orthant, where biological systems are typically confined), up to technical details; for instance, the possible presence of equilibria on the boundary needs to be carefully handled (cf. Section 4.5).

Concerning the applicability of the presented results, it must be underlined that they hold for systems in which interactions between nodes are *independent*. Hence, they are not applicable to models with structural cross-constraints among functions (for instance, models built using mass action kinetics). For instance, take the reaction $A \xrightarrow{g} B$. The dynamics of a will include a term $-g(a)$, representing consumption of A; the same term will appear, with opposite sign, in the dynamics of b. Constraints are therefore present, which do not allow to independently scale the magnitude of the Jacobian entries.

Example 8.3. *[BFG14] Consider the reactions*

$$X_0 \xrightarrow{1} X, \quad X \xrightarrow{g_X} Y, \quad Y \xrightarrow{g_Y} Z, \quad pX + Z \xrightarrow{g_{XZ}} \emptyset,$$

where all the reaction rates are increasing functions, corresponding to the differential equation model

$$\begin{cases} \dot{x} = x_0 - g_X(x) - p g_{XZ}(x, z) \\ \dot{y} = g_X(x) - g_Y(y) \\ \dot{z} = g_Y(y) - g_{XZ}(x, z). \end{cases}$$

The Jacobian

$$J = \begin{bmatrix} -(\alpha + p\mu) & 0 & -p\nu \\ \alpha & -\beta & 0 \\ -\mu & \beta & -\nu \end{bmatrix},$$

where, for a fixed equilibrium, all Greek letters represent positive constants, has dependent entries. Although it presents both negative and positive cycles, this structure may only undergo oscillatory transitions to instability (hence, it is a candidate oscillator in the strong sense). In fact, the characteristic polynomial has only positive coefficients and cannot admit real positive roots. This is not in contradiction with the presence of the positive cycle $1 \to 3 \to 1$ and does not invalidate the results in this chapter. Simply, the proposed classification does not apply to systems with cross-constraints among Jacobian entries (such as the fact that $J_{22} = -J_{32}$).

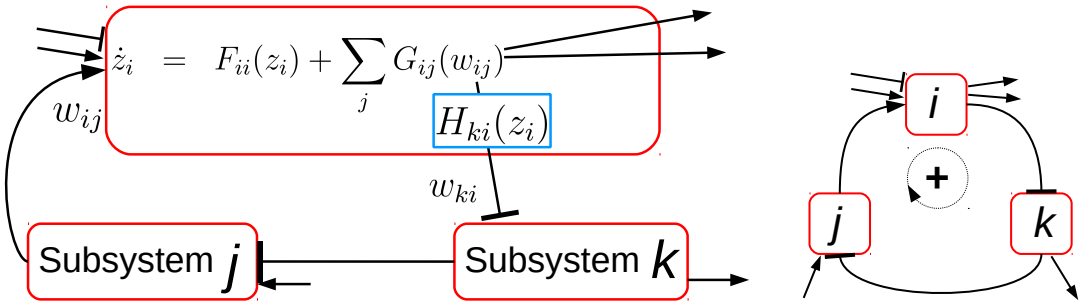

Figure 8.4: Sketch of a portion of an aggregate monotone system: the interconnection of monotone subsystems (8.15)-(8.16) (left) and the corresponding graph, where each monotone subsystem is collapsed in a single node (right).

For systems with cross-constrained dynamics, algorithmic and numerical methods (as those based on the BDC-decomposition, presented in Chapters 6 and 7) can be a much preferable approach to discriminate admissible transitions to instability. Sufficient conditions for potential oscillations (and perfect adaptation) in systems with cross-constrained Jacobian entries based on the system BDC-decomposition have been proposed in [BFG12], see Section 5.4.

8.4 Oscillations and Multistationarity in Monotone Aggregates

Following [BFG15b], the structural results in [BFG14] can be extended to aggregate systems that are composed of stable monotone components.

Precisely, an aggregate system is the interconnection of N subsystems

$$\dot{z}_i(t) = F_{ii}(z_i(t)) + \sum_{j\in\mathcal{J}_i} G_{ij}(w_{ij}(t)), \tag{8.15}$$

$$w_{ki}(t) = H_{ki}(z_i(t)), \quad k \in \mathcal{K}_i, \tag{8.16}$$

where $i = 1, ..., N$, $z_i(t)$ is the state vector associated with subsystem i, $w_{ij} \in \mathbb{R}$ are the subsystem inputs and $w_{ki} \in \mathbb{R}$ are its outputs. Subsystem i receives inputs from subsystems $j \in \mathcal{J}_i$, and sends an output to subsystems $k \in \mathcal{K}_i$, where $\mathcal{J}_i$ and $\mathcal{K}_i$ are the sets that index all the subsystems having respectively an upstream or downstream connection with subsystem i (see Fig. 8.4). Assume that $F_{ii}(\cdot)$, $G_{ij}(\cdot)$ and $H_{ki}(\cdot)$ are sufficiently smooth functions. Function $G_{ij}(w_{ij}(t))$ models the influence of subsystem j on subsystem i through $w_{ij}(t)$, output of subsystem j.

Assumption 8.4. *The input-to-state mappings G_{ij} are either non-decreasing or non-increasing: $w_{ij} \geq \hat{w}_{ij}$ implies either $G_{ij}(w_{ij}) \geq G_{ij}(\hat{w}_{ij})$, or $G_{ij}(w_{ij}) \leq G_{ij}(\hat{w}_{ij})$.*

Assumption 8.5. *Functions $H_{ij}(z_j)$ are non-decreasing.*

Assumption 8.5 enables a simplified analysis without being restrictive: negative interconnection trends among subsystems can be captured by the input functions $G_{ij}(w_{ij})$. For example, consider a generic subsystem 1 and the influence of subsystem 2 on 1 given by w_{12}:

$$\dot{z}_1 = F_{11}(z_1) + G_{12}(w_{12}), \qquad w_{12} = H_{12}(z_2),$$

with H_{12} decreasing. The overall interaction depends on the monotonic compound function $G_{12} \circ H_{12}$, and the decreasing trend can be accounted for with a simple sign change: $\hat{w}_{12} = -w_{12}$. The net effect remains unchanged:

$$\dot{z}_1 = F_{11}(z_1) + G_{12}(\hat{w}_{12}), \qquad \hat{w}_{12} = H_{12}^{-}(z_2),$$

where $H_{12}^{-}(\omega) \doteq -H_{12}(\omega)$ is now increasing.

Definition 8.10. *Subsystem* (8.15)-(8.16) *is* unconditionally stable *iff, for constant input values $\bar{w}_{ij}$, it admits a single equilibrium $\bar{z}_i$, which is the solution of*

$$0 = F_{ii}(\bar{z}_i) + \sum_{j \in \mathcal{J}_i} G_{ij}(\bar{w}_{ij}), \quad \bar{w}_{ki} = H_{ki}(\bar{z}_i), \tag{8.17}$$

and such an equilibrium is asymptotically stable (all of the eigenvalues of the Jacobian $J_i = \frac{\partial F_{ii}}{\partial z_i}\Big|_{\bar{z}_i}$ have a negative real part).

With a slight abuse of notation, a system that is either monotone, or anti-monotone is called simply *monotone*. The definition already given in Chapter 2 (where, however, the distinction between monotone and anti-monotone systems is made) is here reminded.

Definition 8.11. *Subsystem* (8.15)-(8.16)*, with inputs w_{ij}, is* input-to-state monotone *iff, for $w_{ij}(t) \geq \tilde{w}_{ij}(t)\ \forall\ j \in \mathcal{J}_i$, either $z_i(0) \geq \tilde{z}_i(0) \implies z_i(t) \geq \tilde{z}_i(t)$, $t \geq 0$, or $z_i(0) \leq \tilde{z}_i(0) \implies z_i(t) \leq \tilde{z}_i(t)$, $t \geq 0$.*

Assumption 8.6. *The considered aggregate systems are composed of subsystems* (8.15)-(8.16)*, each unconditionally stable as in Definition 8.10 and input-to-state monotone as in Definition 8.11.*

Given an input-output monotonicity characterisation for all the subsystems, each subsystem can be collapsed into an equivalent *aggregate node*. Then an *aggregate graph* can be defined (cf. Fig. 8.4, right), whose nodes correspond to the aggregate nodes, and whose signed arcs represent the influence of subsystem j on subsystem i. The sign of each arc depends on the trend of the associated input-to-state mapping $G_{ij}(w_{ij})$: positive (resp. negative) arcs are associated with non-decreasing (resp. non-increasing) mappings.

Based on the cycles formed by the arcs connecting aggregate nodes in the aggregate graph, structural oscillatory and multistationary behaviours can still be classified, by providing necessary and sufficient conditions for an aggregate monotone system to be a strong candidate oscillator (every transition to instability is an OTI) or a strong multistationary system (every transition to instability is an RTI).

Theorem 8.1. *Consider an aggregate system, formed by the interconnection of strongly connected*[9] *subsystems of the form* (8.15)-(8.16)*, satisfying Assumptions 8.4, 8.5 and 8.6. The aggregate system is structurally a candidate*

i) oscillator in the strong sense iff all the cycles in the aggregate graph are negative;
ii) multistationary system in the strong sense iff all the cycles in the aggregate graph are positive.

Remark 8.2. *Positive cycles are generally present* within the monotone subsystems. *However, if all the cycles in the aggregate graph are negative, the aggregate system is* not *a weak candidate multistationary system, due to the assumption of unconditional stability for each subsystem.*

In order to prove Theorem 8.1, a preliminary lemma is needed.

Given an aggregate system, under the assumptions of Theorem 8.1, for constant input values $\bar{w}_{ij}$, each subsystem admits a single equilibrium $\bar{z}_i$, which is implicitly defined by the steady-state condition (8.17) and is globally asymptotically stable. Define

$$A_{ii} = \left.\frac{\partial F_{ii}}{\partial z_i}\right|_{\bar{z}_i}, \quad B_{ij} = \left.\frac{\partial G_{ij}}{\partial w_{ij}}\right|_{\bar{w}_{ij}}, \quad C_{ki} = \left.\frac{\partial H_{ki}}{\partial z_i}\right|_{\bar{z}_i}.$$

In the corresponding aggregate graph, whose nodes are associated with the monotone subsystems, the sign of the directed arc connecting subsystems j and i depends on the trend of function $G_{ij}(w_{ij})$, *i.e.*, on the sign of B_{ij}.

Lemma 8.1. *If the steady-state input-to-output mapping in system* (8.15)-(8.16) *is monotone, then the input-to-output mapping between each pair* (w_{ij}, w_{ki}) *is implicitly defined by* (8.17)*, and*

$$\frac{\partial w_{ki}}{\partial w_{ij}} = -C_{ki} A_{ii}^{-1} B_{ij}$$

is either a positive or a negative scalar, depending on the sign of the elements of B_{ij}*.*

Proof. As a consequence of monotonicity and unconditional stability, A_{ii} is an asymptotically stable Metzler matrix. Therefore, all the entries of its inverse A_{ii}^{-1} are non-positive. Due to Assumption 8.5, C_{ki} has non-negative elements, while Assumption 8.4 ensures that B_{ij} has all non-negative elements or all non-positive elements, depending on the type of interaction. Hence, the sign of $\partial w_{ki}/\partial w_{ij}$ depends on the sign of B_{ij} only. □

[9]Recall that a graph is *strongly connected* if an oriented path exists connecting each pair of nodes.

Proof of Theorem 8.1

i): Sufficiency requires showing that, if exclusively negative cycles are present in the aggregate graph, then the Jacobian of the system cannot have real non-negative eigenvalues (hence, only oscillatory destabilisation is possible); *i.e.*, denoting by A the Jacobian of the aggregate system,

$$\det(\lambda I - A) \neq 0 \qquad \forall \;\; \lambda \in \mathbb{R}, \qquad \lambda \geq 0.$$

By contradiction, assume that A admits a real non-negative eigenvalue λ. Denoting the ith linearised subsystem by

$$\dot{\zeta}_i(t) = A_{ii}\zeta_i(t) + \textstyle\sum_{j\in\mathcal{J}_i} B_{ij}\omega_{ij}(t), \quad \omega_{ki}(t) = C_{ki}\zeta_i(t),$$

any eigenvalue λ must satisfy the equation

$$\lambda\zeta_i \;\; = \;\; A_{ii}\zeta_i + \sum_{j\in\mathcal{J}_i} B_{ij}\omega_{ij},$$

where $\zeta = [\zeta_1 \cdots \zeta_i \cdots \zeta_N]^\top$ is the associated eigenvector. Hence,

$$\zeta_i = -(A_{ii} - \lambda I)^{-1} \sum_{j\in\mathcal{J}_i} B_{ij}\ \omega_{ij},$$

where all the elements of $(A_{ii} - \lambda I)^{-1}$ are non-positive because of monotonicity. In fact, A_{ii} is a stable Metzler matrix; $(A_{ii} - \lambda I)$ is still a stable Metzler matrix, because $\lambda \geq 0$; thus all the elements of $(A_{ii} - \lambda I)^{-1}$ are non-positive.

Then, for all $k \in \mathcal{K}_i$,

$$\omega_{ki} = \sum_{j\in\mathcal{J}_i} \; -C_{ki}(A_{ii} - \lambda I)^{-1}B_{ij}\ \omega_{ij} = \sum_{j\in\mathcal{J}_i} \pi^i_{kj}\ \omega_{ij}, \tag{8.18}$$

where $\pi^i_{kj} \doteq -C_{ki}(A_{ii} - \lambda I)^{-1}B_{ij}$ are scalars. Equations (8.18) are linear in ω_{ij} and can be compactly rewritten as

$$\omega = \Pi\omega, \tag{8.19}$$

where ω is a vector including all the arc variables ω_{ij}, which define the interconnections in the aggregate system. In the aggregate graph, the sign of the arc from node i to node k depends on the sign of $\pi^i_{kj} = -C_{ki}(A_{ii} - \lambda I)^{-1}B_{ij}$. Therefore, matrix Π in (8.19) has the same cycles as the Jacobian A of the aggregate system. Let Σ_Π be the sign matrix corresponding to Π. Every cycle in the aggregate graph corresponds to a cycle in matrix Σ_Π. For example, the sign matrix Σ_Π associated with the aggregate graph in Fig. 8.5, left, is a 5×5 matrix, since there are 5 arcs. If the arc variables are ordered as $\omega = [\omega_{21} \;\; \omega_{32} \;\; \omega_{43} \;\; \omega_{14} \;\; \omega_{24}]^\top$, then

$$\Sigma_\Pi = \begin{bmatrix} 0 & 0 & 0 & - & 0 \\ + & 0 & 0 & 0 & - \\ 0 & + & 0 & 0 & 0 \\ 0 & 0 & + & 0 & 0 \\ 0 & 0 & + & 0 & 0 \end{bmatrix}. \tag{8.20}$$

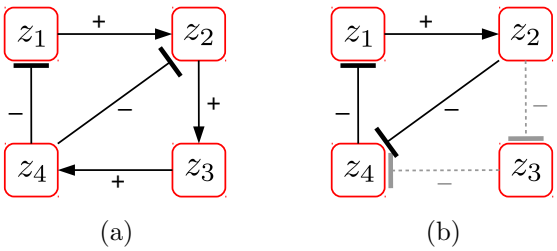

Figure 8.5: Left: aggregate graph corresponding to the sign matrix (8.20). Right: aggregate graph with emphasis on the selected positive cycle (solid); excluded arcs are dashed, light gray.

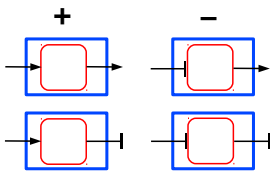

Figure 8.6: Rules for determining the sign of interactions in matrix Σ_Π.

The sign of the interaction depends on that of the incoming arc, related to B_{ij}, as shown in Fig. 8.6. Therefore, if all the cycles in the aggregate graph are negative, then all the cycles in matrix Σ_Π are negative as well. Then Property 8.1, from Theorem 3.1 in [MQ69], can be exploited. Since all the cycles in Π, hence in $(\Pi - I)$, are negative, then sign $[\det(\Pi - I)] = \pm 1$. Relation (8.19) is equivalent to $(\Pi - I)\omega = 0$ and thus implies $\det(\Pi - I) = 0$. Yet, if all the cycles are negative, $\det(\Pi - I) \neq 0$, hence (8.19) cannot be true for $\omega \neq 0$. Therefore, the system cannot admit real non-negative eigenvalues $\lambda \geq 0$ and is a candidate oscillator in the strong sense.

i): Necessity can be proved by contradiction. Suppose that a positive cycle of order m exists in the aggregate graph. Then, by means of $\nu_{\epsilon,\kappa}$ differential scaling maps, the arcs *connecting the aggregate nodes* can be modified without compromising stability of the monotone subsystems,[10] scaling the κ parameter so as to enhance the considered positive cycle only ($\kappa_{ij} = 1$) and virtually exclude all the other arcs ($\kappa_{ij} \ll 1$). For instance, in the structure in Fig. 8.5, right, the cycle formed by subsystems 1-2-3 can be selected and all the other arcs in the aggregate graph can be neglected. By suitably reordering the nodes, a realisation can be found which corresponds to a monotone system (see [BFG15b] for details). Hence, it has a real dominant eigenvalue and can be destabilised only due to a real root which crosses the imaginary axis through the origin, yielding an RTI. This contradicts the assumption; therefore, only negative cycles can be present in the aggregate graph.

ii). Sufficiency: if positive cycles only are present in the aggregate graph, then

[10]It is not possible to scale up a single positive cycle inside a monotone subsystem in order to induce an RTI, because parameter variations are assumed to preserve stability of each monotone subsystem. Hence, only arcs connecting different subsystems can be scaled.

the overall system is monotone (hence it has a dominant real eigenvalue and only real destabilisation is possible). **Necessity:** if a negative cycle exists, then it can be enhanced through a differential scaling map $\nu_{\kappa,\epsilon}$, as in the necessity proof of i), and thus a realisation can be found that admits an OTI, contradicting the assumption.

8.5 Examples of Oscillatory and Bistable Biomolecular Systems

Nature provides many excellent examples of aggregate monotone systems. For instance, in the MAPK pathway, each stage of the phosphorylation cascade can be regarded as an unconditionally stable monotone module [AFS04, FB13] and, depending on the active feedback loops, the network can generate bistable or oscillatory behaviours [AFS04, SVB07, QNKS07, FB13].

Also, several *artificial* biochemical networks can be viewed as aggregate monotone systems: monotonicity is often embedded by design in such networks, indeed, in view of its structural nature [KWW06, KW11, BCFG14, MTF14]. Hence, the proposed classification can be applied to structurally evaluate the behaviour of biomolecular networks expressly engineered to exhibit either periodic or bistable dynamics. When these artificial systems turn out to be candidate oscillators or multistationary systems in the strong sense, this indicates that their bottom-up design is fundamentally sound. Structural analysis, thus, reveals to be a powerful aid for streamlining the synthesis of robust biochemical networks.

Oscillators

Example 8.4. *Consider a model for an artificial oscillating system built with minimal transcriptional modules, adapted from [KW11, FB12]. Genes X_1 and Z_1 produce RNA species X_3 and Z_3, respectively; X_1 is activated by species X_2, while Z_1 is inhibited by species Z_2. RNA Z_3 inhibits active X_1, while X_3 activates inhibited Z_1. The system can be described by the following chemical reactions (species marked by a * are inactive compounds).*

$$
\begin{array}{ll}
X_3 + Z_1^* \xrightarrow{\alpha_z} Z_1 & X_2 + X_1^* \xrightarrow{\alpha_x} X_1 \\
Z_1 \xrightarrow{\beta_z} Z_3 + Z_1 & X_1 \xrightarrow{\beta_x} X_3 + X_1 \\
Z_2 + Z_1 \xrightarrow{\delta_z} Z_1^* & Z_3 + X_1 \xrightarrow{\delta_x} X_1^* \\
\emptyset \xrightarrow{z20} Z_2 \xrightarrow{\rho_z} \emptyset & \emptyset \xrightarrow{x20} X_2 \xrightarrow{\rho_x} \emptyset
\end{array}
$$

with mass conservation constraints $x_1^{tot} = x_1 + x_1^*$, $z_1^{tot} = z_1 + z_1^*$. *The system obtained by using the law of mass action is*

$$\begin{cases} \dot{z}_1 = \alpha_z(z_1^{tot} - z_1)x_3 - \delta_z z_1 z_2, \\ \dot{z}_2 = z_{20} - \rho_z z_2 - \delta_z z_1 z_2, \\ \dot{x}_3 = \beta_x x_1 - \alpha_z(z_1^{tot} - z_1)x_3, \\ \dot{z}_3 = \beta_z z_1 - \delta_x x_1 z_3, \\ \dot{x}_1 = \alpha_x(x_1^{tot} - x_1)x_2 - \delta_x x_1 z_3, \\ \dot{x}_2 = x_{20} - \rho_x x_2 - \alpha_x(x_1^{tot} - x_1)x_2. \end{cases}$$

The Jacobian of this system is sign-definite and, after the change of variables $\hat{z}_2 := -z_2$, $\hat{z}_3 := -z_3$, *has the following structure:*

$$\begin{bmatrix} -\alpha_z\bar{x}_3 - \delta_z\bar{z}_2 & \delta_z\bar{z}_1 & \alpha_z(z_1^{tot} - \bar{z}_1) & 0 & 0 & 0 \\ \delta_z\bar{z}_2 & -\delta_z\bar{z}_1 - \rho_z & 0 & 0 & 0 & 0 \\ \alpha_z\bar{x}_3 & 0 & -\alpha_z(z_1^{tot} - \bar{z}_1) & 0 & \boxed{\beta_x} & 0 \\ \boxed{-\beta_z} & 0 & 0 & -\delta_x\bar{x}_1 & \delta_x\bar{z}_3 & 0 \\ 0 & 0 & 0 & \delta_x\bar{x}_1 & -\alpha_x\bar{x}_2 - \delta_x\bar{z}_3 & \alpha_x(x_1^{tot} - \bar{x}_1) \\ 0 & 0 & 0 & 0 & \alpha_x\bar{x}_2 & -\alpha_x(x_1^{tot} - \bar{x}_1) - \rho_x \end{bmatrix}$$

This corresponds to the negative feedback of two monotone subsystems (z_1-z_2-x_3 *and* z_3-x_1-x_2) *which are unconditionally stable (the corresponding matrices are irreducibly diagonally dominant with negative diagonal entries). Hence, the system is a candidate oscillator in the strong sense. It is indeed the simplified model of a biochemical circuit that, if driven to instability, exhibits sustained oscillations, as shown in [KW11, FB12].*

Example 8.5. *A simplified model is proposed in [BCFG14] for an artificial oscillator where transcriptional regulation is achieved with RNA aptamers (namely, RNA molecules whose sequence is synthetically evolved to bind and modify the properties of a desired target). In this system, two aptamers* X_1 *and* X_3 *are transcribed by RNA polymerases* X_2 *and* X_4 *respectively. Aptamer* X_1 *inactivates polymerase* X_4, *while aptamer* X_3 *activates polymerase* X_2. *The overall list of reactions is*

$$X_2 + G_1 \xrightarrow{k_1} X_2 + X_1 + G_1 \qquad X_4 + G_2 \xrightarrow{k_2} X_4 + X_3 + G_2$$
$$X_1 \xrightarrow{\delta_1} \emptyset \qquad X_3 \xrightarrow{\delta_2} \emptyset$$
$$X_2^* + X_3 \xrightarrow{\gamma_1} X_2 \qquad X_4 + X_1 \xrightarrow{\gamma_2} X_4^*$$
$$X_2 \xrightarrow{\beta_1} X_2^* \qquad X_4^* \xrightarrow{\beta_2} X_4$$

where G_1 and G_2 are genes, whose concentration is constant; defining the new constants $\kappa_i = k_i g_i$, $i = 1, 2$, the resulting system is

$$\begin{cases} \dot{x}_1 = \kappa_1 x_2 - \delta_1 x_1 - \gamma_2 x_4 x_1 \\ \dot{x}_2 = -\beta_1 x_2 + \gamma_1 (x_2^{tot} - x_2) x_3 \\ \dot{x}_3 = \kappa_2 x_4 - \delta_2 x_3 - \gamma_1 (x_2^{tot} - x_2) x_3 \\ \dot{x}_4 = \beta_2 (x_4^{tot} - x_4) - \gamma_2 x_4 x_1 \end{cases} \tag{8.21}$$

In [BCFG14], it is shown that the solutions of system (8.21) *are bounded for any nonnegative initial condition such that $x_2(0) \leq x_2^{tot}$ and $x_4(0) \leq x_4^{tot}$. In fact, $0 \leq x_2(t) \leq x_2^{tot}$ and $0 \leq x_4(t) \leq x_4^{tot}$, from the second and fourth equations in* (8.21). *Moreover, by applying the comparison principle [Kha02], it can be seen that $x_1(t)$ is upper bounded by the solution of $\dot{x}_1 = \kappa_1 x_2^{tot} - \delta_1 x_1$, since $\dot{x}_1 \leq \kappa_1 x_2 - \delta_1 x_1 \leq \kappa_1 x_2^{tot} - \delta_1 x_1$. Hence $x_1(t) \leq x_1^+ + [x_1(0) - x_1^+] e^{-\delta_1 t}$, where $x_1^+ = \frac{\kappa_1}{\delta_1} x_2^{tot}$. Analogously, $x_3(t) \leq x_3^+ + [x_3(0) - x_3^+] e^{-\delta_2 t}$, where $x_3^+ = \frac{\kappa_2}{\delta_2} x_4^{tot}$. Therefore, as long as the conditions $0 \leq x_1(t) \leq x_1^+$ and $0 \leq x_3(t) \leq x_3^+$ are satisfied for $t = 0$, they will be fulfilled for each time $t > 0$; furthermore, they are asymptotically satisfied for any initial state.*

Boundedness implies the existence of an equilibrium point inside the nonnegative box delimited by the quantities x_1^+, x_2^{tot}, x_3^+, x_4^{tot} ([Srz85], see also [RW02, RW04]). Equilibrium conditions for the model are shown to be given by the intersection of two nullclines having a monotonic trend (one increasing and the other decreasing), hence system (8.21) *admits a unique equilibrium.*

The Jacobian matrix

$$J = \begin{bmatrix} -\gamma_2 \bar{x}_4 - \delta_1 & \kappa_1 & 0 & -\gamma_2 \bar{x}_1 \\ 0 & -\beta_1 - \gamma_1 \bar{x}_3 & \gamma_1 (x_2^{tot} - \bar{x}_2) & 0 \\ 0 & \gamma_1 \bar{x}_3 & -\gamma_1 (x_2^{tot} - \bar{x}_2) - \delta_2 & \kappa_2 \\ -\gamma_2 \bar{x}_4 & 0 & 0 & -\beta_2 - \gamma_2 \bar{x}_1 \end{bmatrix}$$

is sign definite and, through a state transformation

$$T = \begin{bmatrix} 0 & 0 & 0 & -1 \\ 0 & 1 & 0 & 0 \\ 1 & 0 & 0 & 0 \\ 0 & 0 & 1 & 0 \end{bmatrix},$$

it is similar to a matrix $\tilde{J} = T^{-1} J T$:

$$\begin{bmatrix} -\gamma_1 (x_2^{tot} - \bar{x}_2) - \delta_2 & \gamma_1 \bar{x}_3 & \boxed{\kappa_2} & 0 \\ \gamma_1 (x_2^{tot} - \bar{x}_2) & -\beta_1 - \gamma_1 \bar{x}_3 & 0 & 0 \\ 0 & 0 & -\beta_2 - \gamma_2 \bar{x}_1 & \gamma_2 \bar{x}_4 \\ 0 & \boxed{-\kappa_1} & \gamma_2 \bar{x}_1 & -\gamma_2 \bar{x}_4 - \delta_1 \end{bmatrix}$$

The overall system, formed by the negative feedback interconnection of two unconditionally stable aggregate monotone subsystems, is thus a strong candidate oscillator: instability can only occur due to an OTI. It can be checked, actually, that the coefficients of the characteristic polynomial are all positive: therefore, the characteristic polynomial does not have positive real solutions and instability can just be due to a complex pair of unstable eigenvalues. The system is indeed the simplified model of a biochemical circuit that, if driven to instability, exhibits sustained oscillations, as shown by simulation results in [BCFG14] for some choice of the parameters.

Switches

Example 8.6. *Consider a model adapted from [KWW06], which proposes the experimental realisation of a minimal, artificial transcriptional network exhibiting bistability. Genes X_1 and Z_1 produce RNA species X_3 and Z_3 and are respectively activated by species X_2 and Z_2, inhibited by RNA species Z_3 and X_3. A simplified description of the system is provided by the following chemical reactions.*

$$
\begin{array}{ll}
Z_2 + Z_1^* \xrightarrow{\alpha_z} Z_1 & X_2 + X_1^* \xrightarrow{\alpha_x} X_1 \\
Z_1 \xrightarrow{\beta_z} Z_3 + Z_1 & X_1 \xrightarrow{\beta_x} X_3 + X_1 \\
X_3 + Z_1 \xrightarrow{\delta_z} Z_1^* & Z_3 + X_1 \xrightarrow{\delta_x} X_1^* \\
\emptyset \xrightarrow{z_{20}} Z_2 \xrightarrow{\rho_z} \emptyset & \emptyset \xrightarrow{x_{20}} X_2 \xrightarrow{\rho_x} \emptyset
\end{array}
$$

Under mass action kinetics assumptions, the chemical reactions, along with mass conservation constraints $x_1^{tot} = x_1 + x_1^*$, $z_1^{tot} = z_1 + z_1^*$, correspond to the system

$$
\begin{cases}
\dot{z}_1 = \alpha_z(z_1^{tot} - z_1)z_2 - \delta_z z_1 x_3 \\
\dot{z}_2 = z_{20} - \rho_z z_2 - \alpha_z(z_1^{tot} - z_1)z_2 \\
\dot{x}_3 = \beta_x x_1 - \delta_z z_1 x_3 \\
\dot{x}_1 = \alpha_x(x_1^{tot} - x_1)x_2 - \delta_x x_1 z_3 \\
\dot{x}_2 = x_{20} - \rho_x x_2 - \alpha_x(x_1^{tot} - x_1)x_2 \\
\dot{z}_3 = \beta_z z_1 - \delta_x x_1 z_3.
\end{cases}
$$

After the change of variables $\hat{x}_3 := -x_3$, $\hat{z}_3 := -z_3$, the system Jacobian, which is sign-definite, becomes

$$
\begin{bmatrix}
-\alpha_z\bar{z}_2 - \delta_z\bar{x}_3 & \alpha_z(z_1^{tot} - \bar{z}_1) & \delta_z\bar{z}_1 & 0 & 0 & 0 \\
\alpha_z\bar{z}_2 & -\alpha_z(z_1^{tot} - \bar{z}_1) - \rho_z & 0 & 0 & 0 & 0 \\
\delta_z\bar{x}_3 & 0 & -\delta_z\bar{z}_1 & -\beta_x & 0 & 0 \\
0 & 0 & 0 & -\alpha_x\bar{x}_2 - \delta_x\bar{z}_3 & \alpha_x(x_1^{tot} - \bar{x}_1) & \delta_x\bar{x}_1 \\
0 & 0 & 0 & \alpha_x\bar{x}_2 & -\alpha_x(x_1^{tot} - \bar{x}_1) - \rho_x & 0 \\
-\beta_z & 0 & 0 & \delta_x\bar{z}_3 & 0 & -\delta_x\bar{x}_1
\end{bmatrix}
$$

The system is composed of two unconditionally stable monotone subsystems (z_1-z_2-x_3 and x_1-x_2-z_3), which form a positive cycle. Hence, it is a candidate multistationary system in the strong sense: instability can only occur due to an RTI.

Example 8.7. *A simplified model is proposed in [MTF14] for an artificial bistable network where transcriptional regulation is achieved with RNA aptamers. Aptamers X_1 and X_3 are transcribed by polymerases X_2 and X_4 respectively; X_1 represses polymerase X_4 and X_3 represses polymerase X_2. The corresponding system is*

$$\begin{cases} \dot{x}_1 = \kappa_1 x_2 - \delta x_1 - \gamma x_4 x_1 \\ \dot{x}_2 = \beta x_2^{tot} - \beta x_2 - \gamma x_2 x_3 \\ \dot{x}_3 = \kappa_2 x_4 - \delta x_3 - \gamma x_2 x_3 \\ \dot{x}_4 = \beta x_4^{tot} - \beta x_4 - \gamma x_4 x_1 \end{cases}$$

A state transformation yields the Jacobian

$$\begin{bmatrix} -\beta - \gamma\bar{x}_3 & \gamma\bar{x}_2 & 0 & 0 \\ \gamma\bar{x}_3 & -\gamma\bar{x}_2 - \delta & \boxed{\kappa_2} & 0 \\ 0 & 0 & -\beta - \gamma\bar{x}_1 & \gamma\bar{x}_4 \\ \boxed{\kappa_1} & 0 & \gamma\bar{x}_1 & -\gamma\bar{x}_4 - \delta \end{bmatrix}$$

The overall system, formed by the positive feedback interconnection of two unconditionally stable monotone subsystems, is thus a strong candidate bistable network. Actual bistability of the system is shown by simulation results in [MTF14] for some choice of the parameters.

Based on the results presented in this chapter, many other examples of synthetic transcriptional circuits can be analysed to show that, by design, they are structurally capable of oscillations or multistationarity [CGK+16, CGBF16].

III

Network-Decentralised Control of Dynamical Networks

9

Network-Decentralised Control Strategies for Stabilisation

Most often, as seen in the previous chapters, huge and complex natural networks coordinate their global behaviour thanks to local interactions, based on local dynamics. This is exactly the concept of *network-decentralised control*, introduced earlier in Chapter 3. Having understood that nature efficiently exploits a decentralised "control", for instance in biological and biochemical networks, it is now worth wondering how a network-decentralised control can be synthesised in artificial networks.

This part of the thesis is therefore dedicated to the *control* of network systems: the viewpoint switches from a system-theoretic perspective (analysing a given system to assess its properties and its natural behaviour) to a control-theoretic perspective (given a system, synthesising a proper controller in order to achieve the desired behaviour). In particular, the considered controllers must satisfy specific constraints depending on the *structure* of the network system, *i.e.*, on its interconnection topology.

A class of linear systems composed of a set of dynamically decoupled subsystems, interconnected through a set of control agents, is considered in this chapter, based on [BFG13, BFG15a]. In this case, subsystems that are naturally independent become interconnected when a control is applied. The novel contribution with respect to previous literature is that, in the proposed framework, subsystems having their own *arbitrary* dynamics are considered. The architecture of any system in this class can be visualised as a graph, whose nodes are associated with subsystems and whose arcs are associated with control agents. Hence, the interconnection between subsystems is determined by the structure of the overall input matrix of the system, and the decisions of each control agent can directly affect exclusively the subsystems-nodes connected by the corresponding arc.

The goal is to stabilise the system by means of a control that satisfies the following constraint: each control agent can use information exclusively about the state components of the subsystems-nodes that the corresponding arc interconnects (*i.e.*, the subsystems that the control agent directly influences). Controllers satisfying this constraint are said to be *network-decentralised*, or *decentralised in the sense of networks*. This problem setup involves block-structured matrices, with structural zero blocks: the rule of the game for network-decentralised stabilisation (each control

agent must make its decisions based on the information about the nodes it affects, only) imposes that the feedback matrix has structural zero blocks, depending on the graph topology. As shown in the following, the design of a suitable network-decentralised controller requires a block-structured feedback matrix with the same structure as the transpose of the overall input matrix of the system.

It is shown that a stabilisable network system can be always stabilised by means of a network-decentralised state-feedback control law, provided that the subsystems do not have common unstable eigenvalues. The general case is still open, but sufficient conditions for solvability can be provided.

Moreover, when the system is formed by identical subsystems and each input agent controls a pair of subsystems with input sub-matrices having opposite sign (as typically happens in the case of flow networks), stabilisation is shown to be possible if and only if at least one of the agents affects one subsystem only (in this case, the system is said to be *externally connected*, or *connected with the external environment*).

The proposed results are based on constructive proofs that lead to structured *Linear Matrix Inequalities (LMIs)*. The advantages of LMIs are worth underlining:

- they can express a variety of classical control constraints (including Lyapunov and Riccati inequalities) for general dynamical systems;
- they are readily solvable with commonly available software; hence, the sought network-decentralised controller can be found efficiently.

9.1 Background

In a wide range of applications, complex systems consisting of independent subunits, which become interactive once a control action is applied, must be controlled or coordinated.

A typical example is provided by water distribution systems [BBGP13, LK69]. The water level in each reservoir has its own dynamics; yet, for a proper management of the system, incoming or outgoing water fluxes need to be regulated. In this case, the reservoirs are pairwise connected by pipes in which the fluxes are controlled to achieve an efficient distribution service. Electrical power distribution networks can also be considered [DPB13].

Platoons of autonomous vehicles [RI96, D'A98, RBA07] and distributed traffic control [Ift96, Ift99] are another significant example. In large platoons, equipping each vehicle with a control that includes information from neighbouring vehicles can assure optimal speed and safety distance: this increases the overall throughput and, at the same time, avoids collisions and congestions [Ift96, D'A98, Ift99]. If a control acting pairwise (*e.g.*, each vehicle must keep a certain distance from the one in front and from the one behind) is added, subsystem that are, by their nature, completely independent (individual vehicles) become globally interacting. Also in the case of

formation flight of aircrafts [WCS96, D'A98], independently piloted aircrafts can be cooperatively controlled, for instance, in order to keep a common height; the case of satellite formations [SMH99] has been investigated as well.

Additional examples include transportation networks [AI98, MOnL08], routing in large telecommunication and data communication networks [MS82, MP95, EV89, ID90, ID02], inventory management and production-distribution systems [SP85, BYZ95, BRU97, BMU00, BT06, SPTK08, BBP10] and network flows in general [AZ07, OnZ07, BBP10, WvdS13a, WvdS13b, DBO$^+$13]. All of these systems can be seen as naturally independent units that interact through the designed control action.

In these large-scale networked control systems, it is often inefficient, too expensive or physically impossible (also due to limitations on energy resources and communication bandwidth, to computation constraints, and to delays) to implement a centralised controller deciding an optimal strategy based on information about *all of the subsystems*. This is the case, for example, of a very large number of subsystems that are geographically sparse. Therefore, control tasks have to be performed collectively, by a network of independent agents, each *autonomously* deciding a local control law relying on *local* information and making *localised* computations (however, autonomous agents are allowed to communicate, according to the given network topology). This type of control, in which the controller acting on a certain *subset of subsystems* decides its strategy based on information about that subset of subsystems only, is called *network-decentralised*. In the past decades, literature on decentralised networked control has flourished [Bak08, CYRC13], yielding a variety of approaches to the stabilisation [ID90, D'A98], the coordination [JML03, CMKB04, Cor09], and the synchronisation [OSM04, RBA07] of large sets of systems, resorting to locally computed controllers only. Distributed control and optimisation of large-scale multi-agent systems have been motivated by several applications, including smart grids and sensor networks able to collect and process information in a distributed fashion, formations of vehicles and networks of robots, spread in a wide region, designed to autonomously perform a global task. It has been shown that system positivity and monotonicity can be exploited, when dealing with large scale control systems, to synthesise distributed controllers [Ran15]. Consensus problems have become increasingly popular for distributed computation (see [OSM04, RBA07] and the references therein); however, in the present chapter the focus is on stabilisability and control of the overall system, rather than agreement among the nodes seen as autonomous agents.

In a wide class of applications, the *same* controller may affect *simultaneously* several subsystems in the network. For instance, in water distribution networks [LK69, BBGP13] the flow controlled in a pipe affects the upstream and the downstream reservoirs simultaneously; in transportation networks, traffic control in a communication route affects at once the density of vehicles at both extremities of the route [AI98, MOnL08]. If a graph is associated with this kind of network systems, dynamically independent subunits are associated with the nodes, while

controllers are associated with the arcs connecting them. The design and synthesis of this type of controllers has been pioneered in [ID90, Ift99, ID02]; more recent contributions are [BMU00, BBGP13], although essentially limited to the case in which the subsystems are first-order integrators. The network-decentralised control is intrinsically different from decentralised control frameworks proposed in the past, where several naturally interacting subsystems are equipped with their own local controller [WD73]: the subsystems considered here are naturally decoupled and the control agents are associated with flow arcs (and not with subsystems).

In this chapter, the case is considered in which the nodes are arbitrary linear subsystems with their own, possibly unstable, dynamics. Under stabilisability assumptions, a linear *network-decentralised* [ID90, Ift99, ID02, BMU00, BBGP13] state-feedback controller is sought in which each control agent (*arc*) can use information exclusively from the subsystems (*nodes*) it connects. As will be seen in Section 9.2, this is equivalent to imposing that the feedback matrix has the same structure as the transpose of the overall input matrix of the system.

The main result in this chapter shows that, if the subsystems do not have common unstable eigenvalues, the problem is solvable; in the case of possibly shared unstable eigenvalues, general structural sufficient conditions, including a constrained LMI, can be provided for the solvability of the problem. In general, the obtained LMI-based condition is sufficient only, because there are systems that admit a network-decentralised stabilising state-feedback control, even though the constrained LMI is not feasible. In the case of a single shared eigenvalue (which is typical in distribution systems), it is shown that the problem is solvable if and only if the LMI is feasible. Finally, in the special case in which all subsystems are equal, each control agent regulates at most two nodes, and the input matrices in these nodes have opposite sign (typical in flow and platoon problems), a necessary and sufficient condition for solvability is the presence of a connection with the external environment.

9.1.1 Arbitrary Node Dynamics

In the literature on network-decentralised dynamic flow, nodes are usually buffers modelled by simple integrators [Ift99, ID02, ID90]. Remarkable exceptions are represented by first-order node dynamics [ID90, BMU00] and systems with a Laplacian state matrix [BBGP13]. The general equation for the class of buffer systems is

$$\dot{x}(t) = Bu(t) + Dd(t) \tag{9.1}$$

where $x \in \mathbb{R}^n$ is the state vector, $u \in \mathbb{R}^m$ is the controlled flow vector, $d \in \mathbb{R}^q$ is an external signal (accounting for a disturbance, or an unknown demand), $B \in \mathbb{R}^{n \times m}$ is the flow matrix and $D \in \mathbb{R}^{n \times q}$ is a suitable disturbance/demand matrix.

However, the nodes often have more complex local processing dynamics, which have to be taken into account. This happens, for instance, in the following examples.

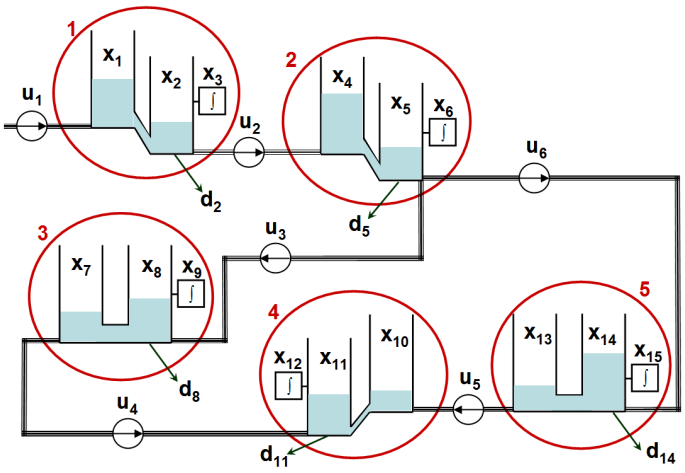

Figure 9.1: The water distribution network in Example 9.1 and in Section 9.5.2. [BFG15a]

Example 9.1. *Fig. 9.1 shows the model of a water distribution system: each node (circled) represents a subsystem with its internal dynamics and includes two reservoirs, where water exchange is spontaneous and depends on their relative levels. Different subsystems are connected by pipes whose flow u can be controlled and the network has a constant demand vector d. Furthermore, supplementary integrators are added to some reservoirs, so that they can asymptotically achieve the exact desired levels. Indeed, as shown in previous work [BMU00, BBGP13], for buffer systems of the form* (9.1)*, zero steady-state error cannot be assured using static continuous controllers; yet, discontinuous controllers may not be applicable in flow networks. In this example, zero steady-state error can be guaranteed, for any demand vector d, for all the reservoirs equipped with a supplementary integrator. This example will be reconsidered in Section 9.5.2.*

Example 9.2. *In large traffic networks, such as data networks [MS82, EV89, ID90, ID02], the traffic arriving at one node is naturally split in several streams with different destinations (as in Fig. 9.2, where α, β and γ are the splitting rates). Traffic splitting at each node can be represented by a continuous-time stochastic matrix, namely, a Metzler matrix with zero sum columns. This example will be reconsidered in Section 9.5.3.*

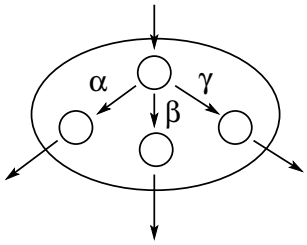

Figure 9.2: The traffic splitting model in Example 9.2 and in Section 9.5.3.

The above examples motivate the study of complex systems composed of subsystems characterised by *arbitrary dynamics*, for which it is interesting to seek *stabilising network-decentralised control strategies*.

9.2 Network-Decentralised Control

Consider a class of linear, interconnected systems consisting of N subsystems, each having its own dynamics:

$$\dot{x}_i(t) = A_i x_i(t) + \sum_{j \in \mathcal{C}_i} B_{ij} u_j(t) + D_i d(t),$$

where $x_i(t) \in \mathbb{R}^{n_i}$, $i = 1, \ldots, N$, is the state of the ith subsystem; $u_j \in \mathbb{R}^{m_j}$, $j = 1, \ldots, M$, are the control subvectors, named *agents*; $\mathcal{C}_i$ is the set that indexes the agents affecting the ith subsystem; $B_{ij} \in \mathbb{R}^{n_i \times m_i}$ represents the effect of the control agent u_j on the ith subsystem; d is an external, non-controllable signal that affects the ith subsystem through matrix D_i. The overall system can be written as

$$\dot{x}(t) = Ax(t) + Bu(t) + Dd(t), \tag{9.2}$$

where $x(t) \in \mathbb{R}^n$ includes the state variables associated with each subsystem, $u(t) \in \mathbb{R}^m$ is the control vector, $d(t) \in \mathbb{R}^n$ is the vector representing the external, non-controllable signal affecting the system, $D \in \mathbb{R}^{n \times n}$ is a generic square matrix, while A and B are block-structured: $A \in \mathbb{R}^{n \times n}$ is a block-diagonal matrix

$$A = \text{blockdiag}\{A_1, A_2, \ldots, A_N\} = \begin{bmatrix} A_1 & 0 & \ldots & 0 \\ 0 & A_2 & \ldots & 0 \\ \vdots & \vdots & \ddots & \vdots \\ 0 & 0 & \ldots & A_N \end{bmatrix}, \tag{9.3}$$

while matrix $B \in \mathbb{R}^{n \times m}$ is a suitably *structured* matrix. For instance, B may have the structure

$$B = \begin{bmatrix} B_{**} & B_{**} & \mathbf{0} & \mathbf{0} & \ldots & \mathbf{0} \\ B_{**} & \mathbf{0} & B_{**} & \mathbf{0} & \ldots & \mathbf{0} \\ \mathbf{0} & \mathbf{0} & B_{**} & \mathbf{0} & \ldots & B_{**} \\ \vdots & \vdots & \vdots & \vdots & \ddots & \vdots \\ \mathbf{0} & \mathbf{0} & \mathbf{0} & B_{**} & \ldots & B_{**} \end{bmatrix},$$

where $\mathbf{0}$ are structural zero blocks, while B_{**} are arbitrary blocks.

All the block dimensions must be compatible with the block structure of A:

$$\sum_{i=1}^{N} n_i = n \quad \text{and} \quad \sum_{i=1}^{M} m_i = m.$$

The following standing assumption is made.

Assumption 9.1. (A, B) *is stabilisable.*

System (9.2) can be naturally represented by means of a hypergraph having N nodes, associated with the N subsystems (corresponding to the diagonal blocks of matrix A), where control agents are associated with hyperarcs. For the sake of simplicity, in the following hypergraphs and hyperarcs will be referred as graphs and arcs. Each control component u_j, $j = 1, \ldots, M$ is a vector in $\mathbb{R}^{m_j}$ associated with a block column of B. Such a block column has zero blocks $B_{ij} \in \mathbb{R}^{n_i \times m_j}$ corresponding to all the nodes not directly affected by agent u_j: formally, $B_{ij} = 0$ if and only if $j \notin \mathcal{C}_i$. Denoting by $\mathcal{N}_j$ the set that indexes the nodes affected by agent j, it can also be written that $B_{ij} = 0$ if and only if $i \notin \mathcal{N}_j$.

Example 9.3. *To illustrate the system framework and its graph representation, consider a system with four subsystems (nodes) and six control agents (arcs), where*

$$A = \mathit{blockdiag}\{A_1, A_2, A_3, A_4\},$$

$$B = \begin{bmatrix} B_{11} & B_{12} & \mathbf{0} & \mathbf{0} & B_{15} & \mathbf{0} \\ \mathbf{0} & B_{22} & B_{23} & B_{24} & \mathbf{0} & \mathbf{0} \\ \mathbf{0} & \mathbf{0} & \mathbf{0} & B_{34} & \mathbf{0} & B_{36} \\ \mathbf{0} & \mathbf{0} & B_{43} & B_{44} & B_{45} & B_{46} \end{bmatrix},$$

$$D = \mathit{blockdiag}\{0, 0, -I, -I\}.$$

$\mathcal{C}_1 = \{1, 2, 5\}$, $\mathcal{C}_2 = \{2, 3, 4\}$, $\mathcal{C}_3 = \{4, 6\}$ *and* $\mathcal{C}_4 = \{3, 4, 5, 6\}$. *The agents control the following nodes:* $\mathcal{N}_1 = \{1\}$, $\mathcal{N}_2 = \{1, 2\}$, $\mathcal{N}_3 = \{2, 4\}$, $\mathcal{N}_4 = \{2, 3, 4\}$, $\mathcal{N}_5 = \{1, 4\}$, $\mathcal{N}_6 = \{3, 4\}$. *The graph corresponding to* B *(and* D*) is shown in Fig. 9.3.*

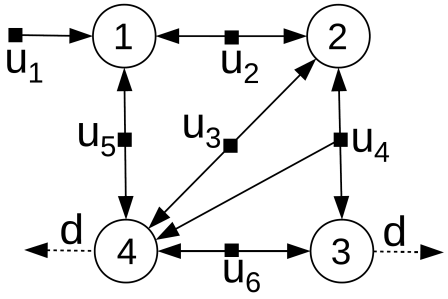

Figure 9.3: The graph corresponding to Example 9.3: circles are the nodes associated with subsystems, solid arcs represent controlled signals, while dashed arcs represent external, non-controllable signals.

In the considered network-decentralised control problem, each control component, affecting a certain subset of nodes, has information about the state components associated with those nodes only. Therefore state-feedback controls restricted to the class

$$u_j = \phi\left(x_i,\ i \in \mathcal{N}_j\right)$$

are considered, where each control agent u_j can have information on the state of nodes in $\mathcal{N}_j$ only. In the case of a linear state feedback, the network-decentralised constraint forces the feedback matrix K to have the same structure as $B^\top$ (this can be written as $K \in \mathcal{S}(B^\top)$), and the following equivalent definition can be provided.

Definition 9.1. *A control $u = -Kx$ is* network-decentralised*, or* decentralised in the sense of networks*, if K has the same structural zero blocks as $B^\top$.*

Example 9.4. *For the system in Example 9.3, a state-feedback controller is network-decentralised provided that K has the following structure:*

$$K = \begin{bmatrix} K_{11}^\top & K_{12}^\top & \mathbf{0} & \mathbf{0} & K_{15}^\top & \mathbf{0} \\ \mathbf{0} & K_{22}^\top & K_{23}^\top & K_{24}^\top & \mathbf{0} & \mathbf{0} \\ \mathbf{0} & \mathbf{0} & \mathbf{0} & K_{34}^\top & \mathbf{0} & K_{36}^\top \\ \mathbf{0} & \mathbf{0} & K_{43}^\top & K_{44}^\top & K_{45}^\top & K_{46}^\top \end{bmatrix}^\top.$$

This constraint on K reflects the restricted information condition that is implicit in the network-decentralised framework. For instance, the second component of the control is the sub-vector

$$u_2(t) = K_{12}x_1(t) + K_{22}x_2(t),$$

so that the control component $u_2(t)$, which affects $x_1(t)$ and $x_2(t)$, has to be decided without any information about $x_3(t)$ and $x_4(t)$.

Remark 9.1. *As a special case, when $A = 0$, the class of buffer systems (9.1) is recovered. For these systems, the control $u = -\gamma B^\top x$, with $\gamma > 0$, is actually a network-decentralised solution: if B has full row rank, then the closed-loop system is asymptotically stable. In the case of a constant $d(t) = d$,*

$$\dot{x}(t) = Bu(t) + Dd,$$

optimality of the control $u = -\gamma B^\top x$ has been proved even under saturation [BBGP13].

9.3 Distinct Unstable Eigenvalues

In this section it is shown that system (9.2) can be always stabilised by means of a network-decentralised controller under the following assumption.

Assumption 9.2. *Two different subsystems do not share unstable eigenvalues.*[1]

This is a *generic property*[2]: it holds almost surely, practically "with probability 1", for any randomly generated instance of the problem.

Before stating the main result of the section, a definition and some preliminary findings need to be provided.

[1] All the eigenvalues whose real part is not strictly negative are denoted as *unstable eigenvalues*.

[2] Formally, a property is *generic* for a set if the subset for which the property holds is dense in the initial set.

Definition 9.2. *The system is* node-stabilisable *if any subsystem i can be stabilised using the control inputs in $\mathcal{C}_i$: $(A_i,\ [B_{i1}\ B_{i2}\ \dots\ B_{iM}])$ are stabilisable for all i.*

Example 9.5. *For the system in Example 9.3, node-stabilisability means that all of the four state-input matrix pairs $(A_1,\ [B_{11}\ B_{12}\ B_{15}])$, $(A_2,\ [B_{22}\ B_{23}\ B_{24}])$, $(A_3,\ [B_{34}\ B_{36}])$ and $(A_4,\ [B_{43}\ B_{44}\ B_{45}\ B_{46}])$ are stabilisable.*

Claim 9.1. *Given any state-input matrix pair (F, G), there exists a Kalman-like transformation such that*

$$T^{-1}FT = \begin{bmatrix} S & R \\ 0 & U \end{bmatrix}, \quad T^{-1}G = \begin{bmatrix} V \\ 0 \end{bmatrix},$$

where (S, V) is a stabilisable pair and U contains unreachable unstable eigenvalues only.

Claim 9.2. *Consider any system of the form*

$$F = blockdiag\{F_1, \dots, F_r\}, \quad G = [G_1^\top \dots G_r^\top]^\top,$$

where G_i have the same number of columns and F_i, F_j do not share unstable eigenvalues for $i \neq j$. Then, if (F_i, G_i) are stabilisable pairs, the system is stabilisable. In particular, node-stabilisability and stabilisability are equivalent.

The detailed proof, based on the Popov criterion, can be found in [BFG15a].

Theorem 9.1. *Under Assumption 9.2, the following conditions are equivalent:*

i) the system is stabilisable;
ii) the system is node-stabilisable;
iii) the system can be stabilised by means of a network-decentralised control.

Proof. Since the subsystems do not share unstable eigenvalues, *i)* $\Leftrightarrow$ *ii)* immediately follows in view of Claim 9.2. Obviously, *iii)* $\Rightarrow$ *i)*. The fact that (node) stabilisability implies decentralised stabilisability can be proved by means of the iterative procedure adopted in [BFG15a]: the inputs u_i are considered one at a time, starting from u_1, and at each time the system is rewritten by applying a Kalman-like transformation to the subsystems that can be stabilised by u_i and grouping them in the first columns of matrices A and B; then, the states associated with these subsystems are fed back in order to stabilise the corresponding portion of the system. By rearranging the blocks, a block-triangular form is obtained at each step and the procedure is iterated by considering the remaining (not yet stabilised) part of the system. The procedure is guaranteed to terminate successfully in view of the assumed node-stabilisability. □

The constructive procedure employed in the proof provides a control which might take advantage of only a subset of the control agents. If this is an issue, it is possible to fully exploit the available arcs according to this algorithm: i) find a structured

feedback $u = -\bar{K}x$, ii) solve the Lyapunov equation to find a P for the closed-loop system, and finally iii) derive a more suitable K with this P by solving the convex optimisation problem

$$\min \|K\|_2 : \ (A - BK)^\top P + P(A - BK) \prec 0, \quad K \in \mathcal{S}(B^\top). \tag{9.4}$$

Theorem 9.1 guarantees that the convex optimisation problem (9.4) is always feasible. Now, the obtained control exploits all available control agents.

9.4 Shared Unstable Eigenvalues

In the case of common unstable eigenvalues, first a general sufficient condition is provided in terms of a structured LMI. This condition, if satisfied, guarantees that the system (9.2) can be stabilised through a decentralised state-feedback control and also provides the expression of the controller. Unfortunately, in general this condition is merely *sufficient* and not necessary. It will be shown that such a condition becomes necessary and sufficient under additional assumptions.

9.4.1 Sufficient LMI Condition

Consider a system of the form (9.2), with A block-diagonal and B block-structured: the following result holds in the general case in which the system can be marginally stable or unstable (*i.e.*, at least one of the subsystems A_i is marginally stable or unstable).

Proposition 9.1. *Given system* (9.2)*, with A block-diagonal and B block-structured, if the following LMI*

$$SA^\top + AS - 2\gamma BB^\top \prec 0, \qquad \gamma > 0 \tag{9.5}$$

has a solution $S \succ 0$ with the same block-diagonal structure as A, in the form

$$S = P^{-1} = \mathit{blockdiag}\{P_1^{-1}, P_2^{-1}, \ldots, P_N^{-1}\}, \tag{9.6}$$

with P_k of the same dimensions of A_k, then the system admits a network-decentralised stabilising feedback control.

Proof. The LMI is solvable if and only if

$$(A - \gamma BB^\top P)^\top P + P(A - \gamma BB^\top P) \prec 0 \tag{9.7}$$

with $P = S^{-1}$, [BEGFB94], which is assured by the choice of the network-decentralised control $K = \gamma B^\top P$. □

Then, a decentralised control $u = -\gamma B^\top S^{-1}x = -\gamma B^\top Px$ exists if (9.5) holds for a block-diagonal $S \succ 0$, or, equivalently, if $A^\top P + PA - 2\gamma PBB^\top P \prec 0$ holds for a block-diagonal $P = S^{-1} \succ 0$.

Why the Condition Is Not Necessary

The LMI condition is sufficient, but not necessary, for network-decentralised stabilisability. In fact, an example is provided in [BFG13] of a system which *can* be stabilised by means of a proper network-decentralised control, even though it is *impossible* to find a block-diagonal P satisfying the inequality. This example, reported below, shows that the existence of a block-diagonal matrix $P \succ 0$, having the same structure as A, such that the inequality $A^\top P + PA - 2\gamma PBB^\top P \prec 0$ holds is just a sufficient, but not a necessary condition for guaranteeing the existence of a stabilising network-decentralised control.

Consider the system

$$\dot{x}(t) = Ax(t) + Bu(t),$$

where

$$A = \begin{bmatrix} 0 & 0 & 0 \\ 0 & \psi & 0 \\ 0 & 0 & 0 \end{bmatrix} \quad \text{and} \quad B = \begin{bmatrix} 1 & 0 \\ -1 & -1 \\ 0 & 1 \end{bmatrix},$$

with $\psi > 0$ (therefore the system is unstable).

In order to find a state-feedback control $u = -Kx$, it is necessary to look for a matrix $K \in \mathcal{S}(B^\top)$:

$$K = \begin{bmatrix} a & -b & 0 \\ 0 & -c & d \end{bmatrix}.$$

Therefore

$$A - BK = \begin{bmatrix} -a & b & 0 \\ a & \psi - (b+c) & d \\ 0 & c & -d \end{bmatrix}$$

and it is possible to freely assign the eigenvalues of $A - BK$ in order to obtain an asymptotically stable system. For instance, when taking $a = b = c = 10\psi$ and $d = -\psi$, a stable matrix is obtained.

Hence, the system can be stabilised by means of a suitable *network-decentralised* state-feedback control. However, there is no stabilising network-decentralised control of the form $u = -\gamma B^\top Px$, where $P \succ 0$ satisfies the Lyapunov condition $(A - BK)^\top P + P(A - BK) \prec 0$, *i.e.*, $A^\top P + PA - 2\gamma PBB^\top P \prec 0$. In fact, by choosing

$$P = \operatorname{diag}\{p_1, p_2, p_3\} \succ 0,$$

then

$$\begin{aligned} -(A^\top P + PA) + 2\gamma PBB^\top P &= \begin{bmatrix} 0 & 0 & 0 \\ 0 & -2p_2\psi & 0 \\ 0 & 0 & 0 \end{bmatrix} + \begin{bmatrix} 2\gamma p_1^2 & -2\gamma p_1 p_2 & 0 \\ -2\gamma p_1 p_2 & 4\gamma p_2^2 & -2\gamma p_2 p_3 \\ 0 & -2\gamma p_2 p_3 & 2\gamma p_3^2 \end{bmatrix} \\ &= \begin{bmatrix} 2\gamma p_1^2 & -2\gamma p_1 p_2 & 0 \\ -2\gamma p_1 p_2 & 4\gamma p_2^2 - 2p_2\psi & -2\gamma p_2 p_3 \\ 0 & -2\gamma p_2 p_3 & 2\gamma p_3^2 \end{bmatrix} \end{aligned}$$

should be positive definite, so all the leading principal minors should be positive. This can be true for the first two, yet it is *impossible* for the matrix determinant (which is equal to $-8\gamma^2 p_1^2 p_2 p_3^2 \psi$) to be positive, since $\psi > 0$.

9.4.2 Solvability Conditions in Particular Cases

Necessary and sufficient conditions for solvability can be provided under additional assumptions.

A Single Shared Unstable Eigenvalue

In Example 9.1, the subsystems share a single unstable eigenvalue ($\lambda = 0$), as is common in distribution systems. In this case, if the system is stabilisable, then the LMI is feasible (hence, the system admits a network-decentralised stabilising control).

Proposition 9.2. *Assume that all the matrices A_i have a single unstable eigenvalue $\lambda \geq 0$ of ascent 1 (*i.e.*, the largest Jordan block associated with λ has dimension 1). Then the following conditions are equivalent:*

i) the system is stabilisable;
ii) the system can be stabilised by means of a network-decentralised control;
iii) the LMI (9.5) *has a structured solution* (9.6).

Proof. It is just necessary to show that *i)* $\Rightarrow$ *iii)* (the remaining implications *iii)* $\Rightarrow$ *ii)* and *ii)* $\Rightarrow$ *i)* are trivial). This can be proved by applying to each block A_k a different transformation T_k, in order to separate the unstable and the stable parts of the system: $T_k^{-1} A_k T_k = \text{blockdiag}\{\lambda I_k, \hat{A}_k^S\}$, where the stable part admits the identity as a Lyapunov matrix. By rearranging all the blocks and joining all λI_k, the system matrices can be then decomposed as

$$\hat{A} = \begin{bmatrix} \lambda I & 0 \\ 0 & \hat{\Lambda}_S \end{bmatrix}, \quad \hat{B} = \begin{bmatrix} \hat{B}_\lambda \\ \hat{B}_S \end{bmatrix},$$

where $\hat{\Lambda}_S = \text{blockdiag}\{\hat{A}_1^S, \hat{A}_2^S, \ldots, \hat{A}_N^S\}$ is stable. Being the system stabilisable, $\hat{B}_\lambda$ must have full row rank and a proper network-decentralised stabilising control can be found: given $u = -\gamma[\hat{B}_\lambda^\top \;\; 0]x = -\hat{K}x$, with γ large enough, the candidate block-diagonal matrix

$$\hat{S} = \begin{bmatrix} I & 0 \\ 0 & \mu I \end{bmatrix}$$

ensures that

$$\hat{S}(\hat{A} - \hat{B}\hat{K})^\top + (\hat{A} - \hat{B}\hat{K})\hat{S} \prec 0 \tag{9.8}$$

for μ large enough. Then, by restoring all the blocks to the original position with the backward transformations, a structured $S \succ 0$ can be found that satisfies (9.5). Details are in [BFG15a]. □

Further examples of this kind of systems will be given in Section 11.1.

Triangularisable and Locally Stabilisable Systems: the Case of Flow Networks

Stronger solvability conditions can be provided in another particular case (for systems with possibly repeated unstable eigenvalues). To this aim, first some preliminary definitions are introduced.

Definition 9.3. *The network is* locally stabilisable *if each agent u_i can (separately) stabilise each of the subsystems in $\mathcal{N}_i$.*

Local stabilisability by no means implies that the control agent can stabilise simultaneously more than one subsystem in $\mathcal{N}_i$. For instance, the non-stabilisable system

$$\begin{cases} \dot{x}_1 = x_1 + u, \\ \dot{x}_2 = x_2 + u, \end{cases}$$

is locally stabilisable.

Definition 9.4. *The system is* structurally triangularisable *if there exist a) an ordering of the nodes and b) a selection and ordering of the agents such that the resulting B has a block triangular structure.*

For instance, the system in Example 9.3 is structurally triangularisable by ordering the nodes as 1, 2, 4, 3 and disregarding the last two agents (*i.e.*, selecting the first four).

In the following an extended system is defined, to consider the case in which some of the subsystems are open-loop stable.

Definition 9.5. *Given the structured system (A, B), the* extended system (A, B_{ext}) *can be defined as follows. For each asymptotically stable node i, B is extended by adding a fictitious block with n_i columns, which has an identity matrix corresponding to A_i and zero blocks elsewhere.*

For instance, if in the system of Example 9.3 the second subsystem is asymptotically stable, B must be extended as

$$B_{ext} := \left[B \,|\, [\, \mathbf{0}\ I\ \mathbf{0}\ \mathbf{0}\,]^\top \right]$$

The following theorem holds.

Theorem 9.2. *If the extended system is triangularisable and locally stabilisable, then* (9.5)-(9.6) *are feasible.*

Proof. In view of the triangularisability and local stabilisability assumptions, B has a suitable "block-triangular" structure and, by properly reorganising the blocks and individually stabilising all of the unstable subsystems, a closed-loop matrix is achieved that is block-triangular and asymptotically stable. Hence, it admits a block-diagonal Lyapunov matrix such that (9.5)-(9.6) are feasible. Details can be found in [BFG15a]. □

Theorem 9.2 has demanding assumptions. However, there are interesting structural assumptions under which LMI solvability is guaranteed, such as when each control agent is associated with an *arc* (not a hyperarc) of a proper *graph* (not a hypergraph), thus affects *at most two* subsystems.

The definition of externally connected graph (a concept already discussed in Chapters 3 and 4) is reported here for convenience.

Definition 9.6. *A network is* connected *if the corresponding graph is connected (namely, each of its nodes can be reached starting from any other, by following the existing arcs); it is* connected with the external environment *if, in addition, the input matrix B has at least one block-column with a single non-zero block.*[3]

Corollary 9.1. *Assume that the system is locally stabilisable and that each agent controls at most two subsystems. If the system is connected with the external environment, then* (9.5)-(9.6) *are feasible, hence a decentralised stabilising control exists.*

The proof is immediately based on Theorem 9.2: in view of the external connection assumption, it is always possible to find a spanning tree and form the triangular structure of B starting from a node connected with the external environment.

An interesting case is that of flow networks, composed of a family of identical subsystems, in which each network arc connects a pair of nodes so that its action has opposite effects (inflow and outflow).

Proposition 9.3. *Given a connected network, assume that all the diagonal blocks of matrix A are equal, $A_i = A_{bl}$, for $i = 1, \dots, N$, and that all non-zero blocks of B are $\pm B_{bl}$. Assume that there are at most two non-zero blocks in each block column of matrix B and that, if they are two, they have opposite sign. Then the following conditions are equivalent:*

i) the system is stabilisable;
ii) the system is locally stabilisable;
iii) the structured LMI is solvable;
iv) either A_{bl} is stable or the network is connected with the external environment.

[3] As discussed in Chapter 3, this can be seen as a connection of the system with an additional node, implicitly present in each graph, that stands for the "external environment".

Proof. Ignoring the trivial case of A_{bl} stable, based on the Popov criterion it is possible to show that both $i) \Rightarrow iv)$ and $i) \Rightarrow ii)$ (see [BFG15a] for details); the rest of the proof follows from Corollary 9.1. □

Remark 9.2. *It is apparent from Proposition 9.3 that requiring connection with the external environment is a crucial assumption: in fact, the presence of a connection with the external environment, in the case of a flow system, is indeed equivalent to stabilisability. Interestingly, external connections are absent in the example in Section 9.4.1, highlighting how the LMI-based conditions are, in general, sufficient but not necessary.*

9.5 Numerical Examples

9.5.1 Double Integrator

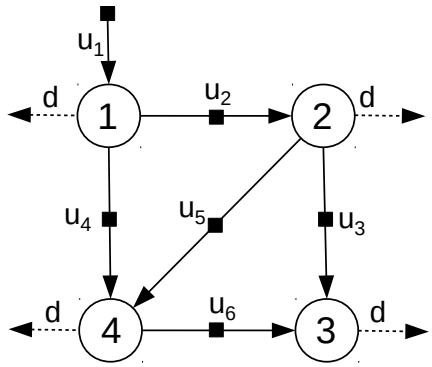

Figure 9.4: Network graph corresponding to the example in Section 9.5.1.

Consider the flow network represented by the graph in Fig. 9.4. Each node corresponds to a buffer (or a reservoir), while the arcs are associated with controlled flows. All the nodes are equipped with a supplementary integrator, to ensure that, at steady state, they all reach the exact prescribed level, fixed as 0 without loss of generality (any given point can be shifted to zero after a suitable change of coordinates). This system can be represented by the eight-state model

$$\dot{x} = Ax + Bu + Dd,$$

with

$$A = \begin{bmatrix} A_2 & \mathbf{0} & \mathbf{0} & \mathbf{0} \\ \mathbf{0} & A_2 & \mathbf{0} & \mathbf{0} \\ \mathbf{0} & \mathbf{0} & A_2 & \mathbf{0} \\ \mathbf{0} & \mathbf{0} & \mathbf{0} & A_2 \end{bmatrix}, \quad A_2 = \begin{bmatrix} 0 & 1 \\ 0 & 0 \end{bmatrix},$$

$$B = \begin{bmatrix} B_2 & -B_2 & \mathbf{0} & -B_2 & \mathbf{0} & \mathbf{0} \\ \mathbf{0} & B_2 & -B_2 & \mathbf{0} & -B_2 & \mathbf{0} \\ \mathbf{0} & \mathbf{0} & \mathbf{0} & B_2 & B_2 & -B_2 \\ \mathbf{0} & \mathbf{0} & B_2 & \mathbf{0} & \mathbf{0} & B_2 \end{bmatrix}, \quad B_2 = \begin{bmatrix} 0 \\ 1 \end{bmatrix}, \quad D = -\begin{bmatrix} B_2 \\ B_2 \\ B_2 \\ B_2 \end{bmatrix}.$$

Even states are the effective buffer levels, while odd states are the integral variables, whose derivatives are equal to even states. Vector d represents a constant demand, uniformly affecting each node. This system can be stabilised by the network-decentralised state-feedback controller $u = -Kx = -\gamma B^\top P x$, where γ is a constant scalar and $P \succ 0$ is a Lyapunov block-diagonal matrix. P and γ can be found by numerically solving an LMI, as previously shown in this chapter. However, an analytical solution can be found as well; in fact, it suffices to notice that

$$P = \begin{bmatrix} P_2 & \mathbf{0} & \mathbf{0} & \mathbf{0} \\ \mathbf{0} & P_2 & \mathbf{0} & \mathbf{0} \\ \mathbf{0} & \mathbf{0} & P_2 & \mathbf{0} \\ \mathbf{0} & \mathbf{0} & \mathbf{0} & P_2 \end{bmatrix}, \; P_2 = \begin{bmatrix} 1 & 1 \\ 1 & 2 \end{bmatrix} \quad \text{and} \quad \gamma = 2$$

render the closed-loop system stable.

When starting from any initial condition, the presence of the integral control guarantees the exact recovery of the equilibrium values of even states, as expected (see Fig. 9.5), while odd states are asymptotically constant (Fig. 9.6). In the proposed simulations, $x(0) = [0.71\ 1.03\ 0.97\ -0.43\ 0.62\ -1.32\ 0.82\ -1.87]^\top$. In order to achieve the zero-steady-state-error goal, the integral variables are communicated by each node to the control agents that are connected to it, in a network-decentralised fashion. Although the numerical and the analytical solution differ for the equilibrium values obtained, they both lead to the same steady-state control vector $u = [4\ \ 1.5\ \ 0.5\ \ 1.5\ \ 0\ \ 0.5]^\top$. In both cases, any deviation from the equilibrium values at the nodes is completely eliminated by the integral control.

9.5.2 Water Distribution System

Reconsider the water distribution system presented in Example 9.1 and assume that the nodes in Fig. 9.1 have the following dynamics:

$$A_i = \begin{bmatrix} -\alpha_i & \beta_i & 0 \\ \alpha_i & -\beta_i & 0 \\ 0 & 1 & 0 \end{bmatrix}, \quad \text{where} \;\; \beta_i = 0 \;\; \text{for} \;\; i \in \{1, 2, 4\}.$$

In each node, the first two states are the reservoirs volumes, while the third represents the local integrator. Constants α_i [min^{-1}] and β_i [min^{-1}] depend on the size of the reservoirs and the diameter of the connecting pipes; in the proposed simulation, $\alpha_1 = 15$, $\alpha_2 = 20$, $\alpha_3 = 16$, $\alpha_4 = 16.7$, $\alpha_5 = 14$, $\beta_3 = 12$ and $\beta_5 = 22$.

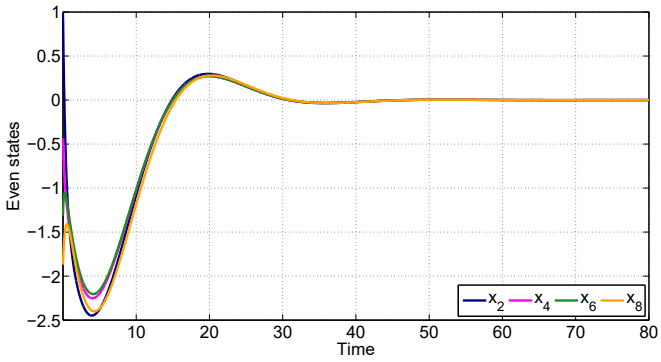

(a) Numerical solution

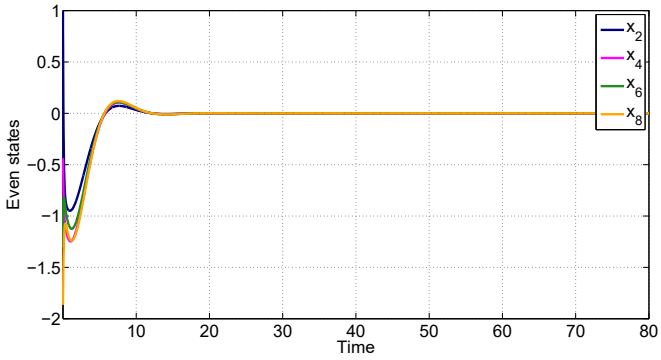

(b) Analytical solution

Figure 9.5: System trajectories for the double integrator in Section 9.5.1: even states (at steady state, $x_4 = x_6$).

The overall system has the same structure as model (9.2), where

$$A = \text{blockdiag}\{A_1, A_2, A_3, A_4, A_5\},$$

$$B = \begin{bmatrix} B_u & -B_d & \mathbf{0} & \mathbf{0} & \mathbf{0} & \mathbf{0} \\ \mathbf{0} & B_u & -B_d & \mathbf{0} & \mathbf{0} & -B_d \\ \mathbf{0} & \mathbf{0} & B_d & -B_u & \mathbf{0} & \mathbf{0} \\ \mathbf{0} & \mathbf{0} & \mathbf{0} & B_d & B_u & \mathbf{0} \\ \mathbf{0} & \mathbf{0} & \mathbf{0} & \mathbf{0} & -B_u & B_d \end{bmatrix},$$

$$B_d = \begin{bmatrix} 0 & 1 & 0 \end{bmatrix}^\top, \quad B_u = \begin{bmatrix} 1 & 0 & 0 \end{bmatrix}^\top,$$

$d = -[0\ 1\ 0\ 0\ 1\ 0\ 0\ 1\ 0\ 0\ 1\ 0\ 0\ 1\ 0]^\top$ and $D = I$. The only unstable eigenvalue is $\lambda = 0$, which has ascent one and is common to all the subsystems. Therefore, the results of Proposition 9.2 can be applied; matrix K of the network-decentralised state-feedback controller is obtained through the direct solution of the LMI (9.5)-(9.6), numerically solved using the MATLAB LMI toolbox [GNLC94]. To enforce a certain speed of convergence, when solving the LMI, A can be replaced with

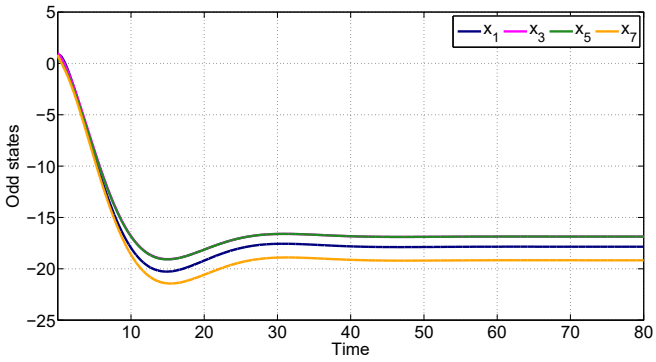

(a) Numerical solution

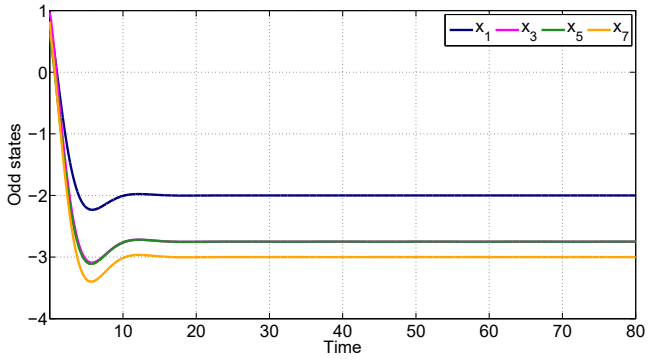

(b) Analytical solution

Figure 9.6: System trajectories for the double integrator in Section 9.5.1: odd states (at steady state, $x_3 = x_5$).

$A + \sigma I$, $\sigma > 0$, so that the closed-loop eigenvalues have real part less than $-\sigma$. The value used in the simulation is $\sigma = 0.15$. In Figs. 9.7 and 9.8, the decentralised control is compared with a centralised LQ control, with state weighting matrix I and input weighting matrix $I/2$; the system is started from the initial condition $x(0) = [2.926\ 4.187\ 5.094\ -4.480\ 3.594\ 3.102\ -6.748\ -7.620\ -0.033\ 9.195\ -3.192\ 1.705\ -5.524\ 5.025\ -4.898]^\top$. The equilibrium values of the states equipped with integral control are smoothly recovered, as expected.

9.5.3 Stochastic Traffic Splitting Dynamics

To control traffic networks with natural splitting dynamics at the nodes, as in Example 9.2, a decentralised approach can be adopted. To study this case via simulation, five interconnected subsystems have been considered with the same network topology as in Fig. 9.1. Instances of the system have been randomly generated in which A_i are continuous-time stochastic matrices, with $0 \leq A_{ij} \leq 1$, $i \neq j$ and $A_{jj} = -\sum_{i \neq j} A_{ij}$, and the entries of the non-zero blocks in B have been randomly

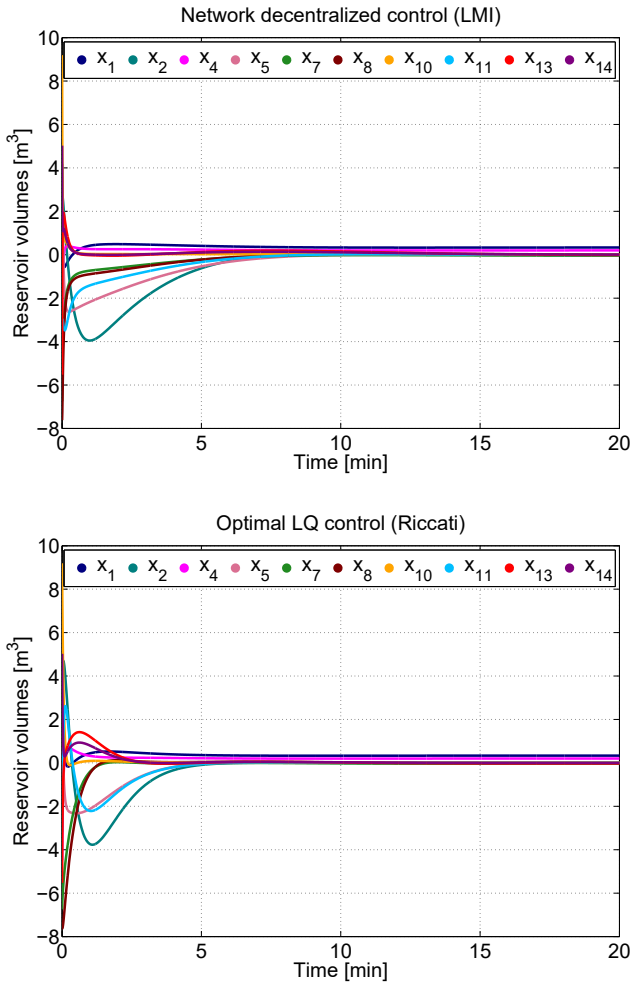

Figure 9.7: Reservoir volumes evolution for the system in Section 9.5.2: decentralised (top) and optimal (bottom) control.

generated as well. In several experiments, the LMI has always been feasible, as expected; the average time T_{n_i} required for its solution, depending on the subsystems dimension n_i, is shown in Table 9.1.

n_i	2	3	4	5	6	7	9	10
$T_{n_i}[ms]$	4	9	13.3	24.7	44.2	73.4	182.7	296.7

Table 9.1: Average time required for LMI solution in Example 9.5.3.

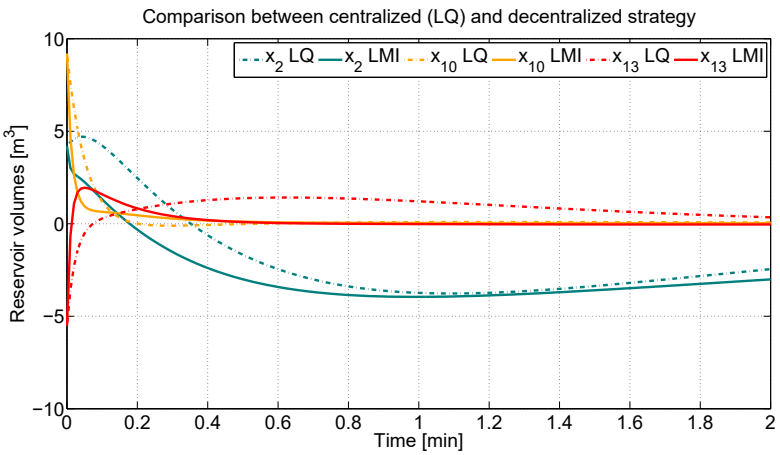

Figure 9.8: Detailed simulation for reservoir volumes x_2, x_{10} and x_{13} (zoomed from Fig. 9.7).

9.6 Remarks

The problem of network-decentralised stabilisation has been shown to be solvable when the subsystems do not have common unstable eigenvalues. In the general case, a structured LMI condition has been provided, which is sufficient only (an example has shown that, in general, satisfaction of the LMI condition is not necessary for decentralised stabilisability); such an LMI is *always feasible* in particular cases of practical interest, *e.g.*, that of flow networks and that of subsystems with a single common unstable eigenvalue of ascent 1. However, unfortunately, the general question whether, under possibly common eigenvalues, stabilisability implies network-decentralised stabilisability is still unsolved and is left as a subject of future investigation.

It is worth pointing out that, in the considered setup, a robust version of the considered LMI can be found when A is a polytopic matrix of the form

$$A_i = \sum_{k=1}^{K} \alpha_k A_{ik}, \quad \sum_{k=1}^{K} \alpha_k = 1, \quad \alpha_k \geq 0.$$

In this case, determining a diagonal P valid for all possible dynamics simply requires the solution of a set of LMIs (one for each vertex of the polytope).

It is also well known that, once the LMI has a solution, the system enjoys the property of infinite gain margin: each agent can increase its gain, independently of the others, without causing instability. This cannot be guaranteed in general, without making use of LMIs.

In Chapter 10, the concept of network-decentralised control will be further developed, considering general nonlinear compartmental systems with uncertain node dynamics and with possibly switching topologies.

The network-decentralised control problem considered in this chapter admits

a dual version; the dual of the assumptions previously introduced for the pair (A, B) should now be considered for (A, C) (namely, the same assumptions are applied to $(A^\top, C^\top)$). Each agent must have access to the information concerning the nodes it connects, so that the output vector can be partitioned into subvectors $y = [y_1\ y_2\ \cdots\ y_m]$ and $y = Cx$, $C \in \mathcal{S}(B^\top)$. For instance, in Example 9.3, the output y_5 of agent 5 would be a linear combination of the states x_1 and x_4. Moreover, local observers are implemented by *estimation node agents* that are informed about the decision of all the control agents $u_j : j \in \mathcal{C}_i$, and two adjacent node estimation agents can exchange the estimated local state. This can be a natural requirement since, by definition, adjacent nodes have common control agents. Then a decentralised observer can be constructed

$$\dot{z}(t) = Az(t) - LC[z(t) - x(t)] + Bu(t),$$

where now L is subject to the dual constraint $L \in \mathcal{S}(C^\top)$. The theory then develops without essential changes. Along these lines, in Chapter 12 network-decentralised estimation will be considered.

10

Compartmental Flow Control: Decentralisation, Robustness and Optimality

The control of large-scale flow networks is relevant in many applications, as discussed in Chapter 9, and often, being global communication impossible, control agents must act based on *locally* available information. In an important case, the involved models can be cast in a compartmental framework, where the compartments (subsystems) frequently exhibit nonlinear dynamics. In this chapter, following [BFG+16], the flow control problem is considered for a general class of nonlinear compartmental systems, in the presence of an external uncontrolled flow, and a stabilising network-decentralised control is sought, such that

- each agent governs a network flow channel (corresponding to an arc of the associated graph) that affects *at most two* subsystems (nodes of the graph);
- each agent decides its actions based exclusively on the states of the subsystems associated with the nodes to which the corresponding arc is directly connected, in the absence of communication with other agents.

As mentioned before, this type of control was considered in [ID90, ID02, Ift99, BMU00] for buffer systems, where the subsystems are first-order integrators; in [BBGP13], a constrained decentralised control law that assures asymptotic optimality in the minimum-norm sense is proposed. A network-decentralised control for linear systems, where nodes represent non-interacting subsystems coupled by the control action, is proposed in [BFG13, BFG15a], see Chapter 9. The novelties in this chapter are the following: *proper* graphs (and not hypergraphs) are considered (since compartmental systems are associated with graphs where each arc, representing a flow link, connects *at most two nodes*) and also nonlinearities in the system dynamics are dealt with.

General necessary and sufficient stabilisability conditions are provided, taking into account decentralisation, control constraints and robustness (*i.e.*, effectiveness of the control regardless of the system parameters). The approach proposed in [BFG+16] is therefore suitable for generic *nonlinear* and *uncertain* compartmental systems.

Under flow constraints, the saturated control proposed in [BBGP13] is adopted, providing necessary and sufficient structural conditions for closed-loop asymptotic stability in terms of connectivity of the network graph. However this control, applied *tout court*, may not be stabilising if the steady state corresponding to the current demand is not exactly known.

A modification of the strategy in [BBGP13] is then proposed: the devised control strategy is still network-decentralised and can stabilise the system robustly (without any knowledge about the system functions, apart from smoothness and monotonicity requirements), under proper assumptions on the network topology.

Moreover, when the overall system is composed of independent, marginally stable compartmental subsystems, a particular network-decentralised saturated control strategy (which can be seen as based on the feedback of the total amounts of resource in the subsystems) is shown to be asymptotically optimal in terms of minimum Euclidean norm: the controlled flow converges to the optimum without requiring communication among agents.

The performances of different network-decentralised strategies, including those proposed in this chapter, are compared by means of simulations in Section 11.1.6.

10.1 Nonlinear Compartmental Models

Consider a class of models of the form

$$\dot{x}(t) = Sg^*(x(t)) + Rh^*(x(t)) + Bu(t) + d(t), \tag{10.1}$$

where $x(t) \in \mathbb{R}^n$ is the state, $u(t) \in \mathbb{R}^m$ is the control input, $d(t) \in \mathbb{R}^n$ is an exogenous signal. Vectors $u_j(t) \in \mathbb{R}$ are referred as control *agents* and vector $d(t)$ as *demand*.

A graph $\mathcal{N}$ with n nodes can be associated with the system. It is assumed that S, R and B are incidence matrices for $\mathcal{N}$: each of their columns has either two non-zero entries, equal to 1 and -1, or a single non-zero entry, equal either to 1 or to -1.

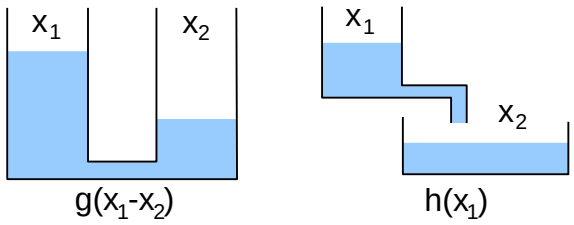

Figure 10.1: g-type (left) and h-type (right) flows in a fluid system.

Vector functions g^* and h^* represent flows between two nodes within the system; application examples include flowing of data, fluids, or currents. Functions g^* and h^* have a different physical meaning: g-type flows, associated with g^*, depend on the difference between the corresponding states, while h-type flows, associated with h^*,

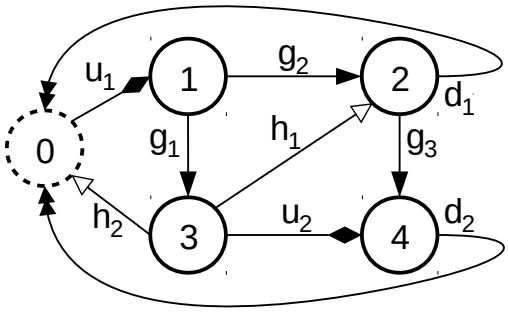

Figure 10.2: Graph of the network in Example 10.1. [BFG+16]

depend on the state of the starting node only. The concept can be better illustrated with the support of Fig. 10.1, representing a fluid system: in this case, g-type flows between tanks depend on the fluid level in both tanks, while h-type flows depend on the fluid level in the upper tank only. Formally:

- $g_j^* = g_j^*(x_k - x_l)$, where $S_{kj} = -1$ and $S_{lj} = 1$;
- $h_j^* = h_j^*(x_k)$, where $R_{kj} = -1$.

Denoting by M_j the jth column of a matrix M, it can be written:

- $g_j^* = g_j^*(-S_j^\top x)$;
- $h_j^* = h_j^*(-\tilde{R}_j^\top x)$, where $[\tilde{R}]_{ij} = \min\{R_{ij}, 0\}$.

Matrix $[S\ R\ B]$ is the overall *incidence matrix* of the graph representing the network. In the network graph, different types of arcs are present: *g-type*, *h-type*, *u-type* and *d-type* arcs are associated respectively with the components of vector g^* (*i.e.*, with the columns of S), of vector h^* (with the columns of R), of the control vector u (with the columns of B) and of the demand vector d.

Recall that, if in a column of matrix R or of matrix B there is a single non-zero entry, then the corresponding arc connects the network with the *external environment*, associated with the *external node* (*node* 0). In general, any arc connected with a single node of the graph (for instance, all arcs associated with vector d) represents a connection with the external environment.

Example 10.1. *The network graph in Fig. 10.2 includes*

- *g-type flows:* $g^*(x) = [g_1(x_1 - x_3)\ \ g_2(x_1 - x_2)\ \ g_3(x_2 - x_4)]^\top$;
- *h-type flows:* $h^*(x) = [h_1(x_3)\ \ h_2(x_3)]^\top$;
- *controlled flows:* $u = [u_1\ \ u_2]^\top$;
- *exogenous flows:* $d = [d_1\ \ d_2]^\top$.

The corresponding system has matrices

$$S = \begin{bmatrix} -1 & -1 & 0 \\ 0 & 1 & -1 \\ 1 & 0 & 0 \\ 0 & 0 & 1 \end{bmatrix}, \quad R = \begin{bmatrix} 0 & 0 \\ 1 & 0 \\ -1 & -1 \\ 0 & 0 \end{bmatrix}, \quad B = \begin{bmatrix} 1 & 0 \\ 0 & 0 \\ 0 & -1 \\ 0 & 1 \end{bmatrix}.$$

The following standing assumptions are made.

Assumption 10.1. *The control is componentwise bounded as* $u_j^- \leq u_j \leq u_j^+$*; with a more compact notation:*

$$u^- \leq u \leq u^+. \tag{10.2}$$

Assumption 10.2. *Functions* g_j^* *and* h_j^* *are smooth and have positive derivative.*

Assumption 10.3. *There are no g-type flows from/to node* 0*.*

Actually, there would be no point in considering g-type flows from/to node 0, since there are no state variables associated with it.

Definition 10.1. *A* path *on the graph is an oriented sequence of distinct arcs, connecting two distinct nodes (and not including node* 0 *as an intermediate node).* Oriented *means that the two paths from node i to node j and from node j to node i are different. A path is* admissible *if: 1) it does not include d-type arcs; 2) whenever it includes h-type arcs, they have path-consistent orientation; other arcs can be included with arbitrary orientation.*[1]

For example, in the graph in Fig. 10.2, the path 4-3-2-1 is admissible, while the path 2-3-4 is not admissible (because it includes h-type arc h_1, whose orientation is opposite to that of the path).

Consistently with the definitions adopted in the previous chapters, the following is introduced.

Definition 10.2. *The graph is* connected *if an oriented path exists connecting each pair of nodes (excluding node* 0*). The graph is* strongly connected *if an oriented* admissible *path exists connecting each pair of nodes (excluding node* 0*). The graph is* externally connected *if, for each node, an oriented admissible path exists leading to node* 0*.*

For instance, the graph in Fig. 10.2 is both strongly connected and externally connected. Conversely, if g-type and h-type arcs are swapped, the resulting graph is no longer strongly connected (because node 1 cannot be reached from the other nodes), but is still externally connected (in fact, from each node, an admissible path leads to node 0). If, instead, in Fig. 10.2 the arcs u_1 and h_2 are removed, then the graph is still strongly connected, but no longer externally connected.

[1] This corresponds to replacing each g-type and u-type arc in the graph by two arcs in opposite directions, and considering directed paths only.

10.2 Stabilisability Conditions

Given a set-point, the goal here is to stabilise the system by means of a network-decentralised control.[2]

Recall that a feedback control is *network-decentralised* if any agent u_j decides its strategy based just on the state variables associated with the nodes to which it is directly connected. In the case of a compartmental system structure, then either $u_j = \Phi_j(x_q, x_p)$, where p and q index the two non-zero elements of column B_j, or $u_j = \Phi_j(x_p)$, where p indexes the unique non-zero element of column B_j. In the example in Fig. 10.2, a control can be denoted as network-decentralised provided that

- u_1 depends on x_1 only;
- u_2 depends on x_3 and x_4 only.

It is fundamental to require that the external demand (assumed to be constant, for the moment being) is compatible with the flow constraints.

Assumption 10.4. *The demand is constant, $d(t) = d$, and an equilibrium vector $\bar{x}$ exists corresponding to a control $\bar{u}$ that strictly satisfies* (10.2)*: $u^- < \bar{u} < u^+$ and*

$$0 = Sg^*(\bar{x}) + Rh^*(\bar{x}) + B\bar{u} + d.$$

Denoting by $v = u - \bar{u}$ and $z = x - \bar{x}$, without restrictions the stabilisation problem can be reformulated for the shifted nonlinear system

$$\dot{z} = Sg(z) + Rh(z) + Bv, \tag{10.3}$$

where g, h are the shifted functions $g(z) = g^*(z+\bar{x}) - g^*(\bar{x})$, $h(z) = h^*(z+\bar{x}) - h^*(\bar{x})$, such that $g(0) = 0$, $h(0) = 0$. The constraints in the shifted framework are

$$v^- \leq v \leq v^+, \tag{10.4}$$

where $v^- = u^- - \bar{u} < 0$ and $v^+ = u^+ - \bar{u} > 0$. Note that stability is now referred to the nominal equilibrium $\bar{z} = \bar{v} = 0$.

Assuming that $\bar{u}$ satisfies the constraints is crucial [BMU00]. Conversely, the requirement that d is constant can be removed. Moreover if, due to parameter uncertainties, the equilibrium condition is not exactly satisfied, so that $Sg^*(\bar{x}) + Rh^*(\bar{x}) + B\bar{u} + d = \Delta \neq 0$, then equation (10.3) becomes $\dot{z} = Sg(z) + Rh(z) + Bv - \Delta$. This is not an issue, because, as shown in the following, the proposed approach relies on Lyapunov functions and is therefore suitable for handling both uncertainties and a time-varying demand. Robustness aspects will be thoroughly discussed in Section 10.4.

[2] A stabilisability problem is dealt with and the equilibrium $(\bar{x}, \bar{u})$ is assumed to be given. The problem of regulating the steady-state value is tackled, for instance, in [HHB06, LA15] (see also the references therein).

Definition 10.3. *Given the vector bound $v^- \leq v \leq v^+$, the* saturation function *is componentwise defined as*

$$[sat(v)]_j = \begin{cases} v_j^+ & if \quad v_j > v_j^+ \\ v_j & if \quad v_j^- \leq v_j \leq v_j^+ \\ v_j^- & if \quad v_j < v_j^- \end{cases} \tag{10.5}$$

The following *saturated network-decentralised control* [BBGP13] is considered:

$$v = \text{sat}(-\gamma B^\top z), \tag{10.6}$$

where $\gamma > 0$.

As will be shown, such a control can globally uniformly stabilise the considered class of systems, according to the following definition.

Definition 10.4. *System $\dot{z}(t) = f(z(t), v(t))$, admitting the equilibrium $\bar{z} = \bar{v} = 0$, such that $f(0,0) = 0$, is* globally uniformly asymptotically stabilisable *(to $z = 0$) if a control law $v(z)$ can be chosen so that:*

- *for all ϵ, a value δ exists such that $\|z(0)\| \leq \delta$ implies $\|z(t)\| \leq \epsilon$ for all $t \geq 0$;*
- *for all $\mu > \epsilon > 0$, a value $T_{\mu,\epsilon}$ exists such that $\|z(0)\| \leq \mu$ implies $\|z(t)\| \leq \epsilon$ for all $t \geq T_{\mu,\epsilon}$.*

Then, the next theorem can be proved.

Theorem 10.1. *Under Assumptions 10.1-10.4, if the system graph is strongly connected, the following statements are equivalent.*

i) System (10.3) *can be globally uniformly stabilised.*
ii) Matrix $[S\ R\ B]$ has row rank n.
iii) The system graph is externally connected.
iv) System (10.3) *can be globally uniformly stabilised by the network-decentralised control* (10.6)*.*

Proof. iv) $\Rightarrow$ i) is obvious.

i) $\Rightarrow$ ii): $\text{rank}[S\ R\ B] < n$ implies the existence of a left kernel. Then, by considering the vector $\zeta \in \mathbb{R}^n$, $\zeta \neq 0$, such that $\zeta^\top [S\ R\ B] = 0$, it follows that

$$\frac{d}{dt}\zeta^\top z = \zeta^\top [Sg(z) + Rh(z) + Bv] = 0.$$

Hence, $\zeta^\top z(t) = \zeta^\top z(0)$ is constant and, if $\zeta^\top z(0) \neq 0$, $z(t)$ cannot converge to 0.

ii) $\Rightarrow$ iii): since the graph is strongly connected by assumption, $\text{rank}[S\ R\ B] = n$ implies connection with the external node 0, *i.e.*, the existence of at least one column having a single non-zero element (see [BFG+16] for more details).

Proving *iii) $\Rightarrow$ iv)* requires a lemma.

Lemma 10.1. *Given functions $g(z)$ and $h(z)$ satisfying the stated assumptions, and matrices B, S and R, there exist positive definite diagonal matrix functions $D_v(z)$, $D_h(z)$ and $D_g(z)$ such that*

$$\begin{aligned} Bsat(-\gamma B^\top z) &= -\gamma B D_v(z) B^\top z, && (10.7)\\ Sg(z) &= -S D_g(z) S^\top z, && (10.8)\\ Rh(z) &= -R D_h(z) \tilde{R}^\top z, && (10.9) \end{aligned}$$

where $\tilde{R} = \min\{R, 0\}$, componentwise. Moreover, in any bounded neighbourhood of $z = 0$, $\|z\| \le \mu$, there exist two numbers $0 < \delta^- < \delta^+$ such that

$$\delta^- \le \; [D_g(z)]_{ii},\; [D_h(z)]_{ii},\; [D_v(z)]_{ii} \; \le \delta^+, \qquad \forall\, i. \tag{10.10}$$

Equation (10.7) immediately follows from a standard property of the saturation function: $\mathrm{sat}(v_i) = [D_v]_{ii} v_i$ componentwise, where $[D_v]_{ii}$ is a suitable number (see for instance [BM15]). The proof of (10.8) (and of (10.9), which is analogous) is based on the integral formula (4.29). In fact, considering the generic column S_j of S and the corresponding $g_j = g_j(-S_j^\top z)$,

$$S_j g_j(-S_j^\top z) = -S_j \underbrace{\left[\int_0^1 g_j'(-\lambda S_j^\top z) d\lambda\right]}_{\doteq D_{jj}(z)} S_j^\top z.$$

$D_{jj}(z)$ is strictly positive, lower and upper bounded in any bounded domain, since it is the integral of a positive continuous function on a non-zero interval.

In view of Lemma 10.1, system (10.3) with the control (10.6) can be written as

$$\begin{aligned} \dot{z} &= -[S D_g(z) S^\top + R D_h(z) \tilde{R}^\top + \gamma B D_v(z) B^\top] z = \\ &\begin{bmatrix} S & R & B \end{bmatrix} \begin{bmatrix} -D_g(z) & 0 & 0 \\ 0 & -D_h(z) & 0 \\ 0 & 0 & -\gamma D_v(z) \end{bmatrix} \begin{bmatrix} S^\top \\ \tilde{R}^\top \\ B^\top \end{bmatrix} z \doteq A(D) z. \end{aligned}$$

Matrix $A(D)$ can be non-symmetric due to h-type arcs. For instance, in Example 10.1, with $D = -\mathrm{diag}(D_1, D_2, \ldots, D_7)$, the closed-loop matrix becomes

$$A(D) = \begin{bmatrix} -(D_1 + D_2 + \gamma D_6) & D_2 & D_1 & 0 \\ D_2 & -(D_2 + D_3) & D_4 & D_3 \\ D_1 & 0 & -(D_1 + D_4 + D_5 + \gamma D_7) & \gamma D_7 \\ 0 & D_3 & \gamma D_7 & -(D_3 + \gamma D_7) \end{bmatrix}.$$

The implication *iii) ⇒ iv)* can now be proved. Matrix $A(D)$, which has strictly negative diagonal entries and non-negative off-diagonal entries, is column diagonally-dominant:

$$-[A(D)]_{jj} \ge \sum_{i=1,\; i \ne j}^{n} [A(D)]_{ij}.$$

Indeed, $A(D)$ is the sum of rank-one matrices of the form $-S_j[D_g]_{jj}S_j^\top$, $-R_j[D_h]_{jj}\tilde{R}_j^\top$ or $-\gamma B_j[D_v]_{jj}B_j^\top$. Each of these matrices has at most four non-zero elements, all of equal magnitude ($[D_g]_{jj}$, $[D_h]_{jj}$ or $\gamma[D_v]_{jj}$), and is (at least weakly) diagonally dominant. Indeed, matrices of the form $-\gamma B_j[D_v]_{jj}B_j^\top$ (or $-S_j[D_g]_{jj}S_j^\top$), where B_j (or S_j) connects two nodes, have four non-zero entries, two negative ones on the diagonal and two positive ones on the corresponding two columns and rows; matrices of the form $-R_j[D_h]_{jj}\tilde{R}_j^\top$, where R_j connects two nodes, have two non-zero entries, a negative one on the diagonal and a positive one on the same column; matrices of the form $-\gamma B_j[D_v]_{jj}B_j^\top$ (or $-R_j[D_h]_{jj}\tilde{R}_j^\top$), where B_j (or R_j) connects with node 0, have a single non-zero entry, negative, on the diagonal.

Note that, since it can be written as $\dot{z} = A(D(z))z$, where $A(D(z))$ is the sum of rank-one matrices, the system admits a BDC-decomposition and its stability can thus be tested by means of the numerical procedure proposed in [BG14] and in Chapter 6. The procedure would actually converge at the first iteration, providing the diamond (the unit ball of the 1-norm) as the unit ball of a polyhedral Lyapunov function for the system. In fact, it can be immediately seen that, since $A(D(z))$ is diagonally dominant and has negative diagonal entries, the function $V(z) = \|z\|_1$ (the 1-norm), is a (weak) Lyapunov function [Wil76, MKO78, BM15]. This proves Lyapunov stability, but unfortunately it does not prove asymptotic stability.

Since the graph is strongly connected, matrix $A(D(z))$ is irreducible, *i.e.*, no ordering of the variables exists such that it assumes a block-triangular form

$$A(D(z)) = \begin{bmatrix} A_{11}(D(z)) & \mathbf{0} \\ A_{21}(D(z)) & A_{22}(D(z)) \end{bmatrix}.$$

Moreover, in view of the assumption of external connection, matrix $[S\ R\ B]$ has at least one column with a single non-zero element; hence, at least one of the terms in the sum of rank-one matrices has a single (negative) diagonal entry. See [BFG+16] for details.

Since $A(D(z))$ is irreducible, has negative diagonal entries and is column diagonally dominant with at least one strictly dominant diagonal entry, the 1-norm is a strong Lyapunov function and $\bar{z} = 0$ is a globally asymptotically stable equilibrium ([Wil76, MKO78]; further details are in Theorems 1 and 2 and the following remarks in [Wil76] and in Theorem 4.60 in [BM15], where a thorough proof is provided). □

More flexibility in the control design can be ensured by choosing different gains for different control components:

$$v = \mathrm{sat}(-\Gamma B^\top z), \tag{10.11}$$

where $\Gamma = \mathrm{diag}(\gamma_1, \ldots, \gamma_m)$ is a positive definite diagonal matrix. It can be shown indeed that Theorem 10.1 equivalently holds if the control (10.6) is replaced by the control (10.11). In fact, from Lemma 10.1, $B\mathrm{sat}(-\Gamma B^\top z) = -(BD_v\Gamma B^\top z) = -(B\tilde{D}_v B^\top z)$, where $\tilde{D}_v$ is still a positive definite diagonal matrix. Hence, all of the derivations can be carried out as in the case of a scalar γ.

In general, if the graph is not strongly connected, then stabilisability and network-decentralised stabilisability are not equivalent, as clarified by the following example.

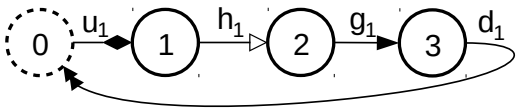

Figure 10.3: The graph in Example 10.2. [BFG+16]

Example 10.2. *The graph in Fig. 10.3 is connected (because* $[S\ R\ B]$ *has rank* $n = 3$*), but not strongly connected (because there is no admissible path leading from nodes* 2 *and* 3 *to node* 1*). Hence, the assumptions of Theorem 10.1 are not satisfied and the results in the theorem cannot be applied to this case. Assuming a linear model* $\dot{z} = Fz + Bv$*, it can be written*

$$F(D) = \begin{bmatrix} -D_2 & 0 & 0 \\ D_2 & -D_1 & D_1 \\ 0 & D_1 & -D_1 \end{bmatrix}, \quad B = \begin{bmatrix} 1 \\ 0 \\ 0 \end{bmatrix}.$$

Although the graph is not externally connected, the system is stabilisable (it is reachable), but not in a decentralised way: in a decentralised framework, v_1 *should be a function of* z_1 *only, but in this case no stabilisation would be possible, since the system is not detectable from output* $y = z_1$*. Hence, agent* v_1 *needs information also from* z_2 *and* z_3*, and no network-decentralised control can stabilise the system.*

The assumption of strong connectivity is now relaxed to provide a weaker result.

Theorem 10.2. *Under Assumptions 10.1-10.4, consider a system of the form* (10.3)*, whose graph is not strongly connected. Then the system can be globally uniformly stabilised by the network-decentralised control* (10.6) *if and only if the graph is externally connected.*

Proof. **Sufficiency**. If the system is not strongly connected, then *maximal strongly connected components* $\mathcal{C}_1, \mathcal{C}_2, \ldots, \mathcal{C}_N$ can be considered (such that, for each pair of nodes $i, j \in \mathcal{C}_k$, *admissible* paths exist in both directions, while for each pair of nodes with $i \in \mathcal{C}_k$ and $j \notin \mathcal{C}_k$, an *admissible* path in at least one direction is missing). The partition in maximal strongly connected components is illustrated in Fig. 10.4. The aggregate oriented graph formed by the strongly connected components, where a directed arc connects component l to component k if an admissible path leads from a node in l to a node in k, is acyclic. Indeed, the presence of a directed cycle, such as $\mathcal{C}_1, \mathcal{C}_2, \ldots, \mathcal{C}_N, \mathcal{C}_1$, would imply that $\mathcal{C}_1, \mathcal{C}_2, \ldots, \mathcal{C}_N$ form a strongly connected component, in contradiction with the fact that $\mathcal{C}_i$ are maximal.

The components can be associated with diagonal blocks of the closed-loop matrix $A(D)$. Since the aggregate graph is acyclic, considering the control (10.6) as before,

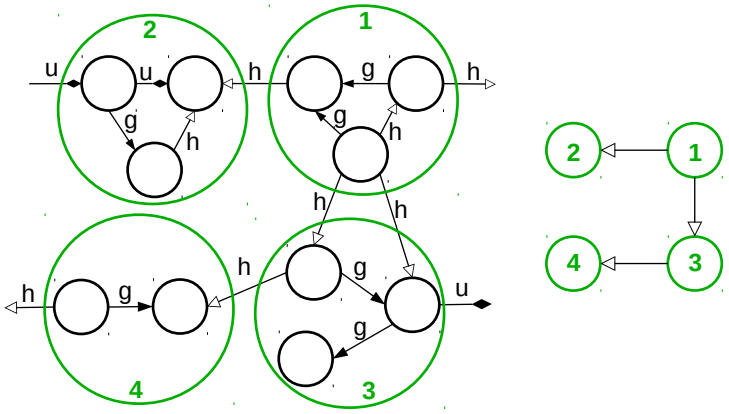

Figure 10.4: A graph where maximal strongly-connected components are encircled (left) and the corresponding aggregate graph (right). [BFG+16]

these blocks can be arranged so that $A(D)$ has a lower triangular form. In the case of Fig. 10.4, for instance,

$$A(D(z)) = \begin{bmatrix} A_{11}(D) & \mathbf{0} & \mathbf{0} & \mathbf{0} \\ A_{21}(D) & A_{22}(D) & \mathbf{0} & \mathbf{0} \\ A_{31}(D) & \mathbf{0} & A_{33}(D) & \mathbf{0} \\ \mathbf{0} & \mathbf{0} & A_{43}(D) & A_{44}(D) \end{bmatrix}.$$

All the diagonal blocks $A_{ii}(D)$ are irreducible matrices, because they correspond to strongly connected components, and are weakly diagonally dominant. Moreover, $A_{ii}(D)$, $i = 1, 2, \ldots N-1$, must have a diagonal entry that is strictly diagonally dominant, referred to $A_{ii}(D)$ (due to a connection either with another block, or with the external node; otherwise there would not be external connection) and $A_{NN}(D)$ must have a strictly dominant diagonal entry (again, due to the assumed external connection). See [BFG+16] for details. Then, since all the $A_{ii}(D)$ are irreducibly diagonally dominant with negative diagonal entries, all the corresponding subsystems are asymptotically stable; in view of the block-triangular form, this implies asymptotic stability of the overall system [BM15].

Necessity. If the system is not externally connected, then it can be partitioned into the subset $\mathcal{C}$ of nodes connected to node 0 and the subset $\mathcal{D}$ of nodes not connected to 0. Then $[S\ R\ B]$ can be partitioned accordingly as

$$[S \mid R \mid B] = \left[\begin{array}{cc|cc|cc} S_1 & \mathbf{0} & R_{11} & \mathbf{0} & B_1 & \mathbf{0} \\ \mathbf{0} & S_2 & R_{21} & R_{22} & \mathbf{0} & B_2 \end{array}\right],$$

where R_{21} is non-negative and all the columns of the sub-matrices S_2, R_{22} and B_2 have two non-zero elements, equal to -1 and 1, hence the sum of the entries in each column is 0 (see [BFG+16] for details).

Let the control be partitioned into two vectors, v_1 and v_2, corresponding to B_1 and B_2. For the control to be decentralised, v_1 must be a function of z_1 only and v_2

of z_2 only: $v_1 = v_1(z_1)$, $v_2 = v_2(z_2)$. The overall system can be written as

$$\begin{cases} \dot{z}_1 = S_1 g_1(z_1) + R_{11} h_1(z_1) + B_1 v_1(z_1) \\ \dot{z}_2 = S_2 g_2(z_2) + R_{21} h_1(z_1) + R_{22} h_2(z_2) + B_2 v_2(z_2) \end{cases}$$

Assume by contradiction that the closed-loop system is stable; if $z_1(0) = 0$, then $z_1(t) = 0$ and $v_1(t) = 0 \; \forall \; t \geq 0$, while

$$\dot{z}_2 = S_2 g_2(z_2) + R_{22} h_2(z_2) + B_2 v_2(z_2).$$

Then, consider the function $\mathrm{sum}(z_2) = \bar{1}^\top z_2$. Its derivative is $\bar{1}^\top \dot{z}_2 = \bar{1}^\top [S_2 g_2 + R_{22} h_2 + B_2 v_2] = 0$, because S_2, R_{22} and B_2 have zero-sum columns. Therefore, if $\mathrm{sum}(z_2(0)) = \kappa \neq 0$, then $\mathrm{sum}(z_2(t)) = \kappa \neq 0 \; \forall \;\; t \geq 0$. Hence, $z_2(t)$ does not converge to 0 and there is no asymptotic stability. □

Remark 10.1. *The control in the original variables has the form*

$$u = \bar{u} + sat[-\gamma B^\top (x - \bar{x})].$$

Therefore, the control agents must know the local *equilibrium values of $\bar{u}$ and $\bar{x}$ associated with the arcs they control and with the nodes to which they are directly connected. This means that the control $u = sat(-\gamma B^\top x)$ considered in [BBGP13], applied* tout court*, may not be stabilising. This issue is further discussed in [BFG+16] by means of an example.*

It is worth stressing that, in the absence of a control action, the stability result provided in [MKO78, JS93] for compartmental systems of the form $\dot{z} = Sg(z) + Rh(z)$ are recovered. In fact, if $B = 0$, then the system (10.3) is asymptotically stable if and only if $\mathrm{rank}[S \; R] = n$. Actually, for systems of the form $\dot{z} = Sg(z) + Rh(z)$, the condition $\mathrm{rank}[S \; R] = n$ is equivalent to the existence of a "path to the outside world" according to Theorem 7 in [MKO78].

10.2.1 A Slightly Different Control Strategy

A control similar to (10.6) can be considered:

$$v = \mathrm{sat}(-\gamma \tilde{B}^\top z), \tag{10.12}$$

where $\tilde{B} = \min\{B, 0\}$, componentwise. This control is suitable for applications in which the controlled flow in each link is decided based on the departure node only (this typically happens, for instance, in data communication networks). The theory is essentially unchanged, apart from Definition 10.1 that must be revised: a path can be considered *admissible* only if both u-type and h-type arcs, whenever included, have path-consistent orientation. Then, along the same lines of the previous theorems, it can be proved that the control (10.12) is stabilising if and only if the overall system is externally connected.

10.3 Decentralised Asymptotic Optimality

Inspired by (10.6), a different network-decentralised strategy is proposed that considers just the marginally stable part of the system and achieves optimality at steady state for any d compatible with the flow constraints (as in Assumption 10.4).

Given a system of the form (10.1), assume that the nodes are grouped into *macro-nodes*. Each macro-node is a subsystem with compartmental dynamics:

$$\dot{x}_i = S_i g_i^*(x_i) + R_i h_i^*(x_i) + \sum_{j \in \mathcal{C}_i} B_{ij} u_j + d_i, \tag{10.13}$$

$i = 1, 2, \ldots, N$, where $x_i(t) \in \mathbb{R}^{n_i}$ and $\mathcal{C}_i$ is the set that indexes control agents $u_j \in \mathbb{R}^{m_i}$ affecting macro-node i. Let $[S\ R] = \left[[S_1\ R_1]^\top\ [S_2\ R_2]^\top \ldots [S_N\ R_N]^\top\right]^\top$. This model accounts for the case in which there is no shared dynamics between the macro-nodes, except that pairs of them can be influenced by the same control agent u_i. This is relevant, for instance, when modelling traffic between nodes, where at each node the traffic splits in several direction according to some dynamic model (examples of such models will be considered in Chapter 11, Section 11.1).

According to [BFG+16], the following assumption is required.

Assumption 10.5. *The uncontrolled system* (10.1)*, composed of subsystems of the form* (10.13) *with* $u_j = 0$*, is* input-to-state stable within the left kernel of $[S\ R]$*: for each perturbation* $\bar{d}$ *that is orthogonal to the left kernel of* $[S\ R]$ *(*i.e.*,* $E^\top [S\ R] = 0$ *implies* $E^\top \bar{d} = 0$*), there exist a unique steady state* $\bar{x}$ *such that* $0 = Sg^*(\bar{x}) + Rh^*(\bar{x}) + \bar{d}$*. Moreover, for all* $\delta \in ker[S\ R]^\top$*,* $\|\delta\| \leq \bar{\delta}$*, such that* $d(t) = \bar{d} + \delta$*, and all initial conditions* $x(0) = \bar{x} + z$*, with* $z \in ker[S\ R]^\top$*, it can be written that*

$$\|x(t) - \bar{x}\| \leq C_1 \bar{\delta} + C_2 \phi(t) \|x(0) - \bar{x}\|,$$

where C_1 *and* C_2 *are positive constants, while* $\phi(t)$ *is a continuous positive function, strictly decreasing and converging to* 0 *as* $t \to \infty$*.*

Linear marginally stable systems with an eigenvalue at $\lambda = 0$ satisfy Assumption 10.5 (see Proposition 11.3, Section 11.1.3, and the examples in Section 11.1).

The original variable x is now reconsidered and it is assumed that 0 is the *reference level* (which is not necessarily the steady state $\bar{x}$). Being the demand d unknown to the controller, exact convergence to the desired value cannot be assured and just convergence to a finite ball can be guaranteed, according to the following result.

Lemma 10.2. *Under Assumptions 10.1-10.5, denote by* $E^\top$ *a basis of the left kernel of* $[S\ R]$*:* $E^\top [S\ R] = 0$*. Then the control*

$$u = sat(-\gamma B^\top E E^\top x) \tag{10.14}$$

assures that, from any initial condition, the system converges to a finite ball $\|x\| \leq \mu$*, for some* $\mu > 0$*, if and only if*

$$u^- < -E^\top d < u^+. \tag{10.15}$$

Proof. By applying the transformation $e = E^\top x$ and $f = F^\top x$, with $[E\ F]$ invertible, the system can be represented as

$$\begin{cases} \dot{e} = E^\top B u + E^\top d \\ \dot{f} = F^\top S\hat{g}(e,f) + F^\top R\hat{h}(e,f) + F^\top B u + F^\top d \end{cases} \tag{10.16}$$

where the e-subsystem can be stabilised if and only if $u^- < -E^\top d < u^+$ [BMU00]; provided that the demand is compatible with the constraints, the control $u = \mathrm{sat}(-\gamma B^\top E e)$ assures convergence of e to some $\bar{e}$. Hence, considering the f-subsystem, in view of Assumption 10.5, it can be shown that also $f(t)$ converges to a bounded equilibrium (see [BFG+16] for details). □

The set of all equilibrium conditions $\bar{x}$ and $\bar{u}$ is parameterised by the equation $Sg(\bar{x}) + Rh(\bar{x}) + B\bar{u} + d = 0$; equivalently,

$$S_i g_i(\bar{x}_i) + R_i h_i(\bar{x}_i) + \sum_{j \in \mathcal{C}_i} B_{ij}\bar{u}_j + d_i = 0, \quad \forall\ i. \tag{10.17}$$

Lemma 10.3. *Let d and $\bar{x}$ be as in Assumption 10.5. Then, $\bar{u}$ is an admissible steady-state control input if and only if*

$$\bar{u} \in \Omega(d) = \{u \in \mathcal{U} :\ E^\top B u + E^\top d = 0\}. \tag{10.18}$$

The proof is based on Lemma 10.2 and on the transformation (10.16). The next property from [BBGP13] is valid for pure buffer systems (namely, systems of the form $\dot{x} = Bu + d$).

Theorem 10.3. *[BBGP13] Assume $E = I$ (the identity), $S = 0$, $R = 0$ and the set $\Omega(d)$ in* (10.18) *has a non-empty interior. Then the (network-decentralised) control* (10.14) *assures convergence to some equilibrium $\bar{x}$ and the corresponding control value at steady state has minimum Euclidean norm:*

$$\lim_{t\to\infty} u(t) = \bar{u} = \arg\min_{u \in \Omega(d)} \|u\|. \tag{10.19}$$

The asymptotic minimum-norm property holds as well in the case of compartmental systems.

Theorem 10.4. *If condition* (10.15) *of Lemma 10.2 is satisfied and Assumptions 10.1-10.5 hold, then the control* (10.14) *is asymptotically optimal,* i.e.*, converges to the vector in $\Omega(d)$ having minimum Euclidean norm in the sense of* (10.19).

Proof. Since the control is stabilising and continuous, $u(t) \to \bar{u}$, where $\bar{u}$ is a finite value; from (10.16), the variable $e(t)$ converges to some finite $\bar{e}$ and, by assumption, the variable $f(t)$ converges to some finite $\bar{f}$.

The control $u = \text{sat}(-\gamma B^\top E E^\top x) = \text{sat}(-\gamma B^\top E e)$ is a function of $e = E^\top x$ only and Theorem 10.3 can be applied to the e-subsystem

$$\dot{e} = E^\top B \text{sat}(-\gamma B^\top E e) + E^\top d,$$

considering $\tilde{B} = E^\top B$ and $\tilde{d} = E^\top d$. Hence, the control u converges to the minimum norm control $\bar{u}$ inside $\Omega(d)$. □

A suitable choice of matrix E can guarantee asymptotic optimality in a network-decentralised way. To this aim, the concept of network-decentralised control must be extended to the macro-node case.

Denoting by $\mathcal{S}_j$ the set that indexes macro-nodes directly affected by agent u_j, *i.e.*, subsystems associated with the non-zero components of the block-column B_j, the control is *network-decentralised* if any agent $u_j \in \mathbb{R}^{m_i}$ decides its action based on the state variables in $\mathcal{S}_j$ only: $u_j = \Phi_j(x_k,\ k \in \mathcal{S}_j)$. For instance, if $B_j = [\ 0\ \ B_{2j}^\top\ \ 0\ \ B_{4j}^\top\ \ B_{5j}^\top\ ]^\top$, then u_j is a function of vectors x_2, x_4, and x_5.

The control (10.14) is network-decentralised if matrix E is chosen of a proper block-diagonal form.

Proposition 10.1. *Given the system composed by decoupled subsystems of the form* (10.13)*, take matrix E as*

$$E^\top = \text{blockdiag}\{E_1^\top, E_2^\top, \ldots, E_N^\top\}, \tag{10.20}$$

where $E_i^\top$ is a basis of the left kernel of S_i: $E_i^\top S_i = 0$. Then the control (10.14) *is network-decentralised.*

The proof follows immediately from the fact that $EE^\top$ is block-diagonal.

Remark 10.2. *The control $u = sat(-\gamma B^\top x)$ in [BBGP13] is asymptotically optimal if $A = 0$. However, unlike* (10.6) *($u = \bar{u} + sat[-\gamma B^\top (x - \bar{x})]$) and* (10.14)*, such a control is not optimal when $A \neq 0$. In this case, it might even lead to instability, even if the demand flow is compatible with the constraints, as already mentioned in Remark 10.1 and as more thoroughly discussed in [BFG+16].*

Remark 10.3. *The proposed control choice minimises the* controlled flow *(not the overall flow). Optimality with respect to the weighted norm $u^\top \Sigma^2 u$, with diagonal Σ, can be easily achieved by scaling the columns of matrix B as $B\Sigma^{-1}$. It must be stressed that achieving a minimum* overall flow *is not a simple task in this* structural *setup, since the functions g and h are unknown.*

10.4 Robustness

Since functions g^* and h^* are not known, the proposed control is intrinsically robust. As mentioned earlier, thanks to the fact that the achieved results are based on

Lyapunov functions, the control is robust even under switching topologies and when the unknown exogenous demand d is time-varying.

Robustness under switching topologies comes from the fact that the closed-loop system has been absorbed in a linear differential inclusion $\dot{z} = A(D)z$. If the matrices S, R, B are switching inside a set $\{S_k, R_k, B_k\}$, and the conditions of Theorems 10.1 or 10.2 are satisfied for each k, the resulting switching system corresponds to a set of linear differential inclusions $\dot{z} = A_k(D)z$, all sharing the 1-norm as a Lyapunov function. Therefore, asymptotic stability of the closed-loop system is preserved [BM15].

Dealing with an unknown exogenous demand d that is time-varying, possibly due to uncertainties on the equilibrium condition, is not an issue in the proposed setup. In fact, if a perturbation is present, then

$$\dot{z}(t) = A(D(t))z(t) + \Delta(t).$$

Clearly, exact convergence to 0 cannot be assured. However, if $\|\Delta(t)\| \leq \Delta_{max}$, a robust asymptotic bound of the form

$$\limsup_{t\to\infty} \|z(t)\| \leq Z$$

can be guaranteed if the linear differential inclusion is stable. The size of Z depends on Δ_{max} and on the specific parameters; hence, stability/boundedness can be assured only if the value of Δ_{max} is compatible with the control constraints.

10.5 Positivity Constraints

Compartmental systems are positive (*i.e.*, the positive orthant is positively invariant) and positivity of the variables naturally follows from physical considerations on the real systems modelled by the equations; hence, in some applications, positivity (or at least non-negativity) of the variables is necessary, because negative values of the variables would not be reasonable. A control action might thus be required to preserve the system positivity.

For the sake of simplicity, the linear case is considered, in which A_i are Metzler matrices. When the control $u = \text{sat}(-\gamma B^\top x)$ is applied, since the term $B\text{sat}(-\gamma B^\top x)$ can be written as $[-\gamma B D_v(x) B^\top]x$, for some state-dependent positive diagonal matrix $D_v(x)$ (see Lemma 10.1), the system can be rewritten as

$$\dot{x} = Ax - \gamma B D_v(x) B^\top x + d.$$

If B is an incidence matrix, $[-\gamma B D_v(x) B^\top]$ is a Metzler matrix. Hence, provided that d is a positive vector, the overall system is positive.

Conversely, the control (10.14), $u = \text{sat}(-\gamma B^\top E E^\top x)$, does not preserve the positivity of the system. In practical applications such as flow systems, where

non-negativity of the variables is required, whenever a buffer becomes empty and a control agent tries to force an outgoing flow, that control must be inhibited. This might introduce chattering. An alternative solution might consist in imposing a non-zero reference level, greater than the physical zero level.

10.6 Buffer Systems with Integral Control

To ensure that the proposed control quickly drives the state variables sufficiently close to the desired set-point, it may be necessary to resort to a very large $\gamma > 0$. However, a too large γ results in an over-exploitation of the actuators, making the control infeasible in practice. Moreover, the control $\mathrm{sat}(-kx)$ for large k becomes close to the discontinuous control $\mathrm{sat}(-x)$, hence it becomes "almost chattering". To *exactly* reach the desired set-point, at least for some of the variables, with a value of γ that is not too large, it is possible to suitably equip the control arcs with integrators. A similar strategy, adopting a saturated proportional-integral control for port-Hamiltonian systems, has been proposed in [WvdS13a, WvdS13b, Wei16].

Given $\dot{x} = Bu + d$, where $x \in \mathbb{R}^n$, B corresponds to a strongly connected and externally connected graph, and d is a constant demand, assume that there is the need to drive the state x to its exact set-point value, regardless of the unknown demand. To this aim, consider the augmented system

$$\begin{cases} \dot{x} = Bu + d \\ \dot{\xi} = x \end{cases} \tag{10.21}$$

along with the saturated control strategy

$$u = \mathrm{sat}[-\gamma B^\top (x + \alpha\xi)], \quad \text{where} \quad \gamma,\ \alpha > 0. \tag{10.22}$$

Let the system state be $v_o = [x\ \xi]^\top$ and the overall demand $d_o = [d\ 0]^\top$; denoting by I_n the identity matrix of dimension n, the system can be written as

$$\dot{v}_o = A_o v_o + B_o u + d_o, \quad \text{where} \quad A_o = \begin{bmatrix} \mathbf{0} & \mathbf{0} \\ I_n & \mathbf{0} \end{bmatrix} \quad \text{and} \quad B_o = \begin{bmatrix} B \\ \mathbf{0} \end{bmatrix}.$$

The equilibrium, corresponding to the desired set-point, is given by

$$\begin{cases} B\bar{u} + d = 0 \\ \bar{x} = 0 \end{cases}$$

hence

$$B\mathrm{sat}[-\alpha\gamma B^\top \bar{\xi}] + d = 0.$$

This saturated control has exactly the same asymptotic expression of that previously discussed; therefore, it is still asymptotically optimal in terms of minimum Euclidean norm: $u = \mathrm{sat}(-\alpha\gamma B^\top \xi) = \arg\min_u \|u\|$ s.t. $Bu + d = 0$.

The new variable $z \doteq \frac{x}{\alpha} + \xi$ can be defined, so that the state vector becomes $v = [z \;\; \xi]^\top$. The corresponding state transformation leads to the transformed matrices

$$\hat{A} = T^{-1}A_oT = \begin{bmatrix} I_n/\alpha & I_n \\ \mathbf{0} & I_n \end{bmatrix} \begin{bmatrix} \mathbf{0} & \mathbf{0} \\ I_n & \mathbf{0} \end{bmatrix} \begin{bmatrix} \alpha I_n & -\alpha I_n \\ \mathbf{0} & I_n \end{bmatrix} = \begin{bmatrix} \alpha I_n & -\alpha I_n \\ \alpha I_n & -\alpha I_n \end{bmatrix},$$

$$\hat{B} = T^{-1}B_o = \begin{bmatrix} I_n/\alpha & I_n \\ \mathbf{0} & I_n \end{bmatrix} \begin{bmatrix} B \\ \mathbf{0} \end{bmatrix} = \begin{bmatrix} B/\alpha \\ \mathbf{0} \end{bmatrix}.$$

The transformed system is then $\dot{v} = \hat{A}v + \hat{B}u + \hat{d}$, where $\hat{d} = d_o/\alpha$. Since $\text{sat}[-\alpha\gamma B^\top z] = -\alpha\gamma D_u(z)B^\top z$, for a suitable $D_u(z)$, the closed-loop matrix is

$$\hat{A}_{cl} = \begin{bmatrix} \alpha I_n - \gamma B D_u B^\top & -\alpha I_n \\ \alpha I_n & -\alpha I_n \end{bmatrix}.$$

Adopting $P = I$ as a Lyapunov matrix, it can be seen that

$$\begin{aligned} v^\top(\hat{A}_{cl} + \hat{A}_{cl}^\top)v &= \begin{bmatrix} z^\top & \xi^\top \end{bmatrix} \begin{bmatrix} 2(\alpha I_n - \gamma B D_u B^\top) & \mathbf{0} \\ \mathbf{0} & -2\alpha I_n \end{bmatrix} \begin{bmatrix} z \\ \xi \end{bmatrix} \\ &= 2z^\top(\alpha I_n - \gamma B D_u B^\top)z - 2\alpha\|\xi\|^2 < 0 \end{aligned} \tag{10.23}$$

for any $v \neq 0$, provided that α is small enough and γ large enough. Hence, given γ, for a suitable choice of α, the system admits a quadratic Lyapunov function $V(v) = \|v\|^2$ that guarantees asymptotic stability. This ensures that the desired set-point $\bar{x} = 0$ is exactly reached at steady state. Note that, given a domain $\mathcal{B}_\mu$ (a ball of radius μ), we have a positive lower bound on the components of D_u. Hence, the following result can be stated.

Theorem 10.5. *An extended system of the form* (10.21)*, where B is a full rank matrix, can be uniformly stabilised by the control* (10.22)*, with a given domain of attraction $\mathcal{B}_\mu$, provided that $\alpha > 0$ is small enough and $\gamma > 0$ large enough. This control assures exact convergence of x to $\bar{x} = 0$ and is asymptotically optimal in norm.*

The ratio γ/α, according to (10.23), depends on μ: a larger μ requires a larger γ/α. Fig. 10.5 shows the simulations corresponding to system (10.21) with $n = 5$,

$$B = \begin{bmatrix} 1 & -1 & 0 & 0 & 0 & 0 \\ 0 & 1 & -1 & 0 & 0 & 0 \\ 0 & 0 & 1 & -1 & 0 & 0 \\ 0 & 0 & 0 & 1 & -1 & 0 \\ 0 & 0 & 0 & 0 & 1 & 1 \end{bmatrix}, \qquad d = \begin{bmatrix} 1 \\ -2 \\ 3 \\ -4 \\ 5 \end{bmatrix},$$

with the application of a control of the form (10.22), componentwise bounded in the interval $[-8\ 8]$, with $\alpha = 0.2$ and $\gamma = 10$, starting from initial conditions with components randomly generated in $[-5\ \ 5]$: $x(0) = [-4.07\ 0.37\ -4.91\ 4.15\ -1.43]$, $\xi(0) = [4.99\ -4.70\ 2.92\ -0.45\ 3.73]$. As expected, the desired set-point value $x = 0$ is exactly achieved at steady-state. The steady-state value of ξ is $\bar{\xi} = [0.25\ 0\ 0.75\ 0\ 1.25]$, while the steady-state control value is $\bar{u} = [-0.5\ 0.5\ -1.5\ 1.5\ -2.5\ -2.5]$.

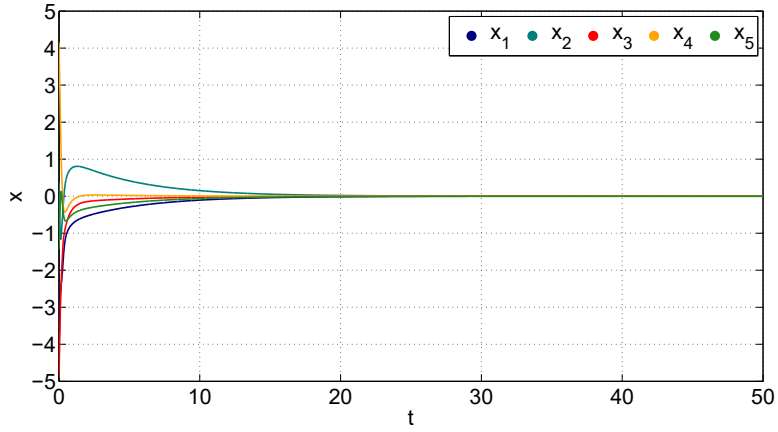

(a) Time evolution of x.

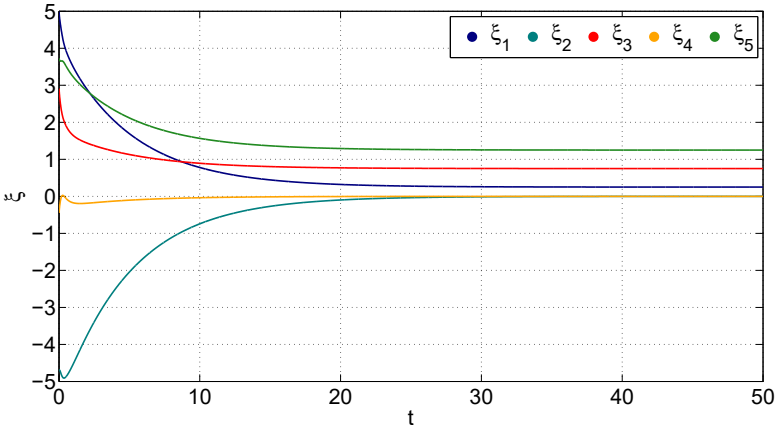

(b) Time evolution of ξ.

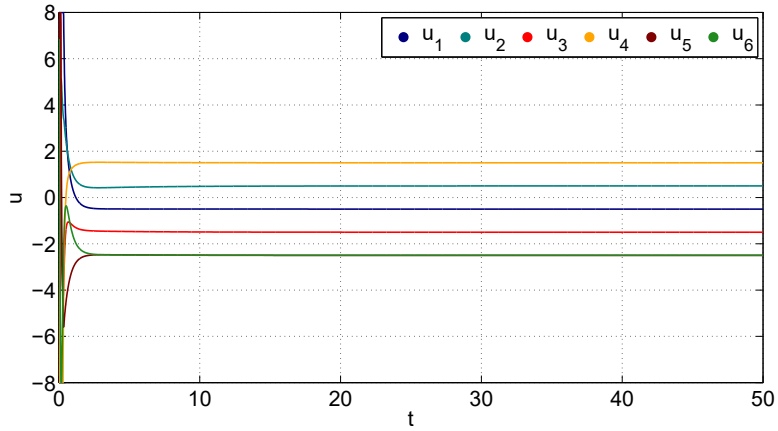

(c) Time evolution of u.

Figure 10.5: Simulation of the system in Section 10.6.

11

Network-Decentralised Control: Applications

In this chapter, various system are considered, pertaining to heterogeneous application domains ranging from computer and data-communication networks to clock synchronisation and vehicle platooning. They do not have much in common, apart from the fact that, in all of the proposed application examples, the overall system can be visualised as a graph (see Fig. 11.1), where the nodes correspond to individual subsystems with their own dynamics, while the arcs represent connections between the subsystems and are each associated with a control agent u_{ij}; also arcs associated with external, uncontrollable signals d_k may be present.

A control implementing a network-decentralised strategy will be applied to each example and its effectiveness will be shown via simulations.

11.1 Network-Decentralised Traffic Control

The relevance of flow control has been thoroughly discussed in Chapter 9; in particular, traffic and congestion control is crucial in several applications, ranging from packet forwarding and node-to-node data transfer in telecommunication networks to vehicle traffic regulation in transportation networks.

Any flow control problem is typically defined on a network that can always be associated with a graph, whose nodes represent buffers (subsystems) and whose arcs represent flow channels; the flow through an arc can be either spontaneous or controlled, according to a given strategy or protocol. Yet, traffic control problems have a peculiarity: the flow is formed by individual units, namely, by distinct elements (packets, vehicles, components to be assembled or delivered) each having an "identifier" and a precise destination node; hence, when arriving at each node, units must be redirected towards different directions (*i.e.*, different adjacent nodes), according to their destination node. This is evident in the case of computer networks, where the routers receive packets that must be forwarded towards different other routers, and in the case of vehicles, which at each intersection, crossroad or fork must take a different road; in both situations, the decision depends on the final destination,

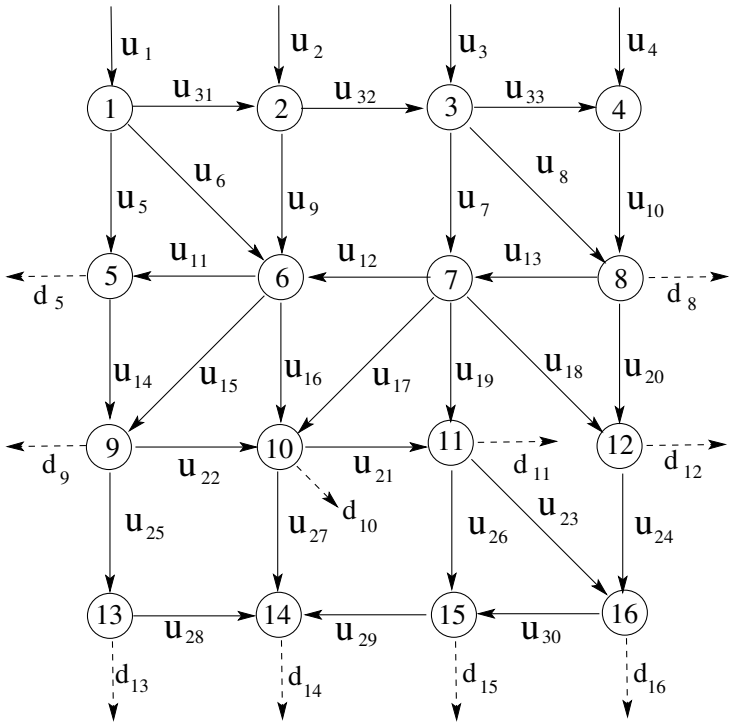

Figure 11.1: Example of a network graph.

routing criteria and available information about the traffic situation in the network. This feature of traffic systems highlights a remarkable difference with respect to other distribution systems; for instance, in the case of a water distribution system, molecules of water are not labelled with a precise destination and the demand can be satisfied by simply providing the required amount of water, regardless of its source. In traffic systems, conversely, traffic at each node (buffer) is naturally split in several queues (associated with flow streams having different forwarding directions), which can be characterised based on statistics and on *a priori* historical data about the flow splitting at the nodes.

This must be taken into account in an appropriate modelling framework. [BGM14] Therefore, assuming that a statistical distribution is available about the exit directions of the units composing the traffic stream, each node can be associated with a continuous-time stochastic matrix (a Metzler matrix with zero-sum columns), whose dynamics represent the internal traffic splitting; some of the states are associated with the different queues, hence with the arcs leaving the node (state j represents the amount of traffic waiting to be directed through arc j). A traffic-splitting model has been already discussed in Example 9.2 (Section 9.1.1) and in Section 9.5.3 of Chapter 9.

Given a network graph associated with a system having these peculiar properties, a solution is sought for the traffic control problem by means of a linear *network-decentralised* strategy [BFG13, BFG15a]: hence, the flow through each arc is

controlled by an agent having exclusively information about the congestion situation at the nodes it directly connects/affects (as illustrated in Chapter 9, this is equivalent to imposing that the state-feedback matrix has the same structure as the transpose of the overall input matrix of the system). At each node, the traffic partition in queues associated with different directions is not a controlled variable: in itself, this would not be an issue. The strategy in Chapter 9 can be applied, indeed, when the nodes are arbitrary subsystems, having their own, possibly unstable, dynamics; yet, it requires the knowledge of the node dynamics, while the stochastic matrices in traffic systems are typically uncertain and can even depend on external factors. In fact, they are likely to be time-varying (for instance, traffic of both packets in computer networks and vehicles in the streets completely changes, in terms of intensity and of distribution, at different times of the day) and completely unknown to the controller (estimates based on historical data would be definitely unreliable for control purposes). To face this major challenge, a "robust" version of the network-decentralised strategy must be devised to assure stability regardless of the stochastic parameters (which are not known to the control agents).

Indeed in this section, following [BGM14], a robust network-decentralised control strategy is proposed under the assumption that zero is a simple eigenvalue for all of the stochastic matrices associated with the nodes (which is always true in the case of irreducible matrices). With this strategy, each control agent needs just to have cumulative information about the total amount of traffic (congestion) at each of the nodes it affects, and can ignore the actual traffic splitting distribution at the nodes.

Remarkably, the control proposed in [BGM14] can stabilise the system without requiring any knowledge of both: (a) the internal traffic splitting statistics at the nodes (namely, the entries of the stochastic matrices); (b) the actual distribution of the traffic among the different queues at the nodes (namely, the internal state variables of the subsystems).

This network-decentralised strategy is shown to be

- robust (since stability is ensured independent of the particular values of the stochastic matrix entries),
- effective even in the presence of flow capacity constraints (which extends the results in [BBGP13]),
- asymptotically optimal in terms of minimum Euclidean-norm (as follows from the results in Chapter 10); this is an important feature in a traffic control framework, since it assures fairness, *i.e.*, an equally distributed traffic load among the controlled flow arcs.

Also the case in which zero is a multiple eigenvalue for at least one stochastic matrix is briefly discussed. [BGM14]

Further developments may consider constraints on both state and flow control variables. In particular, dealing with positivity constraints and with upper bounds due to the buffer size is important, as mentioned in Chapter 10.

11.1.1 Networks with Node Traffic Splitting

A portion of a typical network, whose nodes represent buffers and are connected by arcs representing flow channels, is sketched in Fig. 11.2. Each connection between two nodes includes one or two directed arcs, denoted as u_k, and is controlled by an agent, denoted as v_h: the presence of a pair of directed arcs, in opposite directions, indicates that the same agent can control the flow in both directions. Conversely, arcs denoted as d_j represent an exogenously determined flow. At each of the nodes

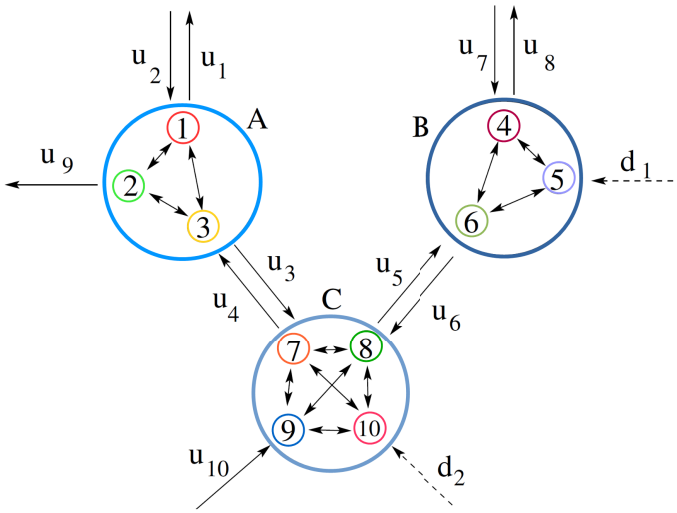

Figure 11.2: An example of network with traffic splitting dynamics inside each node.

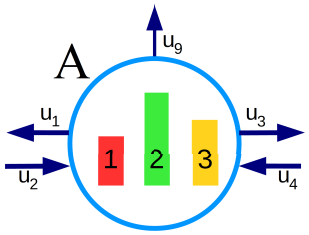

Figure 11.3: At each node, the traffic is split into queues having different destinations.

in Fig. 11.2, denoted by A, B and C, the traffic is split in queues with different destinations. In node A, the different queues are associated with subnodes 1 (traffic directed to the north), 2 (traffic directed to south-east) and 3 (traffic directed to the west); the partition into queues is illustrated in Fig. 11.3. In node B, the different queues are associated with subnodes 4 (traffic directed to the north) and 6 (traffic directed to south-west), while subnode 5 is associated with uncontrolled incoming traffic from the east. In node C, the queues are associated with subnodes 7 (traffic directed to north-west) and 8 (traffic directed to north-east), while subnode 9 is

associated with controlled incoming traffic from south-west and subnode 10 with uncontrolled incoming traffic from south-east.

Traffic splitting among different directions can be modelled as a dynamic process, represented by a stochastic matrix: for instance, the traffic splitting dynamics of node A in Fig. 11.2, whose internal queues are visualised in Fig. 11.3, could be represented by the matrix

$$M_A = \begin{bmatrix} -(\alpha+\beta) & \zeta & \varepsilon \\ \alpha & -(\zeta+\delta) & \varphi \\ \beta & \delta & -(\varepsilon+\varphi) \end{bmatrix},$$

where Greek letters denote splitting rates. Hence, each traffic unit reaching subnode 1 is directed either towards subnode 2 or towards subnode 3, with splitting rates $\alpha > 0$ and $\beta > 0$ respectively; each traffic unit reaching subnode 2 is directed either towards subnode 1 or towards subnode 3, with splitting rates $\zeta > 0$ and $\delta > 0$ respectively; each traffic unit reaching subnode 3 is directed either towards subnode 1 or towards subnode 2, with splitting rates $\varepsilon > 0$ and $\varphi > 0$ respectively. Assume, for the moment being, that $\zeta = \delta = \varepsilon = \varphi = 0$; then, all the units at subnode 1 are transferred either to subnode 2 or to subnode 3, with a proportion given by the values α and β. Starting from initial conditions of the form $x_1(0) = \xi$, $x_2(0) = x_3(0) = 0$, in the absence of external arc flows (namely, $u_i = 0$ and $d_i = 0$ for all i), the corresponding asymptotic value of the state is

$$[x_1(\infty) \quad x_2(\infty) \quad x_2(\infty)] = \frac{\xi}{\alpha+\beta} \quad [0 \quad \alpha \quad \beta].$$

The arc flows u_1, u_9 and u_3 redirect to other nodes the units in subnodes 1, 2 and 3 (respectively) of node A. The transfer process can be seen as exponential, associated with mode $e^{-(\alpha+\beta)t}$ (an instantaneous transfer process would be unrealistic). Then, the magnitude of $\alpha+\beta$ is associated with the speed of the transfer process, while the relative magnitudes $\alpha/(\alpha+\beta)$ and $\beta/(\alpha+\beta)$ are associated with the traffic splitting distribution. The overall traffic distribution at node A can be modelled, of course, by considering positive α, β, ζ, δ, ε and φ.

More in general, a class of linear, interconnected subsystems is considered [BGM14]

$$\dot{x}_i(t) = A^{(i)} x_i(t) + \sum_{j \in \mathcal{C}_i} B_{ij} v_j(t) + D_i d(t),$$

where $x_i(t) \in \mathbb{R}^{n_i}$, $i = 1, \ldots, N$, is the state of the ith buffer; $v_j(t) \in \mathbb{R}^{m_j}$, $j = 1, \ldots, M$, are the control agents; $\mathcal{C}_i$ is the set that indexes the agents affecting the ith buffer; B_{ij} represents the effect of the control agent v_j on the ith buffer; $d(t)$ is an external, non-controllable signal, bounded in a compact and convex set $\mathcal{D}$, affecting the ith buffer through matrix D_i. Matrices $A^{(i)}$ are continuous-time stochastic matrices.

Assumption 11.1. *For all i, matrix $A^{(i)}$ is a Metzler matrix with zero sum columns:*

$$[A^{(i)}]_{kj} \geq 0, \quad k \neq j, \qquad \sum_{k=1}^{n_i} [A^{(i)}]_{kj} = 0.$$

Equivalently, it can be written that

$$\bar{1}_{n_i}^\top A^{(i)} = 0,$$

where $\bar{1}_{n_i}$ is the ones vector having size n_i. The symbol $e_n = \bar{1}_{n_i}/\sqrt{n_i}$ is introduced to denote the averaged unit vector with n_i components:

$$e_{n_i} = \left[\begin{array}{ccc} \frac{1}{\sqrt{n_i}} & \frac{1}{\sqrt{n_i}} \cdots & \frac{1}{\sqrt{n_i}} \end{array} \right]^\top.$$

The overall system can be written in the same form considered in (9.2) (and in [BFG13, BFG15a]):

$$\dot{x}(t) = Ax(t) + Bu(t) + Dd(t), \tag{11.1}$$

where $x(t) \in \mathbb{R}^n$ includes the state variables associated with each buffer, $u(t) \in \mathbb{R}^m$ is the control vector including all the agents $v_j(t)$, $d(t) \in \mathbb{R}^n$ is the vector representing an external, non-controllable signal affecting the system through the generic matrix D, while A and B are block-structured; in particular, $A \in \mathbb{R}^{n \times n}$ is the block-diagonal matrix

$$A = \text{blockdiag}\{A^{(1)}, \ldots, A^{(N)}\}. \tag{11.2}$$

All the considerations in Section 9.2 hold, concerning the dimension of the blocks, the special structure of matrix B and the associated hypergraph representation.

The system equilibrium, which can be the desired set-point in the case of buffers, is set to 0 without loss of generality (it is always possible to reduce the problem to this case by means of a variable translation).

Assumption 11.2. *(A, B) is stabilisable.*

Under stabilisability assumption, a network-decentralised control is sought. Hence, each agent v_j can have information from nodes in $\mathcal{N}_j$ only, $v_j = \varphi(x_i,\ i \in \mathcal{N}_j)$ and, in the case of a linear state-feedback control $u = -Kx$, K must have the same structural zero blocks as $B^\top$ (cf. Chapter 9 and [BFG13, BFG15a]).

Example 11.1. *In the case of Fig. 11.2, there are* 3 *nodes (A is labelled as node* 1*, B as node* 2 *and C as node* 3*) and* 6 *agents: $v_1 = [u_1^\top\ u_2^\top]^\top$, $v_2 = [u_3^\top\ u_4^\top]^\top$, $v_3 = [u_5^\top\ u_6^\top]^\top$, $v_4 = [u_7^\top\ u_8^\top]^\top$, $v_5 = u_9$, $v_6 = u_{10}$. The sets of agents affecting each of the nodes are: $\mathcal{C}_1 = \{1, 2, 5\}$, $\mathcal{C}_2 = \{3, 4\}$, $\mathcal{C}_3 = \{2, 3, 6\}$. The agents control the following nodes: $\mathcal{N}_1 = \{1\}$, $\mathcal{N}_2 = \{1, 3\}$, $\mathcal{N}_3 = \{2, 3\}$, $\mathcal{N}_4 = \{2\}$, $\mathcal{N}_5 = \{1\}$, $\mathcal{N}_6 = \{3\}$. Matrices B and D are*

$$B = \left[\begin{array}{cccccc} B_{11} & B_{12} & \mathbf{0} & \mathbf{0} & B_{15} & \mathbf{0} \\ \mathbf{0} & \mathbf{0} & B_{23} & B_{24} & \mathbf{0} & \mathbf{0} \\ \mathbf{0} & B_{32} & B_{33} & \mathbf{0} & \mathbf{0} & B_{36} \end{array} \right], \qquad D = \left[\begin{array}{cc} \mathbf{0} & \mathbf{0} \\ D_{21} & \mathbf{0} \\ \mathbf{0} & D_{32} \end{array} \right].$$

In this case, K should have the structure

$$K = \begin{bmatrix} K_{11}^\top & K_{12}^\top & \mathbf{0} & \mathbf{0} & K_{15}^\top & \mathbf{0} \\ \mathbf{0} & \mathbf{0} & K_{23}^\top & K_{24}^\top & \mathbf{0} & \mathbf{0} \\ \mathbf{0} & K_{32}^\top & K_{33}^\top & \mathbf{0} & \mathbf{0} & K_{36}^\top \end{bmatrix}^\top .$$

11.1.2 A Robust Network-Decentralised Solution

A robust solution can be achieved under the following assumption.

Assumption 11.3. *The eigenvalue $\lambda = 0$ of $A^{(i)}$ is simple for all i and all other eigenvalues have a strictly negative real part.*

The assumption holds if each $A^{(i)}$ is irreducible (namely, it cannot be recast in a block-triangular form by means of a variable permutation). However, this is a sufficient, but not a necessary condition; in fact, there are reducible matrices for which zero is a simple eigenvalue, as in the following example.

Example 11.2. *The matrix*

$$A^{(i)} = \begin{bmatrix} -(\alpha+\beta) & 0 & 0 \\ \alpha & -\zeta & \delta \\ \beta & \zeta & -\delta \end{bmatrix}, \quad \textit{with} \quad \alpha,\, \beta > 0 \quad \textit{and} \quad \zeta,\, \delta \geq 0,$$

is reducible and its spectrum is $\sigma(A^{(i)}) = \{-(\alpha+\beta), -(\zeta+\delta), 0\}$. Hence the eigenvalue 0 has multiplicity 2 if $\zeta = \delta = 0$, but is simple otherwise.

In view of Assumption 11.3, the following proposition is immediate.[1]

Proposition 11.1. *(A, B) is stabilisable iff rank$[A \;\; B] = n$.*

To robustly solve the stabilisation problem for the considered class of systems, a control can be sought of the form [BGM14]

$$u(t) = -\gamma B^\top H x(t), \tag{11.3}$$

where $\gamma > 0$ and

$$H = \text{blockdiag}\{e_{n_1} e_{n_1}^\top, \ldots, e_{n_i} e_{n_i}^\top, \ldots, e_{n_N} e_{n_N}^\top\}. \tag{11.4}$$

The candidate control (11.3)-(11.4) enjoys some relevant properties:

(a) it is network-decentralised (since matrix H is block-diagonal);

[1] Actually, it holds for generic extended buffer systems, see Definition 11.1, following as a special case of Theorem 10.1.

(b) it is robust (in fact, its expression does not depend on the parameters of the stochastic matrices);
(c) each control agent needs to know the cumulative buffer content only, and not its internal distribution. In fact, notice that

$$e_{n_i} e_{n_i}^\top = (\bar{1}_{n_i}/\sqrt{n_i})\ (\bar{1}_{n_i}^\top/\sqrt{n_i}) = \bar{\mathbf{1}}_{\mathbf{n_i}}/n_i,$$

where $\bar{\mathbf{1}}_{\mathbf{n_i}}$ is an $n_i \times n_i$ matrix of ones. Then

$$u(t) = -\gamma B^\top \begin{bmatrix} \frac{\bar{1}_{n_1}}{n_1} & \mathbf{0} & \dots & \mathbf{0} \\ \mathbf{0} & \frac{\bar{1}_{n_2}}{n_2} & \dots & \mathbf{0} \\ \vdots & \vdots & \ddots & \vdots \\ \mathbf{0} & \mathbf{0} & \dots & \frac{\bar{1}_{n_N}}{n_N} \end{bmatrix} \begin{bmatrix} y_1(t) \\ y_2(t) \\ \vdots \\ y_N(t) \end{bmatrix}, \qquad y_i(t) = \bar{1}_{n_i}^\top x_i(t), \qquad (11.5)$$

where $y_i(t)$ is the cumulative stock of buffer i, namely, the sum of all the state variables of the ith subsystem (node).

In principle, to check whether the stabilisability Assumption 11.2 is satisfied, according to Proposition 11.1 the matrices $A^{(i)}$ should be known (in order to compute rank$[A \;\; B]$). Yet, interestingly, this is not necessary if Assumption 11.3 holds.

Corollary 11.1. *Under Assumption 11.3, stabilisability is equivalent to*

$$\mathit{rank} \left(\begin{bmatrix} \bar{1}_{n_1}^\top & \mathbf{0} & \dots & \mathbf{0} \\ \mathbf{0} & \bar{1}_{n_2}^\top & \dots & \mathbf{0} \\ \vdots & \vdots & \ddots & \vdots \\ \mathbf{0} & \mathbf{0} & \dots & \bar{1}_{n_N}^\top \end{bmatrix} B \right) = N.$$

The proof of Corollary 11.1 is provided within the proof of the following theorem, which is the main result of this section.

Theorem 11.1. *Under Assumptions 11.2 and 11.3, the network-decentralised control (11.3)-(11.4) robustly stabilises the system.*

Proof. Let E_n denote the orthonormal complement of vector e_n: $\begin{bmatrix} e_n^\top \\ E_n^\top \end{bmatrix} \begin{bmatrix} e_n & E_n \end{bmatrix} = I_n$. Since all of the matrices $A^{(i)}$ have zero sum columns,

$$\begin{bmatrix} e_{n_i}^\top \\ E_{n_i}^\top \end{bmatrix} A^{(i)} \begin{bmatrix} e_{n_i} & E_{n_i} \end{bmatrix} = \begin{bmatrix} 0 & 0 \\ E_{n_i}^\top A^{(i)} e_{n_i} & E_{n_i}^\top A^{(i)} E_{n_i} \end{bmatrix},$$

where $E_{n_i}^\top A^{(i)} E_{n_i}$ has only negative real part eigenvalues (0 is a simple eigenvalue).

Consider the orthonormal transformation given by the square matrix

$$T = [\text{blockdiag}\{e_{n_k}\} \;\; \text{blockdiag}\{E_{n_k}\}], \quad k = 1, \dots, N,$$

with $T^\top T = I_n$. Hence $T^\top AT = \begin{bmatrix} \mathbf{0} & \mathbf{0} \\ G & F \end{bmatrix}$, where both $G = \text{blockdiag}\{E_{n_k}^\top A^{(k)} e_{n_k}\}$, $F = \text{blockdiag}\{E_{n_k}^\top A^{(k)} E_{n_k}\}$, $k = 1, \dots, N$, are block-diagonal and F is stable. The transformed input matrix is then $T^\top B = \begin{bmatrix} B_0 \\ B_S \end{bmatrix}$. Since

$$HT = [\text{blockdiag}\{e_{n_k}\} \;\; \text{blockdiag}\{\mathbf{0}\}], \quad k = 1, \dots, N,$$

the transformed control (11.3) can be expressed as

$$\hat{u} = -\gamma B^\top HT\hat{x} = -\gamma \left[\begin{array}{cc} B_0^\top & \mathbf{0} \end{array} \right] \hat{x} \tag{11.6}$$

and the closed-loop matrix is

$$T^\top AT - \gamma T^\top BB^\top HT = \left[\begin{array}{cc} -\gamma B_0 B_0^\top & \mathbf{0} \\ G - \gamma B_S B_0^\top & F \end{array} \right]. \tag{11.7}$$

In view of the Popov criterion, since 0 is the only unstable eigenvalue, stabilisability is equivalent to

$$\text{rank}[A|B] = \left[\begin{array}{cc|c} \mathbf{0} & \mathbf{0} & B_0 \\ G & F & B_S \end{array} \right] = n,$$

hence B_0 has rank N (the last claim proves Corollary 11.1). Then, the $N \times N$ matrix $-\gamma B_0 B_0^\top$ is negative definite. Since F is stable, this in turn implies stability of the overall system. □

11.1.3 Robust Solution Under Saturation

Addressing Flow Constraints

Along the lines in [BBGP13], it can be shown that, in the presence of flow constraints, the proposed network-decentralised stabilising control is effective as well.

Suppose that control flows are subject to capacity constraints in a box, $u(t) \in \mathcal{U} \doteq \{u \in \mathbb{R}^m : u_i^- \leq u_i \leq u_i^+, \, \forall i\}$; then, a saturated network-decentralised control can be considered:

$$u(t) = \text{sat}[-\gamma B^\top Hx(t)], \tag{11.8}$$

with $\gamma > 0$ and H as in (11.4), such that $u(t) \in \mathcal{U}$.

Proposition 11.2. *Under the assumptions of Theorem 11.1, the network-decentralised saturated control* (11.8) *robustly stabilises system* (11.1) *in the presence of a constant vector $d \in \mathcal{D}$, provided that $D\mathcal{D} \subset -int(B\mathcal{U})$.*

Proof. In the presence of a saturated control and a suitable disturbance vector, the closed-loop system becomes

$$\left[\begin{array}{c} \dot{x}_0 \\ \dot{x}_S \end{array} \right] = \left[\begin{array}{c} B_0 \text{sat}(-\gamma B_0^\top x_0) \\ Gx_0 + B_S \text{sat}(-\gamma B_0^\top x_0) + Fx_S \end{array} \right] + \left[\begin{array}{c} \hat{d}_0 \\ \hat{d}_S \end{array} \right].$$

Since matrix B_0 has full row rank and matrix F is stable, stability of the overall system, regardless of the stochastic parameters, follows from [BBGP13] (see [BGM14] for details). □

Asymptotic Optimality

Asymptotic optimality of the saturated robust control follows from the results of Section 10.3, Chapter 10, which clearly hold as well when the functions g and h are linear: (10.13) becomes

$$\dot{x}_i = A^{(i)} x_i + \sum_{j \in \mathcal{C}_i} B_{ij} u_j + d_i, \tag{11.9}$$

where $A^{(i)}$ are Metzler matrices (namely, $[A^{(i)}]_{pq} \geq 0$ for $p \neq q$).

Definition 11.1. *System* (11.9) *is a* buffer system *if* $A^{(i)} = 0$. *It is an* extended buffer system *if* $A^{(i)}$ *is either asymptotically stable or marginally stable with marginally stable eigenvalue* $\lambda = 0$ *(of any multiplicity).*

For the systems considered here, Assumption 10.5 in Chapter 10 is equivalent to requiring that A is either asymptotically stable, or marginally stable without purely imaginary eigenvalues.

Proposition 11.3. *An extended buffer system of the form* (11.9) *is stable in the left kernel,* i.e.*, satisfies Assumption 10.5.*

Proof. By means of a suitable transformation, the overall system matrix can be recast in a block-diagonal form, where each diagonal block has the form

$$\begin{bmatrix} \mathbf{0} & \mathbf{0} \\ P_k & Q_k \end{bmatrix},$$

with zero sub-blocks of the same dimension of the left kernel of $A^{(i)}$ (since the system is stable by assumption, the eigenvalue 0 does not have Jordan blocks of dimension greater that 1), while matrices Q_k have no zero eigenvalues, hence are asymptotically stable. If d is orthogonal to the left kernel of A, then the transformed $\hat{d}$ has zero components corresponding to the zero blocks of $\hat{A}^{(i)}$ and the system $\frac{d}{dt}\hat{x}(t) = \hat{A}\hat{x}(t) + \hat{d}$ is the parallel of systems of the form

$$\frac{d}{dt}\hat{x}_i(t) = \begin{bmatrix} \mathbf{0} & \mathbf{0} \\ P_i & Q_i \end{bmatrix} \hat{x}_i(t) + \begin{bmatrix} \mathbf{0} \\ \hat{d}_i \end{bmatrix},$$

which satisfy Assumption 10.5, because their state is bounded. Hence the overall system satisfies the assumption. Details are provided in [BFG+16]. □

Based on these results, it can be shown that, in the special case in which $A^{(i)}$ are continuous-time stochastic matrices, the robust network-decentralised strategy is also asymptotically optimal.

Theorem 11.2. *If the dominant eigenvalue $\lambda = 0$ is simple for all matrices $A^{(i)}$, the network-decentralised control* (11.3)-(11.4) *robustly stabilises the system and is asymptotically optimal in norm.*

11.1.4 A Non-Robust Network-Decentralised Solution

In general, when $\lambda = 0$ cannot be assumed to be a simple eigenvalue for all $A^{(i)}$, it might not be possible to find a robust network-decentralised control. Only a control depending on the $A^{(i)}$ can be found:

$$u(t) = -\gamma B^\top W x(t), \tag{11.10}$$

with $\gamma > 0$ and

$$W = \text{blockdiag}\{V_{n_1}V_{n_1}^\top, \dots, V_{n_i}V_{n_i}^\top, \dots, V_{n_N}V_{n_N}^\top\}, \tag{11.11}$$

where V_{n_i} denotes any orthonormal basis of the left kernel (namely, the left eigenspace of the 0 eigenvalue) of matrix $A^{(i)}$: $V_{n_i}^\top A^{(i)} = 0$.

Theorem 11.3. *Under Assumption 11.2, the network-decentralised control (11.10)-(11.11) stabilises the system.*

The proof is analogous to that of Theorem 11.1. However, V_{n_i} are functions of the parameters. The exact knowledge of the parameters is not a realistic assumption in most cases and resorting to approximated values can lead to a non robust solution. In short: the control (11.10)-(11.11) is not robust, while the robust control (11.3)-(11.4) is no longer suitable when $\lambda = 0$ is a multiple eigenvalue. This can be better understood by considering the simple example provided in [BGM14].

Example 11.3. *Consider a system composed of a single subsystem-node with a single control agent, whose state matrix A is identical to the reducible matrix considered in Example 11.2 (for which $\lambda = 0$ is a multiple eigenvalue if $\zeta = \delta = 0$, a simple eigenvalue otherwise) and whose input matrix is $B = \begin{bmatrix}1 & 0 & 0\end{bmatrix}^\top$. The system is stabilisable if and only if either ζ or δ (or both) are strictly positive. Conversely, if $\zeta = \delta = 0$, independently of u the distribution of the queued traffic between nodes x_2 and x_3 is an invariant (uncontrollable) variable. In fact, since $\beta\dot{x}_2 - \alpha\dot{x}_3 = \beta(\alpha x_1) - \alpha(\beta x_1) = 0$, the quantity $\beta x_2 - \alpha x_3$ is constant. Also, if the total stock at the node, $y = \bar{1}_3^\top x = x_1 + x_2 + x_3$, is taken as output variable, then stabilisability by means of an output-feedback control is impossible (independently of the chosen output-feedback control).*

Indeed, it can be shown that the condition in Assumption 11.3 ($\lambda = 0$ being a simple eigenvalue) is not only sufficient, but also necessary.

Theorem 11.4. *Under Assumption 11.2, the control* (11.5) *is stabilising if and only if Assumption 11.3 holds.*

Proof. Sufficiency has been proved in Theorem 11.1. Since stabilisability implies detectability (*i.e.*, observability of all the unstable eigenvalues), necessity follows from the application of the Popov observability criterion (for the unstable eigenvalue 0) to the system with output y, in view of the block-diagonal structure of the corresponding matrices C and A. The proof also exploits the fact that, in a Metzler matrix with zero sum columns, the ascent of the eigenvalue 0 is necessarily 1 (*i.e.*, the largest Jordan block associated with 0 has dimension 1), because the system is marginally stable. Details are provided in [BGM14]. □

11.1.5 A Traffic Control Problem

A traffic-splitting model has been already proposed in Example 9.2 (Section 9.1.1) and the effectiveness of the network-decentralised stabilising control $u = -\gamma B^\top P x$ (where $\gamma > 0$ and $P \succ 0$ is a block-diagonal solution of the LMI $A^\top P + PA - 2\gamma PBB^\top P \prec 0$) has been tested based on the generation of random instances in Section 9.5.3.

Also the network-decentralised control scheme proposed in this section for network systems with stochastic traffic splitting at the nodes can be tested by generating random instances of large networks. There is a remarkable progress with respect to the example in Chapter 9, where the control was found by solving a suitable LMI depending on the state matrix. Here, a *robust* solution is proposed, based on the control (11.5), which does not depend on the stochastic parameters (hence, it is independent of the state matrix of the system).

Systems of the form (11.1), with $D = I$, have been considered so as to carry out numerical experiments according to the following procedure.

1) Fix a number of nodes N and a maximum node size $\bar{n}$.
2) Randomly generate a graph based on the probabilities P_c and P_e: each pair of nodes i-j is connected with probability P_c, while each node i is connected with the external environment with probability P_e.
3) For each pair of connected nodes i-j, generate a control associated with the corresponding arc by adding to matrix B a column k whose elements are all null except for B_{ik} and B_{jk}, which are non-negative and non-positive respectively.
4) Apply the proposed control to the randomly generated network and simulate the behaviour of the closed-loop system.

Since the matrices $A^{(i)}$ are randomly generated, they have distinct eigenvalues with probability 1 (in fact, as remarked in Section 9.3, this is a generic property); therefore, 0 is a simple eigenvalue. Hence, the control (11.5) can be applied. It is worth pointing

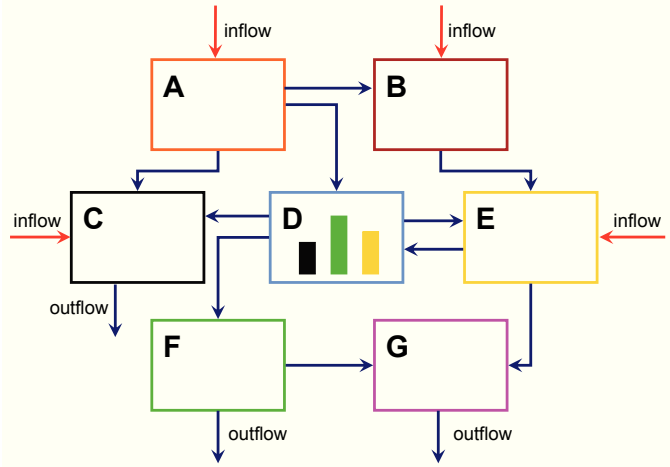

Figure 11.4: A traffic control problem where the incoming traffic at each node is split in different buffers, according to the forwarding direction. [BGM14]

out that, in general, a random instance might not be stabilisable (*i.e.*, it might be that $\text{rank}[A\ B] < n$), due to a lack of connectivity. Whenever the system is stabilisable, however, the robust control (11.5) turns out to be stabilising, as expected.

The congestion control problem is illustrated in Fig. 11.4: each traffic unit, having its own destination, enters the network at some node, through an inflow arc, and leaves the network through an outflow arc. At each node, the traffic is logically (but not necessarily physically) split in queues of units having different directions. For instance, as shown in Fig. 11.4, at node D there are three queues, composed of units directed to nodes C (black buffer), E (yellow buffer) and F (green buffer). If Assumption 11.3 is satisfied, any control agent can perform its action based exclusively on the knowledge of the total congestion at the nodes connected by the corresponding arc. For instance, the controller that governs the flow along the arc connecting node D to node F does not need any knowledge of the internal splitting at node D; yet, the actual controlled flow transfers elements of node D exclusively from the queue directed to F (the green buffer inside node D, in Fig. 11.4).

The results of a numerical random experiment are presented in Fig. 11.5. The fixed number of nodes is $N = 10$, the maximum node size is $\bar{n} = 5$, while the probabilities are $P_c = 0.25$ and $P_e = 0.2$. Based on these values, matrices A and B are randomly generated. The resulting overall system has dimension $n = 38$, with $n_1 = 2$, $n_2 = 5$, $n_3 = 4$, $n_4 = 4$, $n_5 = 5$, $n_6 = 3$, $n_7 = 4$, $n_8 = 3$, $n_9 = 5$, $n_{10} = 3$; the number of controlled arcs is $m = 29$ and the graph results to be connected, and connected with the external environment. The external disturbance vector d, randomly generated as well, with elementwise maximum size 0.1, is held constant. The control (11.5) is applied, with $\gamma = 2$, after checking that the generated system is both controllable and observable. The simulation results, in Fig. 11.5 (a), show the evolution of the buffer levels for the controlled system starting from random

initial conditions in the range [0 10]. The reference level for the buffers is set to zero; however, due to the presence of the persistent disturbance d, the desired set-point is not exactly reached. Convergence to the steady state is smooth and fast, and is assured *without requiring any knowledge of the internal dynamics of the nodes and of the internal traffic distribution at the nodes*, since the stochastic parameters are unknown to the controller and only information about the cumulative buffer content is used for control purposes. The proposed robust control can be compared with a different strategy, which however needs the knowledge of the subsystem states and not just of the cumulative stock: $u = -\gamma BB^\top$, with again $\gamma = 2$. This is the network-decentralised control proposed in Chapter 10; such a choice is suitable, since the closed-loop system with $A_{cl} = A - \gamma BB^\top$ admits the 1-norm as a Lyapunov function. The corresponding evolution of the buffer levels is shown in Fig. 11.5 (b), and is very similar to that of Fig. 11.5 (a), even though convergence is slightly faster and the state variables reach smaller values during their transient.

11.1.6 A Data Transmission System

A problem of data flow control in computer networks [BFG+16] is here proposed as a benchmark to compare the performance of the different network-decentralised control strategies devised in this part of the thesis.

Consider a data transmission system (as in Fig. 11.6), in which the macro-nodes are routers, internally modelled as a network with a central node, providing switching capabilities, and border nodes, representing the queues and the interfaces towards physical links. In the communication network, data packets can be transmitted from a router (macro-node) to another (see Fig. 11.7), making the buffer levels in each router vary, due to three types of flows:

- the uncontrolled flow coming from the internal network and directed elsewhere;
- the controlled flow coming from other routers and directed to the internal network;
- the controlled transiting flow, coming from and directed to other routers.

In the figures, plain arrows represent controlled flows, while dashed arrows represent uncontrolled flows. The internal traffic in each macro-node splits in buffers with different destinations according to some probability distribution (see Fig. 11.8): traffic splitting in each macro-node is modelled as a continuous-time Markov chain. Disk-headed arrows represent stochastic splitting.

Consider for instance the macro-node A in Fig. 11.8. All the traffic arriving at the central node, denoted by IA, splits in several directions, namely, from IA to AB, AC, AD, and to AA, the buffer for the data directed into the local network A. However, in case of congestion of some link, the traffic directed to some node can be reconsidered, with a probability originated by an unknown re-routing criterion. This is represented by the arrows from AB, AC, AD to IA. The internal dynamics of

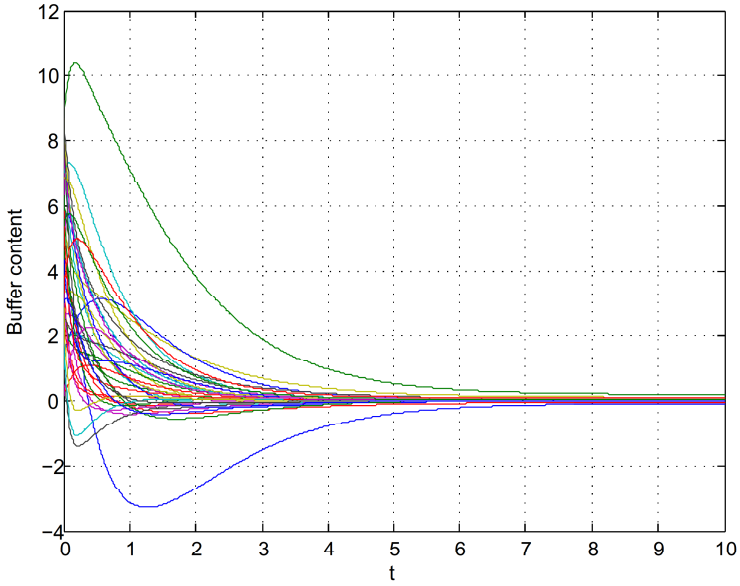

(a) Buffer level evolution with the robust control (11.5), $\gamma = 2$.

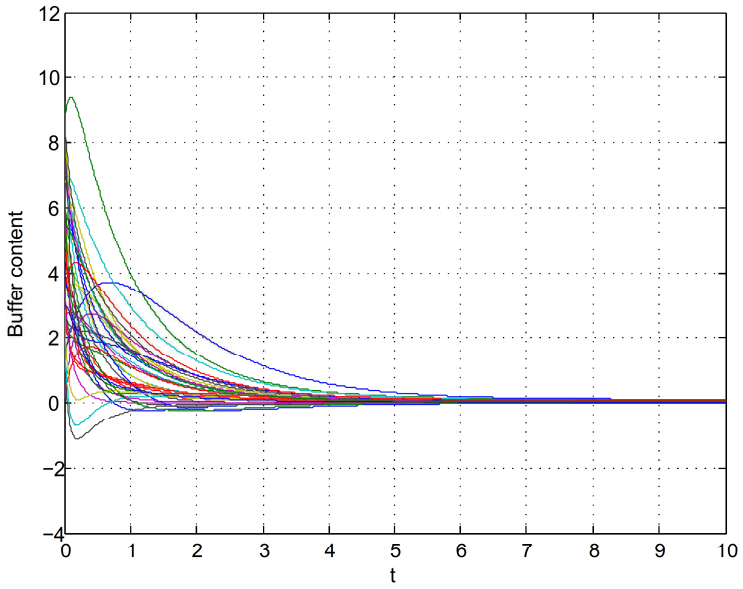

(b) Buffer level evolution with the control $u = -\gamma BB^\top$, $\gamma = 2$.

Figure 11.5: Simulations for the example in Section 11.1.5, comparing two different control strategies.

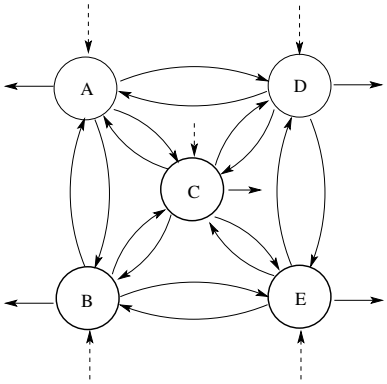

Figure 11.6: A communication network: packets flow among five routers (macro-nodes). [BFG+16]

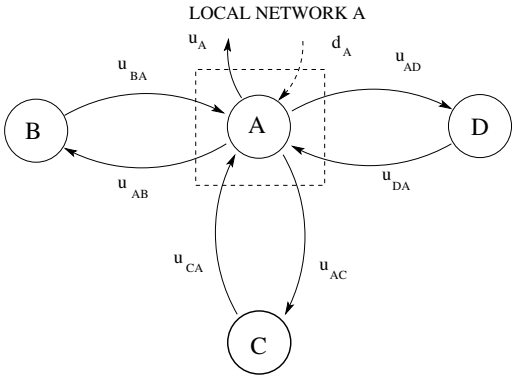

Figure 11.7: Data flows among routers (macro-nodes). [BFG+16]

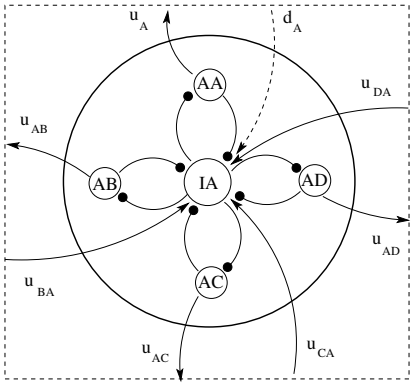

Figure 11.8: Router A seen as a macro-node with splitting dynamics. [BFG+16]

each macro-node is modelled by a continuous-time Markov matrix:

$$A_A = \begin{bmatrix} -(\alpha_{AA}+\alpha_{AB}+\alpha_{AC}+\alpha_{AD}) & \alpha_{BA} & \alpha_{CA} & \alpha_{DA} & \alpha_{AA'} \\ \alpha_{AB} & -\alpha_{BA} & 0 & 0 & 0 \\ \alpha_{AC} & 0 & -\alpha_{CA} & 0 & 0 \\ \alpha_{AD} & 0 & 0 & -\alpha_{DA} & 0 \\ \alpha_{AA} & 0 & 0 & 0 & -\alpha_{AA'} \end{bmatrix}.$$

The first variable represents the arrival node; α_{AA}, α_{AB}, α_{AC}, α_{AD} are the probabilities that, in time dt, a packet is transferred to AA, AB, AC, AD. Conversely, α_{BA}, α_{CA}, α_{DA}, $\alpha_{AA'}$ are the probabilities that, in time dt, a packet is sent back to IA, from AB, AC, AD or AA, for re-routing. The matrices for the other macro-nodes can be determined likewise.

Matrix B is an incidence matrix: each column B_j corresponds to a controlled arc connecting two macro-nodes, or leaving a macro-node. The columns are determined as follows.

- If an arc connects a macro-node to the local network, there is a -1 in the row corresponding to the exit node of the macro-node, directing the traffic to the local network (node AA in Fig. 11.8).
- If an arc connects two macro-nodes, for instance A to B , there is a -1 in the row corresponding to the node AB of macro-node A (directing the traffic to B) and a 1 in the arrival node IB of macro-node B.

At each node, the probability distribution is assumed to be *unknown*, hence it cannot be used for control purposes. Given the transmission network in Fig. 11.6, it is interesting to compare the behaviour of the network when three different control strategies are applied:

- the saturated control $u = \text{sat}(-\gamma B^\top x)$ in (10.6);
- the H-saturated control $u = \text{sat}(-\gamma B^\top H x)$ in (11.3)-(11.4);
- the control $u = \text{sat}(-\gamma \tilde{B}^\top x)$ in (10.12).

In all of the reported simulations (performed with MATLAB), showing for each strategy the evolution of the buffer levels x (starting from random initial conditions) along with the evolution of the control u, the control components are bounded in the interval $[0 \;\; 1]$ Mpackets/s.

In the simulations shown in Fig. 11.9, the component of d affecting node D is suddenly increased to three times its initial value, to represent the case in which node D suddenly increases its traffic in all directions. Parameter values for macro-node A are $\alpha_{AA} = \alpha_{AB} = \alpha_{AC} = \alpha_{AD} = 1$, $\alpha_{BA} = \alpha_{CA} = \alpha_{DA} = 0.25$, $\alpha_{AA'} = 0.05$, and analogously for the other macro-nodes. The value of d is initially $[0.2 \;\; 0.6 \;\; 0.8 \;\; 0.4 \;\; 1.2]^\top$, then at $t = 500$ ms it is switched to $d = [0.2 \;\; 0.6 \;\; 0.8 \;\; 1.2 \;\; 1.2]^\top$. It can be seen that, with a suitable choice of γ (it is chosen $\gamma = 0.1$ for all of the control strategies), the H-saturated control guarantees the fastest convergence and the shortest queues in the

buffers. Buffer queues are an important merit figure, since they are related to delays in the network. The asymptotic value of the control is optimal, as expected: $u = [0.658\ \ 0.742\ \ 0.800\ \ 0.892\ \ 0.908\ \ 0\ \ 0.083\ \ 0\ \ 0.141\ \ 0\ \ 0.233\ \ 0\ \ 0.058\ \ 0\ \ 0.167\ \ 0\ \ 0.092\ \ 0\ \ 0.108\ \ 0\ \ 0.017]^\top$ is the minimum norm control, as it has been independently checked via CVX, by solving the corresponding optimisation problem in a "centralised way".

If γ is taken too large, as in Fig. 11.10, where $\gamma = 0.4$, the H-saturated control may no longer ensure positivity of the state variables. However, a negative value of the buffer levels is not reasonable. Hence, to ensure non-negativity of the buffer levels, it is mandatory to stop the flow (forcing $u = 0$) associated with all of the arcs coming out from empty buffers. This discontinuity in the control may cause chattering, as shown in Fig. 11.10 (b), but guarantees that the buffer levels have non-negative values, as in Fig. 11.10 (c). Interestingly, from several tests it has been noticed that, even in the presence of chattering, the average value of u in the last part of the simulation is very close to the asymptotically optimal value: in the case of Fig. 11.10 (where the value of d is initially $[0.6\ \ 0.2\ \ 0.7\ \ 0.5\ \ 1.2]^\top$ and is then switched to $d = [0.6\ \ 0.2\ \ 0.7\ \ 1.5\ \ 1.2]^\top$ at $t = 150$, while macronode parameters are as in Fig. 11.9), the norm of the difference is 0.040.

The simulation in Fig. 11.11 shows the case in which, instead, the internal parameters of the Markov chains are suddenly changed: $\alpha_{DE}, \alpha_{EB}, \alpha_{BB}$ are switched from 0.05 to 1. This models the case in which node D increases the traffic to node E and node E the traffic to node B, resulting in a large traffic through nodes D-E-B. The disturbance is fixed: $d = [0.2\ \ 0.6\ \ 0.8\ \ 1.2\ \ 1.2]^\top$. For all the macro-nodes $k \in \mathcal{M} = \{A, B, C, D, E\}$, $\alpha_{kk'} = 0.05$ and $\alpha_{*k} = 0.25$ (where $*$ denotes any macro-node in $\mathcal{M}$ suitably connected to k). For macro-nodes A and C, $\alpha_{A*} = \alpha_{C*} = 1$. For macro-nodes B, D and E, $\alpha_{B*} = \alpha_{D*} = \alpha_{E*} = 0.05$; then, at $t = 500$, $\alpha_{BB} = \alpha_{DE} = \alpha_{EB} = 1$. For all of the controls, it is chosen $\gamma = 0.04$. Again, the H-saturated control ensures a much faster convergence, lower buffer levels and smoother transitions (conversely, the other controls are discontinuous when the network changes its behaviour). The resulting asymptotic value $u = [0.675\ \ 0.758\ \ 0.833\ \ 0.908\ \ 0.925\ \ 0\ \ 0.083\ \ 0\ \ 0.158\ \ 0\ \ 0.233\ \ 0\ \ 0.075\ \ 0\ \ 0.167\ \ 0\ \ 0.075\ \ 0\ \ 0.092\ \ 0\ \ 0.017]^\top$ is optimal (CVX-tested).

11.2 Channel Sharing Communication

Communication protocols able to adapt to sudden changes in the network topology are crucial in highly dynamic mobile scenarios (*e.g.*, vehicle-to-vehicle communication [Eic07], swarm robot systems [Sah05], and many others [MPD05, EP05]); yet, often no fraction of the overall available bandwidth can be used for network discovery, coordination and connection setup, hence any coordination and control strategy needs to be decentralised (and also simple, since it must be implemented on low-computation-power devices with limited energy consumption and it must not suffer

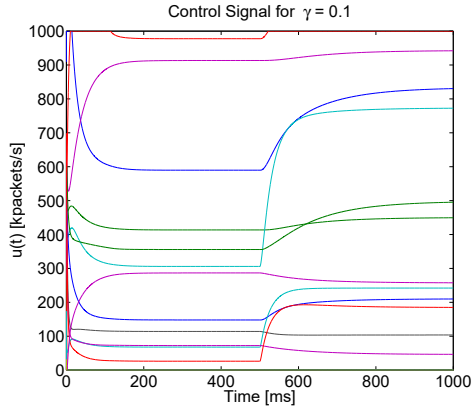

(a) $u = \mathrm{sat}(-\gamma B^\top x)$

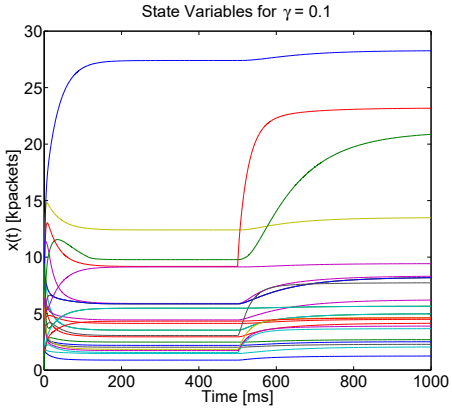

(b) x with $u = \mathrm{sat}(-\gamma B^\top x)$

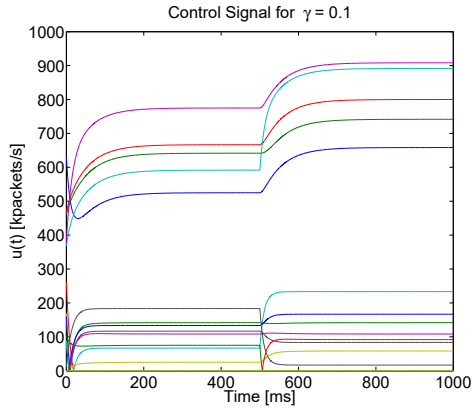

(c) $u = \mathrm{sat}(-\gamma B^\top H x)$

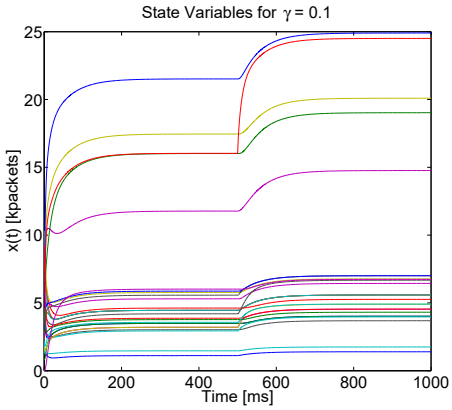

(d) x with $u = \mathrm{sat}(-\gamma B^\top H x)$

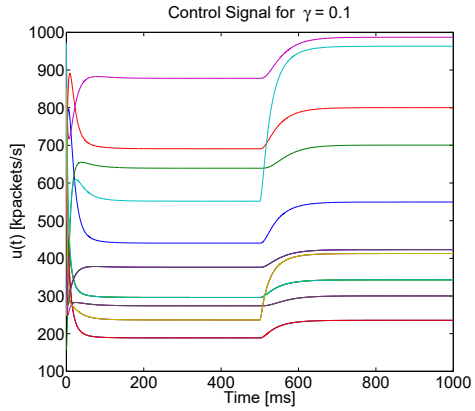

(e) $u = \mathrm{sat}(-\gamma \tilde{B}^\top x)$

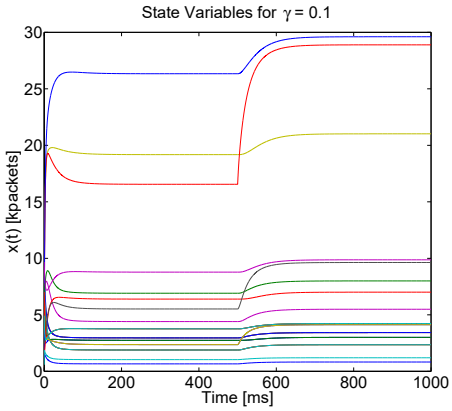

(f) x with $u = \mathrm{sat}(-\gamma \tilde{B}^\top x)$

Figure 11.9: Simulations of the network in Fig. 11.6 when d is suddenly changed (at time $t = 500$ ms). Given $\gamma = 0.1$ and common random initial conditions, the three considered control strategies are compared: for each strategy, both the evolution of the control action u and of the buffer levels x are shown.

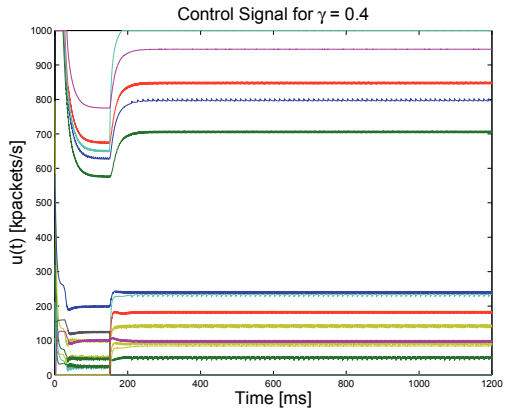

(a) $u = \mathrm{sat}(-\gamma B^\top H x)$

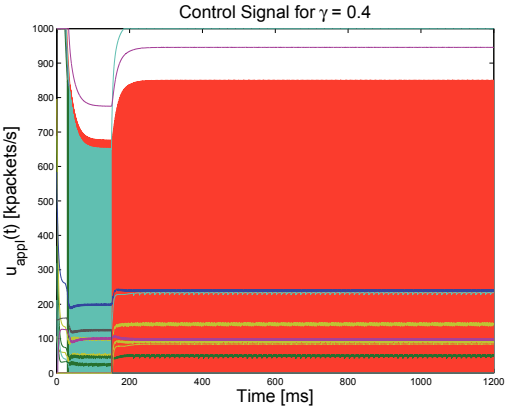

(b) Applied control (discontinuous)

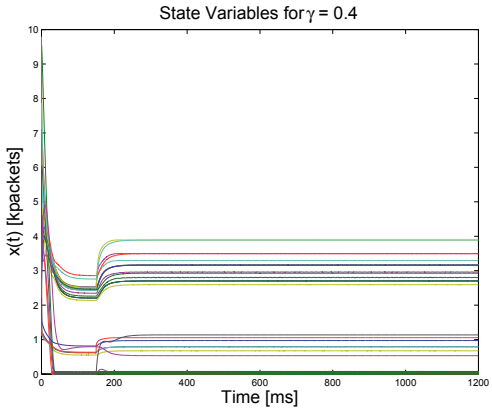

(c) Buffer levels

Figure 11.10: Simulations of the network in Fig. 11.6, with $u = \mathrm{sat}(-\gamma B^\top H x)$ and $\gamma = 0.4$. To ensure positivity of the state variables, the control actually applied is forced to zero for all the arcs which are leaving a node i with $x_i = 0$.

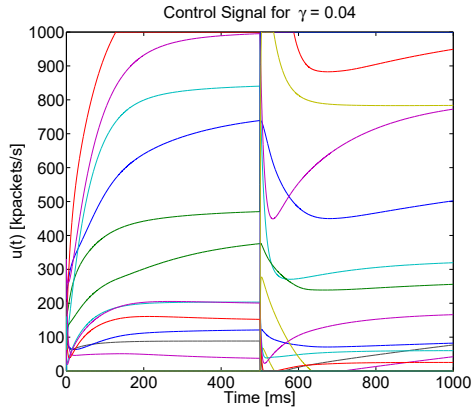

(a) $u = \mathrm{sat}(-\gamma B^\top x)$

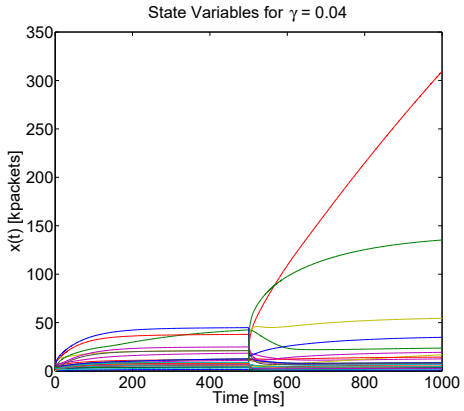

(b) x with $u = \mathrm{sat}(-\gamma B^\top x)$

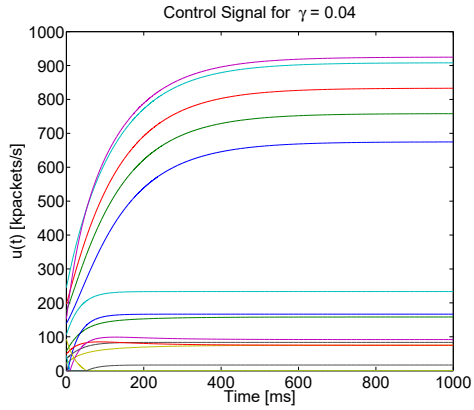

(c) $u = \mathrm{sat}(-\gamma B^\top H x)$

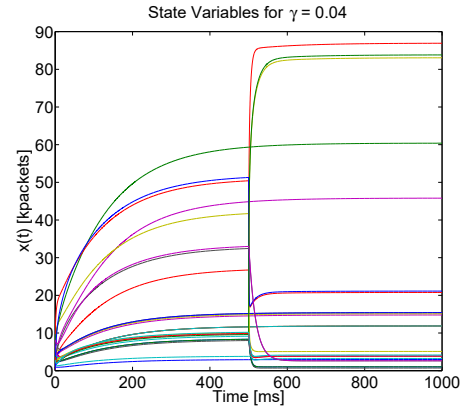

(d) x with $u = \mathrm{sat}(-\gamma B^\top H x)$

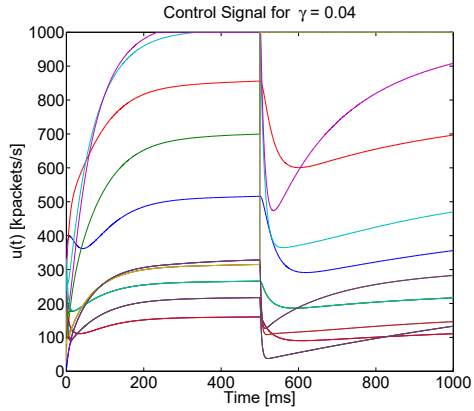

(e) $u = \mathrm{sat}(-\gamma \tilde{B}^\top x)$

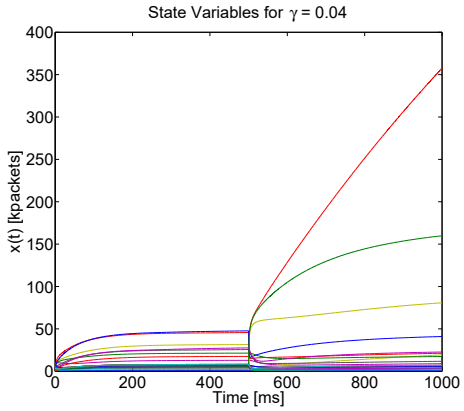

(f) x with $u = \mathrm{sat}(-\gamma \tilde{B}^\top x)$

Figure 11.11: Simulations of the network in Fig. 11.6 when there is a sudden traffic increase through nodes *D-E-B* at time $t = 500$ ms. Given common random initial conditions, the three considered control strategies with $\gamma = 0.04$ are compared: the evolution of u and of x is shown.

of fragility phenomena in the presence of network variations [BLT02]).

Decentralised algorithms have been proposed for power control in wireless communication networks, such as the Foschini-Miljanic algorithm [FM93, DL14, FCJ14].

Concerning instead bandwidth allocation, the Carrier Sense Multiple Access (CSMA) p-persistent protocol family represents an interesting solution for coordinator-free *ad hoc* networks [Abr70, BCG03, Eic07, Miś07, WAKP08]. In wireless communication networks, fairness is not less important than the maximisation of channel utilisation [LL07, MLAM10, LPRK13]; concurrently fulfilling both design goals is challenging and crucial.

An improvement of the p-persistent protocol, based on a decentralised and distributed control paradigm [Tsi84], has been proposed and analysed in [BCM11, BDMP12, BCGM16]; this channel sharing communication protocol is here presented and it is shown that it actually implements a network-decentralised strategy.

Consider the problem of n transmitters (associated with the nodes of a graph), sharing a common communication channel having a known bandwidth (assumed to be unitary, without loss of generality). Each transmitting node has to autonomously decide its transmission rate, based on the knowledge of its own rate and of the aggregate transmission rate of the other nodes (which is related to bandwidth occupancy). The following variables need to be defined:

- $x_i(t) \in \mathbb{R}$: transmission rate of the ith node, $i = 1, \dots, n$;
- $y(t) = \sum_{i=1}^{n} x_i(t) \in \mathbb{R}$: total message rate;
- $u_i(t)$: control signal at the ith node;
- $z_i(t) = \sum_{j \neq i} x_j(t) = y(t) - x_i(t)$: aggregate message rate of the nodes complementary to the ith node.

Each node autonomously controls its own transmission rate, according to the following equation:

$$\dot{x}_i(t) = u_i(t). \tag{11.12}$$

The overall control goal is the ideal steady-state condition

$$\lim_{t \to \infty} \; x_i(t) = \frac{1}{n}, \quad \forall i, \tag{11.13}$$

which implies fairness and full exploitation of the overall available bandwidth (since $\lim_{t \to \infty} \; y(t) = 1$).

A centralised control law of the form $u_i = u_i(x)$ would require either full connection (*i.e.*, each node should be connected to all the others, so as to receive information about their state) or the presence of a centralised supervisor that has information about the state of the whole system. Yet this is not always possible and decentralised algorithms need to be devised.

Definition 11.2. *Let $\mathcal{C}_i$, for $i = 1, \dots, n$, index the set of nodes connected to node i. The* connectivity degree *is $c_i = |\mathcal{C}_i|$.*

Then $\sum_{j\in\mathcal{C}_i} x_j(t)$ denotes the aggregate transmission rate of the nodes in $\mathcal{C}_i$.

The algorithm works as follow. Any node increases/decreases its transmission rate with speed u_i, according to

$$u_i(t) = -\alpha(1+\mu)x_i(t) - \alpha\sum_{j\in\mathcal{C}_i} x_j(t) + \alpha, \tag{11.14}$$

where α and μ are positive parameters.

In the absence of communication among nodes, the control would be $u_i(t) = -\alpha(1+\mu_i)x_i(t) + \alpha$, which means that asymptotically

$$x(t) \to \frac{1}{(1+\mu)},$$

which is close to 1 for μ small. Note that $\mu > 0$ is necessary for stability.

In the presence of connections among nodes, the transmission control u_i is decreased of a quantity $\sum_{j\in\mathcal{C}_i} x_j(t)$, due to the presence of other nodes that are sharing the same channel.

In [BDMP12] it is shown that in the case of full connection, *i.e.*, when

$$\sum_{j\in\mathcal{C}_i} x_j(t) = \sum_{j\neq i} x_j(t) = z_i(t),$$

the control law (11.14) renders system (11.12) asymptotically stable and that

$$\lim_{t\to\infty} x_i(t) = \frac{1}{n+\mu}. \tag{11.15}$$

Therefore, in the case of full connection, (11.13) can be satisfied up to an arbitrarily small tolerance. The case in which there is no full connection deserves some attention. A *connection* from j to i is present if

$$j \in \mathcal{C}_i;$$

the connection is said to be *symmetric* if

$$j \in \mathcal{C}_i \iff i \in \mathcal{C}_j,$$

non-symmetric otherwise.

The system described by (11.12) and (11.14) can be represented as

$$\dot{x}(t) = Ax(t) + \alpha\bar{\mathbf{1}} \tag{11.16}$$

where $\bar{\mathbf{1}} \doteq [\ 1\ 1\ \dots\ 1\ ]^\top$ and

$$A = \alpha \begin{bmatrix} -(1+\mu) & -\delta_{12} & -\delta_{13} & \cdots & -\delta_{1n} \\ -\delta_{21} & -(1+\mu) & -\delta_{23} & \cdots & -\delta_{2n} \\ -\delta_{31} & -\delta_{32} & -(1+\mu) & \cdots & -\delta_{3n} \\ \vdots & \vdots & \vdots & \ddots & \vdots \\ -\delta_{n1} & -\delta_{n2} & -\delta_{n3} & \cdots & -(1+\mu) \end{bmatrix}, \tag{11.17}$$

with $\delta_{ij} = 1$ if node j is linked to node i, $\delta_{ij} = 0$ if it is not. Compactly, it can be written

$$A = -\alpha[(\mu + 1)I + \Delta],$$

where Δ is the adjacency matrix associated with the system graph. This matrix is symmetric iff all connections are symmetric.

The control (11.14) can be thus seen as a special case of network-decentralised control. In fact, any connection from node j to node i is associated with a control signal αx_j, acting on node i, that depends on x_j only.

In general it can be shown that, in the absence of full connection, stability cannot be ensured for any $\mu > 0$. It turns out, however, that stability can be ensured provided that $\mu > 0$ is taken large enough. The following result is proved in [BCGM16].

Proposition 11.4. *Stability of system* (11.16) *with matrix* A *as in* (11.17) *is ensured for any matrix* Δ*, possibly non-symmetric, if*

$$\mu > \frac{n}{2} - 1. \tag{11.18}$$

In [BCGM16] it is also shown that the bound in (11.18) cannot be improved, in general, since it is tight in the symmetric-connection case. Robustness of the proposed control with respect to time-varying network topologies and delays is also discussed.

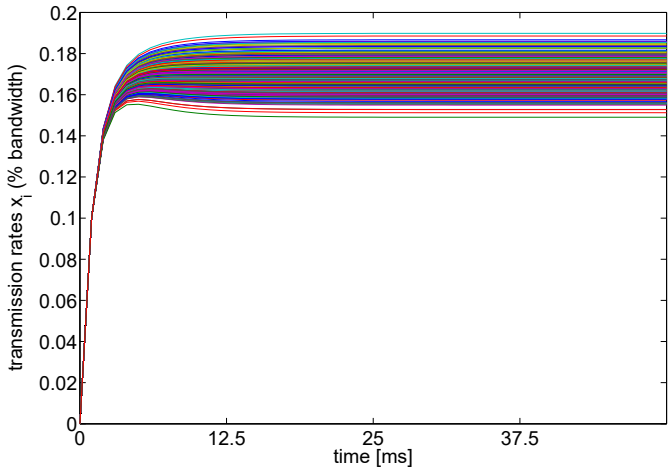

Figure 11.12: Channel sharing protocol: time evolution of the transmission rates, expressed in terms of percentage of the overall bandwidth.

The effectiveness of the proposed control is here shown by the simulations in Fig. 11.12, obtained starting from zero initial conditions in the case of $n = 500$ transmitters, with $\alpha = 1$, $\mu = 250$ and a randomly generated symmetric matrix

Δ (nodes are connected with probability $p = 0.8$). It can be seen that the control naturally achieves not only stability, but also a good compromise between fairness and maximal bandwidth exploitation. In fact, the channel exploitation is "almost equal" for all transmitters (at steady state, all x_i are in the range $0.15\% - 0.19\%$ of the total bandwidth) and the overall bandwidth is "almost fully" exploited (y is almost 85% of the total bandwidth at steady state).

11.3 Clock Synchronisation

Clock synchronisation is a particular case of the general and well studied class of consensus problems [OSM04, OSFFS06, BGP06, OSFM07, RBA07, CFSZ08, CMA08, GG08, KWLB08, TKY08], where the goal is to drive the state variables to a common value. The clock synchronisation problem has been widely investigated: the interested reader is referred to [SS07, CCSZ08, SWX08, SAS10, CCSZ11, CZ14] and the references therein for a deep inquire into the subject, and also to [LL88, SBK05, PB09, HLST11, SF11, HSV12], which deal in particular with synchronisation protocols and algorithms. Here, a particular discrete-time formulation of the problem (a similar problem, in a continuous-time setting, has been considered in [BM15], Chapter 12.6.3) is considered as a benchmark to show how synchronisation can be achieved by means of a network-decentralised strategy. The obtained results are comparable to the state of the art.

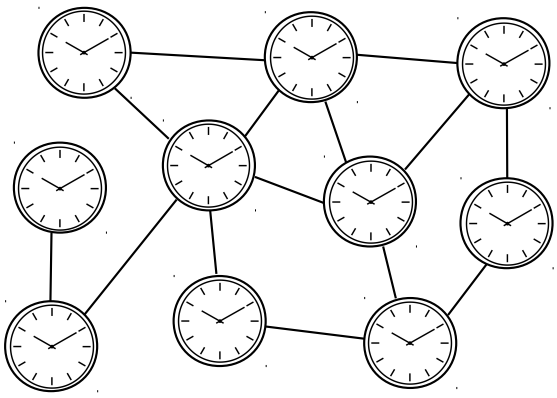

Figure 11.13: The clock synchronisation network.

Consider N clocks, each having its own inner period, whose time indications need to be synchronised. The clocks are not directly connected: they communicate with one another by periodically emitting a beep (according to their inner period), which is sensed by a subset of the other clocks only (in real applications this may be due, for instance, to the fact that the sound intensity fades beyond a certain physical distance). This situation can be represented by a graph, as in Fig. 11.13, where the

presence of an arc connecting two clocks (nodes) means that each of the two clocks can sense the beep emitted by the other.

A particular interpretation of the connection graph is the following. Each clock senses the beeps emitted by the other clocks within a time window (a listening window), symmetrically centered in its own beep instant. This concept is illustrated in Fig. 11.14. It is assumed that the listening window has the same length for all of the clocks. This implies symmetry: if clock i is in the window of clock j, then also clock j is in the window of clock i. In the graph modelling the interactions among clocks, the ith clock is then connected only to the clocks that beep within its listening window $\mathcal{W}_i$ and the connection between clocks i and j means that each is in the time window of the other.

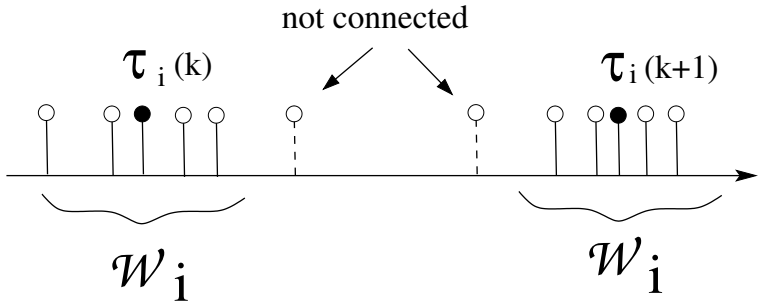

Figure 11.14: The time windows.

Assume that the resulting graph is always fully connected and denote by

- $\tau_i(k)$ the beep time of the ith clock, expressed according to the *universal time*;
- $\hat{\tau}_i(k)$ the beep time of the ith clock, expressed according to the *inner time* of the ith clock itself;
- d_i the conversion factor between universal and internal time, such that $\tau_i(k) = d_i\hat{\tau}_i(k)$;
- $T_i(k)$ the (internal) time period of the ith clock.

Hence, each clock emits a beep in the time instants $\tau_i(k)$ and has an *adjustable* period whose length, expressed in universal time, is $d_iT_i(k)$.

A general formulation of the problem can be provided as follows. Given N clocks, the spontaneous (uncontrolled) evolution of the system would be:

$$\begin{cases} \tau_i(k+1) = \tau_i(k) + d_iT_i(k), \\ T_i(k+1) = T_i(k), \end{cases}$$

for $i = 1, \ldots, N$. The aim is to synchronise the N clocks, *i.e.*, to achieve for all of them the same time indication and the same period: asymptotically, $\tau_i = \bar{\tau}\ \forall i$ and $T_i = \bar{T}\ \forall i$. To achieve synchronisation, each clock, which perceives the beeps emitted by some of the other clocks, can modify its behaviour accordingly. As previously

seen, for each clock the following beep emission instant and the following period will depend only on the beeps sensed *inside a certain time window* centered at the present beep emission instant. To synchronise the clocks, correction factors of the form

$$c_i(k) = \sum_{j \in \mathcal{W}_i} (\tau_i(k) - \tau_j(k)) \tag{11.19}$$

can be considered, depending on the beep emissions of all the other clocks indexed in the set $\mathcal{W}_i$ associated with the time window of the ith clock. The correction factor for the ith clock depends exclusively on information coming from a subset of the other clocks, those which are beeping in the time window $\mathcal{W}_i$ and are hence connected with the ith clock in the associated graph. Therefore, this can be seen as a *network-decentralised control strategy*, implemented by the combined action of several local agents $u_{ij} = \tau_i(k) - \tau_j(k)$.

The system equations become then

$$\begin{cases} \tau_i(k+1) = \tau_i(k) + d_i T_i(k) - \gamma \sum_{j \in \mathcal{W}_i} (\tau_i(k) - \tau_j(k)), \\ T_i(k+1) = T_i(k) - \alpha d_i^{-1} \sum_{j \in \mathcal{W}_i} (\tau_i(k) - \tau_j(k)), \end{cases}$$

for $i = 1, \ldots, N$, where γ and α are positive correction coefficients that will be analysed later.

If the clock inner implementation is considered, the system evolution is

$$\begin{cases} \hat{\tau}_i(k+1) = \hat{\tau}_i(k) + T_i(k) - \gamma \sum_{j \in \mathcal{W}_i} (\hat{\tau}_i(k) - \hat{\tau}_{i,j}(k)), \\ T_i(k+1) = T_i(k) - \alpha \sum_{j \in \mathcal{W}_i} (\hat{\tau}_i(k) - \hat{\tau}_{i,j}(k)), \end{cases}$$

for $i = 1, \ldots, N$, where $\hat{\tau}_{i,j}(k)$ is the beep time of the jth clock expressed according to the inner time of the ith clock. From the above equations, it is apparent that the knowledge of the conversion factor d_i is not necessary at all for the practical implementation of the algorithm in the logic of each clock.

The following convergence analysis proves that the proposed network-decentralised algorithm assures synchronisation with a period T that is

- asymptotically constant;
- equal to the average of the initial period values of all the clocks.

Define

$$\tau(k) = \begin{bmatrix} \tau_1(k) \\ \vdots \\ \tau_N(k) \end{bmatrix} \quad \text{and} \quad T(k) = \begin{bmatrix} T_1(k) \\ \vdots \\ T_N(k) \end{bmatrix},$$

to compactly write the discrete-time system as

$$\begin{bmatrix} \tau(k+1) \\ T(k+1) \end{bmatrix} = \begin{bmatrix} I_N - \gamma L & D \\ -\alpha D^{-1} L & I_N \end{bmatrix} \begin{bmatrix} \tau(k) \\ T(k) \end{bmatrix}, \tag{11.20}$$

where $D = \mathrm{diag}\{d_1, \ldots, d_N\}$ is the time conversion matrix, while $L \in \mathbb{R}^{N\times N}$ is the Laplacian matrix of the graph. Among the several interesting properties of the Laplacian matrix, remind that L is positive semidefinite and the algebraic multiplicity of its zero eigenvalue is equal to the number of connected subgraphs. Hence, if the whole graph is connected (as in the present case), zero has multiplicity equal to one and the corresponding eigenvector is the vector of ones: $L\bar{1} = 0$.

If the state transformation

$$\begin{bmatrix} \tau(k+1) \\ T(k+1) \end{bmatrix} = \begin{bmatrix} I_N & 0 \\ 0 & D^{-1} \end{bmatrix} \begin{bmatrix} \tilde{\tau}(k+1) \\ \tilde{T}(k+1) \end{bmatrix}$$

is applied, the dynamic matrix of system (11.20) becomes

$$A = \begin{bmatrix} I_N & 0 \\ 0 & D \end{bmatrix} \begin{bmatrix} I_N - \gamma L & D \\ -\alpha D^{-1} L & I_N \end{bmatrix} \begin{bmatrix} I_N & 0 \\ 0 & D^{-1} \end{bmatrix} = \begin{bmatrix} I_N - \gamma L & I_N \\ -\alpha L & I_N \end{bmatrix},$$

resulting in the transformed system

$$\begin{bmatrix} \tilde{\tau}(k+1) \\ \tilde{T}(k+1) \end{bmatrix} = \begin{bmatrix} I_N - \gamma L & I_N \\ -\alpha L & I_N \end{bmatrix} \begin{bmatrix} \tilde{\tau}(k) \\ \tilde{T}(k) \end{bmatrix}. \tag{11.21}$$

Consider the orthonormal matrix Q which diagonalises L: $Q^\top L Q = \Lambda$, where Λ is a diagonal matrix with the same eigenvalues of L, hence $\Lambda_i \in \mathbb{R}$ may be either zero or positive. Matrix Q defines a transformation that changes matrix A as follows:

$$Q^\top A Q = \begin{bmatrix} I_N - \gamma\Lambda & I_N \\ -\alpha\Lambda & I_N \end{bmatrix}.$$

Suitably changing the order of rows and columns, a block diagonal matrix is obtained having diagonal blocks

$$\begin{bmatrix} 1 - \gamma\Lambda_i & 1 \\ -\alpha\Lambda_i & 1 \end{bmatrix}.$$

The characteristic polynomial of the ith block is

$$p_i(z) = z^2 + (\gamma\Lambda_i - 2)z + 1 + (\alpha - \gamma)\Lambda_i, \tag{11.22}$$

whose stability properties can be easily studied by applying the transformation that maps the open unit disk to the real negative half-plane (thus transforming stable eigenvalues of the discrete-time system into stable eigenvalues of a fictitious continuous-time system):

$$z = \frac{s+1}{s-1}.$$

The transformed characteristic polynomial is

$$p_i(s) = [\alpha\Lambda_i]s^2 + [2\Lambda_i(\gamma - \alpha)]s + [4 + \Lambda_i(\alpha - 2\gamma)], \tag{11.23}$$

whose roots can have negative real part if and only if all the coefficients are positive. Thus, assuming that $\Lambda_i \neq 0$, the following inequalities must be satisfied:

$$\begin{cases} \alpha > 0, \\ \gamma > \alpha, \\ (2\gamma - \alpha) < \frac{4}{\Lambda_i} \qquad \forall i. \end{cases}$$

By considering the largest eigenvalue of matrix L, $\Lambda_M = \max_i(\Lambda_i)$, the following bound is obtained:

$$\begin{cases} \alpha > 0, \\ \gamma > \alpha, \\ (2\gamma - \alpha) < \frac{4}{\Lambda_M}. \end{cases} \tag{11.24}$$

Remark 11.1. *By exploiting the fact that the largest eigenvalue of a Laplacian matrix L can never be greater than N, another bound could be obtained by considering $\Lambda_M = N$. The control parameters could then be chosen without computing the eigenvalues of L (and without even knowing the Laplacian matrix itself, provided that the corresponding graph is connected).*

Since both α and γ must be positive, the system of inequalities in (11.24) plus $\gamma > 0$ identifies a stabilising set which is a triangle in the plane (α, γ), represented in Fig. 11.15. The triangle barycenter has coordinates $(\alpha_B, \gamma_B) = (\frac{4}{3\Lambda_M}, \frac{2}{\Lambda_M})$: this can be considered as the optimal value of the pair of parameters.

If the system parameters are chosen inside the triangle, stability is guaranteed for all the eigenvalues *different from the two on the unitary circumference*: in fact, for $\Lambda_i = 0$, $p(z) = z^2 - 2z + 1 = (z-1)^2$, hence there is the eigenvalue $\lambda = 1$, with algebraic multiplicity $m_a = 2$. Since the geometric multiplicity of the eigenvalue $\lambda = 1$ is $m_g = 1$, denoting by e the normalised unit vector, $e = \frac{\bar{1}}{\sqrt{N}}$, the associated eigenspace is generated by the eigenvector

$$\begin{bmatrix} e \\ 0 \end{bmatrix}$$

and the generalised eigenvector

$$\begin{bmatrix} 0 \\ e \end{bmatrix},$$

and the discrete-time modes associated with the eigenvalue $\lambda = 1$ are 1 and k. All the other modes are asymptotically stable, hence the solution of the system converges to the eigenspace associated with $\lambda = 1$:

$$\begin{bmatrix} \tau \\ T \end{bmatrix}_\infty = (\mu + \nu k) \begin{bmatrix} e \\ 0 \end{bmatrix} + (\rho + \sigma k) \begin{bmatrix} 0 \\ e \end{bmatrix},$$

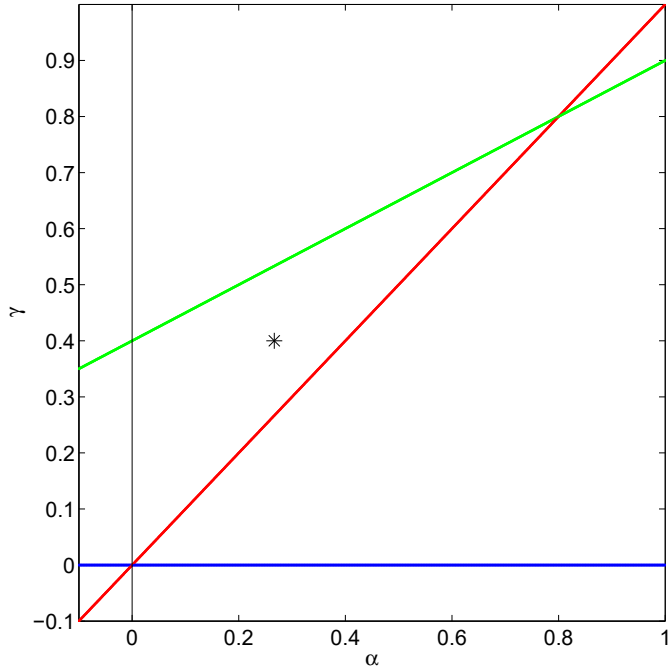

Figure 11.15: The triangle in the upper half-plane, formed by the black, red and green sides, is the set of the stabilising pairs (α, γ) for a clock interconnection graph with $\Lambda_M = 5$. The blue line is $\alpha = 0$, the red line is $\gamma = \alpha$, the green line is $(2\gamma - \alpha) - \frac{4}{\Lambda_M} = 0$, the black line is $\gamma = 0$ and the black star inside the triangle denotes its barycenter.

for some constants μ, ν, ρ, σ. Since the solution must satisfy system (11.21), it must be that $\sigma = 0$ and $\rho = \nu$. Therefore, the generic asymptotic solution is

$$\begin{bmatrix} \tau \\ T \end{bmatrix}_\infty = \begin{bmatrix} (\mu + \nu k)e \\ \nu e \end{bmatrix}$$

and the synchronisation goal is fully achieved:

- the clocks are synchronised;
- the period is the same for all of them (and is equal to the average of the initial periods).

In fact, it can be shown that the average of the periods is invariant: since $e^\top L = 0$,

$$\bar{m} = e^\top T(k) = e^\top T(k+1).$$

Fig. 11.16 reports the simulation results of a clock synchronisation process based on the proposed network-decentralised strategy. $N = 10$ clocks are considered and a connection graph is randomly generated with connectivity (connection probability) $c = 0.7$. The initial conditions are randomly chosen in the interval $[0 \;\; 10]$, and for α

and γ the optimal value is picked, corresponding to the barycenter of the triangular shape seen above. Matrix $D = I + \Delta$, where Δ is a diagonal matrix whose diagonal entries are randomly generated in the interval $(-1 \;\; 1)$. The time indication quickly becomes the same for all of the clocks, and is asymptotically linear, while the period indication is asymptotically constant and reaches, for all of the clocks, a common value (5.53 time units) expressed according to the universal time, which is equal to the average of the random initial values. Interestingly, time synchronisation occurs much faster than period synchronisation.

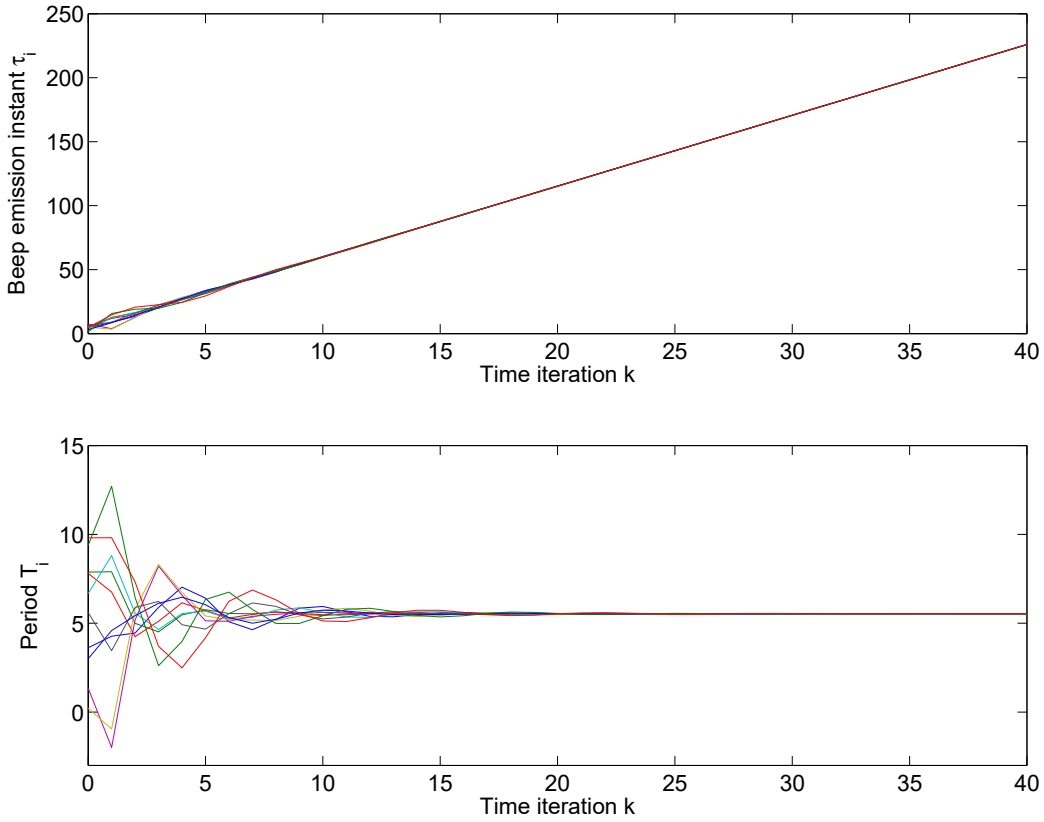

Figure 11.16: The clock synchronisation transient: evolution of the time indication (top) and of the period (bottom), both expressed according to the universal time.

11.4 Vehicle Platooning

In this section, a wireless-communication-based network-decentralised control for platoons of vehicles is considered.

In the proposed framework, all the vehicles in the platoon are enabled to share information about one another by wireless communication in order to automatically follow the reference vehicle, called the *leader* (whose dynamics is decided, *e.g.*, by a

human driver). This evolution of the standard Adaptive Cruise Control (ACC) is named CACC (Cooperative ACC), because wireless communication among vehicles allows them to share information so as to efficiently cooperate. The aim is often to minimise inter-vehicle spacing (thus reducing fuel consumption by better exploiting the aerodynamic effects due to platooning) and to prevent extraneous vehicles from inserting between two vehicles of the platoon. For controlling the longitudinal dynamics of N vehicles in a platoon, many different schemes have been proposed. Two are analysed here: the former ensures constant spacing among vehicles; the latter, based on an analogy with impedance matching in transmission lines, is designed for reducing oscillations along the platoon.

In the following, all the physical quantities will be referred to a reference frame that moves with a constant speed, considered as the nominal one. Denoting by y_i, $\dot{y}_i$ and $\ddot{y}_i$ $(i = 0, 1, \ldots, N)$ the position, speed and acceleration of the ith vehicle, respectively, the dynamics of the leader can be described by

$$\dot{y}_0 = \beta(u_0 - y_0),$$

where u_0 is the position control input (provided, for instance, by a human driver). In general, y_0 and $\dot{y}_0$ are assigned inputs for the system. The acceleration control input for each vehicle of the platoon is u_i and the equation representing the dynamics of the ith vehicle is then

$$\ddot{y}_i = a_i,$$

where two cases can be considered:

- if the effect of vehicle dynamics is neglected (thus assuming infinite bandwidth associated with the lower level controller), $a_i = u_i$;
- if the finite bandwidth associated with the lower level controller is considered and its effect is expressed by a lowpass filter, a_i is derived by the equation

$$\dot{a}_i = \frac{1}{\tau_F}(u_i - a_i), \qquad \tau_F > 0.$$

Constant spacing control. If the control is designed for obtaining constant spacing among the vehicles in the platoon, the acceleration control input is [Raj12]

$$u_i = \alpha_1 \ddot{y}_{i-1} + \alpha_2 \ddot{y}_0 - \alpha_3(\dot{y}_i - \dot{y}_{i-1}) - \alpha_4(\dot{y}_i - \dot{y}_0) - \alpha_5(y_i - y_{i-1} + l_{i-1} + g_d),$$

for $i = 1, \ldots, N$, where α_j are positive design parameters, l_i is the length of the ith vehicle and g_d is the desired inter-vehicle spacing.

A faster alternative is achieved by considering for control purposes, instead of the actual acceleration of other vehicles, their *desired* acceleration:

$$u_i = \alpha_1 u_{i-1} + \alpha_2 u_0 - \alpha_3(\dot{y}_i - \dot{y}_{i-1}) - \alpha_4(\dot{y}_i - \dot{y}_0) - \alpha_5(y_i - y_{i-1} + l_{i-1} + g_d),$$

for $i = 1, \ldots, N$.

In both cases, only "local" information regarding the vehicle in front and the leader is required: this is therefore an example of *network-decentralised control*, where each vehicle-node is connected with the leader-node and, moreover, with the node corresponding to the vehicle in front.

Consider the whole platoon and the state variable $x = [x_0\ x_1\ \dots\ x_N]^\top$, where $x_0 = [y_0\ \dot{y}_0]^\top$, while $x_i = [y_i\ \dot{y}_i\ \ddot{y}_i]^\top$, $i = 1, \dots, N$. Assuming for simplicity $l_i = l$ for all i, this leads to the continuous-time system

$$\dot{x} = \left[\begin{array}{c|ccccc} A_0 & \mathbf{0} & \mathbf{0} & \mathbf{0} & \cdots & \mathbf{0} \\ \hline A_4 & D_c & \mathbf{0} & \mathbf{0} & \cdots & \mathbf{0} \\ A_4 & X & D_c & \mathbf{0} & \cdots & \mathbf{0} \\ A_4 & X & X & D_c & \cdots & \mathbf{0} \\ \vdots & \vdots & \vdots & \vdots & \ddots & \vdots \\ A_4 & X & X & X & \cdots & D_c \end{array}\right] x + \left[\begin{array}{c} B_0 \\ \hline B_2 \\ B_2 \\ B_2 \\ \vdots \\ B_2 \end{array}\right] \left[\begin{array}{c} u_0 \\ l \\ g_d \end{array}\right],$$

where $\mathbf{0}$ are zero-blocks,

$$A_0 = \left[\begin{array}{cc} 0 & 1 \\ 0 & 0 \end{array}\right],\ A_4 = \left[\begin{array}{cc} 0 & 0 \\ 0 & 0 \\ 0 & \alpha_4 \end{array}\right],\ B_0 = \left[\begin{array}{ccc} 0 & 0 & 0 \\ 1 & 0 & 0 \end{array}\right],\ B_2 = \left[\begin{array}{ccc} 0 & 0 & 0 \\ 0 & 0 & 0 \\ \alpha_2 & -\alpha_5 & -\alpha_5 \end{array}\right],$$

X are matrices whose entries depend on the influence of the dynamics of the vehicles in front and the diagonal blocks are

$$D_c = \left[\begin{array}{ccc} 0 & 1 & 0 \\ 0 & 0 & 1 \\ -\alpha_5 & -(\alpha_3 + \alpha_4) & -1/\tau_F \end{array}\right].$$

Since the dynamics of the leader is to be considered as an assigned and non-controllable input, the stability of the system can be studied by considering just the subsystem formed by the followers, having dynamic matrix

$$D_p = \left[\begin{array}{ccccc} D_c & \mathbf{0} & \mathbf{0} & \cdots & \mathbf{0} \\ X & D_c & \mathbf{0} & \cdots & \mathbf{0} \\ X & X & D_c & \cdots & \mathbf{0} \\ \vdots & \vdots & \vdots & \ddots & \vdots \\ X & X & X & \cdots & D_c \end{array}\right].$$

Since D_p is block-triangular, its eigenvalues correspond to those of the diagonal block D_c (each with multiplicity N). Denoting $k = \alpha_5$ and $h = \alpha_3 + \alpha_4$, the stability of D_c can be studied by means of the Routh-Hurwitz table:

$$\begin{array}{cc} 1 & h \\ \frac{1}{\tau_F} & k \\ h - k\tau_F & 0 \\ k & 0 \end{array}$$

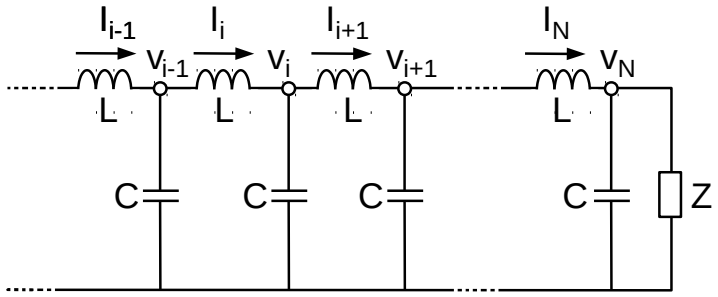

Figure 11.17: A transmission line: impedance matching is achieved for $Z = \sqrt{\frac{L}{C}}$.

Therefore, the system is asymptotically stable (all of the eigenvalues have negative real part) provided that $k > 0$ and $h > \tau_F k$.

When the leader has a constant speed $\dot{y}_0 = \bar{v}$ (hence $u_0 = 0$), being matrix D_p non-singular, the unique solution is $\dot{y}_i = \bar{v}$ and $y_{i-1} - y_i = l_{i-1} + g_d$ for all $i = 1, \ldots, N$, corresponding to the case in which all of the vehicles have the same speed (imposed by the leader) and keep a constant spacing.

Impedance-matched control. An analogy with impedance matching for transmission lines can inspire an acceleration control input having the form

$$u_i = -k(y_i - y_{i-1}) - k(y_i - y_{i+1}) - h(\dot{y}_i - \dot{y}_{i-1}) - h(\dot{y}_i - \dot{y}_{i+1}), \quad i = 1, \ldots, N-1 \quad (11.25)$$

for the intermediate vehicles and

$$u_N = -k(y_N - y_{N-1}) - h(\dot{y}_N - \dot{y}_{N-1}) - \alpha \dot{y}_N \quad (11.26)$$

for the last vehicle of the platoon (which is in charge of implementing "impedance matching"). This can be seen a network-decentralised control, associated with a given "interconnection topology" (corresponding to a path) among the vehicles: each vehicle needs information exclusively about the vehicle in front and the vehicle behind (apart from the last vehicle, which of course needs just information about the vehicle in front). In fact, if a control agent is associated with each arc of the interconnection graph, it can be written that

$$u_i = u_{i,i-1} + u_{i,i+1} \quad \text{where} \quad u_{i,j} = -k(y_i - y_j) - h(\dot{y}_i - \dot{y}_j).$$

The constants k, h and α are design parameters and their value can be chosen, as mentioned, based on an impedance-matching-like criterion. In fact, consider the ideal case of the transmission line in Fig. 11.17. Then, for all $i = 1, \ldots, N-1$, $LC\ddot{v}_i = L\dot{I}_i - L\dot{I}_{i+1} = v_{i-1} - v_i - v_i + v_{i+1}$, hence

$$\ddot{v}_i = k(v_{i-1} - 2v_i + v_{i+1}), \quad \text{where} \quad k = \frac{1}{LC},$$

which does not depend on the voltage derivatives $\dot{v}_i$ if an ideal lossless line is considered. However, adding an analogous term depending on $\dot{v}_i$ leads to the strategy

in equation (11.25). Moreover, $LC\ddot{v}_N = L\dot{I}_N - \frac{L}{Z}\dot{v}_N = v_{N-1} - v_N - \frac{L}{Z}\dot{v}_N$, hence

$$\ddot{v}_N = k(v_{N-1} - v_N) - \frac{1}{CZ}\dot{v}_N,$$

where, as is well-known, the choice $Z = \sqrt{\frac{L}{C}}$ corresponds to the matched impedance. With this choice, $\ddot{v}_N = k(v_{N-1} - v_N) - \frac{1}{\sqrt{LC}}\dot{v}_N$.

The impedance-matching analogy then leads to the choice $\alpha = \sqrt{k}$ in (11.26) (and then also in (11.25)). For the sake of symmetry, it may be chosen $h = \sqrt{k}$ as well. Since $\sqrt{k}$ corresponds to the propagation speed along the platoon, it can be expected that the higher is k, the more "reactive" is the system. By simulation, it can be seen that the proposed network-decentralised control, along with the matched-impedance parameter choice, is effective: the vehicles smoothly follow the leader, without oscillations due to "reflections" (see Fig. 11.18).

The proposed control protocol has two fundamental aspects:

- it works in the absence of communication with the leader;
- vehicle N, the matching vehicle, must automatically recognise to be the last and apply the matching impedance control.

It should be noticed that, with this control strategy, the inter-vehicle spacing

$$y_i - y_{i-1} = \frac{\bar{v}}{\sqrt{k}}$$

in no longer constant, since it depends on both k and the cruising speed $\bar{v}$.

Since the considered system is based on a finite number of vehicles, the transmission line analogy provides just a physical intuition. A numerical criterion can be proposed, however, to show that, indeed, the system behaves like an "impedance matched" line, without reflections. Denoting by u_0 the reference input for the leader, with respect to a frame moving at the desired speed, consider a bounded input

$$|u_0(t)| \leq u_{max}$$

representing the maximum allowable deviation from the current position in the moving frame. If the infinity norm of a scalar signal f is introduced as

$$\|f(t)\|_\infty \doteq \sup_{t \geq 0} |f(t)|,$$

then the maximum relative deviation of each follower $y_i(t)$ can be assessed by introducing the functional (norm)

$$J_i = \sup_{\|u_0\|_\infty \neq 0} \frac{\|y_i\|_\infty}{\|u_0\|_\infty},$$

which can be computed as

$$J_i = \int_0^\infty |F_i(t)|dt,$$

where $F_i(t)$ is the impulse response of the ith follower due to an impulse applied to the leader reference.

The example of a platoon composed of a leader and 10 followers has been simulated with the choice $\tau_F = 0.5$, $k = h = 0.5$ and $\alpha = \sqrt{k}$. The integrals have been numerically evaluated as

1.01 1.0097 1.0179 1.0228 1.0227 1.0169 1.0133 1.0131 1.0128 1.0125 1.0122

and the corresponding step response is reported in Fig. 11.18.

In the case of an ideal transmission line, the signal propagates as a wave (an electromagnetic wave, indeed) and, if impedance matching is implemented, there are no reflected waves coming backwards.[2] Hence, the wave simply propagates the signal of the leader, unchanged, but delayed. In the case of a step response, the ideal behaviour is that in which there is no reflection and all of the quantities become equal to 1 after a certain delay. Fig. 11.18 shows a behaviour that is very close to the ideal case: the step response presents almost no oscillations. Instead, oscillations (due to reflections in the transmission line analogy) are present whenever α is different from the matching value. For instance, if $\alpha = \frac{1}{2}\sqrt{k}$,

1.01 1.1544 1.2993 1.4269 1.5324 1.6141 1.6734 1.7136 1.7385 1.7521 1.7571

and, if $\alpha = 2\sqrt{k}$,

1.01 1.1466 1.2802 1.3881 1.4573 1.4728 1.4193 1.2879 1.0962 0.9205 0.8930.

Note that a generic formation of vehicles (not necessarily aligned in a longitudinal platoon) can be controlled by decomposing the problem in the two directions associated with the x-axis and the y-axis, and independently controlling the spacing in each direction (see Fig. 11.19).

As a future direction, it would be interesting to investigate a saturated type of control for vehicle platoons, and to assess its advantages and disadvantages with respect to the impedance-matched control.

[2] In fact, a signal travelling along an ideal transmission line can be partly or fully reflected back in the opposite direction only if there is a discontinuity in the characteristic impedance of the line, or if the far end of the line is not terminated in its own characteristic impedance. Impedance matching ensures that the line is terminated in its own characteristic impedance, thus preventing reflections: the signal propagates as if the line were infinitely long.

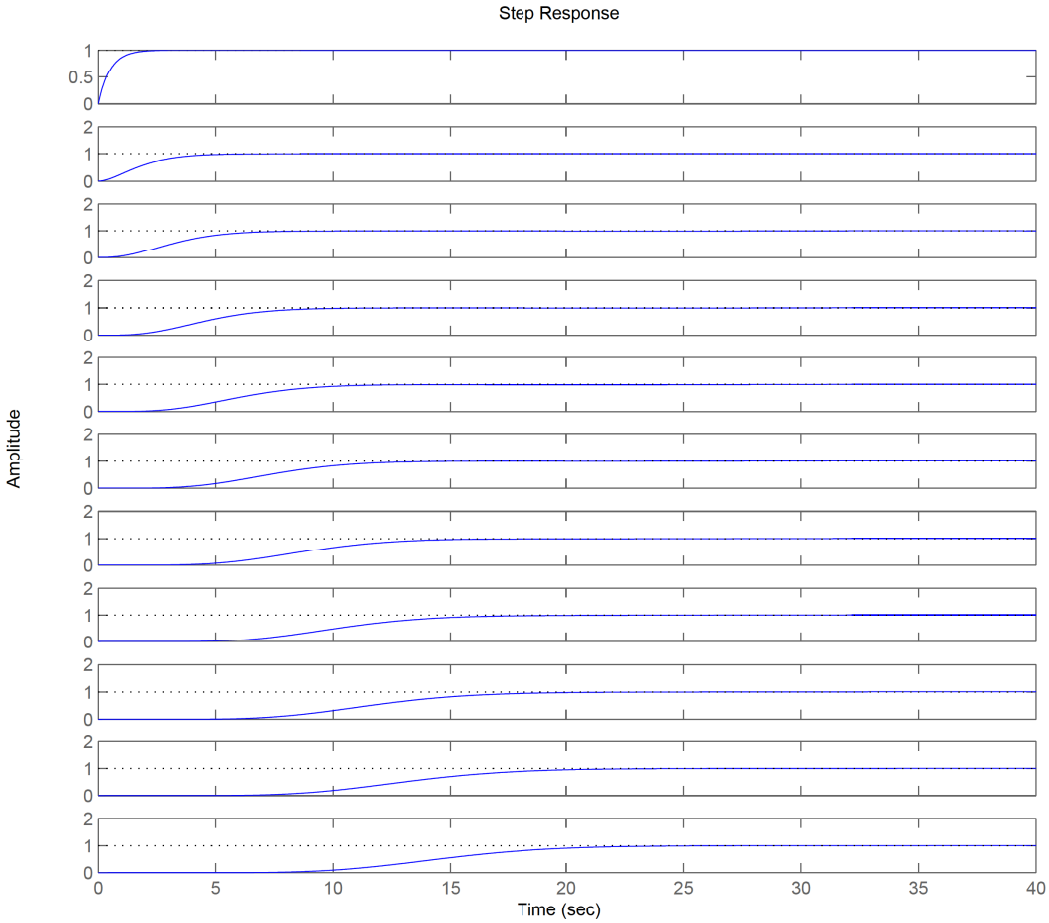

Figure 11.18: The step response for a platoon with 10 cars following a leader. The same "good" behaviour has been verified for quite larger numbers of vehicles, *e.g.*, $N = 30$.

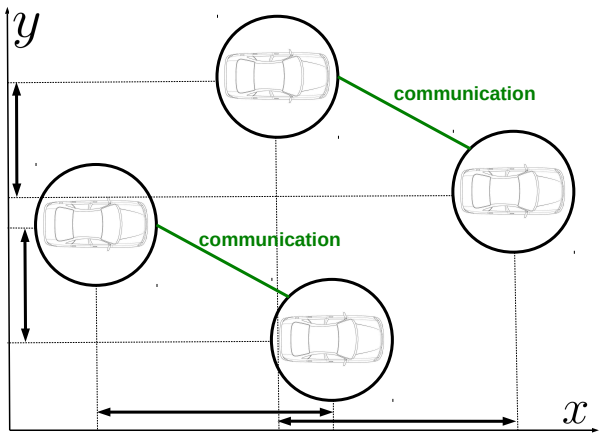

Figure 11.19: The vehicle formation problem in two dimensions.

12

Network-Decentralised Estimation

The dual problem of network-decentralised control is *network decentralised-estimation*, which consists in designing an observer for a network of several agents, where each agent (associated with a node of the network) asymptotically estimates its own state based on information exchanges with the neighbouring agents only. [GBF+15]

In the network-decentralised control case, agents are associated with control components, hence with the arcs of the network. In the case of network-decentralised estimation, agents implement local state observers and are associated with the nodes. The decentralised control of naturally decoupled subsystems is performed by independent agents that decide their strategy relying on restricted information [BMU00, BFG13, BGM14, BFG15a]; analogously, the need of synthesising decentralised observers arises whenever several subsystems, corresponding to the nodes of a network, aim at asymptotically estimating their own state by exchanging local measurements, without having access to the whole network information (*e.g.*, due to security issues [FG14] or operational limitations [KFRC13]).

Distributed estimation and observer design [SH07, SSS09, ISKI11, BDvdWH13, DPB13, LZ15] is a challenging problem, especially for large-scale systems. However, it is crucial for tackling, for instance, formation problems in the absence of a global coordinate system [Cor09, SS09, Zho13, ALNSZ15], when the control can benefit from estimating the states of neighbouring agents, as well as for common reference frame estimation [FG14] and localisation [GJWL05, ABGS08].

It is worth stressing that the network-decentralised estimation problem proposed in [GBF+15] is different from the network-distributed (global) estimation problem: in the latter case, in fact, each agent aims at determining the overall system state (see [Ugr13] and the references therein), while in the former case a local estimation problem is formulated, in which each agent aims at estimating its own state only and it *has not even the knowledge* about the existence of the agents with which it cannot directly communicate. In a network-decentralised estimation framework, it is therefore assumed that the network topology is unknown to the nodes, which can rely on information about their neighbouring nodes only.

In the case of identical agents, along the lines of the previous chapters, it is shown that a basic necessary and sufficient condition for global convergence is that the network is connected to the external environment: necessity is intuitive (for

instance, to achieve localisation, at least one of the communicating agents must have information on its absolute position), while sufficiency can be proved constructively.

Following [GBF+15], a network-decentralised estimation scheme can be designed by starting from local observers (typically chosen as optimal filters) and then adapting the gain so as to globally ensure stability and global robustness. In this second phase, the network connectivity must be taken into account and the smallest eigenvalue of the generalised Laplacian matrix plays a key role. In fact, to ensure robust stability of the system, the gain has to be greater than a threshold value depending on this eigenvalue (which is strictly positive as long as the graph includes a connection with the external environment, in contrast to the smallest eigenvalue of the standard Laplacian matrix, which is zero; in fact, the generalised Laplacian matrix is positive definite, while the standard Laplacian is positive semi-definite).

In this chapter, the results in [GBF+15] about the smallest eigenvalue of the generalised Laplacian matrix are presented, along with an application to estimation for a network of agents.

Along with a result on the *worst-case* smallest eigenvalue of the generalised Laplacian matrix for connected graphs with an external connection, it is also shown that the worst-case graph is a path graph. This result suggests that poorly connected networks are more fragile than highly connected networks. The characterisation of the worst-case is fundamental to face uncertain network topologies and situations in which only the maximum number of nodes is known.

Applied to the network-decentralised estimation problem, the results on the smallest eigenvalue of the generalised Laplacian matrix provide therefore a non-conservative bound that ensures robustness under arbitrary, unknown and possibly time-varying (switching) network topologies.

Finally, some application examples are proposed, which show interesting properties in themselves; for instance, when the node dynamics are integrators, the proposed scheme achieves the optimal (least-square) solution.

12.1 Generalised Laplacian: Smallest Eigenvalue

The second smallest eigenvalue of the standard Laplacian matrix (*i.e.*, the first positive one, since the smallest is zero) has been widely investigated as a measure of connectivity [Fie73, Mer94, RBA07, BGP09]. In the case of an externally connected graph, the smallest eigenvalue of the generalised Laplacian, which is positive, may be considered as a connectivity measure.

In [GBF+15] it is shown that, for all the N-node networks connected with the external environment, the smallest possible eigenvalue is lower bounded as $\lambda^*_{min}(N) \geq 1/\sigma_{max}(\Phi_N)$, where $\sigma_{max}(\Phi_N)$ is the largest eigenvalue of the symmetric matrix Φ_N, with entries $[\Phi_N]_{ij} = N + 1 - \max\{i, j\}$; it is also shown that the worst-

case topology, which reaches the bound (hence, the bound is tight), corresponds to a path graph, namely, to a tree with a single leaf (in [WRL14] it was suggested, although not proved, that a "chain" topology is the worst-case scenario).

Consider a directed graph with N nodes and arcs that can either connect two nodes (internal arcs) or connect one of the nodes with the external environment (external arcs). In the generalised incidence matrix G that characterises the graph (previously introduced in Chapter 4, where it was called B), the jth column is zero, apart from

- a -1 in the kth position and a 1 in the hth position, if arc j connects node k to node h;
- a 1 in the kth position, if arc j connects node k with the external environment.

To characterise the smallest eigenvalue of the generalised Laplacian $L = GG^\top$, some preliminary results are needed.

Lemma 12.1. *Matrix G is totally unimodular.*[1]

Proof. The incidence matrix of a directed graph is always totally unimodular [VF21, Sch86]. The generalised incidence matrix G is totally unimodular as well, being a sub-matrix of an incidence matrix G_0 (which can be obtained by explicitly considering the external node 0 as a node of the graph). □

Definition 12.1. *A graph is* internally connected *if each pair of nodes are the extrema of a path. A graph is* externally connected *if, for each node, there exists a path connecting it to a node adjacent to node* 0 *(namely, a path leading to the external environment). A graph is* connected *if it is both internally and externally connected.*

Although the incidence matrix G characterises a directed graph, the direction of the arcs is no longer relevant when the Laplacian matrix is considered. In fact, if the sign of any column of G is changed, the Laplacian $\mathcal{L} = GG^\top$ is the same. For this reason, in the previous definitions, the direction of the arcs is neglected.

Denote by λ_{min} the smallest eigenvalue of the generalised Laplacian matrix $L = GG^\top$ and by $\lambda^*_{min}(N)$ the smallest generalised Laplacian eigenvalue of all connected graphs with N nodes.

Note that the generalised Laplacian matrix $L = GG^\top$ is non-singular (equivalently, $\lambda_{min} > 0$) if and only if the graph is externally connected [BBGP13].

Proposition 12.1. *Consider two graphs represented by the generalised incidence matrices G and G'. If the arcs of G are a proper subset of those of G', then*

$$\lambda_{min}[GG^\top] \leq \lambda_{min}[G'G'^\top].$$

[1] Namely, the determinant of each square sub-matrix achieved by selecting k rows and k columns of G is either 0, -1 or 1.

Proof. The columns of G' can be ordered so that $G' = [G\ \Delta]$, where Δ includes all column vectors associated with the arcs in G' that are not in G. Then

$$G'G'^{\top} = GG^{\top} + \Delta\Delta^{\top}.$$

Weil's inequality [Fra93] can be exploited, which states that, if a positive definite matrix $GG^{\top}$ is perturbed by adding a semi-definite matrix $\Delta\Delta^{\top}$, then the new ordered eigenvalues λ'_k are not smaller than the original ordered ones λ_k: $\lambda'_k \geq \lambda_k$. □

If a graph is not internally connected, it can be partitioned into *internally connected components*, each formed by a subset of nodes, such that:

- each component is internally connected;
- if two nodes i and j belong to two distinct components, there is no internal path[2] connecting them.

Remark 12.1. *Two internally connected components can be both connected to the external environment. Hence, a graph which is not internally connected is externally connected iff each of its internally connected components is externally connected.*

If the graph can be partitioned into C internally connected components, then, by suitably reordering the nodes, the generalised Laplacian can be written in the block-diagonal form

$$GG^{\top} = \text{blockdiag}\{G_1G_1^{\top}, G_2G_2^{\top}, \ldots, G_CG_C^{\top}\},$$

where $G_jG_j^{\top}$ is the generalised Laplacian matricx associated with the jth internally connected component. Since the spectrum of $GG^{\top}$ is the union of the spectra of $G_jG_j^{\top}$, $j = 1, \ldots, C$, to characterise the smallest eigenvalue, the case of a connected graph (composed of a single internally connected component) can be analysed without restriction.

In standard graph theory, a *tree* defined on N nodes is an internally connected graph having the smallest number $(N-1)$ of internal arcs (equivalently, an internally connected graph without cycles); a generalised tree can be defined as a tree with a single additional external arc, connecting one of the nodes to node 0. A generalised tree is a *path graph* if it has a single branch (namely, each node is connected with at most two other nodes, including node 0).

Recall that a connected graph is internally connected and has at least one external connection.

Proposition 12.2. *Among all connected graphs with N nodes, the graph corresponding to $\lambda^*_{min}(N)$ is a generalised tree.*

Proof. Any connected graph can be achieved by adding arcs to a tree and, in view of Proposition 12.1, adding connections does not decrease the smallest eigenvalue. □

[2] An internal path is a path not including node 0 (the external environment).

Therefore, the graph providing $\lambda^*_{min}(N)$ is to be sought among all generalised trees. This is expected, since trees have the minimal connectivity. Precisely, $\lambda^*_{min}(N)$ is achieved when the tree is a path graph.

Theorem 12.1. *Consider all possible generalised trees with N nodes. Then,*

$$\lambda^*_{min}(N) = \frac{1}{\sigma_{max}(\Phi_N)},$$

where $\sigma_{max}(\Phi_N)$ denotes the largest eigenvalue of matrix

$$\Phi_N = \begin{bmatrix} N & N-1 & \dots & 1 \\ N-1 & N-1 & \dots & 1 \\ \vdots & \vdots & \ddots & \vdots \\ 1 & 1 & \dots & 1 \end{bmatrix}.$$

Moreover, the tree corresponding to $\lambda^*_{min}(N)$ is a path graph.

Proof. A sketch of the complete proof is here reported.

- Since a generalised tree with N nodes has N arcs, the generalised incidence matrix G is square. By suitably ordering the nodes of the tree, so that node 1 is connected with the external environment, matrix $G^\top$ becomes lower triangular, with unitary diagonal entries and just one other non-zero entry, equal to -1, in each row.
- Then $-G^\top$ is a Metzler matrix with negative-real-part eigenvalues, hence $(G^\top)^{-1}$ is non-negative [BP94] and lower triangular with unitary diagonal entries.
- Due to Lemma 12.1, $G^\top$ is totally unimodular, along with its inverse. Therefore, any entry in the lower triangular part of $(G^\top)^{-1}$ is either 0 or 1.
- Among all possible matrices $(G^\top)^{-1}$ corresponding to generalised trees, that corresponding to the path graph is the most populated by ones. In fact, in the case of a path graph, $[(\bar{G}^\top)^{-1}]_{ij} = 1$ for all $i \geq j$.
- Let $G^\top$ correspond to any generalised tree. Denoting by $y = G^\top x$, in view of the invertibility of $G^\top$ (due to the external connection), $x = (G^\top)^{-1}y$. The value λ_{min} solves the following optimisation problem:

$$\lambda^{1/2}_{min} = \inf_{x \neq 0} \frac{\|G^\top x\|}{\|x\|} = \inf_{y \neq 0} \frac{\|y\|}{\|(G^\top)^{-1}y\|} = \left[\sup_{y \neq 0} \frac{\|(G^\top)^{-1}y\|}{\|y\|}\right]^{-1}.$$

  Namely, $\lambda^{1/2}_{min}$ is the inverse of the induced norm of $(G^\top)^{-1}$, which is the square root of the maximum eigenvalue of $(G)^{-1}(G^\top)^{-1}$.
- Due to the structure of matrix $(G^\top)^{-1}$, the largest norm is achieved for $(\bar{G}^\top)^{-1}$, where $\bar{G}$ is the incidence matrix of the path graph.
- $\Phi_N = (\bar{G})^{-1}(\bar{G}^\top)^{-1}$.

The detailed proof is provided in [GBF+15]. □

Corollary 12.1. *$\sigma_{max}(\Phi_N)$ is a non-decreasing function of N.*

Proof. The result follows since matrix Φ_{N+1} is achieved by adding a non-negative matrix to $\tilde{\Phi}_N = \begin{bmatrix} 0 & 0 \\ 0 & \Phi_N \end{bmatrix}$, whose eigenvalues are those of Φ_N and the zero eigenvalue (hence, $\sigma_{max}(\tilde{\Phi}_N) = \sigma_{max}(\Phi_N)$). See [GBF+15] for details. □

The non-connected case. Consider an externally connected graph with N nodes, which is not internally connected and is composed of C internally connected components (necessarily, each externally connected). By suitably reordering the nodes, its Laplacian matrix can be written as a block-diagonal matrix $L = \text{blockdiag}\{L_1, \ldots, L_C\}$, where each of the diagonal blocks corresponds to the Laplacian matrix of an internally connected component. Hence, denoting by $\lambda_{min}^{(i)}$ the smallest eigenvalue of matrix L_i, the smallest eigenvalue of L is $\lambda_{min} = \min\{\lambda_{min}^{(1)}, \ldots, \lambda_{min}^{(C)}\}$. The next corollary then immediately follows from Theorem 12.1 and Corollary 12.1.

Corollary 12.2. *Consider all possible externally connected graphs with N nodes and $C \leq N$ internally connected components. Then,*

$$\lambda_{min}^{*}(N) = \frac{1}{\sigma_{max}(\Phi_K)},$$

where $K \leq N$ is the number of nodes in the largest internally connected component and $\sigma_{max}(\Phi_K)$ is defined as in Theorem 12.1. Moreover, the subgraph corresponding to the largest internally connected component is a path graph.

It follows that, in general, the worst case is given by a fully connected graph whose unique internally connected component is a path graph.

12.2 Network-Decentralised Detectability

To formulate the network-decentralised estimation problem, N agents are considered, with dynamics

$$\dot{x}_i = A_i x_i + B_i u_i, \quad i = 1, ..., N,$$

where $x_i \in \mathbb{R}^{n_i}$, $u_i \in \mathbb{R}^{m_i}$. Each agent has a (non-empty) set of neighbours $\mathcal{O}_i$. Measurements are associated with arcs in the network of agents; for example the jth arc, connecting two agents i and k, is associated with a relative measurement $y_j = (C_{ji} x_i + C_{jk} x_k)$. Each agent runs a local estimator defined as:

$$\dot{z}_i = A_i z_i + B_i u_i + \sum_{j \in \mathcal{O}_i} L_{ij}(\hat{y}_j - y_j). \tag{12.1}$$

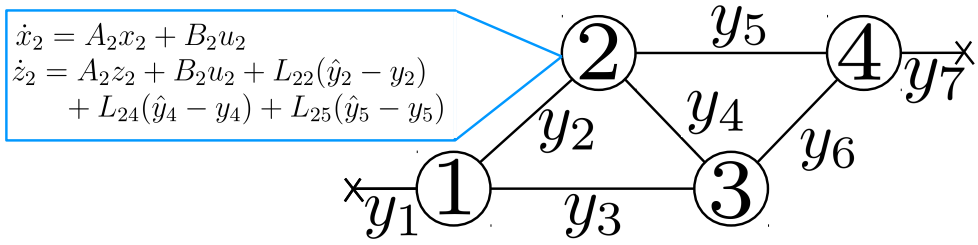

Figure 12.1: Graph corresponding to the four-agent model in Example 12.1; external connections are indicated by crosses.

The estimated measurement $\hat{y}_j$ of each arc is:

$$\hat{y}_j = \sum_{k \in \mathcal{N}_j} C_{jk} z_k,$$

where $\mathcal{N}_j$ is the set that indexes the nodes connected by arc j.

It is worth underlining that this expression is valid in general, even in the presence of hyperarcs connecting more than two nodes.

Example 12.1. *Consider the communication topology among four agents shown in Fig. 12.1. The agents, associated with the nodes of the graph, exchange information about their state; measurement signals y_i are associated with the arcs. Crosses indicate connections with the external environment: since nodes* 1 *and* 4 *are adjacent to node* 0, *y_1 depends exclusively on the state of agent* 1, *y_7 depends exclusively on the state of agent* 4. *Consider for instance agent* 1, *with dynamics $\dot{x}_1 = A_1x_1 + B_1u_1$. Since it has knowledge about y_1, y_2 and y_3, its local observer will be:*

$$\dot{z}_1 = A_1z_1 + B_1u_1 + L_{11}(C_{11}z_1 - y_1) + L_{12}(C_{21}z_1 + C_{22}z_2 - y_2) + L_{13}(C_{31}z_1 + C_{33}z_3 - y_3).$$

Agent 1 *measures the common inputs y_2 and y_3, receives the estimated outputs $C_{22}z_2$ from agent* 2 *and $C_{33}z_3$ from agent* 3, *respectively, and computes its estimated outputs $C_{21}z_1$, which it transmits to agent* 2, *and $C_{31}z_1$, which it transmits to agent* 3. *Besides, since node* 1 *is externally connected, agent* 1 *receives the actual output y_1 from the anchor (the cross) and compares it with the estimated output $C_{11}z_1$.*

The dynamics of the overall system of agents, along with their observer, is:

$$\begin{cases} \dot{x} = Ax + Bu \\ y = Cx \\ \dot{z} = Az + Bu - Ly + LCz \end{cases} \tag{12.2}$$

where matrix $A \in \mathbb{R}^{n \times n}$ is a block-diagonal matrix, whose blocks are the individual agent matrices A_i, B is a generic input matrix and matrix $C \in \mathbb{R}^{p \times n}$ has a block structure that depends on the agents communication topology. The dynamics of the estimation error $e = x - z$ are:

$$\dot{e} = Ae + L(y - Cz) = (A + LC)e. \tag{12.3}$$

Definition 12.2. *The observer defined by matrix L is a* network-decentralised observer *if L has the same block structure as $C^\top$.*

Definition 12.3. *System* (12.2) *is* network-decentralised detectable *if the error dynamics* (12.3) *are asymptotically stable.*

Remark 12.2. *The structure of L corresponds to that of the incidence matrix G of the interconnection graph. System* (12.2) *is externally connected iff the corresponding block-row in matrix C has a single non-zero block.*

Example 12.2. *In Example 12.1 (Fig. 12.1), the output matrix and the overall estimator matrix are, respectively,*

$$C = \begin{bmatrix} C_{11} & 0 & 0 & 0 \\ C_{21} & C_{22} & 0 & 0 \\ C_{31} & 0 & C_{33} & 0 \\ 0 & C_{42} & C_{43} & 0 \\ 0 & C_{52} & 0 & C_{54} \\ 0 & 0 & C_{63} & C_{64} \\ 0 & 0 & 0 & C_{74} \end{bmatrix} \quad \textit{and} \quad L = \begin{bmatrix} L_{11} & L_{12} & L_{13} & 0 & 0 & 0 & 0 \\ 0 & L_{22} & 0 & L_{24} & L_{25} & 0 & 0 \\ 0 & 0 & L_{33} & L_{34} & 0 & L_{36} & 0 \\ 0 & 0 & 0 & 0 & L_{45} & L_{46} & L_{47} \end{bmatrix}.$$

Nodes 1 *and* 4 *are connected with the external environment; consistently, the first and last row of matrix C have a single non-zero block.*

Denote as *unstable* an eigenvalue having a non-negative real part and recall that a system is detectable if all of its unstable eigenvalues are observable. Then, based on the stabilisability results in [BFG15a], the detectability result immediately follows from duality.

Theorem 12.2. *If A_i do not share unstable eigenvalues, then system* (12.2) *is network-decentralised detectable if and only if it is detectable.*

It is unclear, at this moment, whether the property holds or not, in general, in the case of common unstable eigenvalues. However, there are special cases in which interesting results can be found.

12.2.1 Identical Agents

Systems associated with proper graphs (where, therefore, matrix C has at most two non-zero blocks for each row, since each arc connects at most two nodes, and its non-zero blocks, if they are two, are opposite), where matrices A_i are equal for all the agents arise, for instance, in distributed localisation problems.

Assumption 12.1. *$A_i = A_1$ and $C_{ij} = \pm C_1$, for all non-zero blocks. Moreover there are at most two non-zero blocks C_1 for each block-row of C; if the non-zero blocks are two, they are opposite.*

In the case of Example 12.1, it would be $C_{11} = C_1$, $C_{21} = -C_1$, $C_{22} = C_1$, $C_{31} = -C_1$, $C_{33} = C_1$, and so on.

Assumption 12.2. *(A_1, C_1) is detectable.*

This assumption is not restrictive, since it can be immediately seen that the problem cannot be solved if this assumption is not verified.

As previously seen, the information exchange can be represented by a directed graph with incidence matrix G. In particular,

$$C = G^\top \otimes C_1,$$

where $\otimes$ denotes the Kronecker product (hence, C is the expansion of $G^\top$ achieved by replacing $\{-1, 0, 1\}$ entries respectively by $\{-C_1, 0 \times C_1, C_1\}$). Note also that

$$A = I \otimes A_1.$$

Example 12.3. *Consider a system with the structure described in Example 12.1, in which each agent aims at reconstructing its position in the plane by exchanging information with its neighbours. Denoting by $r_i \in \mathbb{R}^2$ the position of agent i (unknown to the agent itself), each agent exchanges information about its own estimated position with all of its neighbours. If all the agents are standing still, the equations are $\dot{r}_i(t) = 0$, hence $A_1 = \mathbf{0}_2$, the 2×2 zero matrix. Each agent can update its own estimated position, $z_i(t)$, by communicating with the others. In this case, all the non-zero blocks in C are either I_2 or $-I_2$, where I_2 is the 2×2 identity matrix. Then the updating equation for agent 1 is*

$$\dot{z}_1 = B_1 u_1 + L_{11}(z_1 - \underbrace{r_1}_{y_1}) + L_{12}(z_1 - z_2 - \underbrace{(r_1 - r_2)}_{y_2}) + L_{13}(z_1 - z_3 - \underbrace{(r_1 - r_3)}_{y_3}).$$

Denoting by $e = z - r$ the estimated error, $\dot{e}(t) = LCe(t)$, where L must have the same block structure as $C^\top$.

Remark 12.3. *It is not necessary for the graph to be connected. It is just required that* each internally connected component is externally connected*: among the columns of the incidence matrix associated with an internally connected component, at least one must have a single non-zero entry (corresponding to a single non-zero block in at least one row of C). Hence, a path exists that connects each node of the graph to the external environment.*

Lemma 12.2. *System* (12.2) *is network-decentralised detectable if and only if there exists $\gamma \geq 0$ such that the following Lyapunov inequality is satisfied:*

$$A^\top P + PA - 2\gamma C^\top C < 0. \tag{12.4}$$

A stable observer is $L = -\gamma P^{-1} C^\top$.

Proof. If the system is network-decentralised detectable, then the observer matrix $(A + LC)$ is stable and satisfies the Lyapunov equation:

$$(A + LC)^\top P + P(A + LC) < 0. \tag{12.5}$$

If $L = -\gamma P^{-1} C^\top$, equation (12.4) is recovered. Conversely, if (12.4) is satisfied and C is block-structured, the choice $L = -\gamma P^{-1} C^\top$ allows to convert equation (12.4) to equation (12.5). □

Theorem 12.3. *Under Assumptions 12.1 and 12.2, system* (12.2) *is network-decentralised detectable if and only if at least one of these conditions holds:*

(a) A_1 is asymptotically stable;
(b) the system is externally connected.

Proof. **Sufficiency.** (a) If A_1 is asymptotically stable, then equation (12.4) holds for any $\gamma > 0$: $P = \text{blockdiag}\{P_1, P_1, \dots, P_1\}$, for any P_1 such that $A_1^\top P_1 + P_1 A_1 < 0$, provides $A^\top P + PA < 0$, hence the system is network-decentralised detectable.

(b) Without loss of generality, consider a connected graph (should the graph be composed of many internally connected components, each externally connected, the same reasoning could be applied to each internally connected component). Even if A_1 is not asymptotically stable, $\gamma > 0$ may be chosen sufficiently large to satisfy (12.4) for the single subsystem, so that $A_1^\top P_1 + P_1 A_1 - 2\gamma C^\top C < 0$. Then, replacing without restriction P_1 with $\tilde{P}_1 \doteq P_1/\gamma$, and keeping on writing P_1 for simplicity, it can be assumed $z_i^\top [A_1^\top P_1 + P_1 A_1 - 2C_1^\top C_1] z_i < 0 \quad \forall\, i$.

Being $z^\top [C^\top C] z \geq 0$, the inequality (12.4), with $P = \text{blockdiag}\{P_1, P_1, \dots, P_1\}$, holds for $\gamma > 0$ large enough if, for any non-zero $z \in \ker(C)$, $z^\top [A^\top P + PA] z < 0$. [BEGFB94] Partitioning the state as $z = \begin{bmatrix} z_1^\top & z_2^\top & \dots & z_N^\top \end{bmatrix}^\top$, in view of Assumption 12.1, for each block-row of C with two non-zero blocks, say h and k, it must be $C_1 z_h = C_1 z_k$. Since the graph is connected, $C_1 z_1 = C_1 z_2 = \dots = C_1 z_N$. Moreover, since the graph is externally connected, it must be $C_1 z_l = 0$ for some l (in fact, for one row the block l only is different from zero). Hence, $C_1 z_k = 0$ for all k. In conclusion, $z \in \ker(C)$ iff $z_i \in \ker(C_1)$. Then $z^\top [A^\top P + PA] z = \sum_{i=1}^N z_i^\top [A_1^\top P_1 + P_1 A_1] z_i < 0$, in view of the detectability assumption on (A_1, C_1). See [GBF+15] for details.

Necessity Assume by contradiction that neither condition (a) nor condition (b) holds. Let λ be an unstable eigenvalue of A_1 and z_1 the corresponding eigenvector of A_1; then $z = [z_1^\top \; z_1^\top \dots z_1^\top]^\top$ is an eigenvector of A. If the graph is not externally connected, then $Cz = 0$ (in each block-row there are two opposite blocks). Then

$$\begin{bmatrix} \lambda I - A \\ C \end{bmatrix} z = 0.$$

Based on the Popov criterion, this means that λ is an unobservable eigenvalue with non-negative real part, hence the system is not detectable. □

12.3 Gain Computation

In the case of unknown topology, a design approach inspired by the proof of Theorem 12.3 can be adopted, which requires solving the following two steps.

- For the single subsystems (A_1, C_1), design a gain $L_1 = -P_1^{-1}C_1^\top$, by means of some optimality criterion (*i.e.*, Kalman gain), where P_1 satisfies
$$A_1^\top P_1 + P_1 A_1 - 2C_1^\top C_1 < 0. \tag{12.6}$$
In this way the system works even for isolated nodes.
- Given a known matrix P_1 satisfying (12.6), to achieve global stability under connections, apply the network-decentralised filter gain
$$L = -\gamma P^{-1} C^\top, \tag{12.7}$$
for some $\gamma > 0$, with
$$P = \text{blockdiag}\{P_1, P_1 \dots P_1\}. \tag{12.8}$$

Theorem 12.3 does not provide any information on how large $\gamma > 0$ should be chosen. If A_1 is asymptotically stable, then any $\gamma > 0$ is suitable. In the interesting unstable case, a lower bound for γ is given by the following theorem, in which the assumption of external connection is crucial.

Theorem 12.4. *Under Assumptions 12.1 and 12.2, let G be the incidence matrix of the graph. If the graph is externally connected, then the overall filter is stable provided that*
$$\gamma > \gamma^* \doteq \frac{1}{\lambda_{min}[GG^\top]}, \tag{12.9}$$
where $\lambda_{min}[GG^\top]$ is the smallest eigenvalue of matrix $GG^\top \in \mathbb{R}^{N\times N}$.

Proof. Denoting by $\tilde{C}^\top\tilde{C} = \text{blockdiag}\{C_1^\top C_1, C_1^\top C_1, \dots, C_1^\top C_1\}$, the inequality (12.4) becomes $(A^\top P + PA - 2\tilde{C}^\top\tilde{C}) + (2\tilde{C}^\top\tilde{C} - 2\gamma C^\top C) < 0$. The first addend in parentheses is negative definite, in view of its diagonal structure and of (12.6). To assess the remaining part $(2\tilde{C}^\top\tilde{C} - 2\gamma C^\top C)$, take $z = \begin{bmatrix} z_1^\top & z_2^\top & \dots & z_N^\top \end{bmatrix}^\top$, $\tilde{y}_k = C_1 z_k$ and $\tilde{y} = \begin{bmatrix} \tilde{y}_1^\top & \tilde{y}_2^\top & \dots & \tilde{y}_N^\top \end{bmatrix}^\top$. The sought condition is
$$z^\top[2\tilde{C}^\top\tilde{C} - 2\gamma C^\top C]z = y^\top 2Iy - y^\top 2\gamma\Gamma\Gamma^\top y = y^\top 2[I - \gamma\Gamma\Gamma^\top]y < 0, \tag{12.10}$$
where $\Gamma = G \otimes I_p$ has the same structure as matrix G (I_p is the identity of dimension p). Hence, $\Gamma\Gamma^\top \in \mathbb{R}^{pN\times pN}$ has the same eigenvalues of $GG^\top \in \mathbb{R}^{N\times N}$, repeated p times. This means that (12.10) is true if (12.9) holds, and the proof is over. □

Remark 12.4. *The requirement* (12.9) *is consistent with the necessity of assuming connection with the external environment. In the absence of external connection, indeed, $\lambda_{min}[GG^\top] = 0$.*

12.4 Unknown and Switching Topologies

A robust bound on γ^* must be determined to assure stability when the network topology is unknown and potentially switching. Assume that the network incidence matrix G_t depends on time (in fact, the network topology is fully characterised by the incidence matrix G).

Assumption 12.3. *The incidence matrix $G_t \in \mathbb{R}^{N\times m_t}$, where N is the number of agents (nodes) and m_t is the number of links, belongs to some given family $\mathcal{G}(N, n_A)$, where n_A is the number of anchors (*i.e.*, of connections with the external environment). Moreover, the current topology G_t is unknown to the agents.*

Given the number N of agents and the number n_A of anchors, a robust bound on $\gamma^* \geq 0$ must be found such that, if $\gamma > \gamma^*$, the network-decentralised observer remains stable under arbitrary switching $G_t \in \mathcal{G}(N, n_A)$.

Before proceeding further, the assumption of full row rank of G needs to be introduced and discussed. Any graph $\mathcal{G}$, not necessarily connected, can be uniquely partitioned into internally connected components $\mathcal{G}_1, \mathcal{G}_2, \ldots, \mathcal{G}_k$ that are connected graphs, each defined on a subset of nodes of $\mathcal{G}$ and such that there is no arc connecting nodes of different components. By means of a proper node and link ordering, the corresponding matrix G can be arranged in a block-diagonal form:

$$G = \text{blockdiag}\{G_1, \ldots, G_k\}. \tag{12.11}$$

Proposition 12.3. *Matrix G has full row rank if and only if each internally connected component of the graph is connected with the external environment, namely, if each block-matrix in* (12.11) *has at least one column with a single non-zero entry.*

Proof. Matrix G has full row rank if and only if there is no row vector $z = [z_1 \;\; z_2 \;\; \ldots z_k] \neq 0$ such that $zG = 0$ (namely, $zG = 0$ implies $z_i = 0$ for all i). If each internally connected component is connected with the external environment, then, for all i, G_i has full row rank, hence $z_i = 0$. Conversely, if one internally connected component is not externally connected, then $\bar{1}^\top G_i = 0$ because each column of G_i has two non-zero entries equal to 1 and -1 respectively. □

Indeed, if the graph has several internally connected components, then each of them must have an anchor (cf. Fig. 12.2).

Theorem 12.5. *Assume that A_1 is not asymptotically stable. Then the two following statements are equivalent.*

i) All of the matrices $G \in \mathcal{G}(N, n_A)$ have full row rank N.
ii) There exists $\gamma^* \geq 0$ such that the network-decentralised observer is stable for $\gamma > \gamma^*$ under arbitrary switching $G_t \in \mathcal{G}(N, n_A)$.

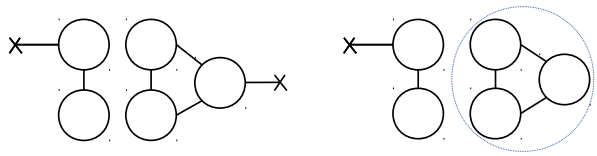

Figure 12.2: Left: each internally connected component has an anchor. Right: there is an isolated component, which may be subject to a "drift".

Proof. i) $\Rightarrow$ ii): if all the matrices G in $\mathcal{G}(N, n_A)$ (which are in finite number) have full row rank, then all the matrices $GG^\top$ have full row rank as well; hence, for any

$$\gamma^* \doteq \min_{G \in \mathcal{G}(N,n_A)} \frac{1}{\lambda_{min}[GG^\top]}, \tag{12.12}$$

P as in (12.8) gives a common quadratic Lyapunov function in view of Theorem 12.4.

ii) $\Rightarrow$ i): by contradiction, assume that some $\tilde{G} \in \mathcal{G}(N, n_A)$ does not have full row rank. Then, if $G_t = \tilde{G}$, there is no asymptotic stability. Hence, there exists at least one internally connected component of the graph that is not connected to the external environment. Since by assumption A_1 is not asymptotically stable, take a (column) eigenvector z_1 associated with an eigenvalue which is not asymptotically stable: $A_1 z_1 = \lambda z_1$. Then, by partitioning A in two diagonal blocks, the first associated with the internally connected component that is not externally connected and the second with the internally connected component that is externally connected, the non-zero vector $z^\top = [z_1^\top \; z_1^\top \ldots z_1^\top \; 0 \; 0 \ldots 0] = [\bar{z}_1^\top \;\; \bar{0}^\top]$ can be considered that selects the first subsystem. Therefore, proceeding exactly as in Theorem 12.3, the system has an unobservable eigenvalue that is not asymptotically stable. Details are in [GBF+15]. □

It is not necessary to identify the set of all possible topologies $G \in \mathcal{G}(N, n_A)$: a robust bound can be provided based on N (the number of nodes) only, according to the next result, whose proof follows directly from Theorems 12.5 and 12.1.

Theorem 12.6. *Let G_t be the incidence matrix of any connected[3] graph with N nodes. Then, stability is assured if*

$$\gamma > \gamma^* \doteq \frac{1}{\lambda^*_{min}(N)} = \sigma_{max}(\Phi_N). \tag{12.13}$$

Moreover, being $\sigma_{max}(\Phi_N)$ an increasing function of N, according to Corollary 12.1, the following result holds.

Corollary 12.3. *Let G_t be the incidence matrix of any connected graph with $N \leq \bar{N}$ nodes. Then, stability is assured if $\gamma > 1/\lambda^*_{min}(\bar{N}) = \sigma_{max}(\Phi_{\bar{N}})$.*

Finally, in an interesting case, it can be shown that any $\gamma > 0$ is suitable.

[3]It is worth reminding that a connected graph is both internally and externally connected.

Proposition 12.4. *Assume that $A = 0$ and C_1 has full column rank.*[4] *Then, if the necessary and sufficient condition i) of Theorem 12.5 is satisfied, the proposed network-decentralised observer with $P = I$ is stable for any $\gamma > 0$.*

Proof. Being externally connected, G_t has full row rank. Hence, $C = G_t^\top \otimes C_1$ has full column rank. The observer error equation is $\dot{e} = -\gamma C_t^\top C_t e$, with $C_t^\top C_t$ positive definite for all t, therefore all matrices $-\gamma C_t^\top C_t$ share the common quadratic Lyapunov function $V(e) = e^\top e$. □

12.5 Application Examples

Example 12.4. Node localisation. *Consider a set of given points r_i, each associated with an agent willing to establish its own position based on absolute information, if available, and by exchanging information with the neighbouring agents only, as in Example 12.3. For instance, some agents in an unknown region could exchange information to construct a topographic map.*

Two communicating agents have to measure their distance and the angle formed by the segment between them and an absolute reference direction. Of course, some of the agents must be externally connected, so that they have information on their absolute position (and any other agent connected with one of these is externally connected as well).

The theory applies quite straightforwardly by taking $P = I$, so that the observer gain matrix is $L = -\gamma C^\top$ and the observer matrix (affecting the dynamics of the error equation) is $-\gamma C^\top C$, which is stable as long as the graph is connected.

An interesting feature of the proposed network-decentralised estimation strategy can be noticed if the effect of additive noise is considered:

$$y = Cx - \delta.$$

The error equation associated with the resulting network-decentralised observer is

$$\dot{e} = -\gamma C^\top C e + \gamma C^\top \delta$$

and, asymptotically, the error becomes

$$e(\infty) = (C^\top C)^{-1} C^\top \delta,$$

which is the least-square solution of the minimisation problem $\min \|Ce - \delta\| = \min \|y - Cz\|$.

To quantify the error filtering property, N–node networks with a varying connectivity degree can be randomly generated: the number of arcs is $m = \frac{N(N-1)}{2}\frac{p}{100}$,

[4] If C_1 did not have full column rank, then (A_1, C_1) would not be detectable, against the stated assumptions.

where $0 < p \leq 100$ *is the connectivity degree and* $m_{max} = \frac{N(N-1)}{2}$ *is the maximum number of internal connections (non-oriented arcs) for a network with* N *nodes. To assure connectivity, at each random experiment* N *arcs have been initially placed, corresponding to a path including an external connection; the remaining arcs have been added by randomly selecting the departure and arrival node and when, by chance, the two coincide, an external connection has been added. A noise* δ *has been then added (so that* $y = Cx - \delta$*) with components* δ_k *uniformly generated in* $[-1 \quad 1]$.

The index

$$J = \frac{var(e)}{var(\delta)}$$

has been computed at steady state, considering $n_s = 1000$ *samples. The results for* $\gamma = 1$ *(which is suitable, in view of Proposition 12.4) are reported in Table 12.1. As expected, noise rejection increases (hence,* J *decreases) with connectivity. Less expectedly, noise rejection increases with* N*, the number of nodes.*

Table 12.1: The index J as a function of the number of nodes N and of the connectivity p.

N \ p	10	20	30	40	50	60	70	80	90	100
30	0.754	0.246	0.14	0.10	0.078	0.063	0.053	0.047	0.041	0.036
40	0.446	0.162	0.101	0.072	0.056	0.046	0.039	0.034	0.029	0.027
50	0.310	0.124	0.077	0.055	0.044	0.036	0.030	0.026	0.023	0.021
60	0.238	0.100	0.062	0.046	0.036	0.029	0.025	0.022	0.019	0.017
70	0.193	0.083	0.053	0.039	0.030	0.025	0.021	0.018	0.016	0.014
80	0.163	0.071	0.045	0.033	0.026	0.023	0.019	0.016	0.014	0.013

Example 12.5. Local altitude detection. *Consider a number of agents that lie on a surface and exchange information with their neighbours to determine their own altitudes. The agents that lie in two points having altitudes* q_i *and* q_j *exchange information about:*

- *their estimated altitude* z_i *and* z_j*;*
- *the difference* $y_{ij} = q_i - q_j$.

The agents are still, hence $\dot{q}_i = 0$*. Also in this case, as in the previous example, the proposed estimation scheme provides the least-square solution.*

To simulate this situation, consider a regular setup with 16 *agents (nodes) that communicate according to the topology shown in Fig. 12.3, where communication channels among nodes are represented by arcs. The first agent is the only one that can communicate with the external environment. It could therefore, in principle, determine its own position; however, it is not aware of receiving an absolute altitude by the external connection and processes the information about the difference between its own altitude and the external reference (which can assumed to be* 0*) as all the other data, ignoring that this information corresponds exactly to its own altitude. Hence, the local observer of agent* 1 *will have a transient as that of all other agents. Matrix* C *has* 25 *columns, corresponding to the arcs of the graph in Fig. 12.3.*

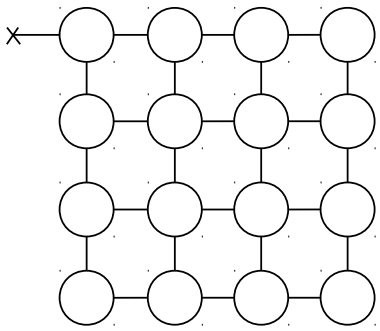

Figure 12.3: The altitude setup problem.

Fig. 12.4 shows the evolution of the decentralised altitude estimation, when the initial value of the observer state is chosen, for all agents, equal to altitude $1/2$*. The first frame shows the actual altitude of the points, randomly generated between* 0 *and* 1*. Frames* 2 *to* 6 *show the evolution of the estimation, with* $\gamma = 5$ *and a time horizon of* $T = 2$ *seconds. The snapshots are taken at non-equidistant time instants, to evidence the initial part of the transient.*

Example 12.6. A network of moving agents. *Consider the planar motion of nodes (agents) representing vehicles, or crafts, confined in a square. Whenever an agent reaches the boundary of the square, it bounces back. The bounces are assumed to be elastic (energy-preserving); hence, whenever a bounce occurs, the component of the agent speed that is orthogonal to the hit surface instantaneously changes its sign. As is known, this represents a discontinuity, equivalent to introducing disturbance impulses* $u_i = \delta_i(t - t_k)$ *in the systems; due to these persistent disturbances, the observer error cannot exactly converge to zero. Uniform linear motion is assumed (the acceleration is zero, hence the speed is constant), apart from bounces instants, and other forces (such as friction) are neglected.*

The agents wish to reconstruct their absolute positions and speeds, under the following rules.

- *If two agents* i *and* j *can communicate, they measure the relative position* $r_i - r_j$ *and they communicate to each other their own estimated positions* $\hat{r}_i$ *and* $\hat{r}_j$*.*
- *If an agent can communicate with an anchor* r_A*, it measures the relative position* $r_i - r_A$ *and receives the anchor position* $\hat{r}_A = r_A$*.*
- *No additional information is available from other agents not connected.*
- *The network topology is unknown and can vary; indeed, communication is possible only if two nodes are within a maximum distance* ρ_{max}*, the effective radius.*

This results in a family of graphs with incidence matrix G_σ *and a set of overall output matrices* C_σ*, such that:*

$$y = C_\sigma x = [G_\sigma^\top \otimes C_1]x.$$

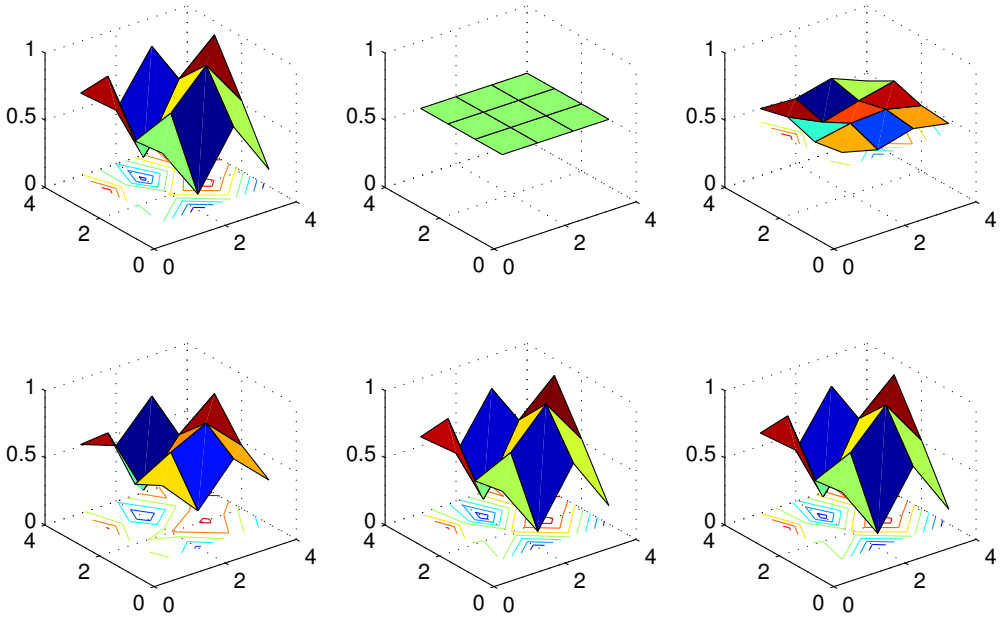

Figure 12.4: The true altitude (first frame) and the altitude detection evolution at times $t = 0,\ 0.01,\ 0.07,\ 0.48,\ 2.00$ seconds. [GBF+15]

The estimator (12.1) *can be applied:*

$$\begin{aligned}\dot{z}_i &= A_1 z_i + B_1 u_i + \sum_{j\in\mathcal{O}_i} L_1[(\hat{r}_i - \hat{r}_j) - (r_i - r_j)] \\ &= \underbrace{A_1 z_i + L_1 \hat{r}_i + B_1 u_i}_{\textit{internal dynamics}} + \sum_{j\in\mathcal{O}_i} \left[L_1 \left(\underbrace{(r_j - r_i)}_{\textit{measured}} - \underbrace{\hat{r}_j}_{\textit{received}} \right) \right]. \end{aligned} \tag{12.14}$$

If a node i communicates with an anchor, since the anchor position is known exactly ($\hat{r}_A = r_A$), then $(r_A - r_i) - \hat{r}_A = r_i$: the node receives precisely its position. Node i does not necessarily know to be communicating with an anchor: it will use the information exactly as if it were communicating with any other node.

The model for each moving agent is:

$$A_1 = \begin{bmatrix} \mathbf{0}_2 & I_2 \\ \mathbf{0}_2 & \mathbf{0}_2 \end{bmatrix}, \qquad B_1 = \begin{bmatrix} \mathbf{0}_2 \\ I_2 \end{bmatrix}, \qquad C_1 = \begin{bmatrix} I_2 & \mathbf{0}_2 \end{bmatrix}.$$

The Kalman gain $L_1 = -Q_1 C_1^\top$ can be chosen for each agent, where Q_1 is the solution of the Riccati equation for the single subsystem:

$$A_1 Q_1 + Q_1 A_1^\top - Q_1 C_1^\top C_1 Q_1 + M = 0,$$

for a suitable $M > 0$; note that $Q_1 = P_1^{-1}$. Applying the network-decentralised estimator leads to the overall filter:

$$\dot{z}(t) = (A - \gamma Q C^\top C)z + Bu + \gamma Q C^\top y,$$

with $Q = P^{-1}$.

Solving the Riccati equation with $M = I_4$, for each subsystem, provides

$$Q_1 = \begin{bmatrix} 1.41 & 0 & 1 & 0 \\ 0 & 1.41 & 0 & 1 \\ 1 & 0 & 1.41 & 0 \\ 0 & 1 & 0 & 1.41 \end{bmatrix}$$

In [GBF+15], a set of 8 agents moving in the (x, y) plane has been considered (see Fig. 12.5, left) and their behaviour has been simulated, with $\gamma = 15$, in the three cases with 1, 2 and 3 anchors respectively. A novel simulation example for this system, with 2 anchors and effective radius $\rho_{max} = 1.5$, is shown in Fig. 12.5, right.

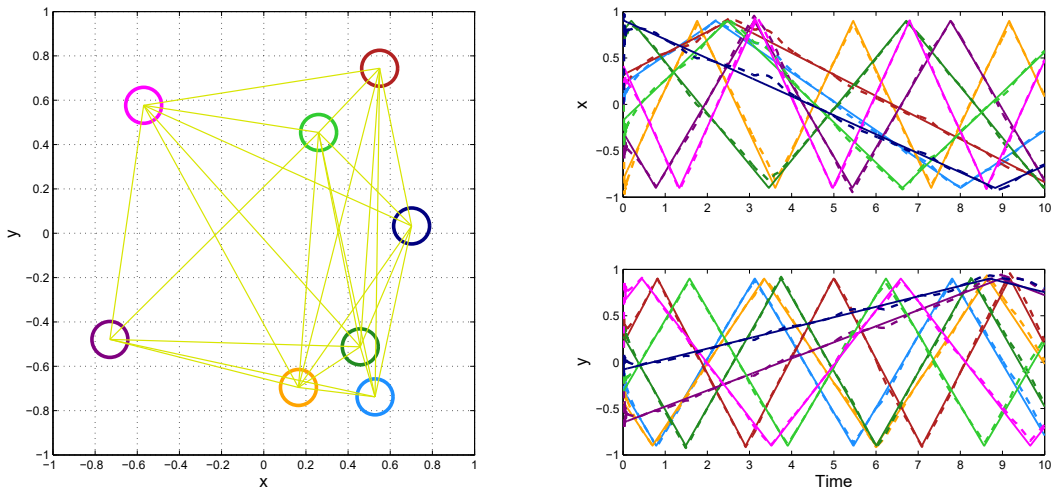

Figure 12.5: The network of eight moving agents confined in a square: setting in the (x, y) plane at time $t = 2$ (left); system evolution over time: solid lines represent the x and y coordinates of the agents, and dotted lines their estimates (right).

As shown in [GBF+15], the values of the smallest eigenvalue of the generalised Laplacian matrix $G(t)$, corresponding to the interconnection configuration at time t, are greater when more anchors are present. It is also shown that the estimation error is very small (albeit not converging to zero because of the persistent disturbances due to bounces), provided that $1/\lambda_{min}$ does not become greater than γ during the whole simulation. According to the provided theoretical results, stability (hence, a negligible error estimation) would be ensured, no matter how the interconnection topology changes during the system evolution, *by choosing $\gamma > \sigma_{max}(\Phi_8) \approx 29.37$.*

Conclusions and Outlook

The analysis and the control of dynamical networks pose a lot of interesting challenges.

Dynamical networks can model any system in which the quantities evolve in time (leading to a dynamical system) and are related by a web of interconnections with a certain topology (namely, a network). Since both dynamics and interconnections are widespread both in natural and in artificial systems, dynamical networks are capable of modelling systems in the most diverse contexts, ranging from ecology, biology and chemistry to physics and engineering.

For instance, dynamical networks in nature can be found at all spacial scales: a set of chemical reactions can be seen as a network of interactions between molecules, leading to the dynamic evolution that transforms the reaction environment; the overall functioning of living organisms is determined by networks of dynamical interactions among proteins, between DNA and proteins (the so-called gene regulatory networks, where gene activity is regulated by proteins called transcription factors), between different RNAs, resulting in very complex networks such as metabolic pathways (which are in charge of converting a substance into another, often thanks to the presence of enzymes that catalyse reactions), signalling pathways (which allow for transducing signals that carry valuable information within or between cells), neuronal networks (the complex and deeply connected networks ruling the functioning of the brain thanks to interactions among neurons). But also organisms and species are related to one another by intricate interactions between prey and predators, since each species can eat or be eaten by another (the so-called food webs, or feeding interactions). Dynamical networks arise as well when social interactions and relations are considered, both between and within species, and when opinion dynamics are studied. Studying these systems in terms of dynamical networks can provide a powerful insight into the mechanisms that regulate nature at all levels.

Also man-made systems are most often comprised of the complex interconnection of several, simpler components: circuits of integrated electronic devices are a small-scale example (in terms of the nanometric dimension, of course, not of the number of components, which is huge and always growing due to the increasing miniaturisation), but also electrical circuits, computer networks, data communication and telecommunication systems all rely on the interconnection of units having their own dynamics. In this context, often the problem of achieving consensus or synchronisation in a dynamical network arises. Optimisation problems need often to be solved in the context of inventory management and production-distribution systems; also in this case, a dynamical network model can be beneficial to study and solve the problem. Flow networks in general can be modelled in the same framework: water distribution networks, transportation networks, traffic and congestion management

systems, formation and coordination of robots, vehicles and aircrafts are all examples of dynamical networks.

The presence of dynamical networks in the natural world and in artificial systems not only motivates their study, but suggests that a virtuous cycle can be triggered, so that analysing nature and its mechanism can help develop bio-inspired control and coordination strategies that mimic those of natural systems, which exhibit an astounding efficiency and robustness to changes in parameters and environmental conditions (thus improving the efficiency and the resilience of artificial systems), while the techniques employed to build from the bottom up artificial systems composed of simple units, which implement a specific functionality, can be adopted also when engineering biomolecular systems to devise innovative biotechnologies and drugs (thus improving human health and quality of life).

In this thesis, some of the problems concerning both analysis and control synthesis have been faced from a structural point of view, providing parameter-free criteria for assessing properties and strategies for control and coordination that rely on the structure of a dynamical network, corresponding to the interconnection topology of an associated graph.

This approach is challenging and powerful: demanding conditions are looked for, therefore they are often difficult to prove, but provide strong indications in case of success.

As a common denominator, all the proposed results rely on a peculiar aspect of dynamical networks: *local* interactions have consequences on the *global* behaviour of the system. Hence, structural analysis can examine what characteristic behaviour can be produced by local interactions having a given structure, or how local interactions with a given structure can result in a given behaviour. The so-called network-decentralised control synthesis aims at obtaining the desired global behaviour by deciding the local interactions with local information only: a global thought and goal is implemented through a set of local actions.

In this respect, the BDC-decomposition of a matrix (which can be the Jacobian matrix of a nonlinear system) can capture the fact that the global behaviour is due to the combination of several local interactions, representing a meaningful picture of the "*local interactions, global behaviour*" effect.

Based on the BDC-decomposition, it has been shown how structural, parameter-free criteria can be devised to assess fundamental properties of the system, such as boundedness, stability, capacity of exhibiting oscillations and perfect adaptation, steady-state input-output behaviour (including the steady-state effect of alterations in parameters).

Boundedness and stability analysis provide structural criteria relying on the computation of a polyhedral Lyapunov function for a linear differential inclusion absorbing the dynamics of the nonlinear system; the vertices and the facets of the unit ball of the polyhedral norm are computed based on a numerical iterative procedure that propagates each of the components associated with the BDC-decomposition. For significant systems, it can be shown that stability can be structurally proved

exclusively by means of polyhedral Lyapunov function.

By exploiting the multi-affinity properties of the BDC-decomposition, numerical procedures can be devised to provide guarantees on the sign of suitable functions in a whole hypercube, based on the computation of the function on its vertices only. This allows the efficient computation of the steady-state influence matrix, representing the steady-state effect on each of the variables of a persistent input applied to each of the system equations, but the same procedure can be applied to assess the effect of variations in significant parameters.

Further results have been presented that lead to a structural classification of candidate oscillatory and multistationary systems, which are applicable to systems with a sign definite Jacobian matrix and to interconnections of unconditionally stable monotone subsystems. These results are useful when analysing models corresponding to artificial biochemical networks and can aid and streamline their synthesis.

As for the control of dynamical networks, network-decentralised state-feedback strategies have been presented, where each control agent is associated with a link of a given interconnection topology and can decide its strategy exclusively based on the state variables associated with the subsystems connected by the link itself. To enforce these restricted information constraints, the feedback matrix must be block-structured: structural zero-blocks are present whenever the information relative to a subsystem is not available to the controller. Interestingly, such a feedback matrix turns out to have the same block structure as the transpose of the overall input matrix of the system.

It has been shown that systems composed of several dynamically decoupled subsystems, interconnected by the control action, can be always stabilised by a network-decentralised controller, provided that the subsystems do not share unstable eigenvalues. For identical subsystems where each input affects a pair of subsystems with input sub-matrices that differ for the sign only (which is typically the case for flow networks), network-decentralised stabilisability is possible if and only if at least an agent is affecting a single subsystem.

Also nonlinear compartmental systems have been analysed. Two different types of flows connecting pairs of compartments have been considered: in the first type, the flow between two compartments depends on the difference between the state of the two compartments; in the second type, it depends on the state of the starting compartment only. A saturated network-decentralised strategy can be considered and necessary and sufficient structural conditions for stabilisability can be achieved. The control has interesting properties in terms of robustness and asymptotic optimality (minimal Euclidean norm of the asymptotic controlled flow). Often, in compartmental systems, positivity of the state must be preserved during the system evolution: this can be guaranteed by a particular network-decentralised control. To ensure exact convergence to the desired set-point, it has been shown that integrators can be suitably adopted in a decentralised framework, and asymptotic optimality is still guaranteed.

Network-decentralised control strategies can be applied in several contexts. The

particular case of traffic control problems has been dealt with, where the traffic inside the nodes splits in queues of units, each associated with a different outgoing arc, and a network-decentralised control can be found that is robust, asymptotically optimal and independent of the traffic splitting rates, relying just on information about the cumulative node content. Besides traffic systems and data transmission systems, an application to a network-decentralised channel sharing communication protocol has been proposed, along with the network-decentralised solutions of a clock synchronisation and of a vehicle platooning problem.

Network-decentralised estimation, the dual of network-decentralised control, has been considered as well, formulating a local estimation problem where each node-agent of the network aims at reconstructing its own state based on information exchanges with the neighbouring agents only. A network-decentralised solution has been provided, which is robust when the topology is unknown and even switching.

However, there are still several open problems that are worth analysing. For instance, methods for assessing global stability of (bio)chemical reaction networks in the absence of the ε-dissipativity and conditions for network-decentralised stabilisation in the case of possibly common unstable eigenvalues are still to be provided. The BDC-decomposition might be further exploited, to consider control problems for linear systems whose state matrix (or for nonlinear systems whose Jacobian matrix) admits a BDC-decomposition, or control problems in which the input matrix or the state-feedback matrix can be expressed in a BDC-form. Moreover, it might be interesting to study a network-decentralised control problem for subsystems that are not decoupled, so that the resulting state matrix is no longer block-diagonal. Several problems in a biochemical and biomolecular context can be recast in a structural formulation, so as to assess properties that are practically independent of parameter values. But also in other traditional domains of engineering, structural, parameter-free properties are often sought (for instance, [BFGP15] investigates model-free plant tuning with a robust Lyapunov approach). Hence, many challenges concerning both analysis and control synthesis are still worth being faced with a structural approach.

A

Catalogue of Tested Biochemical Networks

Madamina, il catalogo è questo
delle belle che amò il padron mio
un catalogo egli è che ho fatt'io:
osservate, leggete con me.
— W. A. Mozart and L. Da Ponte, *Don Giovanni*

This appendix presents a collection of biochemical/chemical reaction networks (most of which already examined in [BG14]), each named after a musician and labelled with a number corresponding to the order of the system. For each network, the following information is reported:

- the graph, where the nodes represent species and the arcs represent reactions according to the legend in Fig. 6.1;
- the system of ordinary differential equations, in the form $\dot{x} = Sg(x) + g_0$;
- the Jacobian matrix $J = BDC$;
- the sign of $\det(-J) = \det(-BDC)$ and, whenever it is suitable, the influence matrix M;
- the number of vertices n_v and of facets n_f of the unit ball of the polyhedral Lyapunov function obtained by means of the stability procedure (whenever it converges; otherwise, the number is replaced by an asterisk).

The exact correspondence between the Greek letters and the partial derivatives in the Jacobian matrix is explicitly indicated in the first example, but is omitted later, since it can be immediately deduced from the context. The influence matrix M is not reported for systems with $\det(-J)$ structurally negative, since it would not be meaningful; for systems with $\det(-J)$ structurally zero, the influence matrix M_{scc} (associated with the impulse response) is reported, if zero is a simple eigenvalue.

Section A.7 provides a synoptic overview of the considered biochemical networks.

A.1 Three Nodes Networks

Albinoni3.

$$\dot{a} = g_{ac}(a^{tot} - a, c) - g_{ab}(a, b)$$
$$\dot{b} = g_b(b^{tot} - b - a^{tot} + a) - g_{ab}(a, b)$$
$$\dot{c} = c_0 - g_{ac}(a^{tot} - a, c)$$

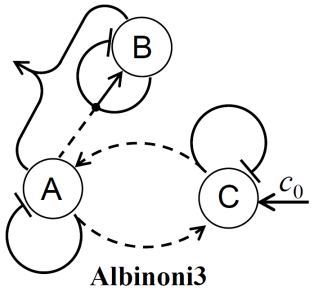

Figure A.1: Graph of Albinoni3.

$$J = \begin{bmatrix} -(\alpha+\beta) & -\gamma & \delta \\ \varepsilon - \beta & -(\varepsilon+\gamma) & 0 \\ \alpha & 0 & -\delta \end{bmatrix}, \qquad M = \begin{bmatrix} + & - & + \\ ? & + & ? \\ + & - & + \end{bmatrix}$$

The partial derivatives are denoted as $\alpha = \partial g_{ac}/\partial a$, $\beta = \partial g_{ab}/\partial a$, $\gamma = \partial g_{ab}/\partial b$, $\delta = \partial g_{ac}/\partial c$, $\varepsilon = \partial g_b/\partial a = -\partial g_b/\partial b$.
$\det(-J) > 0$, $n_v = 14$, $n_f = 12$

Buxtehude3.

$$\dot{a} = a_0 + g_b(b) + g_c(c) - g_a(a)$$
$$\dot{b} = g_a(a) - g_b(b)$$
$$\dot{c} = g_a(a) - g_c(c)$$

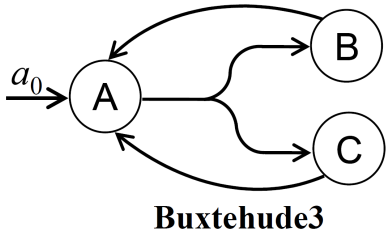

Figure A.2: Graph of Buxtehude3.

$$J = \begin{bmatrix} -\alpha & \beta & \gamma \\ \alpha & -\beta & 0 \\ \alpha & 0 & -\gamma \end{bmatrix}$$

$\det(-J) < 0$, $n_v = *$, $n_f = *$

Corelli3.

$$\dot{a} = a_0 - g_a(a) - g_{ac}(a, c)$$
$$\dot{b} = g_a(a) - g_b(b)$$
$$\dot{c} = g_b(b) - g_{ac}(a, c)$$

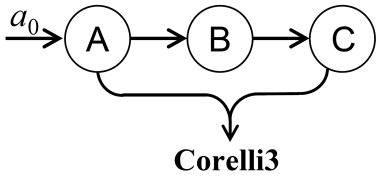

Figure A.3: Graph of Corelli3.

$$J = \begin{bmatrix} -(\alpha+\delta) & 0 & -\gamma \\ \alpha & -\beta & 0 \\ -\delta & \beta & -\gamma \end{bmatrix}, \qquad M = \begin{bmatrix} + & - & - \\ + & + & - \\ ? & + & + \end{bmatrix}$$

$\det(-J) > 0$, $n_v = 6$, $n_f = 6$

Frescobaldi3.

$$\dot{a} = a_0 - g_a(a) - g_{ac}(a,c)$$
$$\dot{b} = g_a(a) - g_{bc}(b,c)$$
$$\dot{c} = g_a(a) - g_{ac}(a,c) - g_{bc}(b,c)$$

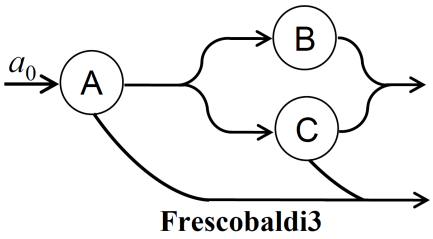

Figure A.4: Graph of Frescobaldi3.

$$J = \begin{bmatrix} -(\alpha+\delta) & 0 & -\varphi \\ \alpha & -\beta & -\gamma \\ \alpha-\delta & -\beta & -(\gamma+\varphi) \end{bmatrix}, \qquad M = \begin{bmatrix} + & + & - \\ + & + & - \\ - & - & + \end{bmatrix}$$

$\det(-J) > 0$, $n_v = *$, $n_f = *$

Pachelbel3.

$$\dot{a} = g_{ac}(a^{tot} - a, c) - g_{ab}(a,b)$$
$$\dot{b} = g_b(b^{tot} - b - a^{tot} + a) - g_{ab}(a,b) - g_{bc}(b,c)$$
$$\dot{c} = c_0 - g_{ac}(a^{tot} - a, c) - g_{bc}(b,c)$$

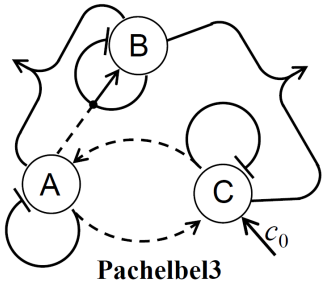

Figure A.5: Graph of Pachelbel3.

$$J = \begin{bmatrix} -(\alpha+\gamma) & -\delta & \beta \\ \varepsilon-\gamma & -(\delta+\varepsilon+\varphi) & -\eta \\ \alpha & -\varphi & -(\beta+\eta) \end{bmatrix}, \qquad M = \begin{bmatrix} + & - & + \\ ? & + & ? \\ ? & - & + \end{bmatrix}$$

$\det(-J) > 0$, $n_v = *$, $n_f = *$

Telemann3.

$$\dot{a} = a_0 - g_a(a) - g_{ac}(a,c)$$
$$\dot{b} = g_a(a) - g_b(b)$$
$$\dot{c} = g_a(a) - g_{ac}(a,c)$$

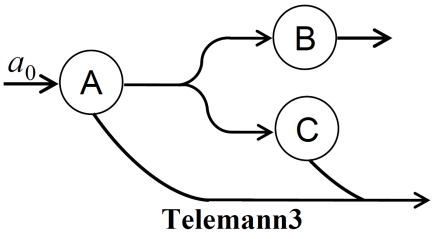

Figure A.6: Graph of Telemann3.

$$J = \begin{bmatrix} -(\alpha+\delta) & 0 & -\gamma \\ \alpha & -\beta & 0 \\ \alpha-\delta & 0 & -\gamma \end{bmatrix}, \qquad M = \begin{bmatrix} + & 0 & - \\ + & + & - \\ ? & 0 & + \end{bmatrix}$$

$\det(-J) > 0$, $n_v = 10$, $n_f = 12$

A.2 Four Nodes Networks

Bach4.

$$\begin{aligned}\dot{a} &= a_0 - g_a(a) + g_d(d)\\ \dot{b} &= g_a(a) - g_{bc}(b,c)\\ \dot{c} &= c_0 - g_{bc}(b,c)\\ \dot{d} &= g_{bc}(b,c) - g_d(d)\end{aligned}$$

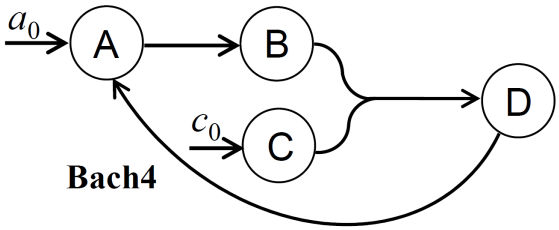

Figure A.7: Graph of Bach4.

$$J = \begin{bmatrix} -\alpha & 0 & 0 & \delta \\ \alpha & -\beta & -\gamma & 0 \\ 0 & -\beta & -\gamma & 0 \\ 0 & \beta & \gamma & -\delta \end{bmatrix}, \qquad M_{scc} = \begin{bmatrix} 0 & 0 & 0 & 0 \\ + & + & 0 & + \\ - & - & 0 & - \\ 0 & 0 & 0 & 0 \end{bmatrix}$$

$\det(-J) = 0$, $n_v = *$, $n_f = *$

Beethoven4.

$$\begin{aligned}\dot{a} &= a_0 - g_a(a) - g_{ab}(a,b) - g_{ad}(a,d)\\ \dot{b} &= b_0 - g_b(b) - g_{ab}(a,b)\\ \dot{c} &= g_{ab}(a,b) - g_c(c)\\ \dot{d} &= g_c(c) - g_{ad}(a,d)\end{aligned}$$

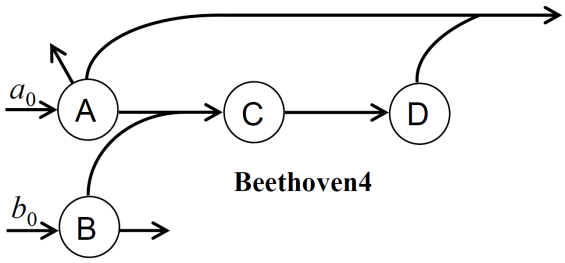

Figure A.8: Graph of Beethoven4.

$$J = \begin{bmatrix} -(\alpha+\gamma+\varepsilon) & -\beta & 0 & -\varphi \\ -\alpha & -(\beta+\zeta) & 0 & 0 \\ \alpha & \beta & -\delta & 0 \\ -\varepsilon & 0 & \delta & -\varphi \end{bmatrix}, \qquad M = \begin{bmatrix} + & - & - & - \\ - & + & + & + \\ + & + & + & - \\ ? & + & + & + \end{bmatrix}$$

$\det(-J) > 0$, $n_v = *$, $n_f = *$

Boccherini4.

$$\begin{aligned}\dot{a} &= a_0 - g_{ab}(a,b) - g_{ac}(a,c) - g_{ad}(a,d)\\ \dot{b} &= b_0 - g_{ab}(a,b)\\ \dot{c} &= g_{ab}(a,b) - g_{ac}(a,c)\\ \dot{d} &= g_{ac}(a,c) - g_{ad}(a,d) - g_d(d)\end{aligned}$$

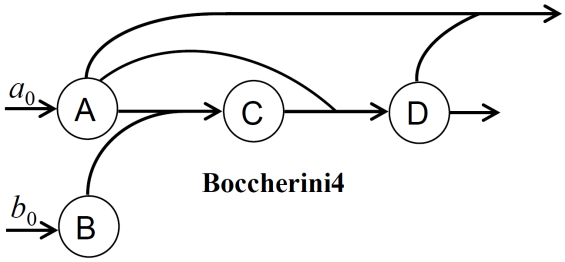

Figure A.9: Graph of Boccherini4.

$$J = \begin{bmatrix} -(\alpha+\delta+\zeta) & -\beta & -\gamma & -\eta \\ -\alpha & -\beta & 0 & 0 \\ \alpha-\delta & \beta & -\gamma & 0 \\ \delta-\zeta & 0 & \gamma & -(\eta+\varepsilon) \end{bmatrix}, \qquad M = \begin{bmatrix} + & - & - & - \\ - & + & + & + \\ - & + & + & + \\ - & + & + & + \end{bmatrix}$$

$\det(-J) > 0$, $n_v = *$, $n_f = *$

Čajkovskij4.

$$\begin{aligned}
\dot{a} &= a_0 - g_a(a) - g_{ab}(a,b) + g_d(d) \\
\dot{b} &= b_0 - g_{ab}(a,b) - g_{bc}(b,c) \\
\dot{c} &= g_a(a) - g_{bc}(b,c) \\
\dot{d} &= g_{bc}(b,c) - g_d(d)
\end{aligned}$$

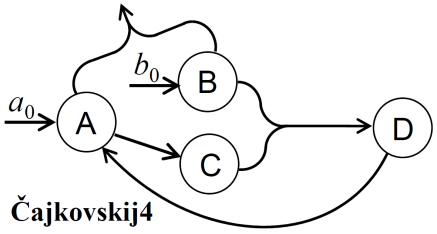

Figure A.10: Graph of Čajkovskij4.

$$J = \begin{bmatrix} -(\alpha+\beta) & -\gamma & 0 & \varphi \\ -\alpha & -(\gamma+\delta) & -\varepsilon & 0 \\ \beta & -\delta & -\varepsilon & 0 \\ 0 & \delta & \varepsilon & -\varphi \end{bmatrix}$$

$\det(-J) < 0$, $n_v = *$, $n_f = *$

Chopin4.

$$\begin{aligned}
\dot{a} &= -g_a(a) + g_d(d) \\
\dot{b} &= g_a(a) - g_b(b) - g_{bd}(b,d) \\
\dot{c} &= g_b(b) - g_c(c) \\
\dot{d} &= g_c(c) - g_d(d) - g_{bd}(b,d)
\end{aligned}$$

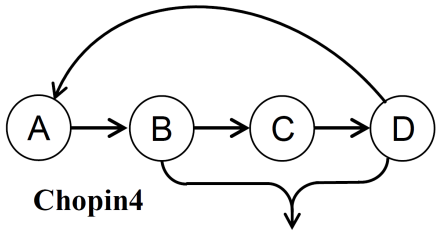

Figure A.11: Graph of Chopin4.

$$J = \begin{bmatrix} -\alpha & 0 & 0 & \delta \\ \alpha & -(\beta+\varepsilon) & 0 & -\varphi \\ 0 & \beta & -\gamma & 0 \\ 0 & -\varepsilon & \gamma & -(\delta+\varphi) \end{bmatrix}, \qquad M = \begin{bmatrix} + & ? & + & + \\ + & + & ? & ? \\ + & + & + & ? \\ ? & ? & + & + \end{bmatrix}$$

$\det(-J) > 0$, $n_v = 8$, $n_f = 14$

Clementi4.

$$\begin{aligned}
\dot{a} &= a_0 - g_{ab}(a,b) - g_{ac}(a,c) + g_d(d) \\
\dot{b} &= b_0 - g_{ab}(a,b) \\
\dot{c} &= g_{ab}(a,b) - g_{ac}(a,c) \\
\dot{d} &= g_{ac}(a,c) - g_d(d) - g_d^*(d)
\end{aligned}$$

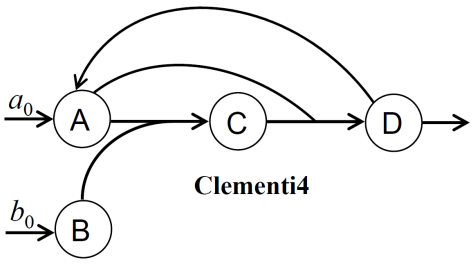

Figure A.12: Graph of Clementi4.

$$J = \begin{bmatrix} -(\alpha+\gamma) & -\beta & -\delta & \varphi \\ -\alpha & -\beta & 0 & 0 \\ \alpha-\gamma & \beta & -\delta & 0 \\ \gamma & 0 & \delta & -(\varphi+\varepsilon) \end{bmatrix}, \qquad M_{scc} = \begin{bmatrix} + & - & - & + \\ - & + & + & - \\ - & + & + & - \\ 0 & 0 & 0 & 0 \end{bmatrix}.$$

$\det(-J) = 0$, $n_v = *$, $n_f = *$

Dvořák4.

$$\begin{aligned}\dot{a} &= a_0 - g_{ab}(a,b)\\ \dot{b} &= b_0 - g_{ab}(a,b) + g_d(d)\\ \dot{c} &= g_{ab}(a,b) - g_c(c)\\ \dot{d} &= g_{ab}(a,b) - g_d(d)\end{aligned}$$

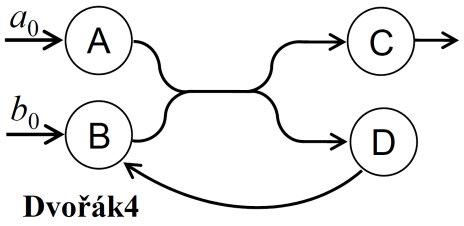

Figure A.13: Graph of Dvořák4.

$$J = \begin{bmatrix} -\alpha & -\beta & 0 & 0 \\ -\alpha & -\beta & 0 & \varepsilon \\ \alpha & \beta & -\gamma & 0 \\ \alpha & \beta & 0 & -\varepsilon \end{bmatrix}, \qquad M_{scc} = \begin{bmatrix} 0 & - & 0 & - \\ 0 & + & 0 & + \\ 0 & 0 & 0 & 0 \\ 0 & 0 & 0 & 0 \end{bmatrix}$$

$\det(-J) = 0$, $n_v = *$, $n_f = *$

Fauré4.

$$\begin{aligned}\dot{a} &= a_0 - g_{ab}(a,b) - g_a(a) + g_d(d)\\ \dot{b} &= b_0 - g_{ab}(a,b) + g_c(c)\\ \dot{c} &= g_{ab}(a,b) - g_c(c) - g_c^*(c)\\ \dot{d} &= g_c^*(c) - g_d(d) + g_a(a)\end{aligned}$$

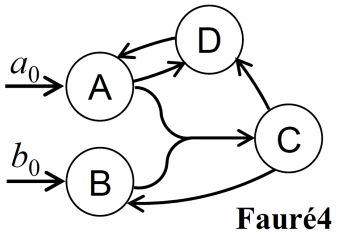

Figure A.14: Graph of Fauré4.

$$J = \begin{bmatrix} -(\alpha+\zeta) & -\beta & 0 & \varepsilon \\ -\alpha & -\beta & \gamma & 0 \\ \alpha & \beta & -(\gamma+\delta) & 0 \\ \zeta & 0 & \delta & -\varepsilon \end{bmatrix}, \qquad M_{scc} = \begin{bmatrix} + & - & ? & + \\ - & + & ? & - \\ 0 & 0 & 0 & 0 \\ + & - & ? & + \end{bmatrix}$$

$\det(-J) = 0$, $n_v = *$, $n_f = *$

Gershwin4.

$$\begin{aligned}\dot{a} &= a_0 - g_a(a) - g_a^*(a) + g_b(b) + g_d(d)\\ \dot{b} &= -g_b(b) - g_b^*(b) + g_a(a)\\ \dot{c} &= -g_c(c) - g_{cd}(c,d) + g_a(a)\\ \dot{d} &= g_a^*(a) - g_d(d) - g_{cd}(c,d)\end{aligned}$$

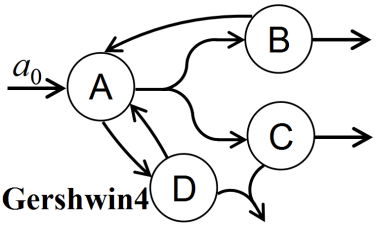

Figure A.15: Graph of Gershwin4.

$$J = \begin{bmatrix} -(\alpha+\rho) & \mu & 0 & \nu \\ \alpha & -(\beta+\mu) & 0 & 0 \\ \alpha & 0 & -(\gamma+\varphi) & -\delta \\ \rho & 0 & -\varphi & -(\delta+\nu) \end{bmatrix}, \qquad M = \begin{bmatrix} + & + & - & + \\ + & + & - & + \\ ? & ? & + & ? \\ ? & ? & - & + \end{bmatrix}$$

$\det(-J) > 0$, $n_v = *$, $n_f = *$

Gluck4.

$$\begin{aligned}
\dot{a} &= a_0 - g_a(a) + g_{bc}(b,c) - g_{ad}(a,d)\\
\dot{b} &= g_a(a) - g_{bc}(b,c) - g_b(b)\\
\dot{c} &= g_a(a) - g_{bc}(b,c) - g_c(c)\\
\dot{d} &= g_c(c) - g_{ad}(a,d)
\end{aligned}$$

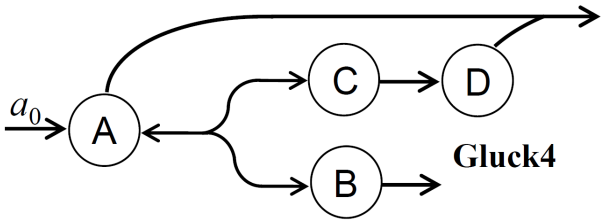

Figure A.16: Graph of Gluck4.

$$J = \begin{bmatrix} -(\alpha+\varphi) & \beta & \gamma & -\zeta \\ \alpha & -(\beta+\delta) & -\gamma & 0 \\ \alpha & -\beta & -(\gamma+\varepsilon) & 0 \\ -\varphi & 0 & \varepsilon & -\zeta \end{bmatrix}, \qquad M = \begin{bmatrix} + & + & ? & - \\ + & + & - & - \\ + & 0 & + & - \\ ? & - & ? & + \end{bmatrix}$$

$\det(-J) > 0$, $n_v = 14$, $n_f = 8$

Gounod4.

$$\begin{aligned}
\dot{a} &= a_0 - g_{ab}(a,b)\\
\dot{b} &= b_0 - g_{ab}(a,b) - g_{bd}(b,d)\\
\dot{c} &= g_{ab}(a,b) - g_c(c)\\
\dot{d} &= g_c(c) - g_d(d) - g_{bd}(b,d)
\end{aligned}$$

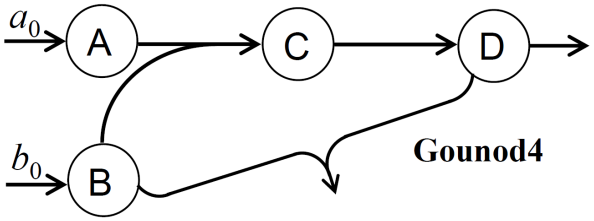

Figure A.17: Graph of Gounod4.

$$J = \begin{bmatrix} -\alpha & -\beta & 0 & 0 \\ -\alpha & -(\beta+\varepsilon) & 0 & -\delta \\ \alpha & \beta & -\gamma & 0 \\ 0 & -\varepsilon & \gamma & -(\delta+\varphi) \end{bmatrix}, \qquad M = \begin{bmatrix} + & - & + & + \\ - & + & - & - \\ + & 0 & + & 0 \\ + & - & + & + \end{bmatrix}$$

$\det(-J) > 0$, $n_v = *$, $n_f = *$

Händel4.

$$\begin{aligned}
\dot{a} &= a_0 - g_a(a) - g_{ab}(a,b)\\
\dot{b} &= g_a(a) - g_{ab}(a,b) - g_{bd}(b,d)\\
\dot{c} &= c_0 - g_c(c) - g_{cd}(c,d)\\
\dot{d} &= g_c(c) - g_{cd}(c,d) - g_{bd}(b,d)
\end{aligned}$$

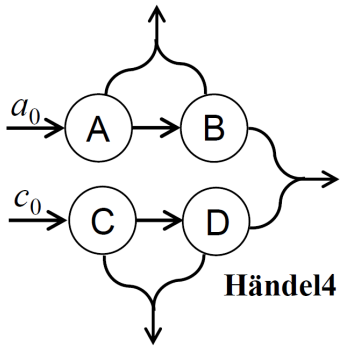

Figure A.18: Graph of Händel4.

$$J = \begin{bmatrix} -(\alpha+\varepsilon) & -\varphi & 0 & 0 \\ \alpha-\varepsilon & -(\gamma+\varphi) & 0 & -\delta \\ 0 & 0 & -(\beta+\zeta) & -\eta \\ 0 & -\gamma & \beta-\zeta & -(\delta+\eta) \end{bmatrix}, \qquad M = \begin{bmatrix} + & - & ? & + \\ ? & + & ? & - \\ ? & + & + & - \\ ? & - & ? & + \end{bmatrix}$$

$\det(-J) > 0$, $n_v = 8$, $n_f = 16$

Haydn4.

$$\begin{aligned}\dot{a} &= a_0 - g_{ab}(a,b) - g_{ac}(a,c)\\ \dot{b} &= b_0 - g_{ab}(a,b)\\ \dot{c} &= g_{ab}(a,b) - g_{ac}(a,c)\\ \dot{d} &= g_{ac}(a,c) - g_d(d)\end{aligned}$$

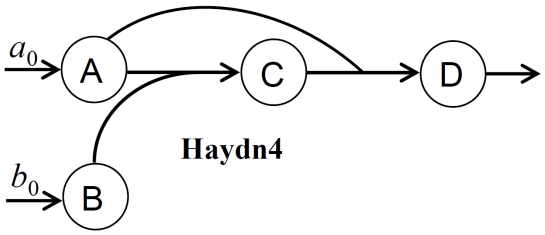

Figure A.19: Graph of Haydn4.

$$J = \begin{bmatrix} -(\alpha+\gamma) & -\beta & -\delta & 0\\ -\alpha & -\beta & 0 & 0\\ \alpha-\gamma & \beta & -\delta & 0\\ \gamma & 0 & \delta & -\varepsilon \end{bmatrix}, \qquad M_{scc} = \begin{bmatrix} + & - & - & 0\\ - & + & + & 0\\ - & + & + & 0\\ 0 & 0 & 0 & 0 \end{bmatrix}$$

$\det(-J) = 0$, $n_v = 16$, $n_f = 18$

Mozart4.

$$\begin{aligned}\dot{a} &= a_0 - g_{ab}(a,b) - g_{ad}(a,d)\\ \dot{b} &= b_0 - g_{ab}(a,b)\\ \dot{c} &= g_{ab}(a,b) - g_c(c)\\ \dot{d} &= g_c(c) - g_{ad}(a,d)\end{aligned}$$

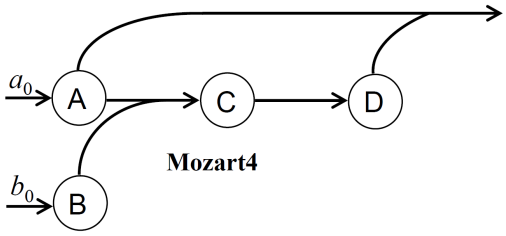

Figure A.20: Graph of Mozart4.

$$J = \begin{bmatrix} -(\alpha+\delta) & -\beta & 0 & -\varepsilon\\ -\alpha & -\beta & 0 & 0\\ \alpha & \beta & -\gamma & 0\\ -\delta & 0 & \gamma & -\varepsilon \end{bmatrix}, \qquad M_{scc} = \begin{bmatrix} + & - & - & -\\ - & + & + & +\\ 0 & 0 & 0 & 0\\ - & + & + & + \end{bmatrix}$$

$\det(-J) = 0$, $n_v = 14$, $n_f = 8$

Offenbach4.

$$\begin{aligned}\dot{a} &= a_0 - g_{ab}(a,b) - g_{ad}(a,d) - g_a(a)\\ \dot{b} &= b_0 - g_{ab}(a,b)\\ \dot{c} &= g_{ab}(a,b) - g_c(c)\\ \dot{d} &= g_c(c) - g_{ad}(a,d)\end{aligned}$$

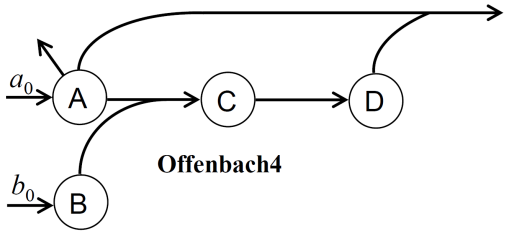

Figure A.21: Graph of Offenbach4.

$$J = \begin{bmatrix} -(\alpha+\gamma+\varepsilon) & -\beta & 0 & -\varphi\\ -\alpha & -\beta & 0 & 0\\ \alpha & \beta & -\delta & 0\\ -\varepsilon & 0 & \delta & -\varphi \end{bmatrix}, \qquad M = \begin{bmatrix} + & - & - & -\\ - & + & + & +\\ 0 & + & + & 0\\ - & + & + & + \end{bmatrix}$$

$\det(-J) > 0$, $n_v = *$, $n_f = *$

Paganini4.

$$\begin{aligned}\dot{a} &= a_0 - g_a(a) + g_d(d)\\ \dot{b} &= g_a(a) - g_{bc}(b,c)\\ \dot{c} &= c_0 - g_c(c) - g_{bc}(b,c)\\ \dot{d} &= g_{bc}(b,c) - g_d(d)\end{aligned}$$

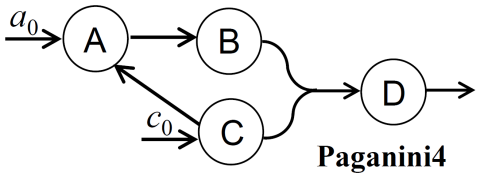

Figure A.22: Graph of Paganini4.

$$J = \begin{bmatrix} -\alpha & 0 & \delta & 0\\ \alpha & -\beta & -\gamma & 0\\ 0 & -\beta & -(\gamma+\delta) & 0\\ 0 & \beta & \gamma & -\varepsilon \end{bmatrix}, \qquad M = \begin{bmatrix} + & - & + & 0\\ + & + & ? & 0\\ - & - & + & 0\\ + & + & + & + \end{bmatrix}$$

$\det(-J) > 0$, $n_v = 14$, $n_f = 18$

Pergolesi4.

$$\begin{aligned}\dot{a} &= a_0 - g_{ab}(a,b) - g_{ac}(a,c)\\ \dot{b} &= b_0 - g_{ab}(a,b) - g_{bd}(b,d)\\ \dot{c} &= g_{ab}(a,b) - g_{ac}(a,c)\\ \dot{d} &= g_{ac}(a,c) - g_{bd}(b,d) - g_d(d)\end{aligned}$$

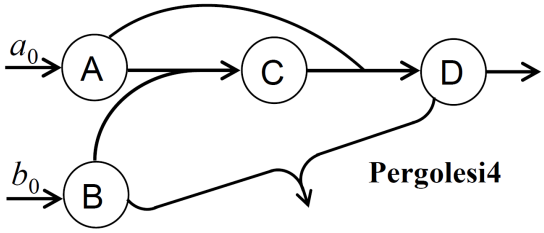

Figure A.23: Graph of Pergolesi4.

$$J = \begin{bmatrix} -(\alpha+\gamma) & -\beta & -\delta & 0\\ -\alpha & -(\beta+\zeta) & 0 & -\varepsilon\\ \alpha-\gamma & \beta & -\delta & 0\\ \gamma & -\zeta & \delta & -(\varepsilon+\vartheta) \end{bmatrix}, \qquad M = \begin{bmatrix} + & - & - & +\\ - & + & + & -\\ ? & + & + & -\\ + & - & 0 & + \end{bmatrix}$$

$\det(-J) > 0$, $n_v = *$, $n_f = *$

Purcell4.

$$\begin{aligned}\dot{a} &= a_0 - g_{ab}(a,b) - g_{ac}(a,c)\\ \dot{b} &= b_0 - g_{ab}(a,b)\\ \dot{c} &= g_{ab}(a,b) - g_{ac}(a,c)\\ \dot{d} &= g_{ab}(a,b) - g_d(d)\end{aligned}$$

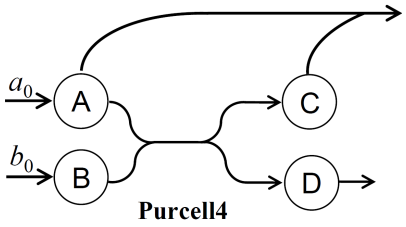

Figure A.24: Graph of Purcell4.

$$J = \begin{bmatrix} -(\alpha+\gamma) & -\beta & -\delta & 0\\ -\alpha & -\beta & 0 & 0\\ \alpha-\gamma & \beta & -\delta & 0\\ \alpha & \beta & 0 & -\varepsilon \end{bmatrix}, \qquad M_{scc} = \begin{bmatrix} + & - & - & 0\\ - & + & + & 0\\ - & + & + & 0\\ 0 & 0 & 0 & 0 \end{bmatrix}$$

$\det(-J) = 0$, $n_v = 16$, $n_f = 18$

Salieri4.

$$\begin{aligned}\dot{a} &= a_0 - g_a(a) - g_a^*(a) + g_d(d)\\ \dot{b} &= g_a(a) - g_{bc}(b,c)\\ \dot{c} &= g_a^*(a) - g_{bc}(b,c)\\ \dot{d} &= g_{bc}(b,c) - g_d(d)\end{aligned}$$

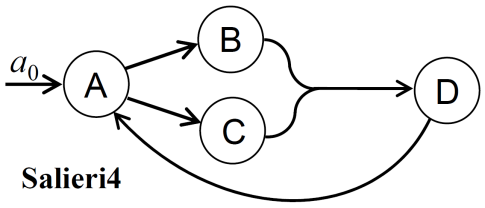

Figure A.25: Graph of Salieri4.

$$J = \begin{bmatrix} -(\alpha+\beta) & 0 & 0 & \varepsilon \\ \alpha & -\gamma & -\delta & 0 \\ \beta & -\gamma & -\delta & 0 \\ 0 & \gamma & \delta & -\varepsilon \end{bmatrix}, \qquad M_{scc} = \begin{bmatrix} 0 & 0 & 0 & 0 \\ ? & + & - & ? \\ ? & - & + & ? \\ 0 & 0 & 0 & 0 \end{bmatrix}$$

$\det(-J) = 0$, $n_v = *$, $n_f = *$

Scarlatti4.

$$\begin{aligned}\dot{a} &= a_0 - g_{ab}(a,b) - g_{ac}(a,c)\\ \dot{b} &= b_0 - g_{ab}(a,b)\\ \dot{c} &= g_{ab}(a,b) - g_{ac}(a,c) + g_d(d)\\ \dot{d} &= g_{ac}(a,c) - g_d(d) - g_d^*(d)\end{aligned}$$

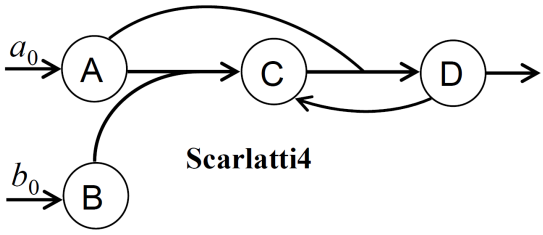

Figure A.26: Graph of Scarlatti4.

$$J = \begin{bmatrix} -(\alpha+\gamma) & -\beta & -\delta & 0 \\ -\alpha & -\beta & 0 & 0 \\ \alpha-\gamma & \beta & -\delta & \varphi \\ \gamma & 0 & \delta & -(\varphi+\varepsilon) \end{bmatrix}, \qquad M_{scc} = \begin{bmatrix} + & - & - & - \\ - & + & + & + \\ - & + & + & + \\ 0 & 0 & 0 & 0 \end{bmatrix}$$

$\det(-J) = 0$, $n_v = *$, $n_f = *$

Schubert4.

$$\begin{aligned}\dot{a} &= a_0 - g_a(a) - g_{ad}(a,d) + g_{bc}(b,c)\\ \dot{b} &= g_a(a) - g_{bc}(b,c) - g_{bd}(b,d)\\ \dot{c} &= g_a(a) - g_{bc}(b,c) - g_c(c)\\ \dot{d} &= g_c(c) - g_{ad}(a,d) - g_{bd}(b,d)\end{aligned}$$

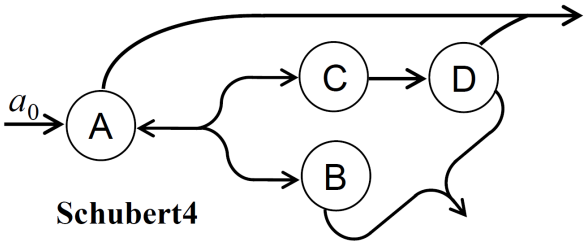

Figure A.27: Graph of Schubert4.

$$J = \begin{bmatrix} -(\alpha+\zeta) & \beta & \gamma & -\eta \\ \alpha & -(\beta+\delta) & -\gamma & -\varepsilon \\ \alpha & -\beta & -(\gamma+\varphi) & 0 \\ -\zeta & -\delta & \varphi & -(\varepsilon+\eta) \end{bmatrix}, \qquad M = \begin{bmatrix} + & + & - & - \\ + & + & - & - \\ ? & ? & 0 & ? \\ - & - & + & + \end{bmatrix}$$

$\det(-J) = ?$, $n_v = *$, $n_f = *$

Schumann4.

$$\begin{aligned}\dot{a} &= a_0 - g_{ab}(a,b) - g_{ac}(a,c)\\ \dot{b} &= b_0 - g_{ab}(a,b) + g_d(d)\\ \dot{c} &= g_{ab}(a,b) - g_{ac}(a,c)\\ \dot{d} &= g_{ac}(a,c) - g_d(d) - g_d^*(d)\end{aligned}$$

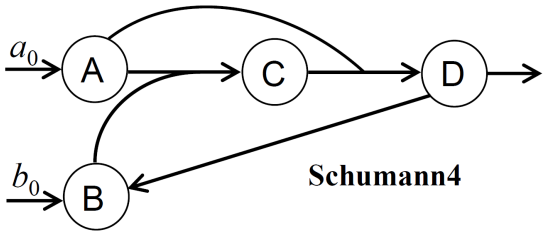

Figure A.28: Graph of Schumann4.

$$J = \begin{bmatrix} -(\alpha+\gamma) & -\beta & -\delta & 0 \\ -\alpha & -\beta & 0 & \varphi \\ \alpha-\gamma & \beta & -\delta & 0 \\ \gamma & 0 & \delta & -(\varphi+\varepsilon) \end{bmatrix}, \qquad M_{scc} = \begin{bmatrix} + & - & - & - \\ - & + & + & + \\ - & + & + & + \\ 0 & 0 & 0 & 0 \end{bmatrix}$$

$\det(-J) = 0$, $n_v = *$, $n_f = *$

Vivaldi4.

$$\begin{aligned}\dot{a} &= a_0 - g_{ab}(a,b) - g_{ac}(a,c)\\ \dot{b} &= b_0 - g_{ab}(a,b) + g_d(d)\\ \dot{c} &= g_{ab}(a,b) - g_{ac}(a,c)\\ \dot{d} &= g_{ab}(a,b) - g_d(d)\end{aligned}$$

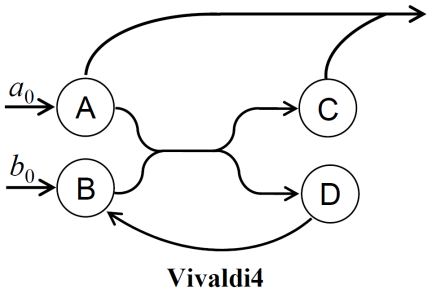

Figure A.29: Graph of Vivaldi4.

$$J = \begin{bmatrix} -(\alpha+\gamma) & -\beta & -\delta & 0 \\ -\alpha & -\beta & 0 & \varepsilon \\ \alpha-\gamma & \beta & -\delta & 0 \\ \alpha & \beta & 0 & -\varepsilon \end{bmatrix}, \qquad M_{scc} = \begin{bmatrix} 0 & - & 0 & - \\ 0 & + & 0 & + \\ 0 & + & 0 & + \\ 0 & 0 & 0 & 0 \end{bmatrix}$$

$\det(-J) = 0$, $n_v = *$, $n_f = *$

A.3 Five Nodes Networks

Berg5.

$$\begin{aligned}\dot{a} &= a_0 + g_e(e) - g_{ab}(a,b)\\ \dot{b} &= b_0 - g_{ab}(a,b) - g_{bc}(b,c)\\ \dot{c} &= c_0 - g_{bc}(b,c)\\ \dot{d} &= g_{bc}(b,c) - g_d(d)\\ \dot{e} &= g_d(d) - g_e(e)\end{aligned}$$

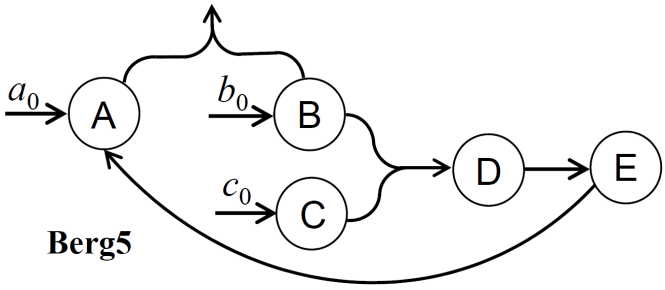

Figure A.30: Graph of Berg5.

$$J = \begin{bmatrix} -\alpha & -\gamma & 0 & 0 & \varphi \\ -\alpha & -(\beta+\gamma) & -\delta & 0 & 0 \\ 0 & -\beta & -\delta & 0 & 0 \\ 0 & \beta & \delta & -\varepsilon & 0 \\ 0 & 0 & 0 & \varepsilon & -\varphi \end{bmatrix}, \qquad M_{scc} = \begin{bmatrix} + & - & + & + & + \\ - & + & - & - & - \\ + & - & + & + & + \\ 0 & 0 & 0 & 0 & 0 \\ 0 & 0 & 0 & 0 & 0 \end{bmatrix}$$

$\det(-J) = 0$, $n_v = 32$, $n_f = 10$

Berlioz5.

$$\begin{aligned} \dot{a} &= a_0 - g_{ab}(a,b) - g_{ae}(a,e) \\ \dot{b} &= b_0 - g_{ab}(a,b) \\ \dot{c} &= g_{ab}(a,b) - g_{cd}(c,d) \\ \dot{d} &= d_0 - g_{cd}(c,d) \\ \dot{e} &= g_{cd}(c,d) - g_{ae}(a,e) \end{aligned}$$

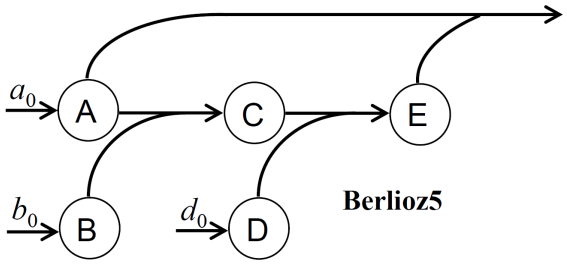

Figure A.31: Graph of Berlioz5.

$$J = \begin{bmatrix} -(\alpha+\varepsilon) & -\beta & 0 & 0 & -\varphi \\ -\alpha & -\beta & 0 & 0 & 0 \\ \alpha & \beta & -\gamma & -\delta & 0 \\ 0 & 0 & -\gamma & -\delta & 0 \\ -\varepsilon & 0 & \gamma & \delta & -\varphi \end{bmatrix}$$

$\det(-J) = 0$ (and the eigenvalue zero has multiplicity 2), $n_v = 32$, $n_f = 10$

Brahms5.

$$\begin{aligned} \dot{a} &= a_0 - g_{ab}(a,b) - g_{ae}(a,e) + g_c(c) \\ \dot{b} &= b_0 - g_{ab}(a,b) + g_c(c) \\ \dot{c} &= g_{ab}(a,b) - g_c(c) - g_c^*(c) \\ \dot{d} &= g_c^*(c) - g_d(d) \\ \dot{e} &= g_d(d) - g_{ae}(a,e) \end{aligned}$$

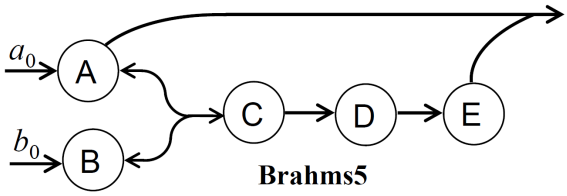

Figure A.32: Graph of Brahms5.

$$J = \begin{bmatrix} -(\alpha+\varphi) & -\beta & \gamma & 0 & -\zeta \\ -\alpha & -\beta & \gamma & 0 & 0 \\ \alpha & \beta & -(\gamma+\delta) & 0 & 0 \\ 0 & 0 & \delta & -\varepsilon & 0 \\ -\varphi & 0 & 0 & \varepsilon & -\zeta \end{bmatrix}, \qquad M_{scc} = \begin{bmatrix} + & - & - & - & - \\ - & + & + & + & + \\ 0 & 0 & 0 & 0 & 0 \\ 0 & 0 & 0 & 0 & 0 \\ - & + & + & + & + \end{bmatrix}$$

$\det(-J) = 0$, $n_v = 32$, $n_f = 10$

Elgar5.

$$\begin{aligned}
\dot{a} &= a_0 - g_a(a) + g_e(e)\\
\dot{b} &= g_a(a) - g_{bc}(b,c)\\
\dot{c} &= c_0 - g_{bc}(b,c)\\
\dot{d} &= g_{bc}(b,c) - g_d(d)\\
\dot{e} &= g_d(d) - g_e(e)
\end{aligned}$$

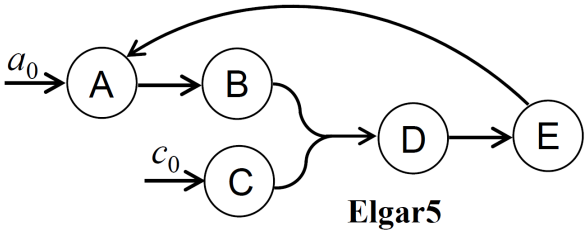

Figure A.33: Graph of Elgar5.

$$J = \begin{bmatrix} -\alpha & 0 & 0 & 0 & \varepsilon \\ \alpha & -\beta & -\gamma & 0 & 0 \\ 0 & -\beta & -\gamma & 0 & 0 \\ 0 & \beta & \gamma & -\delta & 0 \\ 0 & 0 & 0 & \delta & -\varepsilon \end{bmatrix}, \qquad M_{scc} = \begin{bmatrix} 0 & 0 & 0 & 0 & 0 \\ + & + & 0 & + & + \\ - & - & 0 & - & - \\ 0 & 0 & 0 & 0 & 0 \\ 0 & 0 & 0 & 0 & 0 \end{bmatrix}$$

$\det(-J) = 0$, $n_v = *$, $n_f = *$

Grieg5.

$$\begin{aligned}
\dot{a} &= a_0 - g_a(a)\\
\dot{b} &= g_a(a) - g_{bc}(b,c)\\
\dot{c} &= c_0 - g_{bc}(b,c) - g_c(c)\\
\dot{d} &= g_{bc}(b,c) - g_d(d)\\
\dot{e} &= g_d(d) - g_e(e) + g_c(c)
\end{aligned}$$

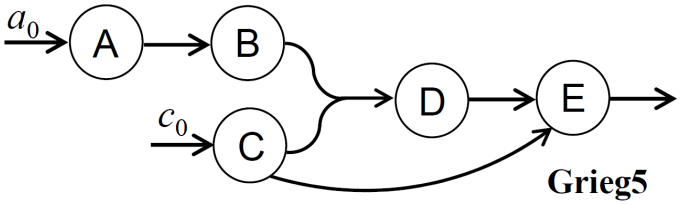

Figure A.34: Graph of Grieg5.

$$J = \begin{bmatrix} -\alpha & 0 & 0 & 0 & 0 \\ \alpha & -\beta & -\gamma & 0 & 0 \\ 0 & -\beta & -(\gamma+\varepsilon) & 0 & 0 \\ 0 & \beta & \gamma & -\delta & 0 \\ 0 & 0 & \varepsilon & \delta & -\varphi \end{bmatrix}, \qquad M = \begin{bmatrix} + & 0 & 0 & 0 & 0 \\ + & + & - & 0 & 0 \\ - & - & + & 0 & 0 \\ + & + & 0 & + & 0 \\ 0 & 0 & + & + & + \end{bmatrix}$$

$\det(-J) > 0$, $n_v = 22$, $n_f = 68$

Liszt5.

$$\begin{aligned}
\dot{a} &= a_0 - g_{ab}(a,b)\\
\dot{b} &= b_0 - g_{ab}(a,b) - g_{bc}(b,c)\\
\dot{c} &= c_0 - g_{bc}(b,c) - g_c(c)\\
\dot{d} &= g_{bc}(b,c) - g_d(d)\\
\dot{e} &= g_d(d) + g_c(c) - g_e(e)
\end{aligned}$$

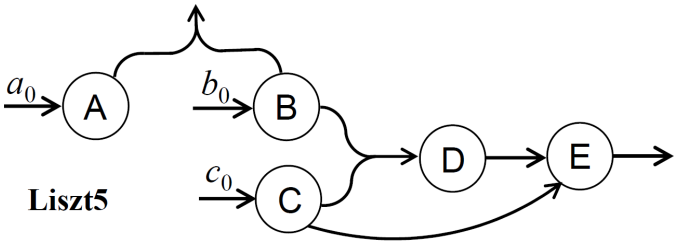

Figure A.35: Graph of Liszt5.

$$J = \begin{bmatrix} -\alpha & -\gamma & 0 & 0 & 0 \\ -\alpha & -(\beta+\gamma) & -\delta & 0 & 0 \\ 0 & -\beta & -(\delta+\varphi) & 0 & 0 \\ 0 & \beta & \delta & -\varepsilon & 0 \\ 0 & 0 & \varphi & \varepsilon & -\zeta \end{bmatrix}, \quad M = \begin{bmatrix} + & - & + & 0 & 0 \\ - & + & - & 0 & 0 \\ + & - & + & 0 & 0 \\ - & + & 0 & + & 0 \\ 0 & 0 & + & + & + \end{bmatrix}$$

$\det(-J) > 0$, $n_v = 28$, $n_f = 66$

Martucci5.

$$\begin{aligned} \dot{a} &= a_0 - g_a(a) - g_{ac}(a,c) \\ \dot{b} &= g_a(a) - g_{bd}(b,d) - g_{be}(b,e) \\ \dot{c} &= g_d(d) - g_{ac}(a,c) \\ \dot{d} &= g_a(a) - g_d(d) - g_{bd}(b,d) \\ \dot{e} &= g_{bd}(b,d) - g_{be}(b,e) \end{aligned}$$

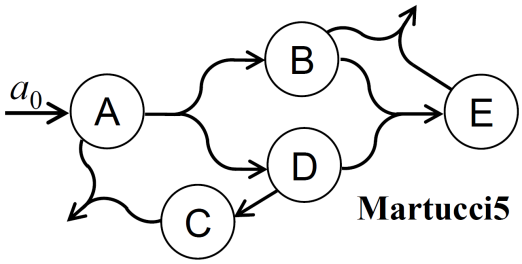

Figure A.36: Graph of Martucci5.

$$J = \begin{bmatrix} -(\alpha+\beta) & 0 & -\gamma & 0 & 0 \\ \alpha & -(\delta+\mu) & 0 & -\varepsilon & -\nu \\ -\beta & 0 & -\gamma & \varphi & 0 \\ \alpha & -\delta & 0 & -(\varepsilon+\varphi) & 0 \\ 0 & \delta-\mu & 0 & \varepsilon & -\nu \end{bmatrix}, \quad M = \begin{bmatrix} + & + & - & - & - \\ ? & + & ? & - & - \\ ? & - & + & + & + \\ + & - & - & + & + \\ ? & ? & ? & ? & + \end{bmatrix}$$

$\det(-J) > 0$, $n_v = *$, $n_f = *$

Mendelssohn5.

$$\begin{aligned} \dot{a} &= a_0 - g_{ab}(a,b) + g_c(c) \\ \dot{b} &= b_0 - g_{ab}(a,b) - g_{bd}(b,d) \\ \dot{c} &= g_{ab}(a,b) - g_c(c) - g_c^*(c) \\ \dot{d} &= g_{ab}(a,b) - g_{bd}(b,d) - g_{de}(d,e) \\ \dot{e} &= g_c^*(c) - g_{de}(d,e) \end{aligned}$$

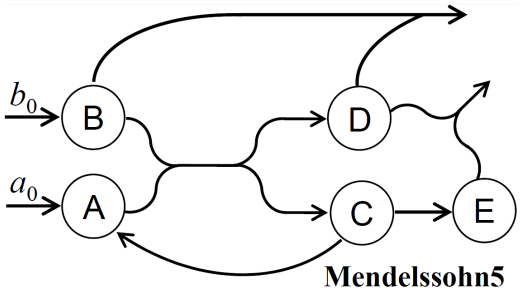

Figure A.37: Graph of Mendelssohn5.

$$J = \begin{bmatrix} -\alpha & -\beta & \gamma & 0 & 0 \\ -\alpha & -(\beta+\varepsilon) & 0 & -\varphi & 0 \\ \alpha & \beta & -(\gamma+\delta) & 0 & 0 \\ \alpha & \beta-\varepsilon & 0 & -(\varphi+\nu) & -\mu \\ 0 & 0 & \delta & -\nu & -\mu \end{bmatrix}, \quad M_{scc} = \begin{bmatrix} + & - & ? & + & - \\ - & + & ? & - & + \\ 0 & 0 & 0 & 0 & 0 \\ + & - & ? & + & - \\ - & + & ? & - & + \end{bmatrix}$$

$\det(-J) = 0$, $n_v = *$, $n_f = *$

Rachmaninov5.

$$\begin{aligned}
\dot{a} &= a_0 - g_{ab}(a,b)\\
\dot{b} &= b_0 - g_{ab}(a,b) - g_{bc}(b,c)\\
\dot{c} &= c_0 - g_{bc}(b,c) + g_e(e)\\
\dot{d} &= g_{bc}(b,c) - g_d(d)\\
\dot{e} &= g_d(d) - g_e(e)
\end{aligned}$$

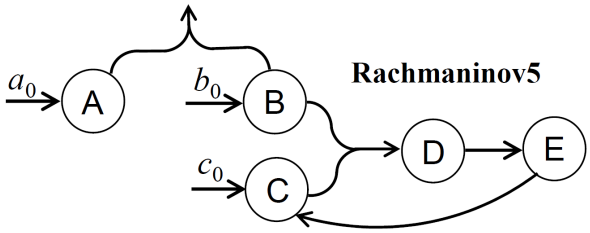

Figure A.38: Graph of Rachmaninov5.

$$J = \begin{bmatrix} -\alpha & -\gamma & 0 & 0 & 0\\ -\alpha & -(\beta+\gamma) & -\delta & 0 & 0\\ 0 & -\beta & -\delta & 0 & \varphi\\ 0 & \beta & \delta & -\varepsilon & 0\\ 0 & 0 & 0 & \varepsilon & -\varphi \end{bmatrix}, \qquad M_{scc} = \begin{bmatrix} 0 & 0 & + & + & +\\ 0 & 0 & - & - & -\\ 0 & 0 & + & + & +\\ 0 & 0 & 0 & 0 & 0\\ 0 & 0 & 0 & 0 & 0 \end{bmatrix}$$

$\det(-J) = 0$, $n_v = *$, $n_f = *$

Ravel5.

$$\begin{aligned}
\dot{a} &= a_0 - g_{ab}(a,b) - g_{ac}(a,c)\\
\dot{b} &= b_0 - g_{ab}(a,b) + g_e(e)\\
\dot{c} &= g_{ab}(a,b) - g_{ac}(a,c)\\
\dot{d} &= g_{ab}(a,b) - g_d(d)\\
\dot{e} &= g_d(d) - g_e(e)
\end{aligned}$$

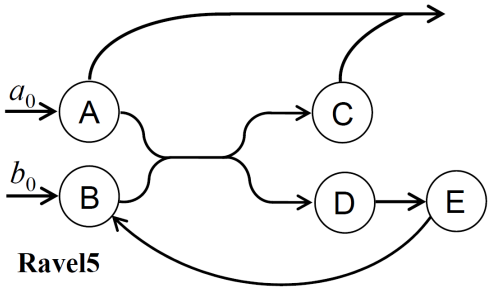

Figure A.39: Graph of Ravel5.

$$J = \begin{bmatrix} -(\alpha+\gamma) & -\beta & -\delta & 0 & 0\\ -\alpha & -\beta & 0 & 0 & \varphi\\ \alpha-\gamma & \beta & -\delta & 0 & 0\\ \alpha & \beta & 0 & -\varepsilon & 0\\ 0 & 0 & 0 & \varepsilon & -\varphi \end{bmatrix}, \qquad M_{scc} = \begin{bmatrix} 0 & - & 0 & - & -\\ 0 & + & 0 & + & +\\ 0 & + & 0 & + & +\\ 0 & 0 & 0 & 0 & 0\\ 0 & 0 & 0 & 0 & 0 \end{bmatrix}$$

$\det(-J) = 0$, $n_v = *$, $n_f = *$

Respighi5.

$$\begin{aligned}
\dot{a} &= a_0 - g_{ab}(a,b) - g_{ac}(a,c)\\
\dot{b} &= b_0 - g_{ab}(a,b)\\
\dot{c} &= g_{ab}(a,b) - g_{ac}(a,c)\\
\dot{d} &= g_{ab}(a,b) - g_d(d)\\
\dot{e} &= g_d(d) - g_e(e)
\end{aligned}$$

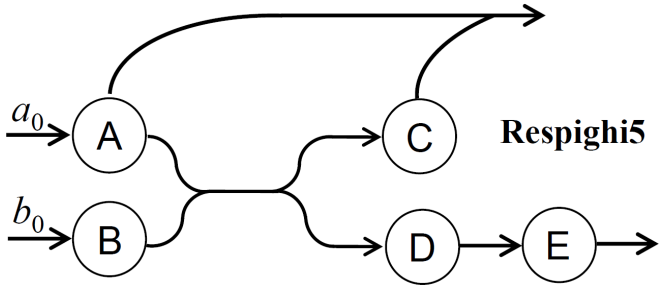

Figure A.40: Graph of Respighi5.

$$J = \begin{bmatrix} -(\alpha+\gamma) & -\beta & -\delta & 0 & 0 \\ -\alpha & -\beta & 0 & 0 & 0 \\ \alpha-\gamma & \beta & -\delta & 0 & 0 \\ \alpha & \beta & 0 & -\varepsilon & 0 \\ 0 & 0 & 0 & \varepsilon & -\varphi \end{bmatrix}, \qquad M_{scc} = \begin{bmatrix} + & - & - & 0 & 0 \\ - & + & + & 0 & 0 \\ - & + & + & 0 & 0 \\ 0 & 0 & 0 & 0 & 0 \\ 0 & 0 & 0 & 0 & 0 \end{bmatrix}$$

$\det(-J) = 0$, $n_v = 32$, $n_f = 32$

RimskijKorsakov5.

$$\begin{aligned} \dot{a} &= a_0 - g_a(a) - g_{ac}(a,c) + g_e(e) \\ \dot{b} &= g_a(a) - \bar{g}_b(b) + g_d(d) - g_b(b) \\ \dot{c} &= g_a(a) - g_{ac}(a,c) \\ \dot{d} &= g_{ac}(a,c) - g_d(d) - g_d^*(d) \\ \dot{e} &= \bar{g}_b(b) - g_e(e) \end{aligned}$$

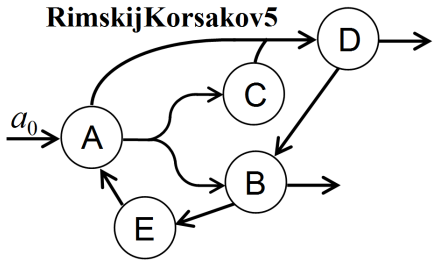

Figure A.41: Graph of RimskijKorsakov5.

$$J = \begin{bmatrix} -(\alpha+\mu) & 0 & -\nu & 0 & \varepsilon \\ \alpha & -(\beta+\rho) & 0 & \delta & 0 \\ \alpha-\mu & 0 & -\nu & 0 & 0 \\ \mu & 0 & \nu & -(\delta+\varphi) & 0 \\ 0 & \beta & 0 & 0 & -\varepsilon \end{bmatrix}, \quad M = \begin{bmatrix} + & + & - & + & + \\ + & + & - & + & + \\ ? & ? & + & ? & ? \\ + & + & + & + & + \\ + & + & - & + & + \end{bmatrix}$$

$\det(-J) > 0$, $n_v = *$, $n_f = *$

Šostakovič5.

$$\begin{aligned} \dot{a} &= -g_a(a) - g_{ab}(a,b) + g_c(c) \\ \dot{b} &= g_a(a) - g_b(b) - g_{ab}(a,b) - g_{bd}(b,d) \\ \dot{c} &= g_b(b) - g_c(c) + g_e(e) \\ \dot{d} &= g_{ab}(a,b) - g_{bd}(b,d) \\ \dot{e} &= g_{bd}(b,d) - g_e(e) \end{aligned}$$

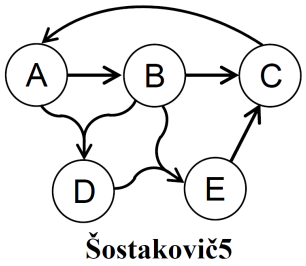

Figure A.42: Graph of Šostakovič5.

$$J = \begin{bmatrix} -(\alpha+\gamma) & -\beta & \varphi & 0 & 0 \\ \gamma-\alpha & -(\beta+\delta+\mu) & 0 & -\nu & 0 \\ 0 & \delta & -\varphi & 0 & \varepsilon \\ \alpha & \beta-\mu & 0 & -\nu & 0 \\ 0 & \mu & 0 & \nu & -\varepsilon \end{bmatrix}, \quad M = \begin{bmatrix} + & + & + & + & + \\ ? & + & ? & - & ? \\ ? & + & + & + & + \\ ? & ? & ? & + & ? \\ + & + & + & + & + \end{bmatrix}$$

$\det(-J) > 0$, $n_v = *$, $n_f = *$

Strauss5.

$$\dot{a} = a_0 - g_a(a) - g_{ac}(a,c)$$
$$\dot{b} = g_a(a) - g_{bd}(b,d) - g_{be}(b,e)$$
$$\dot{c} = c_0 - g_{ac}(a,c)$$
$$\dot{d} = g_a(a) - g_{bd}(b,d)$$
$$\dot{e} = g_{bd}(b,d) - g_{be}(b,e)$$

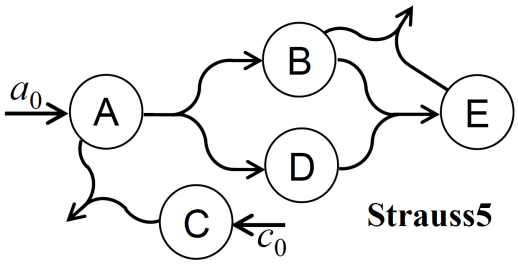

Figure A.43: Graph of Strauss5.

$$J = \begin{bmatrix} -(\alpha+\beta) & 0 & -\gamma & 0 & 0 \\ \alpha & -(\delta+\mu) & 0 & -\varepsilon & -\nu \\ -\beta & 0 & -\gamma & 0 & 0 \\ \alpha & -\delta & 0 & -\varepsilon & 0 \\ 0 & \delta-\mu & 0 & \varepsilon & -\nu \end{bmatrix}, \quad M_{scc} = \begin{bmatrix} 0 & 0 & 0 & 0 & 0 \\ - & + & + & - & - \\ 0 & 0 & 0 & 0 & 0 \\ + & - & - & + & + \\ + & - & - & + & + \end{bmatrix}$$

$\det(-J) = 0$, $n_v = 12$, $n_f = 24$

A.4 Six Nodes Networks

Debussy6.

$$\dot{a} = a_0 - g_{ab}(a,b) - g_{ae}(a,e)$$
$$\dot{b} = b_0 - g_{ab}(a,b)$$
$$\dot{c} = g_{ab}(a,b) - g_{cd}(c,d)$$
$$\dot{d} = d_0 - g_{cd}(c,d)$$
$$\dot{e} = g_{cd}(c,d) - g_{ae}(a,e)$$
$$\dot{f} = g_{ae}(a,e) - g_f(f)$$

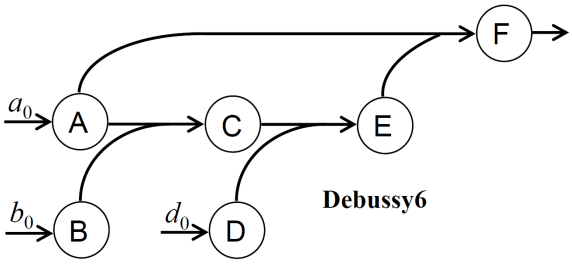

Figure A.44: Graph of Debussy6.

$$J = \begin{bmatrix} -(\alpha+\varepsilon) & -\beta & 0 & 0 & -\varphi & 0 \\ -\alpha & -\beta & 0 & 0 & 0 & 0 \\ \alpha & \beta & -\gamma & -\delta & 0 & 0 \\ 0 & 0 & -\gamma & -\delta & 0 & 0 \\ -\varepsilon & 0 & \gamma & \delta & -\varphi & 0 \\ \varepsilon & 0 & 0 & 0 & \varphi & -\zeta \end{bmatrix}$$

$\det(-J) = 0$ (the eigenvalue zero has multiplicity 2), $n_v = 64$, $n_f = 30$

Dukas6.

$$\begin{aligned}
\dot{a} &= a_0 - g_{ab}(a,b) + g_c(c) + g_d(d)\\
\dot{b} &= b_0 - g_{ab}(a,b) - g_{bc}(b,c) + g_f(f)\\
\dot{c} &= g_{ab}(a,b) - g_c(c) - g_{bc}(b,c) - \bar{g}_c(c)\\
\dot{d} &= \bar{g}_c(c) - g_d(d)\\
\dot{e} &= \bar{g}_c(c) - g_{ef}(e,f) - g_e(e)\\
\dot{f} &= g_{bc}(b,c) - g_{ef}(e,f) - g_f(f)
\end{aligned}$$

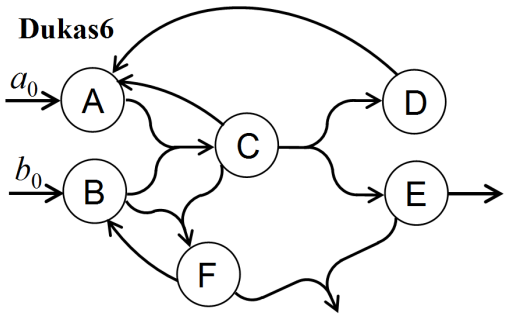

Figure A.45: Graph of Dukas6.

$$J = \begin{bmatrix}
-\alpha & -\beta & \eta & \delta & 0 & 0\\
-\alpha & -(\beta+\mu) & -\nu & 0 & 0 & \rho\\
\alpha & \beta-\mu & -(\eta+\nu+\gamma) & 0 & 0 & 0\\
0 & 0 & \gamma & -\delta & 0 & 0\\
0 & 0 & \gamma & 0 & -(\varepsilon+\zeta) & -\varphi\\
0 & \mu & \nu & 0 & -\varepsilon & -(\varphi+\rho)
\end{bmatrix}$$

$\det(-J) < 0$, $n_v = *$, $n_f = *$

Henze6.

$$\begin{aligned}
\dot{a} &= a_0 - g_{ab}(a,b) - g_{ae}(a,e)\\
\dot{b} &= b_0 - g_{ab}(a,b) - g_b(b) + g_c(c)\\
\dot{c} &= g_{ab}(a,b) - g_c(c) - g_{cd}(c,d)\\
\dot{d} &= g_b(b) - g_{cd}(c,d) - g_{df}(d,f)\\
\dot{e} &= g_{cd}(c,d) - g_{ae}(a,e)\\
\dot{f} &= g_{cd}(c,d) - g_{df}(d,f) - g_f(f)
\end{aligned}$$

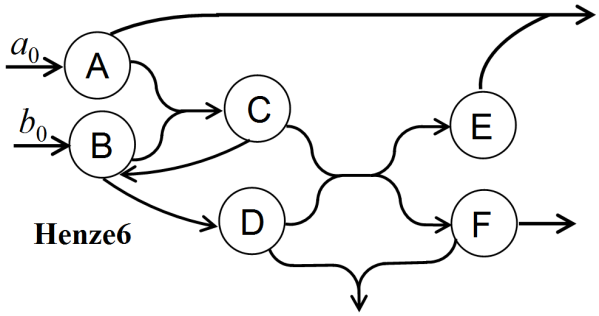

Figure A.46: Graph of Henze6.

$$J = \begin{bmatrix}
-(\alpha+\gamma) & -\beta & 0 & 0 & -\delta & 0\\
-\alpha & -(\beta+\varepsilon) & \zeta & 0 & 0 & 0\\
\alpha & \beta & -(\zeta+\eta) & -\vartheta & 0 & 0\\
0 & \varepsilon & -\eta & -(\vartheta+\kappa) & 0 & -\lambda\\
-\gamma & 0 & \eta & \vartheta & -\delta & 0\\
0 & 0 & \eta & \vartheta-\kappa & 0 & -(\lambda+\varphi)
\end{bmatrix}$$

$\det(-J) > 0$, $n_v = *$, $n_f = *$

$$M = \begin{bmatrix}
+ & - & - & ? & - & ?\\
- & + & + & - & + & +\\
+ & - & + & - & - & +\\
- & + & ? & + & + & -\\
? & + & + & ? & + & ?\\
+ & ? & ? & ? & - & +
\end{bmatrix}$$

Hindemith6.

$$\begin{aligned}
\dot{a} &= a_0 - g_{ab}(a,b) + g_c(c) + g_d(d) + g_e(e)\\
\dot{b} &= b_0 - g_{ab}(a,b) - g_{bc}(b,c)\\
\dot{c} &= g_{ab}(a,b) - g_c(c) - g_{bc}(b,c) - \bar{g}_c(c)\\
\dot{d} &= \bar{g}_c(c) - g_d(d)\\
\dot{e} &= \bar{g}_c(c) - g_{ef}(e,f) - g_e(e)\\
\dot{f} &= g_{bc}(b,c) - g_{ef}(e,f)
\end{aligned}$$

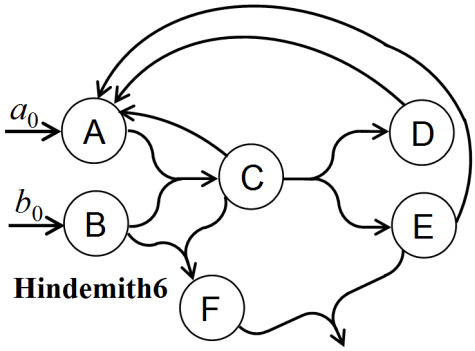

Figure A.47: Graph of Hindemith6.

$$J = \begin{bmatrix}
-\alpha & -\beta & \eta & \delta & \rho & 0\\
-\alpha & -(\beta+\mu) & -\nu & 0 & 0 & 0\\
\alpha & \beta-\mu & -(\eta+\nu+\gamma) & 0 & 0 & 0\\
0 & 0 & \gamma & -\delta & 0 & 0\\
0 & 0 & \gamma & 0 & -(\varepsilon+\rho) & -\varphi\\
0 & \mu & \nu & 0 & -\varepsilon & -\varphi
\end{bmatrix}$$

$\det(-J) < 0$, $n_v = *$, $n_f = *$

Mahler6.

$$\begin{aligned}
\dot{a} &= a_0 - g_a(a) - g_{ae}(a,e)\\
\dot{b} &= g_a(a) - g_b(b) - g_{bd}(b,d)\\
\dot{c} &= c_0 - g_c(c) - g_{cf}(c,f)\\
\dot{d} &= g_c(c) - g_d(d) - g_{bd}(b,d)\\
\dot{e} &= g_b(b) - g_{ae}(a,e)\\
\dot{f} &= g_d(d) - g_{cf}(c,f)
\end{aligned}$$

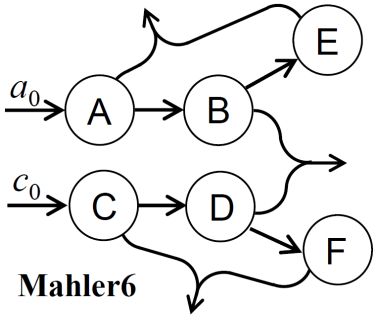

Figure A.48: Graph of Mahler6.

$$J = \begin{bmatrix}
-(\alpha+\zeta) & 0 & 0 & 0 & -\eta & 0\\
\alpha & -(\gamma+\varepsilon) & 0 & -\delta & 0 & 0\\
0 & 0 & -(\beta+\iota) & 0 & 0 & -\lambda\\
0 & -\gamma & \beta & -(\delta+\varphi) & 0 & 0\\
-\zeta & \varepsilon & 0 & 0 & -\eta & 0\\
0 & 0 & -\iota & \varphi & 0 & -\lambda
\end{bmatrix}$$

$\det(-J) > 0$, $n_v = 12$, $n_f = 62$

$$M = \begin{bmatrix} + & - & + & + & - & - \\ + & + & - & - & - & + \\ + & + & + & - & - & - \\ - & - & + & + & + & - \\ ? & + & - & - & + & + \\ - & - & ? & + & + & + \end{bmatrix}$$

A.5 Seven Nodes Networks

Schönberg7.

$$\begin{aligned} \dot{a} &= a_0 - g_a(a) - g_{ae}(a,e) \\ \dot{b} &= g_a(a) - g_b(b) - g_{bd}(b,d) \\ \dot{c} &= c_0 - g_c(c) - g_{cf}(c,f) \\ \dot{d} &= g_c(c) - g_d(d) - g_{bd}(b,d) \\ \dot{e} &= g_b(b) - g_{ae}(a,e) \\ \dot{f} &= g_d(d) - g_{cf}(c,f) \\ \dot{g} &= g_{bd}(b,d) - g_g(g) \end{aligned}$$

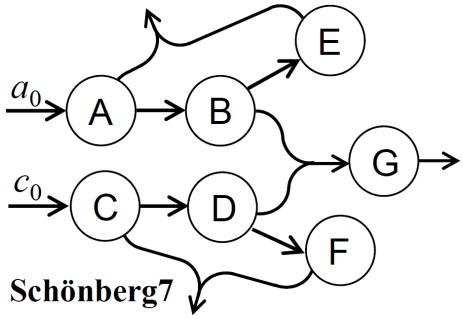

Figure A.49: Graph of Schönberg7.

$$J = \begin{bmatrix} -(\alpha+\zeta) & 0 & 0 & 0 & -\eta & 0 & 0 \\ \alpha & -(\gamma+\varepsilon) & 0 & -\delta & 0 & 0 & 0 \\ 0 & 0 & -(\beta+\iota) & 0 & 0 & -\lambda & 0 \\ 0 & -\gamma & \beta & -(\delta+\varphi) & 0 & 0 & 0 \\ -\zeta & \varepsilon & 0 & 0 & -\eta & 0 & 0 \\ 0 & 0 & -\iota & \varphi & 0 & -\lambda & 0 \\ 0 & \gamma & 0 & \delta & 0 & 0 & -\mu \end{bmatrix}$$

$\det(-J) > 0$, $n_v = *$, $n_f = *$

$$M = \begin{bmatrix} + & - & + & + & - & - & 0 \\ + & + & - & - & - & + & 0 \\ + & + & + & - & - & - & 0 \\ - & - & + & + & + & - & 0 \\ ? & + & - & - & + & + & 0 \\ - & - & ? & + & + & + & 0 \\ + & + & + & + & - & - & + \end{bmatrix}$$

A.6 Eight Nodes Networks

Massenet8.

$$
\begin{aligned}
\dot{a} &= a_0 - g_{ab}(a,b) - g_{ac}(a,c) - g_{ae}(a,e)\\
\dot{b} &= b_0 - g_{ab}(a,b) - g_b(b)\\
\dot{c} &= g_{ab}(a,b) - g_{ac}(a,c) - g_{cd}(c,d) - g_c(c) + g_g(g)\\
\dot{d} &= g_{ac}(a,c) - g_{cd}(c,d)\\
\dot{e} &= g_b(b) - g_{ae}(a,e) - g_e(e)\\
\dot{f} &= g_c(c) + g_e(e) - g_{fh}(f,h)\\
\dot{g} &= g_{fh}(f,h) - g_g(g) - g_g^*(g)\\
\dot{h} &= g_e(e) - g_{fh}(f,h) - g_h(h)
\end{aligned}
$$

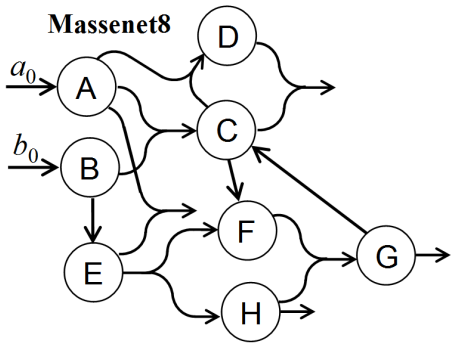

Figure A.50: Graph of Massenet8.

$$
J = \begin{bmatrix}
-(\alpha+\nu+\psi) & -\beta & -\xi & 0 & -\mu & 0 & 0 & 0\\
-\alpha & -(\beta+\lambda) & 0 & 0 & 0 & 0 & 0 & 0\\
\alpha-\psi & \beta & -(\xi+\gamma+\vartheta) & -\delta & 0 & 0 & \omega & 0\\
\psi & 0 & \xi-\gamma & -\delta & 0 & 0 & 0 & 0\\
-\nu & \lambda & 0 & 0 & -(\mu+\varepsilon) & 0 & 0 & 0\\
0 & 0 & \vartheta & 0 & \varepsilon & -\varphi & 0 & -\eta\\
0 & 0 & 0 & 0 & 0 & \varphi & -(\zeta+\omega) & \eta\\
0 & 0 & 0 & 0 & \varepsilon & -\varphi & 0 & -(\eta+\rho)
\end{bmatrix}
$$

$\det(-J) > 0$, $n_v = *$, $n_f = *$

$$
M = \begin{bmatrix}
+ & - & - & + & - & - & - & 0\\
- & + & + & - & + & + & + & 0\\
? & ? & + & - & ? & + & + & 0\\
? & ? & ? & + & ? & ? & ? & 0\\
- & + & + & - & + & + & + & 0\\
? & ? & + & - & ? & + & + & -\\
? & ? & + & - & ? & + & + & 0\\
? & ? & - & + & ? & - & - & +
\end{bmatrix}
$$

Stravinskij8.

$$
\begin{aligned}
\dot{a} &= a_0 - g_{ab}(a,b) - g_{ac}(a,c) - g_{ae}(a,e) + g_g^*(g)\\
\dot{b} &= b_0 - g_{ab}(a,b) - g_b(b)\\
\dot{c} &= g_{ab}(a,b) - g_{ac}(a,c) - g_{cd}(c,d) - g_c(c) + g_g(g)\\
\dot{d} &= g_{ac}(a,c) - g_{cd}(c,d)\\
\dot{e} &= g_b(b) - g_{ae}(a,e) - g_e(e)\\
\dot{f} &= g_c(c) + g_e(e) - g_{fh}(f,h)\\
\dot{g} &= g_{fh}(f,h) - g_g(g) - g_g^*(g)\\
\dot{h} &= g_e(e) - g_{fh}(f,h) - g_h(h)
\end{aligned}
$$

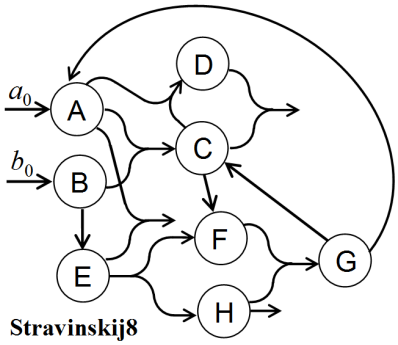

Figure A.51: Graph of Stravinskij8.

$$J = \begin{bmatrix} -(\alpha+\nu+\psi) & -\beta & -\xi & 0 & -\mu & 0 & \zeta & 0 \\ -\alpha & -(\beta+\lambda) & 0 & 0 & 0 & 0 & 0 & 0 \\ \alpha-\psi & \beta & -(\xi+\gamma+\vartheta) & -\delta & 0 & 0 & \omega & 0 \\ \psi & 0 & \xi-\gamma & -\delta & 0 & 0 & 0 & 0 \\ -\nu & \lambda & 0 & 0 & -(\mu+\varepsilon) & 0 & 0 & 0 \\ 0 & 0 & \vartheta & 0 & \varepsilon & -\varphi & 0 & -\eta \\ 0 & 0 & 0 & 0 & 0 & \varphi & -(\zeta+\omega) & \eta \\ 0 & 0 & 0 & 0 & \varepsilon & -\varphi & 0 & -(\eta+\rho) \end{bmatrix}$$

$\det(-J) = ?$, $n_v = *$, $n_f = *$

$$M = \begin{bmatrix} + & ? & ? & ? & ? & ? & ? & 0 \\ - & + & ? & ? & ? & ? & ? & 0 \\ ? & ? & + & - & ? & ? & ? & 0 \\ ? & ? & ? & ? & ? & ? & ? & 0 \\ - & + & ? & ? & + & ? & ? & 0 \\ ? & ? & + & - & ? & + & ? & ? \\ ? & ? & + & - & ? & + & + & 0 \\ ? & ? & - & + & ? & - & ? & ? \end{bmatrix}$$

A.7 Synoptic Overview

An overview of the considered biochemical networks is presented in Table A.1, which summarises the following results.

CV = Convergence of the Stability procedure (Yes/No);
n_V = number of vertices (primal procedure);
n_F = number of facets (dual procedure);
r(S) = rank(S);
NCC = Non-Singularity in the Stoich. Compatibility Class (Yes/No);
MR = Maximum Randomly generated eigenvalue real part;
BO = Boundedness test (Yes/No);
$\det -J$ = Sign of $\det(-J)$.

Table A.1: Summary of the results of the numerical tests

Network	CV	n_v	n_f	r(S)	NCC	MR	BO	det$-J$
Albinoni3	Yes	14	12	3	Yes	< 0	Yes	+
Buxtehude3	No	-	-	3	No	> 0	No	-
Corelli3	Yes	6	6	3	Yes	< 0	Yes	+
Frescobaldi3	No	-	-	3	Yes	< 0	Yes	+
Pachelbel3	No	-	-	3	Yes	< 0	Yes	+
Telemann3	Yes	10	12	3	Yes	< 0	Yes	+
Bach4	No	-	-	3	Yes	0	Yes	0
Beethoven4	No	-	-	4	Yes	< 0	Yes	+
Boccherini4	No	-	-	4	Yes	< 0	Yes	+
Čajkovskij4	No	-	-	4	No	> 0	Yes	-
Chopin4	Yes	8	14	4	Yes	< 0	Yes	+
Clementi4	No	-	-	4	No	0	Yes	0
Dvořák4	No	-	-	3	Yes	0	Yes	0
Fauré4	No	-	-	4	No	0	Yes	0
Gershwin4	No	-	-	4	Yes	< 0	No	+
Gluck4	Yes	14	8	4	Yes	< 0	Yes	+
Gounod4	No	-	-	4	Yes	< 0	Yes	+
Händel4	Yes	8	16	4	Yes	< 0	Yes	+
Haydn4	Yes	16	18	3	Yes	0	Yes	0
Mozart4	Yes	14	8	3	Yes	0	Yes	0
Offenbach4	No	-	-	4	Yes	< 0	Yes	+
Paganini4	Yes	14	18	4	Yes	< 0	Yes	+
Pergolesi4	No	-	-	4	Yes	< 0	Yes	+
Purcell4	Yes	16	18	3	Yes	0	Yes	0
Salieri4	No	-	-	4	No	0	Yes	0
Scarlatti4	No	-	-	4	No	0	Yes	0
Schubert4	No	-	-	4	No	> 0	Yes	?
Schumann4	No	-	-	4	No	0	Yes	0
Vivaldi4	No	-	-	3	Yes	0	Yes	0
Berg5	Yes	32	10	4	Yes	0	Yes	0
Berlioz5	Yes	32	10	3	Yes	0	Yes	0
Brahms5	Yes	32	10	4	Yes	0	Yes	0
Elgar5	No	-	-	4	Yes	0	Yes	0
Grieg5	Yes	22	68	5	Yes	< 0	Yes	+
Liszt5	Yes	28	66	5	Yes	< 0	Yes	+
Martucci5	No	-	-	5	Yes	< 0	Yes	+
Mendelssohn5	No	-	-	5	No	0	Yes	0
Rachmaninov5	No	-	-	4	Yes	0	Yes	0
Ravel5	No	-	-	4	Yes	0	Yes	0
Respighi5	Yes	32	32	4	Yes	0	Yes	0
RimskijKorsakov5	No	-	-	5	Yes	< 0	No	+
Šostakovič5	No	-	-	5	Yes	< 0	Yes	+
Strauss5	Yes	12	24	4	Yes	0	Yes	0
Debussy6	Yes	64	30	4	Yes	0	Yes	0
Dukas6	No	-	-	6	No	> 0	No	-
Henze6	No	-	-	6	Yes	< 0	Yes	+
Hindemith6	No	-	-	6	No	> 0	Yes	-
Mahler6	Yes	12	62	6	Yes	< 0	Yes	+
Schönberg7	No	-	-	7	Yes	< 0	Yes	+
Massenet8	No	-	-	8	Yes	< 0	Yes	+
Stravinskij8	No	-	-	8	No	> 0	Yes	?

B

Code for Testing Biochemical Networks

B.1 Polychem: Polyhedral Functions for Biochemical Systems

MATLAB code has been written to implement the numerical procedure proposed in Chapter 6 and in [BG14], to assess stability and boundedness of biochemical reaction network. The procedure is thoroughly described in Section 6.3.1. The code is available at `https://users.dimi.uniud.it/~franco.blanchini/polychem.zip`, along with the data files for assessing stability and boundedness of most of the networks examined in Appendix A.

In fact, as discussed in Chapter 6, the procedure is the same for testing both boundedness and stability; just the data that need to be provided to the procedure are different. The MATLAB function requires as input: matrices B and C of the BDC-decomposition, the maximum allowed number of iterations, and a flag that is 0 for using the primal procedure, 1 for using the dual. The generated output is a warning that tells whether a fixed point has been reached (the matrix has not changed, successful stop) or the maximum number of iteration has been reached with the matrix still changing (unsuccessful stop). In the former case, the output matrix X is the vertex matrix of the polyhedral Lyapunov function, if the primal procedure is used (the facet matrix if the dual procedure is used). The syntax is

```
X = polychemtest(B,C,max_itera,dual_procedure)
```

A function that provides matrices B and C of the BDC-decomposition based on the system $\dot{x} = Sg(x) + g_0$, requiring matrix S and qualitative information about $g(x)$, is also available online and is presented in Section B.2.

B.2 Computing the Steady-State Influence Matrix

In this section, MATLAB functions are presented that implement the efficient algorithm described in Chapter 7 and in [GCFB15] for computing the Structural Steady-State Influence Matrix (SSIM). These functions constitute the fundamental part of the software package SSIM toolbox (SSIM-Functions) and are the core computational engine for the graphical user interface tackling chemical reaction networks (SSIM-GUI); the whole toolbox, including both general functions and GUI, is online: `https://users.dimi.uniud.it/~franco.blanchini/influence.zip`.

Given a system

$$\dot{x} = f(x) + Eu, \qquad y = Hx, \quad x \in \mathbb{R}^n,\, u \in \mathbb{R},\, y \in \mathbb{R},$$

entry (i, j) of the $n \times n$ SSIM shows the *structural* influence on the ith state variable (seen as an output y) of a constant additive input u applied to the jth state variable: this corresponds to the choice

$$E = E_j = [0 \ \dots \ 0 \ \underbrace{1}_{\text{position } j} \ 0 \ \dots \ 0]^\top, \qquad H = H_i = [0 \ \dots \ 0 \ \underbrace{1}_{\text{position } i} \ 0 \ \dots \ 0].$$

A *structural* influence is identified if the steady-state variation has the same sign for any choice of the parameters. Hence, the entry (i, j) of the SSIM is:

- "+" ("+1" in the MATLAB environment) if a positive input applied to the jth variable always causes an *increase* in the steady state of the ith variable;
- "-" ("-1" in the MATLAB environment) if a positive input applied to the jth variable always causes a *decrease* in the steady state of the ith variable;
- "0" if any input applied to the jth variable always causes *no change* in the steady state of the ith variable;
- "?" ("2" in the MATLAB environment) if an input applied to the jth variable can cause an *increase or a decrease or no change* in the steady state of the ith variable, depending on the choice of parameter values.

The algorithm requires that the Jacobian of the system admits the BDC-decomposition described in Section 4.3: $J = BDC$, where $D \succ 0$ is a diagonal matrix. Chemical reaction networks and all the systems that can be written as

$$\dot{x} = Sf(x) + f_0, \tag{B.1}$$

where $x \in \mathbb{R}^n$, $S \in \mathbb{R}^{n \times m}$ is the stoichiometric matrix, $f(x) \in \mathbb{R}^m$ is a vector of (positive) reaction rates and $f_0 \in \mathbb{R}^n$ is a constant vector, admit a BDC-decomposition under suitable assumptions on $f(x)$ (see Section 4.3).

For computing the SSIM, two *MATLAB functions* have been written that handle a *general class of models* described either by a system of ordinary differential equations of the form (B.1), or by matrices B and C of the BDC-decomposition:

- function `SSIM_general.m` can handle any system that can be written in the form (B.1), since it requires as inputs S and qualitative information about $f(x)$;
- function `SignMatrixGeneration.m` can handle any system that admits a BDC-decomposition, since it requires as inputs matrices B and C.

Computing the SSIM

Function `SSIM_general.m` can be used to compute the structural steady-state influence matrix for any system that can be written in the form (B.1), since it requires only the knowledge of the stoichiometric matrix S and of qualitative information about $f(x)$. The function yields as an output the SSIM and requires either two or three inputs that will be specified below. By typing in the MATLAB command line either

```
M = SSIM_general(S,g);
```

or

```
M = SSIM_general(S,g,comb);
```

the SSIM is both stored in the variable `M` and visualised on the screen, together with information on the structural sign of the opposite of the Jacobian matrix (if this is positive, under boundedness assumptions, uniqueness of the equilibrium can be inferred). The function can also be used inside other MATLAB functions or scripts.

Input Specification. Inputs provided to the function `SSIM_general` must be specified as follows.

- `S`: the stoichiometric matrix S in (B.1).
- `g`: the reaction rate vector $f(x)$, written in a qualitative format. The input `g` is actually a matrix with m rows, each corresponding to an element of vector $f(x)$ in (B.1), and N_{max} columns if the rate function with more arguments depends on N_{max} variables. The elements of its ith row are the indices of the variables on which the ith rate function depends (with a minus sign if the corresponding derivative is negative); if a rate function has less than N_{max} arguments, the corresponding row is completed with zeros.
- `comb`: a column vector with m elements, each associated with an entry of vector $f(x)$ in (B.1). Its ith element is 1 if the corresponding rate function depends on a linear combination of variables, 0 otherwise. This is an optional argument and can be omitted when all of the elements are 0.

To better illustrate how to specify the inputs for the function, examples are provided below.

Example 1: a metabolic network. Consider Example 4.10, Chapter 4, which can be written as in model (B.1) with

$$x = \begin{bmatrix} a \\ b \\ c \end{bmatrix}, \quad S = \begin{bmatrix} -1 & 0 & 0 \\ -1 & 1 & 0 \\ 1 & 0 & -1 \end{bmatrix}, \quad f(x) = \begin{bmatrix} f_{ab}(a,b) \\ f_d(K-b) \\ f_c(c) \end{bmatrix}, \quad f_0 = \begin{bmatrix} a_0 \\ 0 \\ 0 \end{bmatrix}.$$

For this example, the input data are:

• $\mathtt{S} = S$, • $\mathtt{g} = \begin{bmatrix} 1 & 2 \\ -2 & 0 \\ 3 & 0 \end{bmatrix}$, • vector `comb` can be omitted.

The obtained SSIM is consistent with that reported in Example 7.4, Chapter 7.

Example 2: a six-node network. Consider the chemical reaction network named Mahler6 in Appendix A (see also [BG14]), represented by the graph in Fig. A.48; the corresponding ODE system can be recast into the form (B.1). Then the inputs to be provided are:

• $\mathtt{S} = \begin{bmatrix} -1 & 0 & 0 & 0 & 0 & -1 & 0 \\ 1 & 0 & -1 & -1 & 0 & 0 & 0 \\ 0 & -1 & 0 & 0 & 0 & 0 & -1 \\ 0 & 1 & -1 & 0 & -1 & 0 & 0 \\ 0 & 0 & 0 & 1 & 0 & -1 & 0 \\ 0 & 0 & 0 & 0 & 1 & 0 & -1 \end{bmatrix}$, • $\mathtt{g} = \begin{bmatrix} 1 & 0 \\ 3 & 0 \\ 2 & 4 \\ 2 & 0 \\ 4 & 0 \\ 1 & 5 \\ 3 & 6 \end{bmatrix}$

• vector `comb` can be omitted.

The resulting SSIM is that reported in Appendix A.

Example 3: a three-node network. Consider the chemical reaction network named Albinoni3 in Appendix A (see also [BG14]), represented by the graph in Fig. A.1. The corresponding ODE system can be recast into the form (B.1). Then the input data are:

• $\mathtt{S} = \begin{bmatrix} 1 & -1 & 0 \\ 0 & -1 & 1 \\ -1 & 0 & 0 \end{bmatrix}$, • $\mathtt{g} = \begin{bmatrix} -1 & 3 \\ 1 & 2 \\ 1 & -2 \end{bmatrix}$, • $\mathtt{comb} = \begin{bmatrix} 0 \\ 0 \\ 1 \end{bmatrix}$.

The resulting SSIM is that reported in Appendix A.

Function Structure and Intermediate Outputs

Function `SSIM_general.m` is obtained as the cascade of two functions (see Fig. B.1).

The first function is `generateBCmatrices.m`, which receives as inputs `S`, `g` and possibly `comb`, specified as above, and provides as outputs matrices `B` and `C` of the BDC-decomposition. As stressed in Remark 4.3, the BDC-decomposition is not unique and different choices can be made to compute it: *e.g.*, columns of B and rows of C can be arbitrarily permuted, provided that the same permutation is applied on both sides, and also the sign of any column of B can be changed, provided that the sign of the corresponding row of C is changed too (and *vice versa*). Matrices B and C provided by the function are such that B contains columns of S, possibly with changed sign, and an element of C is positive whenever it is the unique nonzero element in the row.

Remark B.1. *This function can also be used as a standalone function to systematically compute the BDC-decomposition for a given system of the form* (B.1) *(see Chapter 4, Section 4.3).*

The second function is `SignMatrixGeneration.m`, which receives as inputs matrices B and C of the BDC decomposition and actually computes the SSIM using the

efficient algorithm described in [GCFB15], Procedure 1, and reported in Chapter 7.

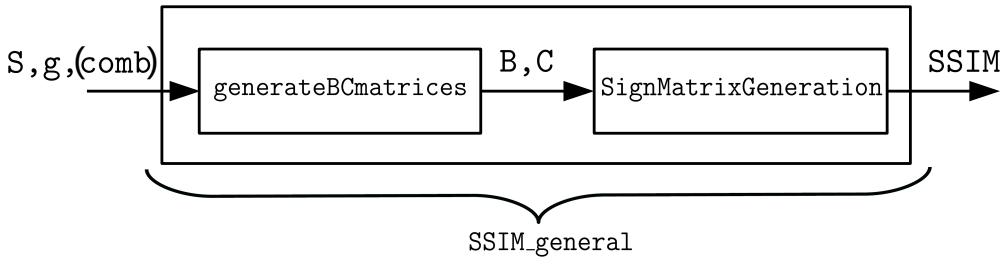

Figure B.1: Function `SSIM_general` as the cascade of functions `generateBCmatrices` and `SignMatrixGeneration`.

Computing the SSIM directly, based on the BDC-decomposition.
The function `SignMatrixGeneration.m` can be used to systematically compute the SSIM for *any system that admits a BDC-decomposition*, even though the system cannot be written in the form (B.1). In this case, it is enough to provide as inputs the matrices B and C of the BDC decomposition.

C

Stability: a Brief Overview

Stability of equilibria is a fundamental issue in dynamical system theory, which has been intensively considered in this thesis. A brief survey about stability and the related results is provided here; the presentation is largely inspired by [BV13, BM15].

Consider the nonlinear autonomous system

$$\dot{x}(t) = f(x(t)), \tag{C.1}$$

where $f : \mathcal{D} \subseteq \mathbb{R}^n \to \mathbb{R}^n$ is assumed to be smooth enough: a minimal requirement is that f is a locally Lipschitz vector field.

Definition C.1. *Given two metric spaces $\mathcal{X}$, with metric $d_{\mathcal{X}}$, and $\mathcal{Y}$, with metric $d_{\mathcal{Y}}$, a function $f : \mathcal{X} \to \mathcal{Y}$ is* Lipschitz continuous *if there exists a real constant $K \geq 0$ such that, for all $x_1, x_2 \in \mathcal{X}$, $d_{\mathcal{Y}}(f(x_1), f(x_2)) \leq K\, d_{\mathcal{X}}(x_1, x_2)$. The function is* locally Lipschitz continuous *if, for any ball $\mathcal{B}$, there exists a real constant $L \geq 0$ such that $d_{\mathcal{Y}}(f(x_1), f(x_2)) \leq L\, d_{\mathcal{X}}(x_1, x_2)$ for all $x_1, x_2 \in \mathcal{B}$.*

In the theory of differential equations, Lipschitz continuity is the central condition of the Picard-Lindelöf theorem that guarantees the existence and uniqueness of the solution to a Cauchy problem (initial value problem). In general, *local* Lipschitz continuity assures *local* existence and uniqueness of the solution, but it does not ensure the existence of a solution that is globally defined. However, in the following, the global existence of the solution will be always assumed.

Denoting by $\varphi(t, x_0)$ the solution at time t of the initial value problem associated with (C.1), with the initial condition $x(0) = x_0 \in \mathcal{D}$, the following general definition can be provided.

Definition C.2. *The solution $\varphi(t, x_0)$ is* stable *(or* Lyapunov stable*) if, for any $\varepsilon > 0$, there exists $\delta > 0$ such that $\|\varphi(t, y_0) - \varphi(t, x_0)\| < \varepsilon$ for all $t \geq 0$ and for all $y_0 \in \mathcal{D}$ such that $\|y_0 - x_0\| < \delta$. The solution is* unstable *if it is not stable, while it is* asymptotically stable *if it is stable and, in addition, a constant $\zeta > 0$ exists such that $\lim_{t\to\infty} \|\varphi(t, y_0) - \varphi(t, x_0)\| = 0$ for all $y_0 \in \mathcal{D}$ such that $\|y_0 - x_0\| < \zeta$. The solution is* marginally stable *if it is stable, but not asymptotically.*

Typically, the main object of the investigation is the stability of equilibria, namely, of solutions that are constant in time (points $\bar{x} \in \mathcal{D}$ such that $f(\bar{x}) = 0$). In

Definition C.2, this amounts to considering $\varphi(t, x_0) \equiv x_0 \doteq \bar{x}$. Note that the above definition concerns *local* behaviours, in the proximity of the equilibrium point. If the basin of attraction[1] is the whole state space, stability is *global*.

In the case of linear systems of the form

$$\dot{x}(t) = Ax(t), \tag{C.2}$$

where $A \in \mathbb{R}^{n\times n}$, stability is an inherent property of the system (the system is stable if and only if its zero solution is stable), and useful and simple stability criteria can be derived.

Theorem C.1. *System* (C.2) *is stable if and only if for all* $\lambda_i \in \sigma(A)$, $\Re(\lambda_i) \leq 0$ *and, whenever* $\Re(\lambda_i) = 0$, *the ascent of* λ_i *is* 1 *(namely, there must not be Jordan blocks with dimension greater than one associated with eigenvalues whose real part is zero). It is unstable if and only if there exists* $\lambda_i \in \sigma(A)$ *with either* $\Re(\lambda_i) > 0$, *or* $\Re(\lambda_i) = 0$ *and ascent greater than* 1. *It is asymptotically stable if and only if for all* $\lambda_i \in \sigma(A)$, $\Re(\lambda_i) < 0$. *The system is marginally stable if and only if it is stable and there exists* $\lambda_i \in \sigma(A)$ *such that* $\Re(\lambda_i) = 0$, *with ascent* 1.

Theorem C.2. *[Bre15] Given matrix* $A \in \mathbb{R}^{n\times n}$, *the following statements are equivalent.*

- *A norm* $\|\cdot\|_a$ *on* $\mathbb{R}^n$ *and a real* $\alpha > 0$ *exist such that, for all* $x \in \mathbb{R}^n$ *and for all* $t \geq 0$, $\|e^{At}x\|_a \leq e^{-\alpha t}\|x\|_a$.
- *For any norm* $\|\cdot\|_c$ *on* $\mathbb{R}^n$, *two reals* $\gamma > 0$ *and* $C > 1$ *exist such that, for all* $x \in \mathbb{R}^n$ *and for all* $t \geq 0$, $\|e^{At}x\|_c \leq Ce^{-\gamma t}\|x\|_c$.
- $\Re(\lambda_i) < 0$ *for all* $\lambda_i \in \sigma(A)$.
- *System* (C.2) *is asymptotically stable.*

The above results hold for continuous-time systems; for discrete-time systems, analogous results can be provided, based on the modulus of the eigenvalues.

The stability properties of the zero solution of linear *hyperbolic* systems (namely, systems whose state matrix has no eigenvalues with zero real part) are *global*: indeed, it can be shown that, if the system is hyperbolic, there are two invariant subspaces $\mathcal{S}$ (stable subspace, such that $\|e^{At}x\|_c \leq Ce^{-\gamma t}\|x\|_c$, for positive constants C, γ, for all $t \geq 0$ and for all $x \in \mathcal{S}$) and $\mathcal{U}$ (unstable subspace, such that $\|e^{At}x\|_c \leq Me^{\mu t}\|x\|_c$, for positive constants M, μ, for all $t \leq 0$ and for all $x \in \mathcal{U}$), with $\mathbb{R}^n = \mathcal{S} \oplus \mathcal{U}$. Conversely, in the non-hyperbolic case, there exists a third invariant subspace $\mathcal{C}$ (center subspace), in which the behaviour is not exponential.

Based on the criteria for the stability of linear systems, it is possible to study *local* stability of the equilibria of nonlinear systems: the principle of linearised stability (introduced by Lyapunov) allows to determine the stability of an equilibrium point

[1] The basin (or domain) of attraction of an equilibrium $\bar{x}$ is the set $\mathcal{A} \subseteq \mathbb{R}^n$ such that $\lim_{t\to\infty} \|\varphi(t, x_0) - \bar{x}\| = 0$ for all $x_0 \in \mathcal{A}$.

of a nonlinear system by linearising the system around the equilibrium and then studying the stability property of the zero solution of the linearised system. The Jacobian of $f(\cdot)$ at the point $\bar{x}$ is denoted as $J_f(\bar{x})$.

Theorem C.3. *Let $\bar{x} \in \mathcal{D}$ be an equilibrium of* (C.1) *and f be smooth enough. Then*

- *if $\Re(\lambda_i) < 0$ for all $\lambda_i \in \sigma(J_f(\bar{x}))$, the equilibrium $\bar{x}$ is asymptotically stable;*
- *if $\Re(\lambda_i) > 0$ for some $\lambda_i \in \sigma(J_f(\bar{x}))$, the equilibrium $\bar{x}$ is unstable.*

The principle of linearised stability does no longer hold when the Jacobian matrix at the equilibrium is not hyperbolic (in this case, considering the linear term is not enough to assess stability of the equilibrium and higher order terms need to be taken into account).

Remark C.1. *In view of the "fragility" of the non-hyperbolic case, usually an eigenvalue is said to be* stable *if it has a strictly negative real part,* unstable *otherwise. This denomination is often used in the thesis.*

Of course, since the linearisation (or linear variational equation) of (C.1) around different equilibrium points has a different state matrix (the Jacobian matrix computed at the equilibrium point, indeed), the stability properties may change when a different equilibrium is considered.

Lyapunov functions provide a powerful alternative to linearisation for assessing the stability properties of equilibria of nonlinear system. Moreover, they allow to study *global* stability of equilibria. Intuitively, Lyapunov functions are chosen as energy functions and the related method is based on the physical consideration that stable equilibria are minima of the energy of the system.

More formally, consider a (possibly uncertain) system

$$\dot{x}(t) = f(x(t), w(t)), \qquad w(t) \in \mathcal{W}, \tag{C.3}$$

such that $f(0, w) = 0$ for all $w \in \mathcal{W}$ (hence, $x(t) \equiv 0$ is a trajectory of the system), and denote by $x(t)$ any solution of (C.3) corresponding to $x(0) \in \mathbb{R}^n$ and $w(t) \in \mathcal{W}$. A Lyapunov function $\Psi : \mathbb{R}^n \to \mathbb{R}$ for the system is a positive definite function that is decreasing along the system trajectories; this property can be checked *without any knowledge of the system trajectories* thanks to the Lyapunov derivative.

If $\Psi(x(t))$ is continuously differentiable, and under regularity assumptions for x, the Lyapunov derivative is

$$\dot{\Psi}(x(t))\Big|_{x(t)=x,\, w(t)=w} = \nabla\Psi(x)^\top f(x, w) = \nabla\Psi(x)^\top \dot{x},$$

where $\nabla\Psi(x) = [\partial\Psi(x)/\partial x_1 \;\; \partial\Psi(x)/\partial x_2 \;\; \dots \;\; \partial\Psi(x)/\partial x_n]^\top$. Otherwise, the upper-right Dini derivative can be used: for a function $\psi(t)$, the upper-right Dini derivative computed at t is $D^+\psi(t) = \limsup_{h\to 0^+} \frac{\psi(t+h)-\psi(t)}{h}$. Hence, it can be shown that

the Lyapunov derivative (the upper directional derivative of Ψ with respect to the system trajectories) becomes

$$D^+\Psi(x,w) \doteq D^+\Psi(x, f(x,w)) = \lim_{h\to 0^+} \sup \frac{\Psi(x + hf(x,w)) - \psi(x)}{h}$$

and, if $\psi(t) = \Psi(x(t))$, $D^+\psi(t) = D^+\Psi(x,w)$ for almost all t [RHL77, BM15].

When considering piecewise-linear functions, the directional derivative has a special form: for instance, for any maximum-type convex Lyapunov function $\Psi(x) = \max_{1\le i\le m} \Psi_i(x)$, with $\Psi_i(x)$ continuously differentiable convex functions for $i = 1,\dots,m$, defining as $\mathcal{I}(x) = \{i : \Psi_i(x) = \Psi(x)\}$ the set of indices where the maximum is achieved, the Lyapunov derivative can be computed as

$$D^+\Psi(x,w) = \max_{i\in\mathcal{I}(x)} \nabla\Psi_i(x)^\top f(x,w).$$

Remark C.2. *The strong relation between Lyapunov (and Lyapunov-like) functions and invariant sets is deeply investigated in the book [BM15]. For instance, if a function Ψ of the state variables is non-increasing along the system trajectories, then the level set*

$$\mathcal{N}[\Psi,\nu] = \{x : \Psi(x) \le \nu\}$$

*is positively invariant for the system (namely, if $x(t_0) \in \mathcal{N}[\Psi,\nu]$, then $x(t) \in \mathcal{N}[\Psi,\nu]$ for all $t \ge t_0$); if the function is strictly decreasing and the derivative is bounded away from zero (*i.e.*, $D^+\Psi(x) < -\kappa$, with $\kappa > 0$) in a set of the form*

$$\mathcal{N}[\Psi,\alpha,\beta] = \{x : \alpha \le \Psi(x) \le \beta\},$$

then $x(t_0) \in \mathcal{N}[\Psi,\alpha,\beta]$ implies that $x(t) \in \mathcal{N}[\Psi,\beta]$ for all $t \ge t_0$ and that $x(t)$ reaches the set $\mathcal{N}[\Psi,\alpha]$ in finite time.

Under the assumption that the system admits a solution for every initial condition and each piecewise continuous input w, and that any solution is globally defined on $\mathbb{R}^n$, the following definitions and results are provided in [BM15].

Definition C.3. *A locally Lipschitz function $\Psi : \mathbb{R}^n \to \mathbb{R}$ is* radially unbounded *if*

$$\lim_{\|x\|\to\infty} |\Psi(x)| = \infty.$$

Definition C.4. *A continuous function $\phi : \mathbb{R}^+ \to \mathbb{R}^+$ is a* κ–function *if it is continuous and strictly increasing, with $\phi(0) = 0$.*

Definition C.5. *The origin as an equilibrium of system* (C.3) *is* (robustly) globally uniformly asymptotically stable *if it is* locally stable *(for all $\epsilon > 0$ there exists $\delta > 0$ such that, if $\|x(0)\| \le \delta$, then $\|x(t)\| \le \epsilon$ for all $t \ge 0$) for all functions $w(t) \in \mathcal{W}$ and* globally attractive *(for all $\mu > 0$ and $\nu > 0$, there exists $T(\mu,\nu) > 0$ such that if $\|x(0)\| \le \mu$ then $\|x(t)\| \le \nu$ for all $t \ge T(\mu,\nu)$) for all functions $w(t) \in \mathcal{W}$.*

In the absence of uncertainties w, the property is simply denoted as global uniform asymptotic stability. In [BM15], a particular definition of positive definiteness is considered.

Definition C.6. *A function* $\Psi : \mathbb{R}^n \to \mathbb{R}$ *is* positive definite *if* $\Psi(0) = 0$ *and there exists a* κ*–function* ϕ_0 *such that*

$$\Psi(x) \geq \phi_0(\|x\|).$$

Definition C.7. *A locally Lipschitz function* $\Psi : \mathbb{R}^n \to \mathbb{R}$ *is a* global Lyapunov function *for the system if it is positive definite, radially unbounded and there exists a* κ*–function* ϕ *such that*

$$D^+\Psi(x, w) \leq -\phi(\|x(t)\|). \tag{C.4}$$

Theorem C.4. *[Lya66] Assume that system* (C.3) *admits a global Lyapunov function* Ψ*. Then the origin is a globally uniformly asymptotically stable equilibrium.*

For differential equations $\dot{x} = f(x)$, with a continuous f and such that $f(0) = 0$, the positive definiteness requirement is simply $\Psi(x) > 0$ for all $x \neq 0$, $\Psi(0) = 0$, and condition (C.4) in Definition C.7 becomes $D^+\Psi(x) < 0$ for $x \in \mathbb{R}^n$, $x \neq 0$; conversely, if $D^+\Psi(x) \leq 0$ for all $x \in \mathbb{R}^n$, Ψ is a *weak Lyapunov function*, and guarantees Lyapunov stability (but not asymptotic stability). A positive definite function for which the condition on the Lyapunov derivative holds in a neighbourhood $\mathcal{B}$ of the origin, and not in the whole space, is a *local* Lyapunov function and can ensure *local* stability (Lyapunov stability if $D^+\Psi(x) \leq 0$ for all $x \in \mathcal{B}$, asymptotic stability if $D^+\Psi(x) < 0$ for all $x \in \mathcal{B}$, $x \neq 0$) of the equilibrium at the origin.

A stronger notion of stability is exponential stability.

Definition C.8. *The origin as an equilibrium of system* (C.3) *is* globally exponentially stable *if there exist* $\mu > 0$ *(transient estimate) and* $\gamma > 0$ *(convergence speed) such that for all* $\|x(0)\|$ *the condition*

$$\|x(t)\| \leq \mu\|x(0)\|e^{-\gamma t}, \tag{C.5}$$

holds for every $t \geq 0$ *and every function* $w(t) \in \mathcal{W}$*.*

Theorem C.5. *Assume that system* (C.3) *admits a positive definite locally Lipschitz function* $\Psi(x)$*, upper and lower polynomially bounded (namely, such that, for some positive reals* α *and* β *and some positive integer* p*,*

$$\alpha\|x\|^p \leq \Psi(x) \leq \beta\|x\|^p, \quad \textit{for all } \ x \in \mathbb{R}^n) \tag{C.6}$$

and such that

$$D^+\Psi(x, w) \leq -\gamma\Psi(x) \tag{C.7}$$

for some positive γ*. Then the origin is a globally exponentially stable equilibrium.*

Global exponential stability implies global uniform asymptotic stability.

Sometimes, global stability can be a too strong requirement, because it can be impossible to require convergence starting from arbitrary initial conditions, or because, due to persistent disturbances, the system trajectories converge to a set that includes the equilibrium, but cannot asymptotically approach the equilibrium. In these cases, Lyapunov functions are a powerful tool to prove local stability and uniform ultimate boundedness. [BM15]

Lyapunov methods and criteria can be provided for discrete-time systems as well.

For a wider classification of stability concepts and for a deep study of stability theory via Lyapunov methods, the reader is referred for instance to [RHL77].

D

Topological Degree Theory

As discussed in Section 4.5, the topological degree theory (see [Sch69, Llo78, Dei85, FG95, OJCC06, Feč08, Ams14] and the references therein) provides powerful tools for the study of dynamical systems and of the stability of their equilibrium points. [Hof90, Zan96, OC95] This fundamental theory is explained more in detail, but still briefly, in this appendix, providing the axiomatic definition of the degree in the finite dimensional case and some essential results that facilitate the understanding of those reported in Section 4.5. The presented material is largely derived from [Zan96] and from the notes of a doctoral course held by Fabio Zanolin.

Let $f : \bar{\mathcal{S}} \to X$ be a continuous function, where $\mathcal{S} \subseteq X$ is an open and bounded set, and let $p \in X$ be a point such that $p \notin f(\partial\mathcal{S})$. Then, $(f, \mathcal{S}, p)$ is an admissible triple and can be associated with an integer $d(f, \mathcal{S}, p)$, the *topological degree*. The topological degree can be defined axiomatically as the unique function $d : A \to \mathbb{Z}$, with

$$A \subset \{(f, \mathcal{S}, p) : f : \mathcal{S} \to X \text{ is continuous}, p \notin f(\partial\mathcal{S})\},$$

which satisfies the following properties:

1. given two open and disjoint subsets of $\mathcal{S}$, $\mathcal{S}_1$, $\mathcal{S}_2 \subseteq \mathcal{S}$ with $\mathcal{S}_1 \bigcap \mathcal{S}_2 = \emptyset$, such that $f(x) \neq p \ \forall \ x \in \bar{\mathcal{S}} \setminus (\mathcal{S}_1 \bigcup \mathcal{S}_2)$, then $d(f, \mathcal{S}_1, p) + d(f, \mathcal{S}_2, p) = d(f, \mathcal{S}, p)$;
2. $d(I_{\mathcal{S}}, \mathcal{S}, p) = 1$ if $p \in \mathcal{S}$ (while $d(I_{\mathcal{S}}, \mathcal{S}, p) = 0$ if $p \notin \bar{\mathcal{S}}$), where $I_{\mathcal{S}}$ denotes the identity mapping of X;
3. if $h : \bar{\mathcal{S}} \times [0 \ \ 1] \to X$ is a continuous homotopy[1] and $p : [0 \ \ 1] \to X$ is a continuous function, with $h(x, \lambda) \neq p(\lambda) \ \forall \ x \in \partial\mathcal{S}$ and $\forall \ \lambda \in [0 \ \ 1]$, then (with the notation $h(x, \lambda) = h_\lambda(x)$ and $p(\lambda) = p_\lambda$) $d(h_\lambda, \mathcal{S}, p_\lambda)$ is constant with respect to λ.

From axiom 3 it immediately follows that $d(h_\lambda, \mathcal{S}, p) = d(h_0, \mathcal{S}, p)$ for all $\lambda \in [0 \ \ 1]$ (it suffices to choose $p(\lambda) \equiv p$) and that $d(f, \mathcal{S}, p) = d(f - p, \mathcal{S}, 0)$ (based on the homotopy $h(x, \lambda) = f(x) - \lambda p$ and $p(\lambda) = (1 - \lambda)p$). Furthermore, for $\varepsilon > 0$ sufficiently small, $d(f_1, \mathcal{S}, p) = d(f_2, \mathcal{S}, p)$ if $\|f_1 - f_2\| < \varepsilon$ on $\partial\mathcal{S}$; in particular, this is true when $f_1 = f_2$ on $\partial\mathcal{S}$. This means that the degree only depends on the behaviour of the function on the boundary of $\mathcal{S}$.

[1] A homotopy is a continuous function $h(x, \lambda)$, with $\lambda \in [0 \ \ 1]$ that describes a continuous deformation of a function $f(x)$ into a function $g(x)$: $h(x, 0) = f(x)$ and $h(x, 1) = g(x)$.

Moreover, from axiom 1 it immediately follows that $d(f, \emptyset, p) = 0$; also, given an open and bounded set $\mathcal{S}_0 \subseteq \mathcal{S}$ such that $f(x) \neq p$ for all $x \in \bar{\mathcal{S}} \setminus \mathcal{S}_0$, then $d(f, \mathcal{S}_0, p) = d(f, \mathcal{S}, p)$. As a corollary, it follows that, if $f(x) \neq p$ for all $x \in \bar{\mathcal{S}}$, then $d(f, \mathcal{S}, p) = 0$. The following theorem holds, ensuring that the equation $f(x) = p$ has at least one solution in $\mathcal{S}$ if $d(f, \mathcal{S}, p) \neq 0$.

Theorem D.1. *(Kronecker) If $(f, \mathcal{S}, p) \in A$ (an admissible triple) and $d(f, \mathcal{S}, p) \neq 0$, then there exists at least one $\tilde{x} \in \mathcal{S}$ such that $f(\tilde{x}) = p$.*

It is then apparent that the topological degree theory is very useful for finding both fixed points and zeros of functions (in fact, a fixed point $\tilde{x}$ of $\psi(\cdot)$, $\psi(\tilde{x}) = \tilde{x}$, corresponds to a zero of $f(x) = x - \psi(x)$, $f(\tilde{x}) = 0$).

That provided above is the axiomatic definition of the topological degree; in Section 4.5 a constructive definition (4.35) is provided. Based on (4.35), properties 1, 2, 3 can be derived as theorems. Conversely, if 1, 2, 3 are assumed as axioms, (4.35) can be derived as a formula to compute the degree (as will be shown in the following).

In finite dimensions ($X = \mathbb{R}^n$), the topological degree is designated as Brouwer degree and it is useful for proving the renowned Brouwer fixed point theorem.

Theorem D.2. *(Brouwer) Let $\mathcal{B} \subset \mathbb{R}^n$ be an open, bounded set such that $\bar{\mathcal{B}}$ is homeomorphic to the closed unit ball $\{x \in \mathbb{R}^n : \|x - x_0\| \leq 1\}$ and let $\psi : \bar{\mathcal{B}} \to \bar{\mathcal{B}}$ be a continuous function. Then ψ has a fixed point in $\bar{\mathcal{B}}$: $\exists\ \tilde{x} \in \bar{\mathcal{B}}$ such that $\psi(\tilde{x}) = \tilde{x}$.*

The topological degree for infinite dimensional spaces (such as metric spaces and normed spaces) has been extended by Schauder and Leray: it takes the name of Leray-Schauder degree and can be defined based on analogous axioms; in this case, an analogous fixed point theorem has been proved by Schauder (see [Maw99] for a thorough survey, and the references therein). Here, however, the focus is on applications to differential equations in finite dimensional spaces, hence Brouwer degree is considered.

In particular, consider $f \in C(\bar{\mathcal{S}}) \bigcap C^1(\mathcal{S})$ and denote by $\mathcal{B}(c, r)$ the open ball of centre c and radius r. For $z \in \mathcal{S}$, the function can be linearised as $f(x) = f(z) + J_f(z)(x - z) + R$, where R is an infinitesimal rest. Then, if $f(x) = p$ has a finite number of solutions $\bar{x}_1, \ldots, \bar{x}_k \in \mathcal{S}$, the degree can be studied just locally, in a neighbourhood of each of these isolated points: by taking $\varepsilon > 0$ such that $\mathcal{B}(\bar{x}_i, \varepsilon)$, $i = 1, \ldots, k$, are pairwise disjoint, it follows from axiom 1 that

$$d(f, \mathcal{S}, p) = \sum_{i=1}^{k} d(f, \mathcal{B}(\bar{x}_i, \varepsilon), p).$$

Definition D.1. *Given $f \in C(\bar{\mathcal{S}}) \bigcap C^1(\mathcal{S})$, a point $\bar{x} \in \mathcal{S}$ is a* critical point *of f if the determinant of the Jacobian matrix evaluated at $\bar{x}$ is zero:* $\det(J_f(\bar{x})) = 0$. *Moreover, let $Z_f = \{x \in \mathcal{S} : \det(J_f(x)) = 0\}$; if $p \notin f(Z_f)$, then p is a* regular value *of f.*

Then, the following results hold, where the case $p = 0$ is considered for the sake of simplicity.

Theorem D.3. *Consider $f \in C(\bar{\mathcal{S}}) \bigcap C^1(\mathcal{S})$ and $z \in \mathcal{S}$ such that $f(z) = 0$ and $\det(J_f(z)) \neq 0$, and denote by $g(x) = J_f(z)(x - z)$. Then, $d(f, \mathcal{B}(z, r), 0) = d(g, \mathcal{B}(z, r), 0)$ for some $r > 0$.*

Corollary D.1. *Let $f \in C(\bar{\mathcal{S}}) \bigcap C^1(\mathcal{S})$ and let 0 be a regular value of f. Then, $f^{-1}(0)$ is finite and*

$$d(f, \mathcal{S}, 0) = \sum_{z \in f^{-1}(0)} d(J_f(z), \mathcal{B}(0, 1), 0). \tag{D.1}$$

The fact that $f^{-1}(0)$ is finite can be shown based on a compactness argument and on the local inversion theorem.

It can also be shown that, if $M \in \mathbb{R}^{n \times n}$ is a non-singular square matrix, $d(M, \mathcal{B}(0, 1), 0) = \text{sign}(\det(M))$, where $\text{sign}(t) = 1$ for $t > 0$ and $\text{sign}(t) = -1$ for $t < 0$ (more in general, $d(M, \mathcal{S}, 0) = \text{sign}(\det(M))$ holds for any $\mathcal{S}$ such that $0 \in \mathcal{S}$). Then, (D.1) is modified as follows:

$$d(f, \mathcal{S}, 0) = \sum_{z \in f^{-1}(0)} \text{sign}(\det(J_f(z))). \tag{D.2}$$

Note that the formula can be applied even though $f(x) = 0$ has no solutions; in this case, $d(f, \mathcal{S}, 0) = 0$. The following theorem corresponds to Lemma 2 in [Hof90].

Theorem D.4. *Assume that the system $\dot{x} = f(x)$, with $f : \mathbb{R}^n \to \mathbb{R}^n$, has solutions that are globally uniformly asymptotically bounded in an open ball $\mathcal{S}$. Then the corresponding degree is $d(f, \mathcal{S}, 0) = (-1)^n$ for any bounded open set $\mathcal{S}$ containing all of the system equilibrium points.*

Based on (D.2), the following corollary is immediate.

Corollary D.2. *Consider the system $\dot{x} = f(x)$, under the assumptions of Theorem D.4. Let it admit $N < \infty$ equilibria $\bar{x}_i$, $i = 1, \ldots, N$, each contained in $\mathcal{S}$, none of which is a critical point. Then*

$$\sum_{i=1}^{N} \text{sign}\left[\det(J(\bar{x}_i))\right] = (-1)^n,$$

or, equivalently,

$$\sum_{i=1}^{N} \text{sign}\left[\det(-J(\bar{x}_i))\right] = 1.$$

Theorem 4.7 in Section 4.5 has thus been contextualised and justified.

Bibliography

[ABGS08] A. Abramo, F. Blanchini, L. Geretti, and C. Savorgnan. A mixed convex/non-convex distributed localization approach for the deployment of indoor positioning services. *IEEE Transactions on Mobile Computing*, 7(11):1325–1337, 2008.

[Abr70] N. Abramson. The Aloha system - another alternative for computer communication. In *Proceedings of AFIPS*, pages 281–285, 1970.

[ABY+10] K. A. Afonin, E. Bindewald, A. J. Yaghoubian, N. Voss, E. Jacovetty, B. A. Shapiro, and L. Jaeger. *In vitro* assembly of cubic RNA-based scaffolds designed in silico. *Nature Nanotechnology*, 5:676–682, 2010.

[AC03] M. Aldana and P. Cluzel. A natural class of robust networks. *Proceedings of the National Academy of Sciences of the USA*, 100(15):8710–8714, 2003.

[ACFO13] D. Acemoglu, G. Como, F. Fagnani, and A. Ozdaglar. Opinion fluctuations and disagreement in social networks. *Mathematics of Operations Research*, 38(1):1–27, 2013.

[ADLS06] D. Angeli, P. De Lenheer, and E. D. Sontag. On the structural monotonicity of chemical reaction networks. In *Proceedings of the IEEE Conference on Decision and Control*, pages 7–12, 2006.

[AdLS07] D. Angeli, P. de Leenheer, and E. D. Sontag. A Petri net approach to the study of persistence in chemical reaction networks. *Mathematical Biosciences*, 210(2):598–618, 2007.

[ADLS10] D. Angeli, P. De Leenheer, and E. Sontag. Graph-theoretic characterizations of monotonicity of chemical networks in reaction coordinates. *Journal of Mathematical Biology*, 61(4):581–616, 2010.

[AFS04] D. Angeli, J. E. Ferrell, and E. D. Sontag. Detection of multistability, bifurcations, and hysteresis in a large class of biological positive-feedback systems. *Proceedings of the National Academy of Sciences of the USA*, 101(7):1822–1827, 2004.

[AI98] B. Ataslar and A. Iftar. A decentralized control approach for transportation networks. In *Proceedings of the 8th IFAC Symposium. on Large Scale Systems*, pages 348–353, 1998.

[AK07] N. Ay and D. C. Krakauer. Geometric robustness theory and biological networks. *Theory in Biosciences*, 125(2):93–121, 2007.

[AL15] C. Altafini and G. Lini. Predictable dynamics of opinion forming for networks with antagonistic interactions. *IEEE Transactions on Automatic Control*, 60(2):342–357, 2015.

[ALNSZ15] M. Aranda, G. López-Nicolás, C. Sagüés, and M. M. Zavlanos. Coordinate-free formation stabilization based on relative position measurements. *Automatica*, 57(7):11–20, 2015.

[Alo03] U. Alon. Biological networks: The tinkerer as an engineer. *Science*, 301(5641):1866–1867, 2003.

[Alo06] U. Alon. *An Introduction to Systems Biology: Design Principles of Biological Circuits*. Chapman & Hall/CRC, 2006.

[Alo07a] U. Alon. Network motifs: theory and experimental approaches. *Nature Reviews Genetics*, 8(6):450–461, 2007.

[Alo07b] U. Alon. Simplicity in biology. *Nature*, 446(7135):497–497, 2007.

[Alt12] C. Altafini. Dynamics of opinion forming in structurally balanced social networks. *PLoS ONE*, 7(6):e38135, 2012.

[Alt13] C. Altafini. Consensus problems on networks with antagonistic interactions. *IEEE Transactions on Automatic Control*, 58(4):935–946, 2013.

[Ams14] P. Amster. *Topological Methods in the Study of Boundary Value Problems*. Springer, 2014.

[And83] D. H. Anderson. Compartmental modeling and tracer kinetics. *Lecture Notes in Biomathematics*, 50, 1983.

[And08] D. Anderson. Global asymptotic stability for a class of nonlinear chemical equations. *SIAM Journal on Applied Mathematics*, 68(5):1464–1476, 2008.

[Ang09] D. Angeli. A tutorial on chemical reaction network dynamics. *European Journal of Control*, 15(3–4):398–406, 2009.

[Ang11] D. Angeli. Boundedness analysis for open chemical reaction networks with mass-action kinetics. *Natural Computing*, 10(2):751–774, 2011.

[AP95] A. Ambrosetti and G. Prodi. *A Primer of Nonlinear Analysis*, volume 34 of *Cambridge Studies in Advanced Mathematics*. Cambridge University Press, Cambridge, 1995.

[AR98] M. R. Anderson and A. C. Robbins. Formation flight as a cooperative game. In *Proceedings of AIAA Guidance, Navigation and Control Conference and Exhibit*, pages 244–251, Boston, MA, 1998.

[AR08] Z. Artstein and S. Rakovic. Feedback and invariance under uncertainty via set iterates. *Automatica*, 44(2):520–525, 2008.

[ARA13] M. A. Al-Radhawi and D. Angeli. Piecewise linear in rates Lyapunov functions for complex reaction networks. In *52rd IEEE Conference on Decision and Control*, pages 4595–4600, 2013.

[ARA14] M. A. Al-Radhawi and D. Angeli. Robust Lyapunov functions for complex reaction networks: An uncertain system framework. In *53rd IEEE Conference on Decision and Control*, pages 3101–3106, 2014.

[ARA15] M. A. Al-Radhawi and D. Angeli. New approach to the stability of chemical reaction networks: Piecewise linear in rates Lyapunov functions. *IEEE Transactions on Automatic Control*, 61(1):76–89, 2015.

[AS03] D. Angeli and E. D. Sontag. Monotone control systems. *IEEE Transactions on Automatic Control*, 48(10):1684–1698, 2003.

[AS04a] D. Angeli and E. D. Sontag. Interconnections of monotone systems with steady-state characteristics. In M. S. de Queiroz, M. Malisoff, and P. Wolenski, editors, *Optimal Control, Stabilization and Nonsmooth Analysis*, volume 301 of *Lecture Notes in Control and Information Sciences*, pages 135–154. Springer, Berlin, 2004.

[AS04b] D. Angeli and E. D. Sontag. Multistability in monotone input/output systems. *Systems and Control Letters*, 51(3–4):185–202, 2004.

[AS08] D. Angeli and E. D. Sontag. Oscillations in I/O monotone systems. *IEEE Transactions on Automatic Control: Special Issue on Systems Biology*, 53:166–176, 2008.

[AS09] D. Angeli and E. D. Sontag. Graphs and the dynamics of biochemical networks. In B. P. Ingalls and P. Iglesias, editors, *Control Theory in Systems Biology*, volume 371, pages 125–142. MIT Press, 2009.

[ASBL99] U. Alon, M. G. Surette, N. Barkai, and S. Leibler. Robustness in bacterial chemotaxis. *Nature*, 397(6715):168–171, 1999.

[ASMN03] M. R. Atkinson, M. A. Savageau, J. T. Myers, and A. J. Ninfa. Development of genetic circuitry exhibiting toggle switch or oscillatory behavior in *Escherichia coli*. *Cell*, 113(5):597–607, 2003.

[ATS09] A. Abate, A. Tiwari, and S. Sastry. Box invariance in biologically-inspired dynamical systems. *Automatica*, 45(7):1601–1610, 2009.

[AVK66] A. A. Andronov, A. A. Vitt, and S. E. Khaikin. *Theory of Oscillators,* translated from the Russian by F. Immirzi, edited and abridged by W. Fishwick. Pergamon Press, Oxford, 1966.

[AWM98] J. Ackermann, B. Wlotzka, and J. S. McCaskill. In vitro DNA-based predator-prey system with oscillatory kinetics. *Bulletin of Mathematical Biology*, 60(2):329–354, 1998.

[AZ07] A. Atamtürk and M. Zhang. Two–stage robust network flow and design under demand uncertainty. *Operations Research*, 55(4):662–673, 2007.

[Bak08] L. Bakule. Decentralized control: An overview. *Annual reviews in control*, 32(1):87–98, 2008.

[Bar94] B. R. Barmish. *New tools for robustness of linear systems.* McMillan, 1994.

[Bar12] A.-L. Barabási. The network takeover. *Nature Physics*, 8(1):14–16, 2012.

[BBGP13] D. Bauso, F. Blanchini, L. Giarré, and R. Pesenti. The linear saturated control strategy for constrained flow control is asymptotically optimal. *Automatica*, 49(7):2206–2212, 2013.

[BBP10] D. Bauso, F. Blanchini, and R. Pesenti. Optimization of long-run average-flow cost in networks with time-varying unknown demand. *IEEE Transactions on Automatic Control*, 55(1):20–31, 2010.

[BBV08] A. Barrat, M. Barthlemy, and A. Vespignani. *Dynamical Processes on Complex Networks.* Cambridge University Press, New York, 2008.

[BC09] M. Banaji and G. Craciun. Graph-theoretic approaches to injectivity and multiple equilibria in systems of interacting elements. *Communications in Mathematical Sciences*, 7(4):867–900, 2009.

[BCFG14] F. Blanchini, C. Cuba Samaniego, E. Franco, and G. Giordano. Design of a molecular clock with RNA-mediated regulation. In *Proceedings of the IEEE Conference on Decision and Control*, pages 4611–4616, Los Angeles (CA), USA, 2014.

[BCG03] R. Bruno, M. Conti, and E. Gregori. Optimal capacity of p-persistent CSMA protocols. *IEEE Communications Letters*, 7(3):139–141, 2003.

[BCGM16] F. Blanchini, D. Casagrande, G. Giordano, and P. L. Montessoro. A robust decentralized control for channel-sharing communication. *IEEE Transactions on Control of Network Systems*, 2016. To appear.

[BCGV15] F. Blanchini, D. Casagrande, G. Giordano, and U. Viaro. Properties of switching-dynamics race models. In *Proceedings of the 14th European Conference on Control (ECC15)*, pages 2907–2912, Linz, Austria, 2015.

[BCGV16] F. Blanchini, D. Casagrande, G. Giordano, and U. Viaro. A switched system approach to dynamic race modelling. *Nonlinear Analysis: Hybrid Systems*, 21(8):37–48, 2016.

[BCM11] F. Blanchini, D. Casagrande, and P. L. Montessoro. Robust stability and performance of a p-persistent communication protocol. In *Proceedings of 18th IFAC world congress*, pages 13251–13256, Milano, Italy, 2011.

[BCV15] F. Blanchini, P. Colaneri, and M. E. Valcher. Switched linear positive systems. *Foundations and Trends in Systems and Control*, 2015.

[BDMP12] F. Blanchini, D. De Caneva, P. L. Montessoro, and D. Pierattoni. Control-based p-persistent adaptive communication protocol. *ACM Transactions on Autonomous and Adaptive Systems*, 7(2):29:1–29:18, 2012. Presented in preliminary form in *Proceedings of the American Control Conference*, pp. 277–282, Baltimore, MD, USA, 2010.

[BDvdWH13] N. W. Bauer, M. Donkers, N. van de Wouw, and W. Heemels. Decentralized observer-based control via networked communication. *Automatica*, 49(7):2074–2086, 2013.

[BEGFB94] S. Boyd, L. El Ghaoui, E. Feron, and V. Balakrishnan. *Linear Matrix Inequalities in System and Control Theory*, volume 15 of *Studies in Applied and Numerical Mathematics*. SIAM, 1994.

[BF02] L. Benvenuti and L. Farina. Positive and compartmental systems. *IEEE Transactions on Automatic Control*, 47(2):370–373, 2002.

[BF11a] F. Blanchini and E. Franco. Multistability and robustness of the MAPK pathway. *Proceedings of the IEEE Conference on Decision and Control*, pages 2214–2219, 2011.

[BF11b] F. Blanchini and E. Franco. Structurally robust biological networks. *BMC Systems Biology*, 5(1):74, 2011.

[BF14] F. Blanchini and E. Franco. Structural analysis of biological networks. In V. Kulkarni, G.-B. Stan, and K. Raman, editors, *A Systems Theoretic Approach to Systems and Synthetic Biology I: Models and System Characterizations*, pages 47–71. Springer, 2014.

[BFBD13] M. Brambilla, E. Ferrante, M. Birattari, and M. Dorigo. Swarm robotics: a review from the swarm engineering perspective. *Swarm Intelligence*, 7(1):1–41, 2013.

[BFG12] F. Blanchini, E. Franco, and G. Giordano. Determining the structural properties of a class of biological models. In *Proceedings of the IEEE Conference on Decision and Control*, pages 5505–5510, Maui (HI), USA, 2012.

[BFG13] F. Blanchini, E. Franco, and G. Giordano. Structured-LMI conditions for stabilizing network-decentralized control. In *Proceedings of the IEEE Conference on Decision and Control*, pages 6880–6885, Firenze, Italy, 2013.

[BFG14] F. Blanchini, E. Franco, and G. Giordano. A structural classification of candidate oscillatory and multistationary biochemical systems. *Bulletin of Mathematical Biology*, 76(10):2542–2569, 2014.

[BFG15a] F. Blanchini, E. Franco, and G. Giordano. Network-decentralized control strategies for stabilization. *IEEE Transactions on Automatic Control*, 60(2):491–496, 2015.

[BFG15b] F. Blanchini, E. Franco, and G. Giordano. Structural conditions for oscillations and multistationarity in aggregate monotone systems. In *Proceedings of the IEEE Conference on Decision and Control*, pages 609–614, Osaka, Japan, 2015.

[BFG+16] F. Blanchini, E. Franco, G. Giordano, V. Mardanlou, and P. L. Montessoro. Compartmental flow control: decentralization, robustness and optimality. *Automatica*, 64(2):18–28, 2016.

[BFGP15] F. Blanchini, G. Fenu, G. Giordano, and F. A. Pellegrino. Plant tuning: a robust Lyapunov approach. In *Proceedings of the IEEE Conference on Decision and Control*, pages 1142–1147, Osaka, Japan, 2015.

[BG06] G. Bastin and V. Guffens. Congestion control in compartmental network systems. *Systems & Control Letters*, 55(8):689–696, 2006. New Trends in Nonlinear Control.

[BG14] F. Blanchini and G. Giordano. Piecewise-linear Lyapunov functions for structural stability of biochemical networks. *Automatica*, 50(10):2482–2493, 2014.

[BG15a] F. Blanchini and G. Giordano. Polyhedral Lyapunov functions for structural stability of biochemical systems in concentration and reaction coordinates. In *Proceedings of the IEEE Conference on Decision and Control*, pages 3110–3115, Osaka, Japan, 2015.

[BG15b] F. Blanchini and G. Giordano. Structural stability of biochemical networks: Quadratic vs. polyhedral Lyapunov functions. In *IFAC Symposium on Robust Control Design (ROCOND'15)*, pages 277–282, Bratislava, Slovakia, 2015.

[BGM14] F. Blanchini, G. Giordano, and P. L. Montessoro. Network-decentralized robust congestion control with node traffic splitting. In *Proceedings of the IEEE Conference on Decision and Control*, pages 2901–2906, Los Angeles (CA), USA, 2014.

[BGP06] D. Bauso, L. Giarrè, and R. Pesenti. Nonlinear protocols for the optimal distributed consensus in networks of dynamic agents. *Systems & Control Letters*, 55(11):918–928, 2006.

[BGP09] D. Bauso, L. Giarré, and R. Pesenti. Distributed consensus in noncooperative inventory games. *European Journal of Operational Research*, 192(3):866–878, 2009.

[BJ11] M. Bailey and J. Joo. Identification of network motifs capable of frequency-tunable and robust oscillation, 2011. arXiv:1110.3041.

[BL97] N. Barkai and S. Leibler. Robustness in simple biochemical networks. *Nature*, 387(6636):913–917, 1997.

[BL00] N. Barkai and S. Leibler. Biological rhythms: Circadian clocks limited by noise. *Nature*, 403(6767):267–268, 2000.

[Bla91] F. Blanchini. Constrained control for uncertain linear systems. *Journal of Optimization Theory and Applications*, 71(3):465–484, 1991.

[BLT02] F. Blanchini, R. Lo Cigno, and R. Tempo. Robust rate control for integrated services packet networks. *IEEE Transactions on Networking*, 10(5):644–652, 2002.

[BM96] F. Blanchini and S. Miani. On the transient estimate for linear systems with time-varying uncertain parameters. *IEEE Transactions on Circuits and Systems*, 43(7):592–596, 1996.

[BM15] F. Blanchini and S. Miani. *Set-theoretic methods in control*. Systems & Control: Foundations & Applications. Birkhäuser, Basel, second edition, 2015.

[BMU00] F. Blanchini, S. Miani, and W. Ukovich. Control of production-distribution systems with unknown inputs and system failures. *IEEE Transactions on Automatic Control*, 45(6):1072–1081, 2000.

[BP94] A. Berman and R. J. Plemmons. *Nonnegative Matrices in the Mathematical Sciences*. Classics in Applied Mathematics. SIAM, 1994.

[BP15] M. Bürger and C. D. Persis. Dynamic coupling design for nonlinear output agreement and time-varying flow control. *Automatica*, 51(1):210–222, 2015.

[BPA15] M. Bürger, C. D. Persis, and F. Allgöwer. Dynamic pricing control for constrained distribution networks with storage. *IEEE Transactions on Control of Network Systems*, 2(1):88–97, 2015.

[BR79] M. J. Berridge and P. E. Rapp. Comparative survey of the function, mechanism and control of cellular oscillators. *Journal Of Experimental Biology*, 81(8):217–279, 1979.

[Bre15] D. Breda. Lyapunov exponents of ordinary differential equations: theory and computation, 2015. Lecture Notes.

[BRU97] F. Blanchini, F. Rinaldi, and W. Ukovich. Least inventory control of multi-storage systems with non-stochastic unknown input. *IEEE Transactions on Robotics and Automation*, 13(5):633–645, 1997.

[BSO+08] F. K. Balagaddé, H. Song, J. Ozaki, C. H. Collins, M. Barnet, F. H. Arnold, S. R. Quake, and L. You. A synthetic *Escherichia coli* predator-prey ecosystem. *Molecular Systems Biology*, 4:187, 2008.

[BSSS11] C. P. Barnes, D. Silk, X. Sheng, and M. P. H. Stumpf. Bayesian design of synthetic biological systems. *Proceedings of the National Academy of Sciences of the USA*, 108(37):15190–15195, 2011.

[BT80] R. K. Brayton and C. H. Tong. Constructive stability and asymptotic stability of dynamical systems. *IEEE Transactions on Circuits and Systems*, 27(11):1121–1130, 1980.

[BT06] D. Bertsimas and A. Thiele. A robust optimization approach to inventory theory. *Operations Research*, 54(1):150–168, 2006.

[BT11] G. Bitsoris and L. Truffet. Positive invariance, monotonicity and comparison of nonlinear systems. *Systems Control Lett.*, 60(12):960–966, 2011.

[BTM+08] N. Bagheri, S. R. Taylor, K. Meeker, L. R. Petzold, and F. J. Doyle III. Synchrony and entrainment properties of robust circadian oscillators. *J. R. Soc. Interface*, 5:17–28, 2008.

[BV13] D. Breda and R. Vermiglio. Numerical Analysis IV: Dynamical systems and numerical analysis, 2013. Lecture Notes.

[BWW+11] C. Breindl, S. Waldherr, D. M. Wittmann, F. J. Theis, and F. Allgöwer. Steady-state robustness of qualitative gene regulation networks. *International Journal of Robust and Nonlinear Control*, 21(15):1742–1758, 2011.

[BYWB07] G. Batt, B. Yordanov, R. Weiss, and C. Belta. Robustness analysis and tuning of synthetic gene networks. *Bioinformatics*, 23(18):2415–2422, 2007.

[BYZ95] E. K. Boukas, H. Yang, and Q. Zhang. Minimax production planning in failure-prone manufacturing systems. *Journal of Optimization Theory and Applications*, 87(2):269–286, 1995.

[CA12] D. Chen and A. P. Arkin. Sequestration-based bistability enables tuning of the switching boundaries and design of a latch. *Molecular systems biology*, 8:620, 2012.

[CB11] C. Cosentino and D. Bates. *Feedback Control in Systems Biology*. Taylor & Francis, 2011.

[CBD11] F. A. Chandra, G. Buzi, and J. C. Doyle. Glycolytic oscillations and limits on robust efficiency. *Science*, 333(6039):187–192, 2011.

[CBHB09] V. Chellaboina, S. P. Bhat, W. M. Haddad, and D. S. Bernstein. Modeling and analysis of mass–action kinetics: nonnegativity, realizability, reducibility, and semistability. *IEEE Control Systems Magazine*, pages 60–78, August 2009.

[CCSZ08] R. Carli, A. Chiuso, L. Schenato, and S. Zampieri. A PI consensus controller for networked clocks synchronization. In *IFAC World Congress on Automatic Control*, pages 10289–10294, 2008.

[CCSZ11] R. Carli, A. Chiuso, L. Schenato, and S. Zampieri. Optimal synchronization for networks of noisy double integrators. *IEEE Transactions on Automat Control*, 56(5):1146–1152, 2011.

[CD02a] J. M. Carlson and J. Doyle. Complexity and robustness. *Proceedings of the National Academy of Sciences of the USA*, 99:2538–2545, 2002.

[CD02b] M. E. Csete and J. C. Doyle. Reverse engineering of biological complexity. *Science*, 295(5560):1664–1669, 2002.

[CDT11] G. C. Calafiore, F. Dabbene, and R. Tempo. Research on probabilistic methods for control system design. *Automatica*, 47(7):1279–1293, 2011.

[CEA08] M. Chaves, T. Eissing, and F. Allgöwer. Bistable biological systems: a characterization through local compact input-to-state stability. *IEEE Transactions on Automatic Control: Special Issue on Systems Biology*, 53:87–100, 2008.

[CF05] G. Craciun and M. Feinberg. Multiple equilibria in complex chemical reaction networks: I. the injectivity property. *SIAM Journal on Applied Mathematics*, 65(5):1526–1546, 2005.

[CF06a] L. Chisci and P. Falugi. Asymptotic tracking for constrained monotone systems. *IEEE Transactions on Automatic Control*, 51(5):873–879, 2006.

[CF06b] G. Craciun and M. Feinberg. Multiple equilibria in complex chemical reaction networks: II. the species-reaction graph. *SIAM Journal on Applied Mathematics*, 66(4):1321–1338, 2006.

[CF12] F. Ceragioli and P. Frasca. Continuous and discontinuous opinion dynamics with bounded confidence. *Nonlinear Analysis: Real World Applications*, 13(3):1239–1251, 2012.

[CFSZ08] R. Carli, F. Fagnani, A. Speranzon, and S. Zampieri. Communication constraints in the average consensus problem. *Automatica*, 44(3):671–684, 2008.

[CFY95] J. Chen, M. K. H. Fan, and C. C. Yu. On D-stability and structured singular values. *Systems and Control Letters*, 24(1):19–24, 1995.

[CGBF16] C. Cuba Samaniego, G. Giordano, F. Blanchini, and E. Franco. Stability analysis of an artificial biomolecular oscillator with non-cooperative regulatory interactions. 2016. In preparation.

[CGK+16] C. Cuba Samaniego, G. Giordano, J. Kim, F. Blanchini, and E. Franco. Molecular titration promotes oscillations and bistability in minimal network models with monomeric regulators. *ACS Synthetic Biology*, 2016. Available online.

[CH08] G. Chesi and Y. S. Hung. Stability analysis of uncertain genetic sum regulatory networks. *Automatica*, 44(9):2298–2305, 2008.

[Cha06] M. Chaves. Stability of rate-controlled zero-deficiency networks. In *45th IEEE Conference on Decision and Control*, pages 5766–5771, 2006.

[CLD95] S. K. Crosthwaite, J. J. Loros, and J. C. Dunlap. Light-induced resetting of a circadian clock is mediated by a rapid increase in frequency transcript. *Cell*, 81(7):1003–1012, 1995.

[CMA08] M. Cao, S. A. Morse, and B. D. O. Anderson. Agreeing asynchronously. *IEEE Transactions on Automatic Control*, 53(8):1826–1838, 2008.

[CMKB04] J. Cortés, S. Martinez, T. Karatas, and F. Bullo. Coverage control for mobile sensing networks. *IEEE Transactions on Robotics and Automation*, 20(2):243–255, 2004.

[Con99] E. D. Conrad. Mathematical models of biochemical oscillations. Master's thesis, Virginia Polytechnic Institute and State University, 1999.

[Cor09] J. Cortés. Global and robust formation-shape stabilization of relative sensing networks. *Automatica*, 45(12):2754–2762, 2009.

[CR02] L. Chong and L. B. Ray. Whole-istic biology. *Science*, 295(5560):1661, 2002.

[Cro78] G. W. Cross. Three types of matrix stability. *Linear Algebra and its Applications*, 20(3):253–263, 1978.

[CTF06] G. Craciun, Y. Tang, and M. Feinberg. Understanding bistability in complex enzyme-driven reaction networks. *Proceedings of the National Academy of Sciences*, 103(23):8697–8702, 2006.

[CWLA05] L. Chen, R. Wang, C. Li, and K. Aihara. *Modeling Biomolecular Networks in Cells*. Springer, 2005.

[CWWL07] B.-S. Chen, W.-S. Wu, W.-S. Wu, and W.-H. Li. On the adaptive design rules of biochemical networks in evolution. *Evolutionary Bioinformatics*, 2:27–39, 2007.

[CYRC13] Y. Cao, W. Yu, W. Ren, and G. Chen. An overview of recent progress in the study of distributed multi-agent coordination. *IEEE Transactions on Industrial Informatics*, 9(1):427–438, 2013.

[CZ14] R. Carli and S. Zampieri. Network clock synchronization based on the second-order linear consensus algorithm. *IEEE Transactions on Automatic Control*, 59(2):409–422, 2014.

[D'A98] R. D'Andrea. A Linear Matrix Inequality approach to decentralized control of distributed parameter system. In *Proceedings of the American Control Conference*, volume 3, pages 1350–1354, Philadelphia (PA), USA, 1998.

[DBC12] S. M. Douglas, I. Bachelet, and G. M. Church. A logic-gated nanorobot for targeted transport of molecular payloads. *Science*, 335(6070):831–834, 2012.

[DBO+13] C. Danielson, F. Borrelli, D. Oliver, D. Anderson, and T. Phillips. Constrained flow control in storage networks: Capacity maximization and balancing. *Automatica*, 49(9):2612–2621, 2013.

[DCB12] S. H. Dandach, R. Carli, and F. Bullo. Accuracy and decision time for sequential decision aggregation. *Proceedings of the IEEE*, 100(3):687–712, 2012.

[Dei85] K. Deimling. *Nonlinear Functional Analysis*. Springer-Verlag, Berlin, 1985.

[DESZ07] B. DasGupta, G. A. Enciso, E. D. Sontag, and Y. Zhang. Algorithmic and complexity aspects of decompositions of biological networks into monotone subsystems. *BioSystems*, 90(1):161–178, 2007.

[DGR+09] J. M. Dambacher, D. J. Gaughan, M.-J. Rochet, P. A. Rossignol, and V. M. Trenkel. Qualitative modelling and indicators of exploited ecosystems. *Fish and fisheries*, 10(3):305–322, SEP 2009.

[DIR+12] C. M. Denby, J. H. Im, C. Y. Richard, C. G. Pesce, and R. B. Brem. Negative feedback confers mutational robustness in yeast transcription factor regulation. *Proceedings of the National Academy of Sciences USA*, 109(10):3874–3878, 2012.

[DJ02] H. De Jong. Modeling and simulation of genetic regulatory systems: a literature review. *Journal of Computational Biology*, 9(1):67–103, 2002.

[DK09] M. Domijan and M. Kirkilionis. Bistability and oscillations in chemical reaction networks. *Journal of Mathematical Biology*, 59(4):467–501, 2009.

[DL14] E. Devane and I. Lestas. Stability of a general class of distributed algorithms for power control in time-varying wireless networks. *IEEE Transactions on Automatic Control*, 59(8):1999–2011, 2014.

[DLAS07] P. De Lenheer, D. Angeli, and E. D. Sontag. Monotone chemical reaction networks. *Journal of Mathematical Chemistry*, 41(3):295–314, 2007.

[DLLR03] J. M. Dambacher, H.-K. Luh, H. W. Li, and P. A. Rossignol. Qualitative stability and ambiguity in model ecosystems. *The American Naturalist*, 161(6):876–888, 2003.

[DLR02] J. Dambacher, H. Li, and P. Rossignol. Relevance of community structure in assessing indeterminacy of ecological predictions. *Ecology*, 83(5):1372–1385, 2002.

[DLR03] J. Dambacher, H. Li, and P. Rossignol. Qualitative predictions in model ecosystems. *Ecological Modelling*, 161(1-2):79–93, MAR 2003.

[DLR05] J. Dambacher, R. Levins, and P. Rossignol. Life expectancy change in perturbed communities: Derivation and qualitative analysis. *Mathematical Biosciences*, 197(1):1–14, SEP 2005.

[DP12] M. Domijan and E. Pécou. The interaction graph structure of mass-action reaction networks. *Journal of Mathematical Biology*, 65(2):375–402, 2012.

[DPB13] F. Dorfler, F. Pasqualetti, and F. Bullo. Continuous-time distributed observers with discrete communication. *IEEE Journal of Selected Topics in Signal Processing*, 7(2):296–304, 2013.

[DRJ07] J. M. Dambacher and R. Ramos Jiliberto. Understanding and predicting effects of modified interactions through a qualitative analysis of community structure. *The Quarterly Review of Biology*, 82(3):227–250, 2007.

[DRO+02] E. H. Davidson, J. P. Rast, P. Oliveri, A. Ransick, C. Calestani, et al. A genomic regulatory network for development. *Science*, 295(5560):1669–1678, 2002.

[Dun99] J. C. Dunlap. Molecular bases for circadian clocks. *Cell*, 96(2):271–290, 1999.

[DUR08] T. Drengstig, H. R. Ueda, and P. Ruoff. Predicting perfect adaptation motifs in reaction kinetic networks. *The Journal of Physical Chemistry B*, 112(51):16752–16758, 2008.

[DVM14] D. Del Vecchio and R. M. Murray. *Biomolecular Feedback Systems*. Princeton University Press, 2014.

[DWS07] D. A. Drubin, J. C. Way, and P. A. Silver. Designing biological systems. *Genes Dev.*, 21(3):242–254, 2007.

[Eic07] S. Eichler. Performance evaluation of the IEEE 802.11p WAVE communication standard. In *Proceedings of the Vehicular Technology Conference*, pages 2199–2203, 2007.

[EK05] L. Edelstein-Keshet. *Mathematical Models in Biology*, volume 46 of *Classics in Applied Mathematics*. SIAM, Philadelphia, 2005.

[EK10] D. Easley and J. Kleinberg. *Networks, Crowds, and Markets. Reasoning About a Highly Connected World*. Cambridge University Press, Cambridge, 2010.

[EL00] M. B. Elowitz and S. Leibler. A synthetic oscillatory network of transcriptional regulators. *Nature*, 403(6767):335–338, 2000.

[Enc05] G. A. Enciso. *Monotone input/output systems, and applications to biological systems*. PhD thesis, Graduate School – New Brunswick, Rutgers, The State University of New Jersey, 2005.

[End05] D. Endy. Foundations for engineering biology. *Nature*, 438(7067):449–453, 2005.

[EP05] N. Eagle and A. Pentland. Social serendipity: Mobilizing social software. *IEEE Pervasive Computing*, 4(2):28–34, 2005.

[ESKD+05] H. El-Samad, H. Kurata, J. Doyle, C. Gross, and M. Khammash. Surviving heat shock: Control strategies for robustness and performance. *Proceedings of the National Academy of Sciences of the USA*, 102(8):2736–2741, 2005.

[ESPP+06] H. El-Samad, S. Prajna, A. Papachristodoulou, J. Doyle, and M. Khammash. Advanced methods and algorithms for biological networks analysis. *Proceedings of the IEEE*, 94(4):832–853, 2006.

[EV89] A. Ephremides and S. Verdú. Control and optimisation methods in communication networks. *IEEE Transactions on Automatic Control*, 34(9):930–942, 1989.

[Far10] H. Farhangi. The path of the smart grid. *IEEE Power and Energy Magazine*, 8(1):18–28, 2010.

[FB12] E. Franco and F. Blanchini. Analysis of a negative feedback biochemical oscillator. In *Proceedings of the American Control Conference*, pages 3445–3450, 2012.

[FB13] E. Franco and F. Blanchini. Structural properties of the MAPK pathway topologies in PC12 cells. *Journal of Mathematical Biology*, 67(6):1633–1668, 2013.

[FCJ14] H. R. Feyzmahdavian, T. Charalambous, and M. Johansson. Stability and performance of continuous-time power control in wireless networks. *IEEE Transactions on Automatic Control*, 59(8):2012–2023, 2014.

[Feč08] M. Fečkan. *Topological Degree Approach to Bifurcation Problems*, volume 5 of *Topological Fixed Point Theory and Its Applications*. Springer-Verlag, Berlin, 2008.

[Fei72] M. Feinberg. Complex balancing in general kinetic systems. *Archive for Rational Mechanics and Analysis*, 49(3):187–194, 1972.

[Fei87] M. Feinberg. Chemical reaction network structure and the stability of complex isothermal reactors: I. the deficiency zero and deficiency one theorems. *Chemical Engineering Science*, 42(10):2229–2268, 1987.

[Fei88] M. Feinberg. Chemical reaction network structure and the stability of complex isothermal reactors: II. multiple steady states for networks of deficiency one. *Chemical Engineering Science*, 43(1):1–25, 1988.

[Fei95a] M. Feinberg. The existence and uniqueness of steady states for a class of chemical reaction networks. *Archive for Rational Mechanics and Analysis*, 132(4):311–370, 1995.

[Fei95b] M. Feinberg. Multiple steady states for chemical reaction networks of deficiency one. *Archive for Rational Mechanics and Analysis*, 132(4):371–406, 1995.

[FFK+11] E. Franco, E. Friedrichs, J. Kim, R. Jungmann, R. Murray, E. Winfree, and F. C. Simmel. Timing molecular motion and production with a synthetic transcriptional clock. *Proceedings of the National Academy of Sciences*, 108(40):E784–E793, 2011.

[FFM08] E. Franco, P.-O. Forsberg, and R. M. Murray. Design, modeling and synthesis of an *in vitro* transcription rate regulatory circuit. In *Proceedings of the American Control Conference*, pages 2786–2791, 2008.

[FG95] I. Fonseca and W. Gangbo. *Degree Theory in Analysis and Applications*, volume 2 of *Oxford Lecture Series in Mathematics and Its Applications*. Oxford University Press, 1995.

[FG14] M. Franceschelli and A. Gasparri. Gossip-based centroid and common reference frame estimation in multiagent systems. *IEEE Transactions on Robotics*, 30(2):524–531, 2014.

[FGFM14] E. Franco, G. Giordano, P.-O. Forsberg, and R. M. Murray. Negative autoregulation matches production and demand in synthetic transcriptional networks. *ACS Synthetic Biology*, 3(8):589–599, 2014.

[FH74] M. Feinberg and F. Horn. Dynamics of open chemical systems and the algebraic structure of the underlying reaction network. *Chemical Engineering Science*, 29(3):775–787, 1974.

[FIA11] G. Facchetti, G. Iacono, and C. Altafini. Computing global structural balance in large-scale signed social networks. *PNAS*, 108(52):20953–20958, 2011.

[Fie73] M. Fiedler. Algebraic connectivity of graphs. *Czechoslovak Mathematical Journal*, 23(98):298–305, 1973.

[FIRT15] P. Frasca, H. Ishii, C. Ravazzi, and R. Tempo. Distributed randomized algorithms for opinion formation, centrality computation and power systems estimation: A tutorial overview. *European Journal of Control*, 24(7):2–13, 2015.

[FJ99] N. E. Friedkin and E. C. Johnsen. Social influence networks and opinion change. In E. J. Lawler and M. W. Macy, editors, *Advances in Group Processes*, volume 16, pages 1–29. JAI Press, 1999.

[FM93] G. J. Foschini and Z. Miljanic. A simple distributed autonomous power control algorithm and its convergence. *IEEE Transactions on Vehicular Technology*, 42(4):641–646, 1993.

[FM08] E. Franco and R. M. Murray. Design and performance of *in vitro* transcription rate regulatory circuits. In *Proceedings of the IEEE Conference on Decision and Control*, pages 161–166, 2008.

[FPK+09] J. E. Ferrell, J. R. Pomerening, S. Y. Kim, N. B. Trunnell, W. Xiong, C.-Y. F. Huang, and E. M. Machleder. Simple, realistic models of complex biological processes: Positive feedback and bistability in a cell fate switch and a cell cycle oscillator. *FEBS letters*, 583(24):3999–4005, 2009.

[FR00] L. Farina and S. Rinaldi. *Positive Linear Systems; Theory and Applications*. John Wiley, Hoboken, 2000.

[Fra93] J. N. Franklin. *Matrix Theory*. Prentice-Hall, 1993.

[Fra11] E. Franco. *Analysis, design, and* in vitro *implementation of robust biochemical networks*. PhD thesis, California Institute of Technology, 2011.

[Fri15] N. E. Friedkin. The problem of social control and coordination of complex systems in sociology. *IEEE Control Systems Magazine*, pages 40–51, June 2015.

[FRTI13] P. Frasca, C. Ravazzi, R. Tempo, and H. Ishii. Gossips and prejudices: Ergodic randomized dynamics in social networks. In *IFAC Workshop on Distributed Estimation and Control in Networked Systems*, pages 212–219, Koblenz, Germany, 2013.

[FWS+05] E. Fung, W. W. Wong, J. K. Suen, T. Bulter, S.-G. Lee, and J. C. Liao. A synthetic gene-metabolic oscillator. *Nature*, 435:118–122, 2005.

[GBF+15] G. Giordano, F. Blanchini, E. Franco, V. Mardanlou, and P. L. Montessoro. The smallest eigenvalue of the generalized Laplacian matrix, with application to network-decentralized estimation. *Submitted to IEEE Transactions on Network Science and Engineering*, 2015.

[GCC00] T. S. Gardner, C. R. Cantor, and J. J. Collins. Construction of a genetic toggle switch in *Escherichia coli*. *Nature*, 403(6767):339–342, 2000.

[GCFB15] G. Giordano, C. Cuba Samaniego, E. Franco, and F. Blanchini. Computing the structural influence matrix for biological systems. *Journal of Mathematical Biology*, 2015. Available online.

[GdOH98] J. C. Geromel, M. C. de Oliveira, and L. Hsu. LMI characterization of structural and robust stability. *Linear Algebra and Its Applications*, 285:69–80, 1998.

[GFM13] G. Giordano, E. Franco, and R. M. Murray. Feedback architectures to regulate flux of components in artificial gene networks. In *Proceedings of the American Control Conference*, pages 4747–4752, Washington (DC), USA, 2013.

[GG08] A. Garulli and A. Giannitrapani. A set–membership approach to consensus problems with bounded measurement errors. In *Proceedings of the IEEE Conference on Decision and Control*, pages 2276–2281, Cancun, Mexico, 2008.

[GGG+12] A. Goldbeter, C. Gérard, D. Gonze, J.-C. Leloup, and G. Dupont. Systems biology of cellular rhythms. *FEBS Letters*, 586(18):2955–2965, 2012.

[GGMF05] J. Gómez-Gardenes, Y. Moreno, and L. M. Floría. On the robustness of complex heterogeneous gene expression networks. *Biophysical Chemistry*, 115:225–229, 2005.

[Gio12a] G. Giordano. Biomolecular rate-regulator circuits. Technical report, 2012. SURF Project at the California Institute of Technology.

[Gio12b] G. Giordano. Structural properties of biochemical systems. Master's thesis, Università degli Studi di Udine, 2012.

[GJWL05] S. Guolin, C. Jie, G. Wei, and K. J. R. Liu. Signal processing techniques in network-aided positioning: a survey of state-of-the-art positioning designs. *IEEE Signal Processing Magazine*, 22(4):12–23, 2005.

[GK09] F. Golnaraghi and B. C. Kuo. *Automatic Control Systems (9th ed.)*. John Wiley & Sons, 2009.

[GNLC94] P. Gahinet, A. Nemirovski, A. J. Laub, and M. Chilali. The LMI control toolbox. In *Proceedings of the IEEE Conference on Decision and Control*, volume 3, pages 2038–2041, 1994.

[God83] K. Godfrey. *Compartmental Models and Their Application*. Academic Press, New York, 1983.

[Gol97] A. Goldbeter. *Biochemical Oscillations and Cellular Rhythms: The Molecular Bases of Periodic and Chaotic Behaviour*. Cambridge University Press, 1997.

[Gol07] A. Goldbeter. Biological rhythms as temporal dissipative structures. In *Special Volume in Memory of Ilya Prigogine*, pages 253–295. John Wiley & Sons, Inc., 2007.

[Gou98] J.-L. Gouze. Positive and negative circuits in dynamical systems. *Journal of Biological Systems*, 6:11–15, 1998.

[GP06] R. Guantes and J. F. Poyatos. Dynamical principles of two-component genetic oscillators. *PLoS computational biology*, 2(3):e30, 2006.

[GR07] A. Gorban and O. Radulescu. Dynamical robustness of biological networks with hierarchical distribution of time scales. *IET Systems Biology*, 1(4):238–246, 2007.

[GS07] T. Gedeon and E. D. Sontag. Oscillations in multi-stable monotone systems with slowly varying feedback. *Journal of Differential Equations*, 239(2):273–295, 2007.

[Han10] K. M. Hangos. Engineering model reduction and entropy-based Lyapunov functions in chemical reaction kinetics. *Entropy*, 12(4):772–797, 2010.

[HC04] W. M. Haddad and V. Chellaboina. Stability theory for nonnegative and compartmental dynamical systems with time delay. *Systems & Control Letters*, 51(5):355–361, 2004.

[HD12] M. E. Harrison and M. J. Dunlop. Synthetic feedback loop model for increasing microbial biofuel production using a biosensor. *Frontiers in Microbiology*, 3:360, 2012.

[HH11] Y. Hori and S. Hara. Time delay effects on oscillation profiles in cyclic gene regulatory networks: Harmonic balance approach. In *Proceedings of the American Control Conference*, pages 2891–2896, 2011.

[HHB06] W. M. Haddad, T. Hayakawa, and J. M. Bailey. Adaptive control for nonlinear compartmental dynamical systems with applications to clinical pharmacology. *Systems & Control Letters*, 55(1):62–70, 2006.

[HHLM99] L. H. Hartwell, J. J. Hopfield, S. Leibler, and A. W. Murray. From molecular to modular cell biology. *Nature*, 402:C47–C52, 1999.

[HHS+00] S. L. Harmer, J. B. Hogenesch, M. Straume, H.-S. Chang, B. Han, T. Zhu, X. Wang, J. A. Kreps, and S. A. Kay. Orchestrated transcription of key pathways in arabidopsis by the circadian clock. *Science*, 290(5499):2110–2113, 2000.

[Hig67] J. Higgins. The theory of oscillating reactions. *Industrial and Engineering Chemistry*, 59(5):18–62, May 1967.

[Hir88] M. W. Hirsch. Stability and convergence in strongly monotone dynamical systems. *Journal für die reine und angewandte Mathematik*, 383:1–53, 1988.

[HJ72] F. Horn and R. Jackson. General mass action kinetics. *Archive for Rational Mechanics and Analysis*, 47(2):81–116, 1972.

[HLMQ14] D. Hale, G. Lady, J. Maybee, and J. Quirk. *Nonparametric Comparative Statics and Stability*. Princeton University Press, 2014.

[HLST11] J.-H. Hoepman, A. Larsson, E. M. Schiller, and P. Tsigas. Secure and self-stabilizing clock synchronization in sensor networks. *Theoretical Computer Science*, 412(40):5631–5647, 2011. Stabilization, Safety and Security.

[Hof90] J. Hofbauer. An index theorem for dissipative semiflows. *Rocky Mountain Journal of Math.*, 20(4):1017–1031, 1990.

[Hop42] E. Hopf. Abzweigung einer periodischen Lösung von einer stationären Lösung eines Differentialsystems. *Berichten der Mathematisch-Physischen Klasse der Sächsischen Akademie der Wissenschaften zu Leipzig*, (XCIV):1–22, 1942.

[Hor73a] F. Horn. On a connexion between stability and graphs in chemical kinetics. I. stability and the reaction diagram. *Royal Society of London Proceedings Series A*, 334(1598):299–312, September 1973.

[Hor73b] F. Horn. On a connexion between stability and graphs in chemical kinetics. II. stability and the complex graph. *Royal Society of London Proceedings Series A*, 334(1598):313–330, September 1973.

[HPDC00] J. Hasty, J. Pradines, M. Dolnik, and J. J. Collins. Noise-based switches and amplifiers for gene expression. *Proceedings of the National Academy of Sciences of the USA*, 97(5):2075–2080, 2000.

[HSV12] F. Heidarian, J. Schmaltz, and F. Vaandrager. Analysis of a clock synchronization protocol for wireless sensor networks. *Theoretical Computer Science - Quantitative Aspects of Programming Languages (QAPL 2010)*, 413(1):87–105, 2012.

[IA09] A. Ipakchi and F. Albuyeh. Grid of the future. *IEEE Power and Energy Magazine*, 7(2):52–62, 2009.

[IA10] G. Iacono and C. Altafini. Monotonicity, frustration, and ordered response: an analysis of the energy landscape of perturbed large-scale biological networks. *BMC Systems Biology*, 108:83, 2010.

[ID90] A. Iftar and E. J. Davison. Decentralized robust control for dynamic routing of large scale networks. In *Proceedings of the American Control Conference*, pages 441–446, San Diego (CA), USA, 1990.

[ID02] A. Iftar and E. J. Davison. Decentralized control strategies for dynamic routing. *Optimal Control Applications and Methods*, 23(6):329–355, 2002.

[Ift96] A. Iftar. A decentralized routing control strategy for semi-congested highways. In *Proceedings of the 13th IFAC World Congress*, volume P, pages 319–324, 1996.

[Ift99] A. Iftar. A linear programming based decentralized routing controller for congested highways. *Automatica*, 35(2):279–292, 1999.

[ISKI11] T. Ishizaki, Y. Sakai, K. Kashima, and J.-i. Imura. Hierarchical decentralized observer design for linearly coupled network systems. In *IEEE Conference on Decision and Control and European Control Conference (CDC-ECC)*, pages 7831–7836, 2011.

[Jac72] J. A. Jacquez. *Compartmental Analysis in Biology and Medicine*. Elsevier, New York, 1972.

[Jia91] J.-F. Jiang. On the global stability of cooperative systems. *Bulletin of the London Mathematical Society*, 26(5):455–458, 1991.

[JMFB15] P. Jia, A. MirTabatabaei, N. E. Friedkin, and F. Bullo. Opinion dynamics and the evolution of social power in influence networks. *SIAM Review*, 57(3):367–397, 2015.

[JML03] A. Jadbabaie, A. S. Morse, and J. Lin. Coordination of groups of mobile autonomous agents using nearest neighbor rules. *IEEE Transactions on Automatic Control*, 48(6):988–1001, 2003.

[JS93] J. A. Jacquez and C. P. Simon. Qualitative theory of compartmental systems. *Society for Industrial and Applied Mathematics Review*, 35(1):43–79, 1993.

[KC08] Y.-K. Kwon and K.-H. Cho. Quantitative analysis of robustness and fragility in biological networks based on feedback dynamics. *Bioinformatics*, 24(7):987–994, 2008.

[KCEO05] K. Kurin-Csörgei, I. R. Epstein, and M. Orbán. Systematic design of chemical oscillators using complexation and precipitation equilibria. *Nature*, 433(7022):139–142, 2005.

[KE09] O. Kartal and O. Ebenhöh. Ground state robustness as an evolutionary design principle in signaling networks. *Public Library of Science One*, 4(12):e8001, 2009.

[KEK81] P. D. Kepper, I. R. Epstein, and K. Kustin. A systematically designed homogeneous oscillating reaction: The arsenite-iodatechlorite system. *Journal of the American Chemical Society*, 103(8):2133–2134, 1981.

[KFRC13] A. T. Kamal, J. Farrell, and A. K. Roy-Chowdhury. Information weighted consensus filters and their application in distributed camera networks. *IEEE Transactions on Automatic Control*, 58(12):3112–3125, 2013.

[Kha02] H. K. Khalil. *Nonlinear Systems*. Prentice Hall, 2002.

[Kit02] H. Kitano. Systems biology: A brief overview. *Science*, 295(5560):1662–1664, 2002.

[Kit04] H. Kitano. Biological robustness. *Nature Reviews Genetics*, 5(11):826–837, 2004.

[Kit07] H. Kitano. Towards a theory of biological robustness. *Molecular Systems Biology*, 3(137):1–7, 2007.

[Kit10] H. Kitano. Violations of robustness trade-offs. *Molecular Systems Biology*, 6:384, 2010.

[KKA84] F. Kajiya, S. Kodama, and H. Abe. *Compartmental Analysis – Medical Applications and Theoretical Background*. Karger, 1984.

[KM11] J. Kim and R. M. Murray. Analysis and design of a synthetic transcriptional network for exact adaptation. In *IEEE Biomedical Circuits and Systems Conference (BioCAS)*, pages 345–348, 2011.

[KNN+06] H. Kageyama, T. Nishiwaki, M. Nakajima, H. Iwasaki, T. Oyama, and T. Kondo. Cyanobacterial circadian pacemaker: Kai protein complex dynamics in the KaiC phosphorylation cycle in vitro. *Molecular Cell*, 23(2):161–171, 2006.

[KST07] M. Kaufman, C. Soulé, and R. Thomas. A new necessary condition on interaction graphs for multistationarity. *Journal of Theoretical Biology*, 248(4):675–685, 2007.

[KTS08] P. D. W. Kirk, T. Toni, and M. P. H. Stumpf. Parameter inference for biochemical systems that undergo a Hopf bifurcation. *Biophysical Journal*, 95(2):540–549, 2008.

[Kuz98] Y. A. Kuznetsov. *Elements of applied bifurcation theory*. Springer-Verlag, New York, NY, 1998.

[KW11] J. Kim and E. Winfree. Synthetic *in vitro* transcriptional oscillators. *Molecular Systems Biology*, 7:465, 2011.

[KWLB08] J. H. Kim, M. West, S. Lall, and A. Banaszuk. Stochastic multiscale approaches to consensus problems. In *Proceedings of the IEEE Conference on Decision and Control*, pages 5551–5557, Cancun, Mexico, 2008.

[KWW06] J. Kim, K. S. White, and E. Winfree. Construction of an *in vitro* bistable circuit from synthetic transcriptional switches. *Molecular Systems Biology*, 1:68, 2006.

[LA15] S. Lee and H. Ahn. Distributed coordination for connectivity adjustment of linear compartmental systems. *IEEE Transactions on Automatic Control*, 60(8):2231–2236, 2015.

[Las11] J. B. Lasserre. A new look at nonnegativity on closed sets and polynomial optimization. *SIAM Journal on Optimization*, 21(3):864–885, 2011.

[LE90] Y. Luo and I. R. Epstein. Feedback analysis of mechanisms for chemical oscillators. In I. Prigogine and S. A. Rice, editors, *Advances in Chemical Physics*, volume 79, pages 269–299. John Wiley & Sons, Inc., 1990.

[Lev68] R. Levins. *Evolution in changing environments: some theoretical explorations*. Princeton University Press, 1968.

[Lev74] R. Levins. The qualitative analysis of partially specified systems. *Annals of the New York Academy of Science*, 231:123–138, 1974.

[Lev75] R. Levins. Evolution in communities near equilibrium. In M. Cody and J. M. Diamond, editors, *Ecology and evolution of communities*, pages 16–50. Harvard University Press, 1975.

[Lev99] O. Levenspiel. *Chemical reaction engineering*. John Wiley & Sons, New York, 1999.

[Lev10] W. S. Levine, editor. *The Control Handbook*. CRC Press, 2010.

[Lew03] J. Lewis. Autoinhibition with transcriptional delay: a simple mechanism for the zebrafish somitogenesis oscillator. *Current Biology*, 13(16):1398–1408, 2003.

[LI02] A. Levchenko and P. A. Iglesias. Models of eukaryotic gradient sensing: application to chemotaxis of amoebae and neutrophils. *Biophysical Journal*, 82:50–63, 2002.

[LK69] R. E. Larson and W. G. Keckler. Applications of dynamic programming to the control of water resource systems. *Automatica*, 5(1):15–26, 1969.

[LL88] J. Lundelius Welch and N. Lynch. A new fault-tolerant algorithm for clock synchronization. *Information and Computation*, 77(1):1–36, 1988.

[LL07] J.-S. Liu and C.-H. R. Lin. Achieving efficiency channel utilization and weighted fairness in IEEE 802.11 WLANs with a p-persistent enhanced DCF. In H. Zhang, S. Olariu, J. Cao, and D. B. Johnson, editors, *Mobile Ad-Hoc and Sensor Networks*, volume 4864 of *Lecture Notes in Computer Science*, pages 174–184. Springer Berlin Heidelberg, 2007.

[Llo78] N. G. Lloyd. *Degree Theory*. Cambridge University Press, 1978.

[Lot20] A. J. Lotka. Undamped oscillations derived from the law of mass action. *Journal of American Chemical Society*, 42:1595–1599, 1920.

[LPRK13] A. Leonardi, S. Palazzo, C. Rametta, and E. W. Knightly. A new adaptive receiver-initiated scheme for mitigating starvation in wireless networks. *Ad Hoc Networks*, 11(2):625–638, 2013.

[LS05] T. Liedl and F. C. Simmel. Switching the conformation of a DNA molecule with a chemical oscillator. *Nano Letters*, 5(10):1894–1898, 2005.

[LSA11] P. Lenz and L. Søgaard-Andersen. Temporal and spatial oscillations in bacteria. *Nature Reviews Microbiology*, 9(8):565–577, 2011.

[LW10] M. C. A. Leite and Y. Wang. Multistability, oscillations and bifurcations in feedback loops. *Mathematical Biosciences and Engineering*, 7(1):83–97, 2010.

[Lya66] A. M. Lyapunov. *Stability of motions.* Academic Press, 1966. English translation of the original work in Russian: Number 7 in Collected Works II, Kharkov Mathematical Society, 1892.

[LYW10] X. Liu, W. Yu, and L. Wang. Stability analysis for continuous-time positive systems with time-varying delays. *IEEE Transactions on Automatic Control*, 55(4):1024–1028, 2010.

[LZ15] H. Liu and T. Zhou. Distributed observer design for networked dynamical systems. In *Chinese Control and Decision Conference (CCDC)*, pages 3791–3796, 2015.

[Maw99] J. Mawhin. Leray–Schauder degree: A half century of extensions and applications. *Topological Methods in Nonlinear Analysis (Journal of the Juliusz Schauder Center)*, 14:195–228, 1999.

[May74] R. M. May. *Stability and Complexity in Model Ecosystems, 2nd ed.* Princeton University Press, 1974.

[MB04] M. Mandal and R. R. Breaker. Gene regulation by riboswitches. *Nature Reviews Molecular Cell Biology*, 5(6):451–463, 2004.

[MC08] M. Mincheva and G. Craciun. Multigraph conditions for multistability, oscillations and pattern formation in biochemical reaction networks. *Proceedings of the IEEE*, 96(8):1281–1291, 2008.

[MCB+10] N. Motee, F. Chandra, B. Bamieh, M. Khammash, and J. C. Doyle. Performance limitations in autocatalytic networks in biology. In *Proceedings of the IEEE Conference on Decision and Control*, pages 4715–4720, 2010.

[MDJ+11] M. P. Marzloff, J. M. Dambacher, C. R. Johnson, L. R. Little, and S. D. Frusher. Exploring alternative states in ecological systems with a qualitative analysis of community feedback. *Ecological Modelling*, 222(15):2651–2662, AUG 2011.

[ME10] M. Mesbahi and M. Egerstedt. *Graph-theoretic Methods in Multiagent Networks.* Princeton University Press, 2010.

[Mei07] J. D. Meiss. *Differential Dynamical Systems*, volume 14. SIAM, Philadelphia, 2007.

[Mer94] R. Merris. Laplacian matrices of graphs: a survey. *Linear Algebra and its Applications*, 197–198:143–176, 1994.

[MF15] A. Mochizuki and B. Fiedler. Sensitivity of chemical reaction networks: A structural approach. 1. Examples and the carbon metabolic network. *Journal of Theoretical Biology*, 367(2):189–202, 2015.

[MGUMvO09] D. Muzzey, C. A. Gómez-Uribe, J. T. Mettetal, and A. van Oudenaarden. A systems-level analysis of perfect adaptation in yeast osmoregulation. *Cell*, 138(1):160–171, 2009.

[MHK04] N. I. Markevich, J. B. Hoek, and B. N. Kholodenko. Signaling switches and bistability arising from multisite phosphorylation in protein kinase cascades. *J. Cell Biol.*, 164(3):353–359, 2004.

[MI02] L. Ma and P. A. Iglesias. Quantifying robustness of biochemical network models. *BMC Bioinformatics*, 3(1), 2002.

[Min11] M. Mincheva. Oscillations in biochemical reaction networks arising from pairs of subnetworks. *Bulletin of Mathematical Biology*, 73(10):2277–2304, 2011.

[Miś07] M. Miśkowicz. On the capacity of p-persistent CSMA. *International Journal of Computer Science and Network Security*, 7(11):38–43, November 2007.

[MJB14] A. MirTabatabaei, P. Jia, and F. Bullo. Eulerian opinion dynamics with bounded confidence and exogenous inputs. *SIAM Journal on Applied Dynamical Systems*, 13(1):425–446, 2014.

[MKO78] H. Maeda, S. Kodama, and Y. Ohta. Asymptotic behavior of nonlinear compartmental systems: Nonoscillation and stability. *IEEE Transactions on Circuits and Systems*, 25(6):372–378, 1978.

[MLAM10] S. Mao, Y. Li, P. Agrawal, and S. F. Midkiff. Toward efficient wireless medium access control. In Y. Xiao, H. Chen, and F. H. Li, editors, *Handbook on Sensor Networks*, pages 69–96. World Scientific Publishing, 2010.

[MMGUvO08] J. T. Mettetal, D. Muzzey, C. Gomez-Uribe, and A. van Oudenaarden. The frequency dependence of osmo-adaptation in saccharomyces cerevisiae. *Science*, 319(5862):482–484, 2008.

[MOnL08] S. Mudchanatongsuk, F. Ordóñez, and J. Liu. Robust solutions for network design under transportation cost and demand uncertainty. *J. Oper. Res. Soc.*, 59(5):652–662, 2008.

[MP86a] A. P. Molchanov and E. S. Pyatnitskii. Lyapunov functions that define necessary and sufficient conditions for absolute stability of nonlinear nonstationary control systems. I. *Autom. Remote Control*, 47(3):344–354, 1986.

[MP86b] A. P. Molchanov and E. S. Pyatnitskii. Lyapunov functions that define necessary and sufficient conditions for absolute stability of nonlinear nonstationary control systems. II. *Autom. Remote Control*, 47(4):443–451, 1986.

[MP86c] A. P. Molchanov and E. S. Pyatnitskii. Lyapunov functions that define necessary and sufficient conditions for absolute stability of nonlinear nonstationary control systems. III. *Autom. Remote Control*, 47(5):620–630, 1986.

[MP89] A. P. Molchanov and E. S. Pyatnitskiy. Criteria of asymptotic stability of differential and difference inclusions encountered in control theory. *Systems & Control Letters*, 13(1):59–64, 1989.

[MP95] J. C. Moreno and M. Papageorgiou. A linear programming approach to large-scale linear optimal control problems. *IEEE Transactions on Automatic Control*, 40(5):971–977, 1995.

[MPD05] P. L. Montessoro, D. Pierattoni, and S. Di Giusto. Designing a pervasive architecture for car pooling services. In *Proceedings of the International Joint Conference on Computer, Information, and Systems Science, and Engineering*, 2005.

[MPS90] J. Mallet-Paret and H. L. Smith. The Poincaré-Bendixson theorem for monotone cyclic feedback systems. *Journal of Dynamics and Differential Equations*, 2(4):367–421, 1990.

[MPS+11] K. Montagne, R. Plasson, Y. Sakai, T. Fujii, and Y. Rondelez. Programming an in vitro DNA oscillator using a molecular networking strategy. *Molecular Systems Biology*, 7(1):466, 2011.

[MQ69] J. Maybee and J. Quirk. Qualitative problems in matrix theory. *SIAM Review*, 11(1):30–51, 1969.

[MS82] F. H. Moss and A. Segall. An optimal control approach to dynamic routing in networks. *IEEE Transactions on Automatic Control*, 27(2):329–339, 1982.

[MTES+09] W. Ma, A. Trusina, H. El-Samad, W. A. Lim, and C. Tang. Defining network topologies that can achieve biochemical adaptation. *Cell*, 138(4):760–773, 2009.

[MTF14] V. Mardanlou, C. H. Tran, and E. Franco. Design of a molecular bistable system with RNA-mediated regulation. In *IEEE Conference on Decision and Control*, 2014.

[MvO09] S. Mukherji and A. van Oudenaarden. Synthetic biology: understanding biological design from synthetic circuits. *Nature reviews. Genetics*, 10(12):859–871, 2009.

[MY10] N. Muranaka and Y. Yokobayashi. A synthetic riboswitch with chemical band-pass response. *Chemical Communications*, 46(36):6825–6827, 2010.

[Nag42] M. Nagumo. Über die Lage der Integralkurven gewöhnlicher Differentialgleichungen. *Proc. Phys-Math. Soc. Japan*, 24(3):272–559, 1942.

[Ngu12] L. Nguyen. Regulation of oscillation dynamics in biochemical systems with dual negative feedback loops. *Journal of The Royal Society Interface*, 9(73):1998–2010, 2012.

[NII+05] M. Nakajima, K. Imai, H. Ito, T. Nishiwaki, Y. Murayama, H. Iwasaki, T. Oyama, and T. Kondo. Reconstitution of circadian oscillation of cyanobacterial KaiC phosphorylation in vitro. *Science*, 308(5720):414–415, 2005.

[Nou06] D. Noutsos. On Perron-Frobenius property of matrices having some negative entries. *Linear Algebra and its Applications*, 412:132–153, 2006.

[NT08] B. Novak and J. J. Tyson. Design principles of biochemical oscillators. *Nature Reviews Molecular Cell Biology*, 9(12):981–991, 2008.

[NYWP07] S. Nikolov, E. Yankulova, O. Wolkenhauer, and V. Petrov. Principal difference between stability and structural stability (robustness) as used in systems biology. *Nonlinear Dynamics, Psychology, and Life Sciences*, 11(4):413–33, 2007.

[OC95] R. Ortega and J. Campos. Some applications of the topological degree to stability theory. In A. Granas, M. Frigon, and G. Sabidussi, editors, *Topological Methods in Differential Equations and Inclusions*, volume 472 of *NATO ASI Series*, pages 377–409. Springer Netherlands, 1995.

[OJCC06] D. O'Regan, Y. Je Cho, and Y.-Q. Chen. *Topological Degree Theory and Applications*, volume 10 of *Series in Mathematical Analysis and Applications*. Chapman & Hall/CRC, 2006.

[OnZ07] F. Ordóñez and J. Zhao. Robust capacity expansion of network flows. *Network*, 50(2):136–145, 2007.

[OSFFS06] R. Olfati-Saber, E. Franco, E. Frazzoli, and J. S. Shamma. Belief consensus and distributed hypothesis testing in sensor networks. In *Networked Embedded Sensing and Control*, pages 169–182. Springer, 2006.

[OSFM07] R. Olfati-Saber, J. A. Fax, and R. M. Murray. Consensus and cooperation in networked multi-agent systems. In *Proceedings of the IEEE*, volume 95, January 2007.

[OSM04] R. Olfati-Saber and R. M. Murray. Consensus problems in networks of agents with switching topology and time-delays. *IEEE Transactions on Automatic Control*, 49(9):1520–1533, 2004.

[PB09] R. M. Pussente and V. C. Barbosa. An algorithm for clock synchronization with the gradient property in sensor networks. *Journal of Parallel and Distributed Computing*, 69(3):261–265, 2009.

[PC66] K. Pye and B. Chance. Sustained sinusoidal oscillations of reduced pyridine nucleotide in a cell-free extract of saccharomyces carlsbergensis. *Proceedings of the National Academy of Sciences of the USA*, 4:888–894, 1966.

[PFR12] A. Padirac, T. Fujii, and Y. Rondelez. Bottom-up construction of *in vitro* switchable memories. *Proceedings of the National Academy of Sciences*, 109(47):E3212–E3220, 2012.

[PIL05] R. J. Prill, P. A. Iglesias, and A. Levchenko. Dynamic properties of network motifs contribute to biological network organization. *Public Library of Science Biology*, 3(11):e343, 2005.

[PL85] C. J. Puccia and R. Levins. *Qualitative Modeling of Complex Systems*. Harvard University Press, Cambridge, MA, 1985.

[Poi92] H. Poincaré. *Les Méthodes Nouvelles de la Mécanique Céleste*. Gauthier-Villars, Paris, 1892.

[Pop34] K. Popper. *Logik der Forschung*. Mohr Siebeck, 1934.

[Pop63] K. Popper. *Conjectures and Refutations*. Routledge, 1963.

[PSF03] J. R. Pomerening, E. D. Sontag, and J. E. Ferrell. Building a cell cycle oscillator: hysteresis and bistability in the activation of Cdc2. *Nat Cell Biol*, 5(4):346–351, 04 2003.

[PSGdB10] O. Purcell, N. J. Savery, C. S. Grierson, and M. di Bernardo. A comparative analysis of synthetic genetic oscillators. *Journal of The Royal Society Interface*, 7(52):1503–1524, 2010.

[PTB03] C. S. Park, M. J. Tahk, and H. Bang. Multiple aerial vehicle formation using swarm intelligence. In *Proceedings of AIAA Guidance, Navigation and Control Conference and Exhibit*, pages 5729–5737, Austin, TX, 2003.

[QBM+10] X. Qin, M. Byrne, T. Mori, P. Zou, D. R. Williams, H. Mchaourab, and C. H. Johnson. Intermolecular associations determine the dynamics of the circadian KaiABC oscillator. *Proceedings of the National Academy of Sciences of the USA*, 107(33):14805–14810, 2010.

[QD92] R. X. Qian and C. L. DeMarco. An approach to robust stability of matrix polytopes through copositive homogeneous polynomials. *IEEE Transactions On Automatic Control*, 37(6):848–852, 1992.

[QNKS07] L. Qiao, R. B. Nachbar, I. G. Kevrekidis, and S. Y. Shvartsman. Bistability and Oscillations in the Huang-Ferrell Model of MAPK Signaling. *Public Library of Science Computational Biology*, 3(9):e184, 2007.

[Raj12] R. Rajamani. *Vehicle Dynamics and Control*. Lecture Notes in Computer Science. Springer, second edition, 2012.

[Ran15] A. Rantzer. Scalable control of positive systems. *European Journal of Control*, 24(7):72–80, 2015.

[Rap76a] P. Rapp. Analysis of biochemical phase-shift oscillators by a harmonic balancing technique. *Journal Of Mathematical Biology*, 3(3–4):203–224, 1976.

[Rap76b] P. Rapp. Mathematical techniques for the study of oscillations in biochemical control loops. *Bull. Inst. Math. Appl*, 12:11–21, 1976.

[RBA07] W. Ren, R. W. Beard, and E. M. Atkins. Information consensus in multivehicle cooperative control: collective group behavior through local interaction. *IEEE Control Systems Magazine*, 27(2):71–82, 2007.

[RBB10] N. Radde, N. S. Bar, and M. Banaji. Graphical methods for analysing feedback in biological networks - a survey. *International Journal of Systems Science*, 41(1):35–46, 2010.

[RC10] W. Ren and Y. Cao. *Distributed Coordination of Multi-agent Networks: Emergent Problems, Models,and Issues*. Springer, 2010.

[RC11] A. Richard and J. P. Comet. Stable periodicity and negative circuits in differential systems. *Journal of Mathematical Biology*, 63(3):593–600, 2011.

[RFTI15] C. Ravazzi, P. Frasca, R. Tempo, and H. Ishii. Ergodic randomized algorithms and dynamics over networks. *IEEE Transactions on Control of Network Systems*, 2:78–87, 2015.

[RGBB09] C. Russo, C. Giuraniuc, R. Blossey, and J.-F. Bodart. On the equilibria of the MAPK cascade: Cooperativity, modularity and bistability. *Physica A: Statistical Mechanics and Its Applications*, 388(24):5070–5080, 2009.

[RHL77] N. Rouche, P. Habets, and M. Laloy. *Stability theory by Liapunov's direct method*, volume 22 of *Applied Mathematical Sciences*. Springer-Verlag, New York, 1977.

[RI96] H. Raza and P. Ioannou. Vehicle following control design for automated highway systems. *IEEE Control Systems*, 16(6):43–60, 1996.

[ROE90] G. Rabai, M. Orban, and I. R. Epstein. Systematic design of chemical oscillators. 64. design of pH-regulated oscillators. *Accounts of Chemical Research*, 23(8):258–263, 1990.

[RW02] D. Richeson and J. Wiseman. A fixed point theorem for bounded dynamical systems. *Illinois Journal of Mathematics*, 46(2):491–495, 2002.

[RW04] D. Richeson and J. Wiseman. Addendum to: "A fixed point theorem for bounded dynamical systems" [*Illinois J. Math.* 46(2):491–495, 2002]. *Illinois Journal of Mathematics*, 48(3):1079–1080, 2004.

[Sah05] E. Sahin. *Swarm Robotics: from Sources of Inspiration to Domains of Application*. Lecture Notes in Computer Science. Springer, 2005.

[SAS10] L. Scardovi, M. Arcak, and E. D. Sontag. Synchronization of interconnected systems with applications to biochemical networks: An input-output approach. *IEEE Transactions on Automatic Control*, 55(6):1367–1379, 2010.

[SBK05] B. Sundararaman, U. Buy, and A. D. Kshemkalyani. Clock synchronization for wireless sensor networks: A survey. *Ad Hoc Networks*, 3:281–323, 2005.

[SCB+08] J. Stricker, S. Cookson, M. R. Bennett, W. H. Mather, L. S. Tsimring, and J. Hasty. A fast, robust and tunable synthetic gene oscillator. *Nature*, 456(7221):516–519, 2008.

[Sch69] J. T. Schwartz. *Nonlinear Functional Analysis*. Gordon and Breach, New York, 1969.

[Sch86] A. Schrijver. *Theory of Linear and Integer Programming*. John Wiley & Sons, 1986.

[SF10] G. Shinar and M. Feinberg. Structural sources of robustness in biochemical reaction networks. *Science*, 327(5971):1389–1391, 2010.

[SF11] L. Schenato and F. Fiorentin. Average timesynch: A consensus-based protocol for clock synchronization in wireless sensor networks. *Automatica*, 47(9):1878–1886, 2011.

[SFM10] C. Sturk, E. Franco, and R. M. Murray. Tuning a synthetic in vitro oscillator using control-theoretic tools. In *Proceedings of the IEEE Conference on Decision and Control*, pages 2554–2559, 2010.

[SGGS09] D. Siegal-Gaskins, E. Grotewold, and G. D. Smith. The capacity for multistability in small gene regulatory networks. *BMC Systems Biology*, 3:96, 2009.

[SGH+10] O. Shoval, L. Goentoro, Y. Hart, A. Mayo, E. Sontag, and U. Alon. Fold-change detection and scalar symmetry of sensory input fields. *Proceedings of the National Academy of Sciences of the USA*, 107(36):15995–16000, 2010.

[SGMGSG11] D. Siegal-Gaskins, M. K. Mejia-Guerra, G. D. Smith, and E. Grotewold. Emergence of switch-like behavior in a large family of simple biochemical networks. *PLoS Comput Biol*, 7(5):e1002039, 2011.

[SH07] R. S. Smith and F. Y. Hadaegh. Closed-loop dynamics of cooperative vehicle formations with parallel estimators and communication. *IEEE Transactions on Automatic Control*, 52(8):1404–1414, 2007.

[SHPB12] W. Saad, Z. Han, H. V. Poor, and T. Basar. Game theoretic methods for the smart grid. *IEEE Signal Processing Magazine*, 29(5):86–105, 2012.

[SKW11] P. Subsoontorn, J. Kim, and E. Winfree. Bistability of an in vitro synthetic autoregulatory switch. 2011. arxiv:1101.0723.

[SKW12] P. Subsoontorn, J. Kim, and E. Winfree. Ensemble bayesian analysis of bistability in a synthetic transcriptional switch. *ACS Synthetic Biology*, 1(8):299–316, 2012.

[SMH99] G. B. Shaw, D. W. Miller, and D. E. Hastings. *The generalized information network analysis methodology for distributed satellite systems*. PhD thesis, 1999.

[Smi08] H. L. Smith. *Monotone Dynamical Systems: An Introduction to the Theory of Competitive and Cooperative Systems*. American Mathematical Society, 2008.

[SMRMA07] G. Shinar, R. Milo, M. Rodrìguez Martìnez, and U. Alon. Input-output robustness in simple bacterial signaling systems. *Proceedings of the National Academy of Sciences of the USA*, 104:19931–199935, 2007.

[Sno98] E. H. Snoussi. Necessary conditions for multistationarity and stable periodicity. *Journal of Biological Systems*, 6(1):3–9, 1998.

[Sol12] S. Soliman. Invariants and other structural properties of biochemical models as a constraint satisfaction problem. *Algorithms for Molecular Biology*, 7(1):15, 2012.

[Son01] E. D. Sontag. Structure and stability of certain chemical networks and applications to the kinetic proofreading model of T-Cell receptor signal transduction. *IEEE Transactions on Automatic Control*, 46(7):1028–1047, 2001.

[Son03] E. Sontag. Adaptation and regulation with signal detection implies internal model. *Systems & Control Letters*, 50(2):119–126, 2003.

[Son05] E. D. Sontag. Molecular systems biology and control. *European Journal of Control*, 11(4–5):396–435, 2005.

[Son07] E. D. Sontag. Monotone and near-monotone biochemical networks. *Systems and Synthetic Biology*, 1(2):59–87, 2007.

[Son14a] E. D. Sontag. Quantifying the effect of interconnections on the steady states of biomolecular networks. In *Proceedings of the IEEE Conference on Decision and Control*, pages 5419–5424, 2014.

[Son14b] E. D. Sontag. A technique for determining the signs of sensitivities of steady states in chemical reaction networks. *IET Systems Biology*, 8(6):251–267, 2014.

[Son15] E. D. Sontag. Lecture notes on mathematical systems biology, 2015.

[Sou04] C. Soulé. Graphic requirements for multistationarity. *ComPlexUs*, 1(3):123–133, 2004.

[SP85] E. A. Silver and R. Peterson. *Decision System for Inventory Management and Production Planning*. Wiley, New York, NY, 1985.

[SP07] A. Serganov and D. J. Patel. Ribozymes, riboswitches and beyond: regulation of gene expression without proteins. *Nature Reviews Genetics*, 8(10):776–790, 10 2007.

[SPO97] P. A. Spiro, J. S. Parkinson, and H. G. Othmer. A model of excitation and adaptation in bacterial chemotaxis. *Proceedings of the National Academy of Sciences of the USA*, 94(4):7263–7268, 1997.

[SPS98] R. Sanchez Pena and M. Sznaier. *Robust systems, Theory and Applications*. Wiley, New York, 1998.

[SPTK08] H. Sarimveisa, P. Patrinos, C. D. Tarantilis, and C. T. Kiranoudis. Dynamic modeling and control of supply chain systems: A review. *Computers & Operations Research*, 35:3530–3561, 2008.

[Srz85] R. Srzednicki. On rest points of dynamical systems. *Fundamenta Mathematicae*, 126(1):69–81, 1985.

[SS61] R. A. Spangler and F. M. Snell. Sustained oscillations in a catalytic chemical system. *Nature*, 191:457–458, 1961.

[SS07] O. Simeone and U. Spagnolini. Distributed time synchronization in wireless sensor networks with coupled discrete-time oscillators. *EURASIP Journal on wireless sensor networks*, 2007.

[SS09] M. V. Subbotin and R. S. Smith. Design of distributed decentralized estimators for formations with fixed and stochastic communication topologies. *Automatica*, 45(11):2491–2501, 2009.

[SSS09] S. S. Stanković, M. S. Stanković, and D. M. Stipanović. Consensus based overlapping decentralized estimator. *IEEE Transactions on Automatic Control*, 54(2):410–415, 2009.

[Str94] S. H. Strogatz. *Nonlinear Dynamics and Chaos*. Perseus Book Publishing, Reading, Massachusetts, 1994.

[SV87] M. A. Savageau and E. O. Voit. Recasting nonlinear differential equations as S-systems: a canonical nonlinear form. *Mathematical Biosciences*, 87(1):83–115, 1987.

[SVB07] S. D. M. Santos, P. J. Verveer, and P. I. H. Bastiaens. Growth factor-induced MAPK network topology shapes Erk response determining PC-12 cell fate. *Nature Cell Biology*, 9(3):324–330, 2007.

[SWSK11] R. Steuer, S. Waldherr, V. Sourjik, and M. Kollmann. Robust signal processing in living cells. *PLoS Computational Biology*, 7(11):e1002218, 2011.

[SWX08] Y. G. Sun, L. Wang, and G. Xie. Average consensus in networks of dynamic agents with switching topologies and multiple time-varying delays. *Systems & Control Letters*, 57(2):175–183, 2008.

[TB05] B. J. Tucker and R. R. Breaker. Riboswitches as versatile gene control elements. *Current Opinion in Structural Biology*, 15(3):342–348, 2005.

[TCM+08] T. Y.-C. Tsai, Y. S. Choi, W. Ma, J. R. Pomerening, C. Tang, and J. E. J. Ferrell. Robust, tunable biological oscillations from interlinked positive and negative feedback loops. *Science*, 321(5885):126–129, 2008.

[TDG+10] M. Tigges, N. Dénervaud, D. Greber, J. Stelling, and M. Fussenegger. A synthetic low-frequency mammalian oscillator. *Nucleic Acids Research*, 38(8):2702–2711, 2010.

[Tho81] R. Thomas. On the relation between the logical structure of systems and their ability to generate multiple steady states or sustained oscillations. In J. Dora, J. Demongeot, and B. Lacolle, editors, *Numerical Methods in the Study of Critical Phenomena*, volume 9 of *Springer Series in Synergetics*, pages 180–193. Springer-Verlag, Berlin Heidelberg, 1981.

[Tho94] R. Thomas. The role of feedback circuits: Positive feedback circuits are a necessary condition for positive real eigenvalues of the jacobian matrix. *Berichte der Bunsengesellschaft für physikalische Chemie*, 98(9):1148–1151, 1994.

[Tia04] T. Tian. Robustness of mathematical models for biological systems. *ANZIAM J.*, 45:C565–C577, 2004.

[TKSS09] M. Takinoue, D. Kiga, K.-i. Shohda, and A. Suyama. Design and numerical analysis of RNA oscillator. In Y. Suzuki, M. Hagiya, H. Umeo, and A. Adamatzky, editors, *Natural Computing*, volume 1 of *Proceedings in Information and Communications Technology*, pages 201–212. Springer Japan, 2009.

[TKY08] K. Topley, V. Krishanmurty, and G. Yin. Consensus formation in a switched markovian dynamical systems. In *Proceedings of the IEEE Conference on Decision and Control*, pages 3547–3552, Cancun, Mexico, 2008.

[TMLSF09] M. Tigges, T. T. Marquez-Lago, J. Stelling, and M. Fussenegger. A tunable synthetic mammalian oscillator. *Nature*, 457(7227):309–312, 2009.

[TSE99] G. Tononi, O. Sporns, and G. M. Edelman. Measures of degeneracy and redundancy in biological networks. *Proc. Natl. Acad. Sci. USA*, 96(6):3257–3262, March 1999.

[Tsi84] J. Tsitsiklis. Problems in decentralized decision making and computation, 1984. PhD Thesis, MIT.

[TWH+13] C. Thomaseth, P. Weber, T. Hamm, K. Kashima, and N. Radde. Modeling sphingomyelin synthase 1 driven reaction at the Golgi apparatus can explain data by inclusion of a positive feedback mechanism. *Journal of Theoretical Biology*, 337:174–180, 2013.

[Ugr13] V. Ugrinovskii. Distributed robust estimation over randomly switching networks using H_∞ consensus. *Automatica*, 49(1):160–168, 2013.

[vB69] L. von Bertalanffy. *General System Theory, Foundations, Development, Applications*. George Braziller, New York, 1969.

[vdH04] G. H. M. van der Heijden. *"Hopf bifurcation", in Encyclopedia of Nonlinear Science*. Routledge, London and New York, 2004.

[VF21] O. Veblen and P. Franklin. On matrices whose elements are integers. *Annals of Mathematics*, 23:1–15, 1921.

[VFFO14] L. Vassio, F. Fagnani, P. Frasca, and A. Ozdaglar. A message passing algorithm for the evaluation of social influence. In *European Control Conference*, pages 190–195, Strasbourg, France, 2014.

[VKBL02] J. M. G. Vilar, H. Y. Kueh, N. Barkai, and S. Leibler. Mechanisms of noise-resistance in genetic oscillators. *Proceedings of the National Academy of Sciences of the United States of America*, 99(9):5988–5992, 2002.

[Vol26] V. Volterra. Fluctuations in the abundance of a species considered mathematically. *Nature*, 118:558–560, 1926.

[vRJ13] A. J. van der Schaft, S. Rao, and B. Jayawardhana. On the mathematical structure of balanced chemical reaction networks governed by mass action kinetics. *SIAM Journal on Applied Mathematics*, 73(2):953–973, 2013.

[VRMG04] A. G. Vitreschak, D. A. Rodionov, A. A. Mironov, and M. S. Gelfand. Riboswitches: the oldest mechanism for the regulation of gene expression? *Trends In Genetics*, 20(1):44–50, 2004.

[Wag05] A. Wagner. Circuit topology and the evolution of robustness in two-gene circadian oscillators. *Proceedings of the National Academy of Sciences of the United States of America*, 102(33):11775–11780, 2005.

[WAJS12] S. Waldherr, F. Allgöwer, E. W. Jacobsen, and S. Streif. Robustness and adaptation of biological networks under kinetic perturbations. In F. Allgöwer, V. Blondel, and U. Helmke, editors, *Control Theory: Mathematical Perspectives on Complex Networked Systems*, pages 663–664. Mathematisches Forschungsinstitut Oberwolfach, 2012.

[WAKP08] Y. Wang, A. Ahmed, B. Krishnamachari, and K. Psounis. IEEE 802.11p performance evaluation and protocol enhancement. In *Proceedings of the IEEE International Conference on Vehicular Electronics and Safety*, pages 22–24, Columbus, OH, USA, 2008.

[Wat07] D. S. Watkins. *The Matrix Eigenvalue Problem: GR and Krylov Subspace Methods*. Society for Industrial and Applied Mathematics, 2007.

[WB05] W. C. Winkler and R. R. Breaker. Regulation of bacterial gene expression by riboswitches. *Annual Review of Microbiology*, 59(1):487–517, 2005.

[WCA06] R. Wanga, L. Chenc, and K. Aiharaa. Construction of genetic oscillators with interlocked feedback networks. *Journal of Theoretical Biology*, 242:454–463, 2006.

[WCS96] J. Wolfe, D. Chichka, and J. Speyer. Decentralized controllers for unmanned aerial vehicle formation flight. *AIAA*, 96–3833, 1996.

[WD73] S. H. Wang and E. J. Davison. On the stabilization of decentralized control systems. *IEEE Transactions on Automatic Control*, 18(5):473–478, 1973.

[Wei16] J. Wei. *Consensus Dynamics in Distribution Networks and Nonlinear Multi-Agent Systems*. PhD thesis, University of Groningen, 2016.

[WGC04] O. Wolkenhauer, B. K. Ghosh, and K. H. Cho. Biochemical networks and cell regulation. Special section on systems biology. *IEEE Control Systems Magazine*, 24(4):30–102, 2004.

[WH95] T. Wilhelm and R. Heinrich. Smallest chemical reaction system with Hopf bifurcation. *Journal of Mathematical Chemistry*, 17(1):1–14, 1995.

[WH96] T. Wilhelm and R. Heinrich. Mathematical analysis of the smallest chemical reaction system with Hopf bifurcation. *Journal of Mathematical Chemistry*, 19(2):111–130, 1996.

[WHO+15] P. Weber, M. Hornjik, M. Olayioye, A. Hausser, and N. Radde. A computational model of PKD and CERT interactions at the trans–Golgi network of mammalian cells. *BMC Systems Biology*, 9(1):9, 2015.

[Wie48] N. Wiener. *Cybernetics or Control and Communication in the Animal and the Machine*. MIT Press, Cambridge, MA, 1948.

[Wil76] J. C. Willems. Lyapunov functions for diagonally dominant systems. *Automatica*, 12(5):519–523, 1976.

[Wil09] T. Wilhelm. The smallest chemical reaction system with bistability. *BMC Systems Biology*, 3(1):90, 2009.

[Win80] A. T. Winfree. *The Geometry of Biological Time*. Springer-Verlag, New York, NY, 1980.

[WLCA10] R. Wang, C. Li, L. Chen, and K. Aihara. Modeling and analyzing biological oscillations in molecular networks. *Proceedings of the IEEE*, 96(8):1361–1385, 2010.

[WLD10] R. W. Whittlesey, S. Liska, and J. O. Dabiri. Fish schooling as a basis for vertical axis wind turbine farm design. *Bioinspiration and Biomimetics*, 5(3):035005, 2010.

[WRL14] S. Wang, W. Ren, and Z. Li. Information-driven fully distributed Kalman filter for sensor networks in presence of naive nodes. *arXiv:1410.0411*, 2014.

[WS08] L. Wang and E. D. Sontag. Singularly perturbed monotone systems and an application to double phosphorylation cycles. *J. Nonlinear Sciences*, 18(5):527–550, 2008.

[WSA12] S. Waldherr, S. Streif, and F. Allgöwer. Design of biomolecular network modifications to achieve adaptation. *IET Systems Biology*, 6(6):223–231, 2012.

[WTL07] W. W. Wong, T. Y. Tsai, and J. C. Liao. Single-cell zeroth-order protein degradation enhances the robustness of synthetic oscillator. *Molecular Systems Biology*, 3:130, 2007.

[WvdS13a] J. Wei and A. J. van der Schaft. Load balancing of dynamical distribution networks with flow constraints and unknown in/outflows. *Systems & Control Letters*, 62(11):1001–1008, 2013.

[WvdS13b] J. Wei and A. J. van der Schaft. Stability of dynamical distribution networks with arbitrary flow constraints and unknown in/outflows. In *Proceedings of the IEEE Conference on Decision and Control*, pages 55–60, Firenze, Italy, 2013.

[XF03] W. Xiong and J. E. Ferrell. A positive-feedback-based bistable memory module that governs a cell fate decision. *Nature*, 426(6965):460–465, 2003.

[YFJ13] Q. Yang and J. E. Ferrell Jr. The Cdk1-APC/C cell cycle oscillator circuit functions as a time-delayed, ultrasensitive switch. *Nature cell biology*, 15(5):519–525, 2013.

[YHSD00] T. M. Yi, Y. Huang, M. I. Simon, and J. Doyle. Robust perfect adaptation in bacterial chemotaxis through integral feedback control. *Proceedings of the National Academy of Sciences of the USA*, 97(9):4649–4653, 2000.

[YKM13] E. Yeung, J. Kim, and R. M. Murray. Resource competition as a source of non-minimum phase behavior in transcription-translation systems. In *Proceedings of the IEEE Conference on Decision and Control*, pages 4060–4067, 2013.

[YM03] N. Yildirim and M. C. Mackey. Feedback regulation in the lactose operon: A mathematical modeling study and comparison with experimental data. *Biophysical Journal*, 84(5):2841–2851, 2003.

[YSHM04] N. Yildirim, M. Santillan, D. Horike, and M. Mackey. Dynamics and bistability in a reduced model of the *lac* operon. *Chaos*, 14(2):279–292, 2004.

[Zan96] F. Zanolin. Continuation theorems for the periodic problem via the translation operator. *Rend. Sem. Mat. Univ. Politec. Torino*, 54:1–23, 1996.

[ZDG96] K. Zhou, J. C. Doyle, and K. Glower. *Robust and Optimal Control*. Prentice-Hall, Englewood Cliff, NJ, 1996.

[Zho13] T. Zhou. Coordinated one-step optimal distributed state prediction for a networked dynamical system. *IEEE Transactions on Automatic Control*, 58(11):2756–2771, 2013.